GEOLOGICAL SURVEY RESEARCH 1981

GEOLOGICAL SURVEY PROFESSIONAL PAPER 1275

A summary of recent significant scientific and economic results accompanied by a list of geologic, hydrologic, and cartographic investigations in progress

UNITED STATES GOVERNMENT PRINTING OFFICE, WASHINGTON, D.C.: 1982

UNITED STATES DEPARTMENT OF THE INTERIOR

JAMES G. WATT, *Secretary*

GEOLOGICAL SURVEY

Dallas L. Peck, *Director*

Library of Congress catalog-card No. 68-46150

For sale by the Superintendent of Documents, U.S. Government Printing Office
Washington, D.C. 20402

CONTENTS

ILLUSTRATIONS

TABLES

ABBREVIATIONS

A ___ angstrom
AAPG ___ American Association of Petroleum Geologists
ABAG ___ Association of Bay Area Governments
ac ___ alternating current
A.D. ___ anno Domini
ADP ___ automatic data processing
AESOP ___ Automatic Surface Observation Platforms
AGID ___ Association of Geoscientists for International Development
AGWAT ___ Ministry of Agriculture and Water
AID ___ Agency for International Development
AIDJEX ___ Arctic Ice Dynamics Joint Experiment
AMRAP ___ Alaska Mineral Resource Assessment Program
ANCSA ___ Alaska Native Claims Settlement Act
AOCS ___ Atlantic Outer Continental Shelf
APD ___ antiphase domain
ARPA ___ Advanced Research Projects Agency
ASL ___ Albuquerque Seismological Laboratory
ASRO ___ Advanced Seismological Research Observatories
atm ___ atmosphere

b ___ barn (area)
bbl ___ barrel
BIA ___ Bureau of Indian Affairs
BLM ___ Bureau of Land Management
BOD ___ biochemical oxygen demand
B.P. ___ before present
Btu ___ British thermal unit
b.y. ___ billion years

°C ___ degrees Celsius
CAI ___ color alteration index
cal ___ calorie
CARETS ___ Central Atlantic Regional Ecological Test Site project
CCD ___ Computer Center Division
CCOP ___ U.N. Committee for Coordination of Joint Prospecting for Mineral Resources in Asian Offshore Areas
CCT ___ computer-compatible tape
C/DCP ___ convertible data-collection platforms
CDP ___ common depth point
CENTO ___ Central Treaty Organization
CEQ ___ Council on Environmental Quality
CFRUC ___ Colorado Front Range Urban Corridor Project
CGIS ___ Canada Geographic Information System
cgs ___ centimeter-gram-second
Ci ___ curie
cm ___ centimeter
COD ___ chemical oxygen demand
COGEODATA ___ Committee on storage, automatic Processing, and Retrieval of Geologic Data
COM ___ computer-oriented microform
COST ___ Continental Off-shore Stratigraphic Test Group
cps ___ counts per second
CPU ___ central processing unit
CRIB ___ Computerized Resource Information Bank
CV ___ characteristic value

d ___ day
D ___ Darcy
db ___ decibel
dc ___ direct current
DCAP ___ Digital Cartographic Applications Program
DCS ___ data-collection system
DEROCS ___ Development of Energy Resources of the Outer Continental Shelf
DMA ___ Defense Mapping Agency
DNPM ___ Departmento Nacional da Producão Mineral
DO ___ dissolved oxygen
DOD ___ Department of Defense
DOE ___ Department of Energy
DOI ___ Department of the Interior
DOMES ___ Deep Ocean Mining Environmental Study
DSDP ___ Deep Sea Drilling Project
dyn ___ dyne

EAO ___ Environmental Affairs Office
EDC ___ EROS Data Center
Eh ___ oxidation reduction potential
EIA ___ Environmental Impact Analysis
EIS ___ environmental impact statement
EM ___ electromagnetic (soundings)
EMRIA ___ Energy Mineral Rehabilitation Inventory and Analysis
emu ___ electromagnetic unit
EPA ___ Environmental Protection Agency
ERDA ___ Energy Research and Development Administration
EROS ___ Earth Resources Observation System
ERTS ___ Earth Resources Technology Satellite
ESCAP ___ Economic and Social Commission for Asia and the Pacific Committeee on Natural Resources
eV ___ electronvolt

FAA ___ Federal Aviation Administration
FAO ___ Food and Agriculture Organization
ft ___ foot
f.l. ___ focal length
FLD ___ Fraunhofer line discriminator
FY ___ fiscal year
FWS ___ Fish and Wildlife Service

g ___ gram
GHz ___ gigahertz
GIPSY ___ General Information Processing System
GIRAS ___ Geographic Information Research and Analysis System
G.M.T. ___ Greenwich mean time
GOES ___ Geostationary Operational Environmental Satellite
GPa ___ gigapascal
GRASP ___ Geologic Retrieval and Synopsis Program

h ___ hour
h ___ height
H ___ Henry
ha ___ hectare
HFU ___ heat-flow unit
HIPLEX ___ High Plains Cooperative Program
hm ___ hectometer
HUD ___ Department of Housing and Urban Development
Hz ___ hertz

IAH ___ International Association of Hydrogeologists
IAHS ___ International Association of Hydrological Scientists
ICAT ___ Inorganic Chemical Analysis Team
IDB ___ Inter-American Development Bank
IDIMS ___ Interactive Display Image Manipulation System
IDOE ___ International Decade of Ocean Exploration
IGCP ___ International Geological Correlation Program
IGU ___ International Geophysical Union
IHD ___ International Hydrological Decade
IHP ___ International Hydrological program
IMW ___ International Map of the World
in ___ inch
IR ___ infrared
ISAM ___ Index Sequential Access Method
ISO ___ International Standardization Organization
IUGS ___ International Union of Geologic Sciences

J ___ joule
JECAR ___ Joint Commission of Economic Cooperation
JPL ___ Jet Propulsion Laboratory
JTU ___ Jackson turbidity unit

K ___ kelvin
kbar ___ kilobar
KCLA ___ Known Coal Leasing Area
KeV ___ kiloelectronvolt
kg ___ kilogram
KGRA ___ Known Geothermal Resources Area
KGS ___ Known Geologic Structure
kHz ___ kilohertz
km ___ kilometer
kn ___ knot
KRCRA ___ Known Recoverable Coal Resource Area
KREEP ___ potassium-rare-earth element-phosphorus
kWh ___ kilowatt-hour

L,l ___ liter
lb ___ pound
LARS ___ Laboratory for Application of Remote Sensing
lat ___ latitude
LMF ___ lithic matrix fragments
long ___ longitude

m ___ meter
M ___ magnitude (earthquake)
m_b ___ magnitude from body waves
M_L ___ Richter magnitude
M_s ___ magnitude from surface waves
mcal ___ millicalorie
mD ___ millidarcy
MEF ___ maximum evident flood
Mg ___ megagram
mg ___ milligram
mGal ___ milligal
mi ___ mile
min ___ minute
ml ___ milliliter
mm ___ millimeter
MM ___ Modified Mercalli intensity
MN ___ meganewton
mo ___ month
mol ___ mole
MPa ___ megapascal
ms ___ milliseconds
MSS ___ multispectral scanner
Mt ___ megaton
mV ___ millivolt
MW ___ megawatt
MWe ___ megawatts electrical
m.y. ___ million years
μ ___ micron
μcal ___ microcalorie
μg ___ microgram
μGal ___ microgal
μl ___ microliter
μm ___ micrometer
μmho ___ micromho
μrad ___ microradian
μstrain/yr ___ engineering shear

NAS ___ National Academy of Science
NASA ___ National Aeronautics and Space Administration
NASQAN ___ National Stream Quality Accounting Network
NAWDEX ___ National Water Data Exchange
NCRDS ___ National Coal Resources Data System
NEIS ___ National Earthquake Information Service
NEPA ___ National Environmental Policy Act
ng ___ nanogram

NGSDC ____National Geophysical and Solar-Terrestrial Data Center
NLCR ____nonlinear complex resistivity
nm ____nanometer
NOAA __National Oceanic and Atmospheric Administration
NOS ____National Ocean Survey
NPRA ____Naval Petroleum Reserve in Alaska
NRA ____National Resources Agency
NRA ____Nuclear Regulatory Agency
NSF ____National Science Foundation
nt ____nanotesla
NTIS ____National Technical Information Service
NTMS ____National Topographic Map Series
NTS ____Nevada Test Site
NURE ____National Uranium Resource Evaluation
NWS ____National Weather Service

OAS ____Organization of American States
OCS ____Outer Continental Shelf
OE ____Oersted
ohm-m ____ohm-meter
OIA ____Office of International Activities
OME ____Office of Minerals Exploration
ORNL ____Oak Ridge National Laboratory
OWDC ____Office of Water-Data Coordination
Ω ____ohm

PAIGH ____Pan American Institute of Geography and History
PCB ____polychlorinated byphenyls
pCi ____picocurie
ppb ____part per billion
ppm ____part per million
psi ____pounds per square inch
PSRV ____pseudorelative velocity

R ____range
rad ____radian
RASS ____Rock Analysis Storage System
RBV ____return beam vidicon
REE ____rare-earth element
RF ____radio frequency
rms ____root mean square
rmse ____root mean square error
R/V ____research vessel

s ____second
SFBRS ____San Francisco Bay Region Environment and Resources Planning Study
SIP ____strongly implicit procedure
SLAR ____side-looking airborne radar
SMS ____Synchronous Meterological Satellite
SOM ____Space Oblique Mercator
SP ____self potential
SRO ____Seismic Research Observatory

t ____tonne
T ____Tesla
TEM ____transmission electron microscopy
TIU ____Thermal-inertia unit
TL ____thermoluminescence
TVA ____Tennessee Valley Authority

UNDP ____U.N. Development Program
UNESCO ___United Nations Educational, Scientific, and Cultural Organization
USAID ____U.S. Agency for International Development
USBM ____U.S. Bureau of Mines
USDA ____U.S. Department of Agriculture
USFS ____U.S. Forest Service
USGS ____U.S. Geological Survey
USPHS ____U.S. Public Health Service
U.S.S.R. ____Union of Soviet Socialist Republics
UTM ____Universal Transverse Mercator

V ____volt
VDETS ____Voice Data Entry Terminal System
VES ____vertical electric soundings
VHRR ____very high resolution radiometer
VLF ____very low frequency
V_p ____velocity of P-waves

W ____watt
WATSTORE ____National Water Data Storage and Retrieval System
WHO ____World Health Organization
wk ____week
WMO ____World Meterological Organization
WRC ____Water Resources Council
WRD ____Water Resources Division
WRDD ____Water Resources Development Department
wt ____weight
WWSSN ____Worldwide Standardized Seismograph Network

yr ____year

SI UNITS AND INCH-POUND SYSTEM EQUIVALENTS

[SI, International System of Units, a modernized metric system of measurement. All values have been rounded to four significant digits except 0.01 bar, which is the exact equivalent of 1 kPa. Use of hectare (ha) as an alternative name for square hectometer (hm^2) is restricted to measurement of land or water areas. Use of liter (L) as a special name for cubic decimeter (dm^3) is restricted to the measurement of liquids and gases; no prefix other than milli should be used with liter. Metric ton (t) as a name for megagram (Mg) should be restricted to commercial usage, and no prefixes should be used with it. Note that the style of $meter^2$ rather than square meter has been used for convenience in finding units in this table. Where the units are spelled out in text, Survey style is to use square meter]

SI unit		Inch-Pound equivalent	
Length			
millimeter (mm)	=	0.039 37	inch (in)
meter (m)	=	3.281	feet (ft)
	=	1.094	yards (yd)
kilometer (km)	=	0.621 4	mile (mi)
	=	0.540 0	mile, nautical (nmi)
Area			
$centimeter^2$ (cm^2)	=	0.155 0	$inch^2$ (in^2)
$meter^3$ (m^2)	=	10.76	$feet^2$ (ft^2)
	=	1.196	$yards^2$ (yd^2)
	=	0.000 247 1	acre
$hectometer^2$ (hm^2)	=	2.471	acres
	=	0.003 861	section (640 acres or 1 mi^2)
$kilometer^3$ (km^2)	=	0.386 1	$mile^2$ (mi^2)
Volume			
$centimeter^3$ (cm^3)	=	0.061 02	$inch^3$ (in^3)
$decimeter^3$ (dm^3)	=	61.02	$inches^3$ (in^3)
	=	2.113	pints (pt)
	=	1.057	quarts (qt)
	=	0.264 2	gallon (gal)
	=	0.035 31	$foot^3$ (ft^3)
$meter^2$ (m^3)	=	35.31	$feet^3$ (ft^3)
	=	1.308	$yards^3$ (yd^3)
	=	264.2	gallons (gal)
	=	6.290	barrels (bbl) (petroleum, 1 bbl = 42 gal)
	=	0.000 810 7	acre-foot (acre-ft)
$hectometer^3$ (hm^3)	=	810.7	acre-feet (acre-ft)
$kilometer^3$ (km^3)	=	0.239 9	$mile^3$ (mi^3)
Volume per unit time (includes flow			
$decimeter^3$ per second (dm^3/s)	=	0.035 31	$foot^3$ per second (ft^3/s)
	=	2.119	$feet^3$ per minute (ft^3/min)

SI unit		Inch-Pound equivalent	
Volume per unit time (includes flow)—Continued			
$decimeter^3$ per second (dm^3/s)	=	15.85	gallons per minute (gal/min)
	=	543.4	barrels per day (bbl/d) (petroleum, 1 bbl = 42 gal)
$meter^3$ per second (m^3/s)	=	35.31	$feet^3$ per second (ft^3/s)
	=	15 850	gallons per minute (gal/min)
Mass			
gram (g)	=	0.035 27	ounce avoirdupois (oz avdp)
kilogram (kg)	=	2.205	pounds avoirdupois (lb avdp)
megagram (Mg)	=	1.102	tons, short (2 000 lb)
	=	0.984 2	ton, long (2 240 lb)
Mass per unit volume (includes density)			
kilogram per $meter^2$ (kg/m^3)	=	0.062 43	pound per $foot^3$ (lb/ft^3)
Pressure			
kilopascal (kPa)	=	0.145 0	pound-force per $inch^2$ (lbf/in^2)
	=	0.009 869	atmosphere, standard (atm)
	=	0.01	bar
	=	0.296 1	inch of mercury at 60°F (in Hg)
Temperature			
temp kelvin (K)	=	[temp deg Fahrenheit (°F) + 459.67]/1.8	
temp deg Celsius (°C)	=	[temp deg Fahrenheit (°F) − 32]/1.8	

GEOLOGICAL SURVEY RESEARCH 1981

MINERAL-RESOURCE INVESTIGATIONS

UNITED STATES AND WORLD MINERAL-RESOURCE ASSESSMENTS

The development of new concepts on the origin and occurrence of mineral deposits can significantly change the United States and world resource picture. Thus, as new data becomes available, it must be analyzed in terms of its impact on the outlook for future supplies of mineral raw materials. In 1980, such analyses led to statements on the resources of a number of commodities.

Aluminum resources of the United States and the world

According to a review by S. H. Patterson, C. L. Neeley, and J. C. Olson of the USGS and H. F. Kurtz of the USBM, the major world bauxite resources are in Africa, Australia, South America, and the Caribbean region; and significant deposits are present in Asia and Europe. The Republic of Guinea has the world's largest bauxite reserves estimated to be 6.5 billion t. Guinea is followed by Australia–4.5 billion, Brazil–2.5 billion, Jamaica–2 billion, and India and Cameroon–1 billion each. Indonesia, Greece, and Guyana each have an estimated 700 million t of reserves, Ghana–570 million, Venezuela–500 million, Surinam–490 million, and Yugoslavia–400 million. Countries having reserves in the 100 to 300 million t range include Costa Rica, Hungary, U.S.S.R., Sierra Leone, and the People's Republic of China. The bauxite reserves in the United States are estimated to be only about 40 million t; and several other countries in the Caribbean region, Europe, and Asia have bauxite reserves of less than 100 million t. Very large subeconomic and virtually certain speculative bauxite resources are located in Africa, South America, and Australia. The other major global regions rank well behind in these categories of resources.

Computerized data bank for mineral occurrences in South America

A project for compilation and synthesis of published and unpublished information about mineral deposits of South America has been initiated as a means of evaluating the mineral potential of the individual countries as well as the region as a whole. According to G. E. Ericksen, summary information, which is being entered in the CRIB computer file, will be used to prepare a series of reports on the principal mineral commodities of South America. It also will be used to establish the parameters of metallogenesis in South America and to determine regional exploration targets. A comprehensive bibliography of the mineral deposits is being compiled and will be published.

Peat occurrences in Maine

During the 1980 field season, 50 areas containing peat deposits in a variety of geologic and physiographic settings were mapped at scales 1:20,000 and 1:15,625 in Piscataquis, Somerset, Kennebec, Waldo, and Aroostook Counties, Maine. C. C. Cameron reported that a total of about 5,580 ha contains commercial quality peat in thickness averaging 1.5 to 5 m. These peat deposits are relatively discrete entities surrounded by bedrock and unconsolidated materials of glacial and fluvial origin, which afford good foundation for access roads and operational plant construction as well as providing materials for operational road construction on the bog. These deposits are in contrast to those on broad expanses of wetlands characteristic of the Atlantic Coastal Plain and the glacial Lake Agassiz Plain in northern Minnesota, where peat suited for resources is more shallow and access across marshlands is more difficult.

The physiography of the Maine deposits, relief and drainage in particular, furnishes clues to quantity and quality of potential peat deposits. For example, deposits in depressions behind natural levees of stream and on fluvio-glacial deltas are apt to be too shallow and have too high an ash content to be of commercial quality, while the best prospects for large peat deposits are in the areas of late Wisconsinan marine readvancement near glacial end moraines.

MINERAL-RESOURCE ASSESSMENTS—LAND AREAS

The USGS systematically assesses the mineral-resource potential of selected 1:250,000-scale quadrangles in the conterminous United States and

Alaska under the Conterminous United States Mineral Resource Assessment Program (CUSMAP) and the Alaska Mineral Resource Assessment Program (AMRAP). In addition, the USGS and USBM assess the mineral-resource potential of areas included or considered for inclusion in the National Wilderness Preservation System.

Regional exploration geochemistry in Alaska

Interpretation of geochemical data for the Chignik and Sutwik Island 1°×2° quadrangles by D. E. Detra showed a trend along the Alaska Peninsula of porphyry-type mineral occurrences lying within Tertiary and Quaternary volcanic-plutonic complexes. These clustered areas of mineralization showed distinct zonal patterns of anomalies of As, Bi, Cu, Au, Pb, Mo, Ag, Sn, W, and Zn. Heavy-mineral-concentrate and stream-sediment data from the Ugashik quadrangle showed clustered anomalies of the same elements plus cadmium, which may indicate an extension of the porphyry-type mineral occurrence trend.

Geochemical anomalies were determined by stream sediment sampling in the Survey Pass quadrangle. Analysis suggested that the known copper- and zinc-bearing stratiform volcanogenic sulfide occurrences found in the Ambler River quadrangle in the Brooks Range extended eastward into the Survey Pass quadrangle. This volcanogenic sulfide mineralization was found in the schist belt located along the southern flank of the Brooks Range. Potential mineralized target areas within the schist belt can be identified by stream sediment geochemistry, magnetic, and lithologic signatures.

W. D. Crim and R. M. O'Leary reported the occurrence of anomalous uranium values in stream-sediment samples from three areas in the Circle 1°×2° quadrangle. One area is in the headwaters of Bear Creek in the west-central part of the quadrangle; the other areas are in the vicinity of Angel Creek and Monument Creek in the southwestern part of the quadrangle.

Aeroradiometric anomalies in the Coastal Plain of Virginia

Andrew Grosz found that with the intensive use of detailed and regional geologic maps, soil maps, land-use and land-cover maps, information on fertilizer use, and ground spectrometer data as filters, aeroradiometric anomalies in the Coastal Plain of Virginia have three general modes of occurrence. First, the most intense anomalies are associated with cultural overprints such as roads made of granitic material. Second, the most frequent anomalies of high-to-intermediate intensity are associated with land used for agricultural purposes, evidently caused by applications of radioactive fertilizer. Third, anomalies of intermediate-to-low intensity are associated with heavy-mineral deposits.

Results of the study showed that aeroradiometric anomalies associated with heavy-mineral accumulations in the Coastal Plain of Virginia have ground radiometric spectra in which thorium is the strongest component with lesser uranium and minor potassium components. Heavy-mineral accumulations in the Coastal Plain of Virginia found by use of the aeroradiometric data are not considered to hold economic importance, mostly because of the low percentage of economic minerals in the heavy-mineral suites, and also due to other factors, such as the very fine-grained nature of the host sediments and competing land use.

Mineral-resource studies in the Ramseys Draft Addition, Virginia–West Virginia

A mineral-resource appraisal of the Ramseys Draft Addition by F. G. Lesure (USGS) and P. C. Mory (USBM) included geologic mapping and geochemical sampling of rocks, soils, and stream sediments. The area is underlain by sedimentary rocks of Late Devonian and Early Mississippian age in a broad syncline. Mineral resources present include sandstone for construction uses, shale suitable for use in brick and tile, and small amounts of sand and gravel. Areas of higher-than-background amounts of copper, lead, and zinc in sandstone of the Hampshire Formation of Late Devonian age form deposits too small to be economic. Structural conditions may be good for the accumulation of natural gas at depth, but no drilling has been done in or near enough to the area to evaluate gas potential.

Oil and gas potential of the Otter Creek and Cheat Mountain Wilderness Areas, West Virginia

Evaluation of subsurface data by E. G. A. Weed indicated that the Paleozoic sedimentary rocks underlying the Otter Creek Wilderness Area and Cheat Mountain Further Planning Area have low-to-moderate potential for natural gas and no potential for oil. Thermal maturation levels of source beds are above the upper limit for oil but are well within the range of dry methane. Thin-skinned faulting in the vicinity decouples surface structures from deeply buried structures along large flat thrusts. Consequently, structures with potential to contain gas in the deeper beds cannot be predicted from surface geology. Prospective structures in the Lower Devonian Oriskany Sandstone or in older strata can be delineated only by seismic profiles and proved by deep drilling. The presence of synclinal structures in the younger Paleozoic rocks does not rule out fault traps in splay faults associated with deeply buried thrusts.

Mineral-resource potential of the North Harpers Creek and Lost Cove RARE II areas

Geochemical and mineralogical studies of heavy-mineral concentrates of stream sediments by W. R. Griffitts, D. F. Siems, and K. A. Duttweiler showed that minerals of vanadium, thorium, niobium, and fluorine are widespread in the North Harpers Creek and Lost Cove RARE II areas. The sources of vanadium, fluorine, and thorium are, at least in part, epigenetic deposits. The bedrock host of the niobium mineral, columbite, has not been found yet.

Mineral-resource studies in the Shining Rock Wilderness Area, North Carolina

Reconnaissance mapping and geochemical sampling by F. G. Lesure (USGS) and M. L. Dunn, Jr. (USBM), showed that the Shining Rock Wilderness Area in the Blue Ridge Mountains of Haywood County, N.C., contains complexly folded, high-grade metamorphic rocks, which contain a few small, uneconomic deposits of sheet muscovite mica. Quartz (SiO_2) and building stone, suitable for crushed rock, are the only potential mineral resources. Other minerals and rocks, such as kaolin, soapstone, copper, corundum, or dunite, have been prospected or mined nearby but have no potential in the Wilderness. A possibility exists for the presence of natural gas at great depth.

Mineral-resource studies in the Big Frog-Cohutta Wilderness Area, Tennessee-Georgia

Reconnaissance geologic mapping and sampling were done by J. F. Slack, assisted by E. R. Force, Andrew Grosz, and Richard Ketelle in the 18.2 km² Big Frog Wilderness Area of southeastern Tennessee and northern Georgia. The area is underlain by the Ocoee Supergroup Proterozoic Y(?) and Z. More than 200 samples of rock, soil, and fine-grained alluvium were analyzed for 31 major, minor, and trace elements. Some rocks contain 5 to 10 percent disseminated sulfides, chiefly pyrite and pyrrhotite, plus tiny intergrowths of chalcopyrite and sphalerite locally, which concentrate copper, zinc, and arsenic at slightly higher than background geochemical values, but produce no significant metal anomalies and are of no current economic interest. No metallic mineral resources are known within the proposed Wilderness. Resources of slate, phyllite, stone, and sand and gravel are present, but are not now economically significant because similar materials exist closer to markets outside the study area. In the adjacent 152 km² Cohutta Wilderness and Hemp Top Further Planning Areas, a similar study was done by J. E. Gair and J. F. Slack, assisted by Richard Ketelle, Andrew Grosz, A. E. Stevenson, D. K. Henry, J. T. Hanley, and T. L. Muzik. Geochemical data from 390 samples of rock and quartz veins, 405 samples of soil, and 231 samples of fine-grained alluvium indicate no potential for resources of copper, zinc, gold, and other metals mined currently or in the past in nearby areas. As in the Big Frog Study Area, resources of rock are present, but there is little likelihood of their exploitation because of inaccessibility and the ready availability of similar materials closer to markets.

Geophysical studies in the Powderhorn Wilderness Study Area, Colorado

R. A. Martin reported that magnetic flows of basalt lava cap the high plateaus in the southern part of the study area and cause intense, steep-gradient magnetic anomalies. North of the plateaus, where the volcanic cover thins, a gentle saddle on a magnetic ridge correlates with the intrusion at Trout Creek. A magnetic high southeast of the Trout Creek intrusion covers an area in which monzonitic and rhyolitic porphyry dikes crop out and suggest the existence of a magnetic body at depth. A magnetic low over basaltic and andesitic flows southeast of the dikes suggests the existence of rocks with low magnetic susceptibility beneath the basalt. The Trout Creek intrusion, the intrusive monzonitic and rhyolitic porphyry dikes, and the elongated southeast-trending magnetic low over basaltic and andesitic flows are located along a steep gradient marking the margin of a major (100×150 km) gravity low.

Mineral-resource studies in the Columbine-Hondo Wilderness Study Areas, New Mexico

Studies by J. C. Reed, Jr., of Precambrian rocks in the Wheeler Peak Wilderness and surrounding areas in the Sangre de Cristo Range disclosed the presence of supracrustal rocks, including layered amphibole gneisses, greenstone, felsic volcanic rocks, layered iron-formation, chert, marble, and phyllite. This terrane is generally similar to the greenstone belt at Pecos mine, but there is no evidence of nearby felsic eruptive centers, so the potential for massive sulfide deposits like that at the Pecos mine is probably low. However, there may be significant potential for disseminated sulfides related to Tertiary intrusive rocks that are widespread in the Precambrian rocks.

Mineral-resource studies in the western Manzano Mountains, New Mexico

Samples of silicified limestone from the Becker SW quadrangle, Socorro County, N. Mex., on the Sevilleta National Wildlife Refuge, were collected by C. H. Maxwell. These samples were submitted by T. S. Lovering to the Branch of Exploration Research for analysis. According to Lovering, anomalous amounts of

Ag, As, B, Ba, Be, Mo, Pb, Sr, W, and Zn in the samples are in amounts similar to known anomalies from fringe areas of silver-lead-zinc mining districts. The silicification was found in faulted, fusulinid-bearing rocks ranging in age from Des Moinesian to late Virgilian or early Wolfcampian. Dikes and a sill of intermediate composition were found in the area and may be associated with the mineralization.

Gravity investigations in the Teton Wilderness Area, Wyoming

D. M. Wilson reported that gravity data indicated that there is a basin between the Washakie and Absaroka Ranges, which is overlain by rocks of the Absaroka Volcanic Supergroup, and that the sedimentary rocks in the Box Creek Downwarp may extend eastward beneath the Buffalo Fork thrust. Elsewhere in Wyoming the sedimentary rocks of the Box Creek downwarp and those postulated in the basin between the Washakie and Absaroka Ranges have significant potential for oil and gas. There is no real evidence that mineable deposits exist within the Wilderness, but possible exploration targets are indicated by negative magnetic anomalies in two locations.

Geologic studies in the Sapphire Wilderness Study Area, Montana

The 200 km^2 intrusive complex present in, and adjacent to, the Sapphire Wilderness Study Area forms a batholith that is elongate in a north-south direction. C. A. Wallace reported that field mapping and preliminary petrographic study suggested that most of the batholith is formed of five plutons, all of quartz monzonite composition. Three of the plutons are biotite-hornblende quartz monzonite, and they occupy most of the batholith. Two plutons of about 15 km^2 are muscovite-biotite quartz monzonite, and they are located in the north-central part of the batholith. Contacts among plutons are gradational, but most plutons have porphyritic border zones where they contact other plutons. Porphyritic border zones are prominent in plutons that contact older sedimentary rocks. The same apparent sequence of crystallization fits all plutons, beginning with zoned sodic plagioclase, then quartz, hornblende plus quartz hornblende plus biotite, (biotite plus muscovite in two plutons), and finally orthoclase or microcline. Pegmatite dikes and quartz porphyry microgranite pods and dikes intrude all plutons. Pegmatites are composed mainly of microline, quartz, and muscovite, with minor biotite. Microgranite is composed mainly of microcline or orthoclase with quartz and minor garnet in the groundmass, with quartz, muscovite, and biotite as phenocrysts. A coarse-grained porphyritic alaskite body is present in the northwestern part of the study area, and the alaskite separates quartz monzonite from country rocks.

Mineral-resource studies in the Middle Mountain–Tobacco Root Wilderness Study Area, Montana

The Middle Mountain–Tobacco Root Further Planning Area (RARE II) of southwestern Montana contains areas of low to high mineral-resource potential, according to J. M. O'Neill. The areas of highest potential are preferentially located in or adjacent to intrusive rocks of Late Cretaceous age. Most of the Further Planning Area is underlain by Archean metamorphic rocks of low-resource potential. These rocks are overlain locally by Paleozoic sedimentary rocks and have been intruded by the Upper Cretaceous Tobacco Root batholith. Metamorphic rocks adjacent to the batholith and metamorphic and sedimentary rocks intruded by plugs and sills satellitic to the batholith commonly show some sulfide mineralization. Disseminated copper and molybdenum sulfides are common in the part of the batholith that extends into the Further Planning Area. Sulfide-bearing breccia pipes are associated with this mineralized zone. Satellitic intrusions are present in the Boulder Lakes cirque, which is partly within the study area. Many of these intrusions bear minor disseminated sulfides, local fluorite, and are associated with veins composed mainly of quartz. A weakly mineralized breccia pipe is present in this area. Gold-bearing quartz veins are being actively mined along the periphery of the Further Planning Area in the Boulder Lakes area and at Beall Canyon vein, and vein systems from these two mines can be traced into the Further Planning Area.

Geologic studies in the Rattlesnake Wilderness Study Area, Montana

C. A. Wallace and D. J. Lidke reported that the Rattlesnake Wilderness Study Area encompasses two structural provinces. The rocks present in the study area are mainly units of the Proterozoic Y Helena Formation and the Missoula Group. The Rattlesnake thrust system occurs in the south part and is characterized by an anastomosing system of thrust faults and isoclinal folds. Gabbroic sills and dikes of probable Proterozoic age and Middle Cambrian sedimentary rocks occur locally in the south part of the area. In the north part of the study area the rocks are autochthonous and the main structural elements are steep northwest-trending faults and open folds.

Mineral-resource studies in the Blue Joint Wilderness Study Area, Montana and Idaho

Geologic mapping of the Blue Joint Wilderness Study Area, western Montana and nearby Idaho, by Karen

Lund, R. B. Hall, C. D. Holloway, F. E. Mutschler, M. E. Palowski, and W. M. Rehn delineated most of a granitic pluton called the Painted Rock pluton: this is of batholith proportions and Eocene in age. The pluton consists of several phases that can be separated on the basis of texture, composition, and structural relations. Compositions vary from gray biotite quartz-monzonite (the oldest phase), through several gray biotite and (or) hornblende granites that make up most of the pluton, to a pink biotite and (or) hornblende synogranite (perhaps the youngest phase). A common feature of the gray granites is horizontal layering caused by cooling textures and differentiation in place and by sheet-like injection of magma.

The west side of the pluton is uplifted relative to the east side and was a zone of late, synplutonic tectonic flow. Rhyolitic to andesitic volcanic rocks present on the structurally lower east side of the pluton are both ash falls and lava flows. Although vent locations are not yet positively known, some of the volcanic rocks can be shown to be intimately related to the younger pink granites.

Known precious metal prospects in the pluton are related to the hydrothermal alteration in the volcanic rocks, anomalous trace element accumulations at the altered zone of the pluton, and late andesite dikes. Trace element evidence suggests that the structurally higher west side of the pluton may represent the root system of a tin-bearing and molybdenum-bearing granite system.

Geophysical studies in the Centennial Mountains Wilderness Area, Montana and Idaho

R. A. Martin reported that aeromagnetic anomalies generally can be explained in terms of mapped geology by low-gradient magnetic features over the Upper Cretaceous and lower Tertiary strata, and high amplitude, steep-gradient anomalies over higher terrain, which is capped with younger, more magnetic rocks. The dominant magnetic anomaly in the eastern Centennials is over elevated crystalline basement rocks. The anomaly apex is near a small pipe about 90 m in diameter with a basaltlike matrix (I. J. Witkind, 1974). Inference can be drawn for the existence of a concealed intrusion related to a diatreme.

Gravity data reflect mild contrast between sedimentary and volcanic rocks in the western Centennials. The broad gravity high over the eastern Centennials reflects older, more dense Precambrian and Phanerozoic rocks, but reconnaissance data show no evidence in support of the magnetic anomaly for a concealed intrusion or diatreme.

Geologic studies in the Jerry Peak Wilderness Study Area, Idaho

The Jerry Peak Wilderness Study Area, south of Challis, Idaho, is underlain principally by two uncomformable volcanic sequences, both of probable Eocene age, according to D. H. McIntyre. The volcanic rocks rest on Mississippian limestone, siliceous mudstone, and chert that crop out near the east margin of the area. The older volcanic sequence has a basal quartzite cobble conglomerate and consists chiefly of nonwelded to moderately densely welded crystal-poor quartz latitic to rhyolitic ash-flow tuff probably derived from a source southeast of the map area. These rocks are broken by numerous small faults, and individual fault blocks are tilted 20° or more.

The younger volcanic sequence, which rests unconformably on these rocks and is much less deformed, began with deposition of a few tens of meters of dacitic to rhyodacitic breccia, lava, and tuff. These rocks are overlain by up to 600 m of potash-rich andesite or banakite lavas and breccias that were erupted from two vents within the area. Locally resting upon these lavas is a sheetlike mass, up to 100 m thick, of flow-layered, crystal-poor rhyolite from a source southeast of the map area. The pumice and shard-rich vitrophyre locally present at the margin of the sheet, and the tabular shape of the unit, suggest that it originated as a very hot ash flow. The area is crossed by two northwest-striking fault zones. The eastern zone locally is invaded by olivine- or hornblende-bearing dike rocks. Fault-associated alteration locally produces celadonite and (or) quartz.

Uranium-resource studies in the Selkirk and RARE II Study Area, Idaho

A zone of fine-grained two-mica granitic rocks in the central part of the Selkirk RARE II Study Area, northern Idaho, yields scintillometer readings that average four times that of other two-mica rocks in the region, according to F. K. Miller. The zone is up to 8 km in length but only about 0.5 km in average width.

These rocks with anomalous uranium are part of an extensive complex of two-mica rocks that underlie about 1800 km^2 bounded by the Purceld trench on the east and the Newport fault on the west. The complex is subdividable into several major two-mica rock units, all of which are extremely heterogeneous with respect to composition and texture, and all contain numerous pods and septa of metamorphic rock.

The uranium-bearing rock is restricted to the east edge of a coarse-grained highly porphyritic biotite quartz monzonite, which appears to be a pre-existing plutonic mass that is intruded by, and caught up in, the

two-mica complex. This coarse-grained rock is more radioactive than most of the two-mica rocks of the complex, but generally is only half as radioactive as the fine-grained rock. Fine-grained two-mica rocks indistinguishable from those containing anomalous uranium occur in other parts of the two-mica complex but have low radioactity in keeping with the complex as a whole. The association of the fine-grained highly radioactive two-mica rocks with the coarse-grained porphyritic quartz monzonite suggests that the latter body may be the source of uranium in the fine-grained rock.

Mineral-resource studies in the Upper Priest Wilderness Study Area, Washington

Analyses of stream-sediment samples and panned concentrates define a large area in northeastern Washington that yielded anomalous silver and gold values. F. K. Miller reported that the area, covering about 55 km^2, lies between the Pend Oreille and Priest River drainages in the northeastern corner of Pend Oreille County, Wash. The anomalous values, ranging from 0.5 ppm to 7 ppm silver and 0.15 ppm to 1.5 ppm gold, were found in samples from streams draining both sides of a northeast-trending ridge underlain by the Proterozoic Shedroof Conglomerate.

The samples were collected an average distance of 3 km from the crest of the ridge and are from streams that drain both sides of an 11-km length of the ridge. The Shedroof Conglomerate in this area is made up of about equal parts conglomerate and phyllite, with a few sills or flows of basalt composition now altered to greenstone. Some of the phyllitic rocks are carbonate-bearing and locally contain relatively pure carbonate beds up to a few cm thick.

Most of the rocks are highly sheared, and in much of the area, primary bedding features have not survived development of schistosity foliation. At several places along the ridgecrest, irregularly shaped, anastomosing quartz veins from less than 1 cm to about 10 cm in thickness are found. No other indications of mineralization were noted, and the source and extent of the anomalies are not presently known. Whatever the source, it is widespread enough to show anomalies on both sides of an irregular ridge for a considerable distance. The configuration of the ridge is such that the anomaly must be at least 1 km wide. Closely spaced sampling of stream sediment and rock for geochemical analyses has been completed, and more detailed geologic mapping is underway. Analytical and geological work is being completed to determine the source, extent, and economic potential of the metalization.

Geologic studies in the Yolla Bolly Wilderness and adjacent RARE II Areas, California

Detailed mapping by M. C. Blake, Jr., and A. S. Jayko in the Yolla Bolly Wilderness and adjacent RARE II Areas, west of Red Bluff in northern California, revealed a complex geologic history. During latest Jurassic (Tithonian) to Early Cretaceous (Valanginian) time, the Franciscan rocks in the areas were deposited as a deep-sea fan complex along the Continental Margin. Thick (up to 50 m) radiolarian cherts, interbedded within the predominant sandstone sequence, distinguish this terrane. Numerous small intrusive and extrusive bodies of basalt and quartz keratophyre also mark this terrane.

Following deposition and subsequent igneous activity, the rocks were subducted to depths of 20 to 30 km, as attested by the development of deformational structure and the widespread occurrence of lawsonite and metamorphic aragonite. The rocks probably were involved in a collision event that imbricated the fan complex and returned them to the surface shortly after subduction (in order to preserve the aragonite). Open folding, along a northwest trend, and northeast-trending normal faulting followed the collision event.

Geochemical exploration of the Hoover Wilderness Area

M. A. Chaffee reported that geochemical analyses of samples of rock, stream sediment, and nonmagnetic heavy-mineral concentrate that were collected in the Hoover Wilderness Area and adjacent study area, California, indicated that there are important anomalies present for elements such as Ag, Au, Cu, Zn, Pb, W, Mo, Sb, Bi, As, Cd, and Ba. Most of these anomalies are related to hydrothermally altered Paleozoic to Jurassic metasedimentary and metavolcanic formations that occur as roof pendants in the Sierra Nevada batholith. The most significant of these anomalies are in the southern part of the areas investigated.

Geologic and mineral-resource studies in the Marble Mountain Wilderness Area, California

M. M. Donato reported that newly completed geologic mapping in the Marble Mountain Wilderness Area, Klamath Mountains, Calif., demonstrated that the Wilderness encompasses two geological assemblages, distinguishable on the basis of grade of metamorphism, structural style, and lithology. In the northern portion of the Wilderness, amphibolite facies metasedimentary, metavolcanic, and metamorphosed ultramafic rock comprise a melangelike terrane characterized by a high degree of lithologic variability and discontinuity. To the south, west, and northwest, a greenschist facies terrane, tentatively correlated with the Hayfork terrane of

Irwin (1972) of the western Paleozoic and Triassic belt, represents a sedimentary and volcaniclastic sequence deposited adjacent to a volcanic island arc. This north-south trending arcuate belt of rocks extends for nearly 200 km along nearly the entire length of the Klamath Mountain geologic province.

The relation of high-grade rocks to the low-grade rocks in the Wilderness is at present unclear; the two may be in contact along a folded thrust fault. Granitic bodies intrude both high- and low-grade rocks. The Wooley Creek pluton, in particular, appears to intrude both and may have been injected along their mutual boundary (Barnes, 1981).

Mineral potential of the Wilderness is low or nil. Small amounts of chromite in ultramafic bodies are uneconomic. Currently available geochemical results show no anomalous concentrations of metals in stream sediments.

Geologic studies in the Condrey Mountain and Orleans Mountain RARE II Areas, California

Geologic mapping in the Condrey Mountain RARE II Area has revealed a complexly folded series of quartz-mica-graphite schists with inter-layered greenschists and blueschists, according to M. M. Donato. The protoliths of these schists were mudstones and shales with a significant volcanic (tuffaceous) component. Volumetrically minor metaserpentinites in the area may represent sedimentary serpentinites deposited adjacent to an oceanic fracture zone or tectonic slivers of serpentinite incorporated in the sequence later in its history. A small massive-sulfide deposit, the site of the Blue Ledge Mine, is located near the RARE II boundary in a more siliceous compositional variety of the metatuff.

The Orleans Mountain RARE II Area is underlain by predominantly metasedimentary and volcaniclastic rocks deposited in proximity to a Mesozoic volcanic arc. These rocks are the northward continuation of a north-south trending arcuate belt of rocks nearly 200 km long, and part of the Hayfork terrane, of Irwin (1972). In the Orleans RARE II Area, these rocks are separated from the western Jurassic belt (Galice) rocks to the west by a complex fault zone separating two major parts of the Klamath Mountain geologic province.

Mineral-resource appraisal of the Rolla 1°×2° quadrangle, Missouri

An appraisal of the mineral-resource potential of the Rolla quandrangle, as of September 1980, was made by the USGS and the Missouri Geological Survey. The appraisal included an analysis of known geologic, geochemical, and geophysical parameters of the quadrangle with respect to recognition criteria for 17 different types of ore deposits, and has identified 3 specific areas in the quadrangle that have a very high potential for Mississippi Valley-type Pb-Zn-Ag-Cu-Ni-Co deposits (Pratt, 1981). It is estimated that each of these areas contains at least one major deposit, and that the metals in the ground in these hypothetical resources have a combined total value on the order of $3 billion. Also of special significance is the amount of cobalt included in the total estimate of base metal potential because it represents nearly a 3-yr domestic consumption of a critical material of which the United States currently imports about 90 percent of its needs.

Three areas have a very high potential for large- to moderate-sized deposits of Precambrian Kiruna-type iron ores: One area has a high potential for small residual barite deposits, at least one area has a potential for Sn-W vein deposits, and much of the quadrangle has a high general potential for Bokan Mountain-type uranium deposits at depths greater than 300 m. Some potential exists, but cannot be evaluated as to high or low, for F-Th-rare earth-bearing kimberlites, uranium in Paleozoic sandstones, and Stillwater-type Fe-Cu-Ni-Co deposits in layered mafic-ultramfic complexes.

Some potential also exists for small deposits of manganese in Precambrian and sedimentary rocks, marcasite-pyrite-hematite, residual iron, and copper in sedimentary rocks, but such deposits would not be commercial because of their small size and (or) unfavorable mineralogy. The quadrangle has low potential for Coastal Plain-type uranium deposits, base and precious metals in Precambrian quartz veins, and massive sulfide deposits.

Regional geophysical studies in the Pueblo 1°×2° quadrangle, Colorado

Interpretation of the gravity and magnetic maps of the Pueblo quandrangle showed that the quadrangle can be divided into three provinces with distinctive geophysical characteristics, according to F. M. Boler, D. P. Klein, and M. D. Kleinkopf. The ridge-trough province west of about long 105°30′ W. showed elongated gravity and magnetic anomalies that reflect the horst and graben-type tectonics associated with the Rio Grande rift. The Front Range province between long 105° and 105°30′ W. showed short wavelength gravity and magnetic anomalies that result from rapid density and magnetization variation, mainly of the Precambrian rocks. The coincident steep-gravity and magnetic gradients dividing these two provinces mark the eastern boundary of the South Park basin, which is a locus of volcanism and some mineralization. The Great Plains province east of long 105° W. showed long wavelength anomalies with east-west trends, which apparently reflect the basement lithologic variations. Correlation

between known mineralization and steep magnetic gradients or gravity gradients indicates that mineralization is controlled by tectonic weakness zones, which are reflected by the gradients.

Mineral resources of the Choteau 1°×2° quadrangle, Montana

The Choteau 1°×2° folio consists of 12 maps published in the USGS Miscellaneous Field Investigations or Open-File Report format, according to R. L. Earhart. The map series consist of geologic, structural, geochemical, aeromagnetic, hydrocarbon potential, and mineral-resource maps. The maps are published as a part of the Conterminous United States Mineral Appraisal Program (CUSMAP) and provide geologic, geochemical, and geophysical data, as well as interpretive information on the distribution of hydrocarbons and mineral resources. Background information and a bibliography are included in a USGS circular by Earhart and others (1981).

Geochemical exploration of Choteau 1°×2°quadrangle, Montana

A possible concealed mineralized porphyry system is outlined by anomalous amounts of metals in rock and stream-sediment samples collected in an area 20 to 40 km north of the Heddleston district in the Choteau 1°×2° quadrangle, Montana. The rock samples contain anomalous amounts of As and Hg, whereas the stream-sediment samples contain anomalous amounts of Pb, Zn, Ag, Cu and Mo. The samples were collected in an area where quartz-calcite veins are exposed at the surface. These results are part of studies made under the Conterminous United States Mineral Resource Assessment Program (CUSMAP) and are contained in reports by Grimes and Leinz (1980) and Leinz and Grimes (1980).

Remote sensing studies in the Walker Lake 1°×2° quadrangle

L. C. Rowan and T. L. Purdy reported that a map showing the distribution of hydrothermally altered rocks has been completed for the Walker Lake, Nevada-California 1°×2° quadrangle. Compilation of this map was accomplished by mapping limonitic bedrock using a Landsat color-ratio composite image and then evaluating these areas in the field to separate the limonitic altered from the limonitic unaltered rocks. Field checking, which was aided substantially by others working in the quadrangle, was also required for mapping some nonlimonitic altered areas and for improving the precision of boundaries, especially where vegetation cover obscured contact zones. Seven subdivisions are shown on the map. Preliminary evaluation of the alteration map showed that most of the altered rocks lie along one of four belts. These belts are also marked by concentrations of lineaments that were delineated in Landsat image. These data will be compared with data acquired using geochemical, geophysical, and field mapping procedures.

GEOLOGIC STUDIES OF MINING DISTRICTS AND MINERAL-BEARING REGIONS

The assessment of the mineral potential of public and other lands requires an ever-increasing knowledge of mineral deposits and the conditions of their formation. This knowledge, obtained through studies of known deposits and districts, can be applied to new areas having similar characteristics. During 1980, field and laboratory studies added to our understanding of mineral deposits in a large number of areas.

Gold placers in the Circle district, Alaska

The source of gold in the Circle district is not immediately clear. There are currently no fossil placers in the area, and a local lode source has not been discovered. W. E. Yeend reported that the gold occurrence, which seemingly is unrelated to out-cropping bedrock types and shows a lack of systematic down-valley increase in the size of gold fragments, suggests a fossil placer source. The few well-rounded zircon grains present in the heavy minerals also suggest a fossil placer. The evidence for this fossil placer interpretation is not conclusive, but bears consideration. Whatever the source, a sizeable amount of gold still remains in the Circle district. Gold-bearing stream channels left largely unmined have become attractive prospects as a result of the recent precipitous increase in gold price. A moderately large, low grade, but as yet largely unevaluated gold resource may be contained in the extensive valley-fill deposits in the lower reaches of Crooked and Birch Creeks as well as the broad topographic trough on the south side of the Crazy Mountains.

Geotectonics, metallogenesis, and resource assessment of southeastern Alaska

The Taku terrane is one of several major tectonostratigraphic terranes recognized in southeastern Alaska (Berg and others, 1978b), and is host to numerous undated stratabound massive sulfide deposits (Berg, 1979). For most of its extent the Taku terrane is fault bounded on the west by Upper Jurassic and Cretaceous flysch and volcanic rocks of the Gravina-Nutzotin belt, which separates the Taku from the Alexander terrane. On the east, the Taku is bounded by the metamorphic and plutonic crystalline complex of the Tracy Arm terrane. Although grossly dissimilar in its

geologic and structural history from adjoining terranes, the Taku is difficult to characterize stratigraphically. Its heterogeneous rocks are complexly deformed, pervasively metamorphosed, and sparsely fossiliferous. Heretofore, only generalized late Paleozoic and Triassic ages have been obtained from the southern part of the terrane near Ketchikan.

In July 1980, more definitive collections of Permian conodonts and brachiopods and of Triassic mollusks were made from the Taku terrane by H. C. Berg, N. J. Silberling, D. L. Jones, and P. J. Coneyu. Conodonts from black crinoidal marble intercalated with phyllite and felsic metatuff about 0.5 km south of Coon Cove include *Neogondolella idahoensis* (Youngquist, Hawley, and Miller) and *Hindeodus* sp. of Leonardian (late Early Permain) age. In keeping with this age, poorly preserved brachiopods from this same locality can be assigned to *Stenocisma* sp. and *Neospirifer*? sp. About 4.5 km south of Coon Cove, ammonites and fragments of halobiid bivalves (probably *Daonella*) are preserved as crushed but undistorted molds in small black, carbonaceous and siliceous concretions within foliated limestone and slate. The ammonites include *Lobites* cf. *L. pacianus* McLearn, *Joannites* sp., and *Meginoceras*? sp. diagnostic of a late Ladinian (latest Middle Triassic) Age. The provisional identification of the Late Triassic genus *Halobia* from this locality by Silberling in Berg and others (1978a) has been revised.

Although the stratigraphy of the Taku terrane is still imperfectly known, these new age determinations reinforce the pronounced stratigraphic differences between the Taku and the Annette subterrane of the Alexander terrane as portrayed by Berg and others (1978b). Briefly stated, in the Annette subterrane, Upper Triasic strata ranging from early to middle Norian in age rest unconformably on Devonian and older metamorphic and plutonic rocks; strata correlative with those of the two fossiliferous localities within the Taku terrane are not represented.

Paleontological studies in mineral-resource assessment of southeastern Alaska

The new fossil discoveries in the Taku terrane have potentially significant metallogenic implications for the stratabound mineral deposits. Many of these deposits are localized in rusty-weathering quartz-muscovite-calcite-pyrite schist similar to the felsic metatuff intercalated with the Permian marble near Coon Cove. The original age of these metamorphosed syngenetic deposits and hosts rocks is unknown, but the similarity in lithology suggests that it may be Permian. If so, many of the numerous stratabound massive sulfide deposits in the Taku terrane may be parts of a heretofore unrecognized metamorphosed and structurally dismembered Permian metallogenic province that stretches for more than 300 km, from Ketchikan to Juneau.

Molybdenum deposits in Idaho

A shallow Paleozoic sedimentary source for much sulfur and perhaps molybdenum in both major molybdenum deposits (Thompson Creek and Little Boulder Creek) in Custer County, Idaho, is indicated by sulfur isotope analyses by J. N. Batchelder, according to C. M. Tschanz. The data suggest a magmatic origin from circulating, partly meteoric fluids in convection cells surrounding Late Cretaceous stocks rather than an origin from strictly magmatic hydrothermal fluids as of most porphyry copper and (or) molybdenum deposits. The two aforementioned deposits, the only ones with proven reserves exceeding 100 million t in Idaho, have much heavier sulfur than most porphry deposits, including other sulfide deposits in the surrounding region.

Molybdenite contains +11.40 per mil $\delta^{34}S$ in the Thompson Creek deposit, compared to +8.55 to +8.70 in the White Cloud (Little Boulder Creek) deposit, and +5.47 in the small Eocene Little Fall Creek deposit. In the Thompson Creek deposit, pyrite contains +9.58 to +9.93 per mil $\delta^{34}S$ and arsenopyrite(?) contains +10.39 per mil compared to +15.57 in sphalerite from the Hoodoo zinc deposit. Comparable high heavy-sulfur values occur in sulfides from the Wood River lead-silver district for which Hall and others (1978, p. 589–591) suggest a similar origin partly because $\delta^{34}S$ values of +10 to +15 per mil are typical of late Paleozoic seawater sulfate.

The molybdenum in the Thompson Creek deposit, a stockwork of quartz-molybdenite veins in the cupola of a small quartz monzonite stock, probably has an igneous source, but that in the White Cloud deposit, a remarkably uniform, disseminated deposit in silicified diopside quartzites in the contact aureole of the White Cloud stock, may be from black Mississippian(?) argillites, which contain more molybdenum than the stock.

Huebnerite veins near Round Mountain, Nevada

D. R. Shawe, E. E. Foord, and N. M. Conklin reported that small huebnerite-bearing quartz veins occur in and near Cretaceous (about 95-m.y. old) granite east and south of Round Mountain. The veins are short and lenticular, and they strike mostly northeast and northwest in several narrow east-trending belts. The quartz veins were formed about 80 m.y. ago near the end of an episode of doming and metamorphism of the granite and emplacement of aplite and pegmatite dikes in and near the granite. An initial hydrothermal stage involved deposition of muscovite, quartz, huebnerite, fluorite,

and barite in the veins. Veins were then sheared, broken, and recrystallized. A second hydrothermal stage, possibly associated with emplacement of a rhyolite dike swarm and granodiorite stock about 35 m.y. ago, had deposition of more muscovite, quartz, fluorite, and barite, and addition of scheelite, tetrahedrite-tennantite, several sulfide minerals, and chalcedony. Finally, as a result of near-surfacing weathering, secondary sulfide and numerous oxides, tungstate, carbonate, sulfate, phosphate, and silicate minerals formed in the veins.

Uranium systems of the Marysvale volcanic field, west-central Utah

According to C. G. Cunningham and T. A. Stevens, the Marysvale volcanic field consists of two contrasting assemblages of rocks—an older calc-alkalic assemblage erupted between 35 m.y. and 21 m.y. ago from coalescing stratovolcanoes, and a younger bimodal basalt-rhyolite assemblage of heterogeneous lava flows and ash-flow tuffs erupted throughout later Cenozoic time. The Mount Belknap Volcanics, 21 m.y. to 14 m.y. old, are the largest accumulation of alkali rhyolite in the bimodal assemblage; they were erupted concurrently from two source areas about 21 km apart, in and just east of the northern Tushar Mountains. Products from the two source areas intertongue complexly. The Mount Belknap magma was anomalously radioactive, and vitrophyres from several different localities average about 14 ppm U. Most of the known uranium deposits and occurrences in the Marysvale volcanic field are associated with the Mount Belknap Volcanics.

Uranium deposits associated closely with igneous centers are epitomized by the hydrothermal uranium-molybdenum-bearing veins in the Central Mining Area, 6 km north of Marysvale, in the eastern source area of the Mount Belknap Volcanics. The veins are localized in a small area of highly fractured ground believed to mark the surface expression above a hidden intrusive that potentially may host a porphyry-molybdenum deposit. Fluorine-rich hydrothermal fluids at 200°C and having low pH and f_{O_2} permeated the broken rocks. At the deepest levels exposed, the fluids and wall rocks interacted to form kaolinitic and sericitic alteration products and to deposit uraninite, coffinite, jordisite, molybdenite, umohoite, fluorite, quartz, and pyrite in open fractures. The fluids were progressively oxidized at higher levels, and sooty pitchblende was the predominant vein mineral deposited. In the highly oxidizing environment at the top of the system, uranium phosphate minerals were deposited by combining either primary or secondary uranium from the vein systems with phosphate derived by leaching apatite from the wall rocks. Some of these oxidized minerals may be of hypogene and some of supergene origin.

In contrast, the Mount Belknap caldera in the western source area was filled to overflowing with uranium-bearing ash-flow tuffs and lava flows. These rocks were widely altered by post-caldera steaming and hydrothermal activity. Much of the rock uranium was dissolved and incorporated into the hydrologic regime. Some of this mobilized uranium was redeposited in favorable environments within the caldera, but much seems to have been transported elsewhere. Some of the fugitive uranium is expected to be redeposited in sedimentary fill in the adjacent Beaver basin and Sevier River Valley.

Bedded Archean iron deposits of southwestern Montana

Metamorphosed iron formation forms distinctive units in the Archean metasedimentary sequences of southwestern Montana according to H. L. James. The iron deposits of the Tobacco Root Mountains occur mainly in a bed about 30 m thick interbedded with schist, quartzite, and dolomite marble. The prinicipal occurrence is in the Copper Mountain area, east of the town of Sheridan; here a bed is exposed for several tens of kilometers along the limbs and axis of a tight anticlinal buckle within a major overturned syncline. The iron content, mostly in the form of magnetite, averages about 35 percent. Gross tonnage in the principal belt of exposure is estimated to be 63 million t to a depth of 100 m.

Proterozoic X mineral resources, Wyoming

R. S. Houston reported that reconnaissance study of metavolcanic rocks in the Sierra Madre, Wyo., suggests that textures and structures in Proterozoic X volcanic rocks are well preserved in an area south of the Cheyenne belt, which separates Archean terrane of the Wyoming province on the north from Proterozoic terrane in the south. The belt of well-preserved metavolcanic rocks contains volcanic cycles that appear to range from basalt and (or) andesite at base to rhyolite at top. The general area is promising for exploration for stratiform sulfide deposits, and mining companies are currently examining several prospects. This volcanic complex in the Sierra Madre is believed to have been formed as an island arc along the southern boundary of the Wyoming Archean province in Proterozoic X time about 1700 m.y. to 1600 m.y. ago.

Relations between tectonism and mineralization in southwestern Colorado

The character and extent of uplift and deformation in two early Mesozoic tectonic episodes in southwestern Colorado have been defined by O. L. Tweto. Faulting,

folding, uplift, and erosion occurred in the Triassic before deposition of the Upper Triassic Chinle (or Dolores) Formation and again in the Jurassic before deposition of the upper Middle Jurassic Entrada Sandstone. Deformation and uplift were most pronounced in a broad belt extending north-northwest across the late Paleozoic Uncompahgre highland, which trended northwest. The early Mesozoic uplifts had the effect of widening the late Paleozoic uplift by adding new areas of uplifted Precambrian basement on both of its flanks. Paleozoic rocks were destroyed in the areas of these uplifts, thus limiting the distribution of certain sedimentary formations that elsewhere contain economic deposits of minerals or fossil fuels.

Pecos contiguous area, New Mexico

It has been recognized that the north-trending Pecos-Picuris fault divides the Precambrian of the southern 60 km of the Sangre de Cristo Range, northeast of Santa Fe, N. Mex., into a predominantly stratified eastern terrane and a western batholithic terrane. The eastern terrane is composed of interstratified quartzite and pelitic schist and coeval to younger metavolcanic and associated rocks of the greenstone belt at Pecos mine (Robertson and Moench, 1979), all of Proterozoic X age (about 1.7 b.y.). Recognized volcanic centers within the belt are host to known volcanogenic mineral deposits, such as the massive sulfide bodies at the Pecos mine. New mapping by R. H. Moench and J. L. Schneider showed that the western batholithic terrane is divisible into two assemblages of granitic rocks of Proterozoic X or Y age, and septums of stratified schists and gneiss that correlate with the rocks of the Pecos greenstone belt east of the Pecos Picuris fault.

During the new mapping an economically important septum in the batholitic terrane was delineated in the area of Thompson Peak and Glorieta Baldy, due east of Santa Fe. Here interbedded quartzite and pelitic schist exposed in the core of a tight east-trending anticline are comformably overlain by intertonguing metabasalt, felsic metatuff, and volcaniclastic metasedimentary rocks. As shown by spectrographic analyses of heavy-mineral concentrates of stream sediments, highly anomalous amounts of tungsten, as scheelite, occur within this area, in a setting that suggests a stratabound source in metavolcanic rocks of the septum. The tungsten anomaly is peripheral to an ancient rhyolitic volcanic center within which abundant evidence was found for possibly important deposits of base- and precious-metals sulfides (Moench and Erickson, 1980).

The structure and distribution of the granitic rocks of the western batholithic terrane indicate that they were emplaced as thin but extensive sheetlike bodies, probably originally subhorizontal but subsequently folded along north-trending axial surfaces. The two assemblages of granitic rocks are (1) gray biotite-rich tonalite, granodiorite, and minor amounts of quartz diorite to gabbro; and (2) younger pink coarse-grained granite, having a thin but extensive roof phase of quartz porphyry and aphanite. Both the tonalitic and granitic rocks are faintly to intensely deformed by secondary foliation, and locally this foliation is further deformed by crenulation folds. The principal sheet of pink granite is no more than 3 km thick, but it is exposed in a narrow hook-shaped strike belt that extends nearly 60 km through the western batholitic terrane. The geochemical data suggest that tin, tungsten, niobium, beryllium, thorium, and rare-earth elements are preferentially associated with the pink granite, but no evidence for an economic deposit of any of these elements was found that might be associated with the granite.

Base-metal fissure veins in the Sandia Mountains

D. C. Hedlund reported that the Sandia Mountains are a part of an eastward-dipping fault block that extends into the Manzano Mountains to the south. The Sandia fault block, which is about 35 km long and up to 19 km wide, is bounded on the north by the Placitas fault and on the south by the Tijeras fault. The Sandia and Rincon faults separate the fault block from the Albuquerque basin on the west.

The steep west-facing range front consists chiefly of the 1,500 m.y. so-called Sandia Granite (Kelley and Northrop, 1975) that intrudes older metapelitic rocks of sillimanite-andalusite grade along Rincon Ridge and metavolcanic rocks of upper amphibolite grade along Tijeras Canyon. The Precambrian metamorphic rocks of Monte Largo are on strike with the Tijeras Greenstone of Kelley and Northrop (1975) but differ in that the rocks are of highly sheared sillimanite-kyanite-bearing quartz-feldspathic and quartz-sericite schist and gneiss with thin intercalated amphibolite and quartzite layers.

The Precambrian basement is capped by the Pennsylvanian Sandia Formation (0–61 m.y.) and overlying Madera Formation (275–396 m.y.). Younger Permian and Mesozoic sedimentary rocks are exposed farther down on the dip slope or in synclinal basins or graben structures, that is, the Hagan basin and the Tijeras graben and basin.

Characteristically, the base-metal fissure veins in this area strike N. 10° to 30° W. and are localized along extensional faults. The veins generally are enriched in galena and (or) sphalerite; copper-bearing minerals are rarely present. Barite is a common gangue mineral and some veins consist entirely of barite and fluorite.

Copper-molybdenum porphyry studies in the eastern United States

About 25 deposits and prospects of andalusite and pyrophyllite are known within two relatively narrow zones of the Carolina volcanic slate belt in North Carolina according to R. G. Schmidt. A few of these showed sparse amounts of Cu, Mo, Sn, As, Bi, and Au associated with them; many contained significant amounts of fluorine, generally in the mineral topaz.

The alteration mineral suite and also the diverse metal suite suggest deposition by high temperature–low pressure hydrothermal solutions close to the surface; these also suggest genetic resemblance to the fluorine-rich systems of the Brewer mine, South Carolina (Cu, Mo, Bi, Sn, As; alteration minerals: pyrophyllite, andalusite, topaz, kaolinite); the Mount Pleasant mine, New Brunswick (Cu, Mo, W, Bi, Sn, Ag?, As, Pb, Zn, Cd; alteration minerals: kaolinite and probably some andalusite, fluorite, and topaz); the Ashio mine, Honshu, Japan (Cu, W, Bi, Sn, Au, Ag, As, Pb, Zn; alteration minerals: pyrophyllite, fluorite, topaz); and the subvolcanic polymetallic deposits of Bolivia (Cu, W, Bi, Sn, Au, Ag, As, Pb, Zn; with fluorite as a common accessory).

A major objective of this study is to determine if the pyrophyllite-andalusite deposits can provide any information that can be used to locate metalliferous deposits, either in unexplored parts of the same hydrothermal systems, or in adjacent areas that may be deduced to be favorable areas for exploration.

Appalachian massive sulfides

Some wall rocks in contact with sulfide orebodies at Great Gossan Lead district, Va., and Ducktown, Tenn., both of which are in Blue Ridge province, flysch-type rift-facies metasedimentary rocks, contain high percentages of either untwinned sodic plagioclase, or biotite-chlorite. Such rocks evidently are absent or exceedingly rare in country rocks away from the ore deposits. Their origin, as yet unexplained, probably is related to metamorphic reactions between sulfide bodies and country rocks, or to chemical deposition or alterations connected with the ore-forming process itself. Samples of drill core collected by J. E. Gair from mineralized zones in the Chopawamsic Formation equivalent of the area of Mineral and Andersonville, Va., are chemically similar to volcanic suites defined by Louis Pavlides farther north in the Chopawamsic Formation. Pavlides distinguished primitive tholeiitic island arc basalts to keratophyres from more evolved calcalkaline felsic and intermediate volcanics on the basis of rare-earth element patterns, niobium content, and La/Yb ratios. In the drill cores, the tholeiitic and calcalkaline rocks are interlayered. Zones containing a high proportion of calcalkaline volcanic rocks are more favorable for the occurrence of large volumes of massive sulfide than are zones containing a large proportion of tholeiitic rock.

Mineralization in Proterozoic Y rocks of the St. Lawrence lowlands, New York

C. E. Brown reported that mineralization in the Grenville lowlands northwest of the Adirondack Mountains can be categorized into four main events or phases as follows: (1) sedimentation and penecontemporaneous introduction of chemical elements into a sedimentary basin in Proterozoic Y time; (2) recrystallization and remobilization of phase 1 elements by regional metamorphism and tectonism about 1000 m.y. B.P.; (3) oxidation and hydrothermal alteration close to the Proterozoic-Paleozoic unconformity between 1,000 m.y. and 500 m.y. B.P.; (4) hydrothermal activity and vein deposition along vertical fractures later than 450 m.y. B.P. The large zinc and talc deposits at Balmat and Fowler, N.Y., are a result of phase 1 mineralization modified by phase 2 recrystallization and mobilization. The hematite deposits mined at Antwerp, N.Y., in the 1800's are a result of phase 3 mineralization. This phase also produced some barite and a wide range of secondary minerals where the Balmat zinc deposits were affected by it. Phase 4 produced the vertical galena-bearing veins previously mined near Rossie and Macomb, N.Y. This type vein is composed mainly of calcite with galena, sphalerite, and fluorite. Some hydrothermal alteration that locally produced epidote, reddened feldspar, and quartz also is related to this mineralization stage. Defining the different mineralization phases aids in exploration through categorizing the geologic features and alteration effects that are guides to each type of mineralization.

The mafic "Chickwolnepy Complex"

Recent mapping by R. H. Moench, J. L. Schneider, and J. E. Selverstone in the Milan 15-min quadrangle and adjacent areas, northern New Hampshire and Maine, has revealed the presence of an igneous complex, herein informally called the "Chickwolnepy complex," composed of metamorphosed gabbro, sheeted diabase dikes, tonalite, and minor trondhjemite. The complex has minimum dimensions of 5×10 km. It is on the north end of the Jefferson dome, the northernmost and largest of the Oliverian domes in New England. Rocks of the complex intrude the Albee Formation and parts of the Middle Ordovician Ammonoosuc Volcanics. The complex is discordantly intruded in turn by foliated pink to

gray granite of the Oliverian Plutonic Suite, dated elsewhere at about 445 m.y. The complex is flanked by extensive and probably exceptionally great thicknesses of metamorphosed felsic tuffs and mixed mafic and felsic volcanic rocks. Although not yet studied in detail, the volcanics and the rocks of the "Chickwolnepy complex" appear to be low-K bimodal mafic-felsic assemblages. Tentatively, the "Chickwolnepy" is interpreted to be a Middle Ordovician subvolcanic complex.

Metavolcanic rocks that flank the "Chickwolnepy complex" in the Milan, Old Speck Mountain, and Percy quadrangles show evidence of extensive premetamorphic hydrothermal alteration. They are host to one known massive sulfide deposit (Milan mine) and several other metallic-sulfide mineral deposits. The known deposits appear to occur marginally to the thickest accumulations of felsic metatuffs, suggesting an association with the margins of deep local basins, possibly cauldrons, of contemporaneous subsidence. Poorly stratified polymictic conglomerate-breccia exposed locally near the base of the volcanic rocks suggest that basement faults were active during the onset of the Middle Ordovician volcanism. In all these respects, the Milan quadrangle and adjacent areas seem remarkably analogous to the middle Miocene kuroko ore districts of Japan, as described in current literature.

Tourmaline in massive sulfides of New England

Recent work by J. F. Slack, based largely on field studies in New England, suggests that tourmaline may be a locally important gangue mineral in some stratabound mineral deposits. Tourmaline appears to be most common in massive sulfide deposits hosted principally by metasedimentary rocks (Sullivan lead-zinc mine, British Columbia; Black Hawk zinc-copper mine, Maine; Elizabeth copper mine, Vermont; Ore Knob copper mine, North Carolina; Blackbird copper-cobalt mine, Idaho). Some volcanic-hosted deposits also contain accessory tourmaline, including those at the Pecos mine, New Mexico, the Kidd Creek mine near Timmins, Ontario, and a few sulfide bodies in the Mineral district, Virginia. Tourmaline typically forms brown, greenish-brown, or black euhedral crystals or crystal aggregates within massive sulfide, fills fractures and joints with sulfide + quartz ± carbonate in wall rocks adjacent to ore zones, and locally at the Elizabeth mine and elsewhere occurs as massive foliated rocks called "tourmalinites." These tourmalinites, which in places have 50 percent or more tourmaline by volume, are stratiform layers conformable to the foliation of enclosing metamorphic host rocks.

Tourmalinites have potential significance for exploration, because they are known to be associated not only with stratabound base-metal sulfides, as at the Sullivan and Elizabeth mines, but also with granitic rocks near these deposits. The distinctive major, minor, and trace-element contents of the ore-related tourmalines indicate that these Mg-tourmalines (dravites) are unrelated to the iron-rich schorls typical of most felsic intrusive rocks. The scarcity of volcanic rocks at or near the stratigraphic horizon of many of the tourmalinites and tourmaline-bearing metal deposits seems to preclude a marine volcanic source for the boron. The tourmalinites may have formed in some places by evaporitic or sabkha processes, locally with related mineralization, that is, Zambian copper belt.

Other geologic evidence, however, suggests that many of the tourmalinites and tourmaline-rich deposits formed in much deeper water, and that significant quantities of boron—as much as 9 percent B_2O_3 or 3 percent boron now present in some rocks—probably were emplaced as subaqueous boron- and metal-rich brines on the sea floor. Boron-rich muds and associated metals are believed to have been deposited as high-density chemical sediments or exhalites from a submarine fumarolic or hot-spring center, and may or may not have emanated from, or coincided with, a volcanic center. In a few mining districts tourmalinites appear to represent facies of ore horizons, and they may be interpreted as boron analogs of the well-known "banded iron-formations" associated with many stratabound sulfide deposits.

Tourmaline appears to have great potential as a prospecting guide for stratabound mineral deposits in metamorphic terranes. Reconnaissance exploration could be directed to search for anomalous amounts of tourmaline in panned concentrates of stream sediment, followed by laboratory studies to determine composition. More detailed exploration programs could search for tourmalinites and for cross-cutting tourmaline-sulfide veinlets. Tourmaline-rich rocks not of obvious granitic or evaporitic origin are considered particularly valuable prospecting guides, especially in dominantly metasedimentary terranes where the lack of pyroclastic rocks hinders identification of ancient volcanic centers—and thus favorable ground for "volcanogenic" mineral deposits. Cross-cutting tourmaline-sulfide veinlets, produced locally by the metamorphism of boron-bearing massive sulfide bodies, are equally significant, and they may be easily identified in outcrop or drill core, considerably enlarging target areas for mineral exploration.

Southern Utah remote sensing for uranium exploration

Limonite anomalies in Beaver Valley, Utah, as defined from Landsat digital data, and postulated areas of ongoing uranium deposition in the subsurface are spatially

but not genetically related according to M. H. Podwysocki. The limonite is not related to an oxidation-reduction "front", but can be attributed to normal soil-forming processes active on valley-fill units deposited in late Tertiary and early Quaternary time.

Band ratio images (1.6/2.2 microns) created from digitally processed airborne multispectral scanner data for the central mining district near Marysvale, Utah, showed localization of intense hydroxyl absorption. These local areas are the remains of late Tertiary hydrothermal cells responsible for the mineralization present in the area. Strong absorption correlates well with areas of alunite and kaolinite. One area of weak hydroxyl absorption correlates with a zeolitized tuff. Another area of weak absorption is coincident with a uranium vein-filling deposit, but this relation is coincidental. The weak hydroxyl anomaly is related to an older period of hydrothermal alteration; the veins of uranium ore are younger, have small alteration haloes, and are not exposed at the surface.

A technique was developed using black and white diazo transparency images to photographically mask areas on digitally processed remote-sensing images so that only a given color—ostensibly related to some desired thematic information contained in the image—may be easily extracted. The technique has wide application, as it may be applied to virtually any type of image and does not necessarily require the use of digital processing.

Remote sensing of porphyry copper

Tests of the use of Landsat-derived spectral reflectance measurements for mineral exploration have been made in the Sonoran desert of southern Arizona according to R. G. Schmidt. In that particular environment, the spectra of hydrothermally altered areas are very similar to those of a variety of unaltered and unmineralized rocks, therefore, making discrimination of hydrothermally altered areas on the basis of Landsat data much more difficult.

Digital classifications of Landsat data were performed using those combinations of spectral reflectances that are present in only parts of the known area of hydrothermally altered rocks at the North Silver Bell orebody, but not commonly associated with any other surfaces. The last two of a series of experimental classification tables used the most discriminant spectral ranges, and both tables yielded good outlines of parts of the North Silver Bell alteration area, but neither delineated the entire area.

Evaluations of 11,000 km^2 of mountains and hilly upland in the region between Tucson and Ajo by the semi-final table cholla-7 and earlier tables identified 18 localities deemed worthy of field checking, and 25 more that seemed to be almost certainly falsely classified. Seven of the most favorable localities were then visited in the field, and none were found to be significantly mineralized. Areas that yielded the most positive results with cholla-7 were also evaluated with the final table, cereus-6, which indicated that no other areas had spectral reflectances like the North Silver Bell orebody. This does not mean that no large orebodies lie hidden beneath alluvium, but it does reduce the likelihood that any large reasonably well-exposed areas of hydrothermally altered rocks are present in the area studied.

GEOCHEMICAL AND GEOPHYSICAL TECHNIQUES IN RESOURCE ASSESSMENTS

GEOCHEMICAL-RECONNAISSANCE RESULTS

Tin potential, Charlotte 1°×2° quadrangle, North Carolina and South Carolina

Tin potential has been found in the Southeast. Heavy-mineral surveys by J. W. Whitlow and W. R. Griffitts show a wide distribution of cassiterite in small streams in the Piedmont of North and South Carolina and the Blue Ridge of west-central North Carolina. Few of the occurrences are of economic importance, but they suggest that placer deposits may have developed in the Coastal Plain in the area between the Pee Dee and Santee Rivers. Most of the cassiterite was removed during the development of the Piedmont Plateau surface, perhaps as long ago as the Eocene, so the postulated placers may be old. G. H. Espenshade has traced a chain of plutons along the Blue Ridge from central North Carolina to central Virginia with potential sources of cassiterite, so the area with placer potential may extend far north of the Pee Dee River. Wolframite and columbite locally associated with the cassiterite probably would not survive the long travel to the Coastal Plains. The tin-spodumene belt in the Carolinas, known for three generations, has been found recently by J. W. Whitlow, W. R. Griffitts, and D. F. Siems, to be part of a much larger mineralized area. Beryllium, tin, niobium, and bismuth are prominent in stream-sediment concentrates taken in an area north and northeast of the apparent northern end of the lithium pegmatite belt; their bedrock sources are not yet known. A similar large area south and southwest of the southern end of the lithium pegmatite belt yields concentrates that contain tin and tungsten in cassiterite and wolframite, respectively, derived from greisen bodies in gneiss and niobium and beryllium with unidentified bedrock sources and mineralogy. The areas show up in a general way in

surveys based on analyses of nonconcentrate-sediment samples. This interpretation is difficult, however, because of erratic high values found in the region. Some clusters of rather high values of beryllium, tin, and niobium may be related to groups of sheet-mica pegmatite deposits, even though no minerals of tin or niobium were found, and few occurrences of beryl were found during examination of more than 100 such mica deposits. High values for beryllium found in sediments of the Carolina slate belt suggest that previously unsuspected deposits of beryllium may be in that region, a suggestion that is reinforced by the finding by Henry Bell of chrysoberyl in South Carolina, not far to the south.

Geochemical sampling, Iron River 1°×2° quadrangle, Michigan and Wisconsin

In the Iron River 1°×2° quadrangle, Michigan and Wisconsin, H. V. Alminas found a number of hydromorphic geochemical patterns strongly indicative of felsic intrusives at depths that have been delineated by B-horizon soil sampling. These areas are defined by an enrichment in Fe, Mg, Ca, Mn, Cr, Sc, Sr, Be, and V. Abnormally high Be/Sr and Mg/Fe ratios are characteristic, and anomalous values in Cu, Co, Ni, Mo, and Ag are associated with these zones. These zones generally occur along or at intersections of gravity and (or) Landsat-imagery-derived lineaments.

Mineral potential, Rolla 1°×2° quadrangle, Missouri

Using spectrographic analyses R. L. Erickson, E. L. Mosier, and S. K. Odland found anomalously high amounts of Mo, As, Pb, Cu, Ni, Co, and Ag in insoluble residue samples of a shallow-water reef and calcarenite facies of the Cambrian Eminence and Potosi Dolomites in the subsurface in southern Missouri in the Rolla 1°×2° quadrangle. The samples are from two drill holes in Douglas County and two in Ozark County. The metal suite is similar to that found in the Viburnum Trend lead deposits except that the molybdenum content is commonly an order of magnitude higher than in the Trend. The principal residence of the metal suite is in or intimately associated with iron sulfide. The shallow-water reef and calcarerite facies of the Eminence and Potosi are lithologically similar to, and may be analgous to, the "white-rock" facies of the ore-hosting Bonneterre Formation in the southeast Missouri lead district. These geochemical and stratigraphic data together suggest that an unknown and untested belt of favorable ground for mineral discovery may be present in the subsurface in southern Missouri.

Mineralization in the Williams Fork, Colorado

P. K. Theobald observed that the headwater area of the Williams Fork in the central Colorado Rocky Mountains has suffered a sequence of chemical and mechanical, rock-destructive events that effectively obscure mineral deposits from discovery by conventional methods of search. Hydrothermal alteration associated with Tertiary mineralization has reduced the erosion resistance in pervasively altered areas that are increasingly numerous toward the east and southeast and in and adjacent to veins and fault zones throughout the area. A period of lateritic weathering proceeded the earliest recognizable glacial features and further reduced the rocks to saprolite beneath an ancient land surface for depths of as much as 100 m. Successive cycles of glacial erosion were most effective where alteration and weathering were most extensive. Major valleys were eroded along the larger altered fault zones. Residual accumulations of ground and lateral till effectively obscure evidence of mineralization along or adjacent to the faults. Altered and weathered zones above the active glacial valleys yielded through periglacial mass movement, producing large terranes of jumbled and slumped ground, again obscuring evidence of mineralization.

Residual accumulation of heavy minerals related to mineralization, fluorite, pyrite, galena, molybdenite, scheelite, powellite, and gahnite, yields fairly coherent patterns of distribution in alluvial deposits reworked from the till along the lower walls of the major valleys. Soils collected along ridge and spur traverses have yielded only occasional erratic, high values reflecting the generally unaltered, unmineralized relics that form the highlands. More direct evidence of mineralization beneath the extensive blankets of transported debris will be required to establish a reliable resource appraisal.

Geochemical anomalies, Silver City 1°×2° quadrangle, Arizona-New Mexico

A geochemically enriched area, which measures approximately 235 km^2, was found in the southern Pinaleno Mountains, Ariz., in the Silver City 1°×2° quadrangle, Arizona-New Mexico. This area is situated on and adjacent to a major regional tectonic feature; but mines in the area do not exist and prospects are few. This geochemical feature was recognized because heavy-mineral geochemical techniques were employed. The intensity of many of the analytical values, using enhancement techniques, suggests that local concentrations of possible ore grade do exist. Leakage along dike-host rock contacts within the many rhyodacite dike swarms

in the area appears to be a main process of metal dispersion. The major regional tectonic feature is the Stockton Pass fault, which trends northwesterly, with a horizontal left-lateral displacement. It is approximately 1.6 km in width and appears to localize metallization because geochemical anomalies in Mo, Bi, W, Ag, Au, As, and the mineral fluorite show close spatial relation to the zone. It also may have controlled the occurrence of a volcanic center to the south that contains geochemical anomalies in the same metals, most prominently for molybdenum and bismuth.

Geochemical survey, Richfield 1°×2° quadrangle, Utah

W. R. Miller, J. B. McHugh, and W. H. Ficklin made a geochemical survey using ground water in the Beaver basin in the Richfield 1°×2° quadrangle, Utah. The results of raw data plots, principal-component analysis, and a solution-mineral equilibria study demonstrate that the chemical environment of the Beaver basin is favorable for the occurrence of sandstone-type uranium deposits. Several areas were identified as possible targets for exploration. The methods described in this study can be used to evaluate other basins in the western United States.

Geochemical sampling of water, Colorado Plateau, Utah

Using field and laboratory data, J. C. Antweiler and J. B. McHugh showed that in some environments water, when available, is superior to other geochemical sampling media for detecting evidence of concealed mineralization. An excellent example is the Long Gulch area of the Colorado Plateau in the Escalante River canyons country, Garfield County, southern Utah. Several uranium prospects have been located in outcrops of the Moenkopi and Chinle (Shinarump Member Formations) (all Triassic in age), but no significant uranium mineralization has been found in the overlying Jurassic rocks such as those in Long Gulch. However, numerous seeps and small springs occur in a fault zone in Long Gulch for a distance of at least 16 km. Water samples from several of those springs carried uranium in amounts up to 480 ppb compared to background levels of about 1 ppb. Fine-grained stream sediments, pan concentrates, and rocks suggested either no or very weak geochemical anomalies. Anomalies of several other cations and anions also are recognized easily by modern analytical techniques applied to water. In areas where the only exposed rocks are thick sequences of Jurassic sandstone, such as in the Escalante River canyons country, water from seeps, springs, intermittent drainages, and fault zones is an excellent sampling medium because it often provides access to mineralization that is entirely concealed. Uranium mineralization is known to occur in Triassic rocks, which in much of the area are not exposed.

Gold anomalies, Butte 1°×2° quadrangle, Montana

Preliminary interpretation of geological and geochemical data by J. C. Antweiler, W. L. Campbell, and R. T. Hopkins, Jr., suggests the presence of several gold resource targets in the Butte 1°×2° quadrangle, Montana.

Several drainages west of the Coloma Mining District in the western part of the Garnet Range were found to contain gold anomalies. Gold compositional studies suggest that gold-source veins may be gold tellurides in some areas and skarn deposits with possible tungsten mineralization in other areas. The Frog Pond basin area in the southern part of the Sapphire Mountains has numerous gold anomalies in drainages west, north, and east of the basin. Other areas that should receive further attention are at least seven target areas of Tertiary gold deposits, including Tertiary pediments on the Sapphire Range and on the flanks of the Flint Creek Range and Tertiary deposits downslope from the Blackfoot and Datlton Mountain stocks. Gold compositional analyses, together with other analytical data, suggest that modeling of suites of anomalous metals may lead to the discovery of unknown mineralized areas.

Geochemical studies of batholiths, Dillon 1°×2° quadrangle, Idaho and Montana

Detailed review of geochemical studies indicated a genetic relation between stockwork molybdenum deposits and leucocratic granitic phases of sodic series (Tilling, 1973) calcalkaline batholiths in the Dillon 1°×2° quadrangle, Idaho and Montana. The leucogranites are commonly two-mica granites and are the youngest phases in the evolutionary history of the batholiths. Earlier granodiorite phases of the batholiths produced tungsten- and copper-bearing skarns, tin-bearing magnetite skarns, and copper-molybdenum gold porphyry-type systems. Complex base-metal sulfide and precious-metal vein occurrences are associated with all of the porphyry-type deposits and may have tin minerals in economic quantities at some localities as suggested by geochemical analyses of ore samples.

Preliminary results from process studies on the movement of trace elements in the weathering environment indicated that streams in southwestern Montana draining areas where there is no significant mineralization reach a steady state with respect to chemical speciation with about 80 percent of the trace elements being

transported as silicates and resistate oxides and most of the remainder being complexed by organic matter. Where there is significant mineralization, the steady state is disrupted at the point of entry of the metals into the stream with organic matter and oxides of ore metals complexing most of the trace metals. Downstream from the metal source the speciation moves systematically back towards the steady-state condition of dominantly silicate and resistate oxide complexing. The total amount of trace metal also decreases downstream. The rate at which the metal anomaly disappears is a function of the mineralogy of the metal complexes entering the streams. Organic complexes appear to flourish on a carbonate substrate.

Geochemical sampling for metallic resources, Chichagof-Yakobi Wilderness Study Area, Alaska

T. D. Hessin collected several types of geochemical samples to evaluate possible metallic resources in the Chichagof-Yakobi Wilderness Study Area, Alaska. Two categories of samples were of primary importance because of the analytical results they have offered. These two sample media are water (filtered and unfiltered) and nonmagnetic heavy-mineral concentrates. Both sulfate and fluoride are excellent associates of many types of mineral deposits and therefore are indicators of mineralization. This becomes quite evident in the former mining districts of Hirst-Chichagof and Apex-El Nido mines, where the sulfate anion analyses were quite anomalous. In correlation, both the nonmagnetic heavy-mineral concentrate sample and the filtered-water sample, taken from the same site, exhibited anomalous amounts of base and precious metals. The same correlation exists between the two media—water (two types) and concentrates—in previously undetermined mineralized areas. Two areas of major importance are Moser Island, located on the east side of the project area on Hoonan Sound and in the vicinity of Stag Bay near Yakobi Island. In addition, anomalous amounts of fluoride (unfiltered water) offer excellent correlation with anomalous amounts of uranium in the filtered-water samples in the proximity of Deep Bay located in the southwest quadrant of Chichagof Island.

The Chichagof-Yakobi Wilderness Study Area is subject to high rainfall, resulting in a strong dilution effect to the collected water samples. In spite of these circumstances, correlation of the water samples and heavy-mineral concentrates was excellent in several areas and warrants continued use in geochemical prospecting.

Prospective copper belt in the Brooks Range, Alaska

J. B. Cathrall reported that the minus 80-mesh stream-sediment geochemical anomalies suggested that the known zone of copper- and zinc-bearing stratiform volcanogenic sulfide occurrences found in the Ambler River quadrangle in the Brooks Range, Alaska, extends eastward into the Survey Pass quadrangle. This volcanogenic sulfide mineralization was found in the schist belt, often referred to as the "copper belt," located along the southern flank of the Brooks Range.

The prospective copper belt in the Survey Pass quadrangle was reflected very well by anomalous drainage areas containing anomalous Cu, Zn, Pb, Ag, Ba, Sb, Mo, W, Bi, and B. The anomalous drainage areas correlate well with areas of mineral occurrences, with areas of pervasive mineralization, and with the approximate location of lode claims. All of these areas were associated primarily with metafelsitic schist, which is associated with mafic metavolcanics. The aeromagnetic data within this section of the schist belt showed that all of the above-mentioned areas have a characteristic magnetic signature. The axes of aeromagnetic highs wrap around these areas, which in turn lie within aeromagnetic lows where magnetic anomalies approximately greater than −20 g are absent.

GEOCHEMICAL CHARACTER OF METALLOGENIC PROVINCES

Concepts and techniques

In a review of concepts and techniques employed in geochemical exploration, W. C. Overstreet and S. P. Marsh observed that the recent accelerated use of geochemical techniques resulted from the increasing need to discover geologically concealed sources of mineral raw materials and geothermal energy. Future research in geochemical exploration can be expected to improve geological perceptions of ore deposits, to establish closer ties with remote sensing of mineralized or geothermal areas, and to provide more sensitive methods of analysis as well as more certain interpretative methods. In the search for concealed mineral deposits and geothermal sources, future improvements in methods of anomaly enhancement are the most significant trend in exploration geochemistry.

Metals in the Ely district, Utah

G. B. Gott determined that there are more than a dozen metals that are enriched above crustal abundance in the most altered rocks in the central part of the Ely district. Copper, iron, and molybdenum are most abundant in the central zone. This zone is overlapped by zinc, which in turn is overlapped by lead. Silver and bismuth are nearly coextensive with lead, and it is likely that these minor elements have been captured in the crystal lattice of galena. Sulfur was probably present throughout the district before oxidation, but it seems to

give way to other anionic forms such as some of the compounds of arsenic, antimony, and tellurium outward from the median line of the district. Gold is most concentrated in a tight circle around the monzonite intrusions. Manganese is most abundant along the outer limits of the district and decreases inwardly; this is inverse to the distribution of copper. Tungsten and tin are most abundant along the contact between the monzonite and sedimentary rocks.

Mineraiization in the Round Mountain area, Nevada

B. R. Berger established that Round Mountain mineralization is characterized as Au, Ag, As, Sb, Tl, W, F, Mo, and Sn with some Zn. Lead and copper are sparse. The gold-silver ratio is nearly one for the district, but gold is slightly more abundant in oxidized ores. Locally manganiferous vein segments are highly enriched in silver. Arsenic is most abundant in argillic- and adjacent silic-altered zones, and decreases outward in phyllic-altered zones. Calcium and manganese are universally depleted in the alunitic and silic zones, whereas copper and manganese contents in the phyllic zone vary with lithology. Metals are concentrated in veins along fractures and disseminated in nonwelded tuffs adjacent to vertical "feeder" structures.

GEOCHEMICAL STUDIES: DESERT ENVIRONMENT

Effect of smelter effluent in soils

M. A. Chaffee found that smelter effluent contaminated soils around some mineralized parts of the Eureka district, central Nevada, and thus soil anomalies related to mineralized areas are difficult to distinguish from those anomalies related to contaminated areas. Soil samples from 274 sites and composite samples of smelter slags were analyzed for 31 chemical elements; geochemical maps were made for selected elements. The elements Ag, As, Au, Cu, Hg, Mo, Pb, Sb, Sn, and Zn are anomalous in various combinations in soils around mineralized areas outside the areas of smelter contamination as well as around the smelter sites. Barium, cobalt, manganese, and vanadium are anomalous in the soils of many known mineralized areas, but are not anomalous in the soils of known contaminated areas. Therefore, anomalous concentrations of these four elements in soils may indicate contaminated, mineralized areas and help to distinguish them from contaminated but unmineralized areas.

GEOCHEMICAL STUDIES: TROPICAL ENVIRONMENT

Deposits in porphyry copper districts, Puerto Rico

R. E. Learned, I. P. Gonzales, and T. H. Hickey made a regional geochemical study covering approximately 500 km^2 around the porphyry copper districts of west-central Puerto Rico. They successfully delineated all the known deposits and prospects in the area and also several new targets warranting further investigation. The study was based on multielement analysis of stream sediments collected at stream junctions at an average sample density of 1/km^2. Factor analysis of the analytical data indicated that several elements play a role in the geochemical characterization of the known copper deposits, including Cu, Au, Mo, Pb, Zn, Mn, Ti, and Zr.

SURFACE AND GROUND WATER IN GEOCHEMICAL EXPLORATION

Mineral patterns in the Baboquivari Mountains, Arizona

W. H. Ficklin, D. J. Preston, Wheeler Preston, A. R. Stanley, and G. A. Nowlan made a study of waters from wells, springs, and streams on the Papago Indian Reservation and extended that study to include the entire Baboquivari Mountains, both on and off the Reservation. The extended study showed definite areal patterns of arsenic, copper, and molybdenum. Some of the patterns are related to various bedrock units within the mountain range, but one of the patterns is made up of anomalous molybdenum in the center, anomalous copper on one side, and anomalous arsenic on the opposite side and appears to be related to mineralization. The area of anomalous molybdenum contains old tungsten mines, and the area of anomalous copper is an old precious- and base-metal mining district.

Uranium potential in the Mineral Mountains, Utah

W. R. Miller, J. B. McHugh, and W. H. Ficklin conducted a geochemical survey in the area. The interpretation of simple plots of uranium concentrations and the results of a *Q*-mode factor analysis indicated that potential exists for uranium deposits within the area. The most favorable areas are in the felsic pluton near its contact with sedimentary and metamorphic rocks. The most likely sources of the uranium anomalies are uraninite-bearing epigenic veins along faults and fractures within the pluton.

MINERALOGICAL RESEARCH

Placer deposits in the Goodnews Bay district, Alaska

Sam Rosenblum, W. C. Overstreet, and R. R. Carlson found platinum-group elements (PGE) in magnetite from placer deposits in the Goodnews Bay district, Alaska. Analyses by R. R. Carlson and J. M. Nishi showed platinum as high as 1,100 ppm (35.37 troy ounces per tonne). Scanning-electron microscope studies showed at least seven phases that contain PGE: Pt-Fe, Pt-As (sperrylite), Ir-Fe, Ir-S-As-Rh-Pt-Fe, Rh-As-S (hollingworthite), Rh-Pd-As-Ni, and Pb-S-Rh-Fe-Ir. In each phase, variable amounts of PGE and minor elements (Cr, Cu, Ni, PGE) make the assignment of definite compositions difficult.

Grain sizes of the various isometric phases range from less than 1 micron (micrometer) to about 65 microns across; the phases are irregular inclusions in magnetite grains that are 200 to 400 microns across. Discrete grains of platinum-iron alloy in two fine-grained concentrates were 25 to 55 and 40 by 80 microns. The average grain size for isometric platinum-iron is about 12 microns, and the average for bladed iridium-iron is about 1 by 12 microns.

Spectrographic analyses of fire-assay magnetic concentrates showed a surprising result in 12 of 14 sets of concentrates. The finest grained fractions contain the greatest amounts of PGE, but the increase in values is not always in direct relation to decreasing grain size. These relations suggest two populations of PGE: a main suite represented by coarse grains, and a finer suite present in late-stage, fine-grained magnetite grains.

PGE phases occur as discrete grains in the magnetic concentrate, as inclusions in magnetite, and PGE are diffused into magnetite adjacent to the borders of PGE phases. Such PGE held in the magnetite lattice may represent a valuable resource.

VOLATILE GASES USEFUL IN GEOCHEMICAL EXPLORATION

Helium and mercury concentrations in the Roosevelt Hot Springs Area, Utah

M. E. Hinkle studied the concentrations of helium and mercury in soils and of helium in soil gases in part of the Roosevelt Hot Springs Known Geothermal Resource Area, Beaver County, Utah, to see what relation helium and mercury concentrations might have to geothermal features of the area. The pattern of high helium concentrations in soils was more dispersed than the pattern of helium in soil gas; however, most of the highest concentrations were over the producing geothermal field, in an area of high-temperature gradients. Low concentrations of helium in soils occurred over an area of visible hydrothermal activity. High concentrations of mercury coincided with areas of high thermal gradients and low resistivity. Concentrations of helium in soils and soil gas could not be related to the depths of geothermal wells.

Helium concentrations in the Long Valley Geothermal Area, California

The concentrations of helium in soil samples in and around the Long Valley geothermal area were studied by M. E. Hinkle, to see what relation helium concentrations might have to geothermal features of the area, and to previously studied mercury anomalies in the area. Anomalously high concentrations of helium occurred over part of the Hilton Creek fault—a major Sierra Nevada frontal fault—and over other faults outside of the caldera. Anomalously low concentrations of helium occurred in several areas of high mercury concentrations, which were also areas of hydrothermal alteration.

INSTRUMENTATION FOR GEOCHEMICAL EXPLORATION

R. C. Bigelow designed and developed detectors and supporting hardware and software for a laser-base differential gas measurement system. The automated system consists of a dye laser, photomultiplier detectors, an analog-to-digital converter, and a HP1000 data processor; the system can make up to 30 readings per second. System accuracy is limited by the 12-bit resolution of the digitizer, about 0.05 percent. This corresponds to a calculated minimum resoultion of about 5000 photons on the photocathode. The previous manual system was limited to average readings at 5-second intervals, 2-percent system accuracy, and a minimum resolution of about $10 \times (Ex;10)$ photons.

ANALYTICAL METHODOLOGY USEFUL IN GEOCHEMICAL EXPLORATION

Partitioning of copper among selected geologic phases

In experiments designed to partition copper among selected geologic phases, R. E. Learned, T. T. Chao, R. F. Sanzolone applied the sequential dissolution procedure to various sample media. The extraction procedure affords a convenient means of determining the copper content of the following fractions: (1) manganese oxides and "reactive" iron oxides, (2) "amorphous" iron oxides, (3) "crystalline" iron oxides, (4) sulfides, magnetite, and other resistant iron oxides, and (5) silicates. The apportionment of copper among phases constituting geologic media is a function of geochemical environment. Geochemical contrasts (anomaly-to-

background ratios) vary widely among the five fractions of each sample media investigated, and at least one fraction of each medium provides substantially stronger contrast than does the bulk medium. Selective extraction procedures appear to have important applications to the orientation and interpretative stages of geochemical exploration. Futher investigation and testing of a similar nature are recommended.

PARTIAL SOLUTION TECHNIQUES APPLIED TO ORE DEPOSITS

A massive sulfide deposit in a humid, subtropical environment

A sequential chemical extraction scheme was used by L. H. Filipek, T. T. Chao, and R. H. Carpenter to determine the geochemical partitioning of copper, zinc, and lead among hydrous manganese and iron oxides, organics, and residual crystalline silicates and oxides in the minus-80-mesh sediments and in boulder coatings from a stream in Lincoln County, Ga. The stream drains an area containing a copper-zinc-lead sulfide deposit (Magruder mine). The boulder coatings contain mainly manganese oxides and organic matter with minor hydrous iron oxides. In the sediments, the chemically active phases are mainly hydrous iron oxides and organics, probably because manganese is leaching out of the sediments and precipitating on the exposed surfaces of boulders. Of the ore metals, zinc is the most mobile and is partitioned most strongly into the coatings. Lead remains mainly in the sediments. In the boulder coatings, competition for copper, zinc, and lead follows the order: copper organics > iron oxides > manganese oxides; zinc, manganese oxides about equal organics > Fe oxides; and Pb, Fe oxides > organics about equal manganese oxides. In the sediments, adsorption sites on clays also appeared to be important as metal scavengers. The mildest extractants (1 mole acetic acid and 0.1 mole hydroxylamine hydrochloride in 0.01 mole nitric acid) gave the best anomaly-to-background contrast in both the boulder coatings and sediments for all three ore metals.

Porphry copper deposit in an arid environment

Using the same extraction scheme, L. H. Filipek and P. K. Theobald analyzed samples of minus-80-mesh sediment rock containing exposed fracture coatings, and jarosite and chrysocolla from an area surrounding the North Silver Bell porphyry copper deposit near Tucson, Ariz. Jarosite and chrysocolla, two major minerals of the North Silver Bell area, were found to dissolve over two or more steps of the extraction scheme. The results suggest that in a semiarid to arid environment where mechanical dispersion of such minerals predominates, uncritical assignment of unique phases such as manganese oxides or organic matter to a given extraction would lead to false interpretations of weathering processes. However, the relative proportions of elements dissolved in each step of the jarosite and chrysocolla extractions could be used as a "fingerprint" for recognition of the presence of these two minerals in the sediment and rock samples. The relative abundance of hydrous iron oxide and jarosite and the alteration zoning could be mapped using data from jarosite and chrysocolla extractions. Manganese oxides were found also to have a greater influence on zinc than on copper or lead during supergene alteration. As with the Magruder mine samples from Georgia, the 1 mole acetic acid extraction gave the greatest anomaly-to-background contrast in the stream sediments at North Silver Bell. However, the residual mineral fraction of these sediments showed the longest dispersion train.

Comparison of two extractions for hydrous iron oxides

A comparison was made by L. H. Filipek, T. T. Chao, and P. K. Theobald of the effectiveness in mineral exploration of two extractions commonly used to dissolve hydrous iron oxides: hot acifidied hydroxlamine hydrochloride and hot oxalic acid. Results obtained on minus-80-mesh stream sediments from the Magruder mine area in Georgia indicate that hydroxlamine hydrochloride enhances the anomaly for copper by a factor of 2 and for zinc by a factor of 1.5, compared to the oxalic method. Analyses of iron-oxide-coated rock samples from the North Silver Bell porphyry copper deposit in Arizona indicate that both techniques effectively outline the zones of hydrothermal alteration. Because the hydroxlamine-hydrochloride extraction also can perform well in high-carbonate or high-clay environments, where other workers have suggested that oxalic acid is not very effective, the hydroxlamine-hydrochloride method is preferable for general exploration use.

APPLICATION AND EVALUATION OF CHEMICAL ANALYSIS TO DIVERSE GEOCHEMICAL ENVIRONMENTS

Recent laboratory investigations by J. G. Viets (USGS) and J. R. Clark (Colorado School of Mines) have developed a synergistic liquid ion exchange-solvent extraction system for the separation and multielement determination of 18 elements of interest in geochemical exploration. The organic separation technique isolates and concentrates the elements of interest away from possible major element interferences such as iron, manganese, calcium, in the sample digestion solution of rocks, soils, and stream sediments. The metals and metaloids in the organic phase may then be determined by flame or graphite furnace atomic absorption spec-

troscopy to near or below crustal abundance levels. Since 18 elements—Ag, Au, As, Bi, Cd, Cu, Ga, Hg, In, Pt, Pd, Pb, Sb, Se, Sn, Te, Tl, and An—are partitioned from a single digestion solution into the organic phase, further investigations will be conducted using various partial leach digestions so that metal contents of specific phases of a sample, such as clays or amorphous oxide coatings, may be determined. Adaptation to induction-coupled plasma emission spectroscopy and rapid automated atomic-absorption instrumentation may allow extremely rapid and sensitive data using this technique.

DEVELOPMENT OF EFFECTIVE ON-SITE METHODS OF CHEMICAL ANALYSIS

W. L. Campbell, using biogeochemical techniques in studies of the mineral potential of the Papago Indian Reservation, found that the plant fluids in succulents can be aspirated directly into an atomic-absorption spectrophotometer. Direct determination of lithium in cactus fluids by conventional atomic-absorption flame photometer was investigated and appeared to warrant further testing as a possible geochemical tool.

RESEARCH IN SPECTROGRAPHIC METHODS

J. M. Motooka and S. J. Sutley developed a new technique using induction-coupled plasma optical emission spectroscopy (ICP-OES) to determine the trace-element content and association in the oxalic acid leachate of stream sediments and soils as an adjunct and (or) replacement method for some existing analytical methods. The ubiquitous nature of iron and manganese oxides, their scavenging ability, and the ease of their selective extraction from stream sediments and soils by a simple oxalic acid leach can be particulary effective in the detection of trace metal associated with concealed orebodies. The direct nebulization of the oxalic acid solution into the plasma reduces sample preparation and analysis time to a fraction of that required by existing procedures. The ICP-OES technique provides a precise, low-detection limit and simultaneous multielement analysis at major, minor, and trace-level concentrations.

BIOCHEMICAL RESEARCH

Trace-element effects on growth of microbes

Using literature and laboratory studies, J. R. Watterson found that trace-element effects on the morphology, motility, gas production, pigmentation, growth, chemotactic behavior, or other specific measurable mutational variation in rapidly responsive, naturally occurring microbes furnish a visible and photo-recordable basis for a new analytical technology applicable to mineral and (or) fuel deposit search.

Using a defined motility medium, Bowdre and Krieg (1974) developed a simple method of using the tumbling aquatic behavior of *Spirillum volutans*, an unusually large bacterium, to detect the presence of Zn, Ni, Cu, Hg, or Pb ions at concentrations of 2 or 3 ppm.

Nieuwoudt and others (1980) showed that selenium in the form of sodium biselenite induces pigmentation in eight group II (colorless) strains of *Serratia marcescens* at concentrations greater than 50 ppm. After the initial color change from white to orange, no further color changes were observed with increasing concentrations of selenium up to 10,000 ppm. Induction of pigmentation did not occur between concentrations of 1 and 45 ppm of selenium, nor was pigmentation induced in these strains with any other of the metals tested. Watterson showed that vanadium causes a color change in pigmented forms of *Serratia marcesens* from orange to rosy red, and tellurium causes a change from orange to brown.

Peyru and Novick (1968) found that an arsenate-sensitive and two cadmium-sensitive plasmid-bearing mutants of *Staphylococcus aureus* were suppressible by streptomycin. The growth of these mutants thus may be made sensitive to a range of concentrations of either Na_2AsO_4 or $Cd(NO_3)_2$ by differential masking of inhibition with streptomycin.

Kikuchi (1965) found that the hydrogen sulfide production of a copper-resistant strain of the sulfate-reducing yeast, *Saccharomyces cerevisiae*, was more than 20 times greater than that of its copper-sensitive parent. In addition to the analytical potential, an acquaintance with metal-microbe interactions also may serve to identify new kinds of measurable primary biogeochemical data. For example, if hyper-hydrogen sulfide production should prove to be a common defense mechanism against heavy-metal poisoning among other sulfate-reducing microbes, this easily measurable parameter might serve as a new tool in the search for concealed mineral deposits.

GEOPHYSICAL EXPLORATION

Remote sensing in the Ajo 1°×2° quadrangle, Arizona

From the analyses of lineaments and regional mapping of hydrothermal alteration using Landsat data, G. L. Raines defined numerous anomalous areas with mineral potential. One of these areas is in the Mohawk Mountains, Yuma County, Ariz. Field studies involving geologic mapping and geochemical surveys, in cooperation with P. K. Theobald, have defined two probable explanations of the anomaly in the Mohawk Mountains. One is that the anomaly is due to a large hydrothermal system intrusive that is mostly concealed on the

pediment east of the mountains, and the second is that the anomaly is associated with extensive large pegmatite dikes that occur in the area.

In the Silver City 2° quadrangle, regional northeast-trending structures were defined from the analysis of lineaments, and there appears to be a relation between these structures and mineralized areas.

NUCLEAR—ELECTRICAL METHODS

Evaluation of coals

J. J. Daniels made hole-to-surface resistivity measurements by placing a current source in a drill hole and measuring the resulting potential distribution on the Earth's surface. This technique has been refined and the surface distribution of the total electric field vector can now be mapped. These measurements can be useful for defining variations in the continuity of coal seams and adjacent beds away from the drill hole. When these measurements are used in conjunction with resistivity well logs and hole-to-hole resistivity measurements, a comprehensive interpretation can be made of both the vertical and horizontal resistivity distribution that is associated with geologic inhomogeneities.

Tests indicated that nonlinear complex resistivity borehole measurements may help to identify clays and sulfides in shallow sedimentary coal environments.

APPLICATIONS OF SEISMIC, GROUND MAGNETICS, AND RESISTIVITY MEASUREMENTS

Chromite deposits in California

In northern California, J. C. Wynn found a combination of refraction seismic, ground magnetic, and complex resistivity methods to be effective in the identification of podiform chromite deposits. All of these methods may be site-specific, however, requiring additional field testing in other areas. It also appears possible to use Landsat imagery to map favorable horizons within the periodotite mass that may host chromite.

Indian Lands in Wisconsin

B. D. Smith made airborne geophysical surveys on selected Indian lands in the Great Lakes region to define anomalies that may indicate the presence of massive sulfide mineralization. Ground geophysical surveys also have been used to define drilling targets. A comparison of ground geophysical techniques has demonstrated that all those tested can detect successfully the airborne anomalies. However, the work to date suggests that conventional geophysical methods should not be used solely as anomaly-finding techniques, but should be interpreted as completely as possible in order to indirectly detect favorable areas for potentially economic mineralization.

Colville Indian Reservation, Washington

V. J. Flanigan and M. S. Sherrard observed that the most prominent feature seen on the recently completed gravity map of the Colville Indian Reservation is a 15 to 20 mGal low associated with less dense volcanic rock and sediments filling the Republic graben. Detail gravity data taken over the Mt. Tolman copper-molybdenum deposit do not show a unique density contrast to unmineralized rocks, hence gravity data probably will be of limited use in delineating other areas of the Republic batholith underlying much of the Reservation which might contain other Mt. Tolman-type mineralization.

RESOURCE INFORMATION SYSTEMS AND ANALYSIS

The Resource Information Systems and Analysis Program is designed to assist the decision-making process for national mineral and fuels policy as well as USGS resource programs. This is done by improving methods for accessing and locating mineral and fuel resources and for the storage, retrieval, manipulation, and display of commodity information for mineral-resource evaluation and prediction. Highlights of this program for fiscal year 1980 follow.

Data processing

The GRASP system was modified to accommodate integer and floating point array data, four new intrinsic functions related to array data were added, and a subscripting capability introduced. A micro-processor version of GRASP was written in BASIC and implemented on the Tektronix 4052.

Remote entry of geochemical data in the field was accomplished with an inexpensive minicomputer, the main computer in Denver being accessed by telephone. Data sets were created to be accessed by statistical programs for geochemical analysis. This ongoing analysis permits reexamination of anomalous areas in the same field season as the sampling.

Bibliographic references

Data fields for the Mineral Data System Reference File (MDSREF) data base were established and a test run made of Idaho citations taken from the CRIB data base. References for a Professional Paper on world

bauxite resources were compiled, edited, and entered on Lexitron diskettes for future entry into MDSREF.

Mineral resources of Alaska in reports covering the last 80 yr were summarized for fourteen 1:250,000 quadrangles, thereby making readily available the information from old and out-of-print reports as well as results of current investigations.

Data bases

The original CRIB file was separated into three component files to form the basic Mineral Data System (MDS). CRIB, now a component file of MDS, consists of point-location data only (mines, prospects, occurrences); the two other basic components are mining district level information (National Atlas File) and summary level information (Summary File). CRIB presently remains the main file of MDS and at the end of 1980 contained 47,023 records. Various types of cooperative programs are continuing. New coops were started in 1980 with the states of South Carolina, Arizona, Colorado, Nevada, and New Mexico. Coops continue with Oregon, Idaho, Alabama, Michigan, Virginia, Tennessee, South Dakota, the BLM, and the State Department.

Resource data retrieval and computerized resource-assessment techniques of the National Coal Resource Data System (NCRDS) are being used interactively by such outside groups as State agencies, in addition to the USGS. Data is continually input from both USGS and external sources, such as State and Federal cooperative programs, to provide a basis for national coal resource assessments. Magnetic tapes of some NCRDS data bases and files were made available through the National Geophysical and Solar Terrestrial Data Center in Boulder, Colo.

In 1980, the Petroleum Data System (PDS) was installed on the Reston computer, and programs were developed to plot PDS data against digitized field outlines. Outlines of geologic provinces were digitized in order to be combined with PDS data.

The Navajo Resources Information System (NRIS) exhibited continued growth, the most actively growing file being a reference data base, "nref," which has over 1200 references. The Navajo Minerals Department constructed a data base, "Landmast," which addresses the land status of potential mineral-resources sites and contains over 5,000 records. Six interrelateable oil and gas data bases were structured to address over 50 different attributes of gas, oil, and helium production on the Navajo Reservation.

The Utah resource-data file currently consists of more than 3,500 records containing locality (UTM, longitude and latitude, and township and range), geologic, and resource information on commodity deposits and occurrences. The file will be corrected and updated annually to maintain accuracy and currency; contributions by users to help keep the file current are welcomed. Rapid selection searches can be made for a complete record, of specified parts, as tabulations, or as map plots for selected fields of interest. A complete description of this file may be found in USGS Open-File Rept. 80–845 by Tooker and Wong (1980).

Twenty mineral-province maps in U.S. Geological Survey Open-File Report 79–576, A through S, (Tooker and others, 1979) for a selected group of critical metal and nonmetal commodities, represent a simplified level 1 evaluation of resource possibilities in favorable areas in the conterminous United States where there is present mining activity, past production, resource indications, or reasonable expectations of undiscovered minerals, and reported but not fully evaluated mineral occurrences. Coproduct and byproduct materials are considered together with primary mineral resources. The maps, as well as the individual authors' reports, summarize present resource availability of Al, Cr, Co, Nb, Cu, F, Au, Fe, Pb, Mg, Hg, Ni, P, Pt, Ta, Sm, Ti, W, V, and Zn. Background information describing province maps and their use may be found in USGS Circular 792 by Tooker (1980).

MINERAL-RESOURCE ANALYSIS

A preliminary Metallogenic Map of North America was completed in draft for editing and display. The data required for preparation of a deposit listing to accompany the map were entered into MULTICS.

One hundred papers on regional-resource assessment of nonfuels were examined and classified according to methods used and form of the products in order to identify possible methods for future assessments. Criteria were found that could be useful in selecting an assessment method, and suggestions were made concerning new methods. A report summarizing these results is being reviewed (Singer and Mosier, 1980). Estimated grades and tonnages for over 700 mineral deposits were published in order to aid others trying to construct grade-tonnage models (Singer and others, 1980).

Preliminary resource assessments of the Walker Lake 2° sheet were constructed, identifying a number of tracts that appear to be permissive for the occurrence of undiscovered porphyry copper, porphyry molybdenum, and epithermal gold-silver deposits. Work is currently underway to examine and evaluate these tracts.

Basic subsurface data collected from over 1,800 boreholes for the Westwater Canyon Sandstone Member of the Morrison Formation in the San Juan basin, N. Mex., have been computerized for the purpose of estimating the potential uranium resources in the San Juan basin. From these data, a genetic-geologic model for the tabular humate-type uranium deposit was

constructed based on the known uranium deposits in the Grants mineral belt. A preliminary estimate of the potential uranium resources in the East Chaco Canyon area, based on these data, suggests that the undiscovered uranium resources are of the same order of magnitude as those already discovered.

It was found that the log grade of mercury data ores has declined in Spain, the United States, and Yugoslavia, in such a way as to remain roughly proportional to the minus 2/3 power of the log cumulative ore mined. In the United States the grade of mercury ores has declined from 36 percent in the middle of the 19th century to 0.5 percent at the recently opened McDermitt mine in Nevada. Extrapolating past trends in ore grades is one way to estimate the grades of ore that will be available for mining in the future and also to estimate the remaining quantity of metal. Similar studies were conducted on copper, byproduct gold and silver, lode gold, uranium, and oil, in the conterminous United States and in the Permian basin. Results of these studies are summarized in tabular form.

Commodity	Limiting point	Remaining quantity	Last year of data
Mercury	Grade = 0.1 percent	54×10^6 kg	1976
Copper	Grade = 0.2 percent	270×10^6 t	1976
Gold (byproduct)	Grade = 0.025 ppm	3,656 t	1976
Silver (byproduct)	Grade = 0.35 ppm	64,676 t	1976
Gold (lode)	Grade = 3.13 ppm	2,076 t	1976
Uranium	Grade = 0.0723 percent	4.5×10^6 sh. tons	1979
Oil (U.S.)	5×10^9 expl. feet	37.64×10^9 bbl	1978

Oil, gas, and coal-resource analyses

A method for evaluating the value of government preleased drilling was developed and applied to a strippable coal deposit in southwestern Wyoming, assuming various drilling intensities and that the government supplied the drilling data to potential bidders. Results showed that the expected value of incremental drilling information should be determined by a tract-by-tract approach with the intensity of the optimal drilling program (to the government) depending on (1) the expected degree of competition for the lease, (2) the risk aversions of bidders, (3) the factors that affect economic rents – thickness of coal seams, proximity to markets and transport facilities, and market conditions – and (4) the spatial correlation characterisics between drill-hole measurements to determine how greatly the standard deviation of the expected value of minable tonnage declines as drill holes are spaced more closely.

SEDIMENTARY MINERAL RESOURCES

MARINE AND NONMARINE EVAPORITE DEPOSITS

Water content of rock salt

Investigations on water content in cored halite samples were determined by T. G. Ging and R. J. Hite; the halite is dissolved in methanol, and the extracted water is measured by Karl Fischer titration. This method eliminates problems attempting to determine water content by heating, then measuring weight loss. Water-content information is needed to evaluate salt beds as possible radioactive-waste-disposal sites. Other advantages of the procedure are that (1) halite is separated from silica, clays, and other minerals so that halite and nonhalite weights can be obtained; (2) calcium, magnesium, and potassium contents of halite waters can be determined; (3) bitumen content of the halite sample can be determined – all from the same sample.

Salt crystallization and diagenesis, Owens Lake, California

Owens Lake, east of the southern Sierra Nevada, Calif., has been a dry salt flat since the early 20th century when its natural inflow from the east slope of the range was diverted to Los Angeles. Uncommonly heavy snowfall in that range during the winters of 1937–38 and 1968–69 led to flooding of the lake floor the following summers, and the inflowing freshwater caused partial solution of the exposed salts.

G. I. Smith, Irving Friedman, and R. J. McLaughlin monitored the lake's 1969 flooding, its desiccation in 1970–71, and the ensuing diagenesis of the new salt bed through 1977. Their observations showed that seasonal phase changes in the accumulating salt layer occurred during its deposition, and that changes in minerology continued after salt deposition was complete. The chemical and isotopic evolution of the brines during lake desiccation was reported earlier (Irving Friedman, G. I. Smith, and K. G. Hardcastle, 1976); study of the crystallization and subsequent diagenesis of the salts is continuing. The saline layers initially had mineralogic and isotopic characteristics that could be related to the temperature and isotopic composition of the lake at the time each of them formed, but diagenesis over 6 yr tended to eliminate those differences. The driving mechanism of diagenesis, as presently inferred, is a pumping effect caused by seasonal temperature changes that lead to the creation of hydrated saline mineral phases during the winter and anhydrous phases during

summer. The interstitial waters act as the early winter source for the required water of crystallization and the early summer reservoir for water that is expelled, and the isotopic character of both salts and interstitial brines becomes more uniform with each seasonal cycle.

CHEMICAL RESOURCES

PHOSPHORITE

Phosphate investigation

The paleooceanographic and paleoclimatic causes of equatorial and trade-wind belt phosphogenesis, which were shown to be mutually exclusive, were postulated by R. F. Sheldon to depend on the dominant mechanism of solar heat transfer from low to high latitudes. If heat transfer is accomplished efficiently by oceanic currents, warm polar climate results from equatorial to polar surficial convection currents, with deep, cold polar to equator return flow. This convection system results in equatorial upwelling and phosphogenesis. If oceanic heat transfer is inefficient, cold polar areas result, and heat transfer is accomplished by atmospheric processes. This results in strong trade winds as shown by trade-wind desert eolian deposits and trade-wind belt eastern boundary current upwelling and phosphogenesis. The efficiency of oceanic equatorial to polar heat transfer is primarily a function of paleogeography and the presence of seaways into polar seas.

This model of paleooceanography and phosphogenesis is supported by studies of marine phosphorite deposits from Proterozoic to Holocene. The presence of Proterozoic marine shelf glacial tillite deposits in equatorial regions interbedded with the normal sequences of phosphorite deposits, dolomites, black shales, and cherts is totally anomalous in the present climatic and sedimentologic regimes. A model of Earth icerings is postulated to account for this tillite-phosphorite-dolomite equatorial association.

LITHIUM

Lithium deposition in Socorro County, New Mexico

Field and laboratory investigations by Sigrid Asher-Bolinder in central New Mexico have determined that the distribution of anomalous to subeconomic deposits of lithium in the Miocene Socorro basin is controlled by the locations of altered ashes within the basin, and by the alteration products of the ashes (primarily smectites and clinoptilolites). In general, lithium distribution increases logarithmically with distance away from the early Miocene caldera contained within the basin, and then drops rapidly a few kilometers farther away. The source for lithium is not easily recognizable.

There are no unequivocal spring deposits present in the sediments of the Miocene Popotosa Formation, but evidence by R. A. Zielinski (1979) suggests that as much as 50 percent of contained lithium may be leached from fresh ashes by alkaline solutions such as might have been the ground water in the Popotosa playa sediments. The caldera contained within the basin may have provided a spring source and (or) heat to drive ground water through the highly permeable and reactive ash beds, leaching lithium and altering the ashes as it passed. As the ground water moved outward from the caldera, leached lithium concentrations would have increased as the solutions cooled. The contained lithium may have been precipitated and incorporated into neoforming smectites or their precursors.

FLUORITE

Fluorite in Cenozoic lacustrine rocks

Fluorite makes up as much as 30 percent of a zeolitic tuff in a Pliocene or Pleistocene lacustrine facies of the Gila Conglomerate that has not been subjected to hydrothermal activity, according to R. A. Sheppard and F. A. Mumpton (State University College at Brockport, N.Y.). Although the fluorite is unevenly distributed throughout a lacustrine sequence at least 20-m thick of tuff, mudstone, and siltstone, concentrations of greater than 20 percent fluorite are in a light-gray zeolitic tuff that is 40 cm thick and that crops out over a 0.5-km^2 area about 2.5 km east of Buckhorn. The fluorite occurs chiefly as prolate pellets and, more rarely, as ooliths 0.1-0.3 mm in size. Broken ooliths are extremely rare. Studies by X-ray diffraction and scanning electron microscopy show that the pellets and ooliths consist mainly of submicrometer-size fluorite and quartz, and that both minerals have poorly defined morphology. The pellets and ooliths are embedded in a matrix that consists chiefly of micrometer-size mordenite and smectite. The pellets and ooliths probably are the result of primary crystallization of fluorite in a saline, alkaline lake that had a high fluorine content. Calcium may have been supplied by springs located marginally to the lake, and the fluorite precipitated where the spring and lake waters mixed. The fluorite pellets were then transported basinward and were incorporated with the reworked vitric ash, which was converted chiefly to smectite and mordenite during diagenesis. The deposit may be of commerical interest because of the areal extent and the ease with which the pellets can be concentrated; however, the quartz content of the pellets may be detrimental.

MINERAL-FUEL INVESTIGATIONS

COAL RESOURCES

FIELD INVESTIGATIONS

The Coal Resources Investigations Program of the Geologic Division classifies the Nation's remaining coal resources into resource and reserve base categories based on geographic and geologic distribution and physical and chemical characteristics. As part of this effort, personnel of the Division in 1980 mapped and assessed coal-bearing lands in Alabama, Alaska, Arizona, Colorado, Georgia, Kentucky, Montana, New Mexico, Pennsylvania, Virginia, West Virginia, and Wyoming. Included in these field investigations were studies conducted on the following Indian Reservations: Blackfoot, Crow, and Fort Peck, Mont.; Alamo, Cañoncito, Jicarilla, Navajo, Ramah, and Zuni, N. Mex.; and Wind River, Wyo. About 35,700 m of air and core drilling was completed in the coal basins of the Rocky Mountains, the Great Plains, and the Colorado Plateau, in coordination with the geological investigations to assess the quantity and quality of buried coal and to provide stratigraphic information. Nearly 800 channel and bench samples of the coal were collected for chemical and physical analyses from 18 States, in cooperation with 4 State Geological Surveys, the Conservation Division, and the Bureau of Land Management.

The USGS also provided geological support to the Energy Minerals Rehabilitation Inventory and Analysis Program of the Bureau of Land Management in the following reclamation areas: North Beulah, Mercer County, N. Dak.; Rattlesnake Butte, Stark County, N. Dak.; and Ojo Encino, McKinley County, N. Mex. Geologic studies of coal-bearing strata were conducted for the USFS, Department of Agriculture, under its Roadless Area Resource Evaluation II Program in the following areas: Burden Falls, Lusk Creek, and Garden of the Gods, Ill.; Troublesome and Cheat Mountain, Ky.; Allegheny Front, Clarion River, and Hickory Creek, Pa.; and Devils Fork, Va. Similar studies were undertaken in the Beaver Creek, Ky., Wilderness Area, also for the USFS.

COAL RESOURCES DATA SYSTEM

The National Coal Resources Data System (NCRDS) continues to grow in size and use under the direction of M. D. Carter and M. A. Carey. The NCRDS has cooperative agreements with 14 State geologic agencies and universities for the collection, correlation, transmission, entry, retrieval, manipulation, and display of drill hole, chemical analyses, and other relevant coal resource-related data. During 1980 approximately 35,000 records of coal resources, chemical analyses, and stratigraphy were added to the system raising the total to 135,000 entries. The data base includes 40,000 coal-resource tonnage records and 55,000 records of USBM proximate and ultimate analyses, mostly reported by coal bed on a State and county basis. The NCRDS also contains 6,000 geodetically located records of proximate, ultimate, major-, minor-, and trace-element analyses and associated data provided by the USGS coal geochemical program, and 30,000 drill-hole and stratigraphic description records. NCRDS software is used to produce log plots, stratigraphic sections, isopach maps, and resource calculations from the point source data in the system.

EASTERN COAL

Age and regional correlation of the Black Creek coal beds, Alabama

New collections and discoveries of plant megafossils by R. W. Cracknell from the roof shales of the Black Creek and Jefferson coal beds of the Pottsville Formation of Alabama were examined by P. C. Lyons and C. R. Meissner, Jr., who were able to correlate the coal-bearing unit with the Lower Pennsylvanian Series in the central Appalachians. The combined floral assemblage, collected over a stratigraphic interval of 15 m, consists of *Lyginopteris hoeninghausii, Mariopteris pottsvillea, Neuropteris smithsii, Neuropteris* cf. *pocahontas* var. *inaequalis, Cyperites longifolium, Lepidostrobophyllum,* sp., *Lepidophlois* sp., *Neuropteris* sp., and *Calamites* sp. The plant fossils correlate with those in the Tumbling Run Member (lower member) of the type Pottsville Formation in the Southern Anthracite Field of Pennsylvania (White, 1899). They also correlate with the flora from the upper half of the Pocahontas Formation or the middle part of the New River Formation in West Virginia; the specific interval containing these fossils ranges from the Pocahontas No. 3 coal bed (Pocahontas Formation) to just above the Sewell coal bed, New River Formation (Gillespie and Pfefferkorn, 1979).

Fluvial depositional model for basal Pennsylvanian sandstone, central Appalachians

Compilation by C. L. Rice of data collected in eastern Kentucky showed that extensive drainage systems were incised in Mississippian strata before deposition of Pennsylvanian strata in Kentucky. Drainage patterns apparently evolved in response to the development (or continuing development) of the Illinois and Appalachian basins. At the end of Mississippian time the two basins were separated by a drainage divide that, in part, extended from southwestern Pennsylvania to south-central Kentucky. In earliest Pennsylvanian time, streams on either side of this divide carried quartz-rich sands and gravels from the northern end of the Appalachian tectonic belt toward depocenters in both basins. Remnants of a major river extending from northwestern Pennsylvania to the Illinois basin are preserved in many channel sandstone deposits from Pennsylvania to western Kentucky. Isopachs of some basal sandstones and conglomerates in southeastern Kentucky, together with the contour map of the base of the Pennsylvanian (Coskren and Rice, 1979), also suggest that those sandstones were deposited in broad valleys incised in Mississippian rocks. Choking of one of these valleys, the Sharon-Brownsville Channel, with coarse clastic rocks in Early Pennsylvanian time appears to have caused floods that breached the low divide between the two basins; subsequent floods resulted in the capture of the upper part of the Sharon drainage system by streams of the Appalachian basin. Extension of the Sharon fluvial system into eastern Kentucky is thought to be responsible for deposition of quartz-rich sands in that area well into Middle Pennsylvanian time. The fluvial model helps explain the stratigraphy of the lower part of the Pennsylvanian section, aids in regional correlation of coal beds, and may be useful in understanding the subsurface distribution of some Lower Pennsylvanian coal beds.

New occurrence of Devonian plant fossils, West Virginia

A new occurrence of Devonian plant fossils in thin coal beds was reported by W. H. Gillespie from a locality near Elkins, W. Va. The collections have proven to be Late Devonian in age (Famennian, probably at the Fa2c-Fa2d boundary) and are the best preserved of any similar Devonian flora in the world. The classic material of this age comes from Belgium and from Bear Island (part of the Spitzbergen Island group). The Elkins flora has all of the genera listed from the classic localities and in addition has them petrified as well as in compression-impression types of preservation. Two spectacular finds are the first pre-Carboniferous coal balls (limestone concretions in coal) and seed-bearing structures somewhat similar to *Archaeosperma*. The site is also significant because the age determination is not solely dependent upon the plant megafossils but is confirmed by a good spore flora collected from throughout the section by associated invertebrate and vertebrate fossils. All lines of information point to a Famennian Age for this unit; and, as a result, about 300 m of presumed Pocono strata are assigned to the Devonian instead of the Mississippian.

An occurrence of Permian strata in western Kentucky

Paleontological studies of fusulinids collected by T. M. Kehn (USGS) and J. G. Beard and A. D. Williamson (Kentucky Geological Survey), from strata previously assigned to the Sturgis Formation of Pennsylvanian and Permian age, indicate that they are of Early Permian age (Douglass, 1979). These strata are preserved in a small down-dropped fault block in the Sturgis, Union County, Ky., area; existence of strata of similar age elsewhere in the eastern interior (Illinois basin) coal field area is unknown. Strata of Permian age probably did cover part or all of this area before being eroded and indeed might have been connected to strata of Permian age in Kansas or Pennsylvania or both.

The section of Permian strata consists of interbedded shale, siltstone, limestone, some sandstone, and coal. These strata have a known thickness of about 130 m, yet may be as much as 400 m thick as suggested by projected structural data; they are assigned to the newly named Mauzy Formation. The boundary between the Pennsylvanian and Permian Systems cannot be defined precisely because the strata everywhere are covered by loess so adequate paleontological, paleobotanical, and stratigraphic data are lacking. For convenience, the formation and systemic boundary is placed tentatively at the base of the limestone sequence lithologically similar to that containing the fusulinids of Permian age. Because deposition appears to have been continuous, all or part of the 110 m of strata between the Sulphur Springs coal bed of the Sturgis Formation of Pennsylvanian age (now stratigraphically restricted) and the overlying fusulinid-bearing limestone bed could be assigned to a transition zone, or the boundaries could be placed elsewhere within the interval.

Sclerotinites in bituminous coals of the central Appalachians

Sclerotinites belonging to the inertinite maceral group were studied by P. C. Lyons, C. L. Thompson, R. B. Finkelman, and F. W. Brown, using a scanning-electron microscope and paleobotanical techniques. The sclerotinites were found in coal samples from the Appalachian basin ranging from the Pocahontas No. 3 coal

bed (Pocahontas Formation, Lower Pennsylvanian) to the Washington coal bed (Washington Formation, Lower Permian). The inertites were shown to be of probable resinous origin and belong to medullosan seed ferns. Fungal sclerotinite was not found. This work agrees with interpretations of similar bodies found in the coals of the Illinois basin (Kosanke and Harrison, 1957).

WESTERN COAL

The Gallup Sandstone, San Juan basin, New Mexico

The Gallup Sandstone in the Gallup sag of the San Juan basin, N. Mex., is divisible into three prograded depositional sequences associated with a wave-dominated delta and with braided fluvial systems. R. M. Flores and J. C. Hohman found that the lowermost sequence consists of shoreface, sheetlike sandstone, siltstone, and shale bodies that coarsen upward into coalesced distributary mouth, bar, and beach sandstones, which in turn are locally dissected and filled by fluvially and tidally influenced distributary channel sandstones. This early depositional sequence is overlain by a constructional delta plain sequence, which consists of meandering distributary channels interspersed with interdistributary crevasse-splay deposits of sandstone, backswamp coal, carbonaceous shale, siltstone, and shale. These deltaic deposits then were partly destroyed with an accompanying development of offshore bars and back-barrier lagoons. The third sequence consists of the sediments filling the back-bay lagoons, largely heavily bioturbated sandstone, siltstone, shale, carbonaceous shale, and coal beds. The coal beds in this sequence are as thick as 1.2 m and extend laterally for distances as great as 6.8 km, in contrast to the few delta-plain coal beds that tend to be thin, discontinuous, and lenticular. The entire deltaic, lagoonal, and offshore bar complex was then covered by many overlapping, lenticular, and varicolored pebbly sandstones deposited by lowly sinuous, braided streams.

The Pictured Cliffs Sandstone, San Juan basin, New Mexico

J. W. Mytton reported that the Upper Cretaceous Pictured Cliffs Sandstone in the eastern part of the San Juan basin, N. Mex., is possibly a modified lower shoreface to transitional facies similar to the middle to lower shoreface to transitional facies described by R. M. Flores in the Bisti-Burnhan area of the western part of the San Juan basin. A thin lenticular coal–carbonaceous shale zone occurs in the Pictured Cliffs Sandstone in the northern part of the Chaco Mesa quadrangle. A lower shoreface sandstone lying above the coal–carbonaceous shale zone is interpreted to represent a minor transgression within the prograding Pictured Cliffs Sandstone. Coal in this zone is less than 0.3 m thick. Remnants of the uppermost Pictured Cliffs Sandstone, interpreted as possible upper shoreface to foreshore deposits, crop out at various localities in the northern part of the Chaco Mesa quadrangle (Star Lake and Wolf Stand 1:24,000-scale quadrangles). Those in the Star Lake quadrangle contain a black sandstone described by W. L. Chenowith, 1957) and referred to by R. S. Houston and J. F. Murphy (1977). During preliminary field studies in the Tinian and Wolfcamp quadrangles, intertonguing of Upper Cretaceous units was seen, including the Cliff House Sandstone with the Lewis Shale and the stratigraphically lower La Ventana Tongue of the Cliff House Sandstone with the Menefee Formation. The transition between the upper part of the Cliff House and its La Ventana Tongue can be traced in the Toran Wash area and supports, in part, the work of D. E. Tabet and S. J. Frost (1979).

Coal compaction in central Utah

The amount of compaction of sediments sustained during lithification is critical in stratigraphic analysis. It is particularly important in the study of coal and coal-bearing strata as the eventual coalificiation of peat involves compaction that is several to many times greater than that of other sediments. Restored cross sections through coal-bearing strata often make better stratigraphic sense when coal-bed thicknesses are expanded to approximately the thickness of precursory peat beds. There is, however, no general agreement on what compaction ratio to use in preparing such reconstructions—estimates of the peat-coal compaction ratio cited in the literature range from 1.4:1 to 30:1. Study by T. A. Ryor of coal beds contained in the Ferron Sandstone Member of the Mancos Shale in central Utah has led to a new estimate of the peat-coal compaction ratio for bituminous coal of Cretaceous age.

Two different methods were used to arrive at this ratio. Detailed stratigraphic study of the *C* coal bed of the Emery coal field permitted development of a refined depositional model explaining the history of accumulation of the peat deposit (Ryer, Phillips, Bohor, and Pollastro, 1980). It was possible to reconstruct the geometry of the basin in which this peat accumulated and, thereby, the original thickness of the peat. Comparison of the thicknesses of the *C* coal bed with the reconstructed thickness of the parent peat indicates a peat-coal compaction ratio of about 11:1, although the data showed a large variance.

The *I* coal bed of the Emery coal field is locally cut by an active channel-fill sequence. The channel fill, which rests erosionally upon a split of the coal bed, shows

evidence of lateral migration followed by channel abandonment and inactive filling with fine-grained sediment. At this location, it is possible to calculate the thickness of peat that was eroded. As the channel deposit thins towards its cutout, the underlying split increases in thickness. Comparison of the relative rates of thinning of the channel-fill sequence and thickening of the coal bed leads to an estimate of the peat-coal ratio of 11.3:1. Variance of the data derived by this method is small. It is concluded that a peat-coal compaction ratio of about 11:1 may be appropriate to use in reconstructing thicknesses of original peats in coal-bearing strata of Cretaceous age in the Rocky Mountain coal province.

Thick coal in the Powder River basin, Wyoming

B. H. Kent and C. L. Molina established that the Tertiary strata in the Powder River basin of northeast Wyoming contain a series of two or more succeeding coal beds that merge locally to form linear, north-trending deposits of unusually thick coal. In the subsurface just east of the Powder River and west of Spotted Horse, Wyo., the Anderson and Canyon coal beds merge to form a single bed 14–25 m thick. Drilling in 1980 confirmed that the merged Anderson-Canyon coal deposit is at least 10 km wide and 30 km long, in which the coal averages 15 m in thickness and lies under a minimum overburden of 200 m. Core samples of coal acquired during drilling were analyzed on an "as-received" basis; the deposit averages 0.3 percent sulfur, 4 percent ash, and its average heat value is 9,000 Btu per pound. The Anderson-Canyon merged coal deposit is too deep to be mined from the surface, yet its exceptional thickness and quality may make it desirable for in-place processing.

Stratigraphy of the Hanna Formation, Wyoming

A coal-resource study of the Hanna basin, south-central Wyoming, conducted by D. E. Hanson, revealed the record of tectonic events and accompanying deposition of coal-bearing strata. Movement along a thrust-fault system on the north side of the Hanna basin during Paleocene time resulted in the filling of an asymmetric foreland by thick, clastic alluvial fans progressively accummulating southward. Remnants of these clastic strata are preserved as steeply dipping beds on the north side of the Hanna basin. The fans subsequently were eroded and the derived sediments were then deposited farther to the south, forming an alluvial plain now crossed by the Medicine Bow River system. The resulting complex stratigrahic unit is known as the Hanna Formation, divisible into an alluvial fan facies and an alluvial plain facies, each of which can be subdivided into smaller units.

The alluvial fan facies contains the coarsest-grained strata, probably derived from the granite core of the Shirley Mountains, although mudstone also may have been furnished through erosion of nearby, thick shale beds of Cretaceous age. The uppermost parts of the alluvial fan facies (its proximal and upper medial parts) have been removed by erosion. Strata considered to represent the lower medial fan facies are still preserved, now exposed in vertical outcrops between Austin and Troublesome Creeks. Beds in this area are thin but laterally broad and consist of large-pebble conglomerate, granular sandstone, and coarse-grained sandstone. Tongues of conglomerate probably were deposited as longitudinal bar deposits. These strata then grade into the lower, or distal, alluvial fan facies, which includes small-pebble conglomerate, granulitic sandstone, coarse-grained sandstone, siltstone, and mudstone. In this part of the alluvial fan facies, much of the sediment dropped out of braided stream systems. The distal alluvial fan facies thins as it approaches the alluvial plain facies and contacts between the two are vague.

The alluvial plain facies can be subdivided into a lower lacustrine and an upper paludal subfacies. The lacustrine subfacies is the thicker of the two, and it overlaps older formations on the southeast side of the basin. It consists of overbank deposits composed chiefly of gray shale-claystone, thin sandstone, siltstone, and thin dark-gray carbonaceous shale. It also contains thick sandstone deposited as channel fill. Coal beds in this lower lacustrine subfacies generally are thin, although some relatively thick coal beds occur near its base. The paludal subfacies also consists of overbank deposits of gray shale, claystone, siltstone, and sandstone, as well as many thick sequences of stacked channel-fill sandstone. The paludal subfacies differs from the lacustrine subfacies in that it contains thick deposits of carbonaceous shale and interbedded mineable coal beds, some as thick as 10 m. Coals in the paludal subfacies consists largely of vitrinite; vitrinitic material also occurs in the associated carbonaceous shales, probably derived from woody matter that could have been floated into place.

Development of the Two Medicine Formation, Montana

The Two Medicine Formation of Late Cretaceous age, in northwestern Montana, was deposited as a nonmarine molasse, according to John Lorenza. Its sediments were derived from highlands created to the west by overthrusting and from the contemporaneous Elkhorn Mountains Volcanics to the southwest. The overthrusting created a supracrustal load that depressed the adjacent lithosphere and created episodes of

contemporaneous low-relief uplift of the adjacent Sweetgrass arch. The arch modified patterns of deposition on the then existing coastal plain where deposition occurred in alluvial flood-plain and delta-plain environments. Thin coals accumulated in the latter behind a wave-dominated deltaic system.

GEOCHEMISTRY

Origin and chemical structure of coal

Studies of humic substances, coals, and kerogens by nuclear magnetic resonance (NMR) have provided insights to their origin, chemical composition, and diagenesis that will undoubtedly lead to reconsideration of previously published concepts. NMR studies have shown that humin is first formed as a residue in both terrestrial and aquatic systems when the more labile plant constituents are preferentially degraded and lost from the sediments. With increasing oxidative exposure, this humin can be oxidized to produce humic acids and also fulvic acids. When buried anaerobically, humin forms coal or aquatic kerogen directly, and humic acids are only products of diagenesis that can be mobilized and lost as the humin undergoes further metamorphosis. Humin that is derived from vascular plants or lignin exhibits a highly aromatic chemical structure that persists to form aromatic structures in coal. Humin that is derived from aquatic plants has a predominantly paraffinic molecular structure that persists to form paraffinic structures observed in kerogens, sapropelic coals, and humic coals. The aromatic and paraffinic structures are considered to exist as distinct, mechanically mixed structures in coals or kerogens having contributions from both terrestrial and aquatic plants.

Chemical impurities in coal

New beds of coal are being opened for mining as national consumption of this fossil fuel is increasing, a trend that undoubtedly will continue. Selection of beds for coal quality until now has been based upon their heat value, ash content, and sulfur content, but Peter Zubovic, F. O. Simon, and Charles Oman note that coal also contains minor and trace amounts of as many as 70 elements, of which 18 are considered to be of environmental concern by EPA and NAS, the concentrations of which differ in each coal bed. The following table shows the minimum, maximum, and geometric mean content of 18 elements that occur in the coals of the eastern half of the United States.

These elements occur in high concentrations in some coals, but the geometric mean content of most of these elements is relatively low. Knowledge of trace-element content of coal can be useful when selecting blocks for mining. Use of coal with low trace-element content could- reduce environmental hazards. Minor and trace elements in some coals could enhance coal processing in future synthetic fuel installations, new power-generating systems, or coal conversion systems. Furthermore, a potential exists for the recovery of elements contained in coal, either as concentrates in the tailings of coal-washing plants, as volatilized elements in stack gasses, or through processing of coal ash. Sulfur is one such element, and certain Illinois coals contain enough sphalerite to be considered as low-grade ore.

Geometric mean and range of identified trace elements in coals of the eastern United States, in parts per million

	Appalachian province (2,390 samples)			Eastern Interior province (370 samples)			Gulf Coast province (40 samples)		
	Min.	Max.	Geom. Mean	Min.	Max.	Geom. Mean	Min.	Max.	Geom. Mean
As	.12	815	9.4	.7	170	6.9	1	26	4.97
Be	.07	25	1.9	.37	16	2.4	.22	17	1.8
Cd	.003	4.09	.08	.009	92	.19	.099	10	.44
Co	.6	927	5.4	.78	32	4.3	1.6	32	5.6
Cr	1.5	130	14	2.8	190	1.7	4.2	48	20
Cu	.08	280	14	2.6	96	10	3.2	85	20
F	11	2100	66	13	415	55	24	250	86
Hg	.010	3.2	.13	.010	.70	.09	.030	1	.16
Li	.64	370	15	.1	.7	.11	.86	150	13
Mm	.75	1400	15	1.4	230	23	7.4	940	100
Mo	.11	32	1.9	.37	45	2.7	.53	10	2.5
Ni	1.1	280	12	1	520	14	3.6	68	14
Pb	.09	130	6.5	.85	350	9.1	4	44	14
Sb	.04	35	.69	.1	15	.73	.19	5.2	.69
Se	.1	150	2.8	.44	13	2.2	1.4	16	4.6
U	.1	22	1.3	.2	20	1.3	.49	17	2.6
V	1.1	160	17	1.1	130	15	5.7	99	35
Zn	1.3	1000	13	3	114	16	5.4	200	26

Electrolytic oxidation of anthracite coal

Although the oxidation of anthracite coal by chemical techniques is extremely difficult, an electrolytic method, devised by F. E. Senftle, A. N. Thorpe, and C. C. Alexander, readily oxidizes anthracite and some high-ash bituminous coals within minutes. The products are humic and subhumic acids. The mechanism of electrolytic oxidation differs from that of chemical oxidation and is not clearly understood. The oxygen formed at the anode, probably in the form of O^{2-} or HO^{2-}, must be in close contact with coal surfaces to affect oxidation.

An anthracite slurry can be oxidized only with difficulty by electrolytic methods when aqueous electrolytes are used and if the slurry is confined around the anode by a porous pot or diaphragm. However, the slurry can be readily oxidized if anthracite itself is used as the anode, in which case porous pots or diaphragms are unneeded. Oxidative consumption of the coal to alkali-soluble compounds is found to proceed preferentially at the edges of the aromatic planes. In a proposed oxidation model the chief oxidants are molecular and radical species form by the electrolytic decomposition of water at the coal surface–electrolyte interface. The proposed oxidation reactions account for the opening of the aromatic rings and the subsequent formation of carboxylic acids. The model also resolves the observed anisotropic oxidation and the

need for the porous pots or diaphragms used in earlier experiments.

It may be possible to carry out electrolytic oxidation of some coal beds in unminable locations or where coal is relatively impure and cannot be used directly as fuel.

Coalification of tissues in a coal ball from the Illinois basin

Plant tissue belonging to a medullosan seed fern from a coal ball was analyzed by P. G. Hatcher, P. C. Lyons, F. W. Brown, and C. L. Thompson through the use of infrared spectroscopy, solid-state C^{13} nuclear magnetic resonance spectroscopy, and chemical techniques. Although the tissue showed the morphology and dark brown color typical of peat, spectral and chemical analyses indicate the absence of lignin and cellulose characteristic of peat. The tissue, therefore, is coalified and has the chemical properties of subbituminous or high-volatile bituminous coal. American investigators have regarded until now the organic material in coal balls as lignocellulosic tissue.

OIL AND GAS RESOURCES

ALASKA

North Slope petroleum exploration history

The petroleum exploration history of the North Slope of Alaska during 40 of the past 60 yr is unusual in that both the federal government and private industry have spent about 20 yr each exploring this area. The two exploratory efforts have been compared and contrasted by K. J. Bird. Although industry has been much more successful in finding petroleum, a strict comparison is not possible because government exploration focused on the National Petroleum Reserve in Alaska (NPRA), and oil apparently is not distributed uniformly on the North Slope. Early government exploration was a pioneering effort and established the basin framework, while later government exploration has been directed toward assessment of all possible plays and not just concentrated on the most promising plays. On the other hand, private industry exploratory efforts have benefited from demonstrated operational techniques and an established geologic framework, as well as from the fortuitous occurrence of Prudhoe Bay and other accumulations in the sector of the North Slope that it explored. Current resource estimates for the North Slope indicate significant amounts of undiscovered petroleum; and, therefore, much work remains to be done before the petroleum potential of the basin is fully explored.

Update of NPRA hydrocarbon resource estimates

The fourth update of hydrocarbon resource estimates in the NPRA was made in May 1980 in order to incorporate new information from wells and geologic and geophysical surveys. The appraisal by the play-analysis method was made by the same group of 10 geologists, who are experts in North Slope geology and resource assessment and who made earlier appraisals. The group reviewed and revised, where necessary, the various geologic input parameters, which were then fed into the Department of Interior computers. The resulting computer estimates of undiscovered in-place hydrocarbons were average oil, 6.4 billion bbl; and average gas, 10.99 trillion ft^3. These values are smaller by about 10 percent and 22 percent, respectively, than the previous estimate made in September 1979.

Two oil conduit systems recognized on North Slope

The North Slope of Alaska is on the southern flank of a ridge system that rifted during Early Cretaceous time to form the Canada basin on the north and the Colville trough on the south. The Barrow arch, the southern flank of the rifted edge, forms a regional high between the Canada basin and the Colville trough and has been the focus for migrating oil from Carboniferous through Cenozoic time. The southern flank of the rifted margin includes sedimentary rocks, designated the "Ellesmerian" sequence, of Carboniferous through Jurassic age. Important reservoir rocks in this sequence are the Lisburne and Sadlerochit Groups, Shublik Formation, Sag River Sandstone, and sands at Kuparuk River. Shales rich in organic material include the Shublik Formation (1–5 wt percent organic carbon (OC)) and the Kingak Shale (2–3 wt percent OC). The Lower Cretaceous (Neocomian) pebble shale unit transgresses and in places truncates the "Ellesmerian" sequence to set the stage for deposition of the "Brookian" sequence, a major sedimentary progradation that includes rocks of Neocomian through Cenozoic age. The pebble shale unit is an important oil source (2–4 wt percent OC) as well as a reservoir seal. The "Brookian" sequence, which includes the Nanushuk and Colville Groups of Cretaceous age and the Sagavanirktok Formation of Tertiary age, contains quartz-poor sandstone and includes at least two marine-shale intervals rich in organic carbons: The Torok Formation (1–2 wt percent OC) and the Seabee Formation (1–5 wt percent OC). L. B. Magoon and G. E. Claypool have postulated at least two hydrocarbon conduit systems for the North Slope on the basis of the two types of oil – the Barrow-Prudhoe and the Simpson-Umiat oils – and of the distribution of mature source rocks. The Barrow-Prudhoe oil was generated downdip of the Barrow arch

in the Shublik Formation, the Kingak Shale, and possibly the Neocomian pebble shale unit. The oil migrated up the flank of the arch until at least latest Cretaceous time through the Sag River Sandstone and other sandstone units to traps in the Point Barrow and Prudhoe Bay areas. The Simpson-Umiat oil was generated from the Neocomian pebble shale unit, the Torok Formation, or the Seabee Formation; and it migrated up deltaic foreset beds into traps in the Nanushuk and Colville Groups in the Umiat and Simpson areas and into traps in Cenozoic rocks in a similar setting east of Prudhoe Bay.

Aerial magnetic surveying discloses possible hydrocarbon-related anomalies in NPRA

Seepage of hydrocarbons from oil and gas pools may, in some cases, cause a mobilization and reduction of iron contained in overlying rocks and soils. The resulting change in state of the iron produces small-scale high-frequency magnetic anomalies. Measurement of the horizontal magnetic gradient enhances these near-surface variations compared with regional or basement-induced anomalies. In order to measure this gradient, a triple-sensor magnetic system was installed in an airplane. The system consists of a total-field proton-precession magnetometer extended from each wing tip and tail. Readings were obtained simultaneously every 0.73 seconds along flight lines, and the gradient was calculated from the readings. Approximately 5,000 line km were flown in the NPRA during June and July 1980 using this system. According to J. D. Hendricks, preliminary results showed that all areas of known oil seepage, as well as all producing areas in the NPRA, have associated high-frequency magnetic anomalies. In addition, several areas devoid of known oil seeps or hydrocarbon production were noted to contain similar magnetic anomalies. These areas warrant further exploration and possibly drilling in search of oil and gas deposits.

Poor reservoir potential of Fortress Mountain Formation north of Brooks Range

The Fortress Mountain Formation of Early Cretaceous (early Albian) age is a clastic wedge, as much as 3,000 m thick, that was deposited in a foredeep in front of the Brooks Range orogen. Stratigraphic field investigations in the central Southern Foothills north of the Brooks Range by C. M. Molenaar, R. M. Egbert, and L. F. Krystinik indicate that this unit consists largely of deep-water deposits that were dumped into a relatively steep-sided basin. The formation appears to have been deposited from many point sources along the ancestral Brooks Range and is composed of a number of separate or overlapping deep-sea fan complexes, each of limited lateral extent. Thick conglomerate units that are common along the southern outcrop belt are mostly of a submarine canyon or inner fan-channel facies. These grade rapidly northward to finer grained turbidite deposits of an outer-fan and basin-plain facies. The outcropping sandstones are poorly sorted graywackes. This lithology, considered together with the expectation of finer grained distal facies basinward, suggests that the Fortress Mountain Formation has poor reservoir potential for hydrocarbons in the subsurface to the north.

Possible hydrocarbon reservoirs in northeastern Alaska

The stratigraphy and depositional history of Cretaceous and lower Tertiary strata in northeastern Alaska was revised by C. M. Molenaar, A. C. Huffman, and A. R. Kirk on the basis of recent fieldwork. The Cretaceous sequence, possibly as thin as 700 m, consists largely of deep-water shale with interbeds of turbiditic sandstone in the Ignek Valley area of the William O. Douglas Arctic Wildlife Range. This area may be a continuation of the Barrow arch. Erosional unconformities are absent within the Cretaceous sequence, and lower Tertiary shales and turbidite deposits overlie it with probable conformity. Paleocurrent direction features observed in exposures of Cretaceous and lower Tertiary turbidite deposits in the area around the Sadlerochit Mountains indicate average current directions to the east-northeast. The turbidite deposits probably were derived from deltas to the west or southwest. The thicker turbidite beds could be hydrocarbon reservoirs in the subsurface to the north.

Hydrocarbon resource estimates for William O. Douglas Arctic Wildlife Range

Assessment of the petroleum potential of the William O. Douglas Arctic Wildlife Range in northeastern Alaska was completed in June 1980. This assessment, using the play-analysis method, was performed at the request of a congressional subcommittee. Nineteen geologists, many of whom participated in the NPRA assessment, appraised the petroleum geology of the Wildlife Range. Their collective estimates of the necessary geologic parameters were fed into Department of the Interior computers. The resulting computer estimates of undiscovered in-place hydrocarbons were average oil, 4.85 billion bbl; and average gas, 11.9 trillion ft^3. Surprisingly, these estimates are nearly the same as those for the NPRA even though the prospective area of the Wildlife Range is only one-tenth that of the NPRA. Most of the petroleum potential in the Wildlife Range is believed to occur in Tertiary rocks, which are not present in most of the NPRA.

Petroleum geology of Alaska Outer Continental Shelf

The Lower Cook Inlet COST No. 1 well is located 70 km southwest of Homer, Alaska, in the Alaska Outer Continental Shelf (OCS) block 489. The well was drilled in 65 m of water to a total depth of 3,776 m to obtain stratigraphic information before lease sale No. CI was held October 27, 1977. Atlantic Richfield Company was the operator for 18 other petroleum companies. Many types of geological, geophysical, and geochemical data were collected. Stratigraphic units penetrated in the COST No. 1 well are the Upper Jurassic Naknek Formation (1,663 m thick), the Lower Cretaceous Herendeen Limestone (572 m thick), the Upper Cretaceous Kaguyak Formation (743 m thick), and the uppermost Paleocene West Foreland Formation (384 m thick). The lithology includes sandstone, siltstone, slate, conglomerate, and coal. Calcareous *Inoceramus* fragments are a major constituent of sandstone in the Herendeen Limestone. The ages of the units are based on detailed analysis of microfossil assemblages utilizing foraminifers, marine and terrestial palynomorphs, calcareous nannoplankton, and radiolarians. The depth or top of each rock unit was judged from wireline well-logging information, lithologic descriptions, and paleontology. The Upper Cretaceous and lower Cenozoic sandstones have the highest potential as petroleum reservoirs. The Upper Jurassic sandstones are cemented with laumontite; and the Lower Cretaceous sandstones are depositionally immature and cemented with calcite, and hence of much lower potential. Content, type, and thermal maturity of organic matter in the sedimentary rocks penetrated in the well are below average in hydrocarbon richness and have poor oil-generating capacity; the Upper Jurassic rocks are marginally mature to mature. From wireline well-logging information the present geothermal gradient is 2.28°C/100 m and too low to mature shales at the bottom of the COST well. Rock units penetrated are not at their historical maximum burial depth or maximum temperature, as indicated by thermal alteration index (TAI), "fossil" laumontite, and the presence of lower Cenozoic strata at a shallow depth. The velocity profile in the COST well was compared to the velocity information derived from the multichanneled seismic data. Of three seismic horizons (A–C) that were mapped on seismic line 752, two horizons were penetrated—one near the base of Cenozoic rocks (A) and the other near the top of Jurassic rocks (C). The third horizon (B) is near the top of Middle Jurassic rocks.

OVERTHRUST BELT

Conodonts and corals in petroleum exploration in western North America

Two fossils of greatly different biologic affinity but of similar ecologic habitat were used by C. A. Sandberg and W. J. Sando to delineate the Mississippian (late Osagean to early Meramecian) shelf margin in western North America. Delineation of this shelf margin is an aid to petroleum exploration, because major facies changes in proximity to it may have produced significant stratigraphic traps within the Overthrust belt of the United States and Canada. The two fossils are the coral genus *Ankhelasma* and the conodont genus *Eotaphrus*, both of which are interpreted to have lived mainly, if not only, on the outer edge of the carbonate platform and adjacent upper foreslope in this formerly tropical region of western North America. *Ankhelasma* has been recognized at three localities in British Columbia; two in Montana; one in Idaho; one in Wyoming; three in Utah; and two in Nevada. *Eotaphrus* occurs mainly below *Ankhelasma* but ranges upward to occur with it at some localities, such as the Arrow Canyon Range, Nev. This conodont has been recognized at more than 20 localities evenly distributed between Arizona and Alaska.

Petroleum potential of Overthrust belt in southwestern Montana

The petroleum potential of a segment of the southwestern Montana Overthrust belt, between Clark Canyon Reservoir and Monida Pass, has been studied by W. J. Perry. This area, 55 km from north to south and 75 km wide, has undergone a relatively mild thermal history despite its position between volcanic rocks of the Snake River Plain to the south and intrusive rocks of the Pioneer batholith to the north. Thermal indexes include conodont color alteration index (CAI) values, organic geochemistry, and vitrinite reflectance. The area comprises, from west to east, (1) the Medicine Lodge thrust sheet, (2) the Tendoy thrust sheet, (3) sub-Tendoy imbricate fault slices associated with a major blind thrust beneath the Lima anticline, and (4) the Blacktail-Snowcrest uplift of Laramide age. The Paleozoic sequence on the Tendoy thrust sheet is similar to that of the Blacktail-Snowcrest uplift, but it is significantly thicker. The geometry of the Cretaceous erosion surface atop the Tendoy thrust sheet indicates that the Tendoy allochthon originated from the southwest-plunging nose of the Blacktail-Snowcrest uplift following initial

development of this basement uplift. Aeromagnetic data support this interpretation. This geometry, the sub-Tendoy imbrication, and the mild thermal history of the area strongly suggest the presence of undiscovered petroleum resources.

Possible Mississippian stratigraphic traps in Idaho

The importance of a recently studied Mississippian sequence at North Georgetown Canyon, in the Aspen Range, Idaho, to petroleum exploration of the Overthrust belt in the western United States has been recognized by W. J. Sando, C. A. Sandberg, and R. C. Gutschick. This sequence, which represents a previously unknown facies belt, includes the westernmost occurrence of the Mission Canyon Limestone. The Mission Canyon or its equivalents contain proven gas and condensate reservoirs in the adjacent western Wyoming part of the Overthrust belt. Westward thinning of the Mission Canyon Limestone from Wyoming into the Aspen Range and its absence farther west in Idaho suggests a westward pinchout that may provide stratigraphic traps for petroleum beneath a seal formed by the basal, phosphatic unit of the overlying "Aspen Range" sequence. Excellent porosity and permeability for reservoirs could be provided by dolomitization of Mission Canyon beds similar to that in the Brazer Dolomite in Utah along the Mississippian shelf margin from the Crawford Mountains south to the Wasatch Mountains.

GREAT PLAINS

Origin of biogenic gas in Upper Cretaceous Gammon Shale

In the Northern Great Plains, isotopically light methane is entrapped at shallow depths in marine rocks of Late Cretaceous age. According to D. L. Gautier, products of early diagenetic decomposition of organic matter in the Gammon Shale support the interpretation that the gas is biogenic and formed at shallow depths early in the burial history of the sediments. This interpretation implies widespread gas occurrence and is consistent with large estimates of gas resources. The Gammon Shale was deposited offshore during a major regression of the epeiric sea. The sediment-water interface was oxygenated, and soft-bodied organisms burrowed the silt-clay sediments. Organic matter was sufficiently abundant for oxygen depletion and bacterial sulfate reduction to occur quickly at shallow depths. This resulted in formation of framboids and octahedrons of pyrite. Abundant concretions and discrete crystals of siderite began forming within tens of meters of the sediment surface. Interstitial waters became saturated with methane; and a free-gas phase, held in siltstone layers by capillary forces, inhibited silicate diagenesis. Methane generation probably continued to burial depths of hundreds of meters. At the maximum burial depth (1,200–1,500 m), interstitial waters contained their maximum dissolved methane, and silt layers still contained free gas. Cenozoic uplift and erosion permitted gas exsolution. Exsolved gas combined with free methane already in the reservoirs to form the gas that is currently being explored and produced.

Distribution of chalk reservoirs in Upper Cretaceous Niobrara Formation

The Niobrara Formation of Late Cretaceous age in the Northern Great Plains includes potential low-permeability reservoirs for natural gas. Subsurface investigations by J. L. Sieverding (USGS) and G. W. Shurr (St. Cloud State University) indicated that three major tongues of chalk are found within the Niobrara. In North Dakota and South Dakota, these tongues grade westward into noncalcareous shale of the Pierre Shale. This facies change contrasts with that in Nebraska where the chalk tongues thicken and grade into calcareous shale within the Niobrara. The lowest tongue of chalk is confined to Nebraska and southern South Dakota, whereas the middle and upper tongues are found throughout Nebraska, North Dakota, and South Dakota. Of the three, the middle tongue is the most widespread and continuous. The interval from the base of the Ardmore Bentonite Beds of the Sharon Springs Member of the Pierre Shale to the base of the Niobrara was mapped throughout the Northern Great Plains. The isopach map shows an oblate area of thin sediments extending from northeast to southwest through southern South Dakota and northern Nebraska. A map of net chalk thickness within the Niobrara reveals thin chalk in the oblate area of thin sediments; however, the thickest chalks are found on the flanks of this feature. The northeast-trending oblate area is interpreted to be a paleotectonic feature that influenced the dispersal of clastic rocks and the accumulation of chalk. Occurrences of natural gas within the Niobrara probably are controlled by the distribution and thickness of chalk and by the depth of burial.

Indigenous biogenic gas in Niobrara Formation, eastern Denver basin

Natural gas is produced from chalk beds of the Upper Cretaceous Niobrara Formation in eastern Colorado and northwestern Kansas. The chalk is fine-grained biogenic limestone, consisting mainly of nannofossils and microfossils, that is characterized by high porosity (30 to 45 percent) and low permeability (about 1 mD). The depth of the gas-productive trend enriched in the

light carbon isotope (C^{12}) increases to the northwest from 270 m to 850 m. The gases are methane-rich ($C_1/C_{1-5}>0.98$), are isotopically light (C^{13} values range from −65 to −55 permil), and become isotopically heavier with increasing depth. The shallow gas in the Niobrara Formation is interpreted by D. D. Rice to be of biogenic origin because of its chemical and isotopic composition, reconstructed maximum depths of burial, and immaturity with respect to thermogenic hydrocarbon formation. The biogenic gas was generated early in the burial history of the chalks by microbial degradation of organic matter in an anaerobic, sulfate-free environment. In situ gas generation is indicated, because low permeability inhibited migration and because organic-rich laminae provided an adequate source for the gas. Organic-carbon values within the chalk sequence average 3.12 percent, and the organic matter consists of hydrogen-rich sapropelic material typical of an open-marine environment. The chalks are overlain by a thick sequence of shale, containing many bentonite beds, in the lower part, which served as a seal for gas after the reservoirs were naturally fractured later in the burial history.

Reservoir properties of Niobrara Formation, Denver basin

The composition and X-ray mineralogy of acid-insoluble residues from chalk and associated rocks in the Niobrara Formation have provided useful information concerning the diagenesis and reservoir properties of these rocks. Approximately 200 samples from five wells within the Denver basin were analyzed by R. M. Pollastro for acid-insoluble residue content and for whole-residue and clay mineralogy. The amount and mineralogy of acid-insoluble residue were found to directly influence geophysical-log response and thus to give an indication of the reservoir properties of the rocks. As in the Pierre Shale, volcanic ash fall was a significant contributor to noncarbonate sediment within the Niobrara. Authigenic noncarbonate minerals in the chalk include pyrite, kaolinite, and highly expansible clay minerals. Most of the authigenic kaolinite was formed by alteration of volcanic detritus within chemical microenvironments created by organic decay. Therefore, microenvironments greatly different from the gross overall environment that formed the chalk can be created within the sediment early in its burial history. Evidence also was found to indicate that clay-mineral transformations correspond to changes in the alteration levels of organic material within the chalk. This study developed several reliable analytical procedures and standards that may be used in similar future studies.

Transgressions and regressions of Cretaceous epeiric sea in Colorado, North Dakota, South Dakota, and Wyoming

Transgressions and regressions of the epeiric sea during early Late Cretaceous (Cenomanian, Turonian, and Coniacian) time were investigated by E. A. Merewether and W. A. Cobban at outcrops in southwestern and northeastern Wyoming, south-central Colorado, eastern South Dakota, and northeastern North Dakota. At these localities, the lower Upper Cretaceous strata consist mainly of shale, siltstone, sandstone, and limestone and were deposited in nonmarine, nearshore-marine, and offshore-marine environments. Molluscan fossils in the marine rocks were used to correlate the outcrop sections. Potassium-argon ages were determined from bentonite beds in the formations (Obradovich and Cobban, 1975). The studied rocks in southwestern Wyoming are assigned to the Frontier Formation and the lower part of the overlying Hilliard Shale. In northeastern Wyoming, strata of the same age are assigned to the Belle Fourche Shale, Greenhorne Limestone, and Carlile Shale, in ascending order. The studied rocks in Colorado consist of the Graneros Shale, Greenhorn Limestone, Carlile Shale, and the lower part of the Niobrara Formation, in ascending order. In South Dakota, they are assigned to the Dakota Sandstone and the overlying Graneros, Greenhorn, Carlile, and Niobrara. The sequence in North Dakota consists of the Belle Fourche, Greenhorn, Carlile, and basal part of the Niobrara. The succession of depositional environments in the lower part of each sequence suggests a continent-wide marine transgression, which continued for about 5 m.y. during Cenomanian and early Turonian time. Depositional environments of the overlying strata indicate that the sea regressed for 0.5 m.y. to 1.0 m.y. during the middle Turonian and, thereafter, transgressed for 1.5 m.y. to 2.0 m.y. in the late Turonian and Coniacian.

Seismic detection of "First Leo" sandstone reservoirs, Powder River basin, Wyoming

The "First Leo" sandstone (an economic subsurface term) is a locally thick sandstone within the middle member (Pennsylvanian) of the Minnelusa Formation in the southern Powder River basin, Wyo. Locally it is very porous, as thick as 18 m, and contains stratigraphically trapped oil. A geologic model of a typical "First Leo" sandstone reservoir and adjacent trap was generated by A. H. Balch, M. W. Lee, J. J. Miller, and R. T. Ryder to determine whether the unit could be detected by seismic exploration methods. One- and two-dimensional

synthetic seismograms suggested that the reservoir unit could be differentiated from the trap facies under the many simplifying assumptions required in the model study. A detailed study of the actual seismic-reflecting properties of the Minnelusa Formation was then made using vertical seismic profiles obtained from an oil well in the Red Bird field, which produces from the 16-m-thick "First Leo" sandstone and from a nearby water well in which the "First Leo" sandstone is very thin or absent. This study corroborated the conclusions obtained from the model study. Finally, a surface seismic profile was run along the east flank of the Old Woman anticline between the wells. The surface profile further supported the hypothesis that a consistent amplitude anomaly accompanies the thick "First Leo" sandstone in the Old Woman anticline area. The near-perfect tie between the well-log data and surface data provided by the vertical seismic profile demonstrates that the thick "First Leo" sandstone is responsible for the observed anomaly.

UTAH

Migration of oil suggested in some Uinta basin oilfields

Evolution of crude oils in the Uinta basin, Utah, follows expected maturation patterns: immature oils are heavy and rich in nitrogen, sulfur, and oxygen; whereas, mature oils are lighter and rich in paraffin. However, preliminary sulfur and carbon isotope analyses and hydrocarbon compositional data gathered by D. E. Anders suggest that some shallow oils, which would be expected to be heavy, have migrated upward from deeper, more mature oil pools. In the Altamont spaced area near the Cedar Rim oilfield, oils being produced between depths of 2,632 m to 2,821 m are probably migrating up from deeper Altamont-Bluebell oils produced at depths of 3,773 m to 4,455 m. Likewise, in the Monument Butte field, shallow oil being produced at a depth of 1,530 m is similar in composition to Altamont-Bluebell oil, produced at depths of 2,753 m to 3,677 m, suggesting possible migration from deeper Altamont-Bluebell pools. The shallow, immature oils produced on the west side of the Altamont spaced area from a depth of 1,433 m in the Black Tail Ridge field are so chemically different from the Altamont-Bluebell oils that they are not likely migrated oils from deeper Altamont-Bluebell pools. In the Bluebell field on the east side of the spaced area, oils at depths of 2,523 m to 2,581 m are dissimilar to deeper oils, suggesting that they are not migrating upward from deeper pools. The Twelve Mile oils produced from smaller fields to the east are distinct in composition. The Horseshoe Bend and Red Wash oils produced from shallower fields even farther east are similar to each other in composition, and this similarity suggests a common source.

Gas exploration on Tavaputs Plateau by location of Cretaceous-Tertiary boundary

The precise position of the boundary between Cretaceous and Tertiary rocks and the time of uplift of the San Rafael structural element have been uncertain in the western Tavaputs Plateau, Utah. Locating the boundary and dating the uplift are important, because natural gas is produced from Upper Cretaceous and Tertiary beds on the Tavaputs Plateau and is locally trapped in anticlines and domes beneath the Cretaceous-Tertiary unconformity. Conglomeratic sandstones that contain Paleocene palynomorphs at Dark Canyon were traced from near the Douglas Creek arch to the area of the San Rafael structural element in the Tavaputs Plateau by T. D. Fouch and W. B. Cashion. Conglomerate unconformably overlies uplifted Upper Cretaceous rocks in the western Book Cliffs. The uplifted area is part of the San Rafael structural element. Conglomerate overlies the oldest Cretaceous rocks at the axis of the uplifted area, and stratigraphic relations indicate the uplift must have occurred between Late Cretaceous (middle Campanian) and middle or late Paleocene time.

Shoaling-upward marine and deltaic sequences identified within Manning Canyon Shale

The Manning Canyon Shale of Mississippian and Pennsylvanian age in the Uinta, Wasatch, Lake, and Oquirrh Mountains of northern Utah comprises parts of two stratigraphic sequences separated by an unconformity. The stratigraphic relations, ages, and succession of the Manning Canyon Shale and Round Valley Limestone in Utah are similar to those of the Big Snowy and Amsden Groups of Montana (Maughan and Roberts, 1967). Formations in both States are considered to contain petroleum source rocks. E. K. Maughan (USGS), J. R. Jennings (Eastern Kentucky University), and W. D. Tidwell (Brigham Young University) found that the lower sequence in northern Utah represents a shoaling-upward marine sequence, in which the rocks grade from dominantly carbonate rocks upward to dominantly carbonaceous mudstone. The lower part of the Manning Canyon bears a Chesterian (Late Mississippian) invertebrate fauna. This sequence thins eastward both depositionally and by truncation beneath the unconformity. Above the unconformity, the upper sequence comprises chiefly mudstone and some sandstone and limestone in deltaic deposits that grade upward to dominantly marine carbonate rocks of the Lower Pennsylvanian Round Valley Limestone.

APPALACHIAN BASIN

Eastern Gas Shales Project (EGSP) Data Systems

The USGS, the Petroleum Information Corporation in Denver, Colo., and the U.S. Department of Energy in Morgantown, W. Va., have created two large data files for the EGSP. All computer-compatible well, outcrop, and sample data generated by EGSP participants from Devonian shales throughout the Appalachian basin are being edited, converted to a database, and accessed to produce digital printouts, charts, and maps. The EGSP Well Data File was developed as an extension of the Petroleum Information Well History Control System (WHCS) and contains geologic, engineering, and production test data for more than 6,000 wells. The EGSP Sample Data File contains geochemical, lithologic, and physical characterization data on more than 50,000 samples from 17 EGSP cored wells and 140 additional wells and outcrops. Well and sample data can be retrieved to produce (1) production test summaries by formation and location; (2) contoured isopach, structure, and trend-surface maps of Devonian shale units; (3) sample summary reports by location, well, contractor, and sample number; (4) cross-sections displaying digitized log traces and geochemical and lithologic data by depth for wells; and (5) frequency distributions and bivariate plots.

EGSP Data System products are being used by EGSP participants to help solve Devonian shale exploration and research problems in the Appalachian basin. Although a portion of the EGSP Well Data file is proprietary and distribution of complete well histories is prohibited by contract, maps and aggregated well data listings can be made available to the public through published reports.

Determination of organic-matter content of Devonian shale

The organic-matter content of Devonian shale of the Appalachian basin is an important parameter for assessing the natural-gas resources of these rocks. Patterns of organic-matter distribution convey information on sedimentary processes and depositional environments. In most of the western part of the Appalachian basin, the organic-matter content of the Devonian shale was estimated by J. W. Schmoker from gamma-ray wireline logs using the equation: $\phi_O=(\gamma_B-\gamma)/1.378A$, where ϕ_O is the organic-matter content of the shale (fractional volume), γ is the gamma-ray intensity (API units), γ_B is the gamma-ray intensity if no organic matter is present (API units), and A is the slope of the crossplot of gamma-ray intensity and formation density (API units/(g/cm^3)). The quantities A and γ_B vary regionally and were mapped using data from gamma-ray and formation-density wireline logs. Organic-matter contents estimated using this equation are compared to direct laboratory analyses for 74 intervals of different thickness and organic-matter content from 12 widely separated wells. Excluding the Cleveland Member of the Ohio Shale and the lower part of the Olentangy Shale, the distribution of the differences between volume-percent organic-matter content measured in core samples and estimated from gamma-ray logs has a mean of 0.44 percent and a standard deviation of 1.98 percent, which indicates that the accuracy of the gamma-ray method is adequate for most geologic applications. The gamma-ray intensity of the Cleveland Member of the Ohio Shale and the lower part of the Olentangy Shale is anomalously low compared to other Devonian shales of similar organic-matter richness, so that organic-matter content computed for each of these units from gamma-ray logs is likely to be too low. Wireline methods for estimating organic-matter content have the advantages of economy, readily available sources of data, and continuous sampling of the vertically heterogenous shale section. The gamma-ray log, in particular, commonly is run in Devonian shale; its response characteristics are well known, and the cumulative pool of gamma-ray logs forms a large and geographically broad data base. The quantitative computation of organic-matter content from gamma-ray logs should be of practical value in studies of Devonian shale in the Appalachian basin.

Geochemical effects of early diagenesis of organic matter in Devonian black shale

The relation between organic carbon and sulfide in Devonian black shale was used by J. S. Leventhal, G. E. Claypool, and M. B. Goldhaber to identify these units as having been deposited in ancient marine euxinic environments. Based on analogy to the modern Black Sea, the euxinic environment is indicated by a positive intercept for sulfur at zero organic carbon on a carbon-sulfur plot. Furthermore, the slope of the plot can be related to position in the basin and to deposition rate. Sulfur-isotope ratios of fine-grained, early diagenetic iron sulfides are typically light, indicating that a majority of the sulfides formed in the water column and near the sediment-water interface. Isolated heavier values are observed, however, which demonstrate that sulfide formation persisted into later diagenesis, at least locally. Carbon and oxygen isotopes of carbonate minerals show the effects of both early diagenesis of organic matter by microbiological processes and later redistribution of carbonate into veins and nodules. A range of values suggests that anaerobic oxidation of organic matter is more important than methane generation for carbonate diagenesis. Trace-element

abundances (U, Mo, V, Ni, Hg) are related to organic-carbon and sulfide-sulfur content. These relations can be explained by invoking an organic-concentration mechanism and aqueous-sulfide protection and redistribution processes. Trace-element to organics and trace-element to sulfide ratios do not change greatly in the basin, although deposition rates vary by more than an order of magnitude.

Hydrocarbon potential of southern Appalachians delimited

Seismic data in the southern Appalachian Mountains suggested to L. D. Harris that the basement beneath the Valley and Ridge and Blue Ridge Provinces and across the Inner Piedmont Province forms a broad shelf that changes eastward into a deep basin. Palinspastic reconstructions of a Proterozoic to Early Ordovician depositional model from rocks exposed at the surface of the Valley and Ridge, Blue Ridge, and Piedmont Provinces confirm the seismic model by showing that shallow-water clastic and carbonate rocks are confined to the shelf; whereas, deep-water clastic and volcaniclastic rocks, now metamorphosed, accumulated in the deep eastern basin. Allegheny thrusting moved the metamorphosed deep-water rocks westward up the basin slope and onto the ancient shelf, burying a large section of shallow-water sedimentary rocks. Structural interpretations suggest that the burial of sedimentary rocks by metamorphic rocks of the Piedmont Province began just east of the Brevard fault zone. As a result, it seems likely that thick sequences of sedimentary rocks with reasonable organic maturation levels may not occur in the subsurface east of the Brevard fault zone. Consequently, the hydrocarbon potential for this province may be restricted to the Blue Ridge area west of the Brevard fault zone.

OTHER STATES

Source-rock potential, South Florida basin

In assessing the source-rock potential of carbonate rocks in the South Florida basin, J. G. Palacas, J. P. Baysinger, C. M. Lubeck, and D. E. Anders found that geochemical parameters appear to be viable indicators of thermal maturation. With reference to bulk geochemical parameters, such as the ratios of extractable hydrocarbons to total organic carbon (TOC), hydrocarbons to extractable bitumen, and saturated to aromatic hydrocarbons, all ratios increase significantly with depth of burial. For example, the relation of hydrocarbons to extractable bitumen, expressed in percent, varies from 25 percent in Paleocene rocks at a depth of 1,500 m to about 75 percent in Lower Cretaceous (Coahuilan) rocks at a depth of 4,500 m. Although changes in geochemical parameters with depth of burial generally reflect increasing degrees of thermal maturation, they may at different stratigraphic levels also reflect distinct differences in organic matter types and lithology. This is particularly evident when comparing bitumen to TOC ratios. Contrary to expectations, some of the highest ratios are found in the younger, more immature rocks. On the molecular level, gas chromatographic analyses of saturated hydrocarbon distributions also are striking maturation indicators. Chromatograms of hydrocarbons from the shallow Paleocene rocks are characterized by a major hump of unresolved naphthenes, maximized at the normal paraffin n-C_{22} region, a narrow range of n-C_{15+} paraffins, and an absence or scarcity of hydrocarbons below n-C_{15}. On the other hand, the hydrocarbon distributions of the deeper and older rocks, such as the Lower Cretaceous Sunniland Limestone, show just the opposite: no hump at the n-C_{22} region, a wide range of n-C_{15+} paraffins, and an abundance of saturated hydrocarbons below n-C_{15}, including gasoline-range hydrocarbons.

Natural gas in sandstone reservoirs, west-central Arkansas

North-south thickness trends in each of five sandstone reservoirs were recognized by B. R. Haley in an area extending 274 km from east to west and 48 km from north to south in the lower part of the Pennsylvanian Atoka Formation in west-central Arkansas. The alignment of these trends agrees with a concept of thicker reservoir areas representing southward-prograding deltaic deposits and thinner reservoir areas representing nearshore marine deposits between the deltas. Wells produce gas from both types of deposits in each of the five reservoirs, but in four of the five, most of the wells produce gas from the uppermost part of the deltaic deposits. In these wells the gas is from sandstone thought to have been deposited in the nearshore marine part of the delta.

Petroleum potential of northeastern Santa Ynez Mountains, California

Reconnaissance mapping by T. H. McCulloh suggested that Paleogene strata north of the Santa Ynez fault and east of State Highway 399 in the northeastern Santa Ynez Mountains, west of Los Angeles, Calif., hold an appreciable potential for petroleum resources. Unlike equivalent strata farther west and unlike those south of the Santa Ynez fault, these rocks do not contain diagenetic laumontite and therefore have not suffered the reservoir destroying or damaging influence of the deep burial conditions implied by that mineral. Indications of mobile hydrocarbons were recorded during

drilling of three of the only four wells that constitute meaningful tests in the region. Additionally, the high temperature (89°C) of the water issuing from Sespe Hot Springs implies a deep, hot source for this connate brine, sufficient for maturity of any source rocks of petroleum.

RESOURCE STUDIES

New estimate of United States oil and natural gas resources

A USGS report (Dolton and others, 1981) set mean estimates for undiscovered recoverable conventional petroleum resources in the United States at 594 trillion ft^3 of gas and 83 billion bbl of oil. These estimates compare with mean estimates made in an earlier USGS study (Miller and others, 1975) of 484 trillion ft^3 of gas and 82 billion bbl of oil. The new study was conducted by a team of USGS specialists in the Resource Appraisal Group working under the direction of G. L. Dolton. More than 80 other specialists throughout the USGS contributed their expertise. The new estimates incorporate geologic and geophysical information compiled since completion of the 1975 study and include assessments for each of 137 petroleum provinces in the country.

New geologic and geophysical information resulted in an increase in the estimates of petroleum potential for some provinces and a reduction in other provinces. For example, drilling in the Overthrust belt of the Western United States revealed a larger potential for both oil and gas than had been projected in the 1975 estimates. This was also true for potential in the offshore North Slope of Alaska on the Beaufort Sea Shelf. On the other hand, results of exploratory drilling in the Gulf of Alaska, the offshore southern California Borderland, and the eastern Gulf of Mexico have been disappointing to date; and geologic information obtained from these provinces indicated a reduced petroleum potential compared to that of the 1975 study. Significant resource potential is projected for areas in the deeper waters offshore for the Atlantic Coast and the deeper Gulf of Mexico.

Part of the increase in natural gas estimates represents increased optimism for prospects in several of the frontier areas. Some of the increase, however, simply reflects an increase in the amount of offshore area assessed in the latest study. In the 1975 study, the offshore areas were assessed out to 200 m water depth. The 1981 study included offshore provinces on the U.S. continental slopes seaward to 2,500 m water depth off the conterminous United States and to 2,400 m off Alaska, thereby increasing the offshore areas assessed for the 1981 study by an additional 1,036,000 km^2. The deeper water areas were included in the new assessment, because current offshore technology has made these areas more accessible to possible development.

The new undiscovered recoverable conventional oil and gas resource estimates were provided at the 95 and 5 percent probability levels and were estimated to range from 64 billion bbl on the low side to 105 billion bbl of oil on the high side—that is, the probability of more than 64 billion bbl is 95 percent, and the probability of more than 105 billion bbl is 5 percent. These estimates compare to the 1975 estimates of 50 to 127 billion bbl of oil. The new undiscovered recoverable conventional gas resource estimates at the 95 and 5 percent probability levels range from 475 trillion ft^3 to 739 trillion ft^3. These estimates compare to the 1975 estimates of 322 to 655 trillion ft^3 of gas.

Sulfur in the world's petroleum reserve

Sulfur recovered from petroleum during its refining now provides more than 5 million t a year to the world's supply, but estimates of tonnage of sulfur in the world's petroleum reserve have been largely conjectural. A recent compilation of the sulfur content and petroleum reserves of each of the world's oil fields by Riva (1980) provides the data needed to establish the tonnage of contained sulfur. A. J. Bodenlos calculated that such sulfur totals 1.4 billion t, of which 1 billion t occur in the oil reserves of the Middle East. About 120 million t occur in the oil reserves of the U.S.S.R., and a similar amount occurs in the oil reserves of Mexico. The balance is divided among the reserves of all other producing nations, including 26 million t of sulfur in the petroleum reserves of the United States. Only a fraction of this large tonnage, perhaps from 20 to 25 percent, can be considered to be a resource, because much sulfur in crude oil is contained in unrefinable asphalt and tars, and because not all recoverable sulfur is extracted in the world's existing petroleum refineries. Potentially recoverable sulfur in the world's petroleum reserve, therefore, consists of a resource of about 300 million t.

NEW EXPLORATION AND PRODUCTION TECHNIQUES

Understanding of hydrocarbon generation and migration by experimentally produced rocks

Continuation of experimental compaction and hydrocarbon-generation experiments in modern lime muds by E. A. Shinn revealed that randomly oriented needlelike fabric prevents compaction to muds with porosities less than 35 percent even when subject to simulated overburden pressures of 3,000 m or more. However, even though porosities remain in the 35 to 45

percent range, sediment thickness is reduced to less than one-half the original thickness, and the resulting "rock" greatly resembles many ancient limestones. Pellets and birdseye structures are mashed, color mottling is produced, fossils are reoriented toward the horizontal (although not broken), and organic seams resembling stylolites are formed. In thin section, such experimentally produced "rocks" resemble well-known source rocks; they contain 2 to 3 percent total organic matter and are in the range of true source rocks. However, because these "rocks" reach minimum porosities within a few days under as little overburden as 300 m, mechanical compaction itself cannot be considered sufficient to force out hydrocarbons. Mechanical compaction alone probably is insufficient to expel hydrocarbons; sufficient heat to crack organic rocks thermally in nature probably is not reached at burial depths less than 3,000 to 4,000 m. To force cooked hydrocarbons from such rocks, therefore, requires "chemical compaction." In other words, the aragonite needles that compose the sediment must be dissolved and the carbonate reprecipitated as closely fitted blocky calcite. This process, in combination with thermal maturation, might be sufficient to expel and cause migration of hydrocarbons.

Importance of high-temperature solubility of crude oil in methane to petroleum generation and maturation

Data gathered by L. C. Price on crude oil solubility in a methane gas phase showed that at temperatures of 100°C and greater and pressures of 7,000 psi and greater, methane has a high carrying capacity for all components of crude oil. These data have strong implications for theories of primary petroleum migration and for the economic feasibility of geopressured geothermal resources. Extensive organic geochemical data of deep, hot well bores are in sharp disagreement with accepted theories of petroleum genesis and maturation. This disagreement suggests that these theories may be in error.

Knowledge of carbon cycle and stable carbon isotopes contributes to source-rock studies

Construction of models for the interaction of the carbon cycle with changes in global climate and sea level and analysis of new isotopic and organic-carbon data, by M. A. Arthur, confirmed that the carbon isotopic values of Cretaceous and Tertiary basinal limestones are related mainly to variations in isotopic composition of the world's oceans. The composition of the oceanic isotopic reservoir, in turn, is a function of the relative ratio of storage in organic carbon versus inorganic carbon reservoirs. Thus, carbon isotopic ratios in pelagic limestones can reflect regional variations in organic-carbon storage; this is one indicator of the source-rock potential of sediments. In rocks that have large organic-carbon to carbonate-carbon ratios, however, diagenetic alteration of the original isotopic composition may have occurred. Therefore, the best analyses come from pelagic carbonate sediments in parts of the basin with minimal organic-carbon preservation. The amount and rate of storage of organic carbon in marine sediments is a complex function of the interaction of global climate, relative sea level, sediment supply, global oceanic fertility, and continental position. However, prediction of the hydrocarbon source-rock potential of upper Mesozoic and Cenozoic strata for a given region reasonably can be made based on knowledge of these parameters. Lower to lower Upper Cretaceous, lower to middle Eocene, and middle to upper Miocene marine strata over much of the world's continental margins probably provide the best overall hydrocarbon source-rock potential.

Confirmation of soil-gas helium surveys as an exploration tool

Previous investigations showed that microseepage from oil and gas reservoirs produces surface indications. One of the observed indicators is the presence of helium in the soil gas overlying reservoirs. In order to further assess the utility of surveying the soil-gas helium concentrations for petroleum exploration, two additional surveys were run by A. A. Roberts and T. J. Donovan.

A regional survey was run in the area surrounding the Velma oilfield in Oklahoma. More than 80 percent of the eastern half of the survey area is underlain by oil or gas reservoirs. A vast majority of the soil-gas samples collected in this half had anomalously high concentrations of helium. In contrast, in the western half of the survey area, where very little oil or gas has been found, almost all samples contained only background concentrations.

Another survey was run over part of the National Petroleum Reserve in Alaska (NPRA). The helium content of more than 700 samples of permafrost collected at 0.75 m depth was measured. A linear pattern of high helium values, about 4 km wide, was observed about 50 km south-southwest of the city of Barrow. This area lies above and parallel to a zone interpreted as a truncation by an intra-Jurassic unconformity of the "Kugrua" sand (a potential reservoir rock in the Jurassic Kingak Shale). The high helium values in the permafrost may reflect microseepage of gas from a stratigraphic trap at this unconformity.

Reservoir properties of submarine-fan sandstones

Petrographic and scanning electron microscope studies of modern submarine-fan sandstones indicated to Hugh McLean and L. F. Krystinik that cementation of

porous and permeable sand can become advanced at burial depths of only a few tens of meters. Calcium carbonate and zeolites are the main cementing agents. Further work is needed from deeper core samples to determine whether precipitation of authigenic cements continues unabated or secondary porosity develops with increasing depth. Reservoir properties in ancient submarine fans are influenced strongly by overall sand to shale ratios. Sand bodies in the inner and middle parts of fan systems, where shale percentage is low, apparently remain porous and permeable to greater depths of burial than sand subjected to abundant dewatering of shale interbeds. However, even sand-rich sequences lose porosity and permeability by mechanical compaction if burial depth and time are sufficient. Early formation and migration of hydrocarbons is critical to preservation of porosity and permeability, especially in tectonically active basins of western California.

Terrain effects of cultural features on shallow borehole gravity data

Borehole gravity surveys of oil and gas reservoirs usually are run at depths of thousands of meters, and such surveys are not likely to be significantly affected by the ordinary works of man. However, borehole gravity surveys for engineering applications and for evaluation of mineral deposits and aquifers may have maximum depths of only a few hundred meters. Therefore, these shallow surveys are more likely to be affected by the gravity fields of manmade surface features, such as basement excavations, quarries, gravel pits, sewage plants, road fills and cuts, storage piles, mine dumps, and tank farms. It is difficult to estimate the terrain effect of cultural features as a function of depth in order to determine the need for terrain corrections. It is also time consuming to compute precise terrain corrections for a cultural feature, because accurate dimensions of the feature often are difficult to obtain, and because its shape may not be well suited to the zones and compartments of conventional terrain-correction schemes. A simple chart was developed by J. W. Schmoker for estimating the significance of the terrain effect of cultural features upon densities computed from borehole gravity data. By signaling the need for data corrections, it can help the user maximize survey accuracy while avoiding unneccessary computations. The chart provides a qualitative estimate of the depth at which the terrain effect of a manmade feature is no longer significant. It is based on a spherical mass anomaly, which can be defined by a minimum of geometric parameters and is best suited to approximately equidimensional cultural features. The chart shows depths below the center of a sphere of a given mass and horizontal distance from the wellbore at which the absolute value of the terrain effect of the sphere upon borehole-gravity density is 0.005 g/cm^3. A terrain effect of this magnitude or greater assumes importance with respect to other experimental errors.

OIL SHALE RESOURCES

Geochemical surveys of oil shale in the Piceance Creek basin, Colorado

Geochemical and mineral analyses of oil shale in a core of the Parachute Creek and Garden Gulch Members of the Green River Formation in the Piceance Creek basin, Colo., were completed by W. E. Dean and J. K. Pitman. Minerals that show the greatest variability within the core are quartz, illite, analcime, and the saline minerals dawsonite and nahcolite. The amounts of Al, Fe, Ti, S, B, Ba, Mo, Pb, Sc, V, and Yb are higher in the clay-rich Garden Gulch Member than in the carbonate-rich Parachute Creek Member, presumably because of concentration in the clay minerals.

Element baselines for the Piceance Creek basin, Colorado

Baselines for 36 major, minor, and trace elements plus pH in soils, 16 elements in DPTA (diehtylene triaminepentacetic acid) soil extracts, and 5 elements in sagebrush and western wheatgrass were established from a regional geochemical survey of these materials in the Piceance Creek basin by Michele Tuttle. The relations among elements in plants, soils, and soil extracts showed that an increase in soil pH generally results in an elevated content of molybdenum, fluorine, copper, and zinc in plants. Activities of zinc and copper generally decrease with increasing pH, which is the opposite of what would be expected and may be the result of interaction between soil carbonate minerals and the plant's root environment. Samples of soils and western wheatgrass were collected from Colorado State University's revegetation plots near Anvil Points, Colo. The plots consist of lysimeters containing spent (burned) oil shale covered with local top soil in amounts varying between 0 and 80 cm. Of the elements fluorine, molybdenum, copper, zinc, only fluorine in soils, copper in soil extracts, and molybdenum and zinc in western wheatgrass showed significant variations between the different top-soil treatments.

Geology and oil shale resources in the Central Roan Plateau, Colorado

Geologic mapping by W. J. Hail in the Circle Dot Gulch quadrangle, Piceance Creek basin, Colo., showed a southward stratigraphic rise, by means of intertonguing, of the contact between the Parachute Creek Member of the Green River Formation and the Uinta

Formation. Within the Circle Dot Gulch quadrangle, three tongues of the Green River Formation merge with the main body of the Parachute Creek Member. These are Coughs Creek Tongue, the Stewart Gulch Tongue, and the marlstone tongue at Jackrabbit Ridge. Oil-shale values increase from north to south in all of these tongues as they approach their junction with the Parachute Creek Member.

NUCLEAR-FUEL RESOURCES

USGS nuclear-fuel studies continued in FY 1980 with the primary objective of achieving the deepest and broadest understanding of the habitats of uranium and thorium and the processes that form deposits in various specific geologic environments in the United States and the world. Known deposits occur in a variety of rock types within sedimentary, igneous, and metamorphic geologic settings. The programmatic approach to the understanding of habitat involves geologic, geochemical, and geophysical studies within known uranium and thorium districts. In addition to habitat studies, the uranium-thorium program involves the development of guides to uranium and thorium exploration, methods of determining uranium and thorium favorability, and resoure estimation using approaches based on geologic-genetic models and data from habitat studies.

Uranium ore-forming processes in the Colorado Plateau

In 1979, H. C. Granger and C. G. Warren presented the framework of a new concept regarding the geochemistry and genesis of vanadium-uranium deposits on the Colorado Plateau. As a part of this process, aluminum-humate complexes in the ground water were said to be destroyed preliminary to vanadium-clay authigenesis, but no mechanism for such destruction was cited. Since that time, it has become evident to Granger and Warren that the most feasible way to destroy the aluminum-humate is by ion exchange with magnesium. Calculations suggest that the required magnesium concentration is quite pH dependent; and, at intermediate pH's, the required magnesium concentration is greater than that generally found in fresh ground waters. This finding may have significant implications regarding the ore-forming environment, because it strongly suggests that one of the reacting solutions was brinelike, perhaps a bittern or evaporite rest fluid. If so, this strengthens previous suggestions regarding the genetic association between evaporites and many uranium deposits both on the Colorado Plateau and elsewhere in the world.

Thorium and rare-earth deposits in the southern Bear Lodge Mountains, Wyoming

Thorium and rare earths occur in large disseminated deposits in the southern Bear Lodge Mountains of northeastern Wyoming. These deposits, according to M. H. Staatz, consist of trachyte and phonolite cut by numerous small crisscrossing veins and are similar in form to copper porphyries. The mineralized trachyte and phonolite make up part of the core of Bear Lodge dome. The most favorable part of the area was outlined by a radiometric survey, and 340 samples were collected over this 10.6 km^2 area. Thorium content of these samples ranged from 9.3 to 990 ppm, and the total rare-earth content ranged from 47 to 27,145 ppm. Contour maps showing the distribution of these elements were constructed. These maps can be used to define the size of the deposit based on whatever cut-off grade may be required. For example, several areas totaling 1.69 km^2 in size are enclosed by the 200 ppm thorium isograd, and several areas totaling 3.22 km^2 in size are enclosed by the 2,000 ppm total rare-earths isoline. Uranium is of little importance in these deposits. The Bear Lodge disseminated deposits have one of the largest resources of both thorium and rare earths in the United States, and although the grade of both commodities is lower than some other deposits, their large size makes them an important future resource.

Origin of uranium-bearing intraformational folds in the Todilto Limestone, northwest New Mexico

The Todilto Limestone of Middle Jurassic age in the Ambrosia Lake uranium mining district of McKinley County, N. Mex., is the host formation for numerous small-to-medium-size uranium deposits that occur in joints, shear zones, and fractures within small- to large-scale intraformational folds in the formation. According to M. W. Green, these folds probably were formed as a result of differential sediment loading, when eolian sand dunes of the overlying Summerville Formation of Middle Jurassic age migrated over soft, chemically precipitated, lime muds of the Todilto shortly after their deposition in a regressive, mixed fresh and saline lacustrine or marginal-marine environment of deposition. Encroachment of Summerville eolian dunes apparently was restricted to relatively narrow beltlike zones trending radially across the Todilto coastline toward the receding Todilto body of water. Intraformational folding is believed to be confined to the pathways of individual eolian dunes or clusters of dunes within the dune belts. During the process of sediment loading by the migrating dunes, layers of Todilto lime mud were differentially compacted, contorted, and dewatered, producing both small- and large-scale plastic deforma-

tion structures including convolute laminations, mounds, rolls, folds, and small anticlines and synclines. During the processes of compaction and dewatering, the mud, in localized areas, reached a point of saturation at which sediment plasticity was lost, causing shearing, fracturing, and jointing of the contorted limestone beds. These areas or zones within the limestone became the preferred sites of uranium mineralization because of the induced transmissivity created by sediment rupture during prolonged sediment loading. Along the Todilto coastline adjacent to the eolian dune belts, both interdune and coastal sabkha environments dominated the Summerville on the margins of the Todilto body of water. Sediment in these areas consists mainly of claystone, siltstone, sandy siltstone, and fine-grained sandstone, which was apparently derived from the winnowing of the finer grained fraction of sediment from adjacent eolian dune fields during eolian activity. Most of the sabkha sediments probably were carried in airborne suspension to the low-lying, ground-water saturated, coastal areas where they were deposited as relatively uniform blanketlike layers. Deposition of sabkha deposits was apparently slow and uniform over most of the Todilto coastal and interdune areas and did not cause the formation of other than small-scale deformation features in underlying Todilto rocks. Large-scale deformational features as well as uranium deposits are notably absent in the Todilto where it is overlain by finer textured sabkha deposits in the Summerville.

Organic geochemistry of uranium in the Grants mineral belt

J. S. Leventhal made additional measurements of organic carbon isotope fractionation that confirm the effect noted earlier in the Grants mineral belt. Samples from Colorado, Wyoming, and Utah showed increases in carbon-13 with increasing ore content (radiation damage). However, carbonate carbon from these areas does not show the unusual light values (from organic matter?) that were observed in samples from Grants. The carbonate oxygen values are very light, relative to normal fresh-water carbonate, which may reflect an exotic origin or diagenesis.

Thorium resource appraisal, Wet Mountains, Colorado

Thorium of potential economic value occurs in several geologic settings in the Wet Mountains area, Colorado, which include quartz-feldspar-barite veins, fracture zones, carbonatites, red syenites, and quartz syenite of the complex at Democrat Creek, according to T. J. Armbrustmacher. All these types of deposits are spacially and genetically related to the Cambrian alkaline complexes of the area. The veins and fracture zones contain the major thorium resources, estimated at about 250,000 t ThO_2. Samples of the veins and fractures average 0.46 percent ThO_2 and range from 0.00075 to 10.2 percent. Uranium is generally present in amounts less than 0.0005 percent U_3O_8, and the average Th/U ratio is 64. Light rare-earth elements (LREE) average 0.18 percent, heavy rare-earth elements (HREE) average 0.12 percent, and the ratio of thorium to total REE is about 2.2. Carbonatites contain thorium resources estimated at about 975 t ThO_2. They average 0.17 percent ThO_2, 0.0031 percent U_3O_8, and 2.15 percent total rare-earth oxides. Additional resources, not yet evaluated, occur in stock-work carbonatite in the Gem Park Complex. Total ThO_2 resources in red syenites are not known, but the rocks average about 0.30 percent ThO_2 and 0.004 percent U_3O_8. Anomalous amounts of lead (0.011 percent), barium (0.33 percent), and rare-earth elements (LREE, 0.078 percent; HREE, 0.077 percent) also occur in these rocks. The quartz syenite of the complex at Democrat Creek may represent a large-tonnage, low-grade, disseminated thorium deposit. Preliminary sampling of the quartz syenite suggests average values near 0.01 percent ThO_2 and 0.0015 percent U_3O_8. The abundance of thorium and the variety of deposits in the Wet Mountains area could make this area one of the most important domestic sources of this element.

Deposition of the uranium-bearing Lance Formation, Niobrara County, Wyoming

Investigation of the Upper Cretaceous Lance Formation along the Cheyenne River, northeastern Niobrara County, Wyo., by H. W. Dodge, Jr., showed a series of lenticular-shaped and vertically stacked sandstone bodies. These sandstones fine upward in grain size and show a decrease in the magnitude of sedimentary structures upwards. Measurements of trough axes or intersections of only large scale cross-strata (large festoons) show a great dispersion, approximately 180° in paleo-current direction. These sandstones are considered to be point-bar deposits, which formed in meandering river systems. Adjacent to the sandstone point-bar deposits are mudstone, silty mudstone, muddy siltstone, and some sandstone. The more sandy deposits are thought to represent proximal crevasse splay, natural levee, and small interfluvial channel paleoenvironments. The finer grained deposits, usually organic rich, represent flood-basin swamps, lakes, and other low-energy environments. The thick flood-basin deposits and thick stacking of point-bar sandstones indicate relatively fixed river systems. Considering previous studies of the Lance Formation southwest of the

Cheyenne River, the regional picture can be extended. This shows a series of relatively fixed parallel river systems meandering across lower portions of a coastal plain.

Geochemical techniques in uranium exploration

Preliminary interpretations were made of correlated abundances of 35 elements in 282 samples of hydrothermal mineral-spring precipitates from 92 localities in the Rocky Mountain and Basin and Range provinces in Colorado, Utah, Arizona, Wyoming, Montana, Idaho, Nevada, California, and Arkansas. The geochemical factors in order of their importance were interpreted by R. A. Cadigan and K. J. Felmlee and are summarized as follows:

- Contamination. Precipitates are contaminated by detrital sand, silt, clay, and rock fragments. Element relative abundances most affected are Cr, V, Cu, Ni, Zr, Al, Ti, Pb, K, Co, Yb, V, Ga, and secondarily Sc, Fe, and Si;
- Dilution. Hot hydrothermal brines from deep sources are diluted in varied proportions by cooler waters from shallow sources, which affects the relative geochemical abundances in precipitates of: Ce, La, Nb, −Si (affected negatively), and secondarily, Co, Li, Zn and W;
- Alkalinity. Increasing alkalinity of mineral spring waters at the surface may affect the geochemical abundances in precipitates of the following: Be, As, Fe, Mn, Mo, W, and Zn;
- Sulfur species. The ratio of carbonate precipitates to sulfate and sulfurous precipitates is negatively affected by the presence of increasing abundances of sulfur species (HS−, S, H_2S) in spring water. The element relative abundances most affected are: S and negatively −Ca, −Mg, and −Sr;
- Barite-radium coprecipitation. Barite is the most common host of radium in mineral spring precipitates. Element relative abundances most affected are Ba, eU (mostly radium), Sc, and secondarily Yb, Mn, and W;
- Evaporation. Formation of minor amounts of evaporites at mineral spring sites affects the following element relative abundances: Na, B, Li, U, and secondarily K, Al, Ti, and Ga. Precipitation occurs at the surface principally as the result of chemical oxidation, loss of dissolved CO_2, loss of heat, and changes in equilibrium resulting from precipitation of sulfates and metal hydroxides. Radioactive elements, chiefly radium-226 and 228 and daughter products, occur with barite and manganese and iron hydrous oxide precipitates. Uranium is not easily precipitated but may occur with evaporite deposits.

Uranium values in stream-sediment samples, Park and Sweet Grass Counties, Montana

Sixty-one stream-sediment samples, collected by K. J. Wenrich-Verbeek from a portion of the North Absaroka study area, Park and Sweet Grass Counties, Mont., in July 1977, were separated into two size fractions (<88 m, and between 88 and 149 m) and analyzed for 80 different elements. Of these elements, 47 showed some variation over the area; 36 met the proper statistical criteria, and were subjected to correlation analysis. Uranium values in the fine size fraction (<88 m) ranged from 2.1 ppm to 430 ppm, with a typical sample containing about 42 ppm uranium. High values (above 100 ppm uranium) were observed along Speculator Creek and Bramble Creek and in drainages on the northwestern and western side of Mt. Douglas. Two high values were found in samples from Falls Creek (north of Boulder Mountain). Fine size fraction sediments containing 410 ppm and 430 ppm, the highest uranium values in the area, were collected from Speculator Creek. The distribution of uranium concentration from this study is somewhat bimodal in both size fractions. Nevertheless, uranium shows a strong correlation with organic carbon (the major component of total carbon in the area) and good correlations (minus sign indicates a negative relation) with Th, $-Al_2O_3$, −Ca, $-Fe_2O_3$, La, −Mg, Pb, −Sc, Se, −Sr, −V, Y, and Yb. Uranium also correlates significantly (at the 99-percent confidence level) with arsenic and −chromium, although the trends are not as well defined as with the elements mentioned above. Uranium decidedly does not correlate with Cu, K, Mn, Na_2O, SiO_2, and Zr. These correlations and the bimodal nature of the uranium suggest that much of the uranium is in a leachable form, hence, the extremely strong correlation with organic carbon, and that some is tied up in resistate minerals such as xenotime, hence, the good correlations with yttrium, thorium, ytterbium, and lanthanum. High molybdenum was evident in some of the same samples that contained high uranium. However, although molybdenum is a good pathfinder for uranium in the water of this area, it is not a good indicator of uranium in the stream sediments.

Uranium in surface waters, North Absaroka area, Montana

Sixty-two surface-water samples, collected by K. J. Wenrich-Verbeek from a portion of the North Absaroka study area, Montana, in July 1977, were analyzed for 52 different variables. Forty-six of these variables are presented in data listings; 27 met the proper statistical criteria and were tested in correlation analysis. Uranium values ranged from 0.04 to 5.1 μg/L, and an average sample contained 0.59 μg/L. The generally low values of uranium in the surface water of this area are in

contrast with high values found in sediments collected at the same sites. However, the maximum uranium concentration was observed in the water of Anomaly Creek, from which previous workers discovered high uranium values in the stream-sediment samples. Out of the 27 parameters treated statistically, uranium correlates only with molybdenum. Uranium does not show correlations with the alkalis or alkaline earths, as was noted in a previous study in New Mexico (Wenrich-Verbeek, 1977b). Arsenic and boron commonly are related to uranium in surface waters (Wenrich-Verbeek, 1977a). However, arsenic analyzed in this area was never above the detection limit of 1 μg/L, and boron showed no correlation with uranium.

Characteristic elemental assemblages associated with uranium deposits at Ambrosia Lake, New Mexico

Statistical treatment of analytical data related to uranium deposits in the Ambrosia Lake area, New Mexico, indicated that, relative to barren rock remote from deposits, the primary ores are enriched in Fe, Mg(?), Ca, Mn, Ba, Be, Cu, Mo, Pb, U, V, Y(?), Na, Se, Sr, organic C, and carbonate C; the secondary ores are enriched in Fe, Ca, Mn, Ba, Cu, Na, Sr, U, V, and carbonate C. The data, compiled and assessed by C. S. Spirakis, C. T. Pierson, and H. C. Granger, indicated that Ca, Ba, Sr, V, and carbonate C are more concentrated in the secondary ore than in the primary ore. Barren rocks adjacent to the ore are enriched in Ca, Ba, Cu(?), Sr, V, U, Na, Se, and carbonate C, compared with barren rock farther from the deposits. The enrichment of these elements in the vicinity of the deposits and the better correlation of them (except for uranium) with eU than with uranium suggest that these elements are mobile and form haloes that may be useful exploration guides. The data also suggest that gallium is depleted in and around the ore. Thus, a decrease in gallium might be an indication of proximity to a deposit.

Geochemistry of mineral-spring waters, Western United States

Preliminary results obtained by K. J. Felmlee and R. A. Cadigan by R-mode factor analyses on water data from 155 mineral-spring sites in the Western United States indicated that three factors have a dominant influence on the water chemistry. These factors can be interpreted on one level as chemical reactions related to salinity, temperature, and alkalinity and on another level as aspects of the hydrogeologic systems that affect chemical reactions. The factors and their parameter groupings are as follows (minus sign indicates a negative relation): (1) Salinity (age of water) Na, specific conductance, Cl, K, Li, B, SO_4, Sr, Fe, Mn; (2) Temperature (depth of water circulation); temperature, F, SiO_2, Rn, $-$Eh, $-$Al, $-$U, $-No_3 + No_2$; (3) Alkalinity (rock composition), pH, $-HCO_3$, $-$Ca, $-$Mg, $-$Ra, $-$Ba. These groupings show that uranium and radium concentrations are generally controlled by reactions related to Eh and pH. Furthermore, radium is commonly higher in deeper circulating, older water, which tends to have higher salinity, higher temperature, lower pH, and lower Eh. Uranium is higher in shallower circulating, younger water, which tends to have lower salinity, lower temperature, higher pH, and higher Eh. Although no uranium-mineralization factor was evident in the factor analysis, consideration of geologic setting indicated that the presence of mineralization may, nevertheless, have a detectable influence on the water chemistry. Some of the highest concentrations of uranium ($>100\mu$g/L), radon ($>10{,}000$pCi/1), or radium (>100pCi/1) were found in spring water near uranium occurrences in the Tallahassee Creek district, Colo., in the Clancy area, Mont., at Spor Mountain, Utah, and in the East Walker River district, Nev.

Helium surveys in Beaver Valley area, Utah

A reconnaissance helium soil-gas survey by G. M. Reimer in the valley surrounding Beaver, Utah, located some areas that were specifically anomalous in helium concentration. Geologic investigations by other researchers have identified the valley as a promising location for possible uranium mineralization based on the nearby location of source rocks, hydrology in the valley, and geochemistry of ground water. The helium anomaly is situated in the southwest portion of the valley near the surface drainage outlet toward Minersville, Utah. That cumulative information strengthened by the helium survey indicates the strong possibility of a localized uranium concentration; and, if subsurface environment favorable for uranium deposition existed in the past, then the presence of an economic uranium deposit in the southwest corner of the valley is extremely likely.

Thorium/uranium ratios for granitic rocks

Th/U ratios for granitic rocks are thought to be normal if they are within the range of 3 to 5. Possible economic significance was proposed for granites with Th/U ratios either below or above this range (Nash, 1979; Stuckless, 1979). Lead isotope analyses by J. S. Stuckless for several suites of peraluminous Precambrian granites showed that Th/U ratios were generally in the range of 1 to 3 throughout most of the history of these granites, but measured Th/U ratios are most commonly in the range of 5 to 10. These high ratios were shown to be due to recent uranium loss through incipient weathering. High Th/U ratios by themselves are not

sufficient to indicate uranium loss by incipient weathering. Data for two granitic suites yield Th/U ratios greater than 10 for both measured and calculated ratios. Such granites may have been derived from a protolith that was enriched in thorium relative to uranium, or uranium may have been lost during the magmatic event. If the latter alternative is true, then these granites are a probable source for uraniferous pegmatites.

Uranium mobility during glass diagenesis

An unusual occurrence of juxtaposed glassy and clay-altered ash was sampled by R. A. Zielinski to determine the extent of element mobility during glass diagenesis. The results are particularly interesting in that major mobilization of uranium is indicated. Closely spaced samples of glassy and clay-altered ash were collected from the same 20 to 50 cm thick stratigraphic horizon in the Troublesome Formation (Miocene) of northwestern Colorado. Sharp contacts exist between glassy ash and underlying pink montmorillonite and may indicate water-saturated conditions restricted to basal ash layers or deposition in a body of water that dried up during the course of eruption. Formation of montmorillonite instead of zeolites indicates that the water was not highly alkaline or saline. Multielement analysis of glassy and clay-altered samples indicates that (1) montmorillonite has 85 to 90 percent less uranium than the coexisting glass. Similarly depleted elements include cesium, rubidium, sodium, and potassium. Much smaller depletions of these elements in some glassy samples serve as particularly sensitive indicators of incipient alteration of this type; (2) the abundances of relatively insoluble elements such as thorium or tantalum are slightly higher (5 to 40 percent) in clay as indicators of the maximum levels of element enrichment in residual material. Greater enrichment of elements such as scandium, strontium, and cobalt indicates adsorptive uptake by clay or by secondary oxides or iron and manganese; (3) the rare-earth-element (REE) patterns and abundances in glass are sufficiently mimicked by detritus-free montmorillonite to document the compositional equivalency of the two.

Origin of roll-type uranium deposits, Ray Point uranium district, south Texas

Detailed studies by M. B. Goldhaber in collaboration with R. L. Reynolds and K. R. Ludwig were conducted on the origin of the Ray Point uranium district of the south Texas coastal plain. Based on petrographic and geochemical studies of mine and core samples and geochemical studies of modern ground water, the following sequence of events was deduced: (1) The host beds were invaded shortly after deposition by fault-leaked oil-field brines derived from depth and transported up the Oakville fault. These brines did not contain H_2S but did contain dissolved organic matter capable of acting as a substrata for sulfate-reducing bacteria. Sulfide produced in this way sulfidized the iron-bearng components of the sediment and produced pyrite; (2) These same brines began to mix with oxygenated-uranium-bearing ground water. This mixing altered the sulfur geochemistry such that marcasite rather than pyrite began to form; (3) Brine ceased to invade the area, but meteoric water recharge did continue and eventually resulted in a roll-type uranium deposit; (4) About 5.07 m.y. ago, the whole deposit was secondarily resulfidized by fault-leaked H_2S from the sour-gas fields of the underlying reef facies of the Edwards Limestone (Cretaceous); (5) Modern-day ground water is similar to step 2, and presently is forming a younger marcasite.

Depositional environment of the White Rim Sandstone Member of the Cutler Formation, Utah

Studies of the White Rim Sandstone Member of the Cutler Formation in the area between the Green and Colorado Rivers in east-central Utah by B. A. Steele-Mallory indicated that the member was deposited in a coastal eolian environment. Sedimentary structures, petrologic features, and stratigraphic relations suggest that the White Rim consists of two major genetic units. These units represent a coastal dune field and related interdune ponds. Distinct sedimentary structures of the dune unit include large- to medium-scale, unidirectional (southeast), tabular planar cross bedding- high-index ripples oriented parallel to dip directions of the foresets, raindrop impressions, slump marks, and coarse-grained lag layers. Distinctive sedimentary structures of the interdune pond unit include wavy horizontally laminated bedding, adhesion ripples, desiccation polygons, and possible evidence of burrowing. A crinoid fragment was discovered, and small amounts of well-rounded, reworked glauconite grains were found in samples from throughout the study area. The White Rim Sandstone Member was deposited during a period of changing sea level and migrating strandlines. Continental sedimentation was dominant in eastern Utah along the ancestral Uncompahgre Mountains, and marine deposition was prevalent in western Utah. Rocks deposited in the two environments interfinger in the study area. The White Rim represents eolian deposition on a prograding shoreline characterized by a semiarid climate and predominately onshore winds.

Sedimentologic relation of the lower part of the Morrison Formation to underlying Jurassic rocks, San Juan basin, New Mexico

The lower part of the Jurassic Morrison Formation appears to be gentically related to strata that underlie it in the San Juan basin of New Mexico, Colorado, Utah, and Arizona. According to R. D. Lupe, the relation of the lower part of the Morrison to the Junction Creek, Bluff, and Cow Springs Sandstones is apparently a vertical and lateral facies change. The lowest member of the Morrison, the Salt Wash Sandstone Member in the north flank of the basin and the Recapture Shale Member elsewhere in the basin, appears to have changed facies from eolian to fluvial. Study of the subsurface strata via oil-well logs points to a diverse and active setting during deposition of the lower part of the Morrison and its facies equivalents. This setting, the San Juan basin, appears to have been the site of actively growing dune fields and migrating rivers on the surface of an abandoned lake or playa. The lake or playa is recorded in the sediments of the underlying Summerville Formation. Formation of perhaps a dozen major dune fields scattered around the basin and deposition in the rivers that migrated around those fields produced a sequence that was many tens of meters thick. Dunes eventually ceased to form, in some places sooner than in others, as is evidenced from variations in dune sediment thicknesses as compared to the overall remarkably constant thickness of the dune and fluvial sediments together. In most places, the entire dune-river depositional episode ended with the onset of an entirely new style of fluvial deposition that originated from a new source—that of the Westwater Canyon Sandstone Member of the Morrison.

Uranium in the White Hills area near Lake Meade

Disseminated intermediate grade uranium in the White Hills area south of Lake Meade is found in the Muddy Creek Formation of Miocene and Pliocene age. Fieldwork by C. S. Bromfield and L. M. Osmonson showed that the uranium occurs near the base of its Hualapi Limestone Member (uppermost). The limestone member in the White Hills overlies a red siltstone and gypsum member. A thin tuff bed is found in the mineralized zone. The Muddy Creek unconformably overlies probable Miocene acid-to-intermediate volcanic rocks. Semiquantitative analyses show an increase in vanadium in uranium-enriched units and in molybdenum, lithium, and gold in some samples.

Volcanic uranium occurrences in the Western United States

Compilation of over 100 uranium occurrences in or interpreted to be related to volcanic rocks in the Basin and Range province was completed by C. S. Bromfield and L. M. Osmonson. Many occurrences are in rhyolite, although host rock types range from rhyolite to andesite. Incomplete data on age of host rocks show a range from Jurassic to Pliocene. Perhaps 20 percent of the occurrences can be interpreted to be related, at least spatially, to calderas; but basic geologic data are scarce in large areas of the Basin and Range. Over two-thirds of all plotted occurrences are clustered in six areas: (1) Mountain City, Nev.; (2) McDermitt, Nev. and Oreg.; (3) Hallelulah Junction, Nev. and Calif.; (4) Thomas Range, western Utah; (5) Pioche-Tushar mineral belt, Utah; and (6) Santa Rita-Ruby area, Arizona.

Stratigraphy of uranium-bearing rocks in the Uinta basin, Utah

The stratigraphic relations of copper-uranium-bearing sandstone beds in the Uinta Formation (Eocene) in the central part of the Uinta basin, Utah, have never been clearly defined. Reconnaissance field investigations by L. C. Craig suggest that widespread lacustrine limestone beds may afford a tie to well-established sections of the Uinta in the western part of the basin, and pebble differences in conglomeratic beds may afford ties to well-established sections in the eastern part of the basin.

Trangressive-regressive relation of Cretaceous rocks in the San Juan basin, New Mexico

Geologic mapping by R. E. Thaden in the Tohatchi 2 NW quadrangle demonstrated several cycles of alternating transgression and regression at the southwest margin of the Cretaceous sea that occupied an area of the San Juan basin. The shaly siltstone of the Satan Tongue of the marine Mancos Shale, for example, transgresses as far southwest as Windy Canyon, overriding the Hosta Tongue of the Point Lookout Sandstone. South and west of that point, the Hosta and the Point Lookout merge to form a single thick shoreface sandstone body. The next regression is demonstrated by the northeastward thinning of the continental Cleary Coal Member of the Menefee Formation, its place being taken northeast of Squirrel Springs by coal-poor beds of the Allison Member of the Menefee, which was deposited higher on the flood plain. Later cycles of transgression and regression cannot be seen, because the Cretaceous beds, dipping 17 to 31 degrees eastward, are overlain to the east and north by the very slightly northeastward-dipping Tertiary Chuska Sandstone.

Radioactive anomalies in the Kootznahoo Formation, Alaska

Radioactive anomalies as high as 50 times background and uranium-bearing samples were discovered in parts of nonmarine Tertiary Kootznahoo Formation in south-

east Alaska by K. A. Dickinson (USGS) and John Mitchell, consultant for Map Co. Inc., Tulsa, Okla. Samples containing as much as 1300 ± 400 ppm uranium measured by beta eU ($2{,}300 \pm 700$ ppm measured by gamma eU) were found. These samples have the highest uranium contents so far reported from Tertiary sedimentary rocks in southeast Alaska. Kootznahoo crops out on Admiralty Kuiu, Kupreanof, and Zerembo Islands. In the Kadake Bay-Port Camden area on Kuiu Island, the Kootznahoo consists of light brown, poorly sorted, very dolomitic sandstone that contains clay clasts, fragments of carbonized wood, and dolomitic concretions. It ranges from silty, fine-grained, thin-bedded sandstone to medium- and coarse-grained partly conglomeratic, medium- to thick-bedded sandstone. Siderite, magnetite, pyrite, and apatite(?) were found in one or more of the samples. Anomalous radioactivity was associated only with carbonized wood fragments on the outcrop. Surface leaching, however, may have removed uranium from the sandstone, especially in the intertidal zone, but unoxidized sandstone containing larger amounts of uranium may be present in the subsurface.

Radioactive volcanic breccia and conglomerate, Norton Bay quadrangle, Alaska

An 80-km-long belt of strongly radioactive volcanic breccia and conglomerate was discovered and mapped by T. P. Miller in the western Norton Bay quadrangle in western Alaska. This belt is a continuation of a horizon of similar rocks first mapped and reported in 1977 in the Candle quadrangle to the north. This discovery gives a total strike length of these anomalously radioactive rocks of about 130 km. Background total radioactivity ranges up to 750 counts per second, and a strong association of anomalous radioactivity with red hematite, purple fluorite, and trachyte was noted.

Rhizocorallum burrows in the Jurassic Todilto Limestone

The lower 40 feet of the clastic sequence overlying the limestone facies of the Todilto Limestone in the Chama basin is tentatively referred to as the Summerville Formation-Wanakah Formation interval. Near the top of this interval, Rhizocorallum burrows were found by J. L. Ridgley at six widely spaced localities along the eastern, southern, and western outcrop belt of the Chama basin. The burrows occur parallel to bedding. Studies of Rhizocorallum burrows from other formations indicate that the burrows are in lower shelf or tidal-flat facies of marine enviroments. Environmental interpretations of the clastic sequence containing the Rhizocorallum burrows in the Chama basin suggest a tidal-flat environment in this case. The problem of whether these burrows may occur in lacustrine environments (as has been postulated for the Todilto Limestone) has not been resolved.

Jasperoid as a possible indicator of uranium source, Pitch mine, Colorado

Continuing studies of the Pitch mine area, Saguache County, Colo., by J. T. Nash focused on jasperoid as a possible indication of a volcanic source for uranium in the ore zone. Several zones up to 150 m^2 of jasperoid occur along the Chester fault zone between the Pitch mine and Little Indian mine 2 km to the north. The jasperoid commonly has a breccia texture that is interpreted to reflect silicification of earlier dolomite breccia. The sequence of events is interpreted to be early Tertiary brecciation along the Chester fault followed by middle-Tertiary silicification. Middle-Tertiary volcanic rocks were present a few tens of meters above the jasperoid and are believed to be the source of silica. Chemical analyses of the Oligocene Rawley Andesite show it to be potassium-rich (5 to 7 percent K_2O) and siliceous (64 to 70 percent SiO_2) rhyodacite and quartz latite with about 10 ppm uranium. Alteration of volcanic rocks produced the silica-rich solutions that probably would have been rich in uranium and are postulated to be the source of uranium for the ore deposits. Because of the proximity and thickness of volcanic flows and tuffs, ground water reacting with the volcanic rocks could have been heated, hence the ore fluid may have had low-temperature meteoric hydrothermal character.

Morphology of uranium ore deposits in the Mariano Lake area, New Mexico

Uranium orebodies in the Mariano Lake mine, McKinley County, N. Mex., occur in fluvial sandstone beds in the lower part of the Brushy Basin Shale Member of the Upper Jurassic Morrison Formation. Mapping by J. F. Robertson showed that the orebodies geometrically have a roll-type configuration, are tabular-elliptical in form with their long dimension oriented to the northwest, and are peneconcordant to bedding though somewhat disconnected by differences in permeability along and across bedding. Orebodies tend to be teardrop shaped in cross section. They have sharp, crosscutting, irregular contact with unmineralized country rock at their thicker northeast end; and they are thinner, fragmented, and have split tails toward the southwest margin where depletion of uranium and post-ore oxidation of pyrite and the host rock is more evident. The general morphology of deposits suggests that the original oxidation-reduction front was on the north margin of the deposit much like that shown in the Ruby Well mines, the Black Jack No. 2 mines, and the Mac mines to the southeast. The mines

appear to line up along a nearly continuous front that extends northwesterly from Smith Lake to Mariano Lake. Some of the orebodies in the Mariano Lake mine are located in the trough of the west-northwest-trending Mariano syncline; some are situated on the south-dipping north flank of the syncline, and exploration drill holes outline mineralized ground and reaction front striking northwest on line with the orebodies on the north flank of the adjacent anticline. It is evident that the line of orebodies and trend of the front cross the fold structures diagonally. A north-northwest-trending normal dip-slip fault in the southeast part of the Mariano Lake mine displaces an orebody as much as 1 m, but shows relatively minor uranium depletion or other alteration along it. There is no suggestion of redistribution of uranium in its vicinity. These observations lend support to the idea that the uranium deposits are primary and were deposited before the folds and faults developed during Laramide time, and are probably pre-Dakota in age.

Uranium content in diatomaceous and porcelaneous rocks, California

Analysis by D. L. Durham of diatomaceous and porcelaneous rocks of the Tertiary Monterey Formation, Calif., and of similar rocks from Peru, Ecuador, Mexico, and the southern California borderland showed that these rocks have more, and for some, considerably more, uranium than do most shaley rocks. On the other hand, analyses showed that chert and dolomite associated with these rocks have only ordinary, or less than ordinary, uranium content, as do siliceous sediments collected away from the continental shelves in the equatorial Pacific Ocean and the Bering Sea. These data are consistent with the idea that areas of upwelling and consequent high productivity are favorable for the accumulation of siliceous sediments with higher than normal uranium content.

Geologic decision analysis applied to uranium resources of the San Juan basin

A systematic matrix of all the known geologic characteristics of a given type of uranium deposit and their corresponding genetic aspects constitute a genetic-geologic model. Such a model may be used to evaluate a similar geologic environment for its favorability to contain undiscovered uranium resources of the type modeled. The system developed by W. I Finch, H. C. Granger, R. D. Lupe, and R. B. McCammon (1980) presented data to indicate whether each geologic attribute is present, absent, or undetermined. The first provisional model was built for the humate uranium deposits in the Morrison Formation in the tabular San Juan basin, and it consists of 140 variables (Granger and others, 1980). Geologic decision analysis has been devised as a method to identify the critical variables and to weight each of several stages of the provisional genetic-geologic model in order to determine favorability (McCammon, 1980). By combining this favorability with grade-tonnage data for deposits and by using prior probabilities of occurrence, one can use geologic decision analysis to estimate the undiscovered uranium resources in a given area. Testing and refinement of the entire resource-assessment methodology outlined above, using the provisional tabular humate uranium deposit model in the San Juan basin, is being carried out to simplify the working model.

Origin of uranium deposits, Date Creek basin, Arizona

According to J. K. Otton, uranium in the Date Creek basin, Arizona, accumulated in small early Micoene interfan lakes developed during a period of rapid alluvial fan growth, decreasing lake size, increasing aridity, and increasing alkalinity and salinity of lake and ground waters. The basin was periodically inundated by silicic volcanic ash. Adjacent mountainous terrains included highly radioactive Precambrian granites. Sedimentation in the lake and on the alluvial fans was dominated by debris flow and turbidite processes. The debris flows, probably initiated by episodic heavy storms, swept ash and plant material across the alluvial fans and into the lake. Where debris flows entered the lake, they formed turbidity currents in which considerable size sorting of plant and other entrained debris occurred. In the center of the lake, thick sections of laminated, carbonaceous, micaceous siltstones accumulated as distal turbidites. Shallow ground waters, moving from sources in the mountains into the basin, leached uranium from granites in the mountains and from arkosic alluvium and volcanic ash in the basin. These waters also leached silica from ash and humate from entrained plant debris in the basin beds. These waters entered the lake in recharge areas around its margin. Uranium, silica, and humate tended to precipitate on the lake bottom most often prefering the carbonaceous siltstone. Precipitation probably was initiated by increases in salinity caused by evaporative concentration of the lake waters. The uranium orebodies thus formed are large, low-grade (average 0.07 percent at the Anderson mine), and stratabound, and are stacked vertically.

Uranium favorbility in the Shiprock 1° × 2° NURE quadrangle, New Mexico and Arizona

All sedimentary, igneous, and metamorphic rock formations in the Shiprock 1° × 2° quadrangle of New Mexico and Arizona were evaluated for their favorability to

contain uranium deposits of at least 45,000 kg and a minimum of .01 percent grade. Favorability was assessed to a depth of 1,500 m using air and ground radioactivity surveys, hydrogeochemical sampling, studies of uranium occurrences, and studies of surface and subsurface geology. Assessment work was conducted during FY 78 and FY 79 under the DOE's National Uranium Resource Evaluation (NURE) Program by M. W. Green and a team of 14 geologists in the Branches of Uranium and Thorium Resources and Central Environmental Geology.

The Recapture Shale and Salt Wash Sandstone Members of the Jurassic Morrison Formation were evaluated to have the most potential for large, and as yet undiscovered, uranium deposits. Uranium deposits in the Salt Wash are clustered in the Shiprock and Chuska mining districts and occur in gray sandstones associated with gray mudstone. The sandstone geometry and thickness, the presence of detrital organics in stream sediments, the depositional environment, and the presence of medium-sized deposits and uranium occurrences make these units conducive to the favorable classification.

The Triassic Chinle Formation and the Cretaceous Toreva Formation also are considered favorable for additional medium-sized uranium deposits. The Chinle Formation deposits are located in Monument Valley in the basal portion of the Shinarump Member within channel sandstones. Deposits in the Toreva Formation occur in the southwest portion of the quadrangle. They are found in the upper part of the lower member of the Toreva Formation. They are located in the fine-grained, carbonaceous, partially abandoned channel-fill deposits of a higher energy meandering stream fluvial complex.

Formations judged to be low in favorability for uranium deposits include the Cretaceous Fruitland Formation and the Point Lookout Sandstone, which contain a number of aerial radiometric anomalies. Other Cretaceous units that contain a significant number of airborne radiometric anomalies include the Menefee Formation and the Mancos Shale. More data need to be obtained, however, before any conclusions can be drawn on the significance of these anomalies.

Other rocks of Precambrian to Cenozoic age also were evaluated but were not considered favorable because of their low radioactivity, their lack of uranium occurrences, and unfavorable environmental and facies characteristics.

Uranium favorbility in the Gallup 1°×2° NURE quadrangle, New Mexico and Arizona

All sedimentary, igneous, and metamorphic rock formations to a depth of 1,525 m in the Gallup 1°×2° quadrangle of northwestern New Mexico and northeastern Arizona were assessed of their favorability of containment of additional uranium deposits of 100,000 t or greater at a minimum grade of 0.01 percent or greater. Favorability assessment work was conducted during FY 78 and FY 79 under the DOE sponsored NURE Program by M. W. Green and a team of 14 geologists in the Branches of Uranium and Thorium Resources and Central Environmental Geology. Results of air and ground radioactivity surveys, hydrogeochemical sampling, uranium occurrence studies, and surface-subsurface geologic studies served as the basis for favorability evaluations.

The Westwater Canyon Sandstone and Brushy Basin Shale Members of the Morrison Formation of Jurassic age throughout their extent in the quadrangle were evaluated to be the most promising for yet undiscovered large uranium deposits. First cycle lithology, facies relation, sandstone geometry, and thickness and depositional environment of the Morrison Formation remain most favorable to depths of 1,000 to 1,500 m north of the Grants mineral belt on the Chaco slope of the southern San Juan basin. This area remains relatively unexplored. The Jurassic Todilto Limestone and the Cretaceous Dakota Sandstone also are considered relatively favorable for additional medium-sized uranium deposits. The Todilto Limestone contains numerous uranium occurrences and deposits near outcrop on the southern edge of the mineral belt. Favorability for additional similar sized deposits at depth within the mineral belt is considered great. Favorability is limited only by extent of Todilto deposition in the quadrangle and depth to the formation. The Dakota Sandstone is considered favorable in the western end of the mineral belt (Church Rock mining district), where pre-Dakota erosion has truncated underlying Brushy Basin impermeable shales to allow access of uranium-bearing ground water from the Westwater Canyon to come into contact with organic-rich sediments of the Dakota Sandstone.

Formations with low favorability, based primarily on scarcity of uranium occurrence, include the Triassic Shinarump Member of the Chinle Formation, the Toreva Formation of Cretaceous age, and the eastern edge of the Tertiary Hopi Buttes volcanic field. Subsurface data on these formations are not sufficient to fully evaluate their potential. Rocks of Precambrian and Paleozoic age, as well as other formations of Mesozoic and Cenozoic age within the quadrangle, are not considered favorable because of low radioactivity, lack of uranium occurrences, and unfavorable environment and facies characteristics.

Uranium favorability in the Aztec 1°×2° NURE quadrangle, New Mexico

All sedimentary, igneous, and metamorphic rock formations in the Aztec 1°×2° quadrangle of northwestern New Mexico were evaluated for their favorability of uranium deposits of at least 45,000 kg and a minimum of .01 percent grade. Favorability was assessed only to a depth of about 1,500 m using hydrogeochemical sampling, uranium occurrence studies, and surface and subsurface geologic studies. Assessment work was conducted during FY 78 and FY 79 under the DOE sponsored NURE Program by M. W. Green and a team of 14 geologists in the Branches of Uranium and Thorium Resources and Central Environmental Geology.

The Burro Canyon(?) Formation of Cretaceous age was determined to be the most promising for large undiscovered uranium deposits. The sandstone geometry, thickness, and apparent presence of reductants downdip are favorable for uranium deposition. Portions of the Burro Canyon were drilled but remain unproductive. However, at least one known deposit was found at fairly shallow depths in this formation; and on the basis of this, it has been considered favorable for uranium deposits. Much more exploration is needed to determine the extent of mineralization. The Westwater Canyon Sandstone and Brushy Basin Shale Members of the Jurassic Morrison Formation also are considered favorable for uranium deposits in the Aztec quadrangle based on their lithology and facies relation with the Westwater Canyon Sandstone and Brushy Basin Members in the Gallup and Albuquerque quadrangles to the south. No uranium deposits were found in these units in the Aztecs area; however, drilling by the D.O.E. has revealed some anomalous, radioactive areas in the subsurface of the southwest corner of the quadrangle. Formations judged to be of low favorability for uranium deposits include the Permian Cutler Formation, the Cretaceous Dakota Sandstone, and the Tertiary Ojo Alamo Sandstone. These formations are considered marginally favorable, because they contain a large number of small occurrences of moderate to low grade. The deposits in the Cutler Formation also are associated with small copper deposits. Results of hydrologic stream and sediment reconniassance data from Los Alamos Scientific Laboratories revealed a number of anomalous sediment and water samples in drainages of the Nacimiento Group; however, these have not been field checked or fully evaluated. Other rocks of Precambrian to Cenozoic age also were evaluated, but they were not considered favorable because of their low radioactivity, lack of uranium occurrences, and their unfavorable environmental and facies characteristics.

Uranium favorability in the Albuquerque 1°×2° NURE quadrangle, New Mexico

All sedimentary, igneous, and metamorphic rock formations in the Albuquerque 1°×2° quadrangle of northwestern New Mexico were evaluated for their favorability to contain uranium deposits of at least 45,000 kg and a minimum of .01 percent grade. Favorability was assessed only to a depth of 1,500 m using air and ground radioactivity surveys, hydrogeochemical sampling, studies of uranium occurrences, and studies of surface and subsurface geology. Assessment work was conducted during FY 78 and FY 79 under the DOE sponsored NURE Program by M. W. Green and a team of 14 geologists in the Branches of Uranium and Thorium Resources and Central Environmental Geology.

The Westwater Canyon Sandstone and Brushy Basin Shale Members of the Jurassic Morrison Formation were evaluated to have the most potential for additional large yet undiscovered uranium deposits. First cycle lithology, facies relation, sandstone geometry, thickness, and depositional environment of the Morrison Formation are conducive to uranium deposition in the quadrangle. The Jurasic Todilto Limestone and the Cretaceous Dakota Sandstone also are considered favorable for additional medium-sized uranium deposits. The Todilto Limestone contains numerous uranium occurrences and small deposits on the eastern edge of the Grants mineral belt. Favorability for the discovery of additional deposits of comparable size at depth within the mineral belt is also good. Favorability is limited only by the areal extent of deposition and depth of Todilto in the quadrangle. The Dakota Sandstone also contains a number of small uranium occurrences on the eastern edge of the San Juan basin. These occurrences are associated with the lignitic or highly carbonaceous Menefee Formation and the Tertiary Galisteo Formation. These units are found within the basin itself and on its eastern edge. Both units contain a number of uranium occurrences that meet the grade and tonnage requirements. The Menefee Formation also contains a large number of aerial radiometric anomalies. Hydrogeologic stream and sediment reconnaissance data from Los Alamos Scientific Laboratories revealed a number of anomalies in the drainages of Precambrian and Tertiary rocks as well as the Jurassic and Cretaceous rocks. These studies are still under investigation, and the results need to be evaluated before conclusions can be made. Formations judged to be of low favorability for uranium deposits include the Permian and Tertiary rocks. These rocks are considered marginally favorable, because they contain a large number of small moderate-to-low-grade occurrences. Other rocks of Precambrian to Cenozoic age also

were evaluated, but they were not considered favorable because of their low radioactivity, lack of uranium occurrences, and unfavorable environmental and facies characteristics.

Uranium favorability in the Pueblo 1°×2° NURE quadrangle, Colorado

Uranium and thorium analyses collected for the NURE Program are used by K. A. Dickinson to evaluate potential uranium source rocks in the northwestern part of the Pueblo 1°×2° quadrangle, Colorado. Thorium to uranium ratios are used as a measure of uranium leaching. A ratio greater than 5:1 is considered to indicate leaching. Proterozoic X granodiorite of Boulder Creek age (1.7 b.y.) and Proterozoic Y granite from the Cripple Creek pluton of Silver Plume age (1.45 b.y.), together with several lower Oligocene units—the Wall Mountain Tuff, the lower member of the Thirtynine Mile Andesite, the tuff of Stirrup Ranch, the Badger Creek Tuff, and The Thorn Ranch Tuff—from the Thirtynine Mile volcanic field, are analyzed. The Wall Mountain Tuff, a silicic tuff, appears to have lost about 5 ppm uranium and is believed to be the primary source of uranium in the area. The tuff of Stirrup Ranch, lithologically similar to but areally much more restricted than the Wall Mountain, and the siliceous Thorn Ranch Tuff also have been leached. The less siliceous lower member of the Thirtynine Mile Andesite does not appear to be leached, but only two samples were available for study. Samples of the tuff of Stirrup Ranch from nearly the same locality but different statigraphic levels have much different uranium contents but are similar in degree of leaching. The Badger Creek Tuff is leached in the Castle Rock Gulch area but not in the Antero basin uranium area. Differences in leachability and uranium content in different layers of the same volcanic unit must be considered in source-rock evaluation. Granodiorite of Boulder Creek age shows an apparent loss of from 2 to 5 ppm uranium. Samples that appear weathered, however, have lost little or no more uranium than those that appear fresh, suggesting that the degree of leaching is not related to the present weathering surface. Leaching in this rock and in the granite of the Cripple Creek pluton may have been complete long before the Tertiary uranium mineralization.

Subdivision of the Morrison uranium-bearing Westwater Canyon Member, San Juan basin, New Mexico

Data gathered by C. E. Turner-Peterson from the west side of the San Juan basin, in the area between Window Rock, Ariz., and Sanostee, N. Mex., suggest that the Westwater Canyon Member of the Morrison Formation may contain at least three major fluvial complexes in this area. A vertical subdivision into lower, middle, and upper parts of the Westwater Canyon can be recognized as far east as Gallup, N. Mex. Near Gallup the middle fluvial complex appears to thin drastically, whereas the lower and upper fluvial complexes apparently persist at least as far east as Laguna, N. Mex.

Western world uranium associated with metamorphosed Proterozoic sedimentary rocks

According to J. T. Nash, approximately 30 percent of Western World uranium reserves, plus a larger percentage of probable resources, occur in or near metamorphosed Proterozoic marginal-marine sedimentary rocks. The chief protolith was carbonaceous pelite; associated sedimentary rocks were carbonate sequences, commonly algal or dolomitic, and sandstone, and generally included interbedded evaporite beds and iron-formation. Stratabound uranium deposits tend to be in rocks of the first Proterozoic marine transgression within about 10 km of Archean granite hills. Sedimentary relations probably are displayed best in the Lower Roan Group, Copperbelt, Zambia-Zaire. Anomalous uranium content generally cannot be demonstrated, but syngenetic or diagenetic enrichment is suggested by the worldwide tendency for stratabound uranium deposits to occur in similar metasedimentary sequences including: Alligator Rivers and Rum Jungle districts, Australia; Bancroft and Athabasca districts, Canada; Front Range, Colo.; Copperbelt and Rossing areas, Africa; and Zechstein area, Europe. The reducing marine environment related to algal bioherms is the major factor in uranium enrichment. Metamorphism to greenschist granulite-grade mobilized uranium, which probably moved less than 1 km into vein unconformity-type, or Rossing-type deposits, depending upon structural setting. Metaevaporite sequences are indicated by widespread scapolite, common uranium-associated magnesian alteration (possibly dependent on diagenetic magnesite), and may have caused reflux of uraniferous brine into carbonaceous-sulfidic zones. Marginal-marine sedimentary preconcentration appears to have been important from the time of atmosphere oxygenation (2.2 b.y.) until the rise of land plants (0.4 b.y.). The characteristic marginal-marine sedimentary package, particularly presence of algal carbonate sequences, is a guide to new hardrock uranium districts.

Stratigraphy and uranium paragenesis, Lake City caldera, Colorado

Fieldwork by K. A. Hon in the interior of the Lake City caldera has led to the refinement of the intracaldera stratigraphy of the Sunshine Peak Tuff through the recognition of an intraunit vitrophyre. He also was

able to map one of the late-stage intracaldera intrusive rocks in enough detail to suggest that it assimilated some of the Sunshine Peak Tuff during intrusion.

Preliminary microscopic and microprobe examination of samples from the Golden Fleece mine by R. I. Grauch showed the following sequence of events in ore paragenesis: (1) alternating deposition of uraninite and silver-tellurides; (2) dissolution of both phases and the deposition of silica (and possibly the alteration of uraninite to coffinite); (3) alternating deposition of uraninite and silver-tellurides; and (4) deposition of silver-gold-tellurides and silica.

Uranium content in Precambrian rocks, Colorado and Wyoming

According to F. A. Hills, aerial radiometric survey maps of six 1° × 2° quadrangles in southern Wyoming (Cheyenne quadrangle) and northern Colorado (Craig, Denver, Greeley, Leadville, and Pueblo quadrangles), produced by contractors for the DOE, indicate that the Proterozoic X gneisses, schists, and igneous rocks (approximately 1,700 m.y. old, synorogenic, Boulder Creek-age group) are approximately normal to only slightly enriched in uranium and thorium as compared with average continental crust. By contrast, with few exceptions, the Proterozoic Y igneous plutons (approximately 1,400-m.y.-old, anorogenic, Silver Plume-age group) contain anomalously high concentrations of uranium and thorium. These generalizations are confirmed by approximately 300 chemical analyses. The "Laramie Anorthosite Complex" (Hodge and others, 1973) (Cheyenne quadrangle) consisting of anorthosite and monzonitic rocks, which have been interpreted as cumulates, comprises the only volumetrically significant pluton of the 1,400-m.y.-age group that shows average or below average uranium and thorium concentrations. Variations in initial strontium isotopic composition in the "Laramie Anorthosite Complex" (Subbarayudu, Hills, and Zartman, written commun.) suggest that the greater part of that complex, formed by crystal settling combined with progressive incorporation of large proportions of ancient country rocks into the differentiating magma. REE compositions (J. C. Fountain, 1980, written commun.) of the anorthosite and associated monzonite are compatible with a cumulate origin for those rocks, and REE compositions of the Silver Plume-age group granites are compatible with an origin as residual liquid from which monzonitic and anorthositic rocks separated. The combined isotopic and REE data suggest that the uraniferous and thoriferous 1,400 m.y.-old-granitic rocks formed by a reaction melting process whereby larger masses of basic magma emplaced into the lower crust provided the heat to zone refine the continental crust. This produced anorthositic and monzonitic cumulates (at depth) that are depleted in incompatible elements such as uranium, thorium, and REE, and granitic rocks (at highest levels in the crust) that are highly enriched in the incompatible elements.

Nonradiometric geophysical surveys in uranium country

Research by B. D. Smith demonstrated that various types of nonradiometric geophysical anomalies can be detected over known areas of uranium mineralization. Anomalies can be related, in many cases, to changes in the physical properties of the host rocks for the uranium mineralization. Research has focused on understanding the relation between the genetic history of uranium mineralization and changes in physical properties of their host rocks that produce geophysical anomalies. This research enables more effective planning of nonradiometric geophysical surveys to explore for and define various types of uranium deposits. A specific objective of the project has been to provide data for uranium mineral resource evaluation of Navajo Indian Lands. Airborne and ground geophysical surveys have been used to isolate areas favorable for sediment-hosted uranium. Large-scale induced polarization–resistivity surveys conducted over the Crown Point district defined shallow (less than 120 m) zones of high-resistivity rocks that have a coincident trend with known deeply buried (approximately 600 m) uranium deposits. There are, at present, no known genetic relation between the shallow geophysical anomalies and the deeper uranium mineralization. However, the correlation of these trends is pronounced enough to warrant further geophysical and geochemical studies. The preliminary data interpretation from the high-resolution airborne total field magnetic survey conducted in the same area suggests that there are low amplitude and long wavelength magnetic anomalies associated with the trend of known uranium mineralization and the zone of anomalously high-resistivity rocks. Further research will be directed toward definition of the source of these geophysical anomalies and their relation to the known uranium mineralization.

Uranium in sagebrush—a possible exploration tool

Results from recent studies of uranium in big sagebrush (*Artemisia tridentata*) from the Western United States suggest that this widespread desert shrub could be used to prospect for uranium. This possibility was tested by J. A. Erdman and J. H. McCarthy at the newly discovered Aurora uranium prospect near the northern edge of the McDermitt caldera complex along the Nevada-Oregon border. The McDermitt is of considerable interest, not only because it is among the

largest known caldera systems, but also because it is the site of (1) large deposits of mercury–including the largest producing deposit in North America; (2) a potentially commercial uranium deposit (buried under 30 m of lake sediments) plus other uranium occurrences; and (3) extensive lithium mineralization.

In 1979, samples of soil, wood, and soil gases from sagebrush were collected along traverses across the Aurora prospect; gross gamma activity along the traverses was measured also. None of the constituents determined in the soils, except for mercury, and none of those determined in the soil-gas samples (H_2, H_2S, CO_2, CH_4) were present in higher than normal concentration over the buried deposit; gross gamma activity also remained constant over the lengths of the traverses. Also, neither lithium and molybdenum in the soils and sagebrush, nor fluorine in sagebrush showed evidence of the presence of the deposit. But uranium in the sagebrush wood and, to a lesser extent, mercury in both sagebrush and soils showed increases over the deposit. The amount of uranium in sagebrush may be an effective guide in exploration for buried uranium deposits.

Uranium ore-forming processes

Literature search and studies by H. C. Granger and C. G. Warren showed that the ore zones richest in vanadium in Plateau-type vanadium-uranium ores are characterized by extensive replacement of quartz-sand grains by vanadium-clay minerals. These clays contain only about half as much silica as does the quartz on a volume-for-volume basis; and as there is no reason to believe that waters percolating through these chert- and quartz-rich host sandstones were ever undersaturated in silica with respect to quartz, it seems to require the solution of quartz in a silica-saturated or supersaturated environment. A possible explanation might be pressure solution of the quartz because many of the recognized characteristics of pressure solution such as microstylolites, clay minerals, and cuspate corrosion are present. However, ghost grains of rounded detrital quartz completely replaced by clay minerals and set in an interstitial matrix of clay can occur adjacent to quartz grains showing no evidence of replacement. The clay and original ghost show no flattening or evidence of pressure. Some partly replaced quartz grains are replaced along all margins rather than just at grain contacts as is usual with pressure solution. Granger and Warren have not determined whether they are working with an unusual manifestation of pressure solution or an entirely new process, but they are satisfied that simple conventional chemistry alone was not responsible for the replacement features.

Age of uranium mineralization at the Midnite mine, Washington

Uranium ores at the Midnite mine near Spokane, Wash., occur in phyllites and calc-silicate rocks of the Proterozoic Y Togo Formation, near the margins of anomalously uraniferous porphyritic quartz monzonite of Late Cretaceous age. The present geometry of the ore zones is tabular with thickest zones above depressions in the pluton country rock contact. Analyses by K. R. Ludwig, J. T. Nash, and C. W. Naeser of high-grade ores from the mine define a $^{207}Pb/^{204}Pb$–$^{235}U/^{204}Pb$ isochron indicating an age of mineralization of 51.0 ± 0.5 m.y. This age coincides with a time of regional volcanic activity (Sanpoil Volcanics), shallow intrusive activity, erosion, and faulting. Uranium-thorium-lead isotopic ages of zircons from the porphyritic quartz monzonite in the mine indicate an age of about 75 m.y.; hence, the present orebodies were formed about 24 m.y. after its intrusion. The 52-m.y. time of mineralization probably represents a period of mobilization and redeposition of uranium by supergene ground waters, perhaps aided by mild heating and ground preparation and preserved by a capping of newly accumulated impermeable volcanic rocks. It seems most likely that the initial concentration of uranium occurred about 75 m.y. ago, probably from relatively mild hydrothermal fluids in the contact-metamorphic aureole of the uranium-rich porphyrite quartz monzonite. Pitchblende, coffinite, pyrite, marcasite, and hisingerite are the most common minerals in the uranium-bearing veinlets, with minor sphalerite and chalcopyrite. Coffinite with associated marcasite is paragenetically later than pitchblende, though textural and isotopic evidence suggests no large difference in the times of pitchblende and coffinite formation.

The uranium-lead isotope systematics of total ores and of pitchblende-coffinite and pyrite-marcasite separates show that whereas open-system behavior for uranium and lead is essentially negligible for large (200–500 g) ore samples, lead migration has occurred on a scale of 1–10 mm out of pitchblende and coffinite and into daughters of ^{238}U (probably ^{222}Rn) has occurred on scales of from 100 cm to 20 cm. The isotopic composition of unsupported radiogenic-lead in pyrite-marcasite seems to depend on the mineralogical microenvironment of the grains so that the radiogenic-lead in pyrite marcasite intimately intermixed with pitchblende-coffinite tends to be deficient in ^{206}Pb, and the radiogenic-lead in pyrite-marcasite in gangue tends to have excess ^{206}Pb. These systematics probably reflect differences between the average distances of lead and ^{222}Rn diffusion since the formation of the ores.

Characteristic differences in Texas roll-type uranium deposits

Studies by R. L. Reynolds and M. B. Goldhaber indicated that a roll-type uranium deposit hosted by the Eocene Jackson Group in Karnes County, Tex., differs in some fundamental geochemical and mineralogic characteristics from uranium deposits hosted by the Miocene Oakville Sandstone in nearby Live Oak County. Reduced sandstone of the Karnes deposit is characterized by the presence of organic carbon and low-sulfur content (<1 percent), and by light sulfur isotopic compositions ($\delta^{34}S$) averaging about −14 permil. Pyrite, the dominant iron disulfide (FeS_2) mineral, occurs commonly as framboids and as replacements of plant fragments and is generallly sparse throughout ore and barren reduced ground. In contrast, the Oakville host beds are virtually devoid of organic matter and contain substantially more sulfur (up to 4 percent) than do host beds for the Karnes deposit. Moreover, the Oakville deposits are characterized in ore and reduced barren ground by abundant ore-stage marcasite ($\delta^{34}S$ as light as −46 permil). An extrinsic sulfide source–fault-leached H_2S–played an important role in localization of the Oakville deposits. Although the Karnes deposit is located near faults and wells that produce oil and sour gas, the deposit lacks geochemical and mineralogic properties, indicating that it formed and (or) was preserved under conditions related to fault-leaked H_2S. Mineralization in the Karnes deposit, rather, appears to have been controlled by intrinsic reductants related to biologic processes.

GEOTHERMAL RESOURCES

Tectonic influences on hydrothermal and magmatic systems in the Geysers–Clear Lake region, California

The Geysers–Clear Lake region is the locus of active volcanism in the Coast Ranges of California and is the site of the largest developed geothermal field in the world. J. M. Donnelly-Nolan, R. J. McLaughlin, and B. C. Hearn, Jr., reported that a shallow silicic magma chamber heated from below by mantle-derived melts underlies the dominantly silicic Clear Lake Volcanics and provides the heat for the accompanying geothermal system. Geophysical evidence for the magma reservoir includes lack of seismic events deeper than 5 km, large P-wave delays, and a circular 30-mGal negative Bouguer gravity anomaly. The hydrothermal systems in the Geysers–Clear Lake region are supplied by varying proportions of meteoric, evolved connate, and metamorphic water. There is no evidence for magmatic water. On the eastern and southeastern periphery evolved connate water plays a larger role, and the high chlorine ion content may have facilitated deposition of gold at Wilbur Springs and at the recent Knoxville discovery. Mercury deposits are widespread in the broad area of young volcanism, abundant thermal springs, and high CO_2 discharge. The specific locations of mineral deposits and thermal springs are controlled by abundant young high-angle faults with a dominant northwest trend. The active hydrothermal systems lie within various thrust-faulted terranes of juxtaposed upper Mesozoic rocks having different ages and physical properties, and all are within a wide area of right-lateral shear of the San Andreas system. This soft plate margin is characterized by pull-apart basins and volcanism increasing younger northward. Models for ascent of magmas into the crust include (1) deep extension and pressure release through strike-slip pull-apart; (2) holes in weak crust resulting from the dynamics of an unstable Pacific-Farallon-North American plate junction; (3) a mantle hot spot.

Temperature gradient map of the conterminous United States

Marianne Guffanti and Manuel Nathenson constructed a preliminary temperature-gradient map of the conterminous United States. The map, which is contoured, displays temperature gradients that can be expected to exist regionally in a conductive thermal regime to a depth of 2 km. Gradients were determined directly from published temperature-depth data for drill holes generally deeper than 600 m. The map will be used in the USGS assessment of low-temperature geothermal energy. A temperature-gradient map of North America was constructed by the AAPG and USGS (1976) using gradients calculated from average annual air temperatures and bottom-hole temperatures for thousands of oil, gas, and water wells. A major difference between the two maps occurs in some central states where the AAPG–USGS map does not indicate a transition between colder eastern and warmer western thermal regimes. The new gradient map agrees more favorably with the heat-flow map of Sass and others (1980) in this regard, with low (<1.5 HFU) heat flow in the east, commonly expressed by gradients <25°C/km, and high (>1.5 HFU) heat flow in the west, generally reflected by gradients >25°C/km.

REGIONAL GEOLOGIC INVESTIGATIONS

NEW ENGLAND

IGNEOUS AND METAMORPHIC ROCKS AND GEOCHEMISTRY

Mineralogic and trace-element basis for subdividing the Monson Gneiss, Connecticut

Further work on the geochemistry of the Monson Gneiss of the Killingworth dome area by R. P. Wintsch (Indiana University) supports the conclusion that it does not constitute a single stratigraphic unit. These plagioclase gneisses can be divided on the basis of gross composition into dacitic gneisses at Bronson Hill and andesitic gneisses of the Waterford Group. The rocks of these two sequences differ also in content of trace elements and in composition of intercalated amphibolites. The gneisses of the Waterford can be further subdivided on the basis of amphibolite composition.

The Orrington-Liberty antiform in Maine and its geologic history

The Orrington-Liberty antiform in Maine trends northeast from the vicinity of Portland to the vicinity of Bangor. It is cored by a pre-Silurian terrane that includes the Cushing, Cape Elizabeth, Spring Point, Diamond Island, and possibly the Spurwink Formations that were first defined near Portland (Katz, 1917; Hussey, 1971). The antiform is flanked to the northwest and southeast by a Silurian turbidite section in south-central Maine. The pre-Silurian terrane plunges northeasterly beneath the Silurian section in the vicinity of Bangor.

The Mesozoic, high-angle Norumbega fault system cuts the core of the antiform longitudinally; it extends from Bangor southwestward to Richmond. This fault system, north of Liberty, consists of two parallel faults whose dip separations are such as to produce a grabenlike wedge of Silurian rocks separating pre-Silurian terrane to the northwest and southeast.

The Orrington-Liberty antiform is complexly deformed. Minor structural features indicate that at least one episode of deformation predates and two episodes postdate the time of development of the antiform. The northwest flank of the antiform is broken by a premetamorphic thrust fault that predates development of the antiform. This thrust fault is truncated in the vicinity of Bangor by the Norumbega fault system.

Correlation of metamorphic rocks of the Presidential Range area, Lewiston 2° sheet, New Hampshire

Restudy by N. L. Hatch, Jr., of the metamorphic rocks of the Presidential Range area of northeastern New Hampshire mapped as Littleton Formation by Billings supports previously hypothesized correlations with sections established to the northeast by R. H. Moench and to the south by J. B. Lyons of Dartmouth College. At the base, the section is well-bedded, gray, nonrusty quartzite, grit, pelite, and conglomerate. Next above is a very rusty, flaggy, hard, sulfidic, biotitic calc-granulite, succeeded by green, white, and tan nonrusty calc-granulite previously mapped as the "Boott Member" of the Littleton. At the top of the section is a gray-brown, medium-bedded, nonrusty pelite and granulite with local coticule overlain by gray, thicker bedded ex-andalusite schist and biotitic quartzite. Graded beds confirm the sequence—the "Boott Member" and lower units, which are at least a thousand meters thick. Proposed correlations are

Central New Hampshire	Northeastern New Hampshire	Western Maine
"Kearsarge Member"	Thick pelite + quartzite	Seboomook Formation
Littleton Formation	Pelite, granulite + coticule	"Carrabassett Formation"
"Warner Formation"	Calc-granulite ("Boott Member")	Madrid Formation
"Francestown Formation"	Rusty granulite	Smalls Falls Formation
Metapelite		Perry Mountain Formation
	Quartzite + conglomerate	Rangley Formation

These correlations and the presumed Silurian age for the Rangeley, Smalls Falls, and Madrid imply abrupt eastward thickening of the Silurian section across New Hampshire from the Bronson Hill area and a southwestward extension of the Silurian tectonic hinge line previously described from western Maine. The apparent absence of the Perry Mountain Formation from New Hampshire could be tectonic or stratigraphic.

GLACIAL GEOLOGY

Glacial Lake Hitchcock, an ice-marginal water body in Long Island Sound

The presence of a large ice-marginal water body in Long Island Sound was suggested by several workers. Data on glacial deltas in south-central Connecticut compiled by J. R. Stone support the presence of such a lake, and indicate that its water plane reached an elevation of about 6 m above present sea level at New Haven.

Because of the concavity of the shoreline toward open water to the south and the southward slope of the water plane (estimated at 0.5 m/km), the zero isobase intersects the shoreline at about Fairfield and Guilford, and only between those points does it lie above present sea level.

The great delta in glacial Lake Hitchcock at the mouth of the Farmington River consists of three segments. The highest segment appears to have been built by ice-contact drainage at a time when the lake extended west through Tariffville gap into the Farmington River valley, and there controlled the level at which other deltaic deposits were being formed. The other two segments were built by the Farmington River to successively lower levels of Lake Hitchcock, the lower of which is consistent with the present floor level of the New Britain spillway.

Connecticut surficial materials map

The surficial materials map of Connecticut, partly compiled by J. R. Stone, J. P. Schafer, E. B. H. London, and W. B. Thompson, is a companion to the surficial geologic map, and is based on that map as well as extensive data on surface and subsurface materials. Most of the map units bear "sandwich" symbols that indicate not only the main materials at the surface (gravel, sand, fines, and others), but also one or more subsurface units. Coarser material overlying finer was a result of deposition in extensive glacial lakes. The reverse relation (coarser underlying finer) is much less common but is locally important as such sequences are a source of ground water. The morphosequence concept provides an important rationale for interpreting the textures of the stratified glacial deposits.

Stratified glacial deposits in Connecticut and their relation to the morphosequence concept

Parts of the surficial geologic map of Connecticut at scale 1:125,000 were compiled by J. P. Schafer, J. R. Stone, E. B. H. London, W. B. Thompson, and W. H. Langer. The accumulated information confirms the productive character of the morphosequence concept as the basis for depiction of the stratified glacial deposits. Successive morphosequences mark successive positions of retreating ice margins and reveal close relation with topography. Comparison of the successions of morphosequences to a generalized curve of ice retreat compiled by J. P. Schafer indicates that retreat northward across the State took about a thousand yr, and that morphosequences were deposited at spacings of perhaps 1 to 4 km or 10 to 75 yr.

Deglaciation and ice-margin retreat of the late Wisconsinan Laurentide ice sheet in Massachusetts

In the compilation of the new Massachusetts State surficial geologic map by B. D. Stone, F. D. Larsen, C. R. Warren, R. N. Oldale, and J. D. Peper, a stratigraphic framework of over 200 map units was established. The resulting map revealed a regional correlation of deglaciation events and a pattern of ice-margin retreat of the late Wisconsinan Laurentide ice sheet. Although upper Wisconsinan till covers about 63 percent of the State, the chronologic framework of ice retreat was established by meltwater deposits. Locally, small moraine segments, isolated high-level kames, and minor readvance features establish the deglacial history. Glaciolacustrine units constitute three-fourths of the total meltwater deposits by area and cover 28 percent of the map area. Glaciofluvial units cover 7 percent, and moraines and glaciomarine units each cover about 2 percent of the map area.

Preliminary synthesis of regional correlations, based on chronology of meltwater deposits, moraines, and ice flow-direction indicators, showed that major topographic features strongly influenced the pattern of retreat across the State of the Laurentide ice sheet. Five glacial lobes formed in lowland areas during thinning and melting back of the ice. During the early stages of ice retreat in southeastern Massachusetts, the Buzzards Bay–Narragansett Bay lobe, Cape Cod Bay lobe, and Great South Channel lobe developed in lowland basins, which were progressively lower in altitude and were larger to the east. Successive overlap of younger deposits to the east indicates that Great South Channel lobe, which occupied the lowest and largest basin, produced sediments that were deposited in plains of the outer cape after the Cape Cod Bay lobe had retreated from most of the bay. North of this area, successive ice-margin positions of the eastern Massachusetts lobe, the Connecticut valley lobe, and the Hudson valley lobe are marked chiefly by ice-margin dams which temporarily impounded numerous proglacial lakes in lowlands across the State.

Lake Passaic sediments and their implications as to gelogic history

Initial coring operations in the Great Swamp basin of Glacial Lake Passaic, northern New Jersey, yielded a nearly complete vertical sequence of lake-bottom sediments at a drill site 8 km south of the late Wisconsinan glacial terminal position. The core, sampled by D. W. Duty, M. J. Pavich, and B. D. Stone, contains 4.1 m of irregularly laminated and deformed silt, clay, and

sand overlying 18.9 m of regularly spaced, alternating silt and clay laminae, which overlie 6.1 m of irregularly laminated silt and clay. Silt-clay couplets of the middle unit, studied by G. E. Reimer and G. M. Ashley, average 3.1 cm thick; clay layers are from 1.5 to 4 times the thickness of superjacent silt layers. When interpreted as varves, these rhythmites indicate a minimum of 600 yr of glacial damming of Lake Passaic during the late Wisconsinan glacial maximum.

SOUTHERN APPALACHIAN HIGHLANDS AND COASTAL PLAINS

PENNSYLVANIA TO ILLINOIS

Thrusting of Proterozoic and lower Paleozoic rocks along the northwestern edge of the Reading prong

Mapping along the northwestern edge of the Reading prong of northern New Jersey and adjacent Pennsylvania reveals regional thrust sheets involving both Proterozoic gneisses and lower Paleozoic carbonate and clastic rocks. The Paleozoic rocks are found both stratigraphically coupled with underlying gneisses and separated from them by a single thrust fault or an imbricate stack of thrusts. The gneisses have a distinct magnetic signature distinguishing them from the weakly magnetic cover rocks. An abrupt drop in magnetic intensity at the northwestern limit of outcropping Proterozoic rocks indicates that these rocks do not extend under the Paleozoic rocks of the Great Valley; and, in fact, are thrust over them as seen in the field.

Two high magnetic anomalies of regional extent northwest of the exposed Proterozoic rocks are interpreted as indicating buried thrust sheets of Proterozoic gneiss. The Catasauqua anomaly was interpreted by Drake (1978) as reflecting the Proterozoic core of the Lyon Station–Paulins Kill nappe at 1.6 km below the surface. A second aeromagnetic anomaly exists farther northwest, near the position of outcropping Silurian rocks between Kingston, N.Y. and Little Gap, Pa. This anomaly was modeled under the assumption that Proterozoic gneisses are the magnetic source. The model suggests a folded southeast-dipping thrust sheet of Proterozoic gneisses at a depth of from 3 to 4.5 km. Seismic data to the southwest in Pennsylvania indicate that autochthonous basement lies below 12 km. It was concluded, therefore, that outcropping Proterozoic gneisses, the buried core of the Lyon Station–Paulins Kill nappe, and the buried Kingston–Little Gap thrust sheet are tectonic slices that have been ramped off the basement along major thrust faults.

Delineation of the northern edge of the Tully Limestone in northwestern Pennsylvania

J. B. Roen reported that the question regarding the presence of the Tully Limestone in the subsurface of northwestern Pennsylvania has been resolved. The assignment of the uppermost Middle Devonian limestone that underlies the equivalents of the Genesee and Sonyea Formations of Late Devonian age in the subsurface of northwestern Pennsylvania has been a controversy since the records of oil and gas wells facilitated the projection of the Devonian stratigraphy from the outcrop in central Pennsylvania and New York westward into the subsurface. Stratigraphic studies based on well records and cuttings have presented opposing views. Jones and Cate (1957) believed the Tully Limestone to be present in northwestern Pennsylvania. The work of Piotrowski and Harper (1979) supports that view. It shows the Tully Limestone to be present throughout all of western Pennsylvania, except for the western part of Mercer and Lawrence Counties and parts of McKean and Warren Counties. Their conclusions are based on a gamma-ray well-log study projected from the outcrop of the Tully Limestone in central Pennsylvania to the subsurface in Erie County. They could find no reason for the Tully not to be present in northwestern Pennsylvania.

On the other hand, Wright (1973), Roen, Wallace, and deWitt (1978a, 1978b), and Wallace, Roen, and deWitt (1977) prepared gamma-ray log cross sections and concluded that the Tully Limestone is not present in the northwestern counties of Pennsylvania. They believed the limestone in question to be older than the Tully and of late Hamilton age. Recently A. G. Harris examined the conodonts from core samples of the questioned stratigraphic interval collected by Roen from the Monsanto Research Corporation, Presque Isle State Park EGSP PA 3 well in Erie County, Pa. In the terms of central New York stratigraphy, Harris reported that the conodonts represent a stratigraphic interval below the Tully Limestone and above the Cherry Valley Limestone Member of the Marcellus Shale. The conodonts identified are from the Varcus zone and are of late Middle Devonian age, probably earliest late Middle Devonian. Interpretation by Roen of surface and subsurface data from the outcrop belt of the Tully Limestone in Tompkins County, N.Y., to the Presque Isle State Park well in Erie County, Pa., concurs with Harris' conodont study and further suggests that the limestone in question is the Tichenor Limestone Member of the Ludlowville Formation and in part may contain beds of the older Centerfield Limestone Member of the Ludlowville. The presence of the Centerfield Limestone

Member is in agreement with earliest late Middle Devonian age suggested by Harris.

In summary, the Tully Limestone is not present northwest of Beaver, Butler, Clarion, Elk, and McKean Counties in northwestern Pennsylvania, and those beds previously thought to be Tully are the older Tichenor Limestone Member and possibly the Centerfield Limestone Member of the Ludlowville Formation.

Distribution of Devonian algae, *Foerstia*, in the Appalachian and Illinois basins

The fossil algae *Foerstia* had been reported from the west side of the Cincinnati arch by Hoskins and Cross (1952). They did not note its stratigraphic position in the Devonian sequence, nor could their localities in the Illinois basin be recovered. Recently, however, R. C. Kepferle (USGS) and J. G. Beard (Kentucky Geological Survey) rediscovered the *Foerstia* zone in the Illinois basin. The algal remains were found in an outcrop and in a drill core from the south side of Buttonmold Knob, a few miles south of Louisville, Bullitt County, Ky. At this locality, the *Foerstia* zone occurs about 2 m below the top of the Clegg Creek Member of Lineback (1968), the uppermost member of the New Albany Shale. Rediscovery of this stratigraphic zone containing *Foerstia* revises an earlier correlation and provides a stratigraphic datum for future correlations of units between the New Albany Shale of the Illinois basin and the Chattanooga and Ohio Shales of the Appalachian basin. The previous correlation of the Devonian shale sequence between the two basins was based on the lithologic similarity of the Three Lick Bed of the Ohio Shale of the Appalachian basin to the lower part of the Camp Run Member which underlies Lineback's Clegg Creek Member of the New Albany Shale in the Illinois basin (Provo and others, 1978, p. 1708).

The position of Three Lick Bed, which occurs above the *Foerstia* zone throughout the Appalachian basin and the Cumberland sag invalidates the correlation of the Three Lick Bed with Lineback's (1968) Camp Run Member of the New Albany Shale. In addition, the Three Lick Bed could not be recognized in the upper 2 m of Lineback's Clegg Creek Member. These data support the contentions of Griffith (written commun., 1977) and Jordan (written commun., 1979) that the Three Lick could not be recognized much beyond the Cincinnati arch in the Illinois basin. Also the rediscovery and stratigraphic placement of *Foerstia* enlarges the extent of a datum for detailed stratigraphic correlations of the black shales of Devonian age between the Appalachian and Illinois basins.

Tentative conclusions based on the relative stratigraphic position of *Foerstia* in the two basins are (1) that the depositional history of the Illinois basin was different from that of the Appalachian basin through much of the Late Devonian, and (2) that the Cincinnati arch, although not necessarily emergent during this time, was a barrier between two independent euxinic basins in which the sedimentation patterns differed.

Correct application of the term "bentonite" to Devonian black shales in the Appalachian basin

Recent studies by J. W. Hosterman and J. B. Roen on the Devonian black shales and associated rocks of the Appalachian basin indicate that the term "bentonite" has been misused in its application to the stratigraphic nomenclature. The Tioga Bentonite Bed is found near the contact between the Onondaga Limestone and Marcellus Shale of the Hamilton Group. The Belpre Bentonite occurs near the base of the Rhinestreet Shale Member of the West Falls Formation. The Center Hill Bentonite Bed is in the upper unit of the Dowelltown Member of the Chattanooga Shale and in the Pipe Creek Shale Member of the Java Formation. These beds are composed of degraded and disordered (Md) illite, kaolinite, and illite-smectite mixed-layer clay. Smectite is a minor constituent in several samples. Bentonite was proposed originally for a soft, soapy-feeling unusually absorbent clay which is composed chiefly of smectite. Because of these unique properties of smectite, bentonite has a high commercial value and a definite meaning in industry.

Because of the obvious mineralogical and physical properties, the established commercial meaning, and the definition that requires smectite to be the major constituent of bentonite, it is recommended that the Devonian bentonite beds be known as Tioga Ash Bed, Belpre Ash Bed, and Center Hill Ash Bed.

Mineralogy of Devonian black shales in the Appalachian basin

A detailed mineralogical study of more than 2,100 samples from 84 drill holes representing 11 units of Devonian black shale in the Appalachian basin has produced some new data, which are summarized in a report by J. W. Hosterman and S. I. Whitlow. The shale is composed of 2M illite, chlorite, mixed-layer clay minerals, and occasionally kaolinite. Quartz and pyrite are usually present, and calcite occurs only in the older units. The 2M illite was derived from degraded and disordered (Md) illite and smectite; chlorite was also derived from smectite; illite-smectite mixed-layer clay was formed from a mixture of Md illite and smectite; and illite-chlorite mixed-layer clay was also formed from Md illite and smectite. Kaolinite, found only in the younger units in minor quantities, is probably the only original detrital clay mineral. The nondetrital quartz resulted from the

formation of the above minerals in the reaction—smectite + $Al^{+3}+K^{+}$ = illite + chlorite + quartz.

Although the shale contains occasional traces of sulfides (galena and chalcopyrite) and sulfates (barite and gypsum), there is no evidence to indicate the existence of a large disseminated mineral deposit. The organic content of the shale can be estimated from the Munsell color value if the amount of calcite is known. For example, a shale with a Munsell color value of 3.5 contains about 12 percent organic carbon if it has more than 5 percent calcite, but with less than 5 percent calcite the same color shale contains only about 4 percent organic carbon. The presence of kaolinite indicates that the source area, during Devonian time, was to the east and northeast of the basin of deposition. The crystallinity variation of the 2M illite supports the conodont color alteration index and indicates that the intensity of low-grade metamorphism increases to the northeastern part of the Appalachian basin.

VIRGINIA

Proterozoic geology of the Blue Ridge province, Marshall and Rectortown 7½-minute quadrangles, Virginia

The Protozoic Y Catoctin Formation (metabasalt breccias and flows) seems to overlie comformably the Fauquier Formation of Furcron (1939) (meta-arkosic sedimentary rocks) in the Marshall quadrangle, Va., according to G. H. Espenshade. Thin, lenticular beds of arkosic quartzite occur at several horizons within the Catoctin. These relations suggest that Catoctin volcanism began suddenly (ending sedimentation) and that eruptions were rapid except for brief periods when Fauquier-like sedimentation was resumed. The Catoctin metabasalts in this region form two chemical suites: a low titanium-high magnesium suite, and a high titanium-generally low magnesium suite. A zone of basaltic breccia, as much as 1000 m thick in the lower part of the Catoctin, belongs to the low-titanium suite. An overlying zone of breccia (of different aspect), perhaps as thick as 900 m, belongs to the high-titanium suite; metabasalt flows above and below the breccia zones, as well as metadiabase dikes, also belong to the high-titanium suite. The breccias, according to R. L. Smith (oral commun., 1980), appear to be agglutinates formed by lava spatter from fissure eruptions. A Proterozoic Z normal(?) fault that occurred at about the start of Catoctin volcanism has been recognized; this fault may have been reactivated during the Alleghanian orogeny in the late Paleozoic.

Petrology of the "Lahore" complex and Ellisville pluton, composite granitoid bodies in the Piedmont of Virginia

Geologic mapping in the Mineral and Lahore quadrangles, Va., by Louis Pavlides and S. L. Cranford indicates that the Ellisville granitoid mass consists of at least two distinct compositional and tectonic bodies, both of which are composite. The older body, in the northwestern part of the mass, is composed of hornblende- and pyroxene-bearing alkali granite and of biotite-hornblende diorite that form an oval-shaped mass, herein named informally the "Lahore" complex, and that partially encloses a smaller serpentinite body at its northern end. The serpentinite of the "Lahore" complex is interpreted to have been intruded and enclosed by the granitoid mass of the "Lahore" prior to the formation of the melange. The rocks of the "Lahore" complex have the same foliation and magnetic signature as the enclosing polydeformed schists, but they have a more distinctive, positive aeroradiometric imprint than the enclosing schist or the granitoid mass to the south. The large granitoid pluton to the south of the "Lahore" complex intruded the schist terrane as well as the "Lahore." The name Ellisville pluton is restricted herein to this composite pluton. The oldest granitoid recognized thus far in the interior of the Ellisville is a coarse-grained porphyritic biotite monzonite with local flow foliation; and it contains macroscopic well-formed epidote and sphene. A fine-grained biotite monzonite cuts the porphyritic monzonite. Locally, leucocratic granite occurs along the margins of the Ellisville pluton.

Based on geologic and geophysical features, the Ellisville pluton is considered to be an intrusive mass emplaced within a melange terrane (Pavlides, 1979) in the Piedmont of Virginia. The "Lahore" complex with its serpentinite inclusion may be an olistolith within the melange. The mafic-ultramafic rootless masses of Green Springs, Diana Mills, and Buckingham, also may be large olistoliths near this melange zone, which is probably coeval with the Baie Verte–Brompton Line of the northern Appalachians.

Structural framework of the Allegheny front in southwestern Virginia

Reconnaissance of structures along the Allegheny front in southwestern Virginia and southeastern West Virginia by R. C. McDowell suggested a new interpretation of the Hurricane Ridge syncline in the juncture zone of the southern and central Appalachians. Instead of curving northward as shown on existing geologic maps, with the southern Appalachian trend gradually changing to a central Appalachian trend, the axis of the

overturned syncline continues northeastward roughly parallel to the St. Clair thrust and appears to "cut off" or override the southern noses of gentle central Appalachian folds. This relation implies that development of the Hurricane Ridge syncline and St. Clair thrust postdate formation of the central Appalachian folds that lie to the northwest.

Geologic evidence of Cenozoic tectonism in the Rappahannock River basin, Virginia

Mapping of Cretaceous and Tertiary stratigraphic units along the Fall Line zone of the Fredericksburg, Va., area by W. L. Newell documented a complex zone of high-angle, northeast-trending reverse faults that juxtapose Paleozoic metasedimentary rocks and Cretaceous and Cenozoic sediments. The reverse faults indicated a regional northwest-southeast compressive stress field with a left-lateral strike-slip component of movement. Thicknesses and spatial distribution of stratigraphic units indicated that fault movement has been sequential and cumulative.

Distribution of younger strata coastward from the Fall Line zone, particularly in the central Rappahannock estuary, suggests that fluvial, estuarine, nearshore-marine, and marine-shelf depositional environments were influenced by sub-Coastal Plain tectonics. East of the Fall Line zone, facies relation and structure contours on the bases of units document a northeast-trending hingeline. Superimposed across this hingeline are southeast-trending troughs. Structure contours on bases of succeedingly older units indicated increasingly steeper gradients across the hingeline and increasing closure on the southeast-trending troughs. The hingeline and troughs are probably underlain by faults that offset Cretaceous and lower Tertiary strata.

Evidence of Quaternary deformation is sparse and subtle. Movement on subsurface structures influenced erosion of upland areas and deposition of surficial deposits in estuarine and peri-estuarine environments adjacent to the upland source areas. The Pliocene to Holocene evolution of the Rappahannock River estuary integrates the effects of tectonism, fluvial to marine depositional processes, weathering and erosional processes, and changing sea levels. Orientation of valley reaches and facies relations of the enclosed deposits indicates response to passive control by the structural and stratigraphic framework, to active control by local and regional uplift, and to glacio-eustatic sea-level changes.

Geologic interpretation of a new simple Bouguer gravity map of the Culpeper basin, Virginia

A new simple Bouguer gravity map of the Triassic-Jurassic Culpeper basin and the adjacent crystalline rock terrane indicates that Mesozoic sedimentary rocks in the basin have only slight effects on the observed anomalies, according to A. J. Froelich. The principal anomalies apparently are caused by the underlying pre-Mesozoic rocks and Jurassic igneous rocks, except in the thickest west-central part of the basin where sedimentary rocks contribute to a weak negative anomaly.

Preliminary calculations of thickness of basin fill from gravity data in the deepest part of the basin indicate a probable maximum thickness of 2 to 3 km. Steeply dipping belts of pre-Mesozoic rocks along the northern part of the basin produce strong alternating linear positive and negative anomalies that extend beneath the basin for tens of kilometers. The basin follows the regional trend of the older rocks in the north, but in the south it cuts abruptly westward across the regional strike. In the south the anomalies associated with pre-Mesozoic rocks can be traced across the basin, which they separate into two subbasins. Jurassic basalt flows and diabase intrusive rocks produce positive gravity anomalies in the northern subbasin; in the southern subbasin, where basalt is absent and diabase constitutes most of the basin fill, the associated positive anomalies are even more pronounced. Steep, north-trending gradients within the basin correspond with contacts between concealed contrasting basement units, intrusive rocks, concealed faults, or combinations of these features.

Evolution of karst terrain in the northern Shenandoah Valley of Virginia

K. Y. Lee reported that in the northern Shenandoah Valley of Virginia, dolines and ponors evolved from limestone and dolomite containing shale, siltstone, and sandstone and have relatively larger values of elongation and relief ratio than those from dense pure limestone and dolomite. The long axes of depressions are generally in the direction of major structural trends. Most deep dolines and ponors are located on uplands near the Shenandoah River and its major tributaries. The dolines are filled with a variety of surficial materials. In areas of limestone and dolomite, as well as areas of limestone and dolomite mixed with other types of rocks, the stratigraphy of the fills is similar. Clayey silt with quartz and quartzite granules, 0.9 m or less thick, is on top. In sinkholes adjacent to major streams, the material in this zone is coarser and thicker. In the center of the depressions, the clayey silt grades downward into alternating sequences of sand and gravel, silt and clay, sand, and gravel. These deposits are as much as 6 m thick in depressions in dolomite and limestone and 5 m in limestone and dolomite mixed with other rock types. The deposits lie on weathered bedrock at the bottom of the sinkhole.

Variable climatic conditions during deposition are indicated by 1 to 3 m of terra-rosa and brown residual clay mantling the limestone and dolomite. About 10 m of yellowish-orange residual clay cover the limestone and dolomite mixed with other rock types.

Relations between Quaternary boulder streams and bedrock, Giles County, southwestern Virginia

Studies of boulder deposits in southwestern Virginia by H. H. Mills have resulted in new information on their origin. Boulder streams in first-order valleys on the flanks of mountains in Giles County have been subdivided into three types on the basis of morphology and sedimentology. Boulder transport for these streams has been traced to either gravity processes, catastrophic floods, or gelifluction-frost heave. Thus, at least some of the boulder streams are apparently relics of Pleistocene events.

Relations between boulder streams and the underlying bedrock suggest that slope retreat occurs by a process of topographic inversion similar to one proposed in 1940 by Kirk Bryan. Armoring of the floors of hollows on the mountain flanks by resistant boulders causes erosion to attack the shale bedrock at the margins of the boulder streams. Thus, the noses between hollows are eventually removed by lateral migration of the hollows, and the original hollows now become noses. The process is repeated through time. This mechanism overcomes the difficulty, in the original concept, of establishing hollows on noses.

Post-Pliocene downcutting in the Potomac River valley

Profiles of major rivers in Maryland and Virginia are generally closely adjusted to the resistance of the rocks over which they flow, but they show major discontinuities at or just above the Fall Line, according to a recent study by J. C. Reed, Jr. The amount of discrepancy at the Fall Line between the actual profiles and the projection of the smooth profiles of the upstream reaches increases from about 27 m at the James River to about 50 m at the Susquehanna River. At the Potomac River it is about 45 m. Detailed study of the terraces along the Potomac in the Piedmont above Washington, DC suggests that the discontinuity in longitudinal profile is the result of post-Pliocene downcutting in response to a lowered base level. The change in base level may be due entirely to sea-level fluctuations during the Pleistocene, but strong circumstantial evidence suggests that it may in part be due to differential uplift of the Piedmont with respect to the Coastal Plain along a zone of flexure or distributed faulting near the Fall Line. Rates of differential uplift calculated from inferred ages of fluvial terraces are in close agreement with those inferred from apatite fission track ages.

KENTUCKY

Structural analysis of Kentucky

An interpretive study of the tectonic evolution of central and eastern Kentucky was completed. D. B. F. Black inferred that the region was subjected to multiple periods of compression and extension. The forces resulted in faults and folds in zones of prior structural weakness. Seismic profiles suggest that tilting and blockfaulting in the basement, possibly coincident with Cambrian sedimentation, created the east- to northeast-trending Eastern Interior aulacogen and the southeast-trending Floyd County aulacogen. On aeromagnetic maps, these features appear to be truncated on the southeast by the northeast-trending New York–Alabama Lineament. The lineament's great size, rectilinear pattern, and associated compressional folds may suggest a major lateral component of displacement. Correlation of features across the lineament was not possible so the amount and sense of lateral offset could not be determined.

Regional north-south compression involving basement rock is suggested by several types of evidence to have occurred in Silurian to Devonian time.

There is some suggestion of structural control of sedimentation along the Borden front and elsewhere during the Mississippian and Pennsylvanian. Rocks as young as Pennsylvanian are displaced in a large conjugate fault system in which the major compression was northwest-southeast.

During the Alleghanian orogeny (Pennsylvanian-Permian), northwest directed thrust faulting occurred in the Pine Mountain fault system. This belt directly overlies the fault zone attributed to the New York-Alabama lineament along the line of seismic profile.

Though only approximately located, centers of maximum intensity for historic earthquakes roughly coincide with structurally and geophysically expressed lineaments.

NORTH CAROLINA–SOUTH CAROLINA–GEORGIA–ALABAMA

Geology of the Kings Mountain shear zone, North Carolina and South Carolina

The north-northeast-striking Kings Mountain shear zone, which separates the Kings Mountain and Inner Piedmont belts near the North Carolina–South Carolina

State line, was traced by J. W. Horton, Jr., from the southern border of the Charlotte 2-degree quadrangle near Gaffney, S.C., to the northern edge of the Lincolnton East 7.5-degree quadrangle near Boger City, N.C. The northern end dips to the northwest, and the southern end dips to the southeast. The Blacksburg Schist and Gaffney Marble are truncated by the zone at Gaffney, and ultramafic bodies lie near the western edge of the Kings Mountain belt in the same area. Lenticular bodies of Pacolet Mills metagranite of Wagener (locally mylonitic) lie along and just northwest of the zone southwest of Gaffney. An isolated stock of Cherryville Quartz Monzonite of Late Mississippian age at Sunnyside, N.C. cuts across the Kings Mountain shear zone without unusual deformation; this provides a minimum age for deformation in the zone.

The Kings Creek shear zone, one of the longest of several within the Kings Mountain belt, terminates a few kilometers north of Bessemer City, N.C. A similar north-northeast-striking ductile shear zone was discovererd a kilometer west of Pasour Mountain. Disseminated pyrite is concentrated in layers parallel to the mylonitic foliation, and quartz veins are abundant. The McCarter Hill, Dixon, and Asbury gold mines, and the Oliver pyrite mine lie along this zone.

The north-northeast-striking Boogertown shear zone marks the boundary between the Kings Mountain and Charlotte belts in York County, S.C., and Gaston County, N.C., but it has not been recognized to the north in Lincoln County, N.C. The boundary between the Kings Mountain and the Charlotte belts is poorly defined in that area and appears to be a series of intrusive contacts. The postmetamorphic biotite granite plutons at York and Clover, S.C., lie within a few hundred meters of the Boogertown zone but show no related deformation, suggesting that mylonite formation preceded emplacement of the granites.

Age and tectonic significance of the Orangeburg scarp southwest of the Cape Fear arch, North Carolina and South Carolina

One of the most prominent geomorphic features in the upper Coastal Plain of North and South Carolina is the Orangeburg scarp immediately southwest of the Cape Fear arch. The age of the sediment which lies at the toe of the scarp has been questionable. J. P. Owens reported that cores were drilled near the toe, and fossiliferous samples were obtained from two localities. Planktic forams (N 21), nannofossils (NN 16) and ostracodes suggest an age of about 3.0 m.y. The highest elevation of these 3.0 m.y.-old deposits on the arch is about 75 m above sea level. The Cape Fear arch, therefore, has been uplifted that amount above sea level since 3.0 m.y. ago.

New evidence of two styles and phases of movement along the Brevard zone, southern Appalachians

There have been at least 19 interpretations of the nature of the Brevard zone in the southern Appalachians. Recent geologic mapping by M. W. Higgins and R. L. Atkins showed that rocks of the Sandy Springs Group, previously thought to crop out only northwest of the zone, are also present southeast of the zone northeast of Atlanta, Ga. Drag folding of the Sandy Springs stratigraphic sequence, and of major, tight, moderately to steeply inclined folds in the Sandy Springs rocks, and elongation of two granitic batholiths due to drag, indicate right-lateral strike-slip movement along the Brevard. The displacement of the Sandy Springs units is right-lateral along the zone, with apparent offset of 35 to 40 km. Because of the tightness of the folds in the Sandy Springs rocks, and the thickness of material that has been removed from this area since metamorphism, the offset must be approximately real and not just apparent. The Brevard cannot have had major normal or reverse displacement since deposition of the Sandy Springs Group. Higgins and Atkins suggest that there were two different phases of movement along the Brevard zone; early reverse faulting was followed by strike-slip faulting. Because the same stratigraphic sequence is present on both sides of the Brevard zone, it is suggested that the zone may not mark the boundary between the Piedmont and Blue Ridge, or "Inner Piedmont" and "Northern Piedmont" in Georgia. This invalidates use of the terms "Inner Piedmont" and "Northern Piedmont" in Georgia.

Metamorphism and structure of the Blue Ridge province, Greenville 2° quadrangle, South Carolina and Georgia

Metamorphic rocks of the Blue Ridge province in the northwestern part of the Greenville 2-degree quadrangle are polydeformed, according to A. E. Nelson. Structural data suggest that at least four fold phases have effected the Blue Ridge rocks. First generation folds (F1) are south-facing recumbent isoclines; their axial planes appear to be coplanar with axial planes of some second generation folds (F2). The F2 folds, which are gently plunging vertical to recumbent isoclinal folds with generally northeast-southwest trending areas, are the major northeast-trending regional folds. Tight upright to overturned folds that trend northerly and westerly represent the third fold phase (F3); these folds generally have lower amplitudes and shorter wave lengths than do the F2 folds. The northerly and westerly F3 folds may each represent a separate fold phase, but evidence suggests they are conjugate folds formed during the same deformational

phase. The fourth generation folds (F4) are represented by the broad warping that forms broad shallow structural basins and domes in the study area.

Some of the westerly and northerly F3 folds have a well-developed axial planar slip or spaced schistosity. In many rock exposures, both F3 schistosities are superposed on the earlier regional foliation, and in places one of the two F3 schistosities form the dominant schistosity.

Metamorphism and structure of the Inner Piedmont province, Greenville 2° quadrangle, South Carolina and Georgia

J. W. Clark reported that at least three generations of folds are present in rock of the Inner Piedmont province. The regional schistosity represents the axial plane foliation of F1 folds. This foliation is folded (F2) in places along steep to vertical areas. Subsequent deformation (F3) has produced chevron folds as well as larger folds that can be mapped. Exposed small-scale folds (up to 30 mm in size) seem to reflect the style and type of the larger F3 folds.

Geologic evidence of Tertiary tectonism in South Carolina

Continuing investigations of Tertiary sediments in the subsurface of the Charleston-Summerville area, South Carolina, showed that most major unconformities are surfaces of considerable stratigraphic relief. Physical evidence of faulting in cores and regional stratigraphic syntheses suggest that middle Tertiary tectonism is at least partly responsible for the delineated geometries of subsurface units.

According to G. S. Gohn, Cretaceous sedimentary rocks and Tertiary sediments as young as middle Paleocene (early Thanetian) have regional dips and locally anomalous thicknesses that are compatible with the location and sense-of-motion of northeast-striking, northwest-dipping reverse faults defined by seismic reflection surveys in the Summerville, S.C. area. The subsurface distribution of upper Paleocene to upper Oligocene sediments cannot be easily related to the sense-of-motion on the seismically defined faults. However, in three of four cores taken in the Summerville area, R. E. Weems and E. M. Lemon found through-going, high-angle fractures (faults?) within (2 cores) or at the top (1 core) of middle Eocene limestone sections. The fracture at the middle Eocene–upper Eocene contact is a true fault with a stratigraphic displacement of 0.5 m. The unexpected high incidence of small-scale structures in these cores suggests that the middle Eocene limestone may be pervasively broken in the study area. The apparent restriction of breakage to this limestone may indicate that it is the only Cenozoic unit that is rigid enough to be fractured; other less competent units would, therefore, be expected to deform by folding. Cumulative local effects of sustained movement on Tertiary fault zones should include (in addition to stratigraphic relief caused directly by folding and faulting) overlap of several older units by each younger unconformity caused by local tilting and erosion, localization and stacking of channels, and restricted geometries of units. One or more of these effects have been documented in the study area for nine units ranging in age from late Paleocene to Pliocene.

Evidence present on a regional scale suggests that the middle to late Eocene was a time of increased tectonism. According to Lucy McCartan, J. P. Owens, and D. C. Prowell, previously documented, widespread, small-scale structures in the upper Coastal Plain of South Carolina and a newly discovered fault zone near the Orangeburg scarp at St. Matthews occur in sediments of possible or probable middle Eocene age. Younger units are not as severely deformed. In addition, along the South Carolina and Georgia coastal margins, the Southeast Georgia Embayment can be shown to be principally a middle to late Eocene basin that is not apparent on ispopach maps of older units.

Middle Cretaceous and younger continental to marine sediment in the Coastal Plain of western Georgia

The Coastal Plain section of western Georgia consists of sedimentary rocks of middle Cretaceous and younger age. Most of the units are unconsolidated clastic deposits having continental to open-shelf facies, according to recent work by A. D. Donovan and Juergen Reinhardt. Texturally, these units range from clay and marl to clean sand. Natural erosional processes have formed a 32-km-long northwest-facing cuesta from Georgetown to Brooklyn, Ga. The cuesta is capped principally by residuum of the Clayton Formation (Paleocene) and is underlain by the Providence Sand (Upper Cretaceous). Formation of the cuesta is clearly related to downcutting by streams draining into the Chattahoochee River. Before settlement of this region, the cuesta margin had a relatively stable, steeply sloping, undulatory surface densely covered by pine and some hardwoods. After settlement in the 1820's, much of the primary forest was removed for farming, and gullies began to form locally near the top of the cuesta margin, apparently along natural swales in the topography that concentrated surface runoff. Once initiated, gullies expanded by the combined processes of downcutting and headward erosion. Today, many large gullies and dendritic gully systems can be seen along the cuesta margin.

In a 33-ha area encompassing Providence Canyon State Park, a single drainage system formed since 1850

produced distinct gullies as much as 400 m long, 180 m wide, and 50 m deep. Between 1850 and 1930, accelerated erosion removed an estimated 1.7×10^6 m^3 of sediment from the gullied areas. Using this figure, an average downcutting rate of 21 cm/yr was calculated for the gully system known as Providence Canyon.

Sedimentology and biostratigraphy of the lower Eocene Hatchetigbee Formation, eastern Alabama and western Georgia

The transgressive-depositional cycle of the Hatchetigbee Formation is well exposed in eastern Alabama and western Georgia. Studies by T. G. Gibson showed that in updip areas the formation consists of crossbedded sand, carbonaceous and laminated silt and clay, and massive sand; these sediments represent deposition in marginal marine (lagoonal) through very shallow marine (lower shoreface) environments. The cycle in downdip areas has glauconitic and marly beds at the base overlain by shelly very fine sand and a thin sequence of laminated silt and clay at the top. These strata represent a basal marine transgression followed by a still-stand period of inner shelf deposition, and then a regressive phase of marginal marine deposition.

The updip sections are considerably thicker (as much as 23 m thick) than the downdip (a maximum of 11 m); the thinning downdip apears to be a primary depositional characteristic. The shelly beds downdip are similar lithologically and in age to the Bashi Marl Member of the Hatchetigbee as developed in western Alabama. Based on mapping and stratigraphic relations in the Chattahoochee area, these beds of the Bashi are a downdip equivalent of the entire Hatchetigbee Formation as seen in the updip thicker exposures and are not just a basal member of the formation. Biostratigraphic ranges of calcareous nannofossils and planktonic Foraminifera place the cycle in the lowest part of the lower Eocene (NP 10 and middle of P6), a duration of no more than one million years. This age relation leaves a considerable time gap between the Hatchetigbee and deposition of the overlying Tallahatta Formation which is generally accepted as upper lower and lower middle Eocene.

Petrology and sedimentology of the Upper Cretaceous Tuscaloosa Formation, eastern Alabama and western Georgia

From the Chattahoochee River valley (Lee and Russell Counties, Ala.) in the west to the Ocmulgee River (Bibb County, Ga.) in the east, the Tuscaloosa Formation (Cenomanian, Upper Cretaceous) can be mapped as a single stratigraphic unit (formation) composed of several characteristic lithologies. Juergen Reinhardt reported that at many localities these lithologies are seen arranged into fining-upward sequences or cycles 3 to 6 m thick. From base to top, a cycle typically contains (1) massive or medium to thickly crossbedded, very coarse feldspathic grit to conglomeratic sand, (2) thinly crossbedded to planar laminated, medium- to fine-grained, commonly micaceous sand, and (3) massive to mottled (red-green) clayey silt and silty kaolinitic clay. The base of the cycle is highly irregular; sediment from the underlying lithofacies is commonly incorporated into the basal part of the cycle. Within the cycle, lithologies and primary sedimentary structures (mostly unidirectional crossbeds) generally record an upward decrease in current energy. Sparse leaf accumulations, lignitized wood, and rare networks of backfilled burrows are the biogenic features in the Tuscaloosa Formation; marine invertebrates are found in outcrop and shallow subsurface in part of the Tuscaloosa Group of western Alabama.

Local highs on aeroradioactivity maps coincide with outcropping Tuscaloosa sediments. Field measurements indicate that both reduced and oxidized flood-plain clays produce 13 to 18 μR/hr, and channel bar sands produce a wider range of values (10 to 20 μR/hr), depending largely on sediment sorting and heavy-mineral content. Preliminary chemical studies and spectrometry suggest that gamma radiation in the clays results from the concentrations of both uranium and potassium, whereas thorium accounts for significant gamma radiation in certain sand intervals.

The geographically extensive fluvial facies represented by the Tuscaloosa in the eastern Gulf Coastal Plain suggest considerable relief and probable uplift in the southeastern United States during the Cenomanian, a time of worldwide marine transgression. The formation of an extensive Coastal Plain during this period profoundly affected the composition and supply of sediment along the margin of this basin for the balance of the Cretaceous.

CENTRAL REGION

METAMORPHIC ROCKS

Metavolcanic rocks and massive-sulfide deposits in northern Wisconsin

Metavolcanic rocks that host the economically significant volcanogenic massive-sulfide deposits (Crandon, Flambeau, and Pelican River) in northern Wisconsin are greenschist facies felsic-mafic rocks that appear to occupy structural basins oriented east-west. Small amounts of basaltic amygdaloidal and pillow lava are interbedded with the felsic volcaniclastic rocks. The largest basin is interpreted from geologic and

geophysical data to be about 90 km long and 8 to 12 km wide. Similar metavolcanic rocks have been mapped to the south in Marathon and Eau Claire Counties by the Wisconsin Geological and Natural History Survey. The metavolcanic rocks in both northern and central Wisconsin have been dated by the U-Pb zircon method as being 1,875 to 1,850 m.y. old (Banks and Rebello, 1969; Van Schmus (personal commun.)). They seem to be grossly correlative with the Marquette Range Supergroup in Michigan but have not been traced laterally into sedimentary or volcanic rocks of the supergroup.

Geology of the metamorphic rocks of the Iron River 2° sheet, Michigan-Wisconsin

A map of metamorphic rocks of the Iron River, Michigan-Wisconsin 1×2° quadrangle has been completed by K. E. Wier as part of a CUSMAP study. Compilation of published and unpublished data supplemented by new petrographic study suggested delineation of two metamorphic isograds not heretofore shown on maps of the area. A kyanite zone is present in Proterozoic rocks in the southwestern part of the map area. Kyanite does not occur in the eastern half of the map area where sillimanite and andalusite occur in amphibolite grade rocks. The age of this metamorphism is about 1.9 b.y. (Proterozoic X). In younger Proterozoic Y Keweenawan volcanic rocks, metamorphism about 1.1 b.y., a pumpellyite epidote zone has been delineated. Significantly, this zone coincides with native copper deposits.

GLACIAL GEOLOGY

Glacial geology in the upper peninsula of Michigan and northern Wisconsin

Mapping of glacial deposits in the Iron River 1×2° quadrangle by W. L. Peterson showed that four glacial lobes were active in the area. The westernmost lobe moved southward out of the Lake Superior basin west of the Keweenaw Peninsula. The next lobe to the east, the Keweenaw Bay lobe, moved southwesterly out of the Keweenaw Bay trough, just east of the Keweenaw Peninsula. The third lobe, that to the southeast of the Keweenaw Bay lobe, moved southwesterly across the area between the present Huron Mountains and Marquette, Mich. The fourth lobe, called the Green Bay lobe, moved westward into the quadrangle from the Green Bay lowland. Within the quadrangle, these four lobes were mostly merged into a large ice mass but had independently acting fronts and built end moraines that are in most areas attributable to individual lobes. A complex series of advances and retreats of the various lobes have been determined.

Glacial deposits mapped in the quadrangle are of Woodfordian Age or younger. A string of abutting moraines deposited, apparently simultaneously, by the four lobes has been traced across the quadrangle from the middle part of the western border to the eastern part of the southern border. With some exceptions, these moraines mark the edge of the red drift. That part of these abutting moraines deposited by the Green Bay lobe probably correlates southward into Wisconsin with deposits of red drift that Mickelson and McCartney (1980) tentatively consider to be of "Port Huron" age. Wood, reported by J. T. Hack (1965), in the northern part of the quadrangle, apparently from the youngest till, showed a radiocarbon age of about 10,000 yr B.P., suggesting that glacial ice from the Lake Superior basin entered the quadrangle at that time. The lobe west of the Keweenaw Peninsula advanced south to the Copper Range. The Keweenaw Bay lobe probably built the youngest of three moraines attributed to that lobe at this time.

GEOLOGIC HISTORY

Geologic history of the Mississippi Embayment

A 70-km-wide northeast-trending graben, indicated by displacement of magnetic basement, extends across northeastern Arkansas and southeastern Missouri. It is overlain regionally by marine Upper Cambrian and younger Paleozoic deposits that thicken gradually toward it rather than abruptly into it, suggesting that the yet undrilled graben fill may be Middle Cambrian or older. During late Paleozoic time the graben flexed upward to form a broad southwest-plunging anticline; the anticline and adjacent areas then remained quiet during 100 m.y. of erosion. The resultant erosional surface was depressed to form a south-plunging trough—the Mississippi Embayment, which was filled with marine and nonmarine Cretaceous and younger deposits. The axis of the 300-km-wide embayment crosses the graben at an angle of about 20 degrees.

Local structures that developed in the area after middle Cretaceous time reflect recurrent tectonic and igneous activity along the trend of the graben. In Arkansas, local uplift of Tertiary deposits that overlie the deeply buried Newport pluton at the northwestern margin of the graben is defined by surface and subsurface data; a post-Cretaceous high-angle reverse fault along the southeastern margin is indicated by subsurface data. Geophysical data outline post-Cretaceous faults in the presently seismically active axial portion of the graben.

An ongoing study suggests that there is no evidence to substantiate the existence of formerly mapped post-Cretaceous faults in the upper part of the Mississippi Embayment, which is well beyond the geographic limits of the graben.

ROCKY MOUNTAINS AND GREAT PLAINS

STRATIGRAPHIC STUDIES

American Stratigraphic Code

Revision of the American Code of Stratigraphic Nomenclature is underway by representatives of numerous Canadian, U.S., and Mexican institutions under the auspices of the North American Commission on Stratigraphic Nomenclature, as reported by S. S. Oriel. Objectives are to respond to the needs of rapidly developing new specialties while rectifying deficiencies in meeting the needs of longer established specialties. Innovative approaches are sought toward promulgating new concepts, principles, and practices, which subsequently may be found worthy of adoption by the IUGS Commission on Stratigraphy.

Liaison has been established with appropriate bodies of the UNESCO IGCP and the IUGS Commission.

Completion of an integrated draft of the new Code is anticipated during calendar 1981.

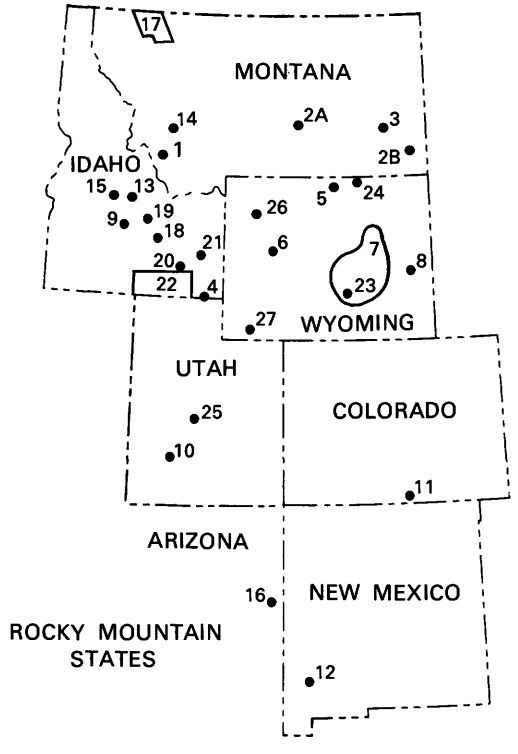

Laramide orogeny timing, Pioneer Mountains, Montana

The youngest sedimentary rock unit mapped in the Vipond Park quadrangle, Pioneer Mountains, Mont. (index map, loc. 1) that predated the Laramide orogeny is a sequence of olive-gray drab-colored fluviatile impure sandstone, argillite, and conglomerate, shale, and volcanic ash, aggregating about 2 km thick, traditionally called the Colorado Group. Knowledge of the younger age limit of this group would define the inception of Laramide orogeny here, but fossils usable for dating have hitherto not been found. A dark-gray shale in the upper member of the unit collected by E-an Zen in 1979 yielded to D. J. Nichols a palynomorph assemblage including the diagnostic mid-Campanian to Maestrichtian forms *Aquilapollenites* sp. *Proteacidites thalmannii*, and *Tricolpites interangulus*. Some of the Colorado Group in the area thus clearly extend into Montana time. This discovery spurred an effort by Zen in 1980 to collect further on a more controlled basis. The youngest sedimentary rocks are overlain by thrust sheets of Proterozoic Y sedimentary rocks, which truncate folded and faulted Phanerozoic rocks and which are in turn intruded by rocks of the Pioneer batholith. Mineral K–Ar and Ar 40/39 ages of Pioneer batholith rocks indicate intrusion during the mid-Campanian-Maestrichtian time. Thus the major events of Laramide orogeny in the Pioneer Mountains apparently were compressed into a brief time span of a very few million years. Early phases of intrusion occurred at a few kilometers depth while a fluviatile depositional system, probably of braided stream, was developing directly above the pluton. This stream system derived its sediments largely from Phanerozoic sedimentary rocks to the west, including upper Paleozoic rocks, fossiliferous cobbles of which are included in the conglomerate of the Colorado Group. The sedimentary cycle was terminated by the movement of allochthonous Proterozoic rocks that destroyed the river system.

Three Proterozoic Y sequences, Pioneer Mountains, Montana

While mapping in the eastern and western Pioneer Mountains, Mont. (loc. 1), E-an Zen recognized that three intergradational lithostratigraphic sequences may be distinguished among the clastic sedimentary rocks of presumed Proterozoic Y age. These rocks are all allochthonous, having been thrust over Phanerozoic sedimentary rocks during the Laramide orogeny. The oldest sequence is characterized by relatively thin bedded, silty to clean, gray to tan quartzite and siltstone that contain sparse detrital feldspar. Mudcracks, "raindrop" impressions, tangential and tabular crossbeds in 10 to 20 cm sets, and wave and current ripple marks including beheaded ripples are abundant and indicate

deposition in a very shallow, at least partly running-water regime. The next younger sequence is dominantly massive-bedded (1–2 m) clean, well-rounded, well-sorted quartzite with little feldspar but with crossbeds and bedding laminations marked by heavy-mineral and clay-rich seams. Internal slumps are common, as are ripple marks. The quartzite is typically light greenish gray, weathers brick red, but light-pink variants appear toward the top of the sequence, and dark steel-blue-gray silty quartzite occurs locally.

The pink quartzite beds grade into the uppermost sequence, which is characterized by pink, salmon, orange, lilac, purple, and maroon highly feldspathic quartzite with mudchip clasts and purple argillite. Cross beds are common, as is coarse polymictic matrix-supported conglomerate dominated by jasper and quartzite clasts.

Units in the three sequences aggregate 3 to 5 km thick and can be assigned to at least two thrust sheets which overlie already folded and faulted Phanerozoic sedimentary rocks as young as late Campanian-Maestrichtian. The thrusting preceded the intrusion of Campanian-Maestrichtian rocks of the Pioneer batholith. Age of the sequences is undefined, but a whole-rock argon 40/39 age determination on an altered mafic dike and a Rb/Sr age determination on a clay gall indicate that the rocks are clearly Precambrian. Paleomagnetic data are being collected in collaboration with D. P. Elston in an effort to obtain independent information on correlation with other sequences of Proterozoic rocks of the northern Rockies.

Holocene eolian features, southeastern Montana

Yardangs, long narrow ridges left by wind erosion, trend southeasterly in and around shale areas exposed in the Porcupine dome and in southeastern Montana (locs. 2a,2b) and indicate severe and continued wind erosion there, according to R. B. Colton. No statistical data have been obtained to show whether wind or water is the dominant erosional process, but the lack of water-eroded channels in many grooves between yardangs suggests that wind erosion may be the dominant process in southeastern Montana. Eolian deposits as much as 4 m thick overlie extensive terrace and fan deposits south of the Yellowstone River and indicate long-continued deposition of silt and sand in areas downwind from areas of wind erosion.

Holocene alluvial features, southeastern Montana

Beaver Flats, 1 to 6 km west of Ekalaka, Mont. (loc. 3), is underlain by thick extensive gravel deposits. Studies by R. B. Colton indicate that fine-to-coarse gravel underlies at least several square kilometers in and around the headwaters of Little Beaver Creek; remnants of these deposits also are scattered along the northwest side of the creek for at least 23 km northeast of Ekalaka. The lithology of well-rounded clasts of quartzitic and igneous rocks suggests that they originated in the Big Horn Mountains. The size of the clasts, as much as 10 cm in diameter, also suggests that a major stream once flowed through the area. The general course of Beaver Creek indicates that the upper part of it was beheaded or captured by the Powder River near the community center of Powderville long ago when the two streams were flowing on a surface 260 m higher than the present Powder River. This figure was determined by subtracting the 900 m altitude of the Powder River at Powderville from the 1160 m altitude at the west end of Beaver Flats. Thus the Powder River has eroded its channel downward at least 260 m since capture occurred. The Powder River now carries gravel of similar lithology to that which underlies Beaver Flats, as well as in several large remnants northeast of Ekalaka. The captured drainage system of upper Beaver Creek includes an area estimated to be 6,000 km^2. The west side of the upper part of the present Powder River drainage basin (the former Little Beaver Creek drainage basin) is the drainage divide of the Bighorn Mountains.

Cambrian-Ordovician relations and paleomagnetics, Bear River Range, Idaho and Utah

An integrated biostratigraphic and magnetostratigraphic study of the St. Charles and overlying Garden City Formations in the Bear River Range, southeastern Idaho and northern Utah (loc. 4), was made in 1979 and 1980 by J. E. Repetski and M. E. Taylor (USGS); S. L. Gillett (State University of New York at Stonybrook), E. W. Landing (New York State Museum and Science Service). Results showed that (1) the Upper Cambrian-Lower Ordovician boundary lies within the upper part of the St. Charles Formation, (2) the sharp contact between coarse-textured, secondary dolomites at the top of the St. Charles and the relatively unaltered lime mudstones and grainstones of the Garden City Formations represents a disconformity. The presence of the disconformity is supported by petrographic evidence and the absence of several conodont subzones at the formational contact. In addition, trilobites from the basal part of the Garden City Formation correlate with the upper *Symphysurina* zone as developed in other parts of the western United States, a correlation which is consistent with the associated conodonts.

Preliminary paleomagnetic data from the St. Charles Formation indicate that this unit is dominantly and perhaps entirely of reversed polarity (declination 179 degrees, inclination −31 degrees), but with much

scatter present. In contrast to this, data from the Garden City Formation show normal polarity (declination 357 degrees, inclination 31 degrees) and are more tightly clustered. The directions obtained are not significantly different from being exactly antipodal, and together they yield a preliminary paleomagnetic pole position at 65 degrees north and 74 degrees east. Age of the magnetization is not well known. A "fold test" shows that the magnetism was emplaced prior to Laramide folding of the Logan Peak syncline. The low inclination yields a paleolatitude of approximately 17 degrees, a position consistent with independent sedimentological evidence for a low-latitude position of the early Paleozoic paleoequator. The change from reversed to normal polarity occurs abruptly at the disconformity between the St. Charles and Garden City Formations and lies within the Lower Ordovician *Symphysurina* zone. Because the paleomagnetic pole position is virtually the same in both formations, it is suggested that the reversed-polarity magnetic signature was imposed on the St. Charles during a time of subaerial exposure and diagenesis prior to Garden City deposition.

Alluvial fan-basin fill relations, Eocene, Powder River and Wind River basins, Wyoming

Eocene alluvial fans along the eastern flank of the Bighorn Mountains bordering the Powder River basin, Wyo. (loc. 5), are being studied by D. A. Seeland. These fans are restricted to a narrow zone a few kilometers wide along the mountain front. Immediately basinward from the fans, the fluvial basin fill consists of a siltstone-coal facies with thin discontinuous sand bodies. The alluvial fans can be correlated spatially with present-day stream valleys that drain the topographically highest part of the range. This correlation suggests persistence of the courses of the major streams since the Eocene.

The segment of the range bordered by alluvial fans also can be identified in the basin-fill sandstones by inflections in the sand-grain shape isopleths; sand grains basinward from the fans are less regular in shape than grains derived from topographically lower parts of the Bighorn Mountains.

Eocene alluvial fans on the Wind River Range margin of the Wind River basin (loc. 6) have an associated sandy facies that extends many kilometers into the basin, rather than terminating abruptly as do the Powder River basin fans. This difference may be explained by the differences in proximity of the structural axes of each basin, the loci of maximum subsidence, to the alluvial fans bordering each basin. These differences in the relations of major sediment source areas and basin axes also may account partially for the presence or absence of uranium deposits adjacent to the various Wyoming uplifts.

Early Tertiary rock volumes, southern Powder River basin, Wyoming

A study of the volume of rock eroded from the Laramie Mountains, adjacent to the southern Powder River basin, Wyo. (loc. 7), since their uplift began in the early Tertiary time, was made by D. A. Seeland and D. J. Hammond. Previous work (Seeland, 1976) showed that a triangular area of the southern Powder River basin bounded by two major rivers of Eocene age has an exclusively southern source and contains nearly all the known commercial uranium concentrations of the basin. The southern source direction precludes the possibility that the host sandstones were deposited by rivers that headed in the Granite Mountains, flowed through the eastern Wind River basin directly across the Casper arch, and into the southern Powder River basin.

It was suspected that the amount of debris shed by the rising Laramie Mountains would be inadequate to account for the volume of Tertiary rocks in the southern Powder River basin. If real, this additional constraint, with assembled paleocurrent data, would provide near-conclusive evidence that the needed additional basin fill was carried by streams that originated in the Granite Mountains and flowed across the Laramie Mountains into the southern Powder River basin, as suggested by the geomorphic characteristics of the Laramie Mountains. The calculations, however, show that the Laramie Mountains could have contributed several times as much lower Tertiary sediment as was deposited in this part of the southern Powder River basin. Therefore the Granite Mountains are not necessarily a source area for these sediments.

In spite of the negative evidence from the sedimentary volume study, however, two lines of evidence still suggest that the uranium deposits of the southern Powder River basin are related genetically to sediment which was deposited from streams that headed in the Granite Mountains and flowed northeastward across the Laramie Mountains. These are the association of several other major uranium deposits with Eocene sedimentary rocks derived from the Granite Mountains and the presence of old stream valleys that traverse the Laramie Mountains.

New Archean stratigraphic nomenclature, Hartville uplift, Wyoming

A new informal nomenclature is proposed by G. L. Snyder for the Whalen Group, an Archean metasedimentary-metavolcanic succession (Snyder, 1979; 1980) in the Hartville uplift of Wyoming (loc. 8). During surface geologic mapping, six newly recognized criteria were used to determine stratigraphic tops. The succession, in descending stratigraphic order, is as follows:

- "Wildcat Hills" unit (top not exposed): siliceous algal dolomite with some interlayered mica schist, amphibolite, and chondrodite dolomite.
- "Silver Springs" schist unit: mica schist and metagraywacke with locally interlayered quartzite, amphibolite, and marble.
- "Mother Featherlegs" metabasalt unit: massive pillowed or amygdular amphibolite with local interlayered schist, metagraywacke, and amphibolite with calc-silicate pods.
- "Muskrat Canyon" unit (base not exposed): tremolite dolomite and algal dolomite with locally interlayered mica schist, graywacke, conglomerate, or quartzite.

Tectonic breccia vs. Hailey Conglomerate Member of Wood River Formation, Boulder Mountains, central Idaho

Mapping and petrographic study in the Boulder Mountains, central Idaho (loc. 9), by W. E. Hall and H. C. Windsor showed that a unit of brecciated rocks as much as 300 m thick originally described by Thomasson (1959) and Bissell (1960) as the Hailey Conglomerate Member of the Wood River Formation of Middle Pennsylvanian age differs in lithology, structural setting, and age from the type Hailey. The breccia in the Boulder Mountains is located within a regional thrust fault zone between the "Salmon River sequence" of Late Mississippian age and the overlying Pennsylvanian and Permian rocks in the Wood River allochthon on the southeast and Permian rocks in the Pole Creek allochthon on the northwest. The breccia zone forms bleached resistant outcrops that locally cut across bedding in both the overlying and underlying allochthons. Clasts in the breccia are mostly irregular angular but locally rounded; they exhibit a pronounced structually alined fabric in which clast boundaries grade into a recrystallized sheared siliceous matrix. Locally, remnant sedimentary bedding structures in the breccia are truncated by shears.

The clasts are argillite and siltite lithologically and texturally similar to the matrix material. Locally the matrix is sheared and recrystallized limestone. Field relations and petrographic studies indicate that this is a tectonic breccia derived primarily from the "Salmon River sequence," and is not equivalent to the Hailey.

Tephrochronology and Tephrostratigraphy of western Utah

The age of basin-fill Cenozoic rocks near Beaver, Utah (loc. 10), ranges from about 3.5 to 0.6 m.y., as reported by G. A. Izett. Dating these rocks reveals the late Neogene tectonic history of the area. The age span of the rocks was determined in three different ways: (1) Isotopic ages were determined for a few of the eight different tephra beds in the basin-fill deposits, (2) Ages for some of the other tephra beds were established by their correlation with isotopically dated tephra beds from other localities in the United States, and (3) A faunal age was established by the discovery of well-preserved fossil mammal remains.

The youngest tephra bed (K-Ar age of 0.53 ± 0.03 m.y.) consists of pumice lapilli that correlates with air-fall pumice of the rhyolite of Ranch Canyon on the west side of the Mineral Mountains. Another widely distributed tephra bed, which underlies the Ranch Canyon tephra bed, correlates with the Pearlette type B bed (2.0 m.y.). A thin (33 m) tephra bed underlies the Pearlette type B ash and correlates with a unit of air-fall pumice near Benton Hot Springs, Calif. The oldest tephra beds lie about 60 m below the Pearlette type B bed; preliminary fission-track ages suggest that these tephra beds are about 3.5 m.y. Blancan fossil mammals (about 2.0–2.5 m.y.) in the deposits include the zebra *Dolichohippus*, the muskrat *Ondatra* cf. *O. idahoensis*, and a microtine rodent *Mimomys meadensis*. These fossils are the first reported fossil land mammals of Blancan Age from Utah.

Precambrian rocks, northern Sangre de Cristo Range, Colorado

Detailed geologic mapping in the Wheeler Peak area, northern Sangre de Cristo Range, Colo. (loc. 11), by J. C. Reed, Jr., showed the presence of a terrane of layered supracrustal rocks, including biotite and amphibole gneiss, amphibolite, greenstone, felsic volcanic rocks, chert, marble, banded iron formation, and phyllite. Some of the volcanic rocks preserve original textures and structures, and a few of the gneisses display relict graded beds. The supracrustal rocks are surrounded by a terrane of massive to rudely layered amphibolite, probably of igneous origin. Both groups of rocks are invaded by foliated granite and tonalite inferred to be related to the 1.7 to 1.8 b.y. igneous rocks that are widespread in Colorado. The Precambrian rocks are cut by diabase dikes, probably of early Paleozoic age. The crystalline rocks in the core of the Sangre de Cristo Range were thrust several kilometers eastward over Paleozoic rocks during the Laramide orogeny and were invaded by dikes, plugs, and batholiths of intermediate to felsic composition during the opening of the Rio Grande rift in the Neogene.

Precambrian dated sequence, Burro Mountains, New Mexico

Geologic field investigations by D. C. Hedlund and radiometric studies by J. S. Stacey and R. F. Marvin established a sequence of Precambrian intrusive activity and metamorphism in the Burro Mountains of

southwestern New Mexico (loc. 12). Older metamorphic rocks of the Bullard Peak Series of Hewitt (1959) characterized by sillimanite-biotite-muscovite gneiss with interlayered hornblende schist, amphibolite, and muscovite quartzofeldspathic gneiss, give zircon U-Pb ages of 1,560 to 1,570 m.y. These metamorphic rocks are intruded by foliated and nonfoliated plagiogranite of the Burro Mountain batholith that has a U-Pb age of $1,450 \pm 50$ m.y. The Burro Mountain batholith is intruded by stocks of granodiorite which is dated by K-Ar methods to be $1,380 \pm 45$ m.y. and by undated stocks and plugs of trondhjemite and rapakivi granite. Smaller lensoid masses of diorite, confined to a zone of migmatized gneiss in the Blackhawk Canyon area, may represent hybrid rocks formed during metamorphism. The migmatized gneiss yields a biotite K-Ar age of $1,410 \pm 50$ m.y. suggesting a metamorphic event of that age. Discordant dikes and plugs of diabase cut both the granite of Burro Mountains and the younger 1,380 m.y. granodiorite. A zircon U-Pb age of 1,535 m.y. from the diabase near Gold Hill is either anomalous, or there are diabases of several ages. Field relations and comparisons with Precambrian diabase in south-central Arizona suggest that the diabase of the Burro Mountains is probably of Proterozoic Y age.

IGNEOUS STUDIES

Batholith-related anticlinorium and intrusive porphyries, central Idaho

Geologic mapping in the Challis $1° \times 2°$ quadrangle, central Idaho (loc. 13), by E. B. Ekren, R. F. Hardyman, and D. H. McIntyre, showed that the Tertiary strata within and adjacent to the Van Horn Peak caldron rocks has been tilted southeastward to form a monocline (Ross, 1934). Tilting ranges from 60 to as much as 90 degrees, and the degree of tilting is greatest adjacent to the northwestern caldron boundary, which closely conforms with the southeast edge of a post-caldron Tertiary batholith, the Casto pluton of Ross (1934). The batholith occupies a northeast-trending structural high, with the tilted Van Horn Peak intracaldron and extracaldron rocks on its southeast flank, and the predominantly northwest-dipping thick caldera and extracaldera rocks of the Thunder Mountain region (Leonard, 1973) on the northwest flank. The Tertiary batholith, therefore, occupies a regionally extensive anticlinorium, which separates two major Tertiary (Challis) volcanic fields and their subsided source areas.

Hypabyssal intrusive porphyries that post date the Casto pluton of Ross are widespread within the Van Horn Peak caldron rocks; and, in places along the northern and northwestern boundaries, their volume equals that of the enclosing ash-flow tuff country rocks. These porphyries are principally of two types: (1) a gray rock of intermediate composition containing 10 to 30 percent phenocrysts of plagioclase as large as 1 cm in diameter; biotite, hornblende, and pyroxene as large as 4 mm; and (2) a pink or tan rhyolite containing 10 to 20 percent phenocrysts of bypyramidal smoky quartz as large as 3 mm in diameter, alkali feldspar as large as 5 mm, and minor biotite. Propylitic alteration is extensive in both of the porphyries and their surrounding country rocks, so that in several places only quartz remains intact. The equigranular or coarsely porphyritic granitic rocks of the Casto pluton are extremely rare within the caldron complex and are confined chiefly to small areas adjacent to the anticlinorium outlined above. There, the intrusive porphyries intrude the granitic rocks and occupy most of the caldron-related ring-fracture zones.

Intrusive complex in Butte quadrangle, Montana

Results from reconnaissance geologic studies of intrusive rocks in the southeastern part of the Flint Creek Range and the northeastern part of the Anaconda-Pintlar Range, Butte 2-degree quadrangle, Montana (loc. 14), by J. E. Elliott indicate the need for revision of previous interpretations and additional mapping and studies of petrography, geochronology, and chemistry. In the southeastern part of the Flint Creek Range in the drainages of Racetrack, Thornton, and Dempsey Creeks, intrusive rocks mapped and described as the "Racetrack pluton" by Hawley (1975) are actually an intrusive complex of various ages and compositions. This complex includes at least three plutonic phases, one (or possibly two) hypabyssal phase represented by dikes, and an episode of quartz veining. This complex was deformed prior to the intrusion of the Mt. Powell two-mica monzogranite batholith and its associated aplite dikes, pegmatites, and quartz veins. Similar plutonic rocks also occur in the northeastern part of the Anaconda-Pintlar Range. These include the "acidic diorite" and "acidic granodiorite" and possibly other units of Emmons and Calkins (1913). In the vicinity of Mt. Haggin and Short Peak, these units are strongly deformed. At one locality a thrust fault is exposed with Proterozoic Y quartzite of the Belt Supergroup overlying and in thrust contact with "acidic granodiorite." Additional work proposed for this region may serve to subdivide and correlate intrusive and structural events and to establish the age and duration of thrusting in this part of the Sapphire thrust system.

"Pre-Tertiary" altered flows in central Idaho are Eocene

Geologic mapping in the Mount Jordan area, Custer County, Idaho (loc. 15), by Fess Foster (University of

Montana) as part of the Challis CUSMAP project, demonstrated that the thick sequence of altered intermediate lavas and breccias exposed near Mt. Jordan is Eocene (McIntyre and Foster, 1981) and not pre-Tertiary as proposed by McIntyre and others (1978). The lavas are in fault contact with 74-m.y.-old granitic rocks of the Idaho batholith and were invaded by a rhyolitic intrusive complex that is compositionally like intrusive rocks of known Eocene age in nearby areas. The probability that similar altered lavas elsewhere in Idaho may be pre-Tertiary is now believed to be remote.

Springerville volcanic field, Arizona

Volcanic rocks of the Springerville–White Mountains volcanic field, at the southern edge of the Colorado Plateau in east-central Arizona (loc. 16), form an extensive late Cenozoic basaltic field developed to the north of a dissected trachyte shield volcano of probable late Miocene age that forms the White Mountains. Studies by Jayne Aubele and L. S. Crumpler (University of Arizona) and C. D. Condit and L. D. Nealey (University of New Mexico) reveal that the basaltic field contains a variety of mildly alkalic lavas of the alkali olivine basalt-hawaiite-mugearite-benmoreite suite, as well as some amphibole-bearing intermediate lavas of uncertain affinity. Several cinder cones with late, more silicic central plugs are known. In the westernmost part of the basalt field, dissected lavas that range in age from latest Miocene to early Pleistocene rest on coarse gravels derived from an area south of the Mogollon Rim. Younger, largely late Pleistocene cones and flows are concentrated in the central interior of the basalt field where cinder cone frequences locally exceed 1 cone/km^2, and cones overlap and bury each other.

TECTONIC AND STRUCTURAL STUDIES

Structural and stratigraphic relations, Precambrian rock, Glacier National Park, Montana

The results of geologic mapping and stratigraphic studies completed in Glacier National Park, Mont. (loc. 17) by R. L. Earhart, O. M. Raup, and J. W. Whipple provide an overview of the geology that greatly modifies previous geological interpretations. The preliminary results of work to date give insight into the structural and stratigraphic relations in the Precambrian rock of the park. Some of the major geologic features recognized from the present investigations include (1) a belt of thrust faulted rocks that trends north to northwesterly on the west side of the park, (2) thrust fault boundaries on the gently folded central core of the park, and (3) the near juxtaposition, of western and eastern facies of the Belt Supergroup rocks, as a result of thrust faulting.

Strucutural sequence in southern Lost River Range and Arco Hills, Idaho

One episode of folding and three subsequent episodes of faulting have involved Ordovician through Permian rocks of the Lost River–Arco Hills allochthon (Skipp and Hait, 1977) exposed in the southern Lost River Range and Arco Hills area, Idaho (loc. 18), as reported by B. A. Skipp. Folds of post-Permian to pre-Eocene age are mostly symmetrical and locally overturned; their axes trend northwest to north-northwest. The folds are displaced by northeast- and northwest-trending normal faults that are, in turn, truncated by north- to north-northeast-trending range front faults. Superimposed on the above structures are large curving, relatively low angle, southward-dipping normal faults that occur in the southernmost part of the Lost River Range and the southwestern part of the Arco Hills. These areas may be large slump blocks that have moved toward the precipitous northwest edge of a proposed caldera complex at the Idaho National Engineering Laboratory (Doherty and others, 1979) on the adjacent Snake River Plain.

Microfabric analysis, Bannock and Albion-Raft River Ranges, southeastern Idaho

Striking consistent results were obtained by R. W. Allmendinger during microfabric analysis of predominantly nonmetamorphosed sediments collected in the Pocatello 1°×2° quadrangle (loc. 22). Dynamic analysis of microstructures in quartz, calcite, and dolomite in oriented samples indicates compression and extension directions of rocks in the Bannock Range and Albion-Raft River Ranges. Compression in all known allochthonous sediments was parallel to bedding and trended approximately east-west. An opposite pattern of vertical compression and horizontal extension is suggested from annealed and slightly restrained crystals in the cover rocks of the core complexes. The age of the latter fabric is not yet known.

Thrusting of Casper Mountain, Laramie Range, Wyoming

D. J. Gable and A. E. Burford reported that northward thrusting of Casper Mountain, in the northernmost Laramie Range, Wyo. (loc. 23), may be of greater magnitude than previously believed. Joint patterns and fault patterns indicate strong movements on and in the vicinity of Casper Mountain since the folding of Cretaceous sediments. Precambrian rocks constituting Casper Mountain may have overridden the southern part of the Emigrant Gap anticline, an important oil-bearing structure. Thus, possible oil-bearing structures may underlie the Casper Mountain anticline.

Fault zone in Sheridan-Buffalo area, Wyoming

Stucture of the Piney lobe was revised on evidence from geologic mapping of the Story and Beaver Creek Hills quadrangles, Sheridan-Buffalo area, Wyoming (loc. 24), by E. N. Hinrichs. The large northwest-trending fault zone, which cuts Moncreiffe Ridge, very probably extends under cover at least as far as Little Goose Creek. The zone probably underlies the east end of Curlew Hill where beds of Cretaceous rocks have been overturned. Confirmation from commercial seismic data will be attempted.

Salt-movement induced arching and diapirism, central Utah

Continued geologic work in central Utah (loc. 25) by I. J. Witkind provides further evidence that much of the deformation in the transition zone between the Colorado Plateau and the Basin and Range province is attributable to multiple episodes of salt diapirism. The salt, contained within the Twelvemile Canyon Member of the Arapien Shale, has moved often seemingly since its deposition in the Middle Jurassic to the present. Much of the movement has been a very slow but persistent upwelling that has forced the mudstones and siltstones of the Twelvemile Canyon to bow up the overlying strata. The resultant slow arching of these younger strata is reflected by depositional thinning of other younger rocks, which overlie the axes of the salt diapirs. Sporadically and repeatedly, this slow upward movement was interrupted by rapid upwelling of the salt diapirs, which deformed the Twelvemile Canyon and younger units into elongate, fan-shaped diapiric folds. It seems likely that all the salt diapirs in the area were reactivated simultaneously during each major diapiric episode. The diapiric folds that formed during each of these episodes were then destroyed by collapse along high-angle normal faults because of salt removal and by erosion. Intense deformation stems from the recurrent growth and collapse of these folds. In general, the renewed folds followed the same trends and occupied the same sites as the parental folds.

The deformation appears to be confined solely to the Arapien Shale and younger overlying units; the Navajo Sandstone, on which the Arapien rests, and older units seemingly were not involved in the deformation.

At least three major episodes of diapirism can be recognized: (1) Late Cretaceous to early Paleocene, (2) early Paleocene to late(?) Oligocene, and (3) late(?) Oligocene to Pliocene(?). Some evidence suggests that cells of salt were active as recently as the Pleistocene.

Holocene fault dating, Lost River Range, Idaho

Radiocarbon dating of organic sediment collected by M. H. Hait, Jr., supports the hypothesis, independently based on scarp morphology, that the central part of the Lost River Range has moved more recently than the southern part. The sediment, from the lower Cedar Creek trench dug across the Lost River Range frontal fault 5 km north-northeast of Mackay, Idaho (loc. 19), has an age of 4,320 ± 130 yr B.P., according to E. C. Spiker (USGS Radiocarbon Lab, written comm. Dec. 12, 1979). This date supports the Holocene range-front movement age postulated by Hait and Scott (1978) for stratigraphic relations in the Willow Creek trench dug across the same fault about 35 km northwest of Mackay.

Stuctural and depositional reconstruction of features exposed in the lower Cedar Creek trench indicates that colluvium with organic material derived from the main Lost River fault scarp was advancing westward across the adjacent antithetic graben which was floored with tan silt. At about the time that the colluvium reached the silty graben surface, part of the graben dropped 75 cm, exposing the tan silt in a scarp that slumped eastward over the toe of the organic layer. The slumped scarp was then overlapped by continued colluvial deposition from the main fault with no subsequent movement on the antithetic fault.

Fault relations, Bannock Range, southeastern Idaho

Several sets of steeply dipping and gently dipping faults in the Scout Mountain and Oxford Mountain parts of the Bannock Range in southeastern Idaho (loc. 20) west of the Idaho-Wyoming foreland thrust belt have been defined by L. B. Platt and S. S. Oriel. The gently dipping faults, along which younger rocks overlie older ones with significant tectonic omissions (Oriel and Platt, 1979), are cut by the steeper faults, which not only bound present ranges but also reflect stress fields that resulted in their rotation as well as tilting of their strata and older flatter faults. Reconstructions of the relations in the Scout Mountain region by L. B. Platt indicate that, prior to tilting, one set of gently dipping faults sloped west and was not associated with folding in either the hanging or foot walls. Another set also dipped west but was associated with folds, which suggests disharmonic folding during the Sevier thrusting of Mesozoic and early Cenozoic age. The first set cuts bedding at a high angle; the secondary nearly parallels bedding of adjacent strata.

The absence of faults along which older rocks have overriden younger ones suggests that subsurface decollement planes of thrust faults, which are exposed farther east, may lie below Scout and Oxford Mountains where the oldest sediment rocks known in southeastern Idaho are exposed.

Geometry of folds and thrust faults, Idaho-Wyoming thrust belt

Recently mapped folds in the Meade plate of the Idaho-Wyoming thrust belt, southeastern Idaho (loc. 21), are described as kink folds that formed over ramps in the basal Meade thrust surface by R. W. Allmendinger (1981). The geometry of the folds is characterized by, from west to east, a moderately steep (40-50 degrees) west-dipping limb, broad crestal region, sharp, narrow hinge zone, and straight planar, overturned eastern limb. The hinge zone was formed over the upper corner of the ramp, then translated passively eastward over the adjoining flat in the thrust surface. The broad crestal region formed over the flat east of the ramp; its width reflects the amount of displacement over the ramp. Finally, the west-dipping limb parallels the underlying ramp, although it may be steepened by later deformation. In the Blackfoot Mountains, imbricate slices in the younger upper plate cut downsection eastward on the steeply west-dipping fold limbs formed during deformation along the basal thrust.

MINERAL-RESOURCE STUDIES

Anomalous metals values in Mississippian black shale, northwestern Wyoming

J. D. Love and J. C. Antweiler reported that a heretofore unnamed and undescribed petroliferous and metalliferous marine black shale in northwestern Wyoming (loc. 26) contains anomalous metals content. The shale, about 15 m thick and at least 26 km^2 in extent, is of Late Mississippian (Chesterian) age. Maximum values in parts per million are Ag 5, Cu 1,500, Mo 200, Ni 300, Pb 150, V 5,000, Zn 1,500, Zr 700, Hg 0.35, Th 20, and U 87. The thickness of beds with the highest metals values ranges from 1–3 cm to 4 m. Although these values are currently too low to be of econimic interest, richer occurrences may be present in adjacent areas. Some beds are moderately radioactive.

Malachite is visible in several units of the black shale. Many of the beds have a petroliferous odor, and some thin partings are combustible. Maximum values of organic carbon are about 10 percent. The shale may have been a significant source rock for oil and gas.

The black shale overlies the Darwin Sandstone Member of the Amsden Formation and underlies the red Horseshoe Shale Member of the Amsden. It is a remnant of a cratonic marine deposit that transgressed from an as yet unknown direction.

Chrome diopside and pyrope garnet in northwestern Wyoming

Chrome diopside and pyrope garnet are associated with kimberlite intrusives in some areas. A rumored occurrence of these minerals in the Green River basin of southwestern Wyoming (loc. 27), 48 km southwest of the town of Green River, was field checked by J. D. Love. The minerals occur in a terrace gravel 3 to 4 m thick, which overlies the Bridger Formation of middle Eocene age. Several tons of chrome diopside as angular fragments were estimated to be present in a mapped area of about 2,450 m $\times$300 m. This mineral is very fragile, and it seems unlikely that is could have survived in the observed fragment sizes and quantity if it had been transported from the nearest Precambrian source in the Uinta Mountains 40 km to the south. Futhermore, the chrome diopside and pyrope garnets disappear abruptly in the terrace gravels to the south toward the mountains. Although these minerals do occur with intrusive kimberlite rocks in some areas, no intrusive rocks of Cenozoic age are known in this area, and no diamonds were found. Further work might determine the western and northern extent of the deposit, the source of the minerals, and the presence or absence of diamonds.

BASIN AND RANGE REGION

MINERAL-RESOURCE STUDIES

Bedded barite in Mississippian rocks of northeastern Nevada

Barite beds in siliceous rocks of Early Mississippian age (Kinderhookian) were recognized by F. G. Poole, K. B. Ketner, and J. F. Smith, Jr., north of Wells in the Snake Mountains, Elko County, Nev. (loc. 1). The sequence consists of intercalated laminated dark-gray mudstone, chert, and laminated to very thin bedded dark-gray, fine-grained barite beds as much as a few meters thick. Conodonts identified by A. G. Harris as Kinderhookian in age were obtained from the siliceous facies north of Wells; the age assignment confirms the lithologic correlation with the type Webb Formation of north-central Nevada. These siliceous rocks, which correlate chronostratigraphically with the type Webb Formation of Early Mississippian age in the Piñon Range of north-central Nevada (loc. 6), were mapped by Brian Oversby (1972) as the lower part of the Chainman Shale. Oversby's Chainman also includes typical Chainman Shale in its upper part. Some of the thicker beds of barite in the Webb Formation in the Snake Mountains are being considered for open-pit mining by several mining companies.

Low-temperature metal deposits in Paleozoic marine shales in Nevada

F. G. Poole and G. A. Desborough reported that low-temperature metal deposits occur in Ordovician and Devonian eugeosynclinal "black-shale" facies in central and northern Nevada. The black-shale facies, which con-

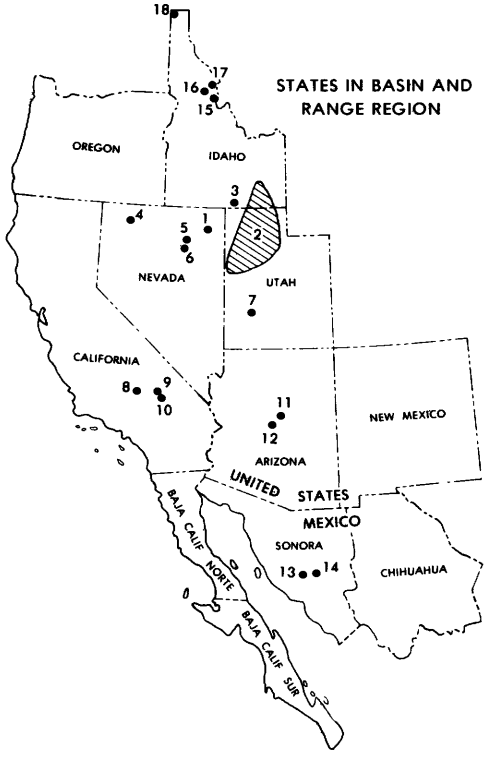

sist of mudstone, siltstone, chert, and minor carbonate strata, contain concentrations of as much as 5,000 ppm V, 1,000 ppm Mo, 18,000 ppm Zn, 350 ppm Se, 10 ppm Ag, 500 ppm Cr, and 20 weight percent organic C. Many of the metalliferous beds are low-grade oil shales (< 60 L of syncrude oil per 1t of rock) indicating thermally immature kerogen-rich organic matter. Most of the vanadium, selenium, silver, and chromium reside in the organic matter; molybdenum resides both in molybdenite and in the organic matter; and zinc resides in sphalerite.

Paleogeographic reconstruction indicates that the metalliferous rocks were deposited on a continental rise at the western margin of Paleozoic North America. Concentrations of metals differ from bed to bed and from area to area, reflecting variations in depositional and chemical conditions as well as distance from sites of submarine discharge of metalliferous hydrothermal fluids.

Conditions necessary for low-temperature (< 50°C) accumulation of significant metal and oil concentrations in shale include (1) marine basinal setting, (2) high content (> 10 weight percent) of organic carbon, (3) low content (< 10 weight percent) of calcium carbonate, (4) high content of sapropel (mostly marine algae) and low content of detritial land plant material, (5) relatively slow rate (< 20 m/m.y.) of deposition of detritus and (or) chemical precipitates, (6) relatively high salinity and density of brines in bottom layers of depression, and (7) anoxic environments of deposition and diagenesis.

STRATIGRAPHIC AND STRUCTURAL STUDIES

Chronometric time scale proposed for the Precambrian

According to J. E. Harrison, time-stratigraphic charts for the Precambrian rocks of the United States and Mexico have been compiled by the International Union of Geological Sciences (IUGS) working group and are scheduled for publication with accompanying texts as chapters in a USGS Professional Paper. The proposed chronometric time scale for the Precambrian, based in part on the data presented in the charts, has been presented to the IUGS Subcommission on Precambrian Statigraphy and to the North American Commission on Stratigraphic Nomenclature. The preliminary proposal for a time scale for the Precambrian of the United States and Mexico has been published along with a request for comments from the geologic profession (Harrison and Peterman, 1980). The proposed scale encompasses the interval from 4,550 to 570 m.y. and includes seven time divisions, in ascending order—pre-Archean, early, middle, and late Archean; Proterozoic X, Y, and Z. This proposed scale requires no stratotype for the time divisions.

Proterozoic Z glaciation in northwestern Utah and adjacent Idaho

Glaciation during Proterozoic Z time is recorded in a number of places extending from the Sheeprock Mountains, Utah, to Pocatello, Idaho, and from Park City (40 km east of Salt Lake City), to the Deep Creek Mountains on the Utah-Nevada line (loc. 2). Throughout this area the glacial deposits form the base of a westward-thickening miogeoclinal wedge. Reanalysis of previous mapping on Fremont Island in Great Salt Lake and the northern Wasatch Mountains by M. D. Crittenden, Jr., and in the Sheeprock Mountains by N. Christie-Blick, shows that glacial episodes are represented either by diamictite or by dropstones enclosed in fine-grained laminated beds. These glacial beds are separated from one another stratigraphically by as much as 1000 m of nonglacial deposits, including black slate, alternating graywacke and siltstone, or quartzite. Using reasonable sedimentation rates for such deposits, they infer that two episodes of glaciation, each probably consisting of multiple advances and retreats, were separated by a nonglacial interval of a few hundred thousand to a few million years duration. Within Utah and southeastern Idaho these glacial deposits can be correlated by means of associated volcanic rocks and by an identical sequence of overlying formations. Throughout other parts of the Cordillera, they are correlated, on the basis of stratigraphic position and their unique glacial history, with similar rocks at the base of the Windermere Group in northeastern Washington, British Columbia, and

Alaska, and with the Kingston Peak Formation of southeastern California.

Conodont color differences fit structure in south-central Idaho

Conodont color alteration index (CAI), determined by B. R. Wardlaw, A. G. Harris, and J. E. Repetski, was an aid in interpreting the structure of the Black Pine Mountains, Cassia County, Idaho (loc. 3), studied by J. F. Smith, Jr. The CAI values are consistently different in samples from blocks north and south of a major fault that transects the range. Conodonts collected north of the fault have CAI values of 4 and below ($<300°C$), whereas those south of the fault have CAI values of 5 and above ($>300°C$). These data suggest that maximum rock temperatures recorded by the conodont colors were attained in different areas with different thermal histories before the blocks were juxtaposed by faulting.

Accreted Mesozoic terrane in northwestern Nevada

Field studies in western Humboldt County, Nev. (loc. 4), by N. J. Silberling (USGS) and in collaboration with R. C. Speed and students (Northwestern University), clarified geologic relations among tectonic-stratigraphic terranes suspected of having been tectonically accreted to the North American Continent during Mesozoic time. Their study in the Jackson Mountains and Pine Forest Range revealed a thick, predominantly volcanic sequence that essentially spans the Norian Stage of the Upper Triassic. This sequence contrasts markedly with the adjacent, largely time-correlative, nonvolcanic Norian-Age strata of the Auld Lang Syne Group (lower part) in northwestern Nevada that represents part of the early Mesozoic miogeocline along the western margin of North America. Recognition of this relation demonstrates major tectonic juxtaposition of one or more accreted terranes against this part of the Mesozoic continental margin in post-Triassic time. This new information is significant, not only in understanding the tectonic evolution of the eastern Pacific margin, but also in delimiting metallogenic provinces in the region.

Revised Paleozoic stratigraphy in northern Nevada

Recently discovered conodonts in a limestone unit in the Swales Mountain quadrangle of the southern Independence Mountains, western Elko County, Nev. (loc. 5), require an important revision of the Paleozoic carbonate stratigraphy there. As originally mapped by J. C. Evans and K. B. Ketner (1971), the Mississippian turbiditic limestone sequence at Camp Creek was underlain by a thick unit of similar carbonaceous limestone turbidites, tentatively identified on the basis of lithic composition and stratigraphic position as the Silurian and Devonian Roberts Mountains Formation. Now, Ketner (USGS) reports that the lower turbiditic limestone unit previously thought to be the Roberts Mountains Formation is actually Lower Mississippian and is part of the Camp Creek sequence based on conodonts identified by A. G. Harris (USGS) from drill core and by Anna Dombrowski and Gilbert Klapper (University of Iowa) from outcrop samples. Total thickness of the Lower Mississippian turbiditic limestone sequence at Camp Creek in the Swales Mountain is, therefore, revised upward to at least 1000 m rather than 220 m as originally reported.

New data on age of the Roberts Mountains thrust

Data on which the widely accepted middle Paleozoic age for the Roberts Mountains thrust in Nevada was based are not adequate to date the thrust, according to K. B. Ketner. A possible Mesozoic age for the thrust in northern Nevada (loc. 6) is indicated by new data on regional stratigraphy and structure that have accumulated in recent years. These data show that in Early Mississippian (pre-Chainman Shale) time the eastern part of the Antler flysch trough received easterly derived limestone turbidite deposits (Tripon Pass Limestone of Oversby (1973) and equivalent limestones) and the western part of the trough received contemporaneous westerly derived siliceous detritus (type Webb Formation). In some places, the siliceous facies has been thrust perhaps tens of kilometers eastward close to the position occupied by the limestone facies. In the Piñon Range (loc. 6) and elsewhere in northern Nevada, this thrust is inferred to be the Roberts Mountains thrust, involving rocks such as the Ordovician Vinini Formation, Devonian Woodruff Formation, and Permian rocks. These geologic relations permit two possible interpretations: (1) The Roberts Mountains thrust is indeed middle Paleozoic (Early Mississippian), but the allochthon has been drastically rearranged in post-Permian time; or (2) The Roberts Mountains thrust is actually of post-Permian age. Recent geologic mapping by Ketner in northern Nevada indicates that the accepted middle Paleozoic age for the Roberts Mountains thrust (Smith and Ketner, 1968) is probably not correct. Permian and Triassic rocks are intimately involved in major thrust and folds, and reinterpretation of previously published data has led Ketner to conclude that the geologic evidence in northern Nevada indicates a post-Paleozoic rather than a Paleozoic age for the Roberts Mountains thrust.

Molasse of the Antler foreland basin in Nevada and Utah

According to F. G. Poole, Antler orogenic deposits include both flysch and molasse in a foreland basin bounded on the west by the Antler orogenic highland (western and central Nevada) and on the east by a carbonate-bank

buildup at the outer margin of the cratonic platform (southern Nevada and western Utah). During Early and early Late Mississippian time, a submarine rise in the central part of the foreland basin separated the western subsiding, elongate, asymmetrical trough from the eastern carbonate shelf and sediment-starved elongate subbasin. Later in Mississippian time, the western trough nearly was filled with deep-marine turbidites and related deposits, and the subsequent combination of uplifts of the orogenic highland and retarded subsidence of the western trough resulted in complete filling of the foreland basin. This Upper Mississippian sedimentary fill consists of eastward prograding molasse facies (Poole *in* Nilsen and Stewart, 1980) that change across the region from alluvial and deltaic conglomerate, sandstone, and siltstone in the area of the western trough and former submarine rise to prodelta shallow-marine siltstone and claystone in the expanded eastern subbasin that included both the former carbonate shelf and starved subbasin. Delta facies are recognized by their characteristic lithologic, faunal, and geometric features. Delta-plain environments include distributary channels and interdistributary flood basins (swamps, marshes, and bays), and delta-front environments include distributary-mouth bars (mostly sand) and distal bars (mostly silt). The starved subbasin in the eastern part of the foreland basin, called the Deseret subbasin, which previously had received only small amounts of orogenic and cratonic sediment, developed into a prodelta subbasin that accumulated a moderate amount of orogenic and cratonic deposits. Most of the prodelta sediments from the west were transported through alluvial valleys and deltaic multiple distributary channels, and cratonic sediments from the east were transported through channels cut into the carbonate platform.

Beaver basin of southwestern Utah

Upper miocene to lower Quaternary basin-fill deposits in the Beaver basin in eastern Beaver County, Utah (loc. 7), recently mapped by M. N. Machette, may be hosts for a possible modern uranium deposit inferred from geophysical measurements and geochemical data. In Pliocene and Pleistocene time, the Beaver basin contained a perennial shallow lake into which as many as eight different felsic volcanic ashes were deposited; the thickest and most widespread ashfall layer in the basin is the 2-m.y.-old so-called "Huckleberry Ridge" ash bed. The lake beds also contained abundant fossils, including ostracodes and diatoms that have been useful in correlation of units and in determining environmental conditions. The basin-fill deposits are extensively deformed, both by major range-front faults and by a north-trending, basin-axis antiform and horst structure. This deformation affected deposits as young as late Pleistocene (125,000–10,000 yr B.P.). Analytical data on soils, dating by the uranium-trend method, and stratigraphic relations establish a well-controlled chronosequence, both for argillic and for calcic soils developed during middle and late Pleistocene time. The Beaver basin currently is being explored for petroleum and uranium by several energy and mining companies.

"Core complexes" of the Cordillera

The "metamorphic core complexes," widespread in the Western Cordillera, are interpreted by W. B. Hamilton to be the tops of large lenses by the separation of Tertiary extension that has been accommodated in the middle continental crust. These complexes consist of rocks that were at least 10 km deep before crustal extension; depth indicators include two-mica granites and the aluminum-silicate triple point in magmatic terrains, and kyanite greenschists in nonmagmatic ones. Ages of dominant metamorphism, and of magmatic rocks where present, range from Archean to Paleogene. The complexes commonly have cataclastic carapaces of Tertiary age, and are overlain tectonically by brittlely deformed upper crustal terranes. Tertiary listric normal faults merge with the upper surfaces of the lenses, and among the tracts typically rotated down on these faults are Tertiary basin strata, including landslide megabreccias from fault scarps, which now dip steeply or moderately into the gently dipping faults that define the tops of the lenses. Seismic-reflection profiles in southern Arizona show that a thickness of the crust of about 12 km beneath the tops of the complexes consists of gently tapered lenses, as wide as tens of kilometers and as thick as 8 km, whereas the lower crust is subhorizontally layered. Apparently the lower crust is extended by smoothly ductile flow, the middle crust by the sliding apart of great lenses, and the upper crust by the collapse of listric normal-fault blocks. Similar complexes occur in extensional terrains around the world. Explanations invoking thrusting, magmatism, or sliding off domes are generally untenable.

Paleozoic siliceous rocks of the northern Mojave Desert, California

According to M. D. Carr and F. G. Poole, Mesozoic deformation and metamorphism and Cenozoic faulting have complicated stratigraphic studies of the Paleozoic siliceous facies in the El Paso Mountains, eastern Kern County, Calif. (loc. 8). However, conodont collections identified by A. G. Harris and B. R. Wardlaw and graptolite collections identified by R. J. Ross, Jr., have provided important new stratigraphic information for previously undated parts of the Garlock Formation. Two contrasting sequences of lower Paleozoic continential rise to slope deposits are recognized in the range. The

western part of the range is comprised of fine-grained siliceous clastic rocks, bedded chert, and greenstone, and contains Ordovician and Devonian fossils (Poole and Christiansen, 1980). The eastern part of the range is characterized by a succession of interbedded argillite, limestone, bedded chert, and quartzite from which Ordovician fossils have been recently obtained. In the central part of the range, rocks of the lower Paleozoic siliceous sequence are overlain with apparent unconformity by a flysch turbidite unit of presumed Carboniferous age, which is in turn overlain by a Lower Permian deep-marine turbidite sequence. Locally, in the eastern part of the range, the lower Paleozoic rocks are unconformably overlain by a Pennsylvanian unit composed of shallower water carbonate rocks. The entire assemblage of Paleozoic rocks in the range was metamorphosed, tightly folded, and faulted in Late Permian to Early Triassic time.

A sequence of rocks similar to the lower Paleozoic siliceous facies in the western part of the El Paso Mountains is also present 60 km to the east on the south side of the Garlock fault in Pilot Knob Valley, northwestern San Bernardino County, Calif. (loc. 9). Devonian conodonts obtained from a distinctive sandy limestone unit, which is also present in the El Paso Mountain assemblage, provide temporal support for the general lithologic correlation of the rocks in the two localities as originally proposed by Smith and Ketner (1970).

A rock sequence that is lithologically and structurally similar to the lower Paleozoic siliceous rocks in the eastern part of the El Paso Mountains is also present in the vicinity of Goldstone in northwestern San Bernardino County, Calif. (loc. 10). Recent discovery of Ordovician graptolites by Poole and Carr in the metamorphosed sequence at Goldstone supports as well the correlation of these rocks with part of the Paleozoic siliceous assemblage in the El Paso Mountains.

Colorado Plateau margin in central Arizona

G. E. Ulrich reported that a combination of late Miocene and Pliocene(?) volcanism, accompanied by extensive erosion and normal faulting, sculptured the present Colorado Plateau margin in eastern Yavapai and southern Coconino Counties, Ariz. (loc. 11). West Clear Creek Canyon cuts through the southwestern margin of the Plateau province for nearly 40 km and emerges westward into the Verde Valley in the transition zone between the Colorado Plateau and the Basin and Range physoigraphic provinces. To the east on the Plateau, thin (15–30 m thick) flows of upper Tertiary basalt disconformably overlie Permian sedimentary rocks. West of there, but still within the physiographically defined Plateau, prevolcanic erosion cut through at least 400 m of Permian rocks, forming a broad paleovalley that appears to trend northeastward. The valley subsequently was filled with a basal conglomerate (0–50 m thick), basalt flows (350–400 m thick), and a few andesites and interbedded silicic ashflow tuffs (0–35 m thick). The topographic margin of the Plateau, which is west of the paleovalley, was a product mainly of prevolcanic erosion. Normal faulting with northwest and northeast trends accompanied and followed the volcanic eruptions. Subsequent erosion has caused the Plateau rim to retreat eastward at least 2 km.

Verde fault of central Arizona

According to E. W. Wolfe, the Verde fault in the southern part of the Verde Valley, eastern Yavapai County, Ariz. (loc. 12), occurs in the trasition zone between the Colorado Plateau and Basin and Range physiographic provinces. The Verde fault, which bounds the Verde basin and marks the depositional edge of basin-fill sediments of the Miocene and Pliocene Verde Formation, forms a north-northwest-trending scarp as high as 1000 m. Except adjacent to the southernmost end of the basin where the Verde fault splays into several high-angle faults of small displacement, this southern part of the Verde fault zone is a single, well-defined, steeply dipping normal fault. Here the upper Tertiary Verde Formation is faulted against Precambrian plutonic and metamorphic rocks that are overlain by gently dipping Paleozoic strata and Miocene basalt of the Hickey Formation. Late Tertiary movements on the Verde fault are recorded by alluvial-fan gravels within the Verde Formation; the gravels are very coarse near the fault and probably resulted from erosion of the fault scarp. Fan deposits in the Verde Formation, however, contain clasts only of Paleozoic strata and Miocene Hickey basalt. Precambrian rocks, now exposed in the lower 400 to 500 m of the fault scarp, are not represented in the conglomerate beds. Apparently more than 400 m of displacement occurred on this segment of the Verde fault since deposition of alluvial fans of the Verde Formation. Younger fan deposits, somewhat dissected and probably of Pleistocene age, also originated at the fault scarp. In contrast to the older fans, these younger fans are dominated by Precambrian detritus and are not displaced by the Verde fault.

New Ordovician locality in central Sonora, Mexico

Miogeosynclinal rocks consisting of interstratified thin-bedded, fine- to coarse-grained limestone, silty and clayey limestone, and intraformational limestone-gravel conglomerate near Rancho Pedregal in central Sonora, Mexico (loc. 13), have been reported by F. G. Poole (USGS) and L. C. Bolich (Minera Baucarit, Hermosillo, Son.). The exposed carbonate rocks (> 200 m thick) have many fossiliferous beds that contain brachiopods,

trilobites, and gastropods. Field recognition by Poole of the lower Middle Ordovician *Orthidiella* brachiopod zone in limestone beds exposed west of Rancho Pedregal establishes a correlation with the Antelope Valley Limestone carbonate-shelf facies in Nevada. The combination of paleontologic and stratigraphic data from the two widely separated regions suggests a physical connection between the limestone deposits in Nevada and Sonora during the early Paleozoic.

Cordilleran eugeosynclinal rocks in central Sonora, Mexico

F. G. Poole, K. B. Ketner, and J. H. Stewart reported that strongly deformed Ordovician, Silurian(?), and Devonian eugeosynclinal rocks exposed near Cobachi and Mazatán in central Sonora, Mexico (loc. 14), are similar in litholgy, fauna, and structural style to eugeosynclinal rocks in Nevada and Texas. In both Sonora and Nevada, economic bedded barite deposits occur in similar Paleozoic facies. An incomplete section of dark-grey shaly argillite (>100 m thick) containing Ordovician graptolites and a superjacent black chert (>20 m thick) containing radiolarians are exposed at Cerro Guayacan near Cobachi (Noll, 1981; Pregger, 1981). These two units in central Sonora probably correlate with similar Middle and Upper Ordovician units in the upper part of the Vinini Formation of northern Nevada. This correlation and other lithologic similarities suggest that the Cordilleran geosyncline was physically continuous around the southwest edge of the North American craton in early and middle Paleozoic time in accord with the paleogeographic belts discussed by Peiffer-Rangin (1979, 1981) and Stewart (1981). The rocks near Cobachi and Mazatán are strongly folded and faulted comparable to allochthonous eugeosynclinal rocks in Nevada. Even if these allochthonous eugeosynclinal rocks are reconstructed to accommodate the middle-Mesozoic left-lateral Mojave-Sonora megashear of Silver and Anderson (1974) and Anderson and Silver (1981), the presence of similar continental-margin rocks in Nevada, Sonora, and Texas supports the concept of an early and middle Paleozoic physical connection around the southwestern edge of North America through northern Mexico in order to connect similar rocks found in Nevada and Texas.

IGNEOUS ROCKS

Mylonitization during emplacement of Bitterroot lobe of the Idaho batholith

Recent field studies in the Selway-Bitterroot Wilderness Area, Idaho County, Idaho, and Ravalli County, Mont. (loc. 15), by Lawrence Garmezy and W. R. Greenwood showed that a north-trending mylonitic zone, characteristic of the eastern margin of the Bitterroot lobe, extends into a similar 16-km-long west-trending zone along the southern margin of the batholith lobe. Features of this west-trending zone do not fit the model of mylonitization involving eastward gliding of a mass over the batholith during Cretaceous time. Along the eastern margin of the Bitterroot lobe, the mylonite forms a 300- to 600-m-thick sheath dipping 20° to 25° east above undeformed foliated granites. At the southeast margin of the lobe, the mylonite dips southerly; farther west, it dips southwesterly. At the southwest margin, strongly mylonitized rocks are interlayered with flow foliated granite. Flow foliation commonly parallels the mylonitic fabric. Biotite streaking lineation and quartz rodding commonly parallel fold axes which trend 110° along both the eastern and southern margins of the Bitterroot lobe. Total symmetry is orthorhombic. Feldspars show both up-dip rotation and down-dip rotation. Early main-phase granites are the most deformed rocks. Later pegmatites display less intense mylonitization; and aplites, which cut the granites and the pegamites, are even less deformed. These features probably formed by progressive injection and flowage of a crystal mush. Mylonite developed by flattening of the mush near the upper contact of the batholith under pressure of newly injected magma along 110° or 290° trends.

Epizonal plutons in Bitterroot lobe of the Idaho batholith

Recent geologic mapping in the Selway-Bitterroot Wilderness Area of northeastern Idaho (loc. 16) by W. E. Motzer and colleagues has increased the previously known outcrop area of Tertiary plutonic rocks from approximately 510 to 880 km^2. Three major epizonal Tertiary granitic plutons intrude the Bitterroot lobe of the Idaho batholith in the wilderness area: the Whistling Pig pluton (WWP), the Running Creek pluton (RCP), and the Bad Luck pluton (BLP). The WPP and RCP consist of main-phase, medium- to coarse-grained granites capped by a chilled margin phase of fine-grained leucogranites. Main-phase modes in the RCP average 47.0 percent orthoclase-perthite, 30.2 percent quartz, 18.6 percent sodic plagioclase, 3.0 percent biotite, and 0.8 percent hornblende. Accessory minerals (0.4 percent) consist of allanite, apatite, baddeleyite, cassiterite, fluorite, iron-titanium(?) oxides, monazite, sphene, thorite, and zircon. The granites have mineralogical, textural, and chemical signatures indicative of *A* or *R* type granites and may represent partially melted lower crust. Structural data, including the orientation of synplutonic, aplite dikes, and postplutonic rhyolite dikes, suggest pluton emplacement during an episode of east-west extension.

Migmatites in Bitterroot lobe of the Idaho batholith

According to Enid Bittner-Gaber, migmatites within the Bitterroot lobe of the Idaho batholith in Idaho County, Idaho (loc. 17), form concordant screens and septa composed of interlayered biotite schist, quartzite, biotite-plagioclase-garnet schist, diopside gneiss, and amphibolite pods. On the eastern margin of the lobe, the migmatites may be roof pendants or large blocks of country rock within lower Tertiary granite plutons. The western side of the lobe consists of screens of tonalite gneiss and migmatites resembling country rocks to the west. Tonalite and granite plutons are separated by but encompass the migmatites on the west. From east to west the foliations and layers strike east-west $\pm 20°$; lineations defined by mica, fold axes, and rodded feldspars bear $290° \pm 10°$. Therefore, petrographic provinces of the migmatites are not uniform from the eastern border to the western border of the Bitterroot lobe. The overall structural concordance of the migmatites with the batholith from east to west may indicate the direction of flow of the magmas.

Petrology and structure of Bitterroot lobe of the Idaho batholith

Geologic mapping by M. I. Toth of approximately 1400 km^2 in the east-central part of the Bitterroot lobe of the Idaho batholith in northeastern Idaho (loc. 17) has delineated two major plutons. The Bear Creek pluton is a medium-grained granite with varying amounts of poorly defined potassium-feldspar phenocrysts and 3 to 5 percent biotite. The younger Cub Creek pluton is a finer grained granodiorite to quartz monzodiorite with well-defined potassium-feldspar phenocrysts, 3 to 5 percent biotite, 3 to 5 percent hornblende, and as much as 3 percent accessory sphene. The Cub Creek pluton is correspondingly higher in CaO, MgO, TiO_2, Cr, V, and Nb, and lower in Na_2O, K_2O, and FeO than the Bear Creek pluton. The areal extent of the Bear Creek pluton has not been determined, but the Cub Creek pluton underlies an area of approximately 300 km^2. The contact between the two plutons is gradational over 250 m due to complex intrusive relations, but it is sharp on outcrop scale. Xenoliths are rare in the interiors of both plutons, but occasional quartzite and calcsilicate xenolith swarms are concentrated along the contact between the plutons. Both plutons have moderate to well-developed flow foliation that decreases in dip upward, suggesting proximity to the roof of the batholith. Primary mineral lineations and small fold axes trend 290° and plunge at shallow angles. Secondary mineral lineations trend 290° and 110° and also plunge at shallow angles with the 110° element increasing in abundance toward the eastern bordering mylonite front. A regional structural discontinuity (the Trans-Idaho discontinuity) trends 290° to 300°, transects the central part of the Bitterroot lobe, and may have been a controlling factor in localizing both the Bear Creek and Cub Creek plutons.

Structure of northern Bitterroot lobe of the Idaho batholith

Mapping by R. R. Reid (University of Idaho) of an area about 15 km north-south by 90 km east-west across the northern part of the Bitterroot lobe of the Idaho batholith in Idaho County, Idaho (loc. 17), revealed that the lobe is asymmetric. Flow foliation along the western margin strikes northwesterly and dips steeply. Within the lobe, migmatite screens dip varying amounts and strike predominantly 90°, near the primary flow-lineation trend. Foliation becomes progressively more intense to the east and dips at shallow angles eastward at the Bitterroot mylonite front. Primary flow foliation is strongly overprinted by a secondary flow foliation trending about 290°. Nonpenetrative blastomylonitic shears of varied trend cut the batholithic rocks west of the Bitterroot mylonite front and intersect in a lineation that plunges at shallow angles toward 290°.

The asymmetric structure began to develop with the rise of magma along a north- to northwest-trending fracture set near the western margin of the lobe; the magma then spread to the east in a sheet that was perhaps controlled by a low-angle thrust. Primary flow foliation formed, and migmatite screens were brought parallel to it. After consolidation, shearing of still-hot rock created secondary foliation and later blastomylonite; the blastomylonite is partly in ductile thrust faults having transport to the east. The shearing seems to have resulted principally from external tectonic forces—Rocky Mountain thrusting, transcurrent movements in the Trans-Idaho discontinuity, crustal thinning, or some combination thereof.

Eastern limit of alkalic intrusive rocks in the northwestern United States

According to F. K. Miller, a small pluton (15 km^2 in area) of hornblende monzonite appears to intrude a highly cataclasized porphyroblastic gneiss in the Selkirk Mountains in northwestern Boundary County, Idaho (loc. 18). This pluton is mineralogically, chemically, and texturally distinct from all other igneous bodies in the region, but it is similar in all respects to relatively sparse and widespread plutons of Triassic and Jurassic age (220 m.y. old) in the Western Cordillera. Like many of the Triassic-Jurassic plutons, the Selkirk mass is leucocratic (color index = 10), contains hornblende with pyroxene cores, has less than 6 percent modal quartz, contains numerous inclusions, and has a highly irregular and variable linear and (or) planar fabric. The rock is locally porphyritic and shows abundant evidence of cataclasis

and late-stage or postemplacement mobility of potassium. It represents the easternmost known occurrence of these distinctive plutons in this part of North America.

If the plutonic rock is Triassic and Jurassic in age and intrudes the porphyroblastic gneiss, the gneiss probably is Precambrian in age, as this region was the site of miogeosynclinal (continental-shelf) sedimentation during early and middle Paleozoic time. The gneiss probably predates the Proterozoic Y Belt Supergroup, as the Belt occurs nearby and is less deformed than the gneiss. The contact between the gneiss and Belt Supergroup does not appear to be a fault and thus may represent one of the few depositional contacts of the basal Belt rocks in the western part of the Belt basin.

PACIFIC COAST REGION

CALIFORNIA

Structural zones extending from the Sierra Nevada Mountains into Oregon

Further work by A. M. Heitanen-Makela has concentrated on synthesizing the structural zones of the northwestern Sierra Nevada Mountains and then comparing them with rocks in eastern Oregon. A major structural zone in the northwestern Sierra Nevada is bordered on the northeast by the Melones fault and on the southwest by the Big Bend fault. This zone includes pieces of oceanic lithosphere, a belt of Pennsylvanian metasedimentary rocks, island-arc type metavolcanic rocks, and melange, all strongly deformed and faulted. This structural zone is a major suture between the Silurian Shoo Fly Formation on the east and the Upper Jurassic rocks on the west. It continues southward including the Foothills fault system and a zone of melange between the Melones and Bear Mountains faults. It can be correlated with similar structures and rock units in the Klamath Mountains, where a belt of Paleozoic and Mesozoic rocks is separated from lower Paleozoic rocks on the east by the Trinity thrust and from Upper Jurassic rocks on the west by a zone of melange.

Paleozoic and Mesozoic rocks exposed in the John Day–Blue Mountains area in eastern Oregon consist of similar metavolcanic and metasedimentary rocks, form melange with ophiolitic rocks, and have northeasterly structural trends. It seems likely that these rocks form a northeastern extension of the same major suture that arches from the western Sierra Nevada through the Klamath Mountains into eastern Oregon around the Paleozoic continental block in northeastern California and northwestern Nevada. This suture includes relict Paleozoic subduction zones, remnants of island-arc volcanic rocks, trench-related ophiolites, and sedimentary rocks deposited in marginal basins. The subduction, volcanism, and sedimentation into minibasins near the continental margin continued over a long period of time. The subduction along the eastern border of the suture system (the Melones fault and Trinity thrust) started in the Devonian and continued locally until the Jurassic. The major subduction in Jurassic time was along the fault zones that border the suture zone on the west (the Big Bend and Bear Wallow faults). The island-arc type volcanic rocks within the suture zone are probably related to an early (Permian?) phase of this subduction. Remnants of sediments deposited on the sea floor that later became a marginal basin floor are preserved between the Paleozoic continental block and the island-arc rocks. Island-arc rocks west of the suture system in California are components of a second arc, related to the subduction along faults in the Coast Ranges. Poor exposure does not allow identification of similar sequence of subduction in eastern Oregon. Rather, remnants of similar rock units along with ultramafic rocks form a zone of mega melange in which the paleontologic ages of shallow-water sediments range from early Paleozoic to Jurassic. Permian and Jurassic time was the major period of island-arc volcanism. Early Triassic time was a period of major tectonism. This zone of melange in eastern Oregon is in the suture zones of the west in its lithology, structure, and time of its formation and presumably in its tectonic significance. All these tectonic zones are marginal to the same Paleozoic block that was accreted to the North American Continent during the Sonoma orogeny.

Faulting in the Sierra Nevada Mountains, California

Four distinct zones of faults comprise the northern third of the Foothills fault system, Sierra Nevada Mountains, Calif., according to D. E. Stuart-Alexander. The eastern three zones are parallel and appear similar in style of faulting, and all include significant bodies of serpentinite and ultramafics; the westernmost is quite different in style, has little-to-no associated serpentine, and strikes at a shallow angle to the other three. From east to west the fault zones are (1) Melones, (2) "Weimar" that may be the southern extension of the Camel Peak fault, (3) Bear Mountains, and (4) The unnamed zone along which the 1975 breaks occurred at Cleveland Hills near Oroville.

The first three zones are compatible with being old subduction zones and probably have been reactivated several times since the Paleozoic. In contrast, the westernmost zone consists of en echelon, relatively narrow shears and does not appear to be a major zone of dislocation, although it too has been reactivated since

the Mesozoic. All four zones appear to have moved during the Cenozoic and appear to be possible sites of renewed activity.

Correlation of Tertiary strata across the San Joaquin Valley

A good correlation between the stratigraphy of the east side and west side of the northern San Joaquin Valley was established by J. A. Bartow by mapping and petrologic studies of outcropping Tertiary strata together with subsurface correlations using data from exploratory wells. The Eocene Ione Formation of the east side apparently does not extend across the valley, but correlative west side strata include a sequence that grades up from marine shale and sandstone to nonmarine shale quartzose anauxitic sandstone and conglomerate nearly identical in lithology and facies to the Ione. The upper Oligocene and lower Miocene Valley Springs Formation of the east side, composed principally of claystone, tuffaceous claystone, and vitric tuff, has been recently identified for the first time on the west side of the valley where it had been mapped previously as part of the upper Miocene Neroly Formation. This identification is supported by very similar trace and minor element chemistry of glass from interbedded vitric tuffs (Andrei Sarna-Wojcicki, written commun., 1980). The Mehrten Formation of the east side is represented in the west side by the Neroly Formation (restricted); both of these formations are composed of andestitic volcaniclastic material from the Sierra Nevada.

A major east-west fault in north-central California

Geologic mapping of the Cenozoic volcanic and alluvial deposits of the northern Sacramento Valley by D. S. Harwood and E. J. Helley revealed a large-scale east-west fault zone. It is named the Battle Creek–Cottonwood Creek fault zone for the two major drainages, which have developed consequent to the faulting. This fault zone can be traced from near Mt. Lassen on the east approximately 80 km west-southwest to its termination against the Coast Range thrust in the Colyear Springs quadrangle. The east side of the fault zone has about 200 m of topographic expression with young volcanic rocks displaced by faulting as well as overlying the fault, thus providing a method to date absolutely the age of faulting. On the west side of the valley, the fault is expressed by a series of offset terrace deposits. The course of the Sacramento River at this latitude is "goosenecked" in large meanders. The river course is controlled structurally by a series of plunging folds, probably related to the faulting. The sense of motion is up to the north on the east side of the valley and up to the south on the west.

Alluviation in the San Joaquin Valley

B. F. Atwater reported that alluvial deposits exposed in a fan-head trench of Marsh Creek, a Coast Range stream of the northwestern San Joaquin Valley, contain charcoal that has a radiocarbon age of $20{,}465 \pm 675$ yr (UM–2053). If widespread, these deposits suggest an episode of alluviation previously unrecognized in the San Joaquin Valley and apparently noncoeval with alluviation by major rivers draining the Sierra Nevada.

Extension of late Cenozoic faulting in northwestern California

R. J. McLaughlin, H. N. Ohlin, R. L. Oscarson, and D. M. Peterson reported that the southwest side of the Elk Creek Rare II Wilderness Areas is transected by a major northwest-trending fault zone that locally exhibits features such as sag ponds, alined springs, and entrenched topography, suggesting late Cenozoic fault activity. The fault zone is traceable on aerial photographs as a series of strong topographic lineaments 45 km southwestward through the Lake Pillsbury area where it joins the Bartlett Springs–Wilson Valley fault zone. The Bartlett Springs–Wilson Valley fault zone cuts Pliocene and Pleistocene gravels of the Cache Formation interbedded with 1.6-m.y.-old volcanic rocks. To the northwest, near Covelo, the fault zone probably joins the active Lake Mountain fault system, recently described by Darrell Herd (1978). Southeast of Clear Lake, the fault zone may connect in a series of en echelon steps with the active Green Valley fault near Lake Berryessa.

Ages of radiolarian cherts in the central Klamath Mountains

The ages of ophiolites and associated sedimentary oceanic rocks and the times of their incorporation into the continental margin as accreted terranes are determined in some instances by study of radiolarians in cherts and tuffs. The North Fork terrane of the central Klamath Mountains was sampled for radiolarian-bearing cherts at many places along its 95-km length by W. P. Irwin and D. L. Jones in an effort to understand the accretionary development of the province and to aid in preparing a tectonostratigraphic map.

Preliminary results of the sampling indicate that the cherts are dominantly late Paleozoic in age in the southern part of the terrane, dominantly Early or Middle Jurassic in the middle latitudes, and dominantly Triassic in the Salmon River region to the north. The late Paleozoic radiolarian fauna found in the cherts of

the southern part of the terrane was previously unknown in North America. The differences in ages of the radiolarian faunas of the various segments suggest that the North Fork terrane is more heterogeneous than previously considered, and it raises the possibility that the various segments may not have accreted to the continental margin as a single unit.

Rand Schist on San Emigdio Mountains

Recent geologic mapping and petrographic study by D. C. Ross revealed a probable fault sliver of Rand Schist along the north flank of the San Emigdio Mountains, Kern County, Calif., considerably west of known Rand Schist slivers along the Garlock fault. The Rand Schist sliver in the San Emigdio Mountains is composed of quartzite and biotite schist layers that contain large dark poikilitic untwinned sodic plagioclase crystals strongly dusted with carbonaceous matter—the very diagnostic black albite of the Rand-Orocopia Pelona terrane. Primary gray chlorite and thick white bull quartz veins also characterize these rocks. The contrast in lithology and metamorphic grade between these presumed Rand rocks and associated andesine- and hornblende-rich dioritic, amphibolitic, and gneissic rocks leaves little doubt that the Rand rocks here are structurally displaced, possibly by significant strike-slip movement on the Pastoria fault zone of Crowell (1952).

OREGON

Tectonostratigraphic terranes of southwest Oregon

Work by M. C. Blake, Jr., and Angela Jayko during FY 79 in the Coos Bay 2° sheet, southwest Oregon, indicates that there are at least nine tectonostratigraphic terranes of late Mesozoic age present. Rather than representing dismembered elements of a former continental margin, these terranes appear to have formed in different areas and were accreted subsequently to the North American Continent by large-scale plate motions.

WASHINGTON

Sedimentation rates in the Puget Sound

The Puget Sound coast is unusual in that 90 to 100 percent of all sediment is derived from bluff erosion as opposed to sediment delivered by rivers. Preliminary results by R. F. Keuler show high rates of sediment productions in the Strait of Juan de Fuca where wave energy is highest; at rapidly eroding sites, typical rates are 7 to 15 m^3/m of shoreline per yr. In sheltered waters that are more representative of the entire region, rates are 1 to 5 $m^3/m/yr$.

Extent of glacial marine drift in the Puget Lowlands

During the course of detailed geologic mapping of deposits of the continental glacier in the Puget Lowlands by J. P. Minard, new outcrops of fossiliferous glacial marine drift were discovered. One outcrop near the mouth of the Stillaguamish River contains an abundant well-preserved suite of shallow-water marine fossils. Radiocarbon dates from peat and shells indicate an age greater than 49,000 yr B.P. Deposits south of Everett push the range of the glacial marine drift farther south than most previously known exposures.

Cretaceous plutons in the Cascades

Recent studies of Upper Cretaceous synkinematic plutons in the North Cascades by R. W. Tabor, V. F. Frizzel, Jr., and M. J. Hetherington confirm the Late Cretaceous age of metamorphism for the crystalline core of the North Cascades and document some of the structural uplift history of the range.

The most northerly pluton, the Sloan Peak, is a tonalite gneiss with mostly crystalloblastic and cataclastic textures. Evidence of its igneous history is preserved in intrusive contacts and relict igneous fabric. The Mount Stuart pluton, lying to the southeast and across the crest of the Cascade Range, displays mostly igneous textures and contact relations.

The Entiat pluton and tonalite of the Chelan pluton, which outcrop roughly 64 km to the east of the Cascade crest, have predominantly metamorphic textures overprinting igneous textures. Lead and lead-uranium isotopes ages of zircons determined by Robert Zartman indicate ages of igneous crystallization of roughly 90 m.y., 96 m.y., 85–90 m.y., and 80 m.y. for the Sloan Peak, Mount Stuart (a mafic phase at Big Jim Mountain), the Entiat, and Chelan plutons respectively.

K-Ar ages of hornblende of the Sloan Peak and the main body of the Mount Stuart are roughly the same as the zircon ages, namely 89 m.y. and 90–95 m.y., respectively. Biotite ages, on the other hand, are degraded to 75 m.y. at Sloan Peak and range from 82 m.y. to 90 m.y. in the Mount Stuart. The concordance of the hornblende and zircon ages at Sloan Peak suggests rapid uplift, but not before biotite had partially degassed. The Mount Stuart was intruded more shallowly than the Sloan Peak and was uplifted to the level where argon is fixed in biotite more rapidly than the Sloan Peak. Hornfels textures at the southern end of Mount Stuart testify to its relatively shallow depth of intrusion.

K-Ar ages of hornblende in the eastern plutons range from 60 m.y. to 74 m.y., and biotite ranges from 56 m.y.

to 74 m.y., suggesting that although the eastern plutons are somewhat younger than the western two plutons, they stayed deeper longer. The migmatization supports the theory that they were deeper during metamorphism and, presumbly, during intrusion.

In summary, following intrusion and metamorphism during the Late Cretaceous, the rocks in the Cascade crest area were uplifted rapidly and were tilted up to the north. The rapid uplift of the Sloan Peak pluton might be ascribed to uplift along the Straight Creek fault, exposed to the west. Farther east, on the flanks of the range, uplift from greater depths was slower and hornblende degassed until about 74 m.y. ago.

The Newport fault

Mapping by F. K. Miller demonstrated that the Newport fault is a thrust fault with a U-shaped trace that straddles the Idaho-Washington State line. It was traced to within about 30 km of the Canadian border on both the east and west arms of the U. The west arm roughly follows the west side of the Pend Oreille River valley to the latitude of Newport, Wash., where it swings eastward, parallel to, but on the north side of the east-west portion of the river. Just north of the town of Priest River, Idaho, the fault swings to a north strike again and roughly follows the east side of the Priest River valley. Where attitudes on the fault can be measured, they all dip into the U at angles ranging from 30 to 60 degrees.

Cataclastic rock and mylonite make up a zone that varies from about 100 to 300 meters in thickness along the fault. Petrographic study of rocks within and adjacent to the zone suggests two distinct and contrasting styles of deformation. The earlier deformation appears to be ductile or semiductile with large crystals showing intense milling and long trains of fine-grained broken and recrystallized minerals. These rocks contain both primary and recrystallized mafic minerals, and they commonly have an oriented fabric. The younger deformation is brittle fracture accompained by intense chloritization. Even though this rock is commonly milled and broken to an aphanitic grain size, it is a hard coherent rock that shows almost no directional fabric. Some attitudes on the younger deformation, where attitudes are obtainable, are slightly steeper than those of the ductile deformation, suggesting that the second stage of movement was not entirely along the preexisting fault.

Young deposits in the Puget Sound area

Compilations of geologic mapping in the Puget Lowland, Wash., by Fred Pessl, Jr., D. P. Dethier, R. F. Keuler, J. P. Minard, and S. A. Safioles have led to broader interpretations of several Holocene or latest Pleistocene deposits. The first of these units are lahars and laharic debris derived from Glacier Peak and deposited along the North Fork Stillaguamish River as far west as Arlington sometime before 10,200 yr B.P., probably between 11,200 and about 12,600 yr B.P. Most of the alluvial fill between Rockport and Mt Vernon, ranging in altitude within 10 m of the Skagit River, consists of material derived from Glacier Peak during the Holocene. At least two separate periods of deposition, about 5000 yr B.P. and about 1800 yr B.P., are indicated by radiocarbon dating of charcoal in the deposits. Deposition of large volumes of volcanic detritus more than 100 km from Glacier Peak suggests that lahars much like those generated at Mount St. Helens in 1980 repeatedly swept down the Skagit River during the Holocene.

Additional deposits include the glacial-marine and marine sediments that are now exposed as much as 90 m above mean sea level, some glacial sediments formed beneath floating ice, and others formed as in a variety of depositional settings including marine beach, tidal flat and estuary, shallow subtidal marine, deeper marine, marine glaciofluvial delta, and marine ice-contact glaciofluvial. Radiocarbon dating of shells preserved in these deposits indicates that the retreat of continental ice was rapid, and that marine waters entered the central Puget Lowland before 12,700 yr B.P. Age differences of approximately 1,000 yr between shallow-marine deposits at similar altitudes suggest differential isostatic rebound, perhaps related to the regional pattern of ice retreat or to inferred crustal structure.

Finally, till deposited during the most recent glaciation of the Clear Lake area, Washington, contains a distinctive suite of locally derived clay minerals. These minerals (serpentine, talc, stilpnomelane, and kaolinite), drumlinoid features, and striations provide specific evidence for basal-ice flow directions to the south and to the east. Tillclast litholigies provide additional evidence of flow direction but are poorer indicators than the clay minerals. Till in the Clear Lake area contains about 70 percent matrix (2 mm) consisting of about 45 percent silt, 45 percent sand, and 10 percent clay.

ALASKA

STATEWIDE

Alaska Mineral Resource Assessment Program

The chief objectives of the Alaska Mineral Resource Assessment Program (AMRAP) are (1) to provide mineral-resource information to Congress, the administration, and the private sector so that decisions can

be made on the allocation and classification of Alaska's Federal lands, particularly in regard to the mandates of the Alaska National Interest Land Conservation Act (ANILCA); (2) to provide geological information to the mineral industry, the natives of Alaska, and other public and private interests concerned with exploration and development of Alaska's mineral resources; (3) to provide comprehensive mineral-resource information to help guide national mineral policy; and (4) to increase the limited knowledge of Alaska's mineral resources even at reconnaissance scale.

AMRAP consists of projects that contribute to four levels of study. The objective of Level I is to publish statewide summaries of Alaska's mineral resources. This project is continuing and is based on past and present investigations by the USGS and by other organizations and agencies. Level II works toward identifying mineral resources likely to occur in a given large area of the State by plotting favorable areas on map generally at a 1:1,000,000 scale and by presenting some measure of the probable size and grade of undiscovered deposits. Level II reports incorporate summaries of the results of Level III studies, which include geologic mapping, aeromagnetic and geophysical surveys, analysis of geochemical samples, and topical studies of known deposits. The Level III studies address 1:250,000-scale quadrangles, each containing about 4.5 million acres, and constitute the main thrust of the program at present. Interdisciplinary teams study each quadrangle for about 3 yr acquiring detailed information. Field studies were completed in 22 quadrangles in 1980 and are underway in 9 additional quadrangles. Level IV investigations focus on individual mineral deposits or mining districts to determine their size, nature, and origin. Such Level IV studies are underway in southeastern Alaska, on the Aleutian Peninsula, and in the Alaska and Brooks Ranges.

Mineral-deposit research problems are being studied in the following mining districts: (1) the Alaska Peninsula porphyry copper district, (2) the Ambler copper district, (3) Willow Creek gold district, (4) Hope gold district, and (5) the Bornite copper deposit. Alaska placer deposits are also being studied.

Metamorphic facies map of Alaska

The map is planned as a contribution to a Map of the Metamorphic Belts of the World, which is sponsored by the Commission for the Geological Map of the World (or the International Geological Congress and the International Union of Geological Sciences) and is a joint USGS–State of Alaska Geological Survey publication. It will show metamorphic facies, facies groups, facies series, selected isograds, and granitic rock bodies in the style of the IUGS (1967) suggested metamorphic facies explanation.

Strato-tectonic terranes in the central Alaska Range

The central part of the Alaska Range near Mount McKinley is composed of eight separate tectonostratigraphic terranes that were accreted in southern Alaska during late Mesozoic time, according to D. L. Jones, N. J. Silberling, and P. J. Coney. These terranes now form long, linear, fault-bounded belts that are subparallel to the Denali fault on the north. From north to south, the major terranes are as follows:

- Yukon-Tanana terrane–Metasedimentary and metavolcanic rocks, mostly undated but including rocks of known late Paleozoic age.
- Pingston terrane–Isoclinally folded Upper Triassic deep-water silty limestone, quartzite, and sooty slate, folded with upper Paleozoic phyllite, chert, tuff, and minor limestone.
- McKinley terrane–Upper Paleozoic flysch, chert, minor limestone; intruded by large gabbro lava. Top of section is thick sequence of upper Mesozoic conglomerate, flysch, chert, and phyllite.
- Dillinger terrrane–Thick sequence of strongly folded lower Paleozoic micaceous sandstone (turbidite beds) and deep-water, poorly fossiliferous limestone; locally overlain unconformably by Jurassic fossiliferous sandstone or Triassic(?) pillow basalt.
- Windy terrane–Heterogeneous assemblage of serpentinite, basalt, tuff, and chert (=ophiolite?) with Paleozoic and Mesozoic flysch and blocks of Paleozoic and Mesozoic fossiliferous limestone.
- Chulitna terrane–Upper Devonian ophiolite overlain by upper Paleozoic chert, volcanic conglomerate, limestone, and flysch, capped by Lower Triassic limestone and Upper Triassic red beds, basalt, and interbedded basalt and limestone; later Mesozoic rocks are sandstone, chert, and argillite.
- West form terrane–Jurassic chert, sandstone, conglomerate, and Triassic(?) and Jurassic crystal tuff.
- Broad Pass terrane–Upper Paleozoic chert, tuff, and argillite, with blocks of Devonian and older limestone weakly associated with serpentinite.

These diverse terranes, of mixed oceanic and continental affinities, are juxtaposed now in a complex sequence of folded, rootless nappes, with major suture zones marked by intensely deformed upper Mesozoic flysch.

NORTHERN ALASKA

Precambrian and early Paleozoic history of the southern Brooks Range

Published and new unpublished geochronology on meta-igneous and metasedimentary rocks of the southern Brooks Range require major changes in interpretation of the tectonic, metamorphic, and magmatic history of this complex region, according to M. L. Silberman, D. B. Brookins, and S. W. Nelson (USGS), and J. T. Dillon (Alaska Division of Geological and Geophysical Surveys). Published U-Pb data from zircons and Rb-Sr data from whole-rock samples of metaplutonic and metavolcanic rocks (1) define a major intrusive and extrusive magmatic event in the middle Paleozoic (centered on the Devonian) that produced high-potassium granitic and felsic volcanic rocks, associated massive-sulfide deposits, and mafic volcanic rocks; and (2) give equivocal evidence for the presence of Precambrian basement. Depending on the minerals dated, published K-Ar ages are interpreted to represent partial argon loss resulting from metamorphism after the Paleozoic magmatic event or to indicate uplift following culmination of metamorphism. A few K-Ar ages support the presence of Precambrian basement in two areas of the region. New Rb-Sr whole-rock data from the Survey Pass quadrangle and K-Ar ages from several other areas confirm the presence of Proterozoic Z rocks and suggest that metamorphic recrystallization began at least as early as the Triassic-Jurassic boundary. In particular, Rb-Sr results from the Arrigetch Peaks and Mt. Igikpak plutons of the Survey Pass quadrangle document a complex pattern of multiple Devonian intrusion of anatectic magma from sources of high but variable initial Sr isotopic composition, and require the presence of much older radiogenic rocks in the source region of the magma.

Basalt in the Tunalik No. 1 test well

A 240-m thick interval of basaltic flows and tuffs was intersected at 5,350 m in the Tunalik No. 1 test well within the Lower Permian limestone and bioturbated mudstone part of the Lisburne Group. A 9-m-long core recovered from the igneous interval was petrographically examined and dated by the K-Ar method, according to M. L. Silberman, J. L. Bentz, I. L. Tailleur, L. B. Gray, and H. W. Yeho. The top and bottom of the core are fine grained and vesicular; vesicles near the top are filled with chlorite, and those near the bottom are filled with calcite plus chlorite. The middle of the core is coarser grained and contains smaller vesicles and inclined stringers of chlorite. The basalt has relict porphyrytic texture, felted microlytic groundmass, and large vesicles; chilled margins suggest that the basalt is a single submarine flow. Six whole-rock K-Ar ages range from 35 m.y. to 110 m.y., are inversely proportional to potassium content, and have the same radiometric argon concentration. Isochron analyses indicate a zero age. The data suggest ongoing thermal homogenization of argon trapped in the volcanic interval by surrounding impermeable sedimentary rocks. Oxygen isotope data from vesicle filling calcite and chlorite suggest isotopic equilibration at about 200° C, near the present temperature, at 5,350 m. The argon and stable isotope results suggest that low-grade metamorphism is still occuring at this depth in the well.

EAST-CENTRAL ALASKA

Sillimanite gneiss in the Big Delta quadrangle

A topographically high, nearly circular area of sillimanite gneiss crops out over approximately 600 km^2 in the Big Delta quadrangle, Yukon crystalline terrane, east-central Alaska, and is being studied by Cynthia Dusel-Bacon and H. L. Foster. Foliation is generally horizontal in the center of the gneiss body and dips outward in all directions. Pegmatite dikes and patches of granitic-appearing aluminun silicate-bearing rocks occur in the central area of gneiss. Quartzite and marble are infolded locally in the gneiss, particularly near its margins. The gneiss is partly surrounded on the north and east by pelitic schist interlayered with lesser amounts of quartizite, marble, and amphibole schist. Two isograds within the schist are concentric to the gneiss body and indicate an increase in metamorphic grade toward the gneiss. The outermost isograd is defined by the appearence of staurolite with biotite at the expense of chlorite and muscovite. Various combinations of the aluminun silicate polymorphs plus garnet plus staurolite are present in quartz-biotite-muscovite schist, and andalusite, kyanite, and sillimanite occur together in thin sections from four separate localities. Textural relations suggest that the polymorphs formed during the same prograde metamorphic event in which pressure-temperature conditions were near the triple point. The innermost isograd, defined by the disappearance of staurolite, closely coincides with the schist-gneiss contact and outlines the proposed dome. Increase in metamorphic grade in the gneiss (quartz plus biotite plus sillimanite plus orthoclase plus plagioclase plus or minus muscovite plus or minus garnet) is indicated by an increase in modal orthoclase and decrease in muscovite plus quartz. Iron-magnesuim distribution between garnet and biotite indicates equilibrium at $535–600 \pm 30$°C for pelitic schist and $655–705 \pm 30$°C for sillimanite gneiss. Evidence that the sillimanite gneiss is a dome consists of (1) topographic expression and radial

drainage pattern, (2) outward dip of foliation, (3) increase in metamorphic grade toward the center of the body, (4) increase in garnet-biotite temperatures inward, and (5) pegmatite dikes and granitic rocks in core, suggesting partial melting.

Plutons of Late Cretaceous and early Tertiary age in the Circle quadrangle

In the Circle quadrangle, tentative potassium-argon age determinations by F. H. Silson and Nora Shew indicate a Late Cretaceous to early Tertiary age (75–55 m.y.) for all plutons studied. This is in contrast to the Big Delta quadrangle to the south where many plutons yield middle Cretaceous ages (110–90 m.y.) (Foster and others, 1979). Mapping by F. R. Weber, H. L. Foster, and F. H. Wilson indicates that, in general, the plutons in the Circle quadrangle are more micaceous than those of the Big Delta quadrangle and include some two-mica granites. These plutons also rarely contain amphibole, unlike the older plutons of the Big Delta quadrangle. Plutons of latest Cretaceous to earliest Tertiary age in the Big Delta quadrangle are similar lithologically to those of the Circle quadrangle. In the Circle quadrangle, two plutons are known to contain up to a few percent tourmaline. One of these is a two-mica granite with pink feldspars, whereas the other contains tourmaline as the only dark mineral and has only accessory muscovite.

Lode gold in the Lost Chicken area

Gold was detected in sheared and altered diorite or quartz diorite in a bedrock cut in the Lost Chicken placer gold mine, Fortymile River area, Alaska, by H. L. Foster. Gold in bedrock only rarely has been found directly associated with placer deposits in the Fortymile River area and other placer districts of the Yukon-Tanana upland. Lost Chicken Creek is a small tributary to the South Fork of the Fortymile River, which has been mined discontinuously since about 1895. In the last few years, the lower part of the valley has been mined by hydraulicking. When the mine was visited in early September 1980, good cuts in greenish-gray, highly sheared diorite or quartz diorite were exposed about 2,000 m above the mouth of the Creek. The rock contained abundant sulfides, and much of it was stained yellow and orange brown. Six grab samples of bedrock were collected from one cut and analyzed for gold by R. M. O'Leary using the atomic absorption method. Two of the six samples contained 0.10 ppm gold. Gold was not detected in the other four samples (limit of detection 0.05 ppm). The samples, which contained gold, were stained orange brown; and one had many visible sulfides. These bedrock analyses suggest that some Lost Chicken placer gold is probably locally derived from sheared mineralized diorite.

Glacial geology of the Yukon-Tanana uplands

A special study was made of the Mt. Prindle area by F. R. Weber. Three major glaciations were recognized, but only one example was found of the most recent Pleistocene advance; and examples of the second oldest advance are greatly restricted. The glacial features seen today are primarily the result of the earliest(?) and most extensive Pleistocene glaciation. The earliest glaciation was studied in the Salcha River, Charley River, and Mt. Harper areas. Evidence is accumulating that suggests that the most extensive glaciation possibly should be viewed as two separate major events. Several new volcanic ash deposit sites were located. A very thin "grass roots" tephra is recognized as the White River Ash Bed of the Engineer Loess, and its location near Joseph in the Eagle quadrangle confirms the maximum extent of this ash deposit as postulated by earlier workers. A second ash found at greater depth in sediments of the Middle Fork of the Fortymile River-Mt. Harper area possibly is related to the episode of maximum Pleistocene glaciation and is therefore much older.

WEST-CENTRAL ALASKA

Mississippian rocks in the Ophir quadrangle

Two extensive, predominantly sedimentary rock units, provisionally assigned a Mississippian to Early Jurassic(?) age, were identified and mapped in the eastern half of the Ophir quadrangle by R. M. Chapman, W. W. Patton, Jr., and E. J. Joll in 1980. Previously, these units were largely unmapped in this area, and their age was uncertain. These rocks form a structurally complex belt, possibly fault-bounded, about 30 km wide and 80 km long that trends northeast from upper Tolstoi Creek to Colorado Creek and into the Medfra and Ruby quadrangles. One unit of radiolarian chert, tuff, argillite, basalt, and a few small bodies of limestone, and a second smaller unit of sandstone, grit, and argillite have been differentiated. The stratigraphic sequence within these units and the ages represented cannot be determined adequately without additional field studies, but the provisional age range is based on a few fossil collections within the Ophir quadrangle and on lithologic correlations with similar rock units that have been mapped and paleontologically dated in the Medfra and Ruby quadrangles (Patton and others, 1980; Chapman and Patton, 1979). Radiolarians in these samples from the Ophir quadrangle have given ages of Mississippian, Early Pennsylvanian, and Late Triassic, respectively

(B. K. Holdsworth, written commun., 1978; D. L. Jones, oral commun., 1980). A mixed, reworked conodont fauna from one of the limestone bodies contains elements of Late Devonian and late Early Mississippian age (A. G. Harris, written commun., 1980). Based on these new lithologic and palentologic data, the Innoko terrane that has oceanic or island-arc affinities can be extended at least 80 km southwest from the northwest part of the Medfra quadrangle where it was originally described by W. W. Patton, Jr.(1978).

Widespread Late Cretaceous and early Tertiary calc-alkaline volcanism in west-central Alaska

Recent reconnaissance mapping by E. J. Moll and W. W. Patton, Jr., documents a major episode of calc-alkalic volcanism of Late Cretaceous and early Tertiary age (70–60 m.y.) in a broad belt stretching from the Bering Sea Shelf eastward to the Alaska Range and northward to the Arctic Circle. The volcanic assemblages are preserved now only as isolated remnants, but the widespread occurrence of contemporaneous hypabyssal intrusive rocks of similar composition suggests that large parts of western Alaska were once covered by these volcanic rocks. The volcanic rocks are studied best in the northern Kuskokwim Mountains where they occur either as elongate fault-bounded synclinal remnants of gently folded flows that trend northeast or as small circular (6 km across) volcanoplutonic complexes along a northeast-trending alinement that extends 250 km from Page Mountain to Horn Mountain. Composition ranges from basalt to rhyolite, but intermediate and siliceous rocks (56–75 percent SiO_2) with high-K (1.9–5.4 percent K_2O) content predominate. The volcanic rocks overlap four tectonostratigraphic terranes: the Nixon Fork, the Innoko-Rampart, the Yukon-Koyukuk, and the Brooks Range-St. Lawrence Island. This overlap established conclusively that all these diverse terranes in western Alaska were sutured together by the end of Late Cretaceous time.

It is tempting to relate this calc-alkalic volcanism to subduction along the Pacific margin, because the volcanic belt lies roughly perpendicular to the probable direction of Kula-plate convergence during Late Cretaceous and early Tertiary time, and because sparse data show an apparent increase in K_2O content landward across the Alaska-Aleutian Range batholith to the volcanic and plutonic rocks of the northern Kuskokwim Mountains. Much additional geologic mapping and chemical data are needed, however, to assess the credibililty of this model.

SOUTHERN ALASKA

Geophysical anomalies over mafic to ultramafic rocks along the north flank of the Chugach Range

Major aeromagnetic and gravity highs occur over mafic, intermediate, and ultramafic plutonic bodies along the flank of the Chugach Mountains in the Valdez 1:250,000 quadrangle of south-cental Alaska. J. E. Case, G. R. Winkler, and Laurel Burns prepared a preliminary interpretation of part of the data. A complex series of aeromagnetic highs, ranging up to 3000 gammas in amplitude, trend about east-west along the north flank of the Chugach Range for a distance of more than 100 km from the western edge of the Valdez quadrangle to near Tonsina and the Copper River. The breadth of this anomaly belt ranges from 5 to 25 km, thus it is of major regional extent. The anomaly belt is caused by a plutonic complex that ranges in composition from gabbro to quartz diorite, with abundant variants such as pyroxenites and anorthositic gabbros. The gabbros are commonly layered, but cumulate textures have not been found in any abundance. Most of the rocks are magnetic, as evident from comparison of the geologic and aeromagnetic maps. Measured susceptibilities of samples range up to 0.0015 cgs units, with many values in the range 0.003 to 0.005 cgs units. Five two-dimensional models have been computed across the belt. Depending on location of the specific profiles, the causative body has a depth extent of 5 to 10 km and a breadth extent of 4 to 10 km, generally increasing with depth for magnetization contrasts of 0.002 to 0.004 emu. Anomalies associated with this plutonic complex evidently extend far to the west toward Anchorage and to the southwest toward Homer, so that the body constitutes a major geologic feature of south-central Alaska.

Residual gravity anomalies across the plutonic complex in the Valdez quadrangle range from +20 to +40 mgals, or more. Preliminary models indicate similar dimensions to those derived from the magnetic models for density contrast of about +0.2 g/cm^3.

SOUTHWESTERN ALASKA

Deep-water marine deposition of the Kuskokwim Group

In its type locality along the Kuskokwim River between the villages of Sleetmute and Aniak, the Cretaceous Kuskokwim Group is composed of moderately folded thin- to thick-bedded graywacke and shale. Study of 16 large cut-bank exposures suggests to J. M. Hoare (USGS) and John Decker (Alaska Division of

Geological and Geophysical Surveys) that most, or all, of the rocks were deposited as meduim- and fine-grained sand and silt turbidite beds in lobes at or near the bottom of a regionally subsiding trough. Rocks of possible shallow marine origin were found in only one or two exposures.

Graywacke sandstone beds range in thickness from less than 1 cm to about 2 m. Beds 2 cm to 10 cm thick are commonly graded. Thick beds locally have channelized bases with rare coarse-grained sand or granule lag deposits and shale rip-ups. Groove casts are common on the base of graywacke beds, but flute casts are rare. Fine carbonized plant material is locally abundant on bedding surfaces.

Stratal disruptions and soft-sediment folds related to submarine slumping and landsliding were seen at one locality and may have been overlooked elsewhere. The ratio of sandstone to shale in the large exposures is estimated to be about 5:1; but this ratio is probably too high, as extensive covered intervals are most likely underlain by more shale-rich sections. In some exposures, the beds occur in systematic megacycles. Of the 16 exposures studied, 4 showed graywacke beds thickening and coarsening upward in megacycles 3 m to 10 m thick. In one exposure, graywacke beds became thinner and finer upward. In about 10 exposures, no megacycles could be recognized. If the section is not repeated by unknown faults or folds, the Kuskokwim Group is at least 12 km thick. The monotonous similarity of the strata suggests that there were deposited in the same deep-marine environment, probably as prodelta lobes in a subsiding continental trough.

Tertiary volcanic and hypabyssal rocks in the Ugashik quadrangle

Potassium-argon dating of volcanic and hypabyssal rocks from the Ugashik quadrangle by F. H. Wilson and Nora Shew indicates that these rocks fall into the same two age groupings as those of the Chignik and Sutwik Island quadrangles to the south. Rocks of late Eocene to earliest Miocene and latest Miocene to Holocene age are found in both areas. Preliminary mapping by R. L. Detterman, J. E. Case, and F. H. Wilson indicates a major break in the trend to the west. This offset occurs in the vicinity of Wide and Puale Bays.

SOUTHEASTERN ALASKA

Basement complex on southern Prince of Wales Island

Regional mapping and U/Pb zircon studies by G. D. Eberlein (USGS) and J. B. Saleeby (Cal Tech) delineated an ensimatic basement complex partly beneath and partly emplaced into the early Paleozoic volcanic arc of southern Prince of Wales Island. The critical assemblages within the complex are basaltic dike swarms (locally sheeted), great masses of diorite-basite migmatite, and irregular intrusive bodies of gabbro, pyroxenite, diorite, and trondhjemite. Combinations of these assemblages occur between Kassan Peninsula and Moria Sound and at Klakas Inlet. Two major igneous stages are recognized. The oldest stage is represented best by the Klakas Island trondhjemite. Concordant ages within the multilple zircon fractions show that this body crystallized at 450 ± 10 m.y. Preliminary discordant ages, permitting a possible Precambrian age, were an artifact of undetected uranorthorite impurities within the zircon populations. The original distribution of the 450 m.y. trondhjemetic basement rock is unknown due to Devonian uplift and erosion and widespread high-temperature remobilization during a second igneous stage. This stage, recognized over a wide area, is marked by a complex family of mafic dikes, significant migmatitic zones, and small plutons of intermediate composition. The migmatitic zones were formed by intermixing of mafic magma and older remobilized basement rock. Inheritance of 450 m.y. zircon and pervasive greenschist metamorphism have prohibited direct dating of the second igneous stage. Existing U/Pb data and geologic considerations constrain this stage to between Devonian and Triassic time. The great swarms of mafic dikes associated with the local occurrence of pillow lava within sheeted intervals indicate rifting and possible displacement of the southern part of the Alexander terrane.

Refinement of Early Silurian time scale

Preliminary determinations of ancient pelagic sedimentation rates by Claire Carter, J. H. Trexler, Jr., and Michael Churkin, Jr., agree with modern rates of about 4 m per million yr. By combining data on the thickness of graptolite zones from the North American Cordillera with data from other parts of the world, they have refined the Early Silurian time scale and have obtained much better resolution than is possible for radiometric dates. The new Early Silurian time scale allows estimation of true rates of change in graptolite diversity. The Llandoverian diversity explosion is twice as rapid as was previously thought. The brevity of diversity lows and rapidity of speciation support modern theories of quantum evolution.

Metamorphic isograds in the Juneau area

Continued study of the isograds in the Barrovian metamorphic belt that forms the southwest side of the Coast Plutonic Complex by A. B. Ford and D. A. Brew has resulted in a major relocation of the "pumpellyite out" isograd and a minor and important adjustment of

the "staurolite in" isograd. The pumpellyite isograd is now recognized north of the Mendenhall Valley to be on the northeast side of the Gastineau Channel fault. This area was considered earlier to be near or above the first appearance of green biotite and is about 4 km distant from the nearest previously known pumpellyite. This new information, together with previous data, requires that the "pumpellyite out," "green biotite in," "brown biotite in," and "garnet in" isograds occur in a zone only 1.5 km wide instead of the common 6-km-wide zone. The cause of this extreme attenuation is not yet known, nor is it known if there is repetition of the "pumpellyite out" isograd on both sides of the Gastineau Channel fault. Possible causes of the attenuation include fault truncation of isograds beneath the Mendenhall Valley and (or) an abrupt change of isograd trend. The pumpellyite-bearing rocks are lithically identical to the Cretaceous augite phenocryst-bearing part of the Douglas Island Volcanics, which had not been known previously to extend across the Gastineau Channel fault. This fault is the local manifestation of the Coast Range megalineament. Thus, the previously suspected presence of Cretaceous rocks northeast of the fault and lineament is supported by the new data.

Interpretation of the heterogeneous rocks in the Duncan Canal area as a Cretaceous melange

The heterogeneous assemblage of rocks of different types and different ages along Duncan Canal currently is interpretated as a fault zone of post-middle Cretaceous–pre-late Tertiary age. An alternative hypothesis, according to D. A. Brew, is that the zone represents a Cretaceous-age melange formed in association with the Gravina terrane volcanic and flyschoid rocks and then further disrupted by younger faulting. Rocks west of the zone consist of slightly to very deformed phyllite of Jurassic and (or) Cretaceous age, obscured in part by relatively undeformed Eocene (?) to Miocene(?) volcanic flows and intrusion. The phyllites probably are derived from distal facies of a turbidite-fan complex. Rocks within the one-to-several- km-wide zone are dominantly phyllite like that to the west enveloping large (km-scale) blocks of older rocks and cut by upper Tertiary basalt plugs. The blocks include fossiliferous Devonian, Permian, and Triassic strata. Most blocks are less than 2 km long and .5 km wide, but one of Triassic(?) age on Woewodski and Zarembo Islands may be as much as 8 km wide and 40 km long. Graywacke, semischist phyllite, some greenschist and minor limestone that probably represent mostly mid-fan facies of the same Jurassic and (or) Cretaceous turbidite fan complex lie to the east of the zone.

To the north, the Duncan Canal zone connects with the Young Bay–Seymour Canal fault zone on Admiralty Island. To the south, it connects beneath the Tertiary volcanic flows, dikes, domes, and plugs of Zarembo Island with the Clarence Straight fault zone or lineament. The Young Bay–Seymour Canal zone has not been reexamined to see if it exhibits any of the features of the Duncan Canal zone. The Clarence Strait zone has been reexamined, and it does contain large blocks of fossiliferous Paleozoic (pre-Permian), Permian, and Triassic strata juxtaposed against Jurassic and (or) Cretaceous flysch to the east.

WATER-RESOURCE INVESTIGATIONS

The mission of the USGS's Water Resources Division (fig. 1) is to provide, to interpret, and to apply the hydrologic information needed for the optimum use and management of the Nation's water resources. This is accomplished, in large part, through cooperative programs with other Federal, State, and local agencies. The USGS also cooperates with the Department of State in providing scientific and technical assistance to international agencies.

The USGS conducts systematic investigations, surveys, and research on the occurrence, quality, quantity, distribution, use, movement, and value of the Nation's water resources. This work includes (1) investigations of floods and droughts and their magnitudes, frequencies, and relations to climate and physiographic factors; (2) evaluations of available waters in river basins and ground-water provinces, including assessments of water requirements for industrial, domestic, and agricultural purposes; (3) determinations of the chemical, physical, and biological characteristics of surface and ground water and the relation of water quality and suspended-sediment load to various parts of the hydrologic cycle; and (4) studies of the interrelation of water supply with climate, topography, vegetation, soils, and urbanization.

One of the USGS' most important activities is disseminating water data and the results of investigations and research by means of reports, maps, computerized information services, and other forms of public releases.

The USGS coordinates the activities of Federal agencies in the acquisition of water data on streams, lakes, reservoirs, estuaries, and ground waters, maintains a national network, conducts special water-data-acquisition activities, and maintains a central catalog of water information for use by Federal agencies and other interested parties.

Supportive basic and problem-oriented research is conducted in hydraulics, hydrology, and related fields of science to improve the scientific bases for investigations and measurement techniques and to provide sufficient information about hydrologic systems so that quantitative predictions of their responses to stress can be made.

During FY 1980, data on streamflow were collected at 8,428 continuous record discharge stations, at 860 lake- and reservoir-level sites, and at 9,015 partial record streamflow stations. More than 13,000 maps of flood-prone areas in all States and Puerto Rico have been completed. Studies of the quality of surface water were expanded; there were 8,913 water-quality stations in the United States and in outlying areas where surface water was analyzed by the USGS. Constituents and properties measured include selected major cations and anions, specific conductance or dissolved solids, and pH. Other constituents, measured as needed, include trace elements, phosphorous and nitrogen compounds, detergents, pesticides, radioactivity, phenols, BOD, and coliform bacteria. Water-temperature records were collected at most of the water-quality stations. Sediment data were obtained at almost 3,000 locations.

Annually, about 500 USGS scientists report participation in areal water-resource studies and research on hydrologic principles, processes, and techniques. There were 1,300 active water-resource projects; 374 of the studies in progress were classed as research projects. Of the current water-resource studies, 81 were related to urban hydrology problems, 176 were energy-related projects, and 71 were related to water use.

In FY 1980, 687 areal appraisal studies were carried out. Maximum and mean areas of the studies were about 1.9×10^6 km^2 and 0.069×10^6 km^2, respectively. Total areal appraisal funding was $60.1 million. Ground-water studies have been made or are currently in progress at some degree of intensity for all of the Nation. Long-term continuing measurements of ground-water levels were made in about 30,000 wells, and periodic measurements in connection with investigations of ground water were made in many thousands of other wells. Studies of saline-water aquifers, particularly as a medium for disposal of waste products, have become increasingly important, as have hydrologic principles and analytic and predictive methodologies for determining the flow of pollutants in ground-water systems. Land subsidence caused by ground-water depletion, the possibilities for induced ground-water recharge, and the practicality of subsurface disposal of wastes were investigated. Ground-water supplies for energy development and the effects of coal-mining activities on both ground- and surface-water resources were intensively studied. FY 1980 marked the beginning of an intensive program designed to monitor and to evaluate hydrologic effects of the Mount St. Helens volcanic eruptions.

The use of computers continued to increase during FY

FIGURE 1. Index map of the conterminous United States showing areal subdivisions used in the discussion of water resources.

1980, in research studies of hydrologic systems, in expanding data storage systems, and in quantifying many aspects of water-resource studies. Records of about 400,000 station-years of streamflow were stored on magnetic tape, and data on about 750,000 wells and springs have been entered in a new automated system for storage and retrieval of ground-water data. Digital computer techniques were used to some extent in almost all of the research projects, and new techniques and programs are being developed continually.

NORTHEASTERN REGION

Half the people in the Nation live and work in the northeastern region—half that number along the Boston-Norfolk corridor. This region continues to have the bulk of the chemical industry along the Atlantic shore and the heavy industrial complex along the shores of the Great Lakes, and is the largest consumer of energy, supporting industry and the demands of its large population. It is little wonder that the water resources of the region are impacted by chemical, industrial, and biological wastes that have accumulated for 200 years, and which continue to increase in spite of modern waste treatment and disposal.

Water-quality activities in the northeastern region have been consistently dynamic in response to and in anticipation of information needed to assess the most significant water-resources issues identified by Federal and other agencies. The major objective in water-quality programming is to insure a balance between project activities and continuous data acquisition at key sites.

Emphasis on data acquisition and interpretative studies in FY 1980 strongly shifted toward assessing the impacts of coal mining on the surface and in the subsurface and acidic components of atmospheric deposition and evaluating the quality of ground water, particularly identifying contaminants introduced by infiltration or by direct contact. Preliminary results from atmospheric-deposition studies indicated that impacts were site- and area-specific, depending largely on the buffering capacity of water and surficial materials. Contamination of both surface- and ground-water bodies was mostly from

synthetic organic compounds and, to a lesser extent, from effluents containing nitrogen and phosphorous.

The Regional Aquifer Systems Analysis (RASA) Program has expanded in the Northeast. An appraisal of the glacial-valley aquifer systems in parts of New York, New England, Pennsylvania, and Ohio will aid in determining the principles governing the distribution of permeable materials in various glacial environments, the geochemical aspects of ground-water quality, and the hydrologic factors controlling stream-aquifier relations.

Flow extremes seemed to be the norm in the Northeast during FY 1980. Flooding was severe on August 15 in parts of Butler, Clarion, and Armstrong Counties in western Pennsylvania because of intense rains. The peak discharge of 115 m^3/s on South Branch Bear Creek at Bruin in Butler County (drainage area 38 km^2) was greater than a 100-year flood, and, in Armstrong County, the peak discharge of 410 m^3/s on Sugar Creek below Brady's Bend (drainage area 44 km^2) was more than five times the 100-year flood at that site.

In the metropolitan area of northeastern New Jersey a water emergency was declared during September as a result of water-level declines in several key reservoirs. The contents of Wanaque Reservoir in the Passaic River basin declined to 38 percent of capacity by the end of October.

Coastal areas of Connecticut had severe floods on October 25 as a result of high tides driven by 120 km/h winds. The 2.7-m tide recorded at Stamford Hurricane Barrier was 1.1 m above the expected high tide.

The drought that developed during FY 1980 affected much of the Northeast and was marked by declines in ground-water levels as well as minimal streamflows along the Atlantic Coastal Plain. This condition posed a potential water-supply crisis and increased concern over deteriorating ground-water quality because of upstream migration of the freshwater-saltwater interface. One of the areas severely effected was the Delaware River basin, which is a major source of water supply for New York City. The city owns three large reservoirs in the upper Delaware and derives 40 percent or more of its water supply from them.

In early May, reservoirs were at 100 percent of capacity, but, with precipitation only 34 percent of average for the month, they began to decline shortly thereafter. The subsequent depletion in storage followed a pattern similar to that of the summer of 1977, and, although reservoir contents were lower than in 1976, 1978, and 1979, supplies seemed adequate until the middle of September.

By September 15, reservoir contents were at 57 percent of capacity, and they were being depleted at rates approaching 53×10^6 m^3 per week. To conserve supplies, the Delaware River Master, appointed under terms of an amended 1954 decree of the United States Supreme Court, proposed immediate reductions in the allowable diversions by New York City and in the quantity to be released from reservoirs to maintain downstream river flows. Under provisions of the decree, the city is allowed an average diversion of 35 m^3/s and a minimum of 50 m^3/s is to be released for downstream users.

In October, the diversions were reduced to 30 m^3/s and releases to 47 m^3/s. New Jersey was restricted to a diversion of 2.8 m^3/s compared with the 4.4 m^3/s authorized by the decree.

With continued lack of adequate precipitation, storage continued to decline, and, by year-end, additional restrictions had been adopted that restricted the city to 23 m^3/s and releases to an amount required to maintain a flow of 43 m^3/s at the USGS gaging station at Montague, N.J.

Mandatory water-use restrictions in northern New Jersey, eastern Pennsylvania, and New York City were effected in September. By the end of the year, it seemed that water savings were in excess of 4.4 m^3/s.

MULTISTATE STUDIES

Water samples were collected from 262 wells tapping the Potomac-Raritan-Magothy aquifer system in the vicinity of its outcrop in New Jersey and Pennsylvania to assess the water quality of the aquifer. According to T. V. Fusillo and J. J. Hochreiter, Jr., samples were analyzed for common inorganic ions, dissolved metals, organic carbon, and volatile organic compounds. Concentrations of many constituents were extremely variable. Specific conductance ranged from 39 to 4,200 μmhos/cm, with a median value of 256 μmhos/cm, while pH ranged from 4.4 to 8.3, with a median of 6.6. Chloride and sulfate concentrations also varied widely, depending on the depth and location of the well. Dissolved iron ranged from 3 to 79,000 $\mu g/L$ in the samples. Volatile organic compounds were not detected in approximately 75 percent of the wells sampled. Benzene, trichloroethylene, tetrachloroethylene and dichloroethylene were the most frequently detected volatile organic compounds. In general, volatile organic contamination appeared to occur as a localized problem in some industrialized areas.

Water and bottom material samples were also collected at 13 sites on the Delaware River estuary and tributaries within the outcrop area. Results indicated a widespread distribution of volatile organic compounds at very low concentrations throughout the estuary. Bottom materials contained significant levels of some pesticides and base neutral extractable organic compounds.

Water quality of Chesapeake Bay Tributaries

Fall-line monitoring of the Susquehanna, Potomac, and James Rivers, which are the three largest tributaries to the Chesapeake Bay, indicated that large concentrations of iron, aluminum, and manganese occurred at high flows, according to D. J. Lang and D. Grason. Total aluminum concentrations exceeding 12,000 μg/L have been observed in the Susquehanna and Potomac Rivers. Total iron concentrations have been recorded as high as 30,000 μg/L in the Potomac River near Washington, D.C. Ammonia nitrogen concentrations in all three rivers have decreased since 1971. Covariance analysis of the water-quality data indicated a significant difference in the means of the two populations at a 5 percent confidence level. No other nutrients showed such a discernible trend.

ILLINOIS

Large yields from glacial drift and bedrock formations

Field data and model results helped W. W. Lapham and L. D. Arihood to define the ground-water resources of the White River basin north of Marion County. Based on field data, the thin discontinuous confined sand and gravel aquifers in the glacial drift averaged about 4.6 m in thickness, whereas the White River outwash aquifer in the downstream part of the project area averaged about 21 m. An average of about 90 m^2/d for bedrock transmissivity was estimated from specific capacity data.

Model results indicated that at places as much as 0.11 m^3/s could be developed from the confined sand and gravel and bedrock aquifers. Overall simulated pumpages ranged from about 0.04 to 0.22 m^3/s. These pumpages usually resulted in a 1.5 m drawdown contour of about 8 km in diameter and no more than a 10 percent reduction in streamflow for streams greater than 0.057 m^3/s. Simulated pumpage from the outwash aquifer was about 1.7 m^3/s and resulted in near-well drawdowns of about 15 m.

Deep test well

A 1,054 m test hole, which is the deepest in this part of the State, has been completed in the northeast corner of Lake County, Ill. midway between Chicago and Milwaukee. According to M. G. Sherrill, project chief for the Illinois part of this Cambrian-Ordovician Regional Aquifer Study, Precambrian granite was encountered at 1,042 m. Preliminary borehole logging and packer testing indicated gradually increasing salinity below the confining units within the Eau Claire Sandstone as the hole entered the Mount Simon sandstone aquifer. At about 533 m below the land surface, the specific conductance of the water was about 20,000 μmhos/cm. Chloride concentrations of 9,000 mg/L were measured in the lower part of the hole during drilling operations.

INDIANA

Preliminary water-quality assessment of Indiana's coal-mining region

A preliminary analysis of water-quality data collected from the coal-mining region, southwestern Indiana, during 1979 by W. G. Wilber, C. G. Crawford, and D. E. Renn indicated that land use (forest, agriculture and reclaimed and unreclaimed mining) was a statistically significant factor controlling water quality for a number of constituents studied. In general, concentrations of dissolved constituents were greatest in streams draining unreclaimed and reclaimed mine areas and lowest in streams draining forested and agricultural watersheds.

During October 1979, the average suspended-sediment concentration of streams draining agricultural and mined watersheds was 1.8 and 2.9 times greater, respectively, than the average concentration of samples from forested watersheds.

The effect of glacial province (surficial geology) on water quality was evident for most dissolved constituents, pH, dissolved solids, alkalinity, acidity, and sulfate in forested and agricultural watersheds. In general, pH and the average concentration of dissolved constituents were significantly higher in the province of Wisconsin Glaciation than in the province of Illinoian Glaciatian and unglaciated region. The effect of surficial geology on water quality is not as significant as the effect of land use and was masked by the effect of surface mining.

MICHIGAN

Wide variations in the chemical and physical characteristics of natural ground waters in Michigan were documented in a recently completed study by T. R. Cummings. Dissolved-solids concentrations ranged from 23 to 2,100 mg/L. Calcium bicarbonate waters were characterizd by low dissolved-solids concentrations. The percentages of sodium, sulfate, and chloride in ground water increased as the dissolved-solids concentration increased. Iron, aluminum, and titanium were higher at some locations than is common in most natural waters. Lead concentrations exceeded desirable limits in drinking water at some locations in the northern part of the Lower Peninsula. Generalized areal patterns of water-quality variation suggested that geology is a primary cause of differences across the State. Examples of chemical association in water suggested that chemical analyses may be valuable in tracing and identifying mineral deposits.

Geology and hydrology for environmental planning in Marquette County

In Marquette County, in the glaciated Upper Peninsula of Michigan, bedrock and glacial deposits contain materials that are good aquifers. A study by F. R. Twenter showed that sedimentary bedrock of Precambrian, Cambrian, and Ordovician age generally yield sufficient water for domestic supply and, in places, may yield more than 5 L/s to large-diameter wells. In the glacial deposits, sand and gravel beds are the principal aquifers; yields to wells range from less than 0.5 to 12 L/s.

In one area, just south of Marquette, the glacial deposits are as much as 122 m thick and inflow from them sustains a constant perennial flow in several streams. Igneous and metamorphic rocks yield little or no water to wells. Quality of water in the county is good. Dissolved-solids concentration of water from wells and streams is low, ranging from 35 to 720 mg/L. The total runoff from the county is about 59 m^3/s, and of this 35 m^3/s to Lake Michigan and 24 m^3/s to Lake Superior.

Suitable sewage and refuse disposal sites were not readily available because of the abundance of wetlands, streams, and lakes susceptible to infiltrating leachate.

MINNESOTA

Water-quality assessment of sand-plain aquifers

A ground-water quality monitoring network comprising 14 wells each in Hubbard, Morrison, Otter Tail, and Wadena Counties, Minn., was established by C. F. Myette. Preliminary results from analyses of samples collected in May and September 1980 indicated that concentrations of dissolved $NO_2 + NO_3$ as nitrogen locally exceeded the drinking-water criteria recommended by Minnesota Department of Health. Graphical representations of nitrogen, chloride, calcium, and dissolved-solids concentrations showed seasonal variations, but further analyses of the data must be made to determine the significance of the variations.

Northern-Midwest Regional Aquifer-System Analysis – Minnesota part

According to D. G. Woodward, regional ground-water movement in the Paleozoic aquifers of southeastern Minnesota is toward the St. Croix and Mississippi Rivers. Potentiometric maps constructed for each aquifer by G. N. Delin suggested a regional ground-water divide in southern Minnesota, separating flow north to the Twin Cities area from flow south into Iowa. Potentiometric-surface values generally decrease with depth. A computerized data base has been created by M. A. Horn to store ground-water pumpage data. Data manipulation and retrieval programs are being developed to categorize pumpage temporally, geographically, by aquifer use, and by application.

Hydrologic and water-quality assessment of the Coon Creek Watershed, Anoka County

A. D. Arntson reported that results of analyses of stream samples taken in 1980 showed the same characteristic distinctions between urban and rural areas as those taken in 1979. Rainfall-runoff characteristics, such as time to peak and peak discharge versus antecedent soil moisture, observed in the watershed in 1980, are generally the same as those observed in 1979 with the exception of two large rain storms of 76 and 100 mm that occurred in August and September 1980. These storms resulted in the longest observed response times of 45 and 55 h. Rainfall response coefficients as the ratio of runoff volume to rainfall volume were found to be greater for the developed areas than for the undeveloped areas for all storms. The response coefficient is dependent upon antecedent soil moisture and rainfall intensity.

Appraisal of the ground-water resources of the Twin Cities metropolitan area

A simplified quasi three-dimensional finite difference ground-water-flow model of major aquifers in the Twin Cities Metropolitan area, Minnesota, was constructed by J. H. Guswa. Sensitivity analyses of 19 parameters and boundary-condition specifications indicated that model results are most sensitive to areal recharge and withdrawal rates and to hydrogeologic variations caused by drift-filled bedrock valleys. D. I. Siegel reported that ground water in the Twin Cities area is generally a mixed calcium magnesium bicarbonate type and that the concentration of dissolved solids in the Prairie du Chien-Jordan and Mount Simon-Hinckley aquifers generally decreases from northwest to southeast. Analysis of area-wide water-level measurements made during the winter and summer of 1980 showed seasonal changes of as much as 20 m in the potentiometric levels in the Prairie du Chien-Jordan and Mount Simon-Hinckley aquifers according to M. E. Schoenberg. Comparison of 1980 potentiometric-level data with similar data collected in 1971 showed that the cone of depression in the Mount Simon-Hinckley decreased in area while the size of the cone in the Prairie du Chien-Jordan increased.

Availability of ground water in Todd County

An evaluation of the availability of ground water for irrigation in Todd County, central Minnesota, has been completed by C. F. Myette. The aquifer with greatest

potential for development of large water supplies is the surficial outwash sand in Long Prairie Valley. The valley is about 60 km long and from 1.5 to 10 km wide. The outwash thickness ranges from 0 to 40 m with depths to water generally less than 5 m. Annual water-table fluctuations are usually less than 2 m. Outwash material is generally a medium to very coarse sand. Aquifer-test results indicated that transmissivities and storage coefficients ranged from about 430 to 1,200 m^2/d and 0.1 to 0.3, respectively. Locally, the aquifer was capable of supplying about 130 L/s to individual wells.

A numerical model of the ground-water-flow system indicated that, with average recharge, the aquifer can sustain additional withdrawals anticipated for increased irrigation with no significant effect on water levels. However, model results also indicated that if natural recharge to the aquifer were reduced by one half during a sustained drought of several years, ground-water levels may decline as much as 3 m and ground-water discharge to streams may be reduced by 45 percent.

Ground-water appraisal in northwestern Big Stone County

Test augering by W. G. Soukup in a recently completed project in Big Stone County, Minn., indicated that a small surficial aquifer south of Beardsely consists of outwash deposits of sand and gravel (Soukup, 1980). The aquifer is elongate, trending northeast-southwest, with a maximum saturated thickness of 13 m and an areal extent of about 13 km^2. Deep test drilling showed that small buried outwash aquifers underlie much of the project area. A major buried outwash aquifer, east of Beardsely, consists of 40 m of fine, uniform quartz sand. The aquifer lies in a steep-sided northwest-southwest trending valley eroded in bedrock and is overlain by 40 m of clayey till. Aquifer-test results indicated that its transmissitivity ranges from 980 to 1,210 m^2/d, and that the storage coefficient ranges from 0.0001 to 0.0002.

Water quality monitoring of Voyaguers National Park

Water samples were collected by G. A. Payne at 14 sites in four lakes in Voyageurs National Park in northern Minnesota as part of a continuing monitoring program. Results of the analyses indicated that water from most of the sampling sites met criteria recommended by the EPA for drinking, recreation, and support of aquatic life. However, water at six sites did not meet criteria for drinking water because of the presence of oil, grease, or phenols. Water from two sites did not meet criteria for the support of aquatic life because of sulfide or ammonia concentrations. Other data indicated that the lakes ranged in trophic state from mesotrophic Sandpoint, Namakan, and Rainy Lakes to eutrophic Kabetogama Lake. Results of analyses showed that there were no differences in nutrient concentrations between waters near developed areas and waters in mid-lake areas. Analysis of the data indicate a good correlation between total phosphorus concentrations and chlorophyll *a* concentrations. Water transparency was inversely related to chlorophyll *a* concentrations and was affected by organic color and resuspended bottom material at some sites.

Effect of acid precipitation on the water quality in the Filson Creek watershed

Monthly mass balances of sulfate were determined for Filson Creek in northeast Minnesota from March to December 1977, and during the snowmelt period in 1979, according to D. I. Siegel (1981). Data indicated that 10.6 k kg/ha of sulfate were retained in 1977, while about 2 kg/ha were retained from March to July 1979. Results suggested that sulfate retention generally occured in the watershed, and probably resulted from the reduction of sulfate in wetlands and sorbtion of sulfate onto sesquioxides in till and soil.

NEW YORK

Integrated Lake-Watershed Acidification Study (ILWAS)

Meteorologic, hydrologic, geologic, limnologic, and water-quality data have been collected since 1978 from three Adirondack lake watersheds that receive similar acidic atmospheric depostion. Basins showed differing responses to neutralization of acid; the pH of lakes varied from acid, (pH–4.5), to intermediate (pH–5.5), to neutral (pH–7.0).

Results as interpreted by N. E. Peters and other participants in ILWAS indicated (1) The degree of lake acidification is a function of the residence time of acid waters in the soils and underlying glacial deposits before being received by the lake. Furthermore, permeability, infiltration rate, thickness of unconsolidated deposits, and the mineral composition combine to yield the degree of neutralization. (2) Acid neutralization occurs predominately through the weathering of hornblende in these basins. (3) A chemical mass balance for the selected heavy metals, Fe, Pb, Zn, and Mn indicate (a) an accumulation of atmospherically derived Pb in all watersheds, (b) weathering and transport of Zn and Mn is positively correlated with acidity, and (c) outflow of all species is highest in the spring, coincident with the release of acid waters from the snowpack. (4) The pH of the lakes and outlets shows a significant decrease ($pH < 5$) with the onset of snowmelt. This pH decrease is confined to the upper 1 to 2 m in the lakes and remains depressed until ice-out when mixing of the more neutral underlying waters restores the normally higher pH to these waters. (5) The pH of ground waters is depressed during recharge from snowmelt. The lack of neutraliza-

tion is a function of the relatively short residence time of these acidic solutions in the overlying unsaturated zone. (6) Release of solutes from the snowpack is not uniform. During the 1979 spring snowmelt, 40 to 83 percent of various constituents were released with only 20 to 30 percent water loss from the snowpack.

Ground-water potential near Smyrna

The glacial sand and gravel aquifer south of Smyrna in central New York is in a Y-shaped cut-off valley not connected hydraulically with the nearby Chenango River. The fact that there is no major stream in the valley means that if these aquifers are a significant source of ground water, they could be developed in the future for municipal or industrial supplies or streamflow augmentation with little risk of induced infiltration that would deplete streamflow in low-flow periods. G. A. Brown reported that preliminary analysis of data from an intensive well inventory, test drilling at five locations, and two seismic lines indicated that the unconsolidated glacial drift generally thickens southward from about 12 m near Smyrna to about 60 m near North Norwich. The aquifer in the northwest branch of the valley, although shallow, is mostly permeable coarse sand and gravel. The eastern branch and southern end of the valley have greater thicknesses of sediments but are generally less permeable fine sands, silts, and silty sands and gravels.

Time-series analysis of a precipitation-chemistry network

The USGS has been operating a nine-station precipitation monitoring network in New York since late 1964. Results from samples collected monthly showed that chemical composition at each station is determined by regional as well as local factors, according to N. E. Peters, R. A. Schroeder, and D. E. Troutman. Local influences result from close proximity to urban centers, the ocean, farms, and trees. Acid precipitation is a regional feature shared by all stations.

The data were examined for trends in chemical concentrations using parametric (linear regression) and nonparametric (seasonal Kendall test) statistical methods. Results indicated that sulfate decreased 2 percent and nitrate increased 12 percent per year since 1964. Although hydrogen ion concentration has not changed for the State as a whole, an increase in precipitation quantity of 3 percent per year has resulted in an increasing load of hydrogen ion.

PENNSYLVANIA

Water monitoring of Big Sandy Creek basin

Suspended sediment and water-quality sampling of Stony Fork, a tributary to Big Sandy Creek, indicated changes have occurred downstream of surface-mined areas according to D. E. Stump, Jr. Suspended-sediment yield increased 100 percent during the first two years of operation when the area affected by mining went from less than 1 to 5 percent of the drainage basin. The suspended-sediment hydrographs, during the second and third years, were characterized by steeper rises, higher peak concentrations, and wider bases. Water quality during low flow fluctuated because of intermittent pumping activities from the surface mine-water treatment facilities.

Assessment of nonpont-source discharges at Pequea Creek

Intensive rainfall, flow, and water-quality data are being collected in a predominantly agricultural region in southeastern Pennsylvania as part of a nonpoint-source discharge study by J. R. Ward. The data are being used to characterize the loadings of suspended sediment, nitrogen, phosphorus, organic carbon, and pesticides to both base flows and storms at six sites of varying land use in Pequea Creek basin. Flows from small basins which contain mostly forest, corn, pasture, residential, and mixed residential and agriculture are monitored during storms and base flows. An additional site monitors flow from mixed land use near the mouth of the 399 km^2 basin.

Yearly suspended-sediment yields averaged 683 Mg/km^2 during 1977–79. Yearly nitrogen and phosphorus yields averaged 4.8 and 0.6 Mg/km^2, respectively, over the same period. Many instances of nitrate contamination of ground water have been documented in the basin. The average nitrate concentration of 40 wells sampled in 1977–78 was 11.6 mg/L.

Residential areas and corn fields seemed to contribute substantial quantities of pesticides to nearby streams. The triazine herbicides atrazine and prometryne, are widely used in the basin, and were present in water samples at high concentrations. Immediately following atrazine applications in a corn field which was being monitored, atrazine concentrations in a nearby stream were as high as 200 $\mu g/L$.

VIRGINIA

Distribution of salt water in Coastal Plain aquifers

A study of the distribution of salt water in the Coastal Plain aquifers of Virginia by J. D. Larson indicated that no significant saltwater intrusion due to human influence had occurred to date. A wedge of saltwater in the aquifers of the York-James Peninsula existed prior to major pumping in the area and corresponded closely with contours of maximum tidal ranges and surface salinity in the Chesapeake Bay.

A contour map of chloride data showed that the altitude of the 250 mg/L chloride concentration varied from less than 30 m below the National Geodetic Vertical Datum of 1929 (NGVD) near the coast and on the York-James Peninsula to greater than 427 m below NGVD on the Northern Neck Peninsula.

A recent report (Hopkins and others, 1981) indicated that heavy pumping in the Coastal Plain Province has drawn down the potentiometric surface to the point that additional pumping increases may induce saltwater intrusion.

WEST VIRGINIA

Water resources of the Guyandotte River basin

A study of the Guyandotte River basin in southwestern West Virginia by J. S. Bader, J. L. Chisholm, R. L. Bragg, and S. C. Downs was designed to provide an understanding of hydraulic conditions. Runoff characteristics of streams were developed and traveltime at different stages indicated that traveltime upstream was greater during low flow than downstream.

Quality of streams ranges from dilute calcuim bicarbonate in the lower part of the basin, to calcium sulfate in the central part, to sodium sulfate and bicarbonate in the upper part. Stream water in mining areas is hard and alkaline and has a dissolved-solids concentration two to five times greater than streams draining unmined areas. Urbanization has resulted in organic pollution as indicated by high fecal coliform populations and high nitrogen and phosphorus concentrations.

Ground water comes from fractures associated with anticlines. Wells in valleys produce water from fractures on the valley walls and beddingplane partings under the valley floor.

Ground-water quality varies areally, from near-neutral dilute calcium and sodium bicarbonate in the upper part of the basin to alkaline, strongly sodium bicarbonate water in the lower part. Water from Upper Pennsylvanian rocks is more mineralized than that from Lower Pennsylvanian rocks; water from both becomes increasingly mineralized with depth. Fresh ground water has been contaminated by brine from oil and gas drilling.

Ground water in Randolph County as a source of public supply

Most public water systems in the Tygart Valley in Randolph County, W. Va., use surface water for public supply. Planners are concerned that enough surface water would not be available during a drought. The main objective of this investigation was to delineate sites in the valley, using remote sensing and other available data and techniques, where water wells could be installed close to existing distribution systems and to determine if enough ground water of suitable quality could be obtained to supplement surface-water sources.

W. A. Hobba, Jr. (1980), concluded from this study that (1) up to 12.6 L/s of ground water can be supplied from the alluvium and the underlying shale; (2) good sites for production wells can be selected using lineaments mapped from satellite imagery and aerial photography; (3) surface electrical-resistivity studies are valuable for mapping buried alluvial sand and gravel and lineaments in shale beneath the alluvium; (4) most of the ground water is stored in the alluvium; (5) low pH and high concentrations of iron, manganese, and chloride may cause water-quality problems; (6) single-well aquifer tests indicate "high yielding" wells are located along lineaments; (7) multiple-well anisotropic aquifer tests indicate maximum permeability parallels lineaments in the shale; (8) it is difficult to predict long-term effects of drawdown because of the fractured nature of the shale beneath saturated alluvium; (9) drawdown may cause the upward migration of salty water, which lies at 30 to 90 m depth.

WISCONSIN

Ground water in sand and gravel aquifers in McHenry County

Four significant sand and gravel aquifers, three semiconfined and one unconfined, are recognized in McHenry County, Wis. According to J. T. Krohelski and J. R. Nicholas, ground-water-level contours and ground-water-flow directions suggest that the shape of the water table roughly coincides with the topography, ground-water divides roughly coincide with surface-water divides, and recharge occurs at higher elevations and discharges to local streams.

Ground water is of the calcium-magnesium-bicarbonate type with little seasonal variation. The range of specific conductance of water from wells sampled was from 260 to 1170 μmhos/cm.

Packer testing in multi-screened wells

The Cambrian-Ordovician aquifer system which underlies approximately 70 percent of Wisconsin is the major source of ground water in the State. Most of the wells penetrating the aquifer system are open to more than one aquifer unit, making it difficult to determine the individual aquifer's contribution to the well. The Wisconsin part of the Upper Midwest Regional Aquifer System Analysis study has conducted aquifer tests using inflatable packers. According to P. J. Emmons, the

packer tests indicated that the potentiometric heads of the aquifers open in a well differ by as much as 36 m. Water-quality analyses indicate that the water is essentially the same quality for each of the packed aquifer zones. The water quality may only be indicative of the aquifer with the highest potentiometric head in the well. The similarity of the water quality in the other zones may be a result of the mixing of water from the zones of higher potentiometric heads.

SOUTHEASTERN REGION

Drought, which struck the southeastern region in the summer of 1980, continued throughout the remainder of the year as fall and winter rains failed to materialize. By the end of the year reservoirs that normally would be full and spilling were at or even below late summer levels. Ground-water levels in aquifers throughout the region showed the usual summer decline. Locally, declines were somewhat steeper than usual because of increased ground-water demand due to the drought. Fall and winter water levels, however, showed little or no recovery. Water managers throughout the Southeast, as a result, have been making preparations for water emergencies in the coming year.

Acreage under irrigation continued to increase, especially in Georgia and Florida. Irrigated acreage in the Dougherty Plain area of south Georgia has continued to grow at an explosive rate. Centerpivot irrigation systems tapping the prolific Tertiary limestone aquifer underlying the Dougherty Plain have been doubling nearly every year for the past 4 years. Potential pumpage from the systems in operation is approaching 7.5 million m^3/d.

Hydrologic activities related to energy development continued strong in the Southeast. Programs for the collection and publication of water-resources data, especially those related to coal, continued. Alabama, Kentucky, and Tennessee have been intensively involved in coal-related programs.

A study of Alabama has resulted in the development of regression equations that relate the chemical constituents common in coal-mine effluent to the age of strip mines. This study indicated that the concentration of chemical constituents reaches a peak 4 or 5 years after a mine is opened and then gradually decreases, taking perhaps 20 years for the constituents to reach pre-mining levels.

A nearly completed study of the wetlands of the Apalachicola River basin has indicated that the wetland forest is a major source of organic detritus. Annual floods carry the detritus downstream to Apalachicola Bay where, according to university investigators, it is vital to the growth of shellfish in the bay. Nitrogen is leached from fallen leaves on the flood plain within a month's time, but phosphorous is released at a constant rate over a period of about 6 months.

Work is continuing on the methodology of predicting trends of selected constituents in the water of major rivers in North Carolina. In several instances, it has been possible to determine a change in trend and then correlate it with the effluent from a newly established industry, the upgrading of a sewage treatment plant, or the change in location of the discharge point of an effluent.

ALABAMA

Hydrologic surveillance of potential coal-mining areas

Celso Puente developed a series of regression equations to estimate regional variations in streamflow and water quality as functions of climate, basin characteristics, and land use. Climatic, physiographic, and hydrologic data from streams in 67 basins, draining mined and unmined areas in the Warrior coal field of Alabama, were analyzed by regressions to derive relations for assessing water quality. Streams in 35 of the basins drained active or inactive surface-mined areas. The remaining basins contain coal deposits but are presently unmined. The streams draining these basins were used to assess pre-mining water-quality conditions.

Mineralization of mine drainage varies as functions of the quantity of water leaving the surface-mined area, presence of reactive minerals in spoil materials, and length of exposure of the reactive materials to weathering. In the regression approach, the dependent variable representing mineralization of mine drainage is specific conductance. Estimates of concentrations represent ranges based on variations in discharge. Verification of estimates was accomplished by sampling at various sites.

Relations between specific conductance and constituent concentrations were also developed to assess the impact of mining on specific constituents in the water of streams.

FLORIDA

Water-quality model of the Hillsborough River

A one-dimensional, steady-state, water-quality model was developed for a 44.7-km reach of the Hillsborough River to evaluate water-quality conditions to be expected from future development. The model was calibrated and verified using water-quality data collected under critical low-flow conditions in April and

December 1978. Dissolved oxygen, ultimate carbonaceous biochemical-oxygen demand, and total coliforms were successfully modeled for most of the study reach.

Model results were used to evaluate impacts of two typical housing developments on water-quality conditions in Tampa Reservoir. One development was located in the Cypress Creek basin near the reservoir, and the other near the upper end of the study reach.

Model results indicated that coliforms significantly affect water quality under conditions tested. Total coliforms at the Tampa Water Treatment Plant ranged from about 2,700 colonies per 100 ml above background, for a 2.59-km^2 development to about 14,000 colonies per 100 ml for a 25.9-km^2 development. Fecal coliforms for the same developments varied from about 350 to 2,000 colonies per 100 ml. Other modeled constituents showed only minor increases in concentration.

NORTH CAROLINA

Water quality of major North Carolina rivers

A study of water-quality variability, pollution loads, and long-term trends of the Yadkin–Pee Dee River in North Carolina, by D. A. Harned and Dann Meyer, showed that suspended sediment, despite a decreasing trend since 1951, is the most significant water-quality problem of the river. Lead concentrations periodically rose above the recommended levels for domestic water use. Mercury concentrations frequently exceeded, and pH levels fell below the recommended levels for protection of aquatic life. Nutrient concentrations were high enough to allow rich algal growth. Anthropogenic pollution makes up from 30 to 60 percent of the total dissolved solids load of the river.

Statistically significant trends showed a pattern of increasing concentration of most dissolved constituents over time, with a leveling off and decline in the mid to late 1970's. These results may be evidence that changes in industrial processes have improved, or at least they have slowed deterioration of water quality in the river system.

Relatively steady increases in sulfate and nitrate, and a steady decrease in pH with time, may have been due to the increasing acidity of atmospheric precipitation.

TENNESSEE

Effects of pumpage monitored at Memphis

According to D. D. Graham, an investigation of three potential problems related to large withdrawals of ground water from the Memphis Sand artesian aquifer (Eocene age) in the Memphis, Tenn., area showed no indication for immediate concern. These potential problems are (1) continual lowering of water levels in response to increased pumpage, (2) contamination of the Memphis Sand by vertical leakage, and (3) land subsidence caused by compaction of fine-grained sediments as a result of water removal.

Prior to 1975 measured pumpage from the Memphis Sand showed a steady upward trend; from 1975 to 1980, however, pumpage has remained essentially steady averaging about 710 m^3/d. A comparison of hydrographs of observation wells and of potentiometric maps prepared for 1975, 1978, and 1980 showed no significant changes in the major cone of depression.

Water-quality analyses for common constituents, selected trace elements and selected organic compounds from one well in each of the six municipal well fields and two industrial wells, gave no evidence of contamination of the Memphis Sand. However, abandoned landfills in the overlying water-table aquifer are known to contain hazardous organic wastes. The possibility of leakage of these wastes from the water-table aquifer to the Memphis Sand makes continued monitoring prudent.

An expanded scale (10:1) extensometer installed in April 1978 below the level of major pumpage in the Memphis Sand recorded an apparent seasonal land surface fluctuation of less than 0.01 m. As yet, no permanent compaction is indicated.

CENTRAL REGION

Hydrologic activities in the central region during FY 1980 continued to emphasize studies related to energy development. Established programs for the collection and publication of diverse water-resources data continued. Intensive hydrologic investigations related to coal development continued in Colorado, Kansas, Missouri, Montana, New Mexico, North Dakota, Utah, and Wyoming; studies related to oil shale in Colorado, Utah, and Wyoming continued at a reduced level of intensity. Water-resource studies of uranium-mining areas of Colorado and New Mexico were continued. Hydrologic studies of small basins that are representative of potential surface coal-mining areas were given continuing attention. Results of these studies are expected to be applied to leasing decisions, environmental impact statements, mining plan formulations and specifications for reclamation of mining areas.

An investigation of special significance to coal development is an evaluation of the water-yielding potential of the Mississippian Madison Limestone—an important deeply buried aquifer underlying large areas in the Powder River Basin in Montana, North Dakota, South Dakota, and Wyoming. The project was completed during 1980 and the final reports are being prepared.

Digital-model analyses are being used for coal and oil shale areas where surface-water supplies are inadequate; the models evaluate availability of ground water and indicate impacts of accelerated energy production on future water resources of the mining areas.

Central region research activities continued to be varied and complex. Sediment research in the central region is directed toward surface-mining effects, channel changes, bedload transport and sampling, and estuarine sediment movement. Estuarine studies are being made on both the Pacific and Atlantic coasts. Particular emphasis is being placed on sediment transport and geomorphologic processes. An intensive historical study of channel changes in the Platte River of Nebraska was completed to aid in the management of a section of the river as habitat for the sandhill crane and the whooping crane. In the East Fork River of Wyoming, an intensive multidiscipline sediment study is underway to evaluate channel changes, sediment transport, and bedload movement as these factors are affected by spring runoff.

Chemical and geochemical studies in the central region included a geochemical survey of water in coal fields, organic determination and definition of waters from oil shale retorting, studies of organic polyelectrolites, and the removal of dissolved organic material by use of selective resins. Such work is a continuation of studies to determine the types and quantities of organic materials in natural waters. Organic fouling of reverse-osmosis membranes used in the desalting process is being investigated. Geochemical kinetic studies, modeling of the chemical changes of water, and transuranium research studies also are underway.

At the Nevada Test Site, intensive investigations of the feasibility of high-level radioactive waste disposal continued. Also, studies in the Paradox Basin of Colorado and Utah to determine the hydrologic conditions that might affect the use of the deeply buried evaporites for waste disposal and related studies in deep evaporite deposit basins of New Mexico and salt-dome provinces of Louisiana and Texas continued.

Methods development for laboratory and field application as well as for increased sensitivity has become a new research endeavor in the central region. Present emphasis is on the analysis of metals and organic compounds in water including pesticides.

Hydraulic modeling continued to be a major factor in central region research. Studies of the relation of lakes to ground water are underway in Colorado, Nebraska, New Hampshire, North Dakota, and Washington. Minnesota and other sites are being evaluated for possible inclusion in the study. Precipitation-runoff modeling research, initially aimed at predicting the effects of surface mining, have received increased emphasis. Work continued in the development of modeling techniques for the prediction of solute transport in ground water and of modified runoff and sediment transport from areas undergoing surface mining in several hydrologic regimes. Development of techniques also continued for estimating numerical values for parameters and boundary-condition values for ground-water systems and research in sediment transport, channel-geometry changes, and fluvial processes.

Studies of regional aquifer systems continued in the northern Great Plains of Montana, North Dakota, South Dakota, and Wyoming, in the High Plains Tertiary Ogallala aquifer and associated systems of Colorado, Kansas, Nebraska, New Mexico, Oklahoma, South Dakota, Texas, and Wyoming. Studies were started in the southwestern alluvial basins in New Mexico and adjacent parts of Colorado and Texas. A study of carbonate aquifers in Arkansas, Colorado, Kansas, Missouri, Nebraska, New Mexico, Oklahoma, South Dakota, and Texas was started. In all of these areas, aquifer-system boundaries and characteristics are being intensively studied to determine storage capacity and natural discharge and withdrawals, sources and amounts of recharge, anticipated yields of wells, and effects of pumping on supplies and water quality. The studies also determine the history of past ground-water development and the effect on the aquifer of future development under various assumptions as to rates and points of withdrawal. Mathematical models of the flow system in the northern Great Plains, High Plains, and southwestern alluvial basins are being prepared.

Field investigations of the hydrology of geothermal systems are continuing in Colorado, Montana, and California. Also, development and testing of instruments, tools, and interpretative techniques for use in the extreme heat of geothermal systems and in possible areas suitable for deep disposal of radioactive and chemical wastes is continuing.

Intensive water-quality studies continued in the coal areas of the central region, especially in parts of Colorado, Montana, New Mexico, North Dakota, Utah, and Wyoming. In other States, attempts are being made to predict how ground- and surface-water systems will have been affected after mining actitivies have ceased.

Lake studies were broadened to include modeling of phosphorus in several reservoirs in Colorado. In addition, a nutrient-primary productivity study is underway in Koocanusa Reservoir, Montana. In Kansas and Oklahoma, limnological studies of strip mine lakes are underway. The effects of acid rain on lakes in western Colorado are being studied.

Surface-water activities continued to be an important part of the regional program. Additions to gaging-station networks were made in coal-development areas

in Montana, New Mexico, North Dakota, Oklahoma, and Wyoming. Most of these new stations were constructed and operated on behalf of the USGS under Government contracts with private engineering firms. The stations were installed to monitor streamflow conditions in coal-development areas and to document changes resulting from mining operations.

Mapping of flood-prone areas continued in several States in the region. HUD Type-15 flood-insurance studies for specific cities continued; however, the program is approaching completion, and few new areas were included. Additional flood-frequency studies are underway in several States.

A major study of the relationship of channel geometry to streamflow characteristics in the Missouri River basin was completed.

MULTISTATE STUDIES

According to E. J. Harvey (1980), average groundwater conditions have not changed significantly in the Springfield-Salem plateaus section of southern Missouri and northern Arkansas during the past 25 years except in the vicinity of well fields. The amount of ground water pumped is approximately 5.7 m^3/s, which is about 5 percent of the total discharged at the 80-percent point on flow-duration curves for major streams. It is estimated that 420 to 2,100 km^3 of water are stored in the aquifers of the region. Main water-yielding zones occur in the Potosi Dolomite and the lower dolomite and sandstone of the Gasconade Dolomite. The source of most of the municipal water supplies is the Potosi Dolomite, which has the largest permeability.

Hydrology of abandoned zinc mines in Oklahoma and Kansas

Over 23 km^2 of northern Ottawa County, and Oklahoma and Cherokee Counties, Kansas, are underlain by many kilometers of interconnected abandoned lead and zinc mine drifts, according to D. L. Bergman. The mine workings have filled with ground water and with appreciable amounts of surface runoff that has entered abandoned shafts, vents, and collapses. The potentiometric surface has risen to the elevation which allows outflow of mine-water to the surface and possibly downward to the Roubidoux aquifer, the major source of drinking water in the area.

Surface runoff and seepage from mine tailings contribute high concentrations of cadmium, lead, fluoride, and zinc to Tar Creek. The addition of direct mine drainage to streamflow has the potential for deleterious effects on the biota of the Neosho River and Grand Lake downstream from Tar Creek.

ARKANSAS

Outcropping Tertiary units

The Tertiary outcrop area in southern Arkansas was mapped by R. L. Hosman in response to a need created by the study of the western Gulf Coast region under the RASA program. The geologic map of Arkansas does not fully differentiate the Tertiary units, especially those of the Claiborne Group. Because major geologic units generally correspond to major hydrologic units in the area, a more detailed geologic map was needed to establish areas of natural recharge.

A 1-yr study was begun October 1, 1979, to map the approximately 25,000-km^2 area using both surface- and subsurface-mapping techniques. About 800 surface exposures were examined, and approximately an equal number of geophysical logs were used for subsurface-to-surface projections and for determination of the surficial unit at each well site. The final map was compiled at a scale of 1:250,000 and will be published at that scale in the USGS' Miscellaneous Investigations Series.

Saline-water encroachment near Brinkley

A recent study by M. E. Broom and F. P. Lyford (1981) outlined an area near Brinkley, Ark., where saline water, containing sodium and chloride as the main constituents, is encroaching on the alluvial aquifer. Dissolved-solids concentrations of as much as 1,500 mg/L have been found in some areas, causing abandonment of some irrigation wells. Apparently, water is moving upward from underlying Tertiary geologic units, which are known to contain sodium chloride water in this area. Saline-water movement has probably been induced by a lowering of the potentiometric surface in the alluvial aquifer, in response to water withdrawals for rice irrigation.

COLORADO

Ground-water resources of the Denver basin

The limit, thickness, and water chemistry of the bedrock aquifers occurring in the Dawson Arkose, Denver, Arapahoe, and Laramie Formations, and in the Fox Hills Sandstone have been mapped in the 1,700-km^2 Denver basin of Colorado by S. G. Robson. Mapping of the hydraulic conductivity and transmissivity of each aquifer indicates that hydraulic conductivity ranges from 0.015 to 4.6 m/d and transmissivity ranges from 0.5 to 250 m^2/d. The greatest hydraulic conductivity and transmissivity occurred in the suburban area south of Denver in the Arapahoe and Laramie-Fox Hills aquifers.

Porosity of the water-yielding materials commonly ranges from 22 to 48 percent. Storage coefficients range from about 0.2 in the unconfined aquifers located near the margins of the basin to about 4×10^{-4} in the confined aquifer located in the central parts of the basin. Both confined and unconfined conditions may occur in the same area of an aquifer due to limited vertical hydraulic connection between upper and lower parts of the aquifer.

R. L. Malcolm and others continued research on the nature and source of natural organic matter in water in an alpine area in the Front Range of the Rocky Mountains. Wetland areas, known as transitional bogs, are responsible for most of the humic matter in the water. Weathering of bedrock in these wetlands was a major source of chemical weathering in these alpine environments. Acidity for weathering of bedrock is derived from the decomposition of organic acids in the transitional bogs.

KANSAS

Sediment and chemical-quality characteristics of a loess-mantled region

The fluvial-sediment and chemical-quality characteristics of selected streams draining the loess-mantled region of northeastern Kansas have been defined by H. E. Bevans. Sediment and water-quality data collected from July 1976 through September 1980 at 21 sites were used to develop regression equations relating specific conductance and stream discharge to concentrations of dissolved solids, selected chemical constituents, and suspended sediment. A regional synthetic flow-duration curve was used to estimate mean annual discharges of both dissolved solids and suspended sediments in each selected stream. Wolf River, near Sparks, Kan., (drainage area, 570 km) was estimated to annually yield 22,140 Mg/km^2 of dissolved solids and 1,208 Mg/km^2 of suspended sediment.

LOUISIANA

Water-quality investigations of the lower Mississippi River

C. R. Demas reported that data collected during the 1980 water year from the Mississippi River and a distributary, Bayou Baptiste Collette, indicated that saltwater does not move up the distributary from Breton Sound into the Mississippi River. Instead, saltwater moves up Southwest pass from the Gulf of Mexico, then up the Mississippi River and back down Bayou Baptiste Collette.

Quarterly samples of benthic invertebrata collected from Bayou Baptiste Collette and the Mississippi River at Venice revealed the presence of the ephemerid type mayfly *Tortopus*. This species was not present at these sites in 1975–76 samplings indicating colonization from upriver.

Saltwater intrusion was monitored in the Mississippi River as far upriver as mile 62 in January 1981. The salt wedge remained near mile 62 for approximately two weeks. The last time the salt wedge moved this far upriver was in 1976.

Water quality of the upper Vermilion River

Analysis of water-quality data collected during 1980 in a reach of the Vermilion River from its headwaters to a point 10 km downstream from Lafayette, La., by D. K. Demcheck indicated that wastewater discharges from the city of Lafayette are not the only cause of the generally degraded quality of water in the river. Nonpoint runoff from upstream agricultural areas appears to be a major cause of relatively low dissolved-oxygen concentrations, relatively high biochemical oxygen demand, and increased fecal coliform bacteria concentrations. Drought conditions existed during most of the study period. An intense rain on May 15, 1980, had a substantial impact on the quality of water in the river. Specific conductance was 158 μmhos/cm in Lafayette on May 13, and 46 μmhos/cm on May 17. Fecal coliform bacteria concentrations in the river within the city limits increased from 450 colonies per 100 mL of water on May 13, to 12,000 colonies on May 17.

Changes in benthic macroinvertebrate populations and in dominant algae downstream from Lafayette indicated that wastewater sources in the city have a detrimental effect on the already degraded water quality of the Vermilion River.

MISSOURI

Water resources of northwestern Missouri

Water supplies and water-resources data are limited for much of northwestern Missouri, according to John Skelton. The largest and most dependable surface-water supplies that can be obtained without storage from tributary streams, based on a 30-day low flow having a recurrence interval of 10 years, potentially are available from the lower Grand River (0.66 to 1.31 m^3/s) and the Nodaway and Chariton Rivers (0.22 to 0.44 m^3/s). Flow of the Missouri River is greater than 425 m^3/s at all points in Missouri.

Surficial deposits containing usable volumes of water include the Missouri River alluvium (well yields as much as 126 L/s), glacial drift (well yields of 1.89 to 31.5 L/s), and alluvium of tributary streams (well yields exceed

3.15 L/s in large basins). The Pennsylvanian bedrock yields very little water to wells.

Areas where additional hydrologic data are needed to provide a data base suitable for use in making decisions regarding future water development include the lower Grand River and Thompson River basins, the Missouri River alluvial aquifer, the Nodaway-Tarkio-One Hundred and Two River basin, the Chariton River basin, and the 19 counties where surface-mineable coal reserves make coal-related industrial expansion possible.

MONTANA

Ground water in the east Big Dry resource area

An appraisal was made by S. E. Slagle of the water resources above the Bearpaw Shale in the east Big Dry resource area, located between the Missouri and Yellowstone Rivers and east of the Big Dry arm of Fort Peck Reservoir in east-central Montana. The results indicated that the most frequently used aquifers are the discontinuous coal and sandstone beds contained in the Tongue River Member of the Fort Union Formation, and sand and gravel of alluvium and terrace deposits. Water is also available from the underlying Lebo Shale and Tullock Members of the Fort Union Formation, the Hell Creek Formation, and the Fox Hills Sandstone which are not frequently tapped because of the availability of water at lesser depths. The Fox Hills–lower Hell Creek aquifer yields are as much as 26 L/s to large-capacity wells. Yields from the Fort Union Formation range from about 0.05 to 3 L/s, but generally are about 0.5 L/s. Yields from alluvium are as much as 63 L/s from coarse gravels along major streams but yields to stock and domestic wells are commonly 2 L/s or less. Water from the Fox Hills–lower Hell Creek aquifer is generally a sodium bicarbonate type having a dissolved-solids concentration of about 770 to 3,700 mg/L. Water from the overlying aquifers is generally a sodium sulfate type containing a dissolved-solids concentration of about 320 to 7,700 mg/L.

NEW MEXICO

RASA study of the Southwest Alluvial Basin (East)

A study was conducted by W. B. Scott and G. A. Hearne of the Southwest Alluvial Basin in the Regional Aquifer System Analysis Program to determine the truncation error associated with vertical grid spacing in alternative models of the Albuquerque-Belen Basin. The cells in the three-dimensional models were brick-shaped volumes that were assigned aquifer characteristics representative of those in the basin. In both models, the top layer was 150 m thick. The remaining layers in the first model were the same thickness. However, in the second model, the thickness of each of the other layers was increased by a factor of 1.5. Each model extended to a depth of 3,000 m below the water table. Steady-state conditions were simulated by both models and the results analyzed by comparing vertical hydraulic-head distribution at selected nodes. The difference was assumed to be a quantitative measure of the truncation error due to the change in layer thickness. The models displayed 0.3 to 2.1 m of truncation error in the steady-state condition.

NORTH DAKOTA

Paleoenvironment controls modern water quality

Detailed lithofacies and thickness maps of the Fort Union Formation near the Gascoyne lignite mine in southwestern North Dakota prepared by R. L. Houghton indicate a nearly stationary system of deltaic stream channels existed during the late Paleocene. Mineralogic and sedimentologic investigations of the Fort Union confirmed the proximity of the site to the Paleocene sea during the depositional period of the Harmon lignite bed of the Tullock Member of the Fort Union.

Major controls on local shallow ground-water composition were determined to be (1) sodium leaching from Tertiary sand channels in and above the Harmon lignite bed, (2) oxidation of pyrite associated with outcropping lignite and with mine spoils, (3) precipitation and dissolution of gypsum during evapotranspiration and infiltration, (4) dissolution of detrital calcite and dolomite, and (5) large-scale divalent-monovalent cation exchange within the lignites and on smectites in the Fort Union sediments. Aromatic-aliphatic, lamellar organic compounds within the lignites have been found to have cation-exchange capacities of as much as three orders of magnitude greater than those of smectite concentrations.

Lignite strip mining appears to have had little effect on ground-water quality except to increase sulfate concentrations by making more pyrite available to the oxidizing environment.

Buried valleys in north-central North Dakota

P. G. Randich reported that test drilling in Towner County, North Dakota, outlined a continuation of the Spiritwood buried-valley aquifer system through central Towner County into Canada. The aquifer ranges in width from 2 to 4 km at depths ranging from 50 to 150 m below land surface datum and consists of sand and gravel deposits having an average thickness of 30 m.

The stratigraphic position of the aquifer deposits indicates that deposition in the area occurred during at least two distinct glacial events during Pleistocene time.

Hydrogeology of Rattlesnake Butte area

The second phase of test drilling and observation-well construction in the Rattlesnake Butte area of North Dakota was completed in 1980. Preliminary interpretations of the data by W. F. Horak indicated the presence of a system of fluvial channel sands of the basal Sentinel Butte Member (Fort Union Formation) that transects the central part of the study area from west to east. These sand beds, as much as 24 m thick in places, constitute an aquifer system. A commercial lignite bed underlies the eastern one-third of the study area and is the only other consistently occurring aquifer within 122 m of the land surface. In areas underlain by neither of these aquifers, water supplies generally were obtained from the basal sands of the Tongue River Member of the Fort Union, at depths ranging from 183 to 244 m.

OKLAHOMA

Geohydrology of the Roubidoux aquifer

The Roubidoux aquifer, in northeastern Oklahoma, consists of sandstone and cherty dolomite of the Roubidoux Formation (Lower Ordovician) that ranges in thickness from 30 to 60 m and averages about 45 m. The Roubidoux occurs at depths generally between 150 and 460 m in the study area.

R. W. Fairchild reported that yields of wells vary in different parts of the area but yield up to 63 L/s; the average yield is about 12.5 L/s.

Population and industrial growth have resulted in increased withdrawal from the Roubidoux aquifer and the development of a cone of depression near the centers of pumpage: water levels range from 30 to over 150 m below land surface. Several wells that tap the aquifer are reported to have flowed early in the 1900's.

The aquifer is recharged where it outcrops is an area about 80 to 240 km east of the study area in the central part of the Ozark Mountains in south-central Missouri and north-central Arkansas. The only known discharge from the aquifer in the study area is by withdrawal from pumped wells. The water is used for municipal, industrial, and rural water district supplies.

Water in the Roubidoux aquifer is generally of good quality but changes in character from a calcium-magnesium bicarbonate type in the eastern part of the study area to a sodium chloride type farther west. The water commonly contains hydrogen sulfide which gives it an unpleasant odor.

Water withdrawn from at least one well in the Roubidoux and used for municipal supply exceeds the recommended the limits for radium. Higher-than-normal radium concentrations have also been reported in water from the aquifer in other parts of the study area.

Water in abandoned zinc mines in the northeastern part of the study area poses a potential threat of contamination to the formations below, including the Roubidoux. A downward hydraulic gradient exists between the water level in the mines and the water level in the Roubidoux aquifer.

Information from geophysical logs suggests that water from an abandoned mine moves downward into the Roubidoux aquifer through leaks in the casing of a deep well that intersects the mine.

Suitability for use of Oklahoma's surface waters

The surface waters of the Arkansas River mainstem and the Verdigris, Neosho, and Illinios River basins in Oklahoma have been examined by J. D. Stoner, using existing data, for suitability of use as irrigation and public water-supply sources. In general, the quality of water in these basins is suitable for irrigation and public supply use. However, in certain specific locations, toxic trace metals occasionally occur in sufficient concentrations to make use as a public supply questionable. In most instances the waters are very hard and have an average total hardness as calcium carbonate generally greater than 180 mg/L. The specific conductance and sodium adsorption ratio in the Arkansas River are occasionally large enough at times to make irrigation use of the water impractical.

High Plains RASA study, Oklahoma

Based on a computer-generated map of water-level changes in the Oklahoma Panhandle from 1938 to 1980, water levels have declined in about 72 percent of the three-county area, according to J. S. Havens. Significant water-level declines (greater than 7.6 m) have occurred in about 34 percent of the area, while water-level rises of more than 7.6 m have occurred in about 8 percent of the area. The greatest water-level decline was about 36.9 m southeast of Guymon, Okla., reflecting heavy irrigation and municipal pumpage.

Geohydrology and numerical simulation of an alluvium and terrace aquifer in Oklahoma

S. C. Christenson reported that a quantitative study of the alluvium and terrace deposits along the North Canadian River from Canton Lake to Lake Overholser in Oklahoma, was made to aid in planning and management of this aquifer.

The aquifer is adjacent to the North Canadian River and underlies approximately 1,036 km^2. It consists of alluvium, low terrace deposits, and high terrace deposits which range from 0 to about 30.5 m in thickness, with an average thickness of about 12.2 m. A thin layer of wind-blown dune sand covers much of the aquifer.

The average saturated thickness of the aquifer is approximately 7.6 m. Recharge to the aquifer is from precipitation and averages about 25 mm/yr. Discharge occurs as base-flow to the North Canadian River and as pumpage for irrigation, public-supply, industry, and domestic use.

A steady-state model of the ground-water system has been completed and work is in progress on projections of future conditions.

WESTERN REGION

Assessments of the hydrologic effects of the cataclysmic eruption of Mount St. Helens on May 18, 1980, have been the most visible activities in the western region, dominating work in the Washington district. Flooding has been the major hazard, and water-quality deterioration a secondary concern, in the months following the blast. The Water Resources Division data program, designed to measure sediment transport, flow, and water quality, has addressed these concerns.

The May 18 blast produced devastating mudflows on most streams draining the mountain and significantly altered the hydrologic processes and characteristics of the drainage basins surrounding the mountain. The direct drainage to the North Fork Toutle River valley was reduced by more than 50 percent. The blast materials blocked the tributary inflow of six streams in the North Fork Toutle River valley (Studebaker, Castle, South Fork, Castle, Jackson, Coldwater, and South Coldwater Creeks), forming natural dams of eruptive debris as much as 80 m high. All but three of the lakes on the debris pile have been breached; Spirit, South Fork Castle, and Coldwater Lakes are continuing to fill, and because of their ultimate possible sizes, they continue to be flood hazards to citizens and property located downstream.

Water quality was affected dramatically in the aftermath of the eruption. Within days of the eruption, concentrations of total iron, manganese, and aluminum increased 100 to 500 times over pre-eruption levels in the Toutle and Cowlitz River basins. These levels of concentration persist.

The interest and concern about volcanic activity of Mount St. Helens has given momentum to studies of other volcanoes and their associated hazards in the western region. The initial work is being carried out in cooperation with the Geologic Division, and it focuses on assessing potential flooding and mudflows, changes in water quality, and disruption of water supplies associated with a variety of eruptive and noneruptive scenarios. The areas of immediate interest include Mount Spurr, Mount Rainer, Mount Hood, Three Sisters (including Broken Top Mountain), Mount Shasta, and Mount Lassen.

In other areas of study, each of the western region states has prepared a 5-year water-use summary. A renewed emphasis on and high Division priority for the cooperative water-use programs reflects the generally increased competition for water. With the addition of Nevada to the cooperative water-use program in February, there is now a program in every state in the region.

Several geothermal projects in the western region are showing results:

- Geopressured geothermal waters exist in California within the miogeosynclinal Great Valley and eugeosynclinal Franciscan sequences in the Coast Ranges and on the west side of the Central Valley. Recent studies by Y. K. Kharaka, M. S. Lico, and W. W. Carothers show that the water salinities in the geopressured zones are generally less than 20,000 mg/L dissolved solids. Lower water salinities in California compared to the Gulf Coast geopressured geothermal waters result in a higher content of dissolved gasses and fewer environment problems.
- A study of the hydrothermal system in southern Grass Valley, about 30 to 50 km south of Winnemucca, Nev., by A. H. Welch, M. L. Sorey, and F. H. Olmsted, indicates that thermal fluids probably circulate to depths of at least 3 km and are derived from precipitation in the region. Numerical modeling suggests that if the present discharge of thermal water, which occurs at Leach Hot Springs, is limited by the hydraulic conductivity of the discharge-conduit system, a deep aquifer might be sufficiently permeable to permit exploitation for electric-power generation. However, if the flow of thermal water is limited by low hydraulic conductivity in the deep aquifer, the potential for exploitation is not large.
- Estimates of pore pressure and temperature gradients in vapor-dominated geothermal reservoirs have been made using a finite-difference fissure-block model developed by A. F. Moench and R. P. Denlinger. These estimates are being used to calculate changes in effective stress in the vicinity of a boiling front in order to account for earthquake activity at the Geysers, Calif.
- Steam-flow experiments in porous materials conducted in the laboratory at various temperatures by W. N. Herkelrath have been successfully simulated

with a finite-difference model that incorporates effects of steam absorption.

- Near Mount Hood, Ore., a program funded by the Department of Energy, Division of Geothermal Energy, to drill geothermal observation wells was continued by J. H. Robison. The wells penetrated andesitic lavas and debris. They range in depth from 220 to 1,220 m, and show temperature gradients as high as 84° C/km. An attempt to obtain geothermal fluid from the deepest well was suspended because of weather; the test will be resumed in 1981.

Regional aquifer studies are continuing or beginning in all the western region states except Alaska. Landsat imagery is becoming a more important tool for analyzing the effects of seasonal changes on hydrologic systems, for estimating irrigated acreage, and for predicting changes in land use.

USGS scientists, in cooperation with the National Oceanographic and Atmospheric Administration (NOAA) and other State and Federal agencies, continued to study the hydrodynamics, water chemistry and ecology of the San Francisco Bay estuarine system. The purpose of these continuing studies is to provide information to legislators, planners, and coastal zone managers so that the valuable system can be manipulated positively and profitably.

Other trends in the western region water resources studies include work on improved network design for both streamflow and water-quality measurements, more attention to flood hazards, and additional studies concerned with ground-water quality and the impacts of contamination. Recent water-quality studies emphasize the significant role of nonpoint sources of pollution. Digital models of aquifer systems, as well as flood runoff, continue to be a requested part of the cooperative program as tools for hydrologic interpretation and innovative water management.

MULTISTATE STUDIES

In March 1980, water levels were measured in about 1,600 wells in southern Idaho and eastern Oregon as part of the Snake River Plain RASA study. Repeat measurements were made in about 800 wells in August 1980, near the peak of the irrigation season. G. F. Lindholm reports that these are the most comprehensive water-level data ever collected for the Snake River Plain and will be used to calibrate regional ground-water flow models that are now in process. Sixty-five wells were added to the observation well network on the Plain.

Data from the Water and Power Resources Service and the Pacific Northwest Regional Basin Commission were used to compile a map of 1979 irrigated acreage. The map shows that about 1.1×10^{10} m^2 were irrigated on the Snake River Plain in 1979, about one-fourth of which were supplied by ground water. A cooperative agreement was made with the Idaho Department of Water Resources to determine 1980 irrigated acreage using Landsat data. Pumpage for irrigation from ground- and surface-water sources is being estimated from power company records. Preliminary estimates are that about 5,500 wells and 400 Snake River pumping plants withdraw water for irrigation within the study area.

Seepage losses from diversion canals are highly variable, but may be as high as 40 percent. Major spring flows were measured every other month to determine seasonal variations in ground-water discharge.

ALASKA

Geohydrology of the Fairbanks North Star Borough

The geohydrologic study of the Fairbanks North Star Borough is a continuing cooperative program designed to provide basic hydrologic information for land-use planning.

In 1980, A. P. Krumhardt published an atlas report on arsenic, nitrate, iron, and hardness in well water in the southwest part of Fairbanks. Collection of similar data continued in other upland areas, primarily along Chena Hot Springs Road.

Increasing pressure to subdivide lots into smaller parcels in the lowlands southeast of town initiated a study of water quality and ground-water-flow direction in these areas. The major concern was that closely spaced, deeply buried private septic systems might contaminate the aquifer which, in many places, lies less than 4.6 m below land surface. Data from approximately eleven newly constructed shallow (1.5 to 6.1 m deep) wells and from six existing observation wells are being used in this study. The first of four planned water-quality sampling sets was completed during FY 1980. Iron, ranging from 0.48 to 57 mg/L, was the only constituent found to exceed limits set by the EPA.

Water-Resources Investigations in the Kenai Peninsula Borough

In 1980, five independent studies of water resources were underway in the Kenai Peninsula Borough. All the studies were part of the USGS' ongoing cooperative program with the Borough. G. I. Nelson (1981) reported that the Fourth of July Creek alluvial fan near Seward contains an unconfined alluvial aquifer that yields water adequate for drinking-water supplies. However, flooding on the fan and a high potential for pollution of the aquifer may be constraints to development.

Studies by Nelson at Soldotna and Nikiski indicate that wells tapping the confined glaciofluvial aquifers were able to supply the 1980 pumping demands without increased drawdown of the area's ground-water levels.

In their study of ground water in part of the lower Kenai Peninsula, Nelson and P. R. Johnson found that the more permeable of the area's shallow aquifers underlie poorly drained lands and are little utilized. Most residential and commercial development has occurred on well-drained moraines where deep wells are usually completed in sandstone. Results of a surface-water study of the lower Kenai Peninsula by D. R. Scully and C. S. Savard showed that, in general, precipitation, peak discharges, low-flow discharge, and unit runoff decrease to the north.

Geohydrology of Anchorage

A multi-phase water-resources program was ongoing during 1980 under joint funding agreements between the USGS and the Municipality of Anchorage. A network of sites provided data on streamflow in major streams, water-level data in wells finished in the water table and in the confined aquifers, and lake levels throughout the Anchorage area. D. J. Cowing found that lake levels were at or near record high levels. The high lake and water-table levels reflected high precipitation during 1979 and 1980 and reduced pumping from two Municipal wells.

A study was begun in 1980 to provide information on water-quality characteristics of three Anchorage streams, and to assess the impact of urban and suburban runoff on water quality. As part of this study, Campbell Creek was intensively sampled during periods of snowmelt in upper and lower parts of the basin, as well as during baseflow conditions and at other times. Cowing reported that the quality of water in the upper Campbell Creek basin is excellent. However, lowland runoff, especially from Little Campbell Creek basin, contributes significant levels of pollutants to the stream system, particularly during periods of low flow and snowmelt.

Hydrologic studies for land-use planning were underway during 1980 in the Potter Creek area in the south part of the Anchorage area, and in the Peters Creek–Eklutna area to the north. Data collection for the Potter creek study was essentially completed in 1980, and a report is being prepared by R. P. Emanuel and D. J. Cowing. Sixty-six well logs from the Potter Creek study area were entered into the System 2000 data base during 1980; 114 well logs now constitute the data base for the Potter Creek area. Emanuel and Cowing reported that more wells tap bedrock than tap sedimentary units in the Potter Creek. The average bedrock well in that area was more than 61-m deep and yielded 0.28 L/s; in contrast, the average well tapping sedimentary units was less than 30.5 m deep and yielded 0.47 L/s. Bedrock crops out over about 30 percent of the Potter Creek study area. About 120 well logs have been obtained from the Peters Creek–Eklutna area. When these are entered into the System 2000 data base, information on about 480 well logs from that area will be available.

An assessment of the ground-water system in Eagle River valley was begun by L. L. Dearborn in 1980. Resistivity and seismic soundings were made along two lines across the middle reach of Eagle River in September 1979, and the analytical results have been published (Dearborn and Schaefer, 1980). Depth to bedrock along the two sounding lines was reported to exceed 107 m. A recent preliminary geologic map of the middle reach of Eagle River (Schmoll Dobrovolny, and Gardner, 1980) will aid in assessing the ground-water resources in that area.

ARIZONA

Organic quality of natural waters in Arizona

The role of natural organic matter in the Yuma Desalting Test Facility near Yuma, Ariz., was studied by R. L. Malcolm. This test facility, which is operated by the Water and Power Resources Service, is a pilot plant that uses reverse osmosis, a type of membrane-filtration technique, to remove salt from the Colorado River. Because of a treaty with Mexico, the United States agreed to maintain a fixed degree of salinity of the Colorado River as it enters Mexico. The purpose of the desalting plant is to meet this treaty agreement by removing salt from the Colorado River.

This study measured how natural organic substances, humic substances from the decomposition of plant and soil organic matter, fouled or plugged the membrane used in this plant. It was found that the fouling was caused by clay rather than organic matter, and the natural organic matter was brominated by chlorine and bromide ions present in the water. Chlorination is part of the purification process. These problems could be alleviated by altering the chlorination procedure to lower the level of brominated-organic substances and improving filtration procedures to remove clay-sized particles before they enter the reverse-osmosis membrane.

CALIFORNIA

Water-quality assessment of Cache Creek

An assessment of water quality in Cache Creek was made to compile and summarize all known water-quality data in the Cache Creek basin, to identify beneficial uses and water-quality criteria as defined by the California Regional Water Quality Control Board, and to define

any existing or potential impairments of water quality which would diminish its beneficial use. The assessment indicated that high suspended-sediment loads and high boron concentrations were the major water-quality problems in Cache Creek. These constituents are probably of natural origin.

HAWAII

Ground-water status of Lahaina, Maui

The Lahaina District, Island of Maui, is typical of coastal areas where little or no coastal sediment impedes the flow of freshwater to the ocean. Water levels range from about 1 m above sea level to a maximum of about 2.4 m, 4.8 km inland. W. R. Souza found that ground-water levels have not changed significantly since the 1930's. However, seasonal fluctuations may occur and declines of 0.3 to 0.6 m have been observed during dry years and during heavy pumping. The major land use is agriculture, with about 14.2 km^2 of pineapple and 39.7 km^2 of irrigated sugarcane. Total water use in the Lahaina district is about 4.38 m^3/s. Ground water supplies about half this use. Souza (1981) estimated the recoverable ground-water supply at about 2.19 m^3/s during an average rainfall year. This draft is possible because of the effective recycling of large quantities of irrigation water to the ground-water system. Samples for water-quality analyses were taken at selected wells during February 1979 and February 1980. Data from these analyses were compared with previous studies. Long-term pumping for sugarcane irrigation has affected the quality of ground water over most of the Lahaina District. Major sources of pollution are from irrigation-water return and the intrusion of saline water.

Dike-impounded reservoirs in Oahu

Ground-water reservoirs impounded by volcanic dikes constitute important reservoirs of high-quality water on the Island of Oahu. In a recently concluded study, K. J. Takasaki and J. F. Mink explained that these dike-impounded reservoirs have high hydraulic heads and are isolated from saline water. The most important and productive of these reservoirs occur in the Koolau Range, where the top of the impounded water ranges to an altitude of 305 m. The storage above sea level of these reservoirs was estimated by the investigators to be about 2.10×10^9 m^3. In the Waianae Range, the top of the impounded water ranges to an altitude of about 610 m and the estimated storage above sea level is about 0.38×10^9 m^3. Water-development tunnels have, by breaching dike controls, reduced storage by at least 0.19×10^9 m^3 in the Koolau Range and by about 0.02×10^9 m^3 in the Waianae Range. A significant part of the storage thus reduced by each of the tunnels could be restored by bulkheading the dike or dikes that impound the most water.

IDAHO

Water quality of the Spokane River

During 1980, H. R. Seitz determined several water-quality characteristics at different flows in the Spokane River between Coeur d'Alene Lake and Post Falls Dam. Velocities in the reach ranged from about 0.61 m/s in June to less than about 0.03 m/s in August and November. Concentrations of nutrients were generally low. An increase in concentration of total ammonia nitrogen was observed in the reach below the outfall from the Coeur d'Alene sewage treatment plant. Dissolved oxygen concentrations were generally within limits established by the Idaho Department of Health and Welfare, Division of Environment. However, at the bottom of several deep stream cross sections, the concentrations were below established limits. Water temperatures ranged from 3°C in March to 20°C in August. With a few exceptions, pH was neutral to slightly basic. Specific conductance was generally less than 75μmhos/cm. Concentrations of selected trace metals were within Idaho water-quality standards.

Ground-water-quality assessment of the eastern Snake River basin

In a study relating 1979 ground-water quality to the hydrogeologic and cultural environments, D. J. Parliman reported that water quality and well construction data for a total of 165 wells were collected in eight eastern Idaho counties in the Snake River basin. Major water-yielding geologic units in these counties include alluvium, basalts, and silicic volcanic rocks of Quaternary, Tertiary, and Cretaceous age, and undifferentiated rocks of pre-Cretaceous age (basement complex).. Recharge to aquifers is principally from precipitation in adjacent mountains and infiltration of surface water in valley lowlands and plains. Infiltration of irrigation water and seepage losses from canals, ditches, lakes, and reservoirs are also important sources of aquifer recharge. The most productive aquifers occur in alluvium, basalts, and silicic volcanics geologic units. Ground-water-quality assessment is based on analyses of water from 165 wells sampled in 1979 and 176 wells sampled prior to 1979. Ground water in all aquifers generally contains calcium, magnesium, and bicarbonate plus carbonate ions and is suitable for most uses. Variations in ground-water composition are most directly related to proximity to sources of recharge and effects of land-use practices such as irrigated acreage, drain wells, landfills and garbage dumps, urban and municipal development, and agricultural wastes.

NEVADA

Water resources of a growing urban area near Reno

Within the 75-km² Cold Spring Valley, ephemeral streamflow and ground water move toward the White Lake playa and adjacent areas, where the water is dissipated by evaporation and transpiration. The estimated system yield for the basin, 1.6 hm³/yr, is based on the assumption that all natural ground-water discharge (0.6 hm³/yr) and about two-thirds of the average stream inflow to White Lake can be captured, according to A. S. Van Denburgh (written commun.). Recycling of water during use, and attendent percolation, would permit a sustained withdrawal significantly greater than the system yield, but also would utimately require water treatment to counter deterioration of quality caused by recycling. As of late 1979, domestic and public-supply withdrawals for the basin-wide population of about 2,000, dependent solely on ground water, totalled about 0.3 hm³/yr, of which about 0.06 hm³/yr was consumed by evapotranspiration, with the remainder returned to the ground-water reservoir by percolation. Irrigation of pasture lands (total, about 50 ha) consumed an estimated 0.2 hm³/yr of streamflow and 0.02 hm³/yr of well water. During 1975–79, ground-water levels declined slightly (0.3–1.2 m) throughout most of the valley, but no local net decline of alarming magnitude related to ground-water has as yet been detected.

Ground-water aquifers near Fallon

Aquifers near Fallon, Nev., can be divided into four interdependent subsystems on the basis of hydrologic characteristics, according to P. A. Glancy (1981). In decreasing order of present use, they are (1) a hydraulically complex, shallow, unconsolidated sedimentary aquifer containing water of variable chemical character; (2) a highly permeable deeper basalt aquifer containing nearly homogeneous, moderately fresh water; (3) an intermediate-depth, unconsolidated sedimentary aquifer locally containing large quantities of freshwater; (4) and a deep sedimentary aquifer that probably contains saline water.

Electrical-resistivity data suggested that the deeply buried basalt aquifer is generally mushroom shaped; characteristically, it overlies the deep sedimentary aquifer and underlies the intermediate aquifer. It is recharged mainly by the freshwater intermediate aquifer, but apparently contains a blend of the freshwater and saline water. In areas of large withdrawals, water from the basalt aquifer exhibits chemical evidence of modern (post-1953) recharge from surface sources. The basalt aquifer is highly transmissive and exhibits a nearly flat potentiometric surface. The shallow sedimentary aquifer is inherently susceptible to pollution, and it contains mainly hard water. The salinity of the shallow ground water is influenced by irrigation-water recharge. Known reserves of freshwater in the intermediate aquifer are expanding with exploration activity. Water from all aquifers contains greater than normal concentrations of dissolved arsenic. Concentrations of arsenic in water from the basalt aquifer, from which the municipal water supply is drawn, are about 0.1 mg/L. Concentrations in the shallow alluvial aquifer are as high as several milligrams per liter in places.

Monitoring network for ground-water quality, Las Vegas Valley

Almost 200 wells and one spring have been selected as preliminary candidates for a monitoring network in Las Vegas Valley, according to A. S. Van Denburgh and others (1981). The wells tap valley-fill sedimentary deposits in three arbitrary depth intervals: (1) the shallow zone, less than about 10 m below the water table, which would be the first to feel the impact of land- and water-use practices; (2) an intermediate zone, about 10 to 60 m below the water table, which is commonly tapped for domestic supplies, and (3) a deep zone, more than 60 m below the water table, which currently yields most of the ground water for public supplies in the valley. Forty-five water-quality characteristics were chosen for monitoring, largely on the basis of drinking-water standards. For each site, the specific array of characteristics and their frequencies of determination (which range from once quarterly to once in 5 years) were based on geographic location and water-yielding zone(s) that were tapped.

Ground-water quality downgradient from copper ore-milling wastes at Weed Heights

Ponds that were used from 1953 until 1978 for disposal of an acid, iron-sulfate-rich brine and an alkaline tailings slurry overlie saturated valley-fill sedimentary deposits. According to H. R. Seitz (written commun.), shallow ground water (1–10 m below land surface) from several test wells closest to the ponds has been contaminated to differing degrees, but comparable water more than about 0.3 km downgradient probably has not. The water-quality data also suggested that the shallow sedimentary deposits through which the waste fluids percolate can deplete several of the more objectionable contaminants, with an effectiveness ranging from moderate to almost complete. Chemical analyses of water from six industrial-supply wells in the same area indicate (1) that deeper ground water (15-140 m below land surface) adjacent to the ponds deteriorated in quality during the period of heavy pumping, which terminated in 1978, and (2) that the chemicals changes may

be due to contamination by percolating acid brine, tailings fluid, or both.

Ground water in Kyle and Lee Canyons, Spring Mountains, Clark County

Rocks in the study area consist of Paleozoic limestone and dolomite, along with unconsolidated to consolidated upper Tertiary(?) and Quaternary alluvium that underlies each canyon floor to depths of as much as 100 m or more. Faults and fractures in the carbonate rocks transmit water to the alluvium. The water then moves down each canyon on gradients that range from 40 to 90 meters per kilometer. Highest gradients occur at the mouths of the canyons, a possible indication of changes in permeability of alluvium, changes in inflow or outflow between carbonates and alluvium, or faulted bedrock. Water-level and water-quality data were collected from wells in both canyons during April 1980–March 1981. Water levels in both canyons rose during late spring early summer in response to the spring snowmelt, and declined through late fall. Absolute water-level changes ranged from 12 to 37 m in Kyle Canyon and from 3 to 10 m in Lee Canyon. Water-quality data indicated little or no contamination of ground water by septic systems in either canyon.

OREGON

Delineation of major aquifers in western Oregon

Aquifers in western Oregon have been grouped into seven major units based on geologic and hydrologic similarities, according to W. D. McFarland. Each aquifer unit has a distinct geologic setting. Bedrock formations in the Klamath Mountains, Coast Range, and the Western Cascade Range generally have low hydraulic conductivities ranging from about 3 mm/d to 6.1 m/d.

In the Klamath Mountains, aquifers consisting of saprolite derived from granitic intrusive rocks are more permeable than surrounding bedrock (hydraulic conductivities range from about 1.5 m/d to 6.1 m/d). Water-bearing characteristics of the volcanic-rock aquifers of the High Cascade Range are largely unknown, but probably are highly variable. The most important aquifer unit in western Oregon consists of Tertiary and Quaternary sediments that occur in lowlands and, most extensively, in the Willamette Valley; hydraulic conductivities of permeable zones range from about 6.1 m/d to 1,830 m/d. Geologic formations in western Oregon are capable of supplying potable water to wells for domestic and stock use. However, available data suggest that the Tertiary marine rocks of the Coast Range commonly contain water with more than 10,000 mg/L dissolved solids at depths greater than 610 m.

WASHINGTON

Hydrologic effects of Mount St. Helens eruption

The cataclysmic eruption of Mount St. Helens on May 18, 1980, produced devastating mudflows on most streams draining the mountain and significantly altered the hydrologic characteristics of and processes occurring in the drainage basins surrounding the mountain. More than 2×10^9 m^3 of unconsolidated rock, pumice, sediment, and debris were deposited in the North Fork Toutle River valley, reducing the direct drainage area of the North Fork Toutle by more than 50 percent. In an attempt to trap some of this sediment, the Corps of Engineers constructed two debris-retention structures. During the fall and winter of 1980, both of these structures filled, and the structure on the North Fork was breached within one month.

The blast materials have blocked the tributary inflow of six streams in the North Fork Toutle River valley (Studebaker, Castle, South Fork Castle, Jackson, Coldwater, and South Coldwater Creeks), forming natural dams of eruptive debris as much as 80 m high. All but three of the lakes on the debris pile have been breached; Spirit, South Fork Castle, and Coldwater Lakes are continuing to fill and, because of their ultimate possible size, continue to represent potential flood hazards to citizens and property located downstream. Estimates are that, with normal rainfall, Coldwater and South Castle Creek lakes will fill in late November 1981, with capacities of 123 hm^3 and 31 hm^3, respectively.

The eruption of St. Helens has also had a pronounced impact on water quality. Within days, total concentrations of iron, manganese, and aluminum increased 100 to 500 times and are persisting in the Toutle and Cowlitz River basins over pre-eruption levels. In the ash-affected basins east of St. Helens, the observed river-quality changes were short-lived and, in general, decreased in magnitude with distance from the volcano. In the immediate blast area, plant and soil organic materials were pyrolized; their byproducts have created a number of organic compounds that have contaminated ash, surface water, and stream-bottom material. Many of the contaminants, including fatty acids, phenols, and resin acids, are similar to those found in effluents from the paper and pulp industry.

The North Fork Toutle River mudflow had a peak sediment concentration greater than 1.8×10^6 mg/L or about 85 percent solids by weight. An estimated 145 Mg of sediment was delivered to the Cowlitz River on May 18–19. A total suspended-sediment discharge of 20 Mg was calculated for the Toutle River for the period May 20 to December 31, 1980; 60 percent of the suspended-sediment discharge was delivered during 8 days of fall and winter storms. Peak concentrations of more than

400,000 mg/L occurred in the Toutle River during the peak flow of February 19, 1981, at which time the instantaneous sediment discharge was 18 Mg/d. Peak sediment concentrations in the North Fork Toutle River commonly exceed 300,000 mg/L, while peak sediment concentrations in the South Fork Toutle River generally were less than 100,000 mg/L.

Transport of ash from Mount St. Helens eruption

Volcanic ash from the May 18, 1980, eruption of Mount St. Helens covered much of northern Idaho to depths of up to 50 mm. Rain and snow have subsequently compacted the ash on flat areas and worked it into the soils. Some of the ash has been transported to stream channels and carried downstream. A sediment sample from the streambed of Big Creek near Calder, Idaho, taken in mid-December 1980, consisted of a mixture of ash, sand, and gravel. Most of the ash could pass through a 63 micron sieve. A flood in late December removed much of the ash from the streambed, although ash is still present locally to depths of 3 mm.

Disposition of mudslide materials from Mount St. Helens

F. P. Haeni reported that 27.2×10^6 m^3 of mudslide material was deposited in the lower Cowlitz and Columbia Rivers, Washington–Oregon, as a result of the May 18, 1980, eruption of Mount St. Helens.

The arrival of this material at the Columbia River during an incoming tidal cycle resulted in the deposition of material that stretched 11.2 km upstream, and 3.2 km downstream from the junction of the Cowlitz River and the Columbia River. The maximum thickness of mudflow material occurred near Coffin Rock where a hole, 42.7 m in depth, was filled with 27.4 m of sediment. Compaction and (or) erosion caused a 3 m depression to form in the surface of the newly deposited material at this location.

The presence of two scour channels, on May 23, 1980, on each side of a 0.99×10^6 m^3 tongue-like delta deposit of very fine sand and silt, indicates that the sediment and water surge on the morning of May 19 initially eroded the lower 0.8 km of the Cowlitz River bed. A minimum of 0.27×10^6 m^3 of material was removed from the Cowlitz River bed and redeposited in the Columbia River.

Preliminary investigation of the water resources of Island County

A preliminary survey of ground-water resources of Island County (Whidbey and Camano Islands) by D. R. Cline and others showed that the pumpage in 1979 was 6.32×10^6 m^3, which was 60 percent greater than in 1963. Although the population has nearly doubled, the quantity pumped in 1979 was not larger because water was imported to supply part of northern Whidbey Island. Public supplies used 66 percent, irrigation 25 percent, and domestic supplies 8 percent of pumpage. About 90 percent of the ground water was pumped from the sea-level aquifer, which is composed of fairly continuous sand and gravel deposits beneath the islands. Locally, one or more water-bearing zones overlie the main aquifer.

Chloride content exceeded 190 mg/L in some areas, mainly northeastern and southern Camano Island and central Whidbey Island.

Water resources of the Yakima Indian Reservation

Present ground-water levels in the lower Satus Creek basin in Washington are so high that some potentially good agricultural lands are of little use because of water logging. A numerical model of the area has been used to estimate the effects on water levels of (1) pumping ground water, (2) reducing the amount of irrigation water used on existing lands in lower Satus Creek basin, and (3) irrigating lands in the Satus uplands. According to E. A. Prych, computations with the model indicate that water levels in some areas would be (1) lowered by up to 3.0 m to 6.1 m by pumping from various numbers of the existing wells, (2) lowered by up to 1.5 m if 10 percent less irrigation water were used on the existing areas in the lower basin, and (3) raised up to 2.7 m or 9.1 m depending on whether 12.1 km^2 or 52.6 km^2 of the Satus upland were irrigated.

Ground-water quality network in Washington

Data from 100 samples collected in the northeastern part of Washington have been evaluated as part of an investigation of the quality of water in the major aquifers in the State. As many as 500 ground-water-quality samples are to be collected from these aquifers.

According to the investigator, J. C. Ebbert, preliminary results indicated that the quality of ground water in the major aquifers of northeastern Washington is suitable for most uses. This evaluation is based on analyses for common ions, nitrates, trace metals, and fecal coliform bacteria. Only a few constituents, chiefly iron and manganese, exceeded EPA primary and secondary drinking water regulations.

SPECIAL WATER-RESOURCE PROGRAMS

DATA COORDINATION, ACQUISTION, AND STORAGE

Office of Water Data Coordination

During FY 1981, progress made in major activities and publications of the Office of Water Data Coordination (OWDC) included the "Index of Water Data Acquisition," "Index to Water Data Activities in the Coal Prov-

inces of the United States," "National Handbook of Recommended Methods for Water-Data Acquisition," the field coordination program, and meetings of OWDC's two advisory committees. A large "Hydrologic Unit Map of the United States" was published at a scale of 1:2,500,000 illustrating all the hydrologic units from regional to cataloging level.

A joint meeting of the Advisory Committee on Water Data for Public Use (ACWDPU) and the Interagency Advisory Committee on Water Data (IACWD) provided recommendations to strengthen coordination of water data aquisition.

In cooperation with the National Water Data Exchange (NAWDEX), the computer file of the "Catalog of Information on Water Data" was updated through 1980. Special editions of the "Index to Water Data Activities in Coal Provinces of the United States" were completed. Volume II, Interior Province, Volume III, Rocky Mountain and Great Plains Provinces, Volume IV, Gulf Coast Province, and Volume V, Pacific Coast and Alaska Provinces complete this series of publications.

The FY 1980–81 coordination cycle was completed with publication of limited editions of indexes to water data activities in each State. These indexes show listings of stations active in FY 1980–81 with summary tables showing tabulations of all water-data collection activities contained in the "Catalog of Information on Water Data." The catalog is a computer file of water-data collection stations and areal investigations of Federal, State, and local agencies.

The "National Handbook of Recommended Methods for Water-Data Acquisition" includes chapters on ground water, sediment, biological quality of water, physical and chemical quality of water, soil moisture, basin characteristics, evaporation and transpiration, snow and ice, and hydrometeorological observations, data handling, and water-use data. The handbook covers almost all phases of hydrology. An appendix provides information on metric units, conversion factors, precision of measurements, and metric conversion of equipment.

Two maps that show national hydrologic units were prepared. One map (scale 1:7,500,000) shows all regional, subregional, and accounting unit boundaries. Another map (scale 1:2,500,000) shows approximately 2,150 cataloging units, as well as the boundaries shown on the smaller-scale map. OWDC prepared a USGS nontechnical pamphlet describing State hydrologic units maps and their uses. The publication shows part of a four-color map with its map legend and gives addresses where the hydrologic unit maps can be obtained. Digitization of all hydrologic unit boundaries at a scale of 1:500,000 was completed, thus permitting (1) computation of all drainage-basin areas (2) computer plotting of boundaries at various scales, and (3) computer conversion of locations from latitude and longitude coordinates into locations by hydrologic unit code.

Plans for water-data acquisition by Federal agencies through FY 1982 were developed by 32 Federal participants. They identify pressing needs for ground-water quantity and quality information, data on acid rain, and water quality in general, as well as real-time transmission.

NATIONAL WATER DATA EXCHANGE

NAWDEX is a national confederation of water-oriented organizations whose purpose is to improve access to water data. It has continued to grow and as of December 1980, the membership, which is voluntary, had increased to 201 organizations.

The national water-data indexing program, operated by NAWDEX in cooperation with the USGS OWDC, continued to expand. By the end of 1980, over 700 organizations had been registered in the computerized Water Data Sources Directory (WDSD), which identifies organizations that are sources of water data or other services and products pertinent to water-data studies and investigations. It also gives the locations within these organizations from which data or service can be obtained, types of data or services available, and the geographic areas in which water data are collected. Also, more than 375,000 sites for which data are available from over 400 organizations have been indexed in the computerized Master Water Data Index (MWDI), which identifies individual sites for which water data are available, the location of those sites, organizations collecting the data, hydrologic disciplines represented by the data, periods of record for which data are available, and the major parameters for which data are available. An automated indexing interface between the MWDI and the Texas Natural Resources Information System (TNRIS) was implemented during 1980 to supplement interfaces already in operation between the WATSTORE of the USGS and the Storage and Retrieval System (STORET) of the EPA.

During 1980, the NAWDEX data bases were used to produce a variety of information products including a 21-volume index to water data acquisition sites, three volumes of a 5-volume index of water-data activities in coal provinces of the United States, a table of sediment data sites for inclusion in a national report on sedimentation activities in the United States in calendar year 1979, a printed version of the WDSD containing information about 553 water-resource organizations, and a report which summarized all water data indexed in the MWDI. In addition, a variety of special catalogs, printed

indexes, and plots of water-data sites were produced to fit the specific needs of individual requests.

NAWDEX services and products are available through a nationwide network of 60 Assistance Centers in 45 States and Puerto Rico. These centers, along with the NAWDEX Program Office located at the USGS National Center in Reston, Va., provide a variety of services to assist users of water data in identifying, locating, and acquiring needed data. Most of the centers have direct access to the WATSTORE system of the USGS, and they provide referral services to many data systems and services available through NAWDEX members. The Program Office in Reston also has direct access to the STORET system of EPA and can provide data from this system upon request.

The third NAWDEX membership conference was held in Falls Church, Va., in November 1980, and representatives from 26 member organizations provided valuable input to matters related to program administration, user services, water-data indexing, and systems development.

WATER-DATA STORAGE SYSTEM

The National Water Data Storage and Retrieval System (WATSTORE) is a large-scale computerized system developed to process and disseminate water-resource data collected by the USGS. Representative WATSTORE products are computer-printed tables and graphs, statistical analyses, digital plots, and data in machine-readable form. The computer system consists of a central computer located in Reston, Va., and remote terminal facilities in nearly every State.

Data for the Station Header File, which contains identifying information for all sites, are stored in the Daily Values, Water-Quality, Peak Flow, and Unit Values Files of WATSTORE. Nearly 263,000 sites are now indexed in the Station Header File.

Geologic and well-inventory data are stored for wells, springs, and other sources of ground water in the Ground-Water-Site-Inventory File. This file continues to grow and currently contains data for nearly 700,000 sites.

The National Water Use Data System collects, stores, and disseminates data about water used in the United States. The data are classified by the following functional use categories: agricultural, commercial, domestic, industrial, irrigational, mining, fossil-fueled power, geothermal power, hydroelectric power, nuclear power, sewage treatment, and water supply. The Water-Use File, containing summary data about the withdrawal, return and use of water throughout the Nation, became part of WATSTORE in 1980. Information from this file can be used to make projections of future water requirements.

A project to test the feasibility of disturbed information processing for the Water Resources Division was completed. Minicomputer systems were installed and evaluated in two district offices and one regional research office.

URBAN WATER PROGRAM

The objective of the USGS urban water program is to provide generalized relationships for estimating (1) hydrologic changes due to urbanization and (2) hydrologic conditions under urbanization. In order to fully meet these objectives, the USGS, in cooperation with EPA, is developing a consistent and accessible urban hydrology data base.

Flood characteristics of urban watersheds in the United States

V. B. Sauer, W. O. Thomas, Jr., V. A. Stricker, and K. V. Wilson assembled a data base of basin, climatic, soils, land-use, urbanization, and flood-frequency characteristics for 269 urban watersheds in 56 cities and 31 States, including Hawaii. They developed regression equations for estimating flood magnitude for the 2-, 5-, 10-, 25-, 50-, 100-, and 500-yr recurrence intervals for ungaged sites. An independent estimate of the equivalent rural discharge for the ungaged basin is of primary importance in these equations. Essentially, the equations adjust the equivalent rural discharge to an urban condition. The primary adjustment factor, or index of urbanization, is the basin development factor. This factor is a measure of the extent of development of the drainage system in the basin and includes evaluations of storm sewers, channel improvements, and curb and gutter streets. The basin development factor is statistically significant and offers a simple and effective way of accounting for drainage development and runoff response in urban areas. Percentage of impervious area is also included in the equations as an additional measure of urbanization and apparently accounts for increased runoff volumes. This factor is not highly significant for large floods, which supports the generally held concept that imperviousness becomes less effective as soils become more saturated during large storms. Other parameters in the equations include drainage area size, channel slope, rainfall intensity, and lake and reservoir storage. The regression equations provide unbiased estimates of urban flood frequency, with average standard errors of regression varying from ±37 percent for the 5-yr flood to ±44 percent for the 100-yr flood and ±49 percent for the 500-yr flood. Several tests for bias, sensitivity, and logic were made that supports the conclusion that the equations are useful throughout the United States.

Pollutant loads in urban runoff in the Tampa Bay area, Florida

Samples of storm runoff from nine urban watersheds with mixed land use, which ranged in size from 0.9 to 8.9 km^2, in the Tampa Bay area were collected.

Concentration of pollutants (five-day BOD, COD, total nitrogen, total organic nitrogen, total phosphorus, and total lead) were determined for up to 10 discrete samples during 21 storms. Total pollutant loads were related to runoff, rainfall, and watershed characteristics by multiple linear-regression analysis. Preliminary results of analysis by R. F. Giovannelli indicated that pollutant loads are a function of runoff volume, rainfall from previous days or period of time since the last storm, and land use. Standard errors of regression ranged from ±41 percent for chemical oxygen demand to ±65 percent for total organic nitrogen.

Quality of urban storm runoff in Illinois

According to R. G. Striegl, water-quality data, which characterized 11 rain storms and 4 low-flow periods in 1980, depicted substantial differences in water chemistry between lake inflows and outflows at a 4.5 km^2 urban storm-water detention lake (Lake Ellyn at Glen Ellyn, Ill). Data indicated that the lake was efficient (greater than 90 percent) in the removal of settleable matrials including suspended sediments, sorbed trace metals and pesticides, and organic debris. Dissolved soilds, on the other hand, often showed higher concentrations at lake outlets than at the primary lake inlet during rain storms. This phenomenon was caused by high dissolved solids loading to the lake during low-flow periods, particularly during the winter road-salting period. These materials were stored in the lake and attenuated in concentration over the year. The net result was an annual dissolved-solids removal efficiency for the lake of near zero.

Nutrient data were more difficult to interpret. Biological assimilation of nitrogen and phosphorus from bottom deposits and the nutrient inputs from resident and migrating waterfowl resulted in a net negative nutrient-removal efficiency for the lake when lake-outflow loads versus runoff-inflow loads were computed.

Storm-water quality in Salem, Oregon

On the basis of storm-water samples collected at 13 reconnaissance sites in the Salem area by T. L. Miller, concentrations of chemical constituents were found to be lower than those in the Portland area. BOD ultimate values have all been less than 14 mg/L. Concentrations of total lead were as high as 370 μg/L. Preliminary results from sampling a storm-water detention basin indicated a sediment-trap efficiency as high as 60 percent. Sediment-trap efficiency for BOD was 15 percent.

Water quality of urban runoff in Salt Lake County, Utah

R. C. Christensen and Doyle Stephens reported that urban runoff in Salt Lake County contains relatively large concentrations of trace metals and nutrients, typically 0.2 to 1.5 μg/L of dissolved phosphorus, 20 to 40 μg/L dissolved copper, 60-400 μg/L dissolved zinc, and minor concentrations of lead and cadmium. Concentrations of dissolved phosphorus in urban runoff exceed the Utah State Water Quality Standard of 0.05 mg/L 60 to 100 percent of the time. The bacterial content of the storm runoff also is large, with fecal-coliform densities of 3,000 to 90,000 per 100 ml of water.

Trace metals found in atmospheric deposition samples are similar to constituents found in urban runoff in Salt Lake County. Data from wetfall deposition indicated dissolved copper and zinc are common constituents (10 to 30 μg/L. Minor concentrations of dissolved cadmium (1 μg/L) and considerable concentrations of dissolved lead (30 μg/L) also are present. Rainfall in this area is only slightly acidic, having a pH of 5 to 5.5, and specific-conductance values generally are less than 25 μmhos/cm. Dryfall deposition exhibits a similar distribution of trace metals with copper, lead, and zinc present in concentrations of 0.5 to 1.5 mg/g when collected over a 1-month period. A sample from one 6-week period contained 5 mg/g of lead, presumably originating from automotive exhaust.

WATER USE

The National Water-Use Information Program which began in 1978 had 48 States and Puerto Rico cooperating by mid-1980. The National Water-Use Data System (NWUDS) has been implemented as part of the USGS WATSTORE data system to handle the water-use data being collected by the States.

Estimated use of water in the United States 1980

C. R. Murray reported that the data for the next USGS 5-yr report has been received from all States. The report will be available for distribution in January 1981.

Water use in New York

Deborah Snavely reported that coordination efforts are continuing with the New York State Departments of Environmental Conservation and Health to collect data on water use. The data are compiled by county and river basin for each use category, such as domestic, industrial,

commercial, etc. Public water supplies and industrial ground-water withdrawal data for Nassau and Suffolk Counties were collected and compiled for the NWUDS. A report was prepared summarizing ground-water withdrawal in Nassau County in 1979. The New York State Department of Health made the necessary changes to their data base to make it compatable with NWUDS. The New York State Department of Environmental Conservation determined the availability of water-use data, evaluated the completeness of the data, and determined additional data needs to complete the NWUDS.

Water use in Montana

According to Charles Parrett, a cooperative water-use data collection program for Montana was initiated by the USGS and the Montana Department of Natural Resources and Conservation. A water-use committee comprised of representatives from six State agencies and the USGS was formed to help determine Montana's water-use data needs and priorities and a data-collection and data-storage strategy. A plan was developed for collecting municipal, industrial, and irrigation water-use data.

Water use in Virginia

H. T. Hopkins reported that the State has completed a report "Virginia Water-Use Data System Pilot Study Area." This report includes an agricultural irrigation survey for the pilot area by the Virginia Department of Agriculture and Consumer Services, Cooperative Crop Reporting Service.

Significant findings are that (1) the quantity of water withdrawn and returned by month and year is not readily available, and, of the data reported, most are estimated; (2) approximately 3 percent of the facilities are metered in the pilot study area; and (3) most of the water used for irrigation was for golf courses and nurseries.

NATIONAL WATER-QUALITY PROGRAMS

National Stream Quality Accounting Network

Operation of the National Stream Quality Accounting Network (NASQAN), the national program of the USGS for uniformly measuring the quality of the major rivers of the United States, continued at its full complement of 516 stations during FY 1980. An extensive list of water-quality characteristics is measured on a continuous, monthly, bimonthly, or quarterly basis at all sites. Locations of NASQAN stations are based on hydrologic accounting units, subdivisions of river basins in the United States that were developed by the USGS' OWDC in conjunction with the U.S. Water Resources Council. The Council's hydrologic subdivisions include 21 regions, 222 subregions, and 352 accounting units. There is at least one NASQAN station in each accounting unit, generally near the most downstream location in the unit. Some complex units contain multiple stations.

Two subnetworks are operated at selected NASQAN sites. These are the Pesticide Subnetwork and the Radiochemical Subnetwork. The Pesticide Subnetwork, operated cooperatively by the USGS and the EPA, consists of 153 stations at which water is sampled quarterly, and bottom (streambed) material is sampled semiannually. The list of pesticides being monitored is presently under review for possible expansion so that the effects of pesticides being applied currently can be observed as well as the residual effects of persistent pesticides applied during prior years.

The Radiochemcial Subnetwork consists of 53 stations, which are monitored semiannually under high-and low-flow conditions for general levels of radioactivity and specific radionuclides.

Data for NASQAN sites are published annually in USGS water-data reports, and summaries of national patterns of water quality that are developed through analysis of NASQAN data are described in periodic special network reports. The data also are available through the USGS computerized hydrologic data system, WATSTORE, and through STORET, the data system operated by EPA. Public access to these data can be faciliated through the use of NAWDEX, which is operated by the USGS. NASQAN data are used by many State, Federal, and private organizations and have been summarized in annual reports of the President's Council on Environmental Quality since 1975.

An active program is underway to develop methods for use in analyzing NASQAN data for evidence of persistent changes with time, or trends, in the quality of the Nation's rivers. The design of the NASQAN program itself is undergoing an intensive review to determine whether the original goals of the program are being achieved, and whether the information derived from operation of the network satisfies the need for a general assessment of the Nation's water quality. Network size, water-quality characteristics measured, and sampling frequency are being evaluated to determine the most efficient and cost-effective way to obtain the data required to make regional and national assessments of water quality.

National Hydrologic Benchmark Network

The Hydrologic Benchmark Network, started in 1958, consists of 57 stations in 37 states located in stream

basins having a wide variety of climate and topography that are expected to be minimally affected by population growth and its attendant impacts on its natural resources. Water-quality samples are collected at 52 sites on a monthly, bimonthly, or quarterly basis, dependent upon station and particular group of constituents. A report summarizing the data collected to date is expected to be published in FY 1982 and, like the NASQAN program, the Benchmark program is being reviewed as a means of determining its future direction.

ATMOSPHERIC DEPOSITION PROGRAM

During 1980 the USGS was an active participant in the Federal interagency effort to develop a national acid-precipitation assessment plan. R. J. Pickering and V. C. Kennedy assisted the Deputy Science Advisor to the Secretary of the Interior in developing a coordinated plan for bureaus in the Department of the Interior. The plan was submitted through the Under Secretary to the Interagancy Task Force on Acid Precipitation as the Department's contribution to the 10-yr research program called for in the plan. The USGS also was asked to act for the Deputy Science Advisor in coordinating the development of a national atmospheric deposition monitoring program for which the Department was assigned lead-agency responsibility in the Plan.

In other acid-rain-related matters, R. J. Pickering represented the Deputy Science Advisor in a bilateral effort between the United States and Canada to develop an agreement on transboundary air pollution. As a first step in the process, a series of bilateral work groups was described as the present state of knowledge of pollution sources, air transport and transformation processes, and environmental impacts. The reports of the bilateral work groups will be used by negotiators for the United States and Canada as a basis for developing the details of the agreement.

The USGS is an other-agency participant in the National Atmospheric Deposition Program of the Department of Agriculture's agricultural experiment stations. In addition to operating several monitoring sites through its Federal/State cooperative program, the USGS provides external quality assurance for the analytical work of the project's Central Analytical Laboratory. L. J. Schroder, W. A. Beetem, and B. A. Malo reported that a number of standard solutions were prepared in quantity for the quality assurance program, analytical methods used in the project were documented, and analyses of "blind" test samples composed of standard solutions showed that the Central Analytical Laboratory is performing well.

Following the eruption of Mount St. Helens on May 18, 1980, the USGS began a program to collect samples of bulk atmospheric deposition for chemical analysis at about 30 sites in Washington, Oregon, Idaho, Montana, and Wyoming. The purpose of the program is to obtain information about the effects of the volcanic activity on the quality of atmospheric deposition in the region surrounding the volcano, according to R. F. Middleburg, program coordinator. On the basis of information derived from the initial data, the program has been scaled back to a core network which includes seven sites in Washington, three in Oregon, two in Idaho, two in Montana, and one in Wyoming. Precipitation samples are collected weekly using automatic samplers and are analyzed for pH, specific conductance, major cations and anions, nitrogen and phosphorus compounds, and some trace metals. A standard raingage is operated at each site as well. The automatic samplers also provide for collection of samples of dry deposition, which will permit the network to double as an ashfall monitoring system during volcanic activity at Mount St. Helens.

REGIONAL AQUIFER-SYSTEM ANALYSIS PROGRAM

The following new regional aquifer studies were initiated in 1980: (1) A study of consolidated rock aquifers of the Central Midwest, (2) a study of alluvial aquifers of the Great Basin, and (3) a study of the unconsolidated aquifers of the Mississippi Embayment Region. Investigations continued in nine ongoing projects including the Snake River Plain, the Atlantic Coastal Plain, the Southwestern Coastal Plain, the Ogalalla Aquifer of the High Plains, the unconsolidated desposits of the California Central Valley, the aquifers of the Northern Great Plains, the sandstone aquifers of the Northern Midwest, the carbonate aquifers of the Southeast, and the alluvial basins of the Southwest.

Calibration of flow simulation models has been completed for the Northern Great Plains and California Central Valley projects, and final reports are in preparation. Numerous interim reports have been completed under these two projects, and under the High Plains and Southeast Carbonate projects.

MARINE GEOLOGY AND COASTAL HYDROLOGY

COASTAL AND MARINE GEOLOGY

INTRODUCTION

During 1980, the USGS program of marine geological research continued to emphasize activities applicable to better management of petroleum operations on the Nation's outer continental shelves. These activities involved the two major thrusts of (1) gaining knowledge about the geologic framework of petroleum occurrence within continental margins, and (2) indentifying and assessing geologic hazards that may affect exploration and production of the resources. The program includes a broad range of supplemental research devoted to other aspects of the continental shelves and to the adjacent coasts, deep oceans, and their mineral resource potentials.

CONTINENTAL MARGIN GEOLOGIC FRAMEWORK

The U.S. continental margins include a range of tectonic frameworks that in turn provide a variety of favorable and unfavorable settings for the occurrence of oil and gas. The differing frameworks and settings correspond generally with the regions identified in the Department of the Interior's lease-management program and have been treated accordingly in the USGS research program. Along the East Coast, particular attention has been devoted to the contribution of basement structures to the configuration of a postulated reef beneath the continental slope and to deformation that may reflect movement of salt deposited during early stages in the birth of the Atlantic Ocean. The results of the deformation may be compared to structures attributed to salt movement beneath the Gulf of Mexico shelf, a region that is much better explored.

The variety of tectonic frameworks that exist off the coasts of the western states and Alaska includes a number of untested basins that have exciting prospects. Of particular note among these is the Navarin basin, discovered in the course of a 1970 joint USGS-Department of the Navy reconnaissance study of the Bering Sea and the subject of a more detailed study during the summer of 1980; it appears particularly promising by comparison with nearby basins in Siberia.

Geologic framework of the Atlantic Continental Margin

K. D. Klitgord and J. A. Grow (1980) used magnetic anomaly and seismic-reflection data to map the structure and character of the basement beneath the U.S. Atlantic Continental Rise seaward of the carbonate bank–paleoshelf-edge complex where significant amounts of gas have been discovered in sedimentary rocks of Jurassic Age. They identify Cretaceous and Jurassic stratigraphic units, which may have a regional role in hydrocarbon generation.

Using a comparable regional synthesis of multichannel seismic-reflection and magnetic-anomaly data, Klitgord and J. S. Schlee determined that Georges Bank is built over a number of buried crustal blocks that subdivide the area into several linear subbasins, a broad sag (flank of LaHave Platform), and a main basin (south central part of bank). Beneath the northwestern half of Georges Bank, these subbasins form narrow discontinuous grabens that are less than 4 km deep and have orientations of 30° to 40°. Beneath the southeastern half of Georges Bank, the main basin contains more than 10 km of sedimentary rocks and along strike to the southwest and northeast connects with linear, complexly faulted troughs that flank the seaward sides of the Long Island and LaHave Platforms.

Schlee also reported an apparent significant influence of basement-block configuration on the internal geometry of the Jurassic shelf-edge carbonate buildup. Along much of the present area of the continental slope, the limestone platform built vertically and its seaward edge may have migrated slightly landward with time. However, near the intersection with the New England Sea Mount Chain, Middle Jurassic carbonate banks built 20 to 30 km seaward from basement blocks along the fractured edge of the Long Island Platform.

The COST wells G–1 and G–2 drilled in the Georges Bank basin were the first to penetrate the complete(?) Jurassic section of the U.S. Atlantic continental margin. Samples from these wells provided an opportunity for R. E. Mattick and his associates to examine their hydrocarbon-generating capacity and reservoir properties. The Jurassic section has thicknesses of 3,000 m in the G–1 well and 4,900 m in the G–2 well. Middle to Upper Jurassic rocks are mostly limestone, and Lower to Middle Jurassic rocks are predominately limestone, dolomite, and anhydrite. Geochemical analyses in-

dicated that the rocks between depths of about 3,000 and 6,000 m are thermally mature with respect to liquid hydrocarbon generation but have organic carbon contents of about 0.2 percent–a value considered low, or perhaps borderline, with respect to good source rock quality for carbonate rocks. Core samples from depths of 3,000 m to 6,000 m have porosities of less than 10 percent and permeabilities of about 0.1 mD. These measurements suggest low probabilities of finding commercial accumulations of hydrocarbons beneath the continental shelf of Georges Bank.

R. E. Miller, H. F. Lerch, D. M. Schultz, M. A. Smith, and G. E. Claypool evaluated the quality (richness), type, and degree of thermal maturity of organic matter in the Cretaceous and Jurassic shale samples from the COST G–1 and G–2 wells. The Cretaceous sedimentary rocks are not considered prospective for oil or gas in the Georges Bank area, because they have poor source rock qualities and are thermally immature. The Middle Jurassic rocks of the COST G–2 well lie at depths of 3,816 to 6,565 m. In the G–2 well the molecular distribution and composition of the saturated paraffin-naphthene hydrocarbons below about 5,640 m indicate the onset of thermal maturation processes . The Middle Jurassic carbonate sequence in the COST G–2 contains total organic carbon values that average 0.25 (weight percent). Although the hydrocarbon quality of source shales and carbonates as source rocks is not directly comparable, the need for a total organic carbon measurement of 0.30 percent, indicated by Hunt (1967), suggests a poor quality range for the organic richness of the Middle Jurassic carbonate rocks in the COST G–2 well. The solid organic matter in the COST G–2 is hydrogen prone, whereas the kerogens of the COST G–1 samples are predominantly hydrogen lean, which probably reflects the influence of nearshore, terrestrially derived organic debris. Whether the thermal maturity data from the COST G–1 and G–2 wells are regionally representative of the entire basin is unknown. It is possible that local "hot spots" and regional paleogeography may be key factors in controlling both the thermal maturity and organic richness of the Lower Jurassic sedimentary rocks beneath Georges Bank.

For the southern Atlantic continental slope and margin, W. P. Dillon and J. A. Grow used seismic-reflection data, which Richard Wise had computer processed as the basis for interpreting the existence of a regional Tertiary unconformity. These data also corroborate previous seismic indications of widespread gas hydrate zones in the area. The gas hydrate zones and the common presence of free gas beneath them are thought to have considerable potential as a future domestic energy source. Wise, Grow, and Dillon also reported that the marine seismic data offer evidence for the presence of numerous salt diapirs–features that are well known as potential traps for petroleum.

Dillon reported the mapping of a growth fault system that is more than 320 km long and lies off the coast of North Carolina on the landward side of the Carolina trough. The system contains one dominant fault but in places has antithetic faults and greater complexity. Maximum throw exceeds 0.4 km at a depth of 4 km and decreases toward the surface. The faulting extends downward nearly to basement at a depth of about 10 km, and upward is apparently present within 10 m of the sediment surface, implying very recent activity. The main fault, a unique feature of the Atlantic continental margin, occurs landward of the paleoshelf edge, is very steep to its greatest depth, and is restricted to the only region of widespread salt diapirism off the Eastern United States. Dillon, therefore, proposes that the faulting is associated with salt tectonics and that it probably resulted from withdrawal of support for a major block of strata by flowage of salt into domes. Such diapiric salt flow has continued until present, as evidenced by diapirs that penetrate the sea floor; and continuing diapirism is consistent with the recency of movement observed on the fault. Conceivably a part of the displacement resulted from a general subsidence of the Carolina trough on the seaward side of the fault. Excluding this possible contribution, however, such faulting requires a significant salt layer. Dillon postulates deposition of this layer in a deep part of the Carolina trough during early stages of continental margin development.

F. T. Manheim investigated interstital waters by analysis of samples from scientific boreholes and interpretation of electric logs of oil industry drill holes and found increasing total salt concentrations with depth beneath Georgia and adjacent offshore areas. The deep hypersaline brine zones form limits for meteoric water penetration and have been earmarked on land as potential waste storage areas. They are linked to buried evaporite deposits of Paleocene and possible Late Cretaceous age.

Geologic framework of the Gulf of Mexico

R. G. Martin and A. H. Bouma have begun a study of movement within diapiric masses of Jurassic salt and Tertiary shale that underlie the northern Gulf of Mexico Continental Slope. Seismic profiles showed evidence that most areas of the slope are undergoing some degree of diapiric uplift and slope steepening. Drill cores indicated that most slope sediments are fine-grained muds and that sand-sized materials are present mainly in canyon axes. Turbidite sands of a core from a diapir adjacent to Gyre basin in the upper slope reflect uplift far above their original depositional levels. Calculations

based on the vertical differential between these sands and equivalent layers in the adjacent basin and on paleontologic age determinations suggest an uplift rate of from 2 to 4 cm/yr since the late Pleistocene. The indicated rate of uplift for this structure is 5 to 10 times greater than rates of movement calculated for salt domes in onshore areas of the world. This relatively rapid rate may reflect (1) greater differential loads on continental slope salt and shale deposits than those on land deposits, and (2) faster growth rates in structurally immature diapirs in the continental slope relative to older domes in onshore basins. No other data are available for calculating rates of uplift in the slope, thus it is not possible to determine if a rate of 2 to 4 cm/yr is high or low for this region. Soil failures resulting from slope steepening over the diapirs can be expected during the lifetime of a producing field, and thus the slopes warrant detailed examination prior to selection of sites for future petroleum facilities.

H. L. Berryhill examined profiles from a high-resolution seismic survey that revealed a buried large submarine canyon at the edge of the continental shelf off southwestern Louisiana. The canyon has a north-south orientation and length of 35 km from head to present edge of shelf. Its length, combined with an elongate sedimentary basin that extends down the continental slope, is at least 72 km. Overall, the size of the buried canyon is comparable to the younger Mississippi trough, which lies 300 km to the east. At its northern terminus, the canyon rim is buried to a depth of 65 m by sediments representing at least two cycles of sea-level fall and rise that preceded the Wisconsinan. At the shelf edge, the sides of the canyon bound a broad swale in the sea floor and a sediment thickness of about 260 m. On the upper slope, continued movement of two large diapirs has narrowed the downslope extension of the canyon and restricted movement of sediment to deeper water. Seismic characteristics suggest that the canyon fill consists of a combination of slumps, mudflows, and deltaic and turbidite deposits. Slumps, mud diapirs, and concentrations of gas are common.

Initially the canyon, an erosional feature, was a major conduit for transporting large volumes of sediment to the shelf edge during at least the last three low stands of sea level, and thus was a site for delta progradation, according to Berryhill. The consequent localization of sediment loading here and elsewhere along the shelf edge has activated salt diapirism. Movement of the salt in turn has accentuated the sedimentary basins and has pulled the sediment up around the rising diapirs. As the sediments eventually filled the basins, they began to spill over into newly formed basins downslope. Lowered sea levels, erosion across the shelf, and deposition in basins caused by diapirism beneath the slope have increased progradation. Because of their organic content, special nature of the sediments, and the structural interaction with salt diapirs, deeply buried submarine canyons are attractive targets for petroleum exploration.

Geologic framework of the California continental margin

Using recently acquired multichannel seismic-reflection profiles, J. G. Vedder found that the sedimentary rocks within three little known basins on the California Continental Borderland south of lat 32°30′ N. may be 5,000 m or more thick. All three basins (West Cortes, East Cortes, and Velero) are in water depths greater than 1,250 m. The comparable San Nicolas and Santa Cruz basins in the relatively well-explored northern part of the borderland have Upper Cretaceous to Holocene sedimentary sequences that are estimated to be 4,500 to 6,000 m thick. In Velero basin, the largest of the southern group, pinchouts in the Tertiary section suggest opposing source areas for the sediments. Along the edges of this basin, Quaternary faults and folds deform the section, and unconformities separate Eocene(?) from Oliogocene(?) strata and Miocene from Pliocene(?) strata. All three basins are considered prospective for future petroleum exploration.

Geologic framework of the southern Alaska continental margin

Exploration of the Kodiak Shelf for hydrocarbons is still at a stage in which direct evidence of source and reservoir rocks remains scant because we lack deep subsurface samples. Indirect information, however, may be inferred from adjacent terranes and from the known geologic history. Roland von Huene and M. A. Fisher found that rocks of Paleogene and Cretaceous age on Kodiak Island are thermally mature with respect to the generation of liquid hydrocarbons. Most of their organic matter is herbaceous and coaly kerogen that could serve as a source of gas and gas condensate for deposits that may have formed beneath the Kodiak Shelf. Paleogene and Cretaceous(?) rocks also form structurally complex framework for offshore Neogene basins. The most likely reservoir rocks in this environment are sand-filled channels and coarse material on buried erosion surfaces. The latter appears to have greatest potential for reservoirs large enough to be economic. Reconstruction of the geologic history suggests probable subaerial erosion of Paleogene and Cretaceous rocks in some areas and deposition of sediment that may contain well-sorted sand during a subsequent trangression, as found in a similar geologic situation off Japan. Such potential reservoir sequences might be defined from careful study of seismic stratigraphy that indicates an extensive unconformity off Kodiak. The generally fine grained Neogene section probably would seal accumulations in stratigraphic or structural traps.

D. W. Scholl and T. L. Vallier described the evolution of the upper 5 to 10 km of the Amlia Sector of the Aleutian Ridge, which is a massive antiform built by volcanic and sedimentary processes during the past 40 m.y. Igneous processes have dominated construction along the crest of the ridge, whereas sedimentary, mass movement, and tectonic processes have shaped the flanks. Widespread igneous activity and tectonic uplift in late Paleogene time elevated the axial part of the ridge above sea level. The crest subsequently subsided, as recorded by the wave-base beveling of the summit platform, and large summit grabens formed and were then filled with upper Miocene and younger beds. Sediment, shed northward from the ridge since Eocene (or older) time, has accumulated on the flanking slope and has lapped onto the igneous crust of the adjacent Bering Sea basin, which probably has a pre-Tertiary age. South of the ridge, lower Tertiary slope deposits can be traced beneath the Aleutian terrace to an area 10 to 15 km seaward of the trench-slope break. Here the deposits terminate at a tectonic contact with a mass of offscraped trench deposits that are only broadly deformed. Cutting of the summit platform and rapid accumulation of upper Miocene and younger beds on the southern slope may have caused massive seaward displacement of Paleogene beds and thereby contributed to the formation of the Aleutian terrace. Alternatively, the subduction of trench turbidite deposits beneath strata of the older series may have elevated them to form the structurally high trench-slope break. Interpretation of structures observed on Aleutian seismic-reflection records in light of the results of DSDP drilling off Japan raises the likelihood of the Aleutian terrace being the structural expression of a deeply (4–8 km) subsided forearc area.

The sediment of the trench's turbidite wedge is believed to have been derived by axial transport from distant Alaskan and Canadian drainages during late Cenozoic time. If a thick wedge existed in Tertiary time, these deposits have been subducted beneath the ridge's lower Tertiary slope deposits. In the vicinity of the trench, reflection profiles and teleseismic data showed that stresses within the subducting oceanic plate are typically relieved by antithetic normal faulting, which elevates blocks of trench turbidite wedges into the accretionary wedge.

Geologic framework of Bering Sea, Alaska

The Gulf of Anadyr and adjacent shorelands of eastern Siberia mark the site of the northwestern portion of the Anadyr basin, a large sediment-filled structural depression that extends seaward beneath U.S. waters of the northern Bering Sea. The basin encompasses a total area of more than 100,000 km^2 and includes an area tentatively scheduled for leasing and hydrocarbon exploration in 1984. The basin is separated from the Navarin basin by a northwest-trending structural high.

During 1980, the USGS collected 3,000 km of gravity, magnetic, and both 24-channel and high-resolution seismic reflection records as well as data from 22 sonobuoy-refraction stations in the Gulf of Anadyr and the northern part of Navarin basin. M. S. Marlow, A. C. Cooper, Jon Childs, and Don Tompkins examined these data and found that the offshore part of Anadyr basin contains 2,000 to 4,000 m or more of strata. Near Cape Navarin these beds have been broadly folded into large antiforms that are tens of kilometers across and may provide traps for hydrocarbons. In the onshore Anadyr basin, Soviet exploration has resulted in discovery of 50 northeast-trending anticlinal structures. The magnetic and seismic refraction data indicate that the Okhotsk-Chukotsk volcanic belt of Eastern Siberia extends offshore southeastward along the inner Bering Shelf and flanks the northern side of Anadyr basin. On the basis of onshore drilling results in the Anadyr basin, Marlow and his associates suspect that there is an offshore section containing Cretaceous and lower Cenozoic rocks that have been folded, uplifted, and eroded during the late Mesozoic and again during the late Miocene to Pliocene, which were times of deformation in the adjacent Koryak Range of Eastern Siberia. Onshore oil shows in lower Tertiary rocks and gas shows in Miocene sandstones of the Anadyr basin suggest the presence of source beds that may extend to offshore parts of the basin and to the nearby Navarin basin. Numerous shallow acoustic anomalies that were detected in records from the Gulf of Anadyr probably indicate shallow gas accumulations.

On the basis of regional geology and the appearance of reflection on seismic profiles, M. A. Fisher concluded that much of the fill in Norton basin may consist of nonmarine deposits. The oldest rocks in the basin are probably Upper Cretaceous or Paleocene and are at depths as much as 7 km, which are great enough to generate hydrocarbons.

GEOLOGIC HAZARDS OF THE OUTER CONTINENTAL SHELF

The USGS investigations of geologic hazards form an integral component of the environmental studies program conducted by the BLM in support of the Department of the Interior's OCS Oil and Gas Leasing Program. As such, many have regional orientations. Like the geologic framework studies described above, regional overlap of activities is greatest among those devoted to the Atlantic Continental Shelf and regional

diversity greatest among those involving the large expanses of the Alaskan shelves.

Geologic hazards include those processes and conditions that affect foundation stabilities and dispersal of sediment-associated pollutants. The distinctive regional aspects of the various processes, conditions, and their combinations are becoming increasingly clear as improved techniques described in last year's report are applied to analyses of bottom disturbances and to measurement of in situ sediment properties, especially those dependent on contained gas.

Geologic hazards, Georges Bank—Baltimore Canyon regions

In the Georges Bank region, M. H. Bothner has continued studies of an area of fine-grained sediments that is thought to be a site of modern deposition on the basis of 140 profiles and many ^{210}Pb inventories for the upper 6 m of fine-grained sediment. The area lies at water depths between 60 and 120 m to the south of Martha's Vineyard, Mass. As Bothner, Bradford, Butnam, and their associates reported previously, net current from the northeast could carry contaminants generated by resource development activities on Georges Bank to this "Mud Patch." The concentration of suspended matter in bottom waters shows a pronounced maximum above the fine-grained sediments during calm conditions, and increases during storms. The resuspension of fine sediments provides a mechanism for striping dissolved contaminants from bottom water during all seasons of the year, and from the entire water column, when it is mixed by winter storms. This mechanism may help explain the distribution of lead with sediment depth. The concentration of stable lead in surface sediments is 30 ppm, about 50 percent higher than background levels measured at depths of 30 cm in these sediments. The increased flux of lead to these sediments probably relates to the discharge of lead from automobile exhaust, which began in 1924.

In a cooperative study, a team from the USGS and Lamont Doherty Geological Observatory of Columbia University used a midrange sidescan sonar system (SEA MARK 1) to obtain information on physiographic details of the Continental Shelf and Slope. B. A. McGregor examined results of a survey in the vicinity of Wilmington Canyon, where a dendritic drainage pattern covers essentially the entire slope and feeds the canyons in a manner that has a striking similarity to that of fluvial systems on land. The canyons are flat floored; but not because they are infilled by sediments. Instead the canyons appear to flush sediments seaward episodically. The morphology of canyon channels varies from a straight, downslope trend to one of tight meanders within an apparent flood plain. McGregor concludes that differences in channel morphology may indicate differing canyon ages.

J. M. Robb, J. S. Booth, J. C. Hampson, Jr., and J. R. Kirby mapped the geology of the continental slope between Lindenkohl and South Toms Canyons off New Jersey on the basis of data from a dense network of high-resolution seismic-reflection profiles, more than 40 sediment cores, 10 submersible dives, and the SEA MARK 1 sidescan sonar system having a 5-km-swath width. Pleistocene deposits cover the upper slope and extend down over the midslope and parts of the lower slope as lobate ridges within a complex system of canyons and valleys. Miocene and Oligocene sediments crop out in canyon and valley bottoms on the midslope, and Eocene sediments are exposed on much of the lower slope. Erosion has deepened and extended valleys and canyons, but the intervalley ridges are primary depositional features of Pleistocene and older age, probably overbank deposits from density currents transporting material downslope. A few small slump features were mapped on the sides and in the heads of canyons and valleys, but seismic-reflection profiles show a general absence of identifiable scars and displaced masses. Most of the topographic surface appears to be relict from late Pleistocene or earlier time and to be covered by a thin layer of undisturbed fine-grained Holocene sediment. However, cores as much as 8 m long commonly have underconsolidated, potentially unstable sediments; and sidescan sonographs provide evidence of gullied canyon walls, bottom current activity, and down-canyon transport of material. Therefore, though evidence for large slope failures is lacking, small-scale processes of submarine erosion and mass wasting seem active at present.

Based on interpretation of 600 km of high-resolution seismic-reflection profiles from a 10×30 km area of the continental slope between Carteret and Lindenkohl Canyons in the Baltimore Canyon area, J. M. Robb attributes much of the complex morphology and many structures in sediments of Pleistocene to Eocene age to turbidite deposition, mass wasting, and erosion. More than 300 m of sediments of Pleistocene age underlie the top of the continental slope, generally thinning to less than 10 m at water depths of 1,000 m. Large masses of Pleistocene materials also are found in the upper rise. Although shallow slump structures are present within the Pleistocene deposits of the upper slope, much of the middle and upper slope topography apparently represents a complex system of depositional leveed channels formed by Pleistocene turbidity currents. Cut-and-fill structures also occur, and a Miocene sequence of complex delta-front deposits crops out at depths greater than 1,000 m. Outcropping Eocene and Miocene sediments of the lower slope are eroded and faulted.

J. S. Booth found a marked difference between the Georges Bank and Baltimore Canyon study areas with regard to evidence of past mass movement and the potential for future mass movement events. For example, in the vicinity of Alvin Canyon off Georges Bank, the continental slope is typified by many scars, allochthonous blocks, and other mass movement features. Geotechnical analyses of cores apparently taken on two differing scars indicated that approximately 10 to 35 m of overburden may have been removed from the sites. Core data also suggest that the surficial sediment elsewhere in the study area tends to be normally consolidated to slightly overconsolidated. Thus, it is probably relatively stable at present. In contrast, the Baltimore Canyon slope area between Lindenkohl and South Toms Canyon offers little topographic evidence of previous mass movement, nor do geologic or geotechnical core data suggest the occurrence of such events. Nevertheless, as noted by Robb and others, above, results of geotechnical tests on the surficial sediment are indicative of underconsolidation, implying relative weakness at many sites. Coupled with the presence of steep slopes and gas at some places, such surficial sediments are probably marginally stable.

Geologic hazards, Southeast Georgia Embayment

Peter Popenoe investigated slump features within and below the lease sale 56 area southeast of Cape Hatteras using records of long-range GLORIA (swath width 22 km) and midrange (swath width 5 km) sidescan sonars. The features were noted during a seismic cruise in 1978 and included low-angle normal faulting and cliffs on the slope that were up to 75 m in height and terminated the bedding abruptly. The long-range sidescan sonar showed the cliffs arcing downslope and wrapping around a breached salt diapir complex. The midrange sidescan sonar confirmed this interpretation and, in addition, showed numerous slide tracks that were normal to the slope and were etched into the bottom to depths of 5 to 10 m. At places the tracks terminated in lobate deposits that are believed to be rubble. These slump features appear to be unique to the area above the breached salt diapirs; and Popenoe, therefore, attributes them to subsidence related to salt removal. Sidescan data over the diapirs showed the bottom to be pocked with probable solution features.

Popenoe also used midrange sidescan sonar (swath width 5 km) to investigate an area of nominated lease tracts due east of Cape Hatteras. The lease tracts straddle the boundary between the shelf and slope in the Monteo quadrangle. The sidescan images showed that they include a slope that is extensively dissected by submarine canyons with depths measured in hundreds of meters. Both thalwegs and divides are steep, suggesting ongoing canyon-cutting processes. Trellis and dendritic drainage patterns are evident on the sides of the canyons.

Geologic hazards, Gulf of Mexico

It has been recognized that biogenic methane exists as free gas in near-surface sediments of certain areas and plays a significant role in their stability. Until recently, however, the amounts of involved methane and the extent to which sediment strengths were reduced could not be accurately assessed due to the severe disruption of samples during core recovery. To circumvent this problem, engineers and geologists at Texas A & M University in cooperation with a USGS team led by L. E. Garrison developed a pressure core barrel that allows retrieval of cores sealed in a container at downhole in situ pressures. After recovery, the container is opened, and the core is tested inside another chamber in which pressure is equalized to original downhole pressure. No significant methane loss or sample disturbance occurs.

The analyses of pressure cores from Mississippi delta sediments show that gas is not ubiquitous, even in those zones where greatest saturation can be inferred from acoustic data. On the contrary, the distribution of methane gas varies vertically and laterally at all locations tested. Gas occurrences were lenticular, with layers only a few feet thick, separated by zones containing only trace amounts of methane. Methane concentrations in pressure cores were as high as 90×10^3 ppm, whereas that of a replicate sample analyzed by conventional procedures was 27×10^3 ppm. In addition, shear strengths in pressure cores were two to three times greater than those measured in replicate samples that had degassed rapidly.

Through monitoring suspended sediment on the South Texas Continental Shelf, G. L. Shideler noted evidence for a regionally persistent turbid benthic nepheloid layer. A time sequence of quasi-synoptic measurements of the water column obtained during six cruises over an 18-month period indicates substantial spatial and temporal variability in the characteristics of the nepheloid layer. Regionally, the shelf nepheloid layer shows trends of increasing thickness both seaward and in a convergent alongshelf direction. Greatest thicknesses occur over a muddy substrate and probably reflect a causal relation; observed maximum local thickness was 35 m along the southern shelf break. Mean concentrations of suspended particulate matter in shelf-bottom waters ranged from 49×10^4 to 111×10^4 particle counts/cc and have a persistent regional trend of increasing shoreward. Bottom particulate matter is predominantly inorganic detritus. Admixtures of organic skeletal par-

ticles, primarily diatoms, are generally present but average less than 10 percent of the total. Texturally, the dominant particulate matter in the bottom waters is poorly sorted very fine silt. (3.9–7.8 μ).

Shideler concluded that the variability in nepheloid-layer characteristics reflects a highly dynamic shelf environment. He suggested a conceptual model for the relation of the layer to hydrographic and substrate conditions, whereby development and maintenance of the nepheloid layer results from sea-floor sediment resuspension that may be attributed to bottom turbulence caused primarily by vertical shear and shoaling of progressive internal waves generated by migrating shelf-water masses, primarily oceanic frontal systems and secondarily shoaling surface gravity waves.

Geologic hazards, Southern California Borderland

H. G. Greene, S. H. Clarke, and M. E. Field used industry and USGS seismic-reflection data to study a structurally deformed zone along the expected offshore extension of the Crisianitos fault zone near San Onofre, Calif. The zone consists of correlatable en echelon faults and folds, many extending into the shallow subsurface strata (probably Neogene in age), and appears fairly continuous, extending south to southwest offshore from the San Onofre nuclear generating station to merge with or be truncated by the Newport-Inglewood-Rose Canyon fault zone. The pattern of these faults suggested a close association with the regime of wrench tectonics active in the Southern California Borderland throughout Neogene time.

In addition to the deformed zone, Greene, Clarke, and Field identified a number of geologic features and conditions that also are potentially hazardous to offshore development in several areas studied in conjunction with the BLM Offshore Petroleum Leasing Program. Prominent geologically young faults associated with the Newport-Inglewood-Rose Canyon and Palos Verdes Hills–Coronado Block fault zones cut the innershelf between San Pedro and San Diego; and prominent northwest-trending faults cut Quaternary sediments in the Gulf of Santa Catalina, in the San Diego trough, and northeast of Thirty Mile Banks. The entire region is active seismically, especially the northern part in the vicinity of the Los Angeles basin. In addition, sediment gravity slides (12 km^2 or more in area and extending to subbottom depths of at least 50 m) were mapped at several localities on the inner shelf between Newport Beach and Point Cavelle, and evidence of old failures and sediment creep is present on the slopes flanking the Gulf of Santa Catalina. The central Santa Rosa–Cortes Ridge and San Nicolas Island Platform are cut by geologically young faults, and evidence of failures in unconsolidated sediments is abundant on the steep slopes. The most prominent potential hazards in the western Santa Barbara Channel–Point Conception area are unstable seafloor conditions. Downslope sediment creep is characteristic of the upper slope between Point Arguello and Point Conception, and evidence of past mass movement is commonplace. In addition, many faults displace the seafloor and the Quaternary and recent sediments in the Point Conception area, a region with active seismic history.

D. S. McCulloch suggested the possible occurrence of active subduction or crustal shortening along the Pacific–North American plate boundary beneath the Santa Barbara Channel and Transverse Ranges to the north on the basis of (1) high modern uplift rates of 10 to 15 mm/yr for as long as 200,000 yr along the southeastern side of the range, (2) a large gravity gradient across the channel exceeding that which can be attributed to accumulated sediment (L. Beyer, pers. comm., 1979), (3) nearby horizontal first motions on earthquake hypocenters beneath the channel that indicate compression directed to the north-northeast, and (4) possible north-south shortening of the geodetic net across the channel west of the Transverse Ranges. The differential plate motion has been accomplished by right-lateral displacement along the seismically active Hosgri fault that serves to decouple the plates. Such a model also could account for the lack of evidence of a southern extension of the Hosgri fault across the Santa Barbara Channel.

In another study of bottom conditions off southern California, D. A. Cacchione collected Geoprobe data at two sites (22 m and 67 m mean water depth) on the San Pedro Continental Shelf off Los Angeles in 1978. He used these data to compute hourly bottom-friction velocities and determine stresses over a 40-d fair-weather period. During two 3- to 4-d segments in this period, long surface swells of 12- to 15-s periods caused increased instantaneous bottom stresses at the shallow site, thereby resuspending the fine sands and other fine materials and accentuating the oscillatory sediment ripples. The ripples observed in the Geoprobe bottom photographs at the shallow site had height and length characteristics predicted by available theories for the measured wave statistics. At the deeper site, the incoming swell waves had no observable effect on the sea floor (as detected in the bottom photographs). Daily offshore net flow of about 1 to 3 cm/s was measured in the lowest 1 m of the water column at both sites and is probably driven by wind-force shelf circulation. This net offshore flow, combined with infrequent fine sequences in which a lateral gradient is caused by swell, induces a net offshore migration of near-bottom and bottom sediments. This process gives rise to slow accumulation of modern

silty sand on the mid to outer shelf that is reworked only during more energetic periods (storms). During storms the fairweather pattern is probably disrupted, and the transport pathways radically changed.

Geologic hazards, northern California–Washington OCS

On the basis of geologic mapping in the offshore Eel River basin, California, and Coos Bay basin, Oregon, S. H. Clarke and M. E. Field reported that the principal hazards off central Oregon appear to be associated with active faulting. Geologically young north- to northwest-trending faults, possibly reflecting a broad zone of shear, cut the inner shelf off Cape Arajo and on Heieta Bank. Some of these faults can be traced for 10 to 15 km and are expressed in seafloor relief. Evidence of modern seafloor mass movement is scant; however, structures that may be attributed to older buried submarines slides are common in seismic profiles across areas of apparently high Pleistocene sediment influx. Subbottom acoustic anomalies thought to reflect accumulations of shallow gas (probably methane) are common; locally these are associated with sea floor dewatering and probable gas seepage into the water column.

Evidence of diapirism and shale flowage along the northern California-Oregon-Washington continental margin has been reported previously. Diapirs on the Washington margin are thought to have associated overpressured zones and shallow gas and could be potentially hazardous if penetrated in offshore drilling activities. In their studies Clarke and Field have mapped youthful diapiric ridges, and piercement structures have been mapped in both the offshore Coos Bay and Eel River basins. Samples of modern unconsolidated sediment ponded near the crest of one of these structures in the Eel River basin contain gasoline range hydrocarbons that are probably thermogenic and are thought to have migrated upward from the underlying Neogene sedimentary section along deep-seated fractures in the diapiric ridges. The offshore Eel River basin also has numerous faults that displace Quaternary sediments on the sea floor and zones of submarine sliding that measure several hundred square kilometers in area and include slump structures extending to depths of 80 m or more beneath the sea floor. The widespread occurrence of sea-floor failure probably reflects the combination of a very high rate of sediment influx (locally, rates of deposition exceed 1 m/1,000 yr), potential triggering events related to high seismicity, and a vigorous wave climate.

Geologic hazards, Gulf of Alaska

Using high-resolution seismic profiles and sediment cores collected during the summer of 1980, M. A. Hampton and his associates now are analyzing the geologic structure, stratigraphy, and the physical and chemical properties of the surficial sediments of Shelikof Strait of the northern Gulf of Alaska. The sea floor of the strait, which trends northeast-southwest between the Kodiak Islands and Alaska Peninsula, is gently sloping and deepens gradually from about 170 m in the northeast to over 200 m northwest of Kodiak Island. Narrow channels border the platform adjacent to the islands and the mainland. Unconsolidated sediment of probable Pleistocene and Holocene age and greater than 200-m thickness covers folded and glacially eroded sedimentary bedrock. Bouldery sediment recovered from the lower part of the unconsolidated section is probably glacial. Surficial sediment grades texturally from muddy sand in the northeast to slightly sandy mud in the southwest and represents a Holocene progradational marine sequence deposited from currents entering the northeast end of the strait. The strait remains a depositional site with no evidence of erosion or large-scale bedform movement as in the nearby Lower Cook Inlet or on the Kodiak Shelf. Accumulation rates judged from sediment thickness overlying a volcanic ash layer from the 1912 Katmai event are on the order of 10 to 15 cm/100 yr. Shallow faults occur in the northeast and central areas near the edges of the strait and near the axis. Some faults that are only a few km in length offset the sea floor up to 100 m, and they are judged to be active. Epicenter plots show only vague concentrations of seismic activity near the high-offset faults. Evidence of slope instability is sparse with only a few small slides identified on fault scarps and channel flanks.

Areal trends in geotechnical properties of sea floor sediment in the Sheikof Strait reflect the northwest to southeast fining in grain size. Water content, plasticity index, and liquidity index increase; whereas, vane shear strength and sensitivity decrease. Levels of light hydrocarbon gases in core samples are low (methane = 30 μl/L), except in one core (methane = 1,600 μl/L), suggesting a general lack of near surface gas-charged sediment. However, acoustic anomalies deeper in the section and sea floor pockmarks may indicate saturation and associated low-shear strength of the sediments at some localities.

Within the northwestern Gulf of Alaska, Hampton reported that the sediments of most areas are either Holocene glacial marine detritus or Quaternary pebbly

muds. The pebbly muds, typically found well offshore (10–40 km), are overconsolidated and have a high in situ shear strength. The nearshore (shallower than the 50 m isobath) Holocene sediments are predominantly sands with some interbedded silts. In situ core penetration measurements indicate medium densities with relatively high slurring resistance. Most glacial marine sediments farther offshore are silts with a few sand layers. Their in situ shear strengths are relatively low indicating normal consolidation or slight overconsolidation. Three examples of mass movement were identified—all in the silty glacial marine sediments. The heads of the slope failures are near the transition from predominantly sand to mostly silt. The failures apparently reflect instability associated with low shear strength of the glacial marine silts and the triggering effect of large storm waves or earthquakes.

Geologic hazards, Bering Sea

The first cruise in Navarin Basin Province, Bering Sea, dedicated to investigate potential sea floor hazards provided about 3,600 km of high-resolution geophysical data and 115 sea floor sediment samples. According to P. R. Carlson and H. A. Karl, gas-charged sediments are the most prevalent potential geohazard of the Navarin Shelf and are most common in the northern part of the province. Many seismic-reflection profiles of the continental slope offer evidence for submarine slides and slumps, especially on the walls and floors of three large submarine canyons that are cut into the western part of Navarin basin. The profiles also provide evidence of shallow faults, especially near the shelf edge. Fields of large sand waves (about 600 m wave length and 10–15 m wave height) have been discovered on the outer shelf and upper slope, associated mostly with the three canyons. More data are needed to determine if these sand waves are presently active.

C. H. Nelson shifted emphasis of his studies in the northern Bering Sea to the western half of the Norton basin, a region known as the Chirikov basin. Here the sea floor apparently has fewer potential geologic hazards than Norton Sound to the east. Acoustic anomalies indicating areas of probable shallow gas-charged sediment are numerous, especially in the eastern half of Chirikov basin adjoining Norton Sound. The muddier transgressive fine to very fine sands in this eastern half, although generally less than 1 m thick, are sufficiently cohesive to trap biogenic methane generated in near-surface Pleistocene peaty muds; however, unlike Norton Sound, gas quantities are not great enough to cause gas crater fields. Fewer acoustic anomalies in the western half of the region correlate with progressively increasing amounts of glacial deposits.

Fields of mobile bedforms are evident at several places in the Chirikov basin. The largest active sand waves occur on large sand ridges (5×30 km) between King Island and Port Clarence; they have wave lengths of about 200 m, wave heights of approximately 2 m, and superimposed small sand waves ($\lambda = 100$ m, $h = 0.5$ m) and ripple fields ($\lambda = 30$ cm, $h = 5$ cm). The small sand waves and ripple fields are active during normal northerly undirectional current flow. When this flow is reinforced by major storm conditions, the large-scale features become intermittently active. Fields of small sand waves and ripples also occur near the northern and western margins of St. Lawrence Island.

H. W. Olsen examined upper Pleistocene transgressive deposits that cover the bottom of Chirikov basin. These deposits include an exposed inner-shelf fine sand underlain by a basal transgressive medium sand on the north and east flanks of the basin. Geotechnical data on the latter, obtained in the sand-wave fields near Port Clarence, show that the material is loose near the surface but becomes firm at shallow depths and could not be penetrated more than about 3 m with an Alpine vibratory sampler. Eastward, Yukon sediment of Holocene age, consisting dominantly of silty fine sand and sandy silt, covers the bottom of central and western Norton Sound, which is a high-energy environment of ice loading, high waves, and strong bottom currents. Olsen reported that the sediment contains significant amounts of sand in some areas and minor amounts of clay-size material ranging from 0 to 20 percent generally. Moreover, the sediment is generally dense, although loose and weak zones occur at the surface and also at depth between relatively dense layers. These features together with evidence of storm sand layers and scour depressions and the preliminary results of analytical studies indicate this sediment is susceptible to liquefaction during major storms.

Pleistocene peaty deposits underlie the Holocene and Pleistocene deposits in Norton Sound and Chirikov basin and are somewhat overconsolidated, probably because of subaerial desiccation during low sea levels of the late Pleistocene. These materials have a higher clay content than the overlying deposits and contain substantial amounts of organic carbon and gas. The presence of gas suggests probable high in situ pore pressures. If so, the strength of the material could be low, even though the material is generally overconsolidated.

Sand bodies of many types can be distinguished on the Bering epicontinental shelf. In a study of these bodies, C. H. Nelson identified the following types: major linear shoals in tidal estuaries, bars paralleling the shore, strandline features, delta-front channel fills, and large leeside sand bodies deposited downstream from land masses that disrupt unidirectional current flow. The

sand bodies range from 5 to 100 km long, from 2 to 15 km wide, and from 5 to 15 m thick. Texturally they range from sorted medium to fine sands in the ancient strandline deposits to very fine sand in the leeside sand bodies. Cross laminations characterize the delta front channel deposits; tabular foresets typify the ancient strandlines where modified by sand waves; and rhythmic parallel laminations distinguish the leeside accumulations. Probable ancient analogs for these modern sequences exist in the Cretaceous deposits of Utah and Colorado.

Geologic hazards, northern Alaskan OCS

P. W. Barnes, Erk Reimnitz, and Dennis Fox determined the sediment content, composition, and ice core stratigraphy of eighteen 1.5-m-long ice cores taken in May 1978 from the seasonal fast ice off northern Alaska. Sediment concentrations in the ice ranged from 3 to more than 1,600 g/m^3. Silt and clay-size particles were dominant and discolored the upper segments of cores to form a layer as much as 1 m thick. The upper 10 cm of ice in almost all cores was less turbid, and the basal relief of the turbid layer was 10 to 20 cm over distances of 1 to 2 m. The known sources and transport relations of suspended sediment do not explain the distribution of turbid ice that is found in the fast-ice zone to distances of 10 to 20 km seaward from the coast. The occurrence of sediment only in the upper part of the seasonal fast ice indicates that the sediment-rich ice forms early during ice growth. The most likely mechanism leading to the formation of sediment-laden ice requires storm resuspension of nearshore bottom sediments accompanied by formation of frazil ice and subsequent offshore advection prior to stabilization of the fast ice. Barnes, Reminitz, and Fox estimated that the amount of sediment incorporated in the 1978 Beaufort sea-ice canopy was at least 5 to 10 percent of the seasonal influx of terrigenous fine-grained sediment. They concluded that the presence of sediment-rich fast ice is a major factor influencing the melting rate, subice photosynthesis, and cross-shelf transport of sediment. The dominance of fine-grained sediments suggest that ice rafting of these size fractions is more voluminous than the "coarse fraction" of traditionally recognized ice-rafted sediments.

BASIC CONTINENTAL SHELF RESEARCH

OCS hard mineral resources

In response to a request from the DOI Outer Continental Shelf Mining Policy Task Force, F. T. Manheim prepared an updated appraisal of OCS resources and concluded that sand, gravel, phosphate, and ferromanganese concretions of the Blake Plateau have near-term economic potential if leasing is implemented. Sand and gravel occur in virtually unlimited quantities on the Atlantic shelf, commonly as coarse sand that is well suited for use as fine building aggregate. Local sand supplies for New York City are expected to be depleted or precluded from use within 5 to 10 yr; offshore supplies may permit both price stability and recovery of capital investment within a few years. The largest known phosphorite deposits of the U.S. continental margins occur in the southeastern U.S. Atlantic; contract studies of deposits off Georgia indicated present feasibility for economic recovery, even in comparsion with land deposits. The Blake Plateau manganese nodules have attracted renewed interest. Though lower in copper and nickel than prime Pacific nodules, they have somewhat higher cobalt (.3 percent) and potential of serving as catalysts for petroleum refining. An estimated startup program of 2 to 3 million t would fulfill most U.S. needs for cobalt (currently 90 percent imported).

Coral reef stress

Based on changes in carbon-14 activity within coral bands extending back to the year 1620, E. A. Shinn, J. H. Hudson, and B. H. Lidz are able to identify clearly the effects of burning fossil fuels since the beginning of the industrial revolution and the widespread effects of atomic testing during the period 1960 to present. In a different but related study, they used the width of coral bands from a large study area to determine the health of corals using the assumption that unhealthy or stressed corals grow more slowly than healthy ones. Preliminary analysis, however, suggests little change in annual growth rates during the past 50 yr in an area heavily stressed by man.

Sediment bedforms and movement

Where bedforms migrate during deposition, they climb upward with respect to the generalized sediment surface. Further sediment that is deposited on each lee slope and not eroded during the passage of a following bedform remains as a cross-stratified bed. Because sediment is thus transferred to underlying strata, bedforms must decrease in cross-sectional area or decrease in number, or both, unless sediment lost from the bedforms is replaced. Thus, D. M. Rubin and R. E. Hunter noted that where sediment is transported solely by downcurrent bedform migration, the mean thickness of cross-stratified beds must be equal to the decrease in bedform cross-sectional area divided by the migration distance over which that size decrease occurs. Also where bedforms migrate more than one wavelength during deposi-

tion, bed thickness can be only a fraction of bedform height. Applications of equations that describe this depositional process help explain the downcurrent decrease in size of tidal sand waves in St. Andrew Bay, Fla., and the downwind decrease in size of transverse eolian dunes on the Oregon coast. Using the same concepts, ancient dunes that deposited the Navajo, De Chelly, and Entrada Sandstones of the Grand Canyon region are calculated to have had mean heights of several tens to hundreds of meters.

In the vicinity of the head of submarine Carmel Canyon off Monterey, Calif., waves have shaped a bed of very coarse grained sand into long-crested oscillation ripples. Using dyed sand tracers to study sediment transport over this ripple bed, J. R. Dingler found that sand moves slowly northward and offshore. Once over the canyon rim, the sand avalanches down angle-of-response slopes to the canyon bottom.

Processes that cause the net transport of sediment normal to the shoreline are not well understood. This is particularly true under high wave-energy conditions, during which the most significant transport occurs. Therefore, to contribute to a better understanding of this cross-shore transport, A. H. Sallenger obtained data from southern Monterey Bay, Calif., that included measurement of changes in the nearshore profile and of waves and currents at different locations on the profile. The data were gathered for breaking waves as high as 5 m. During one high-energy event, extensive erosion was measured across the surf zone. This erosion averaged 35 cm over a shore-normal span of 120 m, and deposition took place offshore in the vicinity of the breaker zone. This pattern of erosion and deposition can be explained by a third moment of measured cross-shore velocities. This third moment is a measure of velocity asymmetry and is thought to be proportional to the rate of sediment transport. In the surf zone, the value of the third moment increased seaward with distance from the shoreline, and its sign indicated offshore sediment transport. Thus, in this area one would expect erosion of the profile as observed. Farther offshore, in the vicinity of the breaker zone, the value of the moment began to decrease with distance from shore. Here one would expect deposition which also was observed. These preliminary results suggest that the third moment of cross-shore current velocities may be important in causing cross-shore sediment transport.

Cyclic deposits containing hummocky cross stratification were found by R. E. Hunter and H. E. Clifton in the Cape Sebastian Sandstone of Dott (1971), a shallow marine sandstone of Late Cretaceous age on the southern Oregon coast. The cycles average 1.6 m in thickness and consist, where complete, of a lower hummocky cross-stratified sandstone, a middle planar- and ripple-bedded sandstone with a shale bed in its middle part, and an upper bioturbated sandstone. Noteworthy features of the hummocky cross stratification include the presence of depositional domes in addition to scoured depressions, the absence of evidence for significant bedform migration, the presence of a small proportion of dip angles greater than the angle of repose, and a large proportion of low dip angles. The lower, stratified, fining-upward part of the cycle (up to the top of the shale bed) is interpreted as having accumulated under conditions of initially great but gradually decreasing current velocity and deposition rate. The currents probably had a strong oscillatory component, and the depositional event is inferred to have been a storm. The part of the planar-and ripple-bedded sandstone above the shale bed was probably deposited during fair weather after the storm but before reestabishment of a normal benthic fauna. The bioturbated sandstone is interpreted to have been deposited during fair weather or during minor storms separated by long intervals of fair weather.

Organic geochemistry of OCS sediments

The combination of high-resolution seismic profiling to locate specific areas where hydrocarbon gases may be present and analyses of core samples from these areas to determine the concentrations, compositions, and isotopic contents of hydrocarbon gases in the sediment forms a prospecting method for oil and gas. The analyses permit distinctions between hydrocarbons from biochemical and from thermochemical sources. Biochemical gas, when generated in large quantities, can establish gas provinces usually at shallow depths; whereas, thermochemically produced hydrocarbons may indicate petroleum (gas and oil) at depth. In tests of these prospecting methods, K. A. Kvenvolden identified biogenic methane-charged sediments in Norton Sound and in the western and eastern Gulf of Alaska. He also found an active submarine seep of mainly carbon dioxide and some petroleumlike hydrocabon gases in the central part of Norton Sound and two minor thermogenic hydrocarbon anomalies at the northern end of St. George basin in the Bering Sea. A preliminary survey of Navarin Basin, also in the Bering Sea, did not show any strong hydrocarbon anomalies. Finally, thermogenic hydrocarbon gas was observed in samples of unconsolidated sediment associated with a diapirlike structure in the Eel River basin, off northern California.

COASTAL INVESTIGATIONS

Massachusetts nearshore environment

R. N. Oldale collected high-resolution seismic data that show a well-developed delta seaward of the Merrimack River valley. The delta most likely was formed

during the postglacial low sea-level stand. Depths to the foreset-topset bed contact will allow estimates of the amount that sea level was lowered following the late glacial high stand and the amount of Holocene sea-level rise.

Oldale also found that in spite of modern techniques that can be used to date glacial and interglacial deposits, there still are no data to firmly establish the ages of such deposits on Cape Cod and the islands to the south. Age estimates of Illinoian or older for the oldest drift and Sangamonian to earliest Wisconsinan for the overlying Sankaty Sand on Nantucket Island are based on paleontologic evidence, radiocarbon dates, and D/L Leucene ratios from the Sankaty Sand. None of these methods, however, provide conclusive age determinations.

Most infer a late Wisconsinan Age for the uppermost drift in southern New England; and although this age seems well established for the youngest drift north of Cape Cod, it is not established for the Cape and islands. For various reasons the radiocarbon dates on material from within or atop the youngest drift cannot be used to fix the age of the drift. Infinite dates on detrital material from the drift are of no use in establishing a "no older than" age, and finite dates on similar material are increasingly suspect because of weathering, recrystallization, and contamination (E. Spiker, written commun., 1979). Dates that stand alone (for example, the 15,300-yr-B.P. date from Zacks Cliff on Martha's Vineyard) are untested and could be wrong. Basal peat dates provide only "no younger than" ages for the underlying drift. However, it can be argued that such dates more or less approximate the age of the drift, because it is unlikely that the drift surface would remain unvegetated for more than a few thousand years. Thus an Illinoian Age or older for the drift below the Sankaty Sand, a Sangamonian to earliest Wisconsinan Age for the Sankaty Sand, and a late Wisconsinan Age for the overlying drift represent best guesses that await confirmation.

C. J. O'Hara obtained high-resolution seismic-reflection profiles that indicate that the most salient submarine topographic features in Nantucket Sound are very large marine bedforms. These include linear sand ridges, broad shoals, beach and bar deposits, tidal deltas, and submerged spit deposits that are, in most cases, acoustically continuous with each other. Together the bedforms blanket 60 percent of Nantucket Sound, underlying the unconformity cut during the Holocene transgression. Their thickness is generally 4 to 6 m, but reaches 13 m at places where they occur as linear ridges (as much as 20 km long and 3 km wide). The large bedforms are believed to have been constructed by wave action and by littoral and tidal currents that reworked the inner-shelf sediments (mostly upper Wisconsinan glacial outwash) and redeposited them onto a nearly flat lying wave-cut surface during the last sea-level rise. Sand waves and megaripples (heights to 4 m and wavelengths to 150 m) locally superpose the larger bedforms, being generally restricted to their flanks but also occurring within the swales or troughs between the shoals and ridges. Where seen, the sand waves and megaripples are mostly well developed and strongly asymmetric in profile, suggesting active near-bottom tidal currents and bedform construction, maintenance, and migration dominated or controlled by the ebbing or flooding phase of each tidal cycle, probably during periods of peak flow. Two very large sand wave fields (covering an area greater than 130 km^2) occur atop a submerged spit-tidal delta complex between Great Point and Monomoy Point, eastern Nantucket Sound. These feaures constitute the most easily recoverable sand and gravel sources from this part of the Massachuetts inner shelf.

A deeply eroded cuesta of seaward-dipping Cretaceous and Tertiary strata that extends from western Long Island Sound to eastern Georges Bank generally has been considered the northernmost limit of submerged Coastal Plain rocks beneath the Inner Continental Shelf of southern New England. In a study of 950 km of high-resolution subbottom profiles, however, C. J. O'Hara reported a much more extensive distribution of the Cretaceous and Tertiary rock beneath Nantucket Sound than previously mapped. Locally, these rocks may extend northward beneath the southern coast of Cape Cod. On the seismic profiles, a prominent, nearly continuous subbottom reflector representing the top of the Coastal Plain deposits delineates numerous northeast-trending, deeply cut valleys with 60 to 110 m relief. Thalweg depths are as much as 150 m below sea level; and the broad, flat-topped interfluves lie about 40 m below sea level. Isolated erosional outliers are present in the north-central part of the sound. All major buried valleys are continuous across the sound, may be locally floored by bedrock in their inner reaches, and are filled with well-stratified glacial drift thought to be mostly of the late Wisconsinan Age. According to O'Hara, the nearshore positions of the valleys correlate remarkably well with large reentrants, estuaries, and salt ponds of the adjacent coastlines. Although many boreholes have been drilled on Cape Cod, all have failed to encounter Coastal Plain strata. The seismic-profiling data indicate that most boreholes were too shallow (less than 30 m below sea level) to penetrate Coastal Plain strata, and the few deeper borings (some to bedrock) were either located over preglacial valleys, between erosional remnants, or north of the cuesta.

Potomac River sediments

Analyses of seismic-reflection profiles, sediment cores, grab samples, and side-scan sonar records by H. J. Knebel permit better definition of the characteristics, distribution, and geologic history of the shallow deposits beneath the Potomac River Estuary. The lowermost strata are sediments of the Chesapeake Group (lower Miocene to lower Pleistocene) that crop out at the shore but are buried as much as 40 m below the floor of the estuary. The top of these sediments is an erosional unconformity that outlines the Wisconsinan valley of the Potomac River. This valley has a sinuous trend, a flat bottom, a relief of 15 to 34 m, and axial depths of 34 to 54 m below sea level. During the Holocene transgression of sea level, the ancestral valley was filled with as much as 40 m of sandy and silty, fluvial-to-shallow estuarine sediments. The fill became the substrate for oyster bars in the upper reaches and now forms most marginal slopes of the estuary. Since sea level approached its present position (2,000–3,000 yr ago), the main channel has become the focus of deposition for watery gray-to-black clay and silty clay, and waves and currents have eroded the heterogeneous Quaternary sediments along the margins, leaving winnowed brown sand on shallow shoreline flats.

Laguna Madre sediments

G. L. Shideler and D. E. Owen obtained nearly continuous cores at six sites distributed through the region of southern Corpus Christi Bay, southern Mustang Island, northern Laguna Madre, and the adjacent mainland. Coring reached depths of 60 m at most sites and provided an average 74 percent recovery for a total 247 m of cores composed of unconsolidated to poorly consolidated sediments. Preliminary determinations suggest an age of late late Pleistocene to Holocene for the penetrated stratigraphic section. Lithologically, alternating sand and mud layers predominate. The sands range from very fine grained to coarse grained and appear to represent at least two distinct facies. The mud layers are multicolored and consolidated to varying degrees. Biogenic gravel beds composed mainly of mollusk shells are present in minor quantities. The section also has a few zones of abundant calcareous nodules and disseminated carbonaceous matter. Tentatively, Shideler and Owen interpreted the cored stratigraphic section to represent a wide variety of late Quaternary paralic environments.

West coast sediments

In continuing studies of San Francisco Bay and its subdivisions, B. F. Atwater concluded that tidal marshes of eastern Suisun Bay underwent a shift from freshwater to brackish-water vegetation about 1,000 to 2,000 yr B. P. The most recent age for this shift is 540 ± 120 yr B.P., a radiocarbon date on rhizomes of *Distichlis spicata* 20 to 25 cm below the surface of a brackish-water marsh at Browns Island; and the maximum age is about 2,000 B. P., based on a date for an older subsurface peat that lacks *D. spicata* rhizomes and instead is dominated by rhizomes of the freshwater *Phragmites australis* and *Scirpus acutus*. In contrast, tidal marshes in central Suisun Bay are underlain by *D. spicata* peat that spans the past $4,150 \pm 100$ yr. Atwater also reported that levee breaks on the Sacramento–San Joaquin delta may be attributed to various error. Chief among natural causes are (1) natural causes in combination with one another and with human negligence or weaknesses of peat and mud beneath the levees akin to the instability of bay muds; (2) rapid (5–8 cm/yr) subsidence of land underlain by peat behind the levees, a process which historically has affected at least half of the delta and continues today; (3) erosion by wind waves, for which modern remedies aid in preserving important habitats of wintering birds and rare plants but sacrifice riparian scenery and other wildlife; and (4) high water in channels, which generally exploits preexisting weaknesses rather than causing levee failure through overtopping.

Wood collected by Larry Phillips at a depth of 10 m from indurated estuarine channel sands within Morro Bay, Calif., had a radiometric carbon-14 date of $27,310 \pm 570$ yr. This date permits identification of the associated estuarine deposits with a late Pleistocene high stand of sea level at 27,000 yr and allows the sediment fill within Morro Bay to be divided into three recognizable stratigraphic sequences that include (1) basal estuarine tidal channel–accretionary bank deposits and possible tidal flat deposits associated with the high stand of sea level the top of which is at a depth of 5.7 m below present sea level and is overlain by (2) indurated and oxidized postglacial (pre-Flandrian) dune-sand deposits that extend up to 3.5 m below sea level, and (3) a thin veneer of Holocene sediment (modern tidal flat deposits and deeper tidal channel deposits). The identification and dating of the high-stand deposits at 27,000 yr also allows the determination of coastal uplift for this region. If compared to published sea-level curves (LaJoie and others, 1979), this coastal region has undergone approximately 38 m of uplift in the last 27,000 yr.

The mid-estuary intertidal flats of Willapa Bay, Wash., are texturally similar to the outer flats near the bay inlet and structurally similar to the inner flats near the rivers. Compostionally, they are transitional between the outer and inner flats, reflecting a mixture of mud supplied by the rivers and components derived

from main sand sources at the bay mouth. Distribution patterns of textural parameters show consistent trends of sediment fining upslope and upestuary, which reflects a response to decreasing hydraulic energy and increasing distance from the sand source at the bay inlet. Where sand occurs, bedforms range from large sand waves to small-scale ripples. Low sedimentation rates on the flats permit extensive biogenic reworking of the sediment, except where local conditions preclude faunal activity. Overall, therefore, bioturbate textured sediments are characteristic of midestuary intertidal deposits. The large subvertical, branching burrows of the ghost shrimp *Callianassa* are the most common preservable trace in sandy sediments. Large *Upogebia* borings are common in exposed, consolidated Pleistocene mud deposits that floor some parts of the intertidal flats.

The floor of Lake Superior

On the basis of bathymetry and underlying bedrock determined from an analysis of 8,000 km of high-resolution seismisc data, R. J. Wold divides Lake Superior into three morphologic regions. The western region is dominated by a more or less continuous bathymetric bedrock valley paralleling the north shore from Thunder Bay, Ontario, to Duluth, Minn. The valley reaches depths of more than 800 m below lake level and contains more than 500 m of unconsolidated sediments near Silver Bay, Minn. This valley probably resulted from differential glacial erosion, where the relatively erodible sandstone of the Bayfield Group is in contact with the underlying relatively resistant Keweenawan volcanic rocks and gabbro of the Duluth Complex. The central region, separated from the western region by a north-south basement ridge, consists of a broad valley with only 8 to 15 m of unconsolidated sediments overlying bedrock. The complex pattern of troughs and shoals of the eastern region forms a north-south dendritic pattern with valleys as much as 100 km long and only 5 to 10 km wide. The bedrock surface is more than 600 m below lake level in some places and is overlain by as much as 300 m of unconsolidated sediments. These eastern valleys probably formed by subglacial stream erosion. Most eastern bedrock valleys are truncated about 15 km from the south shore where the lake floor rises abruptly to the coastline; two valleys extend onshore. Wold concluded that the general morophology of the bedrock surface beneath Lake Superior reflects scour by glacial and subglacial streams with configurations and flow controlled by formation contacts, preexisting topography, and shear zones.

DEEP SEA FLOOR RESEARCH

Deep sea fans

In comparing the Monterey and Delgada fans, which have similar sizes, ages, and crustal settings off California, W. R. Normark found distinct differences in morphologic features that may be related to the grain-size distributions of sediment supplied to the fans. Long, broad, leveed valley systems without branching distributaries are the dominant features on the Delgada fan, where only mud has been recovered by coring. The apparently sandier Monterey fan exhibits a complex system of fan valleys and depositional lobes with distinct distributary channel systems. Analyses of cores from both fans indicate a clear relation between organic carbon contents and sedimentation rates. They also suggest that thick sediments of the upper fan regions preserve sufficient organic carbon to serve as sites for future generation and accumulation of hydrocarbons.

In studies of deep-sea cores, J. V. Gardner found pollen that can be correlated with that recovered from the Clear Lake, Calif., core, which serves as a standard for west coast pollen analyses. The marine sediment also includes planktonic foraminifera that can be analyzed for oxygen isotopes. The oxygen-isotope profile will provide a chronostratigraphy with which to calibrate the Clear Lake record. The two records, once correlated to time, promise further insights to the coupling and decoupling of continental and marine responses to global climatic changes.

In related studies of the upper Neogene and Quaternary cores, Gardner noted a remarkable correspondence of carbonate cycle periodicities from about 3.5 to 7.0 m.y. for carbonate stratigraphies of the Caribbean and eastern equatorial Pacific. The interval from 0 to about 3.5 m.y., however, shows a divergence of periodicities between the Caribbean and Pacific. The timing of the divergence is tied to the emergence of the Isthmus of Panama, which blocked circulation to the west and isolated the Caribbean into a marginal sea. The Pacific record has periodicities of carbonate cycles that range between 60 and 80 thousand years with a predominate periodicity of 60 thousand years. The Caribbean periodicities range between 40 and 60 thousand years. The Pacific record is thought to be the oceanic response to global climatic change, whereas the Caribbean record is oceanic for the interval 3.5 to 7.0+ m.y. but acquired a terrigenous influence following emergence of the Isthmus of Panama when the Magdalena River became the major single input.

Deep sea sediments

Beds of black shale rich in organic matter are common in strata of middle Cretaceous age beneath many parts of the world ocean but particularly the Atlantic Ocean. This observation has led some scientists to speculate that the Atlantic Ocean, and perhaps much of the world ocean, contained stagnant anoxic bottom waters at that time. However, the beds of black shale usually are intercalated with lithologies that are highly bioturbated and poor in organic matter. In a paper presented at the International Geological Congress in Paris, W. E. Dean and J. V. Gardner suggested that the intercalated color variations, characteristic of the so-called black shale sequences of middle Cretaceous age in the Atlantic, are diagenetic in response to variations in rate of influx of organic matter. This hypothesis received further support from cores recovered from the Angola Basin in August 1980, during Leg 75 of the Deep Sea Drilling Project. These cores contain 260 beds of middle Cretaceous black shale, containing as much as 16 percent organic carbon interbedded with red and green claystone or shale. Dean and other shipboard sedimentologists and geochemists attributed the green color of the claystone beds to reduction of iron in predominatly red claystones that are bounded by black beds rich in organic matter. Decreased circulation of bottom waters containing lower concentrations of dissolved oxygen would aid in the formation of reduced sediments, but the primary cause of reduction was oxidation of organic matter, which varied in amount over intervals of hundreds or even thousands of years.

Another aspect of the deposition of organic matter investigated during Leg 75 in the South Atlantic was the development of the Benguela Current upwelling system off southwest Africa. This system supports one of the most organically productive areas of the world ocean, and sediments presently accumulating under the upwelling waters are even richer in organic matter than those deposited during the middle Cretaceous. Continuous, undisturbed cores collected from the Angola basin and adjacent Walvis Ridge using a newly developed hydraulic piston corer show that the Benguela Current upwelling system has existed for about 6 m.y. but was most intense between 1 and 2 m.y. age.

Deep sea manganese

Petrographic and microanalytical studies by R. A. Koski and J. S. Rubin showed that samples dredged from ferromanganese oxide deposits on seamounts in the Gulf of Alaska include both amorphous and crystalline components. Crusts that are 1 to 11 cm in thickness and composed of black amorphous oxide and poorly crystallized MnO_2 coat the surface of alkalibasalt pillows and volcanic breccia. These crusts are characterized by a simple internal stratification caused by isotropic oxide microlaminations of alternating colloform and columnar aggregates. The amorphous crusts have Mn/Fe ratios of 1.5 to 2.5 and relatively high Ni (0.26–0.65 percent), Co (0.23–0.66 percent), and Cu (0.03–0.12 percent). Thin (1–10 mm) crusts, veinlets, and nodular infillings associated with friable tuffaceous sediment consist largely of well-crystallized todorokite and cryptomelane; MnO_2 is a minor constituent. Crystalline oxides occur as broad colloform bands of variably anisotropic radiating fibers, and massive zones of very coarse-grained (>1 mm) strongly anisotropic todorokite or cryptomelane crystals. Crystalline ferromanganese oxide deposits have higher manganese/iron ratios, higher nickel, and lower cobalt. The amorphous and crystalline ferromanganese oxide deposits are thought to result from authigenic and diagenetic processes, respectively.

D. Z. Piper analyzed the sediment and associated manganese nodules of 71 box cores from a small area in the equatorial North Pacific (DOMES Site A). The bathymetry of this area is characterized by a broad east-west-trending valley defined by strongly dissected highlands to the north and south. Sediment from the bounding highlands and from the northern margin of the valley is Quaternary, and the associated nodules tend to be small and poly-nucleated, and all have smooth surface textures. By contrast, cores along the southern margin of the valley contain lower Tertiary sediment and the nodules have a granular surface texture and usually are large and discoidal in shape. Cores from the central part of the valley share properties with each of these environments. The sediment is Quaternary, but the nodules are relatively large and granular. The distribution of sediment and nodules is interpreted to be controlled primarily by the flow of Antarctic bottom water through the valley from west to east.

Preliminary analyses of the chemical compositions of the sediment and nodules provided similar metal ratios (for example, copper:manganese and nickel:manganese) for the sediment and the smooth-textured nodules. The granular nodules from the valley floor, however, are relatively enriched in nickel and copper.

Deep sea alteration

J. L. Bischoff reacted graywacke with seawater and with a saturated NaCl brine containing calcium, magnesium, and potassium, using a solid-liquid ratio of 1 to 10. The degree of reaction was minimal at 200°C but significant at 350°C. In both fluids, anorthite, dolomite, and some illite and quartz, amounting to about 25 percent of the graywacke, were converted to smectite-

chlorite and albite. Both fluids lost all their Mg and gained K, Ca, and CO_2. Only the brine gained and maintained significant concentrations of heavy metals, indicating the importance of chloride complexing. Chloride concentration in seawater is apparently insufficient for extensive complexing under the experimental conditions.

Chloride complexing, however, only serves to maintain metals in solution and to prevent their reprecipitation as alteration products. Alteration involving production and consumption of hydrogen ion is the most common metasomatic process involving the release of metals from the source matrix. In Bischoff's experiments, magnesium metasomatism and dedolomitization provided the H+ for the process. Metal solubilization by the brine followed the order of abundance in the graywacke: Zn>Ni>Cu>Pb>Sb>Cd, suggesting a common matrix and no selective leaching effect. In other words, as a given increment of rock was altered, all of its component metals were released. Therefore, metal concentration in solution represents minimum values.

Changes in the bulk composition of the graywacke were minimal, except for increases in magnesium content, and the final rock would probably not be recognized as an altered source rock in the field. The fluids generated during the experiments probably would subject wall rock at the site of ore deposition to hydrolytic alteration, including potassium-metasomatism.

ESTUARINE AND COASTAL HYDROLOGY

GULF COAST

Appearance and water quality of turbidity plumes in Tampa Bay, Florida

C. R. Goodwin reported that, with one obvious exception, the quality of water collected from turbidity plumes created by dredging in Tampa Bay, Fla. in 1977 and 1978 was the same as the quality of ambient water surrounding the plumes. The exception was water clarity as measured by turbidity, suspended solids, and transparency. Of many types of plumes studied, the most visible were created by open water, pipe-line disposal of material having low clay and silt content during times of maximum tidal flows near the mouth of Tampa Bay. The least visible plumes were created by diked pipeline disposal of material having high clay and silt content in areas of low tidal flows with turbidity barrier containment.

No differences were detected in seasonal turbidity levels between dredging and non-dredging periods in the vicinity of open-water-disposal operations at the mouth of Tampa Bay. Near the head of the bay, seasonal high turbidity levels were unaffected by dredging. Seasonal low turbidity levels, however, were greater during dredging periods by about two nephelometric turbidity units. It is not known whether this difference is environmentally significant.

Hydrology of the Atchafalaya Bay, Louisiana

A rapid building of new delta in the Atchafalaya Bay, an arm of the Gulf of Mexico is taking place, according to G. J. Arcement. The Atchafalaya River receives water diverted from the Mississippi River, resulting in an increased sediment load in the Atchafalaya River basin. As a result of the added sediment load, approximately 100 km^2 of new land has developed in the bay since 1973.

Monthly discharge measurements were made and suspended-sediment samples were collected at eight major distributary channels in Atchafalaya Bay during the 1980 water year. Measured inflows into the bay ranged from a discharge of 2,950 m^3/s with a suspended-sediment load of 29,800 Mg/d to discharge of 5,980 m^3/s with a suspended-sediment load of 103,000 Mg/d

The rapid building of new delta in the Atchafalaya Bay is unique and provides an excellent opportunity to document its development.

Saltwater movement in the Mississippi River

C. R. Demas reported that data collected during the 1980 water year from the Mississippi River and a distributary, Bayou Baptiste Collette, indicate that saltwater does not move up the distributary from Breton Sound into the Mississippi River. Instead, saltwater moves up Southwest Pass from the Gulf of Mexico, then up the Mississippi River and back down Bayou Baptiste Collette.

Quarterly samples of benthic invertebrate collected from Bayou Baptiste Collette and the Mississippi River at Venice revealed the presence of the ephemerid type mayfly *Tortopus*. This species was not present at these sites during 1975–76 samplings, indicating colonization from upriver.

Saltwater intrusion was monitored in the Mississippi River as far upriver as mile 62 during January 1981. The salt wedge remained near mile 62 for approximately two weeks. The last time the salt wedge moved this far upriver was during 1976.

Loxahatchee River Estuary assessment, Florida

B. F. McPherson defined the bathymetric and benthic characteristics of the Loxahatchee River esturary using low altitude aerial photography and ground-truth surveys. Bottom sediments were characterized by

particle-size analyses and organic content, and the distribution and standing crop of sea grass communities were delineated and measured.

Seasonal and tidal changes in water quality, water level, and discharge were measured in the estuary. Data from tidal fluctuations, water velocity, and discharge were used to develop a two-dimensional model of water circulation. Loading of suspended sediment and nutrients from major tributaries was estimated. Concentrations of inorganic nitrogen were used to trace sewage effluent from a treatment pond down the northwest fork tributary to the estuary. Loads of total nitrogen (0.056 Mg/d) and phosphorus (0.029 Mg/d) discharged from the sewage treatment pond were about 6 and 45 times greater than background loads, respectively. Relative input of these nutrients from the pond to the estuary was small, however, because of other large tributary discharges.

ATLANTIC COAST

Potamac River Estuary sedimentation and eutrophication

Nutrient, trace-metal, lead ^{210}, and pollen analyses of 1-m-long cores showed the historical development of sedimentation and eutrophication problems in the Potomac Estuary, and results from an acoustic survey revealed the prehistorical development. Nutrient and trace-metal concentrations decreased with distance seaward from municipal and river sources in the Washington, D. C. area, and with depth in cores. Accumulation rates, computed by E. A. Martin and G. S. Brush from lead ^{210} and pollen analyses, also varied spatially, being rapid in the tidal river, slow in the lower estuary and variable in the transition zone. Acoustic data, analyzed by H. A. Knebel, showed that a silt and clay unit from < 2 to > 6 m in thickness forms the surface deposit in most channels. This unit probably began to accumulate 2,000 to 3,000 years ago and is presently accumulating in the estuary proper at a rate of about 1.5×10^6 Mg per year.

MANAGEMENT OF NATURAL RESOURCES ON FEDERAL AND INDIAN LANDS

The Conservation Division is responsible for carrying out the role of the USGS in classifying leasable mineral and potential water-resources development sites on Federal lands and managing the exploration and development of leasable minerals on Federal and Indian lands, including the Outer Continental Shelf. Primary functions are (1) classification and evaluation of Federal mineral lands for multiple-use management and for leasing, (2) delineation and preservation of potential public-land reservoir and waterpower sites, (3) promotion of orderly exploratory development, conservation, and proper use of mineral resources on Federal lands under lease, (4) supervision of mineral operations to assure protection of the environment, the realization of a fair value from the sale of leases, and satisfactory royalty collection on mineral production, and (5) cooperation with other agencies in the management of Federal mineral and water resources.

CLASSIFICATION AND EVAULATION OF MINERAL LANDS

The organic act creating the USGS gave the Director the responsibility of classifying and evaluating the mineral resources of public-domain lands. There are about 9 million ha of land for which estimates of the magnitude of leasable mineral occurrences only partially have been made. Such appraisals are needed for multiple-use planning by Federal land managers and for leasing by the BLM. Estimates are based on existing data. When additional data are required, field studies and spot checks must be undertaken. Guidelines are prepared from time to time by the USGS to assure uniform executive action in the classification of leasable minerals on Federal lands.

CLASSIFIED LAND

With the passage of the Federal Land Policy and Management Act of 1976, numerous changes occurred in the classification program. For example, classification for retention of mineral rights is no longer appropriate. Also, fair market value is required for exchanges and conveyances of mineral rights. Classification to prevent improvident disposal of Federal mineral rights was a major responsibility under the former classification mission, but was not the only requirement. The Federal lands also were classified as to mineral character to delimit potential leasable mineral resources, conserve natural resources, provide data on Federal lands for multiple-use management, and inventory the resource potential for leasable minerals on Federal lands.

The following classification responsibilities still remain: (1) to identify competitive leasing areas for leasable minerals, (2) to inventory leasable mineral resources, (3) to furnish the Federal land-managing agencies with adequate leasable mineral data on Federal lands for land-use planning and multiple-use or best-use decisions, and (4) to furnish Congress and other Federal agencies leasable mineral data on the Federal lands being considered for withdrawal by Congressional or executive action.

As a result of USGS investigations, large areas of Federal land have been formally classified as mineral land. At the end of calendar year 1980, more than 9 million ha of land had been formally classified, and about 949 million ha had been designated prospectively valuable for a leasable mineral, as shown in the following table:

Lands classified

Commodity	During calendar year 1980		Total at end of calendar year 1980	
	Formally classified (hectares)	Prospectively valuable (hectares)	Formally classified (hectares)	Prospectively valuable (hectares)
Asphaltic minerals	0	416,602	0	7,679,368
Coal	324,304	0	9,099,322	142,040,102
Geothermal resources	0	4,662	0	41,866,764
Oil and gas	0	0	1,714	595,321,498
Oil shale	0	0	0	5,820,728
Phosphate	6,426	0	222,862	12,403,324
Potassium	0	2,331	0	35,678,741
Sodium	0	0	254,536	108,303,594

KNOWN GEOLOGIC STRUCTURES OF PRODUCING OIL AND GAS FIELDS

Under the provisions of the Mineral Leasing Act of 1920, as amended, the Secretary of the Interior is authorized to grant to any qualified applicant a noncompetitive lease to prospect for oil and gas unless the Federal mineral estate is within a Known Geologic Structure (KGS) of a producing oil and gas field. Lands within a KGS must be competitively leased to the highest qualified bidder. During calender year 1980, 706,792 ha of onshore Federal land were classified as

KGS lands, either as a new KGS or as additions to a previously established KGS. The total acreage in KGS's at the end of 1980 was over 8,902,901 ha. The KGS's are summarized in the following table:

Known Geologic Structures (in acres) for calendar year 1980

	End of CY '79	Added in CY '80	End of CY '80
Alabama	38,494	5,680	44,174
Alaska	146,064	0	146,064
Arizona	7,677	0	7,677
Arkansas	328,575	9,600	338,175
California	465,934	1,840	467,774
Colorado	1,195,565	1,080	1,196,645
Florida	160	0	160
Illinois	533	0	533
Indiana	320	5,140	5,460
Kansas	3,329,942	440	3,330,382
Kentucky	15,385	602	15,987
Louisiana	816,793	16,089	832,882
Maryland	2,328	3,200	5,528
Michigan	72,290	80	72,370
Mississippi	95,284	2,135	97,419
Montana	1,357,797	306,202	1,663,999
Nebraska	26,677	920	27,597
Nevada	5,440	0	5,440
New Mexico	4,657,361	159,028	4,816,389
North Dakota	287,584	115,271	402,855
Ohio	244,940	1,400	246,340
Oklahoma	3,859,237	265,054	4,124,291
Pennsylvania	6,708	0	6,708
South Dakota	12,919	11,789	24,708
Texas	146,426	32,612	179,038
Utah	750,391	618,625	1,369,016
Virginia	718	0	718
West Virginia	83,063	0	83,063
Wyoming	2,308,381	199,296	2,507,677
Totals	13,747,642	1,710,197	15,457,839

KNOWN GEOTHERMAL RESOURCE AREAS

The Geothermal Steam Act of 1970 provides for development by private industry of federally owned geothermal resources through competitive and noncompetitive leasing. Those areas that are determined to be within Known Geothermal Resource Areas (KGRA) must be leased competitively. On December 31, 1980, there were 107 KGRA's that contained 3,366,648 acres.

The results of lease sales held in 1980 are summarized in the following table:

KGRA lease sales 1980

Sale date (Total Sales 6)	State	Tracts offered	Acres offered	Tracts leased	Acres leased	Total accepted high bids
12/10/80	California (Heber)	1	10.26	1	10.26	$ 45,176.11
4/22/80	Nevada	15	29,961.09	8	15,904.01	86,569.48
9/23/80	Nevada	13	27,025.07	2	4,515.19	32,934.60
1/8/80	Oregon	62	96,058.79	6	10,605.72	347,943.84
4/29/80	Oregon	64	99,416.96	12	19,664.03	963,182.10
10/23/80	Oregon	2	4,926.46	2	2,360.00	249,617.20
Total		157	257,398.63	31	53,059.21	$1,725,423.30

KNOWN RECOVERABLE COAL RESOURCE AREAS

The Federal Coal Leasing Amendments Act of 1976 provides for the development of federally owned coal lands by private industry through competitive leasing and authorizes the Secretary of the Interior to designate Known Recoverable Coal Resource Areas (KRCRA). During calendar year 1980, 324,304 ha of coal land were classified KRCRA's, bringing the total to 9,099,322 ha. Drilling programs in support of coal land classification during 1980 totaled 13,984 m for 125 holes completed, with an average depth of 111 m/hole.

KNOWN LEASING AREAS FOR POTASSIUM, PHOSPHATE, AND SODIUM

During calendar year 1980, known phosphate leasing areas were increased by 6,426 ha, for a total of 59,764 ha.

WATERPOWER CLASSIFICATION—PRESERVATION OF RESOURCE SITES

Suitable sites for water-resource development are valuable natural resources. The waterpower classification program is conducted to identify, evaluate, and protect from disposal and injurious uses those Federal lands located in sites having significant potential for future development. USGS engineers review maps, aerial photographs, and streamflow records to determine potential dam and reservoir sites. Topographic, engineering, and geologic studies are made of the identified sites to determine whether or not the potential value warrants formal classification of the affected Federal lands. These resource studies provide the land-administering agencies and others with information that is basic to management decisions and effective land-use planning. Previous classifications are reviewed as additional data become available and as funds permit. If the sites are no longer considered suitable for development, revocation of the classification of the affected Federal lands is recommended. If the lands are not reserved for other purposes, they are returned to the unencumbered public domain for possible disposition or other use. During calendar year 1980, about 175 ha of previously classified lands in Idaho were released, and reviews of classifications and other site studies were conducted in river basins in California and Oregon.

To assure consideration of potential reservoir and waterpower sites in the preparation of land-use plans, information concerning such sites was furnished to the BLM and the USFS for several plannng units in the Western States and Alaska.

MANAGEMENT OF MINERAL LEASES ON FEDERAL AND INDIAN LANDS

Supervision of competitive and noncompetitive leases for the development and recovery of leasable minerals in deposits on Federal and Indian lands is a function of the USGS, delegated by the Secretary of the Interior. It includes geologic and engineering examination of applied-for lands to determine whether or not a lease or a permit

is appropriately applicable, approval of operating plans, inspection of operations to insure compliance with regulations and approved methods, and verifications of production, and the collection of royalties (see table 1).

Before recommending approval of a lease or a permit, USGS engineers and geologists consider its possible effects on the environment. Of major concern are the esthetic value of scenic and historic sites, the preservation of fish and wildlife and their breeding areas, and the prevention of land erosion, flooding, air pollution, and the release of toxic chemicals and dangerous materials. Consideration also is given to the amount and kind of mining-land reclamation that will be required.

Onshore oil and gas lease sales

During calender year 1980, there were 23 competitive oil and gas lease sales on Federal lands that resulted in leasing 125,155 acres for the sum of $55,743,355, which equates to $44 per acre. This is a noteworthy increase over the previous years during which 13 sales of this type resulted in the leasing of 58,306 acres for $10,743,926, an average price of $184 per acre. This increase in sales activity reflects the positive efforts of the USGS and BLM to keep pace with industry's search for oil and gas.

The largest sale of onshore Federal lands in calender year 1980 was held in Tulsa, Okla., on December 16. At this sale, 62 parcels comprising 14,281 acres were sold for $15,190,477, an average price of $1,063 per acre.

The high points of Federal land lease sales during calendar year 1980 are summarized in the following table:

Onshore oil and gas lease sales during calendar year 1980

FEDERAL LANDS

Sale date	State	Number of tracts offered	Acres offered	Number of tracts leased	Acres sold	Total accepted high bids
01/08/80	Ala., Mich., Ohio, W. Va., Ark., La.	26	3,907	24	3,907	$ 262,689
01/16/80	Wyoming	39	7,737	39	7,737	2,463,337
01/19/80	Colorado	32	9,825	32	9,825	935,183
03/20/80	Mont. and S. Dak.	19	2,342	19	2,342	252,738
04/02/80	Wyo. and Kans.	22	6,109	22	6,109	525,596
04/15/80	New Mexico	38	8,671	37	8,500	4,541,275
05/20/80	Oklahoma	26	6,335	23	5,058	3,095,262
05/21/80	Mont. and N. Dak.	25	5,727	24	5,687	1,073,895
06/04/80	Wyoming	37	7,725	34	7,165	1,106,216
06/24/80	Texas	18	4,007	18	4,007	1,316,801
06/25/80	Montana	5	440	5	440	49,376
07/17/80	Miss. and Ohio	5	429	5	429	11,264
07/23/80	N. Mex. and Texas	22	7,487	22	7,487	2,033,116
08/06/80	Wyoming	31	7,255	31	7,255	2,122,234
08/20/80	Montana	22	4,395	21	4,315	344,673
09/05/80	Miss. and Ky.	9	2,254	7	2,070	13,751,377
09/09/80	Wyoming	25	5,131	25	5,131	858,532
09/16/80	Okla. and N. Mex.	30	8,533	28	7,998	2,955,242
11/05/80	Wyoming	25	8,106	25	8,106	1,396,063
11/19/80	Montana	12	1,157	12	1,157	142,416
11/26/80	Mich., Ark., and La.	8	626	8	626	886,924
12/10/80	Wyoming	36	5,523	36	5,523	428,669
12/16/80	N. Mex. and Okla.	63	14,363	62	14,281	15,190,477
	Total	575	128,084	559	125,155	55,743,355

There were 26 sales of oil and gas leases on Indian Land during calendar year 1980, about the same as the previous year. These sales resulted in the leasing of 374,663 acres for $38,888,623. The following table is a summary of Indian Land lease sales during calendar year 1980:

Onshore oil and gas lease sales during calendar year 1980

INDIAN LANDS

Sale date	State	Number of tracts offered	Acres offered	Number of tracts leased	Acres sold	Total accepted high bids
01/16/80	Oklahoma	60	5,508	42	3,779	$ 891,741
02/27/80	Montana	61	32,318	56	28,200	213,922
03/04/80	North Dakota	30	4,174	34	4,174	166,226
03/11/80	Oklahoma	108	6,856	65	4,479	407,346
03/13/80	Oklahoma	103	4,964	55	2,573	167,109
03/18/80	Oklahoma	114	7,340	55	3,547	203,295
03/18/80	Oklahoma	100	8,263	65	4,974	1,697,176
03/25/80	Oklahoma	100	6,849	66	4,519	248,844
05/28/80	Oklahoma	297	27,460	110	9,871	1,783,106
07/02/80	Oklahoma	39	3,620	21	1,967	953,406
07/08/80	Oklahoma	88	4,419	40	3,379	240,292
07/08/80	Montana	537	97,720	211	49,028	3,606,570
07/22/80	Oklahoma	23	1,773	23	446	99,978
07/23/80	New Mexico	12	1,842	5	721	639,408
07/29/80	North Dakota	137	11,951	49	4,679	80,881
08/14/80	Oklahoma	81	4,476	50	4,476	126,530
09/04/80	North Dakota	33	3,764	20	2,540	306,689
09/09/80	Montana	549	111,229	512	105,636	6,836,037
09/18/80	Oklahoma	451	818,964	148	8,663	690,796
09/30/80	Oklahoma	44	4,175	17	1,926	74,951
10/14/80	Oklahoma	76	3,470	24	1,109	143,015
10/14/80	Oklahoma	274	23,513	94	7,792	3,173,768
10/21/80	Wyoming	138	76,075	90	47,361	3,759,677
10/29/80	Oklahoma	31	2,656	14	1,093	486,150
12/02/80	Oklahoma	12	1,374	9	921	188,889
12/16/80	Montana	397	72,294	364	66,810	11,702,821
	Total	3,895	1,347,047	2,239	374,663	38,888,623

MANAGEMENT OF OIL AND GAS LEASES ON THE OUTER CONTINENTAL SHELF

The Outer Continental Shelf (OCS) Lands Act of 1953 authorizes the Secretary of the Interior to issue oil and gas leases on a competitive basis in the submerged lands of the OCS. The functions of the USGS, delegated by the Secretary of the Interior, include (1) participation in tract selection and evaluation to insure orderly resource development, protection of the marine environment, and receipt of a fair market value, (2) review and approval or disapproval of proposed exploration plans and development and production plans, (3) inspection of operations to insure compliance with regulations and approved methods, and (4) verification of the amount and value of production and the assessment and collection of rentals and royalties.

The Outer Continental Shelf Lands Act Amendments of 1978 provided the Secretary of the Interior with policy guidance for administration of the leasing provisions of the amended Act and provided an additional enforcement tool in the form of civil penalties. The USGS administers the civil penalties that are assessable for any failure to comply with any provisions of the Act, any

TABLE 1.—*Mineral production, value, and royalty for calendar year 1980*

[All minerals except petroleum products; includes coal, potassium, and sodium minerals, and so forth.]

Lands	Oil (tonnes)	Gas (cubic meters)	Gas liquids (liters)	Other (tonnes)	Value (dollars)	Royalty (dollars)
Public	19,492,610	28,133,095,165	852,341,675	73,672,936	6,271,884,023	662,743,497
Acquired	962,467	674,395,545	14,393,715	756,951	466,551,187	38,683,876
Indian	3,012,574	3,266,378,532	180,545,507	27,594,114	1,002,185,112	119,201,383
Military	51,675	384,818,532	36,328,309	----	22,984,763	3,761,044
Outer Continental Shelf	37,998,490	131,446,061,759	----	----	13,055,515,832	2,136,663,425
Total	61,517,816	163,904,749,533	1,083,609,206	102,024,001	20,819,120,917	2,961,053,225

term of a lease, license, or permit issued under the Act, or any regulation or order under the Act. USGS review and approval of proposed exploration plans and development and production plans also must assure compliance with the new statutory requirement to use the best available and safest technologies on all new drilling and production activities.

Outer Continental Shelf lease sales for oil and gas

Three OCS oil and gas lease sales were held in calendar year 1980. Sales were held for leases in the Gulf of Mexico in September and December, respectively, and in the Gulf of Alaska in October. A summary of the results of these individual lease sales is presented in table 2. For these sales 483 tracts totaling 2.6 million acres were offered for lease. High bids of $3.98 billion were accepted on 218 tracts totaling 1.13 million acres. For the entire Federal OCS, through calendar year 1980, 9,358 tracts totaling 42.8 million acres were offered for lease. High bids of $30.78 billion were accepted on 3,980 tracks totaling 19.1 million acres.

COOPERATION WITH OTHER FEDERAL AGENCIES

The USGS acts as a consultant to other Federal agencies in land-disposal cases. In response to their requests, the USGS determines the mineral character and water-resource development potential of scientific tracts of Federal land under their supervision that are proposed for sale, exchange, or other disposal. About 900 such reports were made during fiscal year 1981.

TABLE 2.—*OCS oil and gas lease sales for calendar year 1980*

[FNPS = Fixed Net Profit Share]

Sale number	Area and date	Tracts offered	Acreage	Tracts leased	Acreage	Total bonus accepted
A62	Central					
	Gulf of Mexico 9/30/80					
	Total	192	909,575	116	551,643	$2,676,927,673
	1/6 Royalty	71	325,804	51	224,408	1,397,437,045
	1/3 Royalty	22	83,946	14	47,872	200,080,628
	Sliding Scale	59	286,721	28	135,243	831,350,900
	FNPS	40	213,103	23	124,120	248,059,100
55	Eastern					
	Gulf of Alaska 10/21/80					
	Total	210	1,195,569	35	199,262	$ 109,751,072
	1/6 Royalty	90	512,387	16	91,091	53,213,147
	Sliding Scale	32	182,182	3	17,080	579,000
	FNPS	88	501,100	16	91,091	55,958,925
62	Western					
	Gulf of Mexico 11/18/80					
	Total	81	458,308	67	383,323	$1,417,961,511
	1/6 Royalty	38	210,628	29	164,443	463,017,160
	1/3 Royalty	11	63,360	8	46,080	204,983,920
	Sliding Scale	10	57,600	10	57,600	533,326,280
	FNPS	22	126,720	20	115,200	216,634,151

GEOLOGIC AND HYDROLOGIC PRINCIPLES, PROCESSES, AND TECHNIQUES

GEOPHYSICS

ROCK MAGNETISM

Paleomagnetic correlations of Proterozoic rocks

D. P. Elston reported that the collection and study of magnetostratigraphic sections in Proterozoic strata in the Western United States is leading to both new and refined correlations among the sections and to correlations with Proterozoic rocks of Lake Superior. Isotopic ages, primarily uranium-lead in zircon and rubidium-strontium isochron ages, accord with the paleomagnetic correlations and provide temporal control. Some discordant isotopic ages, principally from sedimentary rocks, have been found. Correlations based on polar path and polarity zonation have indicated a refined polar wandering path for North America for the interval from 1,450 m.y. to 800 m.y. and a generalized polarity zonation that has potential for intercontinental correlations. The entire Belt Supergroup of Montana and northern Idaho appears to be older than approximately 1,300 m.y. The Missoula Group at the top correlates with the Swauger and Lawson Creek Formations of east-central Idaho, the Pioneer Shale of the Apache Group of central Arizona, and the Sibley Series of Ontario, which is 1,340 m.y. old. Deposition of the Unkar Group of the Grand Canyon Supergroup began between about 1,250 m.y. and 1,200 m.y. ago. Strata of the Unkar Group correlate with sedimentary and volcanic rocks and intrusions of the lower, middle, and upper Keweenawan of Lake Superior, deposited in the interval from 1,200 m.y. to 1,100 m.y. ago. Distinctive characteristics of the paleomagnetic pole path and polarity zonation are helping to identify temporal correlations between the Unkar Group and the Keweenawan Supergroup. Sedimentary strata, lava flows, and intrusions of the Apache Group of central Arizona, above the basal Pioneer Shale, correlate with rocks of early and middle Keweenawan age. The Chuar Group of the Grand Canyon Supergroup was deposited in the interval from approximately 1,000 m.y. to 800 m.y. ago. Paleomagnetic poles and polarities from the Uinta Mountain Goup and the closely adjacent Big Cottonwood Formation of Utah show them to be temporally correlative with the Chuar Group.

Paleomagnetism in northern Alaska

Paleomagnetic determinations from Upper Devonian and Mississippian sedimentary rocks indicate that a large part of the Brooks Range in northern Alaska was remagnetized after major thrusting and folding occurred. J. W. Hillhouse and C. S. Grommé found that the remagnetized zone extends at least 450 km along the northern range front. After partial demagnetization, sandstones interbedded within the Kanayut Conglomerate retain only a magnetic overprint that corresponds to a paleomagnetic pole at 59° N., 197° E., with a 12° uncertainty. Similar overprints were determined from several sites in the Lisburne Group. Rapid uplift and cooling of the northern range front concomitant with underthrusting of the North Slope terrane may account for the simultaneous remagnetization of this immense region. A middle Cretaceous age for the uplift is supported by reset potassium-argon ages in the southern Brooks Range, the history of sedimentation, and by the pole position obtained from the magnetic overprint. Hypotheses concerning counterclockwise rotation of Arctic Alaska cannot be tested in the area sampled because the original magnetic signatures of the Paleozoic rocks have been lost.

Westward extension of known Wrangellia terrane in Alaska

Paleomagnetic results have been obtained from Triassic basalt in the Clearwater Mountains, south-central Alaska, by J. W. Hillhouse and C. S. Grommé. The basalt, identified as part of the Amphitheater Group as used by Smith and Turner (1973), is considered equivalent to the Nikolai Greenstone of the McCarthy quadrangle. The sampling locality in the Clearwater Mountains, 250 km northwest of McCarthy, expands the paleomagnetic investigation of Wrangellia, and new results provide additional evidence supporting large-scale northward drift of Wrangellia. The overall mean magnetic direction that was obtained from seven stably magnetized basalt flows is inclination 32.4° upward, declination 138.4° eastward. The corresponding paleolatitude of 18° N. or 18° S., depending on choice of polarity, is compatible with the anomalously low paleolatitude (15° north or south) of the Nikolai Greenstone determined at McCarthy. The paleomagnetically determined latitude of northern

Wrangellia is at least 25° south (2,700 km) of the Late Triassic latitude (43° N.) predicted for south-central Alaska from plate tectonic reconstructions. If Wrangellia originated in the southern hemisphere, then its northward drift may be as great as 61° (6,800 km).

Paleomagnetic secular variation recorded in volcanic rocks of Long Valley caldera, California

Geologic mapping and radiometric dating showed a periodicity of volcanic eruptions within the late Pleistocene Long Valley caldera in eastern California. Paleomagnetic studies showed that even within each active period, eruptions were not randomly spaced in time but tended to occur in discrete episodes of multiple eruptions. Analysis of paleomagnetic directions by E. A. Mankinen and C. S. Grommé shows that the mean paleomagnetic pole for the volcanic units sampled is indistinguishable from the Earth's rotational axis. This finding contrasts with many other studies, which often yield a pole that is slightly displaced along a line of longitude approximately opposite to the mean site longitude (the "farside" effect). Therefore, in spite of the nonrandom volcanic eruptions, the effects of secular variation of the Earth's nondipole field apparently have been completely averaged in this data set. On the basis of 33 distinct volcanic units, the total dispersion of the ancient geomagnetic field expressed as virtual poles was found to be 16.0°. This value is almost identical to the value found for the Western United States over the past 5 m.y., compiled by previous workers. This agreement suggests that the low paleosecular variation recorded by lava flows of Holocene age may be a fairly recent and unusual feature of the geomagnetic field.

Paleomagnetic evidence for tectonic rotation of the Clarno Formation, Oregon

Andesitic volcanic rocks of the Eocene Clarno Formation cover a widespread area in north-central Oregon; these rocks are the oldest formation of Tertiary age in the area. A paleomagnetic investigation of these lava flows was completed by C. S. Grommé and R. E. Wells, working with M. E. Beck, Jr. (Western Washington University), and D. C. Engebretson (Stanford University). The mean paleomagnetic direction measured in 46 of the lavas has declination 5.5° E. and inclination 64.4° downward, with a 95 percent confidence limit of 5.5°. The inclination is exactly what would be expected for Eocene time at that locality, but the declination is 17.6° east of the expected value, with a cumulative uncertainty of 12.8°. Clockwise deflections of paleomagnetic directions have been reported by many workers for Mesozoic and Tertiary rocks of the Pacific Northwest, and these anomalies now commonly are interpreted as representing tectonic rotations resulting from convergent interactions between the Kula or Farallone and North American lithospheric plates. Rocks near the Pacific Coast showed large clockwise rotations, and middle Tertiary rocks of the Western Cascades also appear to have been rotated, but only about the same amount as the Clarno Formation. Very large rotations have been demonstrated in Mesozoic rocks of eastern Oregon. The new result from the Clarno Formation investigation extends the domain of Tertiary rotations eastward to the longitude of east-central Oregon. East of the Cascade axis, paleomagnetic data from the Columbia River Basalt Group show no rotations, which indicates that this style of tectonic deformation had ceased to occur by middle Miocene time.

Northward movement of the Salinian block, California, indicated by paleomagnetic data

D. E. Champion, C. S. Grommé, and D. G. Howell found that sedimentary rocks from the Campanian and Maestrichtian Pigeon Point Formation possess consistent directions of remanent magnetization. These strata are a submarine fan sequence that occur on the coast of central California west of the San Gregorio fault. Most of the sampled beds indicate mass flow, particularly turbidite depositional processes. Bioturbated and slump-folded units were sampled to test whether the depositional processes caused any systematic errors in the paleomagnetic inclinations. Because the remanent magnetization measured in these different bed forms is coherent everywhere, there appears to be no systematic error, and the magnetization must have been acquired shortly after deposition. Magnetic coercivity of the coarsest layers of the turbidite deposits is lower than that of finer grained layers, and the finer grained layers yield a more precise paleomagnetic record. Simple corrections for the tectonic deformation of the strata leave magnetic directions somewhat scattered in declination due to local tectonic rotations around vertical axes that occurred during Tertiary and Quaternary time. Both normally and reversely polarized sites yield inclination values closely grouped near 40°, clearly different from the expected mean inclination value of 66° at the collecting site for Cretaceous time. Declination values suggest a general rotation of the entire stratigraphic section of approximately 45° in a clockwise sense. The observed shallow inclination implies a 20° to 25° N. latitude of deposition in Cretaceous time, near the present latitude of the Mid-Americas Trench. The conclusion is that the area of the Pigeon Point Formation, and presumably the rest of the Salinian block, has drifted northward as much as 2,500 km since Late Cretaceous time (70 m.y. ago). Neogene right slip between the Pacific and North American plates along the San Andreas fault system can account for no more than 1,000 km of this displacement.

GEOMAGNETISM

Geomagnetic observatories

Under the general direction of J. D. Wood, magnetic observatories at Barrow, College, and Sitka, Alaska, Boulder, Colo., Fredericksburg, Va., Fresno, Calif., and Tucson, Ariz., continue to record the strength and direction of the Earth's magnetic field. Other magnetic observatories at Newport, Wash., San Juan, Puerto Rico, and Guam are operated by the Office of Earthquake Studies, whereas the observatory at Honolulu continues to operate under NOAA. The data are collected, processed, and deposited in the World Data Center A, Boulder, Colo., for worldwide distribution. The data are used in studies of mineral exploration, space physics, solar-terrestrial relations, navigation, surveying, telecommunications, magnetic charting, secular variations, and in development of a better understanding of the processes that occur in the interior of the Earth.

Geomagnetic instrumentation

Acceptance tests were completed by R. W. Kuberry and L. R. Wilson on the production design for 16 microprocessor-based controllers for the newly automated magnetic observatory systems. These devices convert magnetometer outputs into a digital format for on-site recording as well as telemeter the data via telephone lines or the SMS/GOES satellite. At present, magnetic data, operational parameters, and diagnostics from the Boulder Observatory are recorded, analyzed, tested, and modified by a dedicated minicomputer in Denver. The NSF has provided for a two-year extension of the operation of the ground magnetometer stations that comprise the network for the International Magnetospheric Study (IMS). The USGS will continue to provide maintenance and operational support. The quality and volume of data made available by these IMS stations have demonstrated their value as an important magnetospheric research tool.

Repeat magnetic surveys

The magnetic repeat survey work by J. D. Wood is a continuing project of field surveys to determine secular magnetic change patterns. The work is critical to USGS mapping and research studies, and the data acquired provide basic information for various government agencies. In 1980, 10 stations were occupied in Alaska, 4 in Florida, 18 in Alabama, Colorado, Georgia, Illinois, Michigan, Mississippi, North Dakota, South Dakota, Texas, Utah, and Wisconsin, and 5 in the Pacific Islands. All repeat survey data acquired by the USGS are deposited in the World Data Center A, Boulder, Colo. for distribution to the general scientific community. Magnetic induction anomaly surveys were made around the Fresno Magnetic Observatory, the Air Force Geophysics Laboratory near Tampa, Fla., and around the proposed south Texas observatory site. These surveys provide information on induced anomalous variations in the magnetic field, which must be accounted for in various research uses of the data.

Digital processing of geomagnetic data

Computer programs were written by L. R. Wilson to test and verify the reliablility of the automated fluxgate observatory data using a PDP 11/34 minicomputer. Other PDP 11/34 programs, which were written by Terrabit of Salt Lake City, Utah, are being used to transmit magnetic observatory data from the Boulder observatory to the processing center in Denver. These programs also are being used to test the operation of the new microprocessor-based observatory systems.

Magnetic signals from the Earth core

Magnetic signals reaching the surface of the Earth from an oscillating dipole source in the core of the Earth were calcuted by L. R. Alldredge. Oscillation periods from 25 to 250,000 yr were used, and two different mantle conductivity profiles were considered. The results showed that the signals were seen in only a restricted area above the source, so that, for periods of tens of years, very high spherical harmonics would be required to account for the secular variations caused by such sources. These effects are amplified as the mantle conductivity increases. Inadequate representation of short-period variations in spherical harmonic models may be the main cause of the rapid deteriorations of predictive models.

Magsat vector data

The thrust of the work over the past year has been to obtain and analyze the data from the Magsat vector magnetic survey. Much of the effort by J. C. Cain was spent in processing, validating, and inspecting these data. Initial samples of Magsat data were used to augment pre-Magsat results in order to investigate both the crustal magnetic components and the nature of the core-source variations.

Geomagnetic studies of quiet-time field changes

For a year of quiet solar-activity level, geomagnetic records from several American Hemisphere observatories (located between about 0° and 30° N. geomagnetic latitude) were used by W. H. Campbell to compare the annual and semiannual variations of the geomagnetic field associated with three separate

contributions: (1) the quiet-day midnight level, MDT; (2) the solar-quiet daily variation, Sq; and (3) the quiet-time lunar semidiurnal tidal variation, L (12). Four Fourier spectral constituents (24-, 12-, 8-, 6-h periods) of Sq were individually treated. All three orthogonal elements (H, D, and Z) were included in the study. The equatorial annual and semiannual midnight field level variations of the northward and vertical components at quiet periods seem to represent the expected seasonal nighttime magnetospheric distortions. The seasonal equatorial regional solar quiet daily variations in Sq follow closely the annual and semiannual patterns expected to be caused by ionospheric conductivity and heating variations that give rise to a dynamo currrent at E-region heights. The difference in the seasonal changes in MDT and Sq implies that the base line levels for the ionospheric source variations in H and Z would best be taken as the nighttime field levels adjusted for a local-time magnetospheric change of a few percent. The lunar seasonal variations show characteristics of dayside ionospheric electrojet origin; however, the cause of the annual early-February enhancement of the lunar tidal field is unknown, and the explanation should be sought in the atmospheric wind behavior.

PETROPHYSICS

Geophysical logging for geochemistry

G. R. Olhoeft continued the development of the nonlinear complex resistivity logging technique as a system to measure geochemistry in situ. Olhoeft and J. H. Scott (1980) continued to test the technique in a variety of borehole logging environments including sedimentary uranium deposits, massive veined sulfides, coal, and granite. The technique is particularly useful in delineating very subtle changes in lithology, discriminating between fresh and clay-filled fractures, mapping alteration, discriminating redox from ion-exchange-bearing lithologies (such as sulfides versus clays), and in measuring pH and Eh in situ. Olhoeft also has used the technique in the laboratory to study geothermal reactions in high-temperature pressure vessels.

Electrical properties of the crust

G. R. Olhoeft (1980) completed a series of measurements of the electrical properties of wet and dry basalt and granite. The only significant parameters controlling the electrical properties of silicates are water content and temperature. At 1000° C, in order to produce a 1 order of magnitude change in the electrical resistivity of a dry silicate, the oxygen fugacity must be changed by more than 6 orders of magnitude or the dry hydrostatic pressure by 1300 MPa or the temperature by 55° C or the water content by 0.3 weight percent. At lower temperatures, the effects of water are even more pronounced. Further, the water must be present as free water, not structural water as in amphiboles, thus indicating the need for more water in the deep crust than is commonly accepted.

Spectroscopy of rocks and minerals

G. R. Hunt (1980) completed a detailed discussion of the physical basis for the specific variations in the transmitted, reflected, and emitted electromagnetic radiation covering the wavelength range from the ultraviolet to the far infrared (0.2 to 50 μm). Hunt outlined a history of the development of the understanding of the nature of electromagnetic energy and the very specific and different ways in which it interacts with matter. Hunt explained the bulk composition and molecular structure of geologic materials in terms of interpretation of the quantum changes in rotational, vibrational, and electronic energy levels resulting from the interaction of radiation with matter and provided the appropriate theories and nomenclatures necessary to describe these changes. Hunt included discussions of the types of remote-sensing information available at different wavelength ranges that occur as a consequence of the chemistry and molecular geometry of a geological material and of the ways in which the appearance of the natural or intrinsic spectrum can be altered as a consequence of external effects such as sample condition and environmental parameters. Hunt summarized available information resulting from the various electronic and vibrational processes for geologic materials so that the type of information that can and cannot possibly be acquired in a remote-sensing situation using the visible and infrared regions can be specifically defined.

Spectrometer modified to view soils

G. R. Hunt designed and constructed attachments to fit the sample and reference ports of commerically available integrating sphere accessories for visible and near-infrared spectrometers. The attachments, which are essentially light pipes that turn the beams through 90°, allow reflection spectra of geologic surfaces, such as those of soils and particulates, to be recorded from horizontal samples with the energy impinging from above, which no commercially available instruments permit. Using the devices, the greater energy throughput and resolution advantages of the integrating sphere can be achieved and the full integrity of the spectral information that is recorded can be maintained.

Remote cation exchange capacity measurement

G. R. Olhoeft found that the nonlinear complex resistivity technique can measure cation exchange

capacity directly. Laboratory and field studies showed that modern, peptized drilling muds do not interfere with the nonlinear complex resistivity measurement, but that such measures of cation exchange capacity are not precisely measuring the same quantity as conventional laboratory determinations. Such remote measurements of cation exchange capacity are useful in the design of in situ solution mining operations as well as oil and gas exploration.

APPLIED GEOPHYSICS

Resistivity sounding interpretation with a desk top computer

A computer program for the fully automatic interpretation of Schlumberger sounding curves obtained, over horizontal layers, which was previously developed, written, and published (Zohdy, 1973), has been revised and modified significantly by A. A. R. Zohdy. The new version uses O'Neill's instead of Ghosh's filter coefficients. This results in greater computational accuracy in the convolution operation with practically no increase in computational time. The new program is written in HP enhanced BASIC for use with the HP9845B/T desk top computer. The output consists of both tabulated and standard graphical plots on bilogarithmic coordinates. Hence, the interpretation of this universally standard type of sounding curve now can be made with significant savings in computer time expenditures.

Truck-mounted computer for borehole geophysics

A comprehensive system of computer programs was developed by J. H. Scott and J. J. Daniels for an HP9845 minicomputer installed in a field truck that is used for making research borehole geophysical measurements. The computer controls peripheral hardware units such as digital counters, scanners, digitizers, and recorders, which are used for acquiring, editing, formatting, and storing field data in digital form on magnetic tapes or flexible disks. The tapes and disks can be played back, in the field or in the office, and data are processed, analyzed, and plotted to provide publication-grade results as soon as they are needed. The computer system improves the quality, accuracy, and speed with which raw field measurements are converted to a final product ready for interpretation.

Magnetotelluric soundings in the Cascades

Data from over 110 MT soundings were obtained by W. D. Stanley in the Cascades. The data show that there is a major electrical contact in the deep crust that may be observed from Lassen Peak to south of Mt. Hood. This contact occurs approximately at the boundary between the western Cascades and High Cascades to the east. It appears to coincide with gravity and magnetic and thermal anomalies. The western Cascades appear to be more resistive, to depths of about 5 km, and considerably more electrically complex than the High Cascades to the east. Most of the soundings east of the electrical boundary over the area studied, which includes most of central and east-central Oregon and California north of Lassen Peak, are remarkably similar. This implies that the crust is electrically simple. The geoelectric section is essentially composed of four layers—a resistive surface layer of volcanic flows, a conductive layer of altered volcanics, a resistive basement complex, and finally a deep conductive zone at depths of 10 to 20 km similar to that observed on the Snake River Plain and at many other areas in the Basin and Range province.

Airborne electromagnetics in geothermal exploration

In order to test the applicability of airborne electromagnetic methods in geothermal exploration, D. B. Hoover studied the data obtained from INPUT surveys obtained over five Known Geothermal Resource Areas in the Basin and Range province. The INPUT data showed the existence of shallow conductive anomalies associated with deeper conductive zones identified by ground electrical methods. The shallow conductive anomalies are believed to be associated with near-surface thermal waters and alteration products that have migrated along structural boundaries. For certain anomalies there are no obvious surface manifestations associated with the electrical conductive regions. Airborne electromagnetic methods, which previously had not been used in geothermal exploration, now appear to be effective in understanding the near-surface region of such systems.

Electromagnetic field differencing methods

An electromagnetic method in which the difference between corresponding components of the natural magnetic field as measured at two sites was tested by C. K. Moss. Instrumentation was developed for measuring the differences over the frequency range of 4.5–26 Hz. It was found that for this method the use of standard AMT coils is superior to SQUID magnetometers. Theoretical modeling indicated that differences in the natural fields are a sensitive indicator of deeply buried elongated conductors that channel natural electrical currents. Performance of the system was satisfactory during field tests over a mineral deposit in Missouri; however, no large anomalies were found.

Three-dimensional electromagnetic modeling

Mathematical modeling for three-dimensional conductors embedded in a layered Earth model using natural or

controlled electromagnetic sources at the Earth surface is an important problem in electromagnetic prospecting methods. A very fast computer algorithm was developed by W. L. Anderson using related and lagged convolution methods to compute Hankel transforms for various Green's tensor elements needed in the three-dimensional-integral equation formulation.

Geophysical studies in the Beaver basin, Utah

The Beaver basin in Utah is a sediment-filled graben, which is believed to collect uranium leached from the nearby Marysvale volcanic field. Geophysical studies by D. L. Campbell indicated that the basin is at least 1,800 m deep and that it contains material that is electrically very conductive (saline groundwater?). Furthermore, near-surface electrical and IP signatures with substantial horizontal variations indicated complex fault structures that could help trap uranium. Spectral IP studies at Marysvale, Utah, did not show differences between oxidized and reduced sediments as they did in a previous study at Tallahassee Creek, Colo.

Gravity measurements in Glacier National Park

Gravity measurements in and adjacent to Glacier National Park were made by D. M. Kulik. Data from approximately 200 gravity stations were collected in 1980. Eleven gravity base stations were established and tied to gravity base stations of the International Gravity Standardization Net at Cut Bank and Kalispell, Mont. Two NE–SW traverses were completed across the Park, one from Saint Mary to West Glacier along Going-to-the-Sun Road, and one from Lower Two Medicine Lake to Nyack. Additional data were collected to complete an existing traverse at the southern boundary of the Park from East Glacier to Nimrod along U.S. Highway 2. A NW–SE traverse was completed in the valleys of the North Fork and Middle Fork Flathead Rivers, from the U.S.-Canada border to Nimrod, adjacent to the west boundary of the Park; and additional data were collected to complete an existing NW–SE traverse from the U.S.-Canada border to East Glacier, adjacent to the east boundary of the Park. Several local traverses were made near Many Glacier, Lake Josphine, Bowman Lake, and Upper Kintla Lake within the Park, and on the Trail Creek, Tepee Creek, Hay Creek, and North Fork roads west of the Park.

Synthetic seismograms from offshore wells

In order to correlate adjacent USGS seismic-reflection data with data from two deep stratigraphic test wells, COST No. G–1 and G–2, in the Georges Bank area off the northeastern coast of the United States, D. J. Taylor and R. C. Anderson generated synthetic seismograms from sonic and density logs previously run in the wells. The synthetic seismograms then were processed into the seismic-reflection data and correlated with geologic time boundaries and lithology. Working from the well correlations, interpretation of the regional seismic-reflection data can be made with greater accuracy.

Microearthquakes and steam production in The Geysers, California

The large number of earthquakes at The Geysers and the possibility of induced seismicity create a unique laboratory for seismic studies. However, to address these topics properly, it was necesssary to expend considerable effort toward developing a digital seismic system capable of extended dynamic and frequency range beyond the abilities of the existing telemetered seismic network. Significant progress has been made by C. G. Bufe, R. S. Ludwin, P. M. Shearer, W. C. Peppin, C. P. Scofield, and V. J. Cagnetti in relating the seismicity to the production of steam at The Geysers. They reported that a strong correlation exists between microearthquake location and the area of geothermal steam production. Increases in the mean number of events per day and in the magnitude of the largest annual event correlate with increases in steam production. The two largest earthquakes in the steam field occurred near the two injection wells most distant from production wells, and events with magnitudes of 2.5 or greater occurred most frequently during months of peak injection. Spatial seismic clusters in proximity to injection wells have occurred soon after injection began.

Microearthquake studies in The Geysers–Clear Lake region

A fully portable, three-component digital seismograph system was developed to record microearthquakes at The Geysers. This system provides high dynamic range, extended frequency response, and both compressional and shear wave information, which are necessary for the study of the source characteristics of earthquakes. A complementary playback system was developed to read and analyze the seismic field data. The system is now in its final test stage, and source spectra for hundreds of earthquakes recorded by the system at The Geysers are being analyzed. A study comparing earthquakes originating at The Geysers and those from the nearby Alexander Valley was conducted by C. G. Bufe, R. S. Ludwin, P. M. Shearer, W. C. Peppin, C. P. Scofield, and V. J. Cagnetti to determine whether analog or spectral parameters could be used to distinguish geothermal-related earthquakes. They found that neither focal mechanism, spectral corner frequency, seismic moment, Richter magnitude, nor any combination of the above could provide a means to differentiate

induced earthquakes from tectonic earthquakes. This suggests that the induced events are natural earthquakes being triggered by local stress perturbations.

Color enhancement of radiometric data

According to J. S. Duval, the interpretation of aerial radiometric data can be greatly enhanced through the use of composite-color images. These images are produced by assigning one of three basic colors (red, green, blue) to each of three radiometric parameters. Although the basic measurement gives only three parameters—potassium (K), uranium (U), and thorium (Th)—the use of ratios gives nine different radiometric parameters—U, K, Th, U/Th, U/K, Th/K, Th/U, K/U, and K/Th. These nine parameters can be combined three at a time to produce five useful composite-color images. These five images may be described as follows:

1. An element image, which combines U, K, Th, that tends to reflect the lithology.
2. A ratio image, which combines U/Th, U/K, Th/K, that tends to remove variations caused by differences in soil moisture.
3. A uranium image, which combines U, U/Th, and U/K, that emphasizes uranium and highlights areas of potential uranium mineralization.
4. A potassium image, which combines K, K/Th, and K/U, that emphasizes areas of relatively high potassium content.
5. A thorium image, which combines Th, Th/U, and Th/K, that emphasizes areas of relatively high thorium content.

These types of images have been produced for an aerial radiometric survey of the Lake City caldera, Colorado. The various images showed anomalies related to the base metal mineralization in the survey area as well as one location with elevated uranium concentrations.

Uranium and radiometric maps of Iron River 2° quadrangle

A uranium anomaly map and two radiometric unit maps were made by J. A. Pitkin from color composite images of aerial gamma-ray spectrometric data for the Iron River, Mich.-Wis., 2° quadrangle. The uranium anomaly map correlates with three areas of known uranium mineralization or anomalous ground radioactivity. The map includes a cluster of six anomalies that may indicate uranium mineralization because they occur within the outcrop of a black graphitic pyritic slate that has a known occurrence of uranium. In this heavily glaciated area, the radiometric unit maps show little direct correlation with mapped geologic units. The mixing action of repeated glacial advances results in correlations only where the ground source is homogeneous or the covering glacial deposits are thin.

Gravity survey completed in Carson Valley, Nevada

Gravity readings were taken at 260 stations throughout Carson Valley, Nev., to determine the depth and configuration of the bedrock surface underlying the unconsolidated valley-fill sediments. According to D. K. Maurer, the deepest part of the valley, which lies beneath the western half, is approximately 1,600 m below land surface. The average depth to bedrock in the western half of the valley is about 750 m. A conspicuous down-drop to the west occurs in the bedrock surface, roughly along the north-south axis of the valley, forming a major lineament with the west face of two mountain blocks north of the valley and the east edge of the extreme southern end of the valley. East of this scarp, the bedrock is fairly flat and only about 300 m deep, with a small basin approximately 750 m deep near the northeast corner of the valley. Gravity readings showing bedrock near the land surface led to the discovery of previously unmapped bedrock outcrops near the northeast margin of the valley.

Gravity survey of Dixie Valley, Nevada

A gravity survey of Dixie Valley in west-central Nevada was completed, according to D. H. Schaefer. A total of 300 gravity stations were established at 600-m intervals on 8 east-west profiles. Bouguer gravity values in the valley ranged from −180 to about −135 mGal. Residuals gravity values, obtained by correcting for the regional gravity gradient, reached about 30 mGal in the center of the valley. The residuals values were run through a three-dimensional gravity inversion model to determine depth to bedrock, according to D. H. Schaefer. A density contrast of 0.5 g/cm^3 between the valley-fill materials and bedrock was used, resulting in a maximum depth of about 3 km.

GEOCHEMISTRY, MINERALOGY, AND PETROLOGY

EXPERIMENTAL AND THEORETICAL GEOCHEMISTRY

Redox equilibria in the Earth's interior

Motoaki Sato developed a new theoretical method to evaluate whether a mineral assemblage containing an element at a certain depth is stable with respect to the same assemblage or another assemblage containing the same element at a different depth in a planetary interior. The principle of the method is calculation of the fugacities of the element defined by the respective mineral assemblage, temperature, and pressure for the two depths, application of the barometric formula for an ideal gas to correct for the gravitational effect, and their comparison to see if they are compatible. Most of

previous arguments about the core-mantle equilibria have neglected the gravity effect as well as the temperature and pressure effects.

To assess the redox equilibria in the Earth's interior, Sato made extensive computations on the oxygen and iron fugacities of various iron-oxygen assemblages along assumed geotherms and then corrected for the gravity effect. The results showed that to be in equilibrium with the core-mantle boundary (the dominant buffer zone), the mantle is not as oxidized as it should be and has too much iron in the middle to the lower regions. Sato concluded that the Earth has not completed its internal redox differentiation.

Equation describing the solubility of quartz in water

R. O. Fournier and R. W. Potter formulated an equation expressing the solubility of quartz in water from 25 to 900°C at very low to very high pressures. The equation is in the form:

$$\text{Log } S = A + B\text{x}(\text{Log } V) + C\text{x}(\text{Log } V)^2 + D\text{x}(\text{Log } V)^3,$$

where S is the molal concentration of dissolved silica, V is the specific volume of water at the specified temperature and pressure, and *A, B, C,* and *D* are constants that vary with temperature. Substituting the temperature terms for *A, B, C,* and *D* expands the equation to 14 terms. This equation should be useful for incorporation into computer models that assess changes in permeability that are due to quartz solution and deposition occurring where thermal water circulates in the shallow magmatic environment.

Experimental and analytical problems in the system $K_2O - FeO - Al_2O_3 - SiO_2$

A series of published and unpublished studies of phase equilibria in the low-temperature immiscible liquid field in the system leucite-fayalite-silica within the general system $K_2O - FeO - Al_2O_3 - SiO_2$ has yielded in part discordant data on the composition of the two liquids and on the temperature and extent of the field of immiscibility. From a reexamination of the various studies and some interlaboratory comparisons, E. W. Roedder and G. M. Biggar (University of Edinburgh) concluded that there are four major causes for these discrepancies: (1) severe alkali loss in small-volume samples exposed to the furnace atmosphere, particularly in those starting as gels; (2) state of oxidation and local variations in the total iron content within the sample, due to several experimental problems; (3) limited ranges of compositions and temperatures of the quench runs used to delineate the field of immiscibility; and (4) difficulty in obtaining accurate, quantitative, electron microprobe analyses of the glasses, particularly for light and (or) volatile elements in the presence of large and grossly variable amounts of iron. They also concluded that the compositions of individual high-iron or high-silicia melts, along the boundaries of the field of immiscibility (that is, those coexisiting with crystals of silica and (or) fayalite), lie in the plane of the ternary system leucite-fayalite-silica and, hence, represent ternary, not quaternary equilibrium. Experimental and analytical difficulties presently preclude a decision as to whether the conjugate melts in equilibrium with these individual melts along the boundary curves are also in the plane, and, similarly, whether pairs of supraliquidus conjugate melts within the field of immiscibility lie in the plane.

Almost all electron microprobe analyses of pairs of immiscible liquids made from starting compositions in the system leucite-fayalite-silica (that is, with a 1:1 K/Al molar ratio) have ratios less than 1.0 for both melts, and the ratio for the high-iron melt is much lower than that for the conjugate high-silica melt. Roedder and Biggar concluded that these differences stem from a combination of three effects: (1) loss of potassium in the experimental work, (2) low-potassium values in the electron microprobe analysis, particularly on the high-iron melts, and (3) real differences in the partitioning of potassium and aluminum between the two liquids. In support of this last effect, analyses of several examples of natural immiscibility, including some made by classical wet chemistry rather than electron microprobe, show considerably lower values for (K+Na)/(Al) in the high-iron pairs.

Effects of iron and boron-nitride crucibles on experimental determination of phase equilibria

J. S. Heubner, C. R. Thornber, and R. W. Wendlandt critically evaluated two kinds of crucibles used in experimental petrology. Relatively impure electromagnet grade iron, commonly used to contain iron-bearing silicate melts in evacuated sealed silica tubes, can contaminate the charge with manganese and titanium. Both electromagnet grade and high-purity iron commonly reduce the iron-oxide content of the melt by causing metallic iron to precipitate. This iron loss can be minimized (but not eliminated) by annealing the iron capsules in a vacuum or $CO+CO_2$ gas mixture, suggesting that the reducing agent is hydrogen introduced during the manufacturing process.

Boron-nitride crucibles, used in experiments at high pressures (15–30 kbars) by some investigators, pose a similar problem. Such crucibles readily reduce NiO and FeO to metal; the reason appears to be the highly reducing nature of boron nitride itself.

When using iron or boron-nitride crucibles, experimental petrologists must be careful that reduction of oxides of interest, particularly FeO and NiO, does not go undetected, leading to erroneous results.

Computer modeling of binary chemical diffusion

Geological examples of binary chemical diffusion are numerous. They are potential indicators of the duration and rates of geological processes. Analytical solutions to the diffusion equations generally do not allow for variable diffusion coefficients, changing boundary conditions, and impingement of diffusion fields. R. F. Sanford prepared three FORTRAN computer programs, based on Crank-Nicholson finite-difference approximations that can take into account these complicating factors.

Program I describes the diffusion of a component into an initially homogeneous phase that has a constant surface composition. It is written specifically for iron-magnesium exchange in lunar olivine, but other components and phases may be substituted by changing the values of the diffusion coefficient. Program II simulates the growth of exsolution lamellae, such as those so commonly found in pyroxenes. Program III describes the growth of reaction rims, and was specifically intended to model the growth of pigeonite rims or lunar augites. The last two programs are written for pseudo-binary Ca-(Mg,Fe) exchange in pyroxenes. In all three programs, the diffusion coefficients and boundary conditions can be varied systematically with time. To enable users to employ widely different numerical values for diffusion coefficients, diffusion distance, etc., the grid spacing in the space dimension and the increment by which the grid spacing in the time dimension is increased at each time step are input constants that can be varied each time the programs are run to yield a solution of the desired accuracy.

Chemical contrasts between magnetite-bearing and ilmenite-bearing granitoid rocks from Japan

G. K. Czamanske reported petrographic descriptions and electron microprobe analyses of minerals for 35 specimens of rock from 7 suites chosen to examine the transition from magnetite-series to ilmenite-series granitoids along two transects across the Cretaceous-Paleocene Inner Zone batholith of southwestern Japan. Regularities in chemical compositions of amphiboles, biotites, and feldspar suggest that fundamentally similar processes produced the magmas that formed the two series. However, constant or decreasing Fe/(Fe+Mg) for biotites and amphiboles with increasing host-rock silica content, coupled with the absence of early formed magnetite and sphene, suggest that magnetite-series rocks typically became oxidized during crystallization near the level of intrusion through the processes of second boiling and differential loss of hydrogen.

For the Daito-Yokota magnetite-series suites, Fe/(Fe+Mg) for biotites decreased from 0.48 to 0.37 as SiO_2 content of the host rock increased from 55.3 to 75.5 wt. percent; for an ilmenite-series suite from the Takanawa Peninsua, Fe/(Fe+Mg) for biotites increased from 0.51 to 0.77 with an increase in host rock SiO_2 from 53.4 to 75.5. Detailed consideration of amphibole chemistry showed predominance of edenitic and tschermakitic substitution schemes, as well as coupling between substitutions of titanium in octahedral sites and aluminum IV. Interrelations between amphibole and biotite chemistry showed that Fe/(Fe+Mg) and manganese contents can be interpreted in terms of equilibration, whereas titanium content cannot. The chemistry of chlorites correlates well with that of biotites; primary and secondary muscovites in several samples are distinct in composition. Plagioclase in all studied suites showed igneous zoning appropriate to host-rock composition; perthitic alkali feldspars in all samples have lost albite component; and temperatures based on the two-feldspar geothermometers are low. The biotite-apatite geothermometer also is inoperative for this group of samples, because fully fluorinated apatites typically occcur in biotites of modest fluorine content. Whereas magnetites have reequilibrated, analyses of ilmenites for the representative Daito-Yokota and Takanawa suites corroborate biotite compositional data and suggest that fO_2 probably differed by two to three orders of magnitude during crystallization of silicia-rich magnetite- and ilmenite-series granites. Curiously, higher inferred pressures of cyrstallization for ilmenite-series suites are not reflected by considering whole-rock normative data in terms of the system Q-Ab-Or-An H_2O. Whole-rock chemistry supports mineral chemistry in suggesting that the studied granitoids have crystallized from magmas generated in a lower crustal environment by partial melting of source materials with igneous characteristics.

Thermochemical data for siderite, rhodochrosite, orthoferrosilite, and topaz

R. A. Robie, B. S. Hemingway, and H. T. Haselton, Jr., measured the heat capacities of siderite (5–600° K), rhodochrosite (5–650° K), orthoferrosilite (5–1000° K), and topaz (5–1000° K) in order to obtain their standard entropies as a function of temperature. At 298.15° K (25.0°C), the derived entropies are 95.3 ± 0.3, 97.9 ± 0.2, 95.8 ± 0.3, and 105.4 ± 0.2 J/(mol · K) for siderite, rhodochrosite, orthoferrosilite, and topaz, respectively. The Gibbs free energies of formation of fayalite and rhodochrosite were re-evaluated using these new calorimetric entropies together with extant equilibrium data and yielded a Gibbs free energy of formation at 298.15° K $= -818330 \pm 550$ J/mol for $MnCO_3$ and a Gibbs free energy of formation at 298.15° K $= -13795 \pm 2100$ J/mol for Fe_2SiO_4.

Microdetermination of H_2O, CO_2, and SO_2 in silicate glass

A new microscope vacuum heating stage and gas analyzer has been developed by D. M. Harris for measurement of H_2O, CO_2, SO_2, and noncondensable gases (H_2, CO, N_2, Ar, CH_4, etc.) evolved from volcanic glass at temperatures up to 1280°C. The bulk of this development was done at the University of Chicago, and since then a similar unit has been installed at the USGS. The most important application has been to the study of single, well-characterized silicate melt inclusions in volcanic or magmatic minerals, but the system also has been used for studies of fluid inclusions of salt from prospective nuclear waste storage sites. The evolved gas is collected in a liquid nitrogen cold trap. Later, a capacitance manometer records the vapor pressure in a constant-volume gage as the cold trap is heated from 77° to 273° K. Gas components are identified by their characteristic vapor pressures and the temperatures at which solid and vapor are in equilibruim during sublimation of individual components. Partial pressures of CO_2, SO_2, and H_2O are equal to differences in gage readings. The masses of CO_2, SO_2, and H_2O derived from samples and blanks are calculated using the ideal gas law, the molecular weights of the components, and the gage constant. The analytical technique is absolute because the results depend only on measurements of the gage volume and temperature, and the calibration of the manometer is done with a McLeod (absolute) mercury pressure gage. The detection limit is about 10 nanograms for H_2O and 5 nanograms for both CO_2 and SO_2. Determinations of SO_2 in glass inclusions by this technique agree with X-ray fluoresence and electron microprobe determinations of sulfur, but further work is required to increase reliability. Determinations of water by this technique agree with vacuum fusion, microcoulometric, Penfield, and gas chromatographic determinations made in four other laboratories. The principal advantages of this analytical technique are (1) the very small sample required, (2) the simultaneous determination of H_2O, CO_2, and noncondensable gases, (3) the avoidance of calibration procedures dependent on chemical standards, and (4) the visual observations that can be made during sample outgassing.

Hydrogen fugacities over the graphite-methane buffer

I-Ming Chou, using a Ag-AgBr hydrogen sensor technique, measured hydrogen fugacities for the graphite-methane (C-CH_4) buffer assemblage pressure at 2 kbar total from 600° to 800°C. The hydrogen sensors consisted of sealed platinum capsules containing Ag-AgBr-H_2O (sensor A) or Ag-AgBr-1.5 m HBr (sensor B). Each run consisted of four sensor capsules with a graphite filler rod in a conventional cold-seal pressure vessel. One sensor of type A and one of type B were exposed directly to the H_2-CH_4 atmosphere of the vessel, and one each of types A and B were enclosed in separate gold capsules containing a reference Co-CoO-H_2O hydrogen buffer assemblage (Chou, 1978; Myers and Gunter, 1979).

The results indicated that the fH_2 values calculated from thermochemical data for the C-CH_4 buffer at 2 kbar from 700° to 800°C (Eugster and Skippen, 1967) are about 2.5 to 3.0 times higher than those obtained in this study. Because of slow reaction rates, equilibrium fH_2 values for the C-CH_4 buffer at 2 kbar and temperature ≤ 650°C have not been attained in runs having durations of as much as 9 days.

M. J. Rutherford (1969) reported that annite equilibrates with a sanidine + magnetite + vapor assemblage at 2 kbar total pressure and 830 ± 5°C with fH_2 defined by C-CH_4 buffer. The fH_2 at this condition is about 300 bars using Eugster and Skippen's (1967) data, but only about 100 bars using the new data. These results permit, for the first time, internal consistency between the annite decomposition reaction and oxygen buffer reactions most commonly used by experimentalists to determine phase relations and thermochemical data.

Errors in geologic pressure determinations from fluid inclusion studies

In a continuing study of the use of fluid inclusion data in the solution of geologic problems, E. W. Roedder and R. J. Bodnar found that several of the widely used geobarometers based on inclusions are wrong. Fluid inclusions record both temperature at time of trapping (Tt) and pressure at time of trapping (Pt). Laboratory reheating establishes the temperature of homogenization (Th), which may be as much as 300°C below Tt for inclusions trapped at high Tt and Pt. Thus the difference (Tt-Th, the "pressure correction") can be important in evaluating the accuracy of geothermometry. In estimating these procedures, two aspects are frequently misunderstood: (1) calculation of pressure corrections from independent pressure estimates, and (2) use of inclusion data to estimate or place constraints on this pressure (that is, geobarometry). Several commonly used inclusion geobarometers are wrong in theory or practice, or both, and can yield very erroneous values: (1) The "Lemmlein and Klevtsov method" (Klevtsov and Lemmlein, 1959), as used on inclusions homogenizing by solution of an NaCl crystal, has two procedural errors as published, yielding incorrect pressures. We present a new method for such inclusions that presumably yields a good approximation (Roedder and Bodnar, 1980). (2) The "Lyakhov method" (Lyakhov, 1973), for similar inclusions, has an erroneous assumption in the calculation that yields pressure as much as eight times too high. (3) The "Naumov and Malinin method" (Naumov and

Malinin, 1968), for inclusions containing mixed CO_2 and H_2O, resets on a series of assumptions, several of which are dubious. (4) The "Nacken method" (Nacken, 1921), for separate inclusions of CO_2 and H_2O, requires several assumptions that are either difficult to prove or demonstrably invalid. Of the many methods proposed, Roedder and Bodnar believe that the following have the best promise at present: (1) boiling fluids method (and its corollary, solution vapor pressure at Th = minimum pressure for non-boiling fluids); (2) a new daughter-mineral solution method; and (3) Th versus an independent geothermometer (for example, CO_2 in minerals of basalts). All require careful inclusion study and need improved experimental pressure-volume-temperature-composition data on appropriate systems.

The formation of charge transfer complexes in transition metal fulvic and humic acid solutions

The speciation of trace metals in natural waters determines to a large extent the toxicity and nutritional availability of trace metals in soil and natural water systems. The most abundant organic complexing agents in these systems are humic and fulvic acids, which have been shown to form complexes with transition metals. A detailed description of the mechanism of complexation, however, has not been formulated. As a first step in the determination of this mechanism, R. L. Wershaw, D. M. McKnight, and D. J. Pinckney have demonstrated by ultra-violet difference spectroscopy that a charge-transfer complex is formed in copper-humic and fulvic solutions. This complex is evidenced by the appearance of a new spectral band in the region between 40,000 to 42,000 cm^{-1}.

Fulvic acidlike substances from lakes near Mount St. Helens, Washington

One of the major changes in water quality of lakes in the blast zone of Mount St. Helens, Wash., was a large increase in the concentration of dissolved organic material. For example, the concentration of dissolved organic carbon in Spirit Lake increased from 1 to 38 mg/L. Diane McKnight has shown that polymeric organic acids derived from the breakdown of plant and soil material make up most of the organic material isolated from Spirit Lake and West Castle Creek Lake: these acids are similar to aquatic fulvic acids from more typical environments in their concentration of carbon, hydrogen, oxygen, nitrogen, and acidic functional groups, and in their size. However, the Spirit and Castle Creek organic acids do have unusually large concentrations of sulfur (4.3 and 2 percent) and chlorine (1.3 percent), which probably were incorporated into the organic material during pyrolysis in the presence of volcanic gases.

Analysis of the hydroxl groups in humic and fulvic acid by ^{13}C NMR

Carbon-13 nuclear-magnetic-resonance spectroscopy (^{13}C NMR) has proved to be an especially powerful tool for the differentiation of the chemical structure of organic compounds. A number of workers have tried to apply ^{13}C NMR to the study of the natural organic polyelectrolytes, humic and fulvic acid. The spectra obtained generally consisted of broad, poorly defined bands that have not allowed one to unambiguously differentiate between the various functional groups that are present in these compounds. R. L. Wershaw of the USGS, and M. A. Mikita and Cornelius Steelink of the University of Arizona have developed a method for labeling the various hydroxyl groups in a humic or fulvic acid and to obtain ^{13}C NMR spectra of these labeled groups that have sharp, well-defined bands. The technique allows one to calculate the relative abundances of the different hydroxyl groups.

Geochemical kinetics studies

Application of geochemical kinetic principles to understanding natural ground-water systems was emphasized in 1980 by H. C. Claassen. Two ground-water systems were studied: One in New Mexico, containing soluble calcium sulfate, and the other in southern Nevada, composed primarily of tuffaceous alluvium.

Results of the New Mexico study (Claassen, 1981) showed that channels formed by dissolution of the calcium sulfate were the primary conduits by which surface water recharged the aquifer, and that these conduits were growing at the rate of a few tens of millimeters per year. This information will be valuable in evaluating potential leakance at a damsite being planned on the Pecos River upstream from Carlsbad, N. Mex.

The second study in Nevada demonstrated the importance of flood runoff in recharging alluvial aquifers in arid environments. Initially, the quality of ground water in tuffaceous alluvium was expected to be the same regardless of whether the water had originated from direct local recharge through the alluvium or from underlying tuff that had been recharged in more distant upland areas. However, analysis of ground water known to have been recharged in the highlands showed that this water had undergone a greater extent of reaction than the water in the alluvium. Thus, it was concluded that water in the alluvium could not have flowed from the highlands, as previously hypothesized, but rather had recharged locally.

Radioactive and stable-isotope data supported the new hypothesis of direct recharge from runoff and helped to determine the times during which climatic conditions in southern Nevada were favorable for ground-water

recharge. This analysis will impact on the devaluation of potential radioactive waste repositories at the Nevada Test Site.

MINERALOGIC STUDIES AND CRYSTAL CHEMISTRY

Crystal structure of meionite scapolite

In connection with a stability study of the scapolite system, B. Aitken together with J. A. Konnet and H. T. Evans has carried a three-dimensional refinement of a synthetic meionite with composition $(Ca_{3.4}Na_{0.6})(Al_{5.4}Si_{6.6})O_{24}\cdot CO_3$. Previously reported studies have located the carbonate group in disorder on the four-fold symmetry axis in the structure, but its precise disposition has remained uncertain. Extensive refinement of a carefully measured X-ray intensity data set using various special techniques (free atom, constrained atom, rigid molecule, etc.) reduced the reliability factor to R=5.5 percent, but appreciable electron density still remained in the residual map at the carbonate site. Eventually it was discovered that the CO_3 group is divided into two separate positions so that it occupies at random eight positions in disorder around the four-fold axis. The two positions are located symmetrically on either side of a Ca-Ca diagonal axis. This model reduced R to 4.8 percent and removed most of the residual electron density, while retaining normal dimensions for the CO_3 group. This result will give new insight into the behavior of the carbonite anion in the square setting of cations that characterize the scapolite structures.

Decomposition rates in clinopyroxenes

In their continuing collaboration on the kinetics of unmixing of rock-forming pyroxenes, G. L. Nord, Jr. (USGS), and R. H. McCallister (Purdue University) have been studying the coarsening rates in pyroxenes as a function of composition. The width of exsolution lamellae in clinopyroxenes can be used as an indication of cooling rate if the rate of growth is known as a function of time, temperature, and composition. In the simplest case, growth of lamellae can be considered as a reduction of the interfacial area between the two phases. This process is known as coarsening and usually can be described by the relationship wavelength = wavelength (o) + kt to 1/3 power where wavelength (o) is an initial wavelength at t=0, k is a kinetic constant, and t is time. The rate of coarsening in clinopyroxene has been compared for two compositions, Wo27En73Fs0 and Wo25En31Fs44, that differ significantly in Mg/Fe ratio but not in calcium content. For both compositions, coarsening of the exsolution lamellae follows the t to 1/3 power rate law, but the absolute coarsening rate is approximately 10 times faster in Fs44 than in Fs0 at the same temperature. For example, coarsening of the Fs0 composition at 1000°C for 100 days would increase the lamellae wavelength by 60 A whereas coarsening of the Fs44 composition for the identical conditions would increase the lamellae wavelength by 603 A. This change in kinetic behavior is due to the increase in iron content, which in turn has affected the diffusion rate. This comparison showed that the mapping of kinetic behavior with respect to composition will be a necessary step before lamellae size can be used as a quantitative rate tool in geology.

Occurrence of an unusually sodic muscovite

An unusual sodic muscovite was discovered during chemical study of micas recovered from garnet-staurolite grade metapelitic rocks of eastern White Pine County, Nev., by D. E. Lee, R. E. Van Loenen, E. L. Munson Brandt, and W. P. Doering. Gravimetric analysis of this muscovite gave 2.91 percent Na_2O, or about 38 mole percent paragonite. Calculated and observed values for unit-cell volume and density are in good agreement, attesting to the purity of the material analyzed and to the accuracy of the chemical and physical measurements for this mineral (Jackson and others, 1967). It is difficult to reconcile the composition and field setting of this muscovite with the results of experimental work on the stability of paragonitic muscovites. The inferred temperature range of garnet-staurolite grade metamorphism is 400° to 430°C (Hietanen, 1967). According to the data of Eugster and others (1972), only about 10 mole percent solid solution of paragonite in muscovite would be expected at this temperature range.

This sodic muscovite coexists only with quartz, biotite, and sparse amounts of garnet, staurolite, and chlorite. Paragonite is absent, and the biotite coexisting with this sodic muscovite contains only 0.34 percent Na_2O. The simplicity of this mineral assemblage (essentially quartz, sodic muscovite, and biotite) and the chemical data available for the rock, muscovite, and biotite may help to direct future experimental work on the stability of sodium-rich muscovite.

Solid-solid sorption mechanisms for iron oxide coatings on quartz and kaolinite

P. M. Boymel, E. R. Weiner, and M. C. Goldberg examined the solid-solid sorption mechanisms for iron-oxide coatings on quartz and kaolinite as a function of pH and sodium chloride concentration. A method for determining solid-solid sorption was developed which is based on particle-size settling properties and computer-

assisted infrared spectroscopy. The sorption of solid goethite to quartz can be described as purely electrostatic, while the sorption of solid goethite to kaolinite is specific.

Effect of sorbants on the Raman spectrum of gibbsite

A substantial change in the Raman intensities of the $OH-^{1}$ stretching bands of solid, powdred gibbsite (α-$Al(OH)_3$, surface area 10 m^2/g) has been attributed to surface interactions with the sorbates $Ca+^{2}$, $H_xPO_4^{3-x}$, silicic acid, and mixtures thereof. The four OH^- stretching bands of gibbsite occur at 3360, 3430, 3520, and 3618 cm^{-1}; the intensity relative to untreated gibbsite of the 3360 cm^{-1} band was observed to diminish 60 percent upon $CaCl_2$ treatment at one extreme, and to increase 180 percent after H_3PO_4 treatment at the other extreme. Small changes in the relative peak heights of the four bands were observed, depending on the treatment used. The results were interpreted in terms of different surface OH^--adsorbate interactions by other researchers. K. M. Cunningham and M. C. Goldberg of the USGS speculated that such interactions should have little effect on what is virtually a Raman spectrum of bulk OH^-. They examined this system using an internal intensity standard (Na^2Oxalate crystals) and gibbsite with surface area of 1 m^2/g. Adsorbate solutions, treatment regimes, and spectroscopic techniques were similar to previous studies. The results of Goldberg and Cunningham show no effect, within probable error, of the different adsorbates on OH^- band parameters.

VOLCANIC ROCKS AND PROCESSES

MOUNT ST. HELENS

Volcanic events

Results of USGS studies of the 1980 eruptions of Mount St. Helens are reported in Professional Paper 1250 (Lipman and Mullineaux, editors, 1981). Although Mount St. Helens apparently had been dormant since 1857, geologic studies of deposits around the flanks of the volcano indicate that it has erupted frequently in the past and that the modern cone has grown largely in the past 2,500 yr, according to D. R. Mullineaux and D. R. Crandell.

Eruptions of dacite, as pyroclastic flows, air falls, and viscous lava domes, have alternated with lava flows of andesite and basalt. During most eruptive periods, pyroclastic flows and mudflows built fans of fragmental material around the base of Mount St. Helens and partly filled valleys leading away from the volcano. Before 1980, Mount St. Helens was considered by some vocanologists to be the most likely of all Cascade volcanoes to erupt in the near future, and among the most hazardous because of the likelihood of explosive activity and proximity to populated areas.

R. L. Christiansen and D. W. Peterson reported that the 1980 activity of Mount St. Helens began on March 20 with an intensifying swarm of earthquakes. The first steam-blast eruption, a week later, was associated with continued high levels of seismic activity, formation of a summit crater, and beginning of deformation of the north flank of the volcano. These processes continued intermittently through April up to the climactic eruption on the morning of May 18. The May 18 eruption apparently was triggered by a magnitude-5+ earthquake, not appreciably different from many preceding quakes, which caused failure of the bulging north flank and produced a great avalanche of rock debris. Unloading of the volcano by this failure led to a northward-directed lateral blast, probably largely driven by hydrothermal steam explosions that devastated an area of nearly 600 km^2. These events in turn triggered an explosive eruption of dacitic magma that drove a vertical column more than 24 km high, producing visible ash fall for more than 1,500 km to the east and pumiceous pyroclastic flows on the volcano's north flank. Catastrophic mudflows and floods were generated by rapid melting of snow and ice. Smaller magmatic eruptions also occurred on May 25, June 12, July 22, August 7, October 16–18, and in late December, producing pyroclastic flows, airfalls, and several lava domes. Through December 1980, the eruptions tended to become progressively smaller in volume, slightly more mafic in composition, and less explosive.

Geophysical monitoring

The abrupt increase in earthquake activity beginning on March 20 at shallow depth beneath the volcano was recognized as indicating possible impending eruptive activity. With this warning, augmented gesophysical monitoring, photographic documentation, and aerial and ground observation were already under way before initial steam-blast eruptions on March 27. Geophysical monitoring was especially important in April and early May, when continued relatively mild steam-blast eruptions provided little evidence that a catastrophic event was approaching. However, both the sustained high level of seismic activity and of ground deformation on the north flank bulge suggested that the volcano was building toward some major event. Ground deformation was monitored both by geodesy and by photogrammetry. Complementary photogrammetric measurements provided more complete information on the shape of the bulge, but with a greater time lag for data interpretation.

After May 18, patterns of both seismicity and ground deformation changed markedly, but these indicators

continued to provide key information on the readiness of the volcano to erupt and the size and depth of the underlying magma body. Electronic-tilt, microgravity, and magnetic measurements recorded small but significant changes around Mount St. Helens at various times during the 1980 eruptive activity, that offered less clear predictive information, but provided valuable constraints on the geometry of the magma body beneath the volcano.

Seismic studies

Several earthquake types, distinguished by contrasting time-amplitude patterns on seismic records, were important at Mount St. Helens in 1980. High frequency or A-type earthquakes are characterized by distinct impulsive P and S phases, and hypocenter depths are typically 1 to 20 km; this type resembles tectonic earthquakes of nonvolcanic regions and may represent volcanically triggered quakes along regional structures. Low-frequency or B-type events, characterized by emergent P phases and indistinguishable S phases, are limited to depths less than a few kilometers and are typical of subvolcanic swarms. Harmonic tremor is characterized by a nearly continuous train of vibrations on a seismic record. Tremor is thought to reflect subsurface movement of magma and often precedes eruptive activity.

The earthquake swarm at Mount St. Helens preceding the May 18 eruption provided a remarkable opportunity to characterize precursory seismic phenomena associated with andesitic-dacitic volcanism, according to E. T. Endo, C. S. Weaver (USGS), S. D. Malone, and L. L. Noson (University of Washington). Daily earthquake counts gradually increased for 5 days prior to the first major earthquake on March 20, which was of magnitude 4.2 and located at only a few kilometers depth beneath the volcano. The number of earthquakes peaked on March 27, concurrently with the first hydrothermal eruption. A gradual decrease in earthquake counts through April and early May was accompanied by an increasing number of larger magnitude events; as a result, the rate of energy release remained high and nearly constant. These earthquakes were confined to a small volume, less than 2.5 km deep, beneath the growing bulge on the north flank of the volcano. The May 18 eruption was triggered by a magnitude 5.1 earthquake, slightly larger than any previously recorded in 1980. No specific precursory seismicity has been recognized for the May 18 eruption, other than the entire earthquake sequence that started in late March.

C. S. Weaver, W. C. Grant (USGS), and S. D. Malone (University of Washington) noted that marked changes in the seismicity, both local to Mount St. Helens and in the surrounding region, occurred after the May 18 eruption. After May 18, earthquakes beneath the volcano decreased in number and magnitude after the catastrophic eruption, occurred at depths as great as 20 km, and covered zones extending tens of kilometers northwest and southeast of the volcano. Complex earthquake sequences in the crater area, including periods of harmonic tremor, accompanied magmatic eruptions after May 18 and were helpful in forecasting some eruptive activity a few hours to a day in advance. Most focal-mechanism solutions showed right lateral strike-slip faulting, indicative of north-northeast-trending compression, which agrees well with predictions from plate-tectonic subduction models for the Pacific Northwest.

Deformation studies

Mount St. Helens in 1980 has presented an exceptional opportunity to obtain deformation data of types rarely attempted previously. A few base-line distance measurements had been made by D. A. Swanson in 1972 at Mount St. Helens, but these had not been repeated before the beginning of the 1980 activity. Changes on the cone were monitored in 1980 by electronic-distance and theodolite-angle measurements, photogrammetry and topographic mapping, microgravity measurements, and by continuously recording electronic tiltmeters and magnetometers.

Deformation measurements were begun in early April, in an attempt to determine the significance of the ominous fracturing and bulging visible at the summit and upper north slope of the volcano, but poor weather and frequent steam explosions limited these efforts to microgravity readings by R. C. Jachens, D. R. Spydell, Daniel Dzurisin, C. W. Roberts (USGS), and G. S. Pitts (University of Oregon), and several types of tilt measurements by John Dvorak, A. T. Okamura, Carl Mortensen, and M. J. S. Johnston on the lower slopes; these showed relatively small, inconclusive, and partly inconsistent changes.

In mid-April, J. G. Moores, W. C. Albee, Raymond Jordan, and H. H. Kieffer analyzed the first post-eruption vertical aerial photographs and documented startlingly large deformation of the bulge area. About the same time, geodetic measurements by P. W. Lipman, J. G. Moore, and D. A. Swanson of newly established targets high on the north flank showed that deformation was continuing at high rates. The photogrammetric results demonstrated that the upper north slope had moved outward more than 100 m and upward slightly, and the geodetic measurements documented continuing lateral displacements of as much as 2.5 m/day. Despite this extraordinary local deformation, no significant changes were measured on the east, south, or west

slopes. These deformation measurements, along with continued high levels of seismic energy release, provided the primary evidence in April and early May that the volcano could be nearing a major event, despite the seeming mild nature of the intermittent phreatic activity. Concern focused on the probability of landsliding of the north flank, and attempts were made to design a monitoring procedure to obtain advance warning. Even in hindsight, however, no changes in deformation rates preceding the failure on May 18 have been identified. Prior to May 18, the north slope was not sufficiently unstable to fail gravitationally without a trigger, which finally was provided on May 18 by the large earthquake at 0832 PDT.

Since the catastrophic May 18 eruption, a notably different sytle of deformation has characterized Mount St. Helens. D. A. Swanson, P. W. Lipman, J. G. Moore, K. A. Yamashita (USGS), and C. C. Heliker (Western Washington University) found that the entire cone has shown only small changes that are oriented radially with respect to the crater area. The rates of geodetic change slowed during the year, and little analytical significant change was observed on the main cone during the last few months of 1980. Geodetic and electronic-tilt data have shown a general pattern of slow deflation, interrupted by brief small inflationary episodes preceding and accompaning the major pyroclastic eruptions on June 12, July 22, and August 7. Within the crater, larger and more complex deformation seemingly was related to dome growth; the north side (the rampart) of the inner crater has moved northward at rates of as much as several centimeters per day.

Transient magnetic anomalies, recorded during the May 18, May 25, and June 12 eruptions, are thought by M. J. S. Johnston, R. J. Mueller, and John Dvorak to reflect elastic strain release related to the eruptions.

Gas studies

Until recently, volcanic gases have been frustratingly difficult to study quantitatively or to use for monitoring of activity. Major gas vents on volcanoes are often too inaccessible or dangerous to approach, and gas samples from smaller vents commonly contain so much atmospheric air and water vapor that probable magmatic components are difficult to determine. Furthermore, many components of volcanic gases tend to react to form new compounds, even during the collection process, complicating identification of equilibrium volcanic assemblages.

In the last few years, much progress has been made using airborne and ground remote-sensing techniques for measuring volcanic gases. A correlation spectrometer (COSPEC), originally designed to monitor industrial pollutants, has been used successfully for remote monitoring of SO_2 emission at several volcanoes, especially by R. E. Stoiber (Dartmouth College). A recording hydrogen probe, which is essentially a small fuel cell that generates electricity in proportion to the amount of hydrogen available to combine with air, has been operated at Kilauea Volcano in Hawaii since 1973 by Motoaki Sato. Finally, an airborne technique to measure CO_2 in volcanic gas plumes, developed by Sato and D. M. Harris, was used successfully for the first time at Mount St. Helens in 1980.

These ground and airborne techniques, while still partly experimental, already have produced much data on compositions and rates of volcanic gas emissions from Mount St. Helens. Before May 18, SO_2 emissions were at low rates, near limits of COSPEC detectability despite seismic and geodetic evidence for a shallow cryptodome within the volcanic edifice; either the cryptodome was too well sealed for abundant gases to escape, or hydrothermal fluids were absorbing most of the available sulfur gases during this period, according to T. J. Casadevall, D. A. Johnston, D. M. Harris (USGS), W. I. Rose, Jr., T. J. Barnhorst (Michigan Technological University), R. E. Stoiber, L. L. Malinconico, and S. N. Williams (Dartmouth College). N. L. Nehring and D. A. Johnston found that sulfur:chloride ratios in ash leachates, an indirect method of monitoring gas emission, indicated a gradual increase during this period, although no abrupt changes occurred before the May 18 eruption. Plume emissions of SO_2 increased by an order of magnitude after May 18, as shown by airborne COSPEC measurements, and increased markedly again in early June, prior to the June 12 eruption and growth of the first lava dome. These increases probably reflect decreasing depth and less effective sealing of the dacitic magma body. After the June 12 eruption, SO_2 levels remained at high levels but steadily decreased during the rest of the year.

Airborne monitoring of CO_2 in the plume, begun in early July, documented a total flux greater than that of SO_2 and a similar general pattern of gradually decreasing emission rates later in 1980, according to D. M. Harris, Motoaki Sato, T. J. Casadevall (USGS), W. I. Rose, Jr., and T. J. Barnhorst (Michigan Technological University). Pyroclastic magmatic eruptions on July 22, August 7, and October 16–18 appear to have been preceded by several days of significantly decreased CO_2 emissions, a pattern that may help anticipate future explosive eruptions. The total amounts of both CO_2 and SO_2 released to the atmosphere in 1980 exceeded by several times amounts of these gases that could have been derived from the volumes of magma erupted during the monitoring period. Much of the gas appears to have emanated from unerupted magma within the volcano.

Hydrogen concentrations in the ground, relative to the local atmospheric concentration, at a site on the south flank of Mount St. Helens have varied complexly since measurements by Motoaki Sato and K. A. McGee began in July. Smooth diurnal variations probably are related to daily reversals of orographic winds. Short-period irregular increases are interpreted tentatively as evidence of seismically triggered emission of magmatic H_2. Changes in average daily concentrations are thought to reflect varying concentrations in the gas plume; such changes may have preceded by several days the magmatic eruptions in August and October, as well as several prominent gas-emission events and episodes of volcanic tremor.

Direct sampling of fumaroles remains the only way to inventory the range of gas species and to sample for isotopic analyses. Analyses by L. P. Greenland of fumarole samples collected by T. J. Casadevall from the crater indicate that sulfur is released from the magma mainly as H_2S and oxidizes to SO_2 as it cools in the plume. High concentrations of air and water vapor in fumaroles from the flowage deposits confirm that entrainment and heating of nonmagmatic gases contribute to the mobility of pyroclasic flows. A study by T. E. C. Keith, T. J. Casadevall, and D. A. Johnston of encrustations at fumaroles indicates that sublimate mineralogy reflects fumarole temperature and subsequent cooling and hydration history. Isotopic analyses of carbon, oxygen, and hydrogen from fumarolic gases and thermal waters show large deviations from surficial meteoric and organic compositions, according to Ivan Barnes, D. A. Johnston, W. C. Evans, T. H. Presser, R. H. Mariner, and L. D. White. These data demonstrate major volatile contributions from high-temperature environments, in part probably directly from the magma and in part from interactions between ground water and heated rocks.

Thermal studies

Several types of volcanic thermal studies were carried out at Mount St. Helens. Thermal surveillance of large areas, commonly by airborne infrared techniques, was used to monitor changes of thermal expression of internal structural and magmatic features. In addition, measurements were made directly on new volcanic deposits to determine their emplacement temperatures and thermal properties, and eruption and emplacement temperatures also were estimated from effects on vegetation and on manmade materials.

Thermal infrared monitoring by H. H. Kieffer, David Frank, and J. D. Friedman prior to May 18 generally showed only small changes, except in the area of the crater that initially formed on March 27. Of two previously known thermal areas, one on the southwest side of the cone remained unchanged up to May 18. The other historic thermal anomaly, within the deforming area of the bulge on the upper north flank, showed small but gradually increasing heat emission before May 18.

Infrared images from late May through August interpreted by J. D. Friedman, David Frank, and H. H. Kieffer show thermal anomalies associated with the new crater and vent areas, pyroclastic deposits north of the crater and locally on the upper slopes of the cone, and with the successive lava domes that emerged in June and August. En echelon northwest-trending fractures within the crater and on its walls, which are evident on thermal images, may represent local expression of regional structural trends, also expressed seismically, which probably are related to plate subduction and are important structural controls of Cascade volcanoes.

Direct thermocouple measurements by N. L. Banks and R. P. Hoblitt indicated that emplacement temperatures of the May 18 debris avalanche were 70° to 100°C; those of the direct blast ranged from 100° to 300°C and varied with azimuth. Emplacement temperatures of the main pumiceous pyroclastic flows erupted intermittently from May 18 to October 16–18 were 300° to 730°C, and near-vent deposits were emplaced at 750° to 850°C. In general, the later deposits had higher initial temperatures. Except near the vent, temperatures in individual pyroclastic-flow lobes did not decrease substantially along the flow path, and deposits of the directed blast also had similar temperatures over distances as far as 20 km from the vent. Measurements of pyroclastic-flow deposits indicated that, after initial rapid cooling of several hundred degrees by adiabatic expansion and incorporation of air during eruption and development of flowage, the main body of a flow incorporated too little air along the subsequent flow path to cool markedly.

Eruption temperatures of the directed blast, estimated by effects on plastic objects and wood within the devastated zone, are similar to those directly measured. Temperature effects on wood are azimuthally variable and correlate with the amount of juvenile gray dacite in the blast deposit. Effects on plastics indicate only a few minutes of peak temperatures, and the thermal effects decreased markedly near margins of the blast area. Needles of fir trees from the seared zone around margins of the blast area showed cuticular melting patterns that, when compared experimentally with heated needles, suggest temperatures of 50° to 200°C in the seared zone, according to W. E. Winner and T. J. Casadevall.

Remote monitoring

Radar observations from FAA installations at Seattle and near Spokane, Wash., and the National Weather Service system at Portland, Oreg., were used by D. M.

Harris (USGS), W. I. Rose, Jr. (Michigan Technological University), and R. Roe (National Weather Service) to monitor eruptions of Mount St. Helens. Concentrations of ash particles were detectable by radar; moreover, observations could be made at night and in overcast weather when conventional observations were difficult. Radar measurements were especially useful in determining existence, height, and duration of an eruptive column, and direction and rates of ash-cloud movement. Radar observations also may permit estimation of the mass of airborne ash and potential ashfall over specified areas.

The video-survelliance system (a remotely controlled camera 9 km north of Mount St. Helens, a microwave repeater, and viewing and recording equipment in Vancouver, Wash.), became operational in mid-July. The system has been used by C. D. Miller and R. P. Hoblitt to evaluate fluctuations in gas emission, avalanche frequency, wind conditions, blowing ash in potential work areas, to assess eruptive events, and to minimize the risks to personnel on the volcano.

Volcanic deposits

The 1980 eruptions at Mount St. Helens have presented exceptional opportunities to correlate observations of volcanic events with physical features of the resulting deposits. Most geologic studies examine deposits that formed in the past by events and processes that must be inferred from features of the deposits. In many paleovolcanic deposits it is difficult to infer the timing of events, nature and temperature of emplacement processes, composition of associated gases, and original magmatic chemistry of deposits that rapidly alter after emplacement.

The major near-source deposits are (1) deposits of the May 18 debris avalanche that was initiated by landsliding, (2) deposits of the immediately following directed blast, (3) mudflow deposits generated by rapid melting of snow and glacial ice, (4) pumiceous pyroclastic flows that formed later on May 18 and during subsequent magmatic eruptions, (5) lava domes in the crater, and (6) relatively thin air-fall deposits.

Debris-avalanche deposits

The debris-avalanche deposits resulted from landsliding of the north flank at 0832 PDT on May 18 and represented the largest historic gravitational slide known, according to Harry Glicken and R. J. Janda (USGS), Barry Voight (Pennsylvania State University), and P. M. Douglass (Hart-Crowser), having a volume of 2.5 to 3 km^3 and extending about 25 km. The hummocky chaotic debris filled about 60 km^2 of the North Fork Toutle River valley to an average depth of 45 m and raised the level of Spirit Lake 60 m. Seven map units within the avalanche deposits can be correlated with successive slide movements recorded by photographs. Transitory seismic stresses were necessary for initiation of sliding, and additional mechanisms such as liquifaction were necessary to sustain their movement.

Directed-blast deposits

The directed volcanic blast that devasted an area of neary 600 km^2 northwest, north, and northeast of Mount St. Helens within a few minutes on the morning of May 18 is probably the most remarkable aspect of the 1980 eruptions. Similar catastrophic laterally directed explosions have occurred at a few other volcanoes in historic time, notably Bandai-san in Japan in 1888, and Bezymianny and Shiveluch Volcanoes in Kamchatka in 1956 and 1964, but the eruptive mechanism that causes a volcano to vent laterally rather than vertically previously has not been well understood.

J. G. Moore, S. W. Kieffer, R. P. Hoblitt, C. D. Miller, R. B. Waitt, Jr., J. E. Vallance, and T. W. Sisson concluded that the May 18 directed blast was generated by massive explosions, which occurred when an enormous landslide on the north flank released the confining pressure on a shallow dacite cryptodome and its associated hydrothermal system. Propelled by expanding gases and gravity, the mixture of gas, rock, and ice moved as a ground-hugging turbulent hot pyroclastic cloud at initial velocities of as much as 300 m/s. Within a few minutes, the directed blast had extended out about 25 km, had slowed to velocities of 25 to 30 m/s, and had carried off or knocked down all trees in its path. Photographs showed that the pyroclastic cloud remained low, a few kilometers above ground level; then, as forward motion diminished, convecting ash clouds began to billow up. Analysis by S. W. Kieffer indicated that the fluid dynamics of the blast, as representing supersonic expansion of a multiphase mixture (vapor-solid-liquid) from a high-pressure reservoir, accounts for many features of the blast deposits and associated devastation. The total energy released is calculated as about 24 Mt, released over a period of a few minutes. The deposit emplaced directly by the high-velocity blast cloud varies in thickness from more than a meter near the volcano to only about a centimeter near margins of the affected area. A distinctive general feature is the relatively limited maximum thickness of the deposit even in areas of rugged topography, except for local blast-related pyroclastic flows that moved downslope and ponded in valleys. About half the blast deposit consist of fresh, originally hot, gray dacite derived from the exploded cryptodome; the remainder is chiefly mixed lithic fragments from the former north flank of the volcano and entrained soil and organic material. The

blast deposit showed crude normal grading in most places, and at least four subunits were recognized: (1) basal coarse deposit, (2) finer grained middle unit characterized by pyroclastic-surge textural features, (3) secondary blast-related pyroclastic flows, and (4) an upper blast-related air-fall unit containing abundant accretionary lapilli.

Nomenclature applied to the blast and associated deposits has been controversial. Some authors have emphasized the distinctiveness of the laterally directed eruption and associated deposits, referring to the event as a volcanic blast (Kieffer) that produced blast deposits (Hoblitt, Miller, and Vallance); others have interpreted the character of the event as dominantly a pyroclastic surge (Moore and Sisson) or a pyroclastic density flow (Waitt). The terms "directed blast" and "directed-blast deposit" have been used as unambiguous terms to refer to the initial lateral eruptive event and its deposits.

Mudflow deposits

Destructive mudflows commonly accompany pyroclastic eruptions on stratovolcanoes. Because such poorly sorted and unstratified volcaniclastic deposits typically contain abundant coarse fragments, the term lahar commonly is applied to the broad textural range of mudflows and debris flows like those that occurred at Mount St. Helens on and after May 18. The term mudflow commonly is used for flows in which sand, silt, and clay are abundant; debris flows dominantly contain coarser material.

Destructive lahars developed within minutes of the beginning of the May 18 eruption, as hot pyroclastic debris melted snow and glacial ice on upper slopes of the cone, according to R. J. Janda, K. M. Scott, K. M. Nolan, H. A. Martinson, and J. E. Cummans. Large areas of the above-timberline slopes of the volcano were scoured by lahars on the morning of May 18, especially on the east and west flanks. Early lahars descended the Muddy River, Pine Creek, and the South Fork Toutle River. In upper reaches of these drainages, the flows appear to have originated as wet lithic avalanches, locally reaching velocities of as much as 45 m/s as determined by the geometry of cross-valley runups. As velocities decreased downvalley, these avalanches changed into mudflows.

The most voluminous mudflow originated by slumping and flowage of water-saturated deposits of the debris avalanche in the upper North Fork Toutle River valley. This mudflow did not reach peak stage until late afternoon and early evening on May 18, perhaps because of the time required to integrate flowage across the hummocky topography. This mudflow extended more than 120 km downvalley, to the Cowlitz and Columbia Rivers, and caused widespread channel filling, flooding, and damage to roads, bridges, and other structures.

Pumiceous pyroclastic-flow deposits

Pyroclastic flows are high-velocity surface flows of high-temperature fragmental material. Such flows are highly destructive because of their high temperatures and great mobility. Historic flows have been observed to travel a few kilometers from vents at velocities of up to 60 m/s, and analyses of prehistoric deposits suggest that large flows can cover distances of as much as 100 km at velocities of up to 200 m/s.

Pyroclastic flows commonly are subdivided on the basis of constituent materials and grain size into ash flows, pumice flows, lithic pyroclastic flows, block-and-ash flows, etc. Ash flows consist chiefly of ash-size particles of glass shards and phenocrysts; the term pumice flow is applied if pumice lapilli and blocks are dominant. Ash flows are the most common type of pyroclastic flow, especially in large-volume eruptions. Block-and-ash flows contain abundant large fragments and commonly form by explosive disruption or gravitational failure of the flank of a growing lava dome. Many pyroclastic flows are preceded by a ground-hugging hurricanelike surge cloud and accompanied by an overriding ash cloud, each of which may leave recognizable deposits.

Pumiceous pyroclastic flows of mafic dacite occurred during six major eruptions (May 18, May 25, June 12, July 22, August 7, and October 16–18). This sequence presented exceptional opportunities to observe pyroclastic flows in motion, study their primary depositional features, measure thermal and rheological properties, relate size and sorting to eruption characteristics, and monitor compositional changes. In general, time intervals between successive pyroclastic eruptions increased during 1980, and eruptive volumes, area covered, vesicularity, and degree of chemical differentiation decreased.

Pyroclastic flows were first observed shortly after noon on May 18; P. W. Rowley, M. A. Kuntz, and N. S. MacLeod found that resulting deposits extend as much as 8 km from the vent, cover an area of about 15 km^2, and have a bulk volume of about 0.2 km^3. The deposits form a fanlike pattern of sheets, tongues, and lobes of nonwelded and mostly poorly sorted ash and clasts of pumice and dense dacite. Successively younger pyroclastic-flow deposits, in general, cover progressively smaller areas and have smaller volumes. The flows formed simultaneously with, or just prior to, development of large vertical ash columns. Most pyroclastic flows originated when bulbous masses of ash, lapilli, and blocks rose only a short distance above the inner crater before spreading laterally to the north, but some flows were observed to result from gravitational collapse of parts of an accompanying vertical ash column.

Lionel Wilson and J. W. Head (Brown University) concluded that morphologic and rheologic measurements on pyroclastic-flow deposits of July 22 and August 7

indicate that the flows moved as non-Newtonian fluids, most readily modeled as Bingham plastics. Reverse grading of coarse low-density pumice clasts in marginal levee deposits is interpreted as the consequence of briefly increased fluidization, related to interaction between the flow and surrounding air at the time of emplacement.

Petrographic and textural studies by M. A. Kuntz, P. D. Rowley, N. S. MacLeod, R. L. Reynolds, L. A. McBroome, A. M. Kaplan, and D. J. Lidke indicated that all 1980 pyroclastic-flow deposits consist mainly of juvenile dacite, containing plagioclase, hypersthene, hornblende, and Fe-Ti-oxide phenocrysts in a vesicular glassy matrix. In general, successively younger deposits show increasing modal proportions of plagioclase, hypersthene, and Fe-Ti-oxide phenocryst:glass ratios, and decreasing porosity. These relations suggest that successive eruptions have tapped deeper levels in a compositionally zoned magma chamber, have progressively depleted the magma of volatiles, and have been characterized by decreased amounts of vesiculation and gas thrust.

Lava domes

Extrusions of steep-sided domical masses of viscous silicic lava commonly follow discharge of gas-rich, less viscous magma as pyroclastic material. In the past few thousand years, at least a half dozen dacitic domes have formed at Mount St. Helens including the large summit dome that capped the volcano prior to the 1980 eruptions.

Rise of magma to a shallow level beneath the new crater was indicated in early June by increased SO_2 gas emission and by a central warm area detected by airborne radiometers. J. G. Moore, P. W. Lipman, and T. R. Alpha reported that the first dome, of dacitic composition, grew for at least 7 days following the June 12 explosive activity, eventually reaching 365 m in diameter and 45 m in height. The central part of this dome was blown out during the July eruption, and the resulting inner crater largely was filled by a second smaller dome that grew for about a day following explosive eruptions on August 7. A more mafic dome (silicic andesite), intermediate in size between the June and August domes, formed at the same site in about half a day following the October 16–18 pyroclastic eruptions. Between December 27 and January 3, two dacitic dome lobes were erupted from flanks of the October dome without significant premonitory pyroclastic activity. All the 1980 dome units were subcircular in plan and developed apical sags or collapse pits during late stages of growth, due either to lateral spreading, degassing, or to withdrawal of magma from below.

Physical, electrical, and thermomagnetic properties of samples of the June 1980 dome, determined by G. R. Olhoeft, R. L. Reynolds, J. D. Friedman, G. R. Johnson, and C. R. Hunt under laboratory conditions, suggest atypically low oxygen and sulfur activities in the magma, probably due to effective degassing prior to extrusion. The thermal energy of the June dome, calculated from laboratory determinations of physical properties, was used to calibrate energy estimates for other phases of the 1980 eruptions. The total energy yield of the eruptions through October 1980 is estimated by J. D. Friedman, G. R. Olhoeft, G. R. Johnson, and David Frank to be 1.33×10^{25} ergs, similar in yield to the 1950 eruption of Mauna Loa (Hawaii), but only half as great as the 1956 directed-blast eruption of Bezymianny (Kamchatka).

Air-fall deposits

Ash falls accompanied every major eruption in 1980, as well as the steam-blast eruptions prior to May 18. The resulting air-fall ash stratigraphy is complex, but is resolvable, because observations were made after each major eruption. The data collected permit correlations and comparisons between the individual air-fall deposits and variations in eruptive behavior, changing composition and volume of erupted magma, direction and velocity of upper winds, effects of eolian fractionation, and with earlier ash deposits from Mount St. Helens and other similar volcanoes.

During the early steam-blast activity from March 27 to May 18, the volume of ash erupted 8×10^5 m^3 and the areas covered were small according to A. M. Sarna-Wojcicki, R. B. Waitt, Jr., M. J. Woodward, Susan Shipley, and J. R. Rivera. The ash consisted entirely of angular lithic and crystal grains from pre-existing rocks from the conduit. The volume of ash erupted is an order of magnitude less than the volume of the crater formed during the same time interval, mainly because of deformation on the north flank of the volcano and also because of ice in the pre-existing summit crater.

Air-fall deposits of the May 18 eruption studied by R. B. Waitt, Jr., and Daniel Dzurisin display a complex stratigraphy reflecting the multiple eruptive events. Within a few tens of kilometers of the volcano, four principal units were deposited within 12 h: (1) basal gray lithic ash that contains much organic material and is related to the directed blast, (2) tan pumice and lithic lapilli deposited from the plume of the vertical eruptive column, (3) pale-brown vitric ash related to ash clouds generated by pyroclastic flows on the north slope and to large steam explosions near Spirit Lake, and (4) fine gray ash that resulted from the waning eruption late on May 18 and settling out of fines still in the atmosphere from earlier activity. Thus multiple stratigraphic units

can be deposited rapidly during a single eruptive sequence.

More distant ash-fall deposits studied by A. M. Sarna-Wojcicki, Susan Shipley, R. B. Waitt, Jr., Daniel Dzurisin (USGS) and S. H. Wood (Boise State University) show fewer units, as coarser and denser lithic and crystal fragments preferentially settled out, resulting in deposition of a single bed of fine vitric ash at distances of more than a few hundred kilometers from the vent. Ash fall was visible at least 1,500 km to the east. Mapped distributions of the ash-fall deposits differ from radar and satellite locations of the airborne ash cloud, reflecting different wind directions and velocities at different altitudes and times. In thickness and volume, the combined tephra of May 18 is similar to the major 19th-century air-fall deposit (tephra layer T) from Mount St. Helens, but are an order of magnitude less than the largest prehistoric tephra units from Mount St. Helens.

R. A. Zielinski and M. G. Sawyer used an automatic image analyzer to determine the grain size of air-fall ash 100 to 800 km downwind from the May 18 eruption. Nineteen samples ranged from below the 2 μm counting limit to 0.75 mm. Abundant sub-μm sized particles are present as surface coatings (electrostatically attracted?) on larger grains. For coarse-grained fractions (> 63 μm) mean grain diameters range from 183 to 93 μm and show the expected inverse correlation with distance, and likewise, the mass of coarse-grained fractions decreases from 97 to 6 wt. percent. In the fine-grained size fraction (2 to 63 μm), differential rates of settling are not indicated by changes in the mean diameter because of the dominant numbers of particles of 2- to 10-μm diameter. Size frequency histograms indicated at least a bimodal-size distribution with peaks at 80 to 125 and 2 to 8 μm. Grain-shape measurements interpreted as the degree of circularity indicated a statistically significant difference between the circularity means of the two measured size fractions. Fine-grained particles are distinctly more angular and (or) elongate. This observation and the bimodal size distribution suggest that fine-grained particles are produced by abrasion of larger particles during gaseous transport in the volcanic plume.

Air-fall deposits of the explosive eruptions from May 25 through October 16–18 are much smaller than those of May 18, and they generally decreased in volume with time, according to R. B. Waitt, Jr., V. L. Hansen, A. M. Sarna-Wojcicki (USGS) and S. H. Wood (Boise State University). These deposits trend in varying azimuths due to differing wind directions. Each shows offsets in thickness and grain-size axes, which resulted from differing directions and velocities of high- and low-level winds, and each shows a local increase of thickness far downwind from the volcano.

Geochemistry of the deposits

It is difficult to reconstruct magmatic compositional variations from chemical analyses of eruptive products, especially pyroclastic deposits, because of extensive separation of volatiles during eruption, and the instability of quenched porous glassy volcanic materials that are easily hydrated, oxidized, and altered. For prehistoric deposits, timing of eruption and deposition is difficult or impossible to determine precisely. Accordingly, petrologic study of volcanic materials that have been collected immediately after eruption at Mount St. Helens at known times, commonly while still hot, can be especially rewarding, even when the compositional variation is small in comparison to the total compositional range in historic and prehistoric eruptive products.

Precise major-oxide analyses show small but significant variations in compositions of 1980 eruptive products, according to P. W. Lipman, J. J. Norton, J. E. Taggart, Jr., E. L. Brandt, and E. E. Engleman. Compositions of erupted magma generally became more mafic as volumes decreased with time, both during the day on May 18 and during subsequent explosive eruptions from May 25 to October 16–18. All compositions are mafic dacite, transitional to andesite. These changes are thought to represent progressively deeper levels in a compositionally zoned or stratified magma body, similar to progressions in silicic volcanic sequences elsewhere.

Electron-probe analyses of coexisting ilmenite and magnetite indicated crystallization temperatures of about 990°C and oxygen fugacities of about -9.7 ($\log_{10}$), showing no distinct trends with time, according to W. G. Melson (Smithsonian Institution) and C. A. Hopson (University of California, Santa Barbara). Mineral and bulk chemical compositions are similar to 16th–19th century eruptive products, but are less differentiated than some earlier prehistoric pyroclastic deposits. Dark- and light-gray banded layers, which are relatively common in 1980 pumice blocks, contain compositionally varying mineral phases and indicate mixing of different parts of a single magma chamber or of magmas from different chambers.

Active alteration of new deposits studied by D. P. Dethier and David Frank (USGS), and D. R. Pevear (Western Washington University) is indicated by the chemistry of fumarole encrustations and of surface thermal waters, ash-leaching experiments, and scanning electron-microscope studies of mineral and glass surfaces. Calculated stability relations indicate that kaolinite and smectite should be stable alteration phases, but, with the exception of the fumarole incrustations, new secondary minerals were not found in the 1980 deposits, indicating that rates of crystallization are slow.

A. M. Sarna-Wojcicki, C. E. Meyer, M. J. Woodward, and P. J. Lamothe found that chemical compositions of the air-fall ash erupted on May 18 reflect varying mixtures of magmatic constituents and of old volcanic rocks, as well as varying downwind separation of light and dense particles. Because phenocrysts and lithic fragments are concentrated in near-source deposits, and glass shards become more abundant downwind, chemical trends with distance are similar to trends of magmatic crystal-liquid fractionation processes. Such physical mixing and sorting processes obscure any systematic compositional trends in air-fall ash from the post-May 18 eruptions.

HAWAIIAN VOLCANO STUDIES

Movement of magma

There have been no eruptions in Hawaii since the small outbreak at Pauahi Crater on the upper east rift zone of Kilauea Volcano in November 1979. Mauna Loa Volcano continued in repose with a pattern of slow inflation and few earthquakes, but Kilauea had five significant intrusive events during 1980 (March 2, March 10–12, August 27–28, October 22, and November 2). These intrusive events were characterized by shallow earthquake swarms, volcanic-seismic tremor, rapid deflation of the summit area with simultaneous ground deformation in the earthquake swarm area, and for some events, volcanic gas emissions. The events are interpreted to be intrusions of magma into shallow dikes beneath the rift zone. Magma moving into these new fractures apparently is resupplied from the summit reservoir. Rough estimates of the extent and volume of these inferred dikes can be made from the observed data. Seismicity provides the key information to estimate the length, height, depth to top, and propagation rates of the dikes. Subsidence of the summit area provides an estimate of the total volume and rate of supply of magma involved in the intrusions. Gas emissions of CO_2 and SO_2 occurred at the surface over the inferred intrusions during three events. In two of these events, the seismic data also indicated a shallow depth (0.5 km) to the top of the intrusion. The occurrence of five intrusions without eruptions further confirms the major changes in structure and eruption mechanics of Kilauea Volcano caused by the M=7.2 earthquake in November 1975. From 1959 until the major earthquake, Kilauea had 24 eruptions and 12 intrusions without eruptions; since November 1975, Kilauea has had 10 intrusions without eruptions and only two eruptions. The major seaward displacement of the south flank of Kilauea during that M=7.2 earthquake apparently reduced the accumulated stresses across the east rift zone, making it easier for small dike intrusions to dilate the rift zone.

Besides these events of relatively rapid fracturing by magma, longer periods of slow deflation of the summit and slow inflation and dilation of the middle east rift zone from Makaopuhi to the Pahoa-Kaimu highway have continued to occur during 1980. The volume of magma involved in this slow leakage into the rift is difficult to estimate and must be based on an assumed rate of magma supply into the summit reservoir beneath Kilauea. Assuming $100\times10^6m^3$ of magma supplied per year, some $250\times10^6m^3$ of magma could have moved (without magma fracturing) into the middle east rift over a zone 25 km long since October 1977. An alternative estimate based on the cumulative amounts of slow summit deflation since October 1977 indicates $140\times10^6m^3$ of magma may be involved. A blade-shaped body of magma 25 km long and 3 km high would have to dilate 2 to 3 m to accommodate these estimated volumes of additional magma. This amount of displacement seems high but not impossible. Refining these estimates of slow magma movement into the middle east rift of Kilauea and determining how both slow and rapid (magma fracture) intrusion can take place along different segments of the rift is one of the research challenges of the years ahead.

Quantitative forecasting of Kilauea eruptions

An experiment in quantitative forecasting of eruptions of Kilauea on a probabilistic basis was started by Fred Klein in September 1980. It uses summit earthquake counts, tilt amplitude and rates, and the biweekly tidal cycle to estimate the eruption probability of Kilauea for the next day, week, or month. It will take several years to evaluate this dynamic approach as compared to the average probability of eruptions from historic data.

Gas emissions

Daily monitoring of gas emission indicates average daily fluxes of 170 t/d of SO_2 and 3000 t/d of CO_2 from vents located at Kilauea caldera. Halemaumau Crater provided most of the gas emissions from Kilauea in 1980. The 1975 fissure in the Mauna Loa summit caldera produces less than 5 t/d. Observed changes in CO_2/SO_2 and H_2S/SO_2 ratios seem to correlate with intrusions of magma into the summit region and east rift of Kilauea, demonstrating a connection with the major magma system rather than being isolated local phenomena. The monitoring is the first step toward describing the pressure-temperature-composition conditions of the magma and the reactions of the gases during transport.

Earthquakes

Twelve earthquakes of M=4 or greater occurred beneath or near the island of Hawaii in 1980. The largest

was M=4.6 at a depth of 27 km beneath the south flank of Mauna Loa on January 19 at 15:28:49 Hawaii Standard Time. More than 150,000 earthquakes were instrumentally detected, and most of these occurred beneath Kilauea and the southeast flank of Mauna Loa.

Kilauea caldera stratigraphy

A reconnaissance study of the geology of Kilauea caldera was begun in 1979 by Daniel Dzurisin and T. J. Casadevall and expanded during 1980. A 135-m-thick stratigraphic section at Uwekahuna Bluff contains 63 flow units and 2 ash deposits. The uppermost 14 units are distinguished by their lenticularity and by the presence of plagioclase phenocrysts. Macroscopic plagioclase is rare in historic Kilauea summit lavas; interpretation of its significance in the late-prehistoric suite of caldera flows awaits laboratory analysis and further mapping. An intriguing possibility, which is subject to chemical testing, is that some of the flows exposed in Kilauea caldera may have been derived from neighboring Mauna Loa Volcano.

An underlying suite of flows contains little or no macroscopic plagioclase but is remarkably rich in olivine. Individual flow units within the olivine-rich suite are laterally more continuous than overlying plagioclase-bearing units, suggesting a change in source or eruption mechanics. The prevalence of olivine phenocrysts ends abruptly below the Uwekahuna Ash. At the base of Uwekahuna Bluff, this distinctive marker bed drapes a steep slope tentatively interpreted as a structure associated with an ancient buried caldera. Below the ash, flow units are generally aphyric and seemingly more rounded in outcrop than flows above.

Topical studies of the Uwekahuna Ash and of intrusive bodies exposed in the wall of Kilauea caldera are in progress. Results of the ash study reaffirm the potential for violent phreatomagmatic eruptions at Kilauea, perhaps involving pyroclastic surges. We have sampled 16 dikes in the west wall of Kilauea caldera, one of which has been traced to the paleosurface at the base of the 1790 ash of the Keanakakoi Formation of Westworth (1938). In general, dikes that reached the surface display morphologic characteristics that distinguish them from dikes that failed to vent. False or drain-back dikes also can be distinguished on the basis of morphology. Analysis of volatiles (sulfur, chlorine) in intrusive rocks at Kilauea will help assess the importance of shallow intrusions in volcanic outgassing.

HAWAIIAN ISLANDS–EMPEROR SEAMOUNT STUDIES

Hawaiian-Emperor data gap resolved

Two kinematic corollaries of the hot-spot hypothesis for the origin of the Hawaiian-Emperor volcanic chain in the Pacific predict that (1) the ages of the volcanoes should increase away from the active volcanoes of Kilauea and Mauna Loa on the island of Hawaii, and (2) the lavas of the volcanoes should be chemically similar or should show some systematic chemical evolution along the chain. During the past decade or so, these predictions generally have been confirmed, but there are significant gaps in the data set. G. B. Dalyrmple and D. A. Clague (USGS) and Michael Garcia (Hawaii Institute of Geophysics (HIG)) have eliminated one gap by age and petrochemical analyses on dredged samples from Laysan (1976 cruise, USGS R/V *S. P. Lee*) and Northhampton Volcanoes (HIG R/V *Kana Keoki*) located about midway between the Island of Hawaii and the Hawaiian-Emperor bend. The samples from Laysan consist of hawaiite and mugearite from the alkalic (or post-caldera) stage of eruption. The samples from Northhampton are all olivine tholeiites. Major oxide and trace element chemistry shows that Laysan and Northhampton Volcanoes are 19.9 ± 0.3 m.y. and 26.6 ± 2.7 m.y. old, respectively, making a total of 29 radiometrically dated Hawaiian-Emperor Volcanoes. But more importantly, they fill a 1,072-km-long gap in the age-versus-distance and petrochemcial data between French Frigate Shoals and Pearl and Hermes Reef. The data show clearly that the ages of the Hawaiian-Emperor Volcanoes increase from Kilauea, on the Island of Hawaii, to Suiko Seamount, more than half way along the Emperor seamont chain, and that the volcanoes in the chain are chemically similar. These data show that the hot-spot hypothesis is a viable explanation for the origin of this remarkable chain of volcanoes.

CENOZOIC VOLCANISM IN WESTERN UNITED STATES

Long Valley–Mono basin geothermal area, California

Geologic and petrologic studies by R. A. Bailey indicated that Long Valley caldera, the Mono Craters, and the volcanic islands of Mono Lake constitute a south-to-north succession of three progressively younger volcanic complexes, each in a different stage of evolution. Long Valley is the oldest complex (3.0 m.y.–0.5 m.y.) and probably has completed its cycle, having evolved through stages (1) early basalt to quartz latite effusion, (2) precaldera rhyolite ring-fracture extrusion, (3) voluminous ash-flow eruption and caldera collapse, (4) post-caldera structural and magmatic resurgence, and (5) final extrusion of intracaldera rhyolite and quartz latite. The Mono Craters are younger (0.040 m.y.–.001 m.y.) and have evolved through stages 1 and 2. The centers in Mono Lake form the smallest and youngest complex (< 2000 yr) and are in stage 1. Comparison of the sequence of stages in the three complexes suggests that both the Mono Craters and Mono Lake complexes

could evolve in turn through stage 5 of the Long Valley cycle.

The chemically evolved Long Valley magma chamber attained a maximum diameter of 20 to 30 km 0.7 m.y. ago and probably approached within 8 km of the surface before being partially eviscerated by catastrophic ash-flow eruptions. It now is largely congealed but may contain a partially molten core about 10 km in diameter.

The chemical homogeneity of the Mono Craters indicates that they issued from a single chamber that probably is 18 km in diameter, deeper than 10 km, largely molten, and still rising toward the surface. The chemical heterogeneity of the Mono Lake centers indicates that they probably issued from small, multiple, and relatively deep magma bodies that have not yet coalesced. The different ages and stages attained by the three complexes suggest structural models that are comparable to igneous ring complexes, which are considered to be deeper crustal analogues.

Coso Mountains area, California

Five eruptive groups of rhyolite domes and flows can be defined for the last approximately 240,000 yr in the Coso volcanic field on the basis of potassium-argon and obsidian hydration dating, superposition, and extensive trace-element analyses. C. R. Bacon and W. A. Duffield found that the erupted volume of a given group was linearly proportional to the period of repose before emplacement of the next eruptive group. A plot of cumulative erupted volume versus age showed a stair-step, "time-predictable" relation. A line fitted to the four points defined by projecting the cumulative erupted volume for a group to the time of emplacement of the next group gives a long-term rate of eruption of about 5.7 km^3/m.y. This behavior is analogous to that of some faults whose coseismic slip is proportional to the recurrence interval between one earthquake and the next. Analysis of volume and potassium-argon age data for Pleistocene basalts erupted from vents partly surrounding the southern half of the Coso rhyolite field showed the same sort of pattern. The long-term eruption rate is about 2.8 km^3/m.y. for the last approximately 400,000 yr.

The underlying control for the time-predictable nature of both rhyolitic and basaltic volcanism at Coso appears to lie in the extensional tectonics of the Basin and Range province. The long-term rate of extension of the Coso region may be approximately constant. Thus, extensional strain builds up in the crust at a constant rate. If extension within the area of the volcanic field is predominantly taken up by dike injection and if the volume erupted in any given episode is proportional to cumulative dike width, then the following model may well apply: Dikes may be expected to form when magmatic pressure exceeds the sum of lithostatic pressure and the strength of roof rocks, the latter being a function of stored extensional strain. It follows that a given eruptive episode reflects a dike injection event that relieves a certain amount of extensional strain; the period of repose before the next eruption is directly related to the amount of strain relieved by the previous dike injection event. The Coso volume-time data appear to confirm models of Basin and Range heat flow that call for injection of basaltic magma into the crust.

Volcanic evolution of Crater Lake region, Oregon

Eruption of rhyodacite air-fall pumice and subsequent rhyodacitic to andesitic pyroclastic flows eviscerated a shallow magma chamber and resulted in collapse of Crater Lake caldera about 6800 yr B.P. C. R. Bacon reported that the pyroclastic flows carried sufficient dense lithic clasts and traveled with adequate radial velocity to cause significant erosion of features near the present caldera rim. Evidence for such erosion is seen readily in the climactic, bedded air-fall deposits that are present on top of Llao Rock, but have been stripped from the flanks to increasing degrees downslope where they are overlain by lithic-rich deposits of the climactic eruption. The ash-flow surface of the Wineglass Welded Tuff as used by Williams (1942), which was deposited immediately after the climactic air fall, is also eroded, and overlain directly by pyroclastic surge(?) and flow deposits. The erosion must have occurred during the climactic eruption, because hot gases originating in a cooling lava flow beneath the deposits caused fumarolic alteration of the entire section, demonstrating that all units were deposited in a short period of time. The most spectacular evidence for erosion by pyroclastic flows occurs at Grouse Hill, an extensive rhyodacite lava flow and dome known to predate the climactic eruption by no more than about 200 yr. The surface of the Grouse Hill flow must have been fresh at the time of the climactic eruption, yet the original surface is preserved only on the lee side of the flow. Successively deeper levels in the flow are exposed on either flank as the caldera side is approached: pumiceous carapace, obsidian zone, and devitrified felsite. Furthermore, dense scorias and lithic blocks as large as 7 m are piled against the caldera-facing side of Grouse Hill and dunes of similar, though smaller, debris mantle the surface of the lava flow in the lee of the dome, attesting to the power of the pyroclastic flows. Pyroclastic flows from Mt. Mazama traveled more than 40 km down surrounding major drainages.

Columbia River Basalt Group: vent systems in Oregon

The conformable contact between the Picture Gorge and Grande Ronde Basalts is well exposed in the southwestern part of the Pendleton 2° sheet. Most of

the Picture Gorge is best assigned to the N_1 magnetostratigraphic unit of Swanson and others (1979); locally the uppermost flow has reversed polarity and, hence, is assigned to the R_2 unit. No angular discordance between the Picture Gorge and the Grande Ronde (R_2 and N_2) was recognized, but a thin interbed consisting of detritus possibly eroded from the older John Day Formation commonly occurs along the contact. Picture Gorge flows can be traced as far as 15 km north of the axis of the Blue Mountains uplift in the canyons of Juniper and Lone Rock Creeks.

Two north-northwest-trending linear vent systems for two or more flows, probably in R_2 Grande Ronde Basalt, occur between the lower reaches of Lone Rock Creek and the southern edge of the Pendleton 2° sheet at long 119°45′. The eastern vent system, represented by piles of welded spatter, pumice, and thin flows, extends for about 20 km from Buttermilk Canyon to the headwaters of Juniper Creek. The western system, the westernmost yet found for the Columbia River Basalt Group on the Columbia Plateau, occurs for about 17 km along Lone Rock Creek. The western vent system contains elongate tephra cones and ramparts as much as 150 m high; it is the best exposed and most convincing of any vent systems on the plateau. One dike occurs along the western system; it merges upward into highly vesicular flows and tephra. This area also contains a Picture Gorge dike previously recognized by P. T. Robinson, and may represent a zone of crustal weakness considerably west of most such zones in the province.

PLUTONIC ROCKS AND MAGMATIC PROCESSES

Evolution of continental crust by arc magmatism

Arc magmatism (magmatism of Andean type, above subducting slabs of oceanic lithosphere) is deduced by Warren Hamilton to have been the dominant agent in the formation and modification of continental crust throughout Proterozoic and Phanerozoic time. Most exposed middle and deep continental crust consists of igneous rocks plus older rocks equilibrated at magmatic temperatures and subsequently variably metamorphosed. Many terrains can be put in arc-magmatic contexts by their positions beneath obvious shallow arc-magmatic complexes, by their regional tectonic settings, and by their petrologic indicators of depth. Each crustal level displays a typical assemblage of magmatic rock types formed by depth-varying fractionations and equilibrations in continuous magmatic systems. The lower crust is characterized by differentiated layered complexes of mafic and ultramafic rocks, anorthosite, and quartz-poor granite (the latter in part anatectic); premagmatic rocks are subordinate and are in middle-granulite facies. The middle crust consists primarily of migmatites in lower granulite facies in the deeper part and in upper amphibolite facies in the shallower part; voluminous hydrous, aluminous magmas result from dissociation of hydrous wallrocks, and crystallize in part as two-mica granites. The comparatively dry magmas that reach the upper crust are mostly tonalite to adamellite; they spread out in batholiths and erupt as ashflow sheets and as far-traveled volcanic ash.

Volcano "root" in the Sierra Nevada batholith

In the east-central Sierra Nevada, R. W. Kistler has identified a circular-zoned granitic pluton, with an outcrop area of 2.5 km² similar in appearance to the middle-Cretaceous metamorphosed volcanic rocks exposed about 5 km to the south in the western part of the Ritter Range. Samples from the metavolcanic rocks and the pluton yield a Rb-Sr whole-rock isochron age of 99.9 ± 2.2 m.y. with an initial $^{87}Sr/^{86}Sr$ of 0.7048 ± 0.0001. Major element variation diagrams of the pluton and the nearby volcanic rocks define coincidental compositional trends. The pluton is composed of a central body of granite that is intruded into and almost completely surrounded by a crescent-shaped outer rim of quartz monzodiorite. Widely spaced aplite dikes from the granite intrude the quartz monzodiorite along the contact between the granitic rocks. Aplite compositions suggest a minimum crystallization pressure of 0.5 kbar (1–2 km); this depth is consistent with crystallization near the base of a large stratovolcano.

Two-mica S-type granites in northeastern Nevada

During 1969–1976, D. E. Lee visited more than 160 plutons in the course of a systematic sampling of granitoid rocks in the Basin and Range province of Nevada, Utah, California, and Arizona. Among these 160 plutons are 3 two-mica granites that resemble each other and are unlike any of the other plutons observed during this study. These unusual granites occur along a north-south line in northeastern Nevada and are distinguished in part by the presence of large phenocrysts of muscovite, many of which contain small inclusions of euhedral biotite.

High $\delta^{18}O$ and $^{87}Sr/^{86}Sr$ values indicate that all three of these unusual intrusive rocks are S-type granites, derived from continental crust. The chemical compositions and accessory mineral contents of these rocks also are characteristic of S-type granites. The muscovite is phengitic and the biotite contains about 6.0 percent MgO.

From the field and laboratory data available for these three distinctive two-mica granites, it is concluded that they probably result from anatexis of Proterozoic Z argillites under conditions of relatively low oxygen fugacity, along a line that roughly coincides with the westward disappearance of a continental basement.

Distribution of elements of Sierra Nevada batholith

Studies in the central Sierra Nevada batholith by F. C. W. Dodge, H. T. Millard, Jr., and H. N. Elsheimer have led to the determination of the content of several elements of 27 representative granitoid samples and of 36 separates of their major minerals. The chemical data confirm some previously established lateral compositional trends and also demonstrate eastward increase in light rare-earth elements and tantalum across the batholith. These variations are attributable to the heterogeneity of the source regions from which magmas were derived.

Continuous fractionation of ferromagnesian minerals throughout the differentiation history of Sierra Nevada magmas is suggested by systematic decrease of iron and a group of related trace elements with increasing SiO_2. Chemical and mineralogical evidence indicate hornblende dominated fractionation from 55 to 72 percent SiO_2, and at higher SiO_2 levels, iron depletion reflects removal of small amounts of magnetite. Biotite apparently was not an important fractionated phase. Below 72 percent SiO_2, several elemental variations are largely controlled by hornblende fractionation, whereas above 72 percent strontium drops abruptly, and a negative europium anomaly becomes increasingly prominent indicating a shift to plagioclase as a controlling fractionate. The low barium content of a high SiO_2 leucogranite implies depletion of K-feldspar, and the rock may be a true eutectic granite.

New phase diagram for basic magmas

J. S. Huebner has developed a model phase diagram for basic magmas that emphasizes the decrease in Mg/(Mg+Fe) and the changing calcium and silicon contents with fractional crystallization and decreasing temperature that are so clearly recorded by olivine and pyroxene. The diagram showed liquidus and solidus volumes of olivine, three pyroxenes (orthopyroxene, pigeonite, and augite), and silica minerals. Published experimental melt compositions, produced at a pressure of 1 atmosphere and analyzed with the microprobe, were used to locate the various liquidus boundary surfaces. Portions of the three saturation surfaces at which a pyroxene coexists with olivine and plagioclase were located precisely by linear regression analysis, using calcium, magnesium, iron, and titanium in the melt as independent variables. The good fits obtained suggest that different laboratories achieve consistent results and that small amounts of minor elements (sodium, potassium, chromium, manganese) do not markedly affect the equilibria between melt and plagioclase, olivine, and pyroxenes. Using existing knowledge of the tie line orientations between crystals and melt, it appears possible to predict the temperature of magmatic crystallization of most pyroxene+olivine+plagioclase assemblages and to estimate the composition of the melt, given the composition of the pyroxenes and (or) olivine.

Trondhjemitic rocks derived by partial melting of amphibolite

The Ammonoosuc Volcanics of Ordovician age mantle core gneisses of the Oliverian domes along the Bronson Hill anticlinorium in western New Hampshire and adjacent Vermont. Most of the Ammonoosuc lithology is bimodal, comprising metamorphosed oceanic tholeiite and potassium-poor quartz keratophyre tuffs. Recent investigations by G. W. Leo revealed the presence of an intrusive trondhjemitic phase that locally forms abundant sills cutting layered Ammonoosuc. Moreover, the core gneiss in three small domes in entirely trondhjemitic, defining a 100-km-long belt almost free of calc-alkaline rocks.

The metatrondhjemite typically is fine-grained quartz-plagioclase granofels containing about 3 to 6 percent biotite and having the following compositional ranges (16 samples): SiO_2, 73.1 to 79.0 percent; Al_2O_3, 11.3 to 13.5 percent; CaO, 0.9 to 3.1 percent; Na_2O, 3.5 to 5.7 percent; FeO+MgO, 1.6 to 4.8 percent [1]; and K_2O, 0.20 to 1.3 percent. Thus, these rocks effectively meet the chemical criteria of low-Al_2O_3 trondhjemites, but are unusually silicic. Rare-earth-element (REE) patterns show slight enrichment of light REE, pronounced negative europium anomalies, and undepleted heavy REEs. The patterns suggest a plagioclase residue, and appear to be compatible with an origin by partial melting of amphibolite, probably at crustal levels. Such an origin is also suggested by the bimodal Ammonoosuc suite that contains negligible andesite and only minor amounts of other intermediate rocks.

Constraints on the use of ultramafic xenoliths in basalt

The mineralogy and chemical variations resulting from metasomatic interaction of hydrous mineral veins and peridotite wallrock in xenoliths from basaltic rocks in the Western United States were examined by H. G. Wilshire, J. E. N. Pike, and J. T. Nakata. The results revealed chemical trends that differ in important respects, such as the aluminum content of pyroxenes from those already established for pyroxenite veins in peridotite. These differences permit identification of the types of veins responsible for metasomatic alterations of peridotite even when the veins are no longer present in the xenoliths; they also increase the problems of geobarometry based on peridotite mineral compositions. Evidence based on the structure, mineralogy, and com-

[1] Total iron as FeO.

positions of xenoliths from basalts, and on the characteristics of composite xenoliths, show that xenolith suites cannot be used to reconstruct mantle or crustal stratigraphy, but they do yield important information on processes of melting, high-pressure segregation and differentiation of melts, and reaction between melts and wallrock in mobile parts of the upper mantle.

Three distinct magma groups in the Wet Mountains area, Colorado

Major- and minor-element contents of the Cambrian alkaline rocks from the McClure Mountain and Gem Park Complexes and the complex at Democrat Creek, in the Wet Mountains area, Colorado, delineate and define three separate and distinct magma groups. According to T. J. Armbrustmacher, the mafic-ultramafic rocks in the Gem Park and McClure Mountain Complexes and the hornblende-biotite-syenite in the McClure Mountain Complex appear to have been derived from an alkali basalt parent; the nepheline syenite, mafic nepheline-clinopyroxene rock, and carbonatite from the McClure Mountain Complex and the carbonatite of the Gem Park Complex appear to have had a more alkaline parent rock such as nephelinite; and the quartz syenite and mafic-ultramafic rock of the complex at Democrat Creek appear to have evolved from a tholeiitic basalt parent. These magma groups also have been defined by initial $^{87}Sr/^{86}Sr$ ratios and rare-earth-element (REE) patterns.

Quartz syenites from the complex at Democrat Creek contain high concentrations of the lithophile elements, Ba, La, Nb, Y, Zr, REE, U, and Th, relative to crustal abundance and relative to the hornblende-biotite syenites and the nepheline syenites from the McClure Mountain Complex. The quartz syenites are depleted in Ba, Sr, and V relative to the other syenites. The nepheline syenites contain high concentrations of Ni, Co, Cr, and V.

The mafic-ultramafic cumulus rocks from the McClure Mountain and Gem Park Complexes typically contain normative nepheline and normative olivine but lack normative quartz and normative hypersthene; this normative mineral assemblage is characteristic of alkali basalt types. The mafic-ultramafic rocks from the complex at Democrat Creek contain abundant normative hypersthene but lack normative nepheline and normative quartz, as would be expected in crystallization from a saturated tholeiitic basalt.

Delineation of the plutons of the Charlotte belt (North and South Carolina) by geophysical anomalies

Distinct anomaly patterns and intensities on the gravity, aeromagnetic, and aeroradioactivity maps of the Charlotte (N.C.–S.C.) 2° sheet reflect differences in lithology and structure of Charlotte belt plutons, according to F. A. Wilson and D. L. Daniels. Deep magnetic and gravity lows and aeroradioactivity highs clearly outline post-metamorphic granitic intrusions such as the Churchland, Landis, and Clover plutons. Magnetic and gravity lows also suggest unexposed postmetamorphic plutons at Berryhill and Huntersville. In contrast, intense magnetic and gravity highs and aeroradioactivity lows define gabbro (Concord, Mecklenburg-Pinesville-Weddington) and metagabbro plutons with equal clarity. Near Cornelious, N.C., coincident positive magnetic and gravity anomalies much broader than a small outcrop of gabbro suggest a larger pluton at depth.

Gravity models suggest that the gabbro complex in Mecklenburg County is a 3.5 to 5 km thick lopolith and that the gabbro at Weddington may also be a part of the "Mecklenburg" complex. Triangular modal plots of troctolite, olivine gabbronorite, and pyroxene-hornblende gabbronorite, as well as chemical analyses of troctolite and olivine gabbronorite, indicate that the "Weddington" grabbo represents the most mafic of the "Mecklenburg" magmas. Magnetic measurements show that the olivine gabbronorite has a high normal remanent magnetism, and exposures of this rock correlate with some of the highest peaks on the large positive magnetic anomaly over the two gabbro plutons.

A small exposure of postmetamorphic granite on the north side of the "Mecklenburg" gabbro lies within a high aeroradioactivity anomaly that partly encircles the gabbro. This suggests that the granite although not exposed within the anomaly elsewhere forms at least a partial ring around the gabbro. The diameter of this partial ring is 13 km, the same as the diameter of the ring of syenite around the "Concord" gabbro to the northeast. The granite around the "Mecklenburg" gabbro is probably part of a ring structure similar to the "Concord" ring structure. Both are interpreted as subsurface parts of volcanic systems.

Melt inclusions in Murchison chondrite meteorite not solar nebula condensates

Studies of the silicate melt inclusion in the Murchison type II carbonaceous chondrite by E. W. Roedder negate some of the previously published theories of its origin and history. The Murchison chondrite meteorite has been studied extensively. It consists of olivine-pyroxene aggregates and isolated crystals, which formed at high temperatures, in a hydrous, carbonaceous matrix, mainly layer lattice silicates, which formed at low temperatures. The olivine crystals contain calcium-alumium-silicate melt inclusions. Several workers have proposed that the melt inclusions represent globules of melt formed by direct (metastable?) condensation from the solar nebula and that the globules were subsequently enclosed, while still viscous, by

olivine crystals growing from a vapor phase (mainly hydrogen) at about 1,170°C and less than or equal to 10–3 atm. Roedder's studies of the inclusions indicate that this theory is incorrect and that the inclusions and the olivine formed from a gas-bearing melt. The evidence is as follows: (1) glass, which is now phyllosilicate, coats the outer faces of some sharply euhedral olivines; (2) pseudosecondary planes of troilite, glass and "vapor" inclusions are found in olivine; and (3) several about 300 μm iron-rich olivines in diameter were found that have thick, almost inclusion-free rims and sharly defined, more magnesian cores that are densely and uniformly crowded (about $5 \times 10^{10} \cdot cm^{-3}$) with < 1 μm in diameter mainly "vapor"-rich inclusions. These observations, and the lines of evidence presented by other workers, are most compatible with a relatively high-temperature, two-stage formation of the olivine crystals from a gas-bearing olivine-rich silicate melt containing some calcium and aluminum, rather than from a vapor phase.

Electron microprobe analyses of minerals in plutonic rocks of the Pioneer batholith, Montana

J. M. Hammarstrom made electron probe analyses of the plutonic rocks of the Pioneer batholith of southwest Montana. The batholith consists of calc-alkalic Cretaceous quartz diorite, tonalite, granodiorite, and granite plutons and Tertiary muscovite granite bodies. All of the Cretaceous rocks contain calcic amphibole, which is magnesio-hornblende by Leake's (1978) nomenclature. Crystal zoning records a complex history for hornblende. In the most mafic rocks, brown hornblende cores are enriched in aluminum and titanium relative to green rims that are enriched in silica. Rim compositions in the most mafic rocks overlap the range of composition observed for green hornblendes in granodiorite and granite with similar, though less pronounced compositional variations.

Brown biotite, intermediate between ideal phlogopite and siderophyllite compositions, occurs in all rocks. Biotite coexisting with magmatic muscovite is rich in aluminum, iron, and manganese relative to biotite coexisting with hornblende. The ratios of iron to magnesium in biotite and hornblende generally increase from south to north independent of rock type. Average titanium content generally decreases with increasing silica content of the host rock. Magmatic muscovite occurs only in the Tertiary granite bodies. It has a higher ratio of sodium to potassium and a lower content of magnesium than muscovite from other areas. The TiO_2 in the magmatic muscovite ranges from 0.5 to 1.1 wt. percent. Both biotite and muscovite are low in halogens.

Plagioclase ranges from An79 in the quartz diorite to An10 in the muscovite granite. Cores are generally An rich relative to rims, but the cores are commonly reverse zoned and separated from the normally zoned rim by a band of sericitic alteration. Textural relations indicate that the plagioclase began to crystallize early in all rocks, and zoning patterns may reflect water pressure variations accompanying the rise of magma to higher levels in the crust. Potassium feldspar is monoclinic, weakly perthitic, and ranges from Or80 to Or95 with barium-enriched cores. Data on the distribution of the albite component between plagioclase and potassium feldspar, using the two-feldspar geothermometry of Stormer (1975), indicates that the Tertiary muscovite granite, which contains perthitic potassium feldspar phenocrysts, crystallized at about 400° to 450°C and that the Cretaceous granite and granodiorite crystallized at about 500° to 550°C.

These values record reequilibration during cooling. Pure magnetite with hematite lamellae is the only opaque oxide mineral observed in the Cretaceous granite and granodiorite. In the Tertiary muscovite granite, similar magnetite is observed as well as an oxidized extremely manganese-rich ilmenite phase and a titanohematite phase. Titanium-bearing phases only occur within or adjacent to magmatic muscovite-biotite intergrowths. Sphene, which is widespread both as euhedral rhombs and as anhedral grains in biotite in Cretaceous granodiorite and granite, deviates from the ideal sphene formula by the substitution of approximately 40 percent of iron and aluminum for titanium.

METAMORPHIC ROCKS AND PROCESSES

Geology of kimberlite

The Willliams kimberlite diatremes of middle Eocene age contain xenoliths of garnet peridotite (olivine + diopside + enstatite + garnet + phlogopite) that have deformed (porphyroclastic) or recrystallized (equigranular) texture. B. C. Hearn and E. S. McGee found that peridotite garnets have a limited range of Mg/(Mg + Fe), 0.78 to 0.87 percent, and have biomodal CaO contents, 4.2 to 4.9 percent and 5.6 to 6.9 percent that correlate with bimodal Cr_2O_3 contents, 0.8 to 3.1 percent (four red and red-orange garnets) and 4.2 to 7.8 percent (14 purple garnets). The gap in CaO and Cr_2O_3 contents of peridotite garnets is filled by some of the purple colluvial garnets (1–2 mm) that may represent types of garnet peridotites that have not yet been found as xenoliths. Nineteen purple colluvial garnets contain 4.5 to 6.1 percent CaO and 2.4 to 6.1 percent Cr_2O_3, and one contains 6.7 percent CaO and 9.9 percent Cr_2O_3. Colluvial pyrope-rich pink, red, and red-orange garnets containing 1 to 3.5 percent Cr_2O_3 may be from peridotites or may be fragments of megacrysts. Purple chromium-rich garnet is the most distinctive tracer mineral for

prospecting for kimberlites containing upper mantle xenoliths and possibly diamonds.

Temperatures and pressures of equilibration of garnet peridotites calculated by various methods based on pyroxene and garnet compositions fall on either side of the graphite-diamond transition curve in the range 900 to 1,320°C and 33 to 48 kbar, and most of these methods suggest an inflected geotherm that is steeper than normal continental geothermal gradients. Garnet peridotites that have porphyroclastic textures tend to show higher temperatures and pressures than peridotites having equigranular textures. Clots of garnet-diopside-spinel rimmed by phlogopite in some peridotites may indicate reequilibration and (or) metasomatism in the garnet-spinel field. The estimated temperatures and pressures represent a combination of static upper mantle conditions and dynamic conditions resulting from the processes of kimberlite generation.

Hydration reactions during retrograde metamorphism

R. F. Sanford has considered hydration reactions that occur during retrograde metamorphism of igneous or high-grade metamorphic rocks. These reactions show systematic effects due to the lowering of water pressure (PH_2O) below that of pure water at the same temperature and total (rock) pressure (Pt). These effects are (1) equilibrium phase relations are limited to small domains; larger domains may be characterized by more phases than are possible, according to the phase rule, (2) more phases are possible in an equilibrium assemblage during retrograde metamorphism (where, generally, $PH_2O < pt$), than during prograde metamorphism of H_2O-bearing rock (where $PH_2O = pt$), (3) the fluid and minerals tend to be enriched in species that preferentially partition into the fluid, (4) halides and other very soluble phases may precipitate along grain boundaries (5) enrichment of a rock in components that preferentially partition into the fluid is selective, according to the amount of water available for hydration; partially altered rock will show the greatest enrichment. All these features are observed in serpentinized ultramafic rocks. For example, during prograde metamorphism the sequence, chrysotile → antigorite → forsterite (± brucite or talc) is common, but the retrograde sequence is typically forsterite = chrysotile (± brucite or talc). The antigorite stability field may be bypassed commonly because of low PH_2O. Also serpentinites commonly are enriched in chlorine, boron, uranium and other elements that suggest alteration by sea water. Because the fluid phase leaves a signature of its composition in the rock during hydration, it is a potential indicator of the paleocomposition of hydrothermal and metamorphic fluids.

STATISTICAL GEOCHEMISTRY AND PETROLOGY

Trace element partitioning in some micas from the Spokane Formation

Principal components analysis of chemical data on 26 samples of copper-bearing quartzite from the Spokane Formation of Ravalli Group of Belt Supergroup of western Montana by J. J. Connor suggests that the mica in these rocks controls the distribution of 17 elements, including the major cations aluminum, potassium, magnesium, and half of the iron. Petrographic analysis reveals that the dominant mica is illitic, mostly sericite; subordinate muscovite and chlorite are also present. An attempt to determine the partitioning of 13 other elements between two mica phases (sericite-illite-muscovite and chlorite) was undertaken using regression equations of the sort: X = A + B(illite) + C(chlorite), where X is an estimate of the amount of the element in the whole rock, and illite and chlorite are normative quantities (illite computed with 7 percent K_2O and chlorite with 20 percent MgO and 20 percent FeO). The variations in Co, Ni, Sc, Mn, and Zn are explained adequately by equations of this kind, and the coefficients (B and C) suggest the following partitions among the two phases (in parts per million):

	Illite	Chlorite
Cobalt	<1	200
Nickel	8	260
Scandium	10	110
Manganese	<1	7600
Zinc	35	1500

Chlorite appears to accommodate a much larger volume of these ions than does the illitic suite.

Pioneer batholith

L. W. Snee and A. T. Miesch have used extended *Q*-mode factor analysis to develop a differentiation model to explain the chemical variation among 104 samples of granitic rocks (mostly diorites, granodiorites, and quartz monzonites) from the Pioneer batholith of western Montana. The differentiation model includes five end-member phases: (1) a parent magma, (2) a partial melt from the crust, (3) an assemblage of plagioclase, magnetite, and ilmenite, (4) an assemblage of hornblende, plagioclase, magnetite, and ilmenite, and (5) a potash-rich residual fluid. The compositions of all 104 samples can be approximated closely by mixing the parent-magma composition and the composition of the partial melt, subtracting mixtures of the two mineral assemblages, and then adding or subtracting small

amounts of the residual fluid. An alternative model that fits the data equally well in a mathematical sense calls for total assimilation of gneissic rocks rather than incorporation of partial melt and, therefore, is less acceptable.

Granitic rocks of California and Alaska

A *Q*-mode principal components analysis of chemical data on 228 samples of granitic rocks from the Sierra Nevada shows that the data can be well represented as a four-dimensional vector system; the average sample vector communality is 0.9976. This property of the Sierran rocks was noted previously by Miesch and Reed (1979), who also developed from the principal components models similar but independent petrogenetic (differentiation) models for both the Sierra Nevada batholith and the batholith of the Alaska-Aleutian Range. Recent work by A. T. Miesch revealed that the four-dimensional vector space defined by the data for the Sierra Nevada also may be used to define vectors representing the compositions of granitic rocks from both the Alaska-Aleutian Range and from southern California. When vectors representing the compositions of 158 samples from the Alaska-Aleutian Range are projected into four-dimensional space, the average vector communality is 0.9954. When vectors representing the compositions of 480 samples of granitic rocks from the Traverse and Peninsular Ranges of southern California (data from A. K. Baird, Pomona College, Calif., 1980, unpub. data) are projected into the same space, their average vector communality is 0.9950. Attempts to represent the compositions of other granitic rocks, such as those from the Pioneer batholith in western Montana, in the same vector space yield communalities far below these average values. Thus, the results attest to the close chemical similarity among the three groups of granitic rocks from California and Alaska not only in the abundance of each chemical constituent, but in the covariation among the constituents.

Test for geochemical anomalies

A new statistic has been proposed by A. T. Miesch for estimating the geochemical threshold and its statistical significance. The statistic is calculated as the product of the difference between two adjacent values in an ordered array and the expected frequency at the mean of the two values. The values in the ordered array are geochemical values transformed by either ln(x-k) or ln(k-x) and then standardized so that the mean is zero and the variance is unity. The expected frequency is taken from a fitted normal curve with unit area. Adjusted gaps that exceed corresponding critical values may be taken as estimates of the geochemical threshold, and the associated probability indicates the likelihood that the threshold is real. The adjusted gap test may fail to identify threshold values if the variation tends to be continuous from background values to the higher values that reflect mineralized ground. However, the test will serve to identify other anomalies that may be too subtle to have been noted by other means.

Geochemistry of flint clays

Flint clays are unusually hard sedimentary rocks made up chiefly of kaolinite. Such clays are associated at many places with diaspore and boehmite, or contain small admixed amounts of these minerals, according to H. A. Tourtelot and J. G. Boerngen. The origin of such clays is complex but is generally interpreted to involve the progressive leaching of alumnosilicate minerals, and other clay minerals, to form kaolinite. Silica is then leached from the kaolinite to form diaspore and boehmite. The small amounts of fluxing elements in the clays make them suitable for the manufacture of refractory products that are stable under high-temperature industrial uses.

The composition of the flint clays is consistent with their formation by leaching for most trace elements but not for lithium. Using the criterion of differences larger than a factor of two, elements such as Zr and Nb that occur in resistant minerals are enriched in flint clays compared to the average shale, and Ti, Cr, Ga, and Nb are enriched in diaspore-boehmite compared to flint clay.

R-mode factor analysis identified three factors that account for 50 percent or more of the variability of most elements. Ti and Cr are strongly associated together, along with Co, Ni, Nb, and V, to constitute a factor related to the presence of resistate minerals. Fe, Mn, and Zn are associated in a second factor, strengthening the field impression that these elements are secondary additions to the deposits in Missouri. The third factor consists of Ce, Ln, Eu, Y, Yb, Ba, Pb, and Sr, elements that occur together in alumnophosphate minerals that are present in some samples in amounts estimated to be larger than 50 percent. The alumnophosphate minerals seem to have formed in situ by combination of minor constituents that had become concentrated by leaching.

The trace elements Li, B, Mg, and K are a coherent group of elements on factor plots but seem equally related to the resistate mineral factor and to the alumnophosphate factor. Lithium is a principal cation in dioctahedral chlorite identified in both flint clay and diaspore-boehmite samples by X-ray diffraction, and the associated elements are common cations in dioctahedral chlorite.

It does not seem likely that lithium, one of the most mobile trace elements, could have been incorporated in dioctahedral chlorite during progressive leaching that formed flint clay. One alternative is that the

dioctahedral chlorite is a remnant of precursor materials that were leached to form the flint-clay assemblage that we see today. The possible origin of such precursor materials is unknown. Another alternative is that this unusual mineral represents the alteration of flint clay after the deposits were formed. No basis for a choice between these alternatives is yet evident.

ISOTOPE AND NUCLEAR GEOCHEMISTRY

ISOTOPE TRACER STUDIES

Alteration and mobility of elements in Sherman Granite

Chemical, isotopic, radiographic, and rock-leaching data are combined to describe the effects of rock-water interactions in petrographically "fresh" Sherman Granite of Proterozoic Y age in Wyoming. The data serve to identify sensitive indicators of incipient alteration and to estimate the degree, pathways, and timing of element mobilization. The results can be applied to evaluate the geochemical stability of waste disposal sites in granite and to relate the degree of alteration to the mobility of elements of economic interest. Unfractured Sherman Granite is remarkably fresh by most chemical or isotopic measurements of this study. Incipient alteration of unfractured whole-rock samples is best indicated by the abundance and distribution of uranium and the degree of radioactive equilibration of uranium with its decay products. Anomalously variable uranium abundances, which are also out of equilibrium with lead decay products, indicate remobilization of some (3–60 percent) orginal uranium in late Phanerozoic time. Association of uranium with secondary alteration products confirms the fact of remobilization. Near-surface leaching of uranium and reconcentration at depth is suggested by whole-rock analysis and confirmed by isotopic measurements of uranium-lead and uranium decay series disequilibria. The latter measurements indicate that simliar transport pathways are followed today but at a very slow rate. The amount of apparent uranium mobility in unfractured Sherman Granite is small compared to the results of similar studies of Archean granites from nearby localities. Experiments confirm that uranium is preferentially leached from freshly crushed Sherman Granite and that leachable uranium sites are close to the solid/liquid interface; perhaps as uranium along grain boundaries, crystal defects, or cleavage traces of minerals that exclude uranium from their structure. Access of solutions to Sherman Granite is fracture controlled and fracture-zone materials show clear petrographic, chemical, and isotopic evidence of alteration and multielement redistribution.

Strontium isotopic study of rhyolites, Chihuahua, Mexico

M. A. Lanphere, working with K. L. Cameron and Maryellen Cameron of the University of California at Santa Cruz, carried out a strontium isotopic study of voluminous rhyolitic ignimbrites and related rocks in the Batopilas area of western Chihuahua, Mexico. The middle Tertiary ignimbrites of the Sierra Madre Occidental of western Mexico form the largest continuous rhyolitic province in the world. Minor amounts of intermediate lavas occur interlayered with the ignimbrites, and strontium isotope data on the complete range in rock compositions must be considered when evaluating hypotheses for the origin of the rhyolites. Inital $^{87}Sr/^{86}Sr$ ratios of andesites, dacites, and rhyolites lie in the range 0.7042 to 0.7050, showing no systematic variation with rock composition. These data support a crystal fractionation hypothesis for the origin for the voluminous rhyolitic ignimbrites.

Strontium isotopic study of Samail ophiolite, Oman

M. A. Lanphere, working with R. G. Coleman, Field Geochemistry and Petrology Branch, and C. A. Hopson, University of California at Santa Barbara, measured rubidium and strontium concentrations and strontium isotopic compositions in 41 whole-rock samples and 12 mineral separates from units of the Samail ophiolite, including peridotite, gabbro, plagiogranite, diabase dikes, and gabbro and websterite dikes within the metamorphic peridotite. Ten samples of cumulate gabbro from the Wadi Kadir section and nine samples from the Wadi Khafifah section have mean $^{87}Sr/^{86}Sr$ ratios and standard deviations of 0.70314 ± 0.00030 and 0.70306 ± 0.00034, respectively. The dispersion in strontium isotopic composition may reflect real heterogeneities in the magma source region. The average strontium isotopic composition of cumulate gabbro falls in the range of isotopic compositions of modern midocean-ridge basalt. The $^{87}Sr/^{86}Sr$ ratios of noncumulate gabbro, plagiogranite, and diabase dikes range from 0.7034 to 0.7047, 0.7038 to 0.7046, and 0.7037 to 0.7061, respectively. These higher $^{87}Sr/^{86}Sr$ ratios are due to alteration of initial magmatic compositions by hydrothermal exchange with seawater. Mineral separates from dikes that cut harzburgite tectonite have strontium isotopic compositions, which agree with that of cumulate gabbro. These data indicate that the cumulate gabbro and the different dikes were derived from partial melting of source regions that had similar long-term histories and chemical compositions.

Neodymium and lead isotopic study of Hawaiian volcanic rocks

The neodymium and lead isotopic data for Hawaiian volcanic rocks are judged by Mitsunobu Tatsumoto to

indicate that each of the five volcanoes on Hawaii has a distinct isotopic character and that the Mauna Loa and Mauna Kea trends are also isotopically distinct from one another. The neodymium and lead isotopic composition of basalt from the Loihi Seamount suggests that this seamount belongs to the Mauna Loa group. The neodymium and lead isotopic data show that the Hawaiian volcanic rocks did not originate from an isotopically homogenous source, but neither did they originate from randomly heterogeneous mantle. The regular increase in radiogenicity of lead and neodymium towards the southern (younger) volcanoes observed in both the Mauna Loa and Mauna Kea loci, the preservation of isotopic identities for each volcano, and the positive correlation of lead and neodymium isotopes indicate mixing of sources.

Neodymuim isotopic study of kimberlites

Neodymium-isotopes provide important information about the source region of the alkalic ultrabasic kimberlites, the only rock type known to be derived from 200 km in the mantle. The initial $^{143}Nd/^{144}Nd$ ratios of kimberlites, ranging in age from 90 m.y. to 1,300 m.y., from South Africa, India, and the United States, are identical to those ratios in the basaltic achondrite, Juvinas, which represents the bulk chondritic earth in rare-earth elements. This correlation strongly indicates the existence of primeval mantle beneath these continents. Further, carbonatite and melilite basalt from the Cape Verde Islands in the Atlantic Ocean show identical chondritic signature in their $^{143}Nd/^{144}Nd$ ratios, indicating the presence of a primeval layer also in the suboceanic mantle. The neodymium isotopic study of ultramafic xenoliths in both kimberlites and alkali basalts clearly shows that kimberlites are derived from a different (deeper) source than the included xenoliths.

Hafnium isotope variations in oceanic basalts

Routine low-blank chemistry and 0.01 to 0.04 percent precision on the ratio $^{176}Hf/^{177}Hf$ allows study of hafnium isotopic variations, generated by beta-decay of ^{176}Lu, in volcanic rocks derived from the suboceanic mantle. The $^{176}Hf/^{177}Hf$ ranges from 0.2828 to 0.2835, based on 24 basalt samples. The $^{176}Hf/^{177}Hf$ is positively correlated with $^{143}Nd/^{144}Nd$, and negatively correlated with $^{87}Sr/^{86}Sr$ and $^{206}Pb/^{204}Pb$. Along the Iceland-Reykjanes ridge traverse, $^{176}Hf/^{177}Hf$ increases southwards. Sixty percent of the hafnium isotopic variation in oceanic basalts occurs among midocean ridge samples. Lutetium-hafnium fractionation probably decouples from samarium-neodymium and rubidium-strontium fractionation in very depleted source regions, with high lutetium-hafnium, and consequent high $^{176}Hf/^{177}Hf$ ratios developing in mantle residual from partial melting.

Strontium isotopic study of Oregon graywackes

Strontium isotope data collected a number of years ago were re-evaluated to address the provenance problem for lower Tertiary (Eocene) "Flournoy" graywackes (formerly Umpqua Formation) of southwestern Oregon. The Rb/Sr and $^{87}Sr/^{86}Sr$ in graywacke samples are highly correlated to produce a false isochron of about 160 m.y. (three times the depositional age). These systematics are interpreted to have derived from mixing of detritus from two fundamentally different sources—a mafic source with low Rb/Sr and strontium isotope ratios, and a felsic source, probably dominated by Mesozoic supracrustal rocks. Data for overlying graywackes of the Tyee Formation show a distinct isotopic departure from those of the "Flournoy" graywackes generally having higher strontium isotope ratios at the same Rb/Sr values. The isotopic data for the Tyee wackes are coincident with a trend defined by modern sands of the Columbia River. These sands represent a complex provenance including Precambrian rocks of western Idaho and Montana. The sudden change in the strontium isotopic character of turbidite sands in the Eocene is compatible with a postulated clockwise rotation of western Oregon in early Tertiary time. "Flournoy" graywackes were derived largely from the Klamath Mountains and emergent island arcs and oceanic islands. Rotation of this microplate brought the basins into a position to receive detritus from emergent borderlands in eastern Oregon, Idaho, and Montana.

Strontium isotopes in Paleozoic conodonts

Jack Kovach assessed the feasibility of using conodonts to determine the strontium isotopic composition of seawater in the geologic past. The study provided data for middle and late Paleozoic seawater variations.

The conodonts are extremely enriched in strontium (1,500 to 20,000 ppm) and contain negligible rubidium. The isotopic data define several excursions in $^{87}Sr/^{86}Sr$ hitherto unknown. Additional work with R. E. Zartman indicated the potential of using conodonts for U-Pb dating.

Lead-isotope evolution

A model of lead-isotope evolution was developed by R. E. Zartman and B. R. Doe that allows growth curves to be calculated for various geologic environments. This approach to modeling a chemically evolving Earth has been termed "plumbotectonics" in order to emphasize the dynamic interaction envisioned to take place among crustal and mantle reservoirs. The theoretical

background of plumbotectonics and a detailed comparison with observed rock and ore data were completed previously. Now a mathematical derivation of the model that generated the lead growth curves is complete. Some of the numerical parameters are examined in light of current rock and ore data. An HP 9830A BASIC Language Program for plumbotectonics is also complete.

Strontium isotopic study of Marysvale volcanic field, Utah

In conjunction with C. G. Cunningham and T. W. Stevens, C. E. Hedge determined initial Sr^{87}/Sr^{86} ratios for 32 samples from the Marysvale volcanic field, Utah. The range in values is quite limited—0.7044 to 7078. The early (30–21 m.y.) volcanic units of intermediate composition have initial Sr^{87}/Sr^{86} ratios in the range of 0.7050 to 0.7062; and this small variation is, at least in part, a function of geographic location. Most of the latter (21–17 m.y.) more siliceous units have initial Sr^{87}/Sr^{86} ratios like the earlier intermediate rocks. The few exceptions are strontium-poor rhyolitic rocks that may have assimilated a small amount of radiogenic strontium as they differentiated in high-level magma chambers. Basaltic lavas that erupted after the rhyolites show progressively lower initial Sr^{87}/Sr^{86} ratios with the passage of time. The youngest basalt that has been analyzed (7 m.y.) has an initial Sr^{87}/Sr^{86} of 0.7044, whereas the older basalts have values like the intermediate volcanic rocks.

STABLE ISOTOPES

Stable isotope and fluid inclusion study of Thompson Creek and Little Boulder Creek molybdenum deposits

A light-stable isotope and fluid inclusion investigation is being conducted on the Little Boulder Creek and Thompson Creek molybdenum deposits, Custer County, Idaho, by W. E. Hall and J. N. Batchelder. Homogenization and freezing temperature measurements of fluid inclusions indicate temperatures of homogenization from 371° to 377° ± 3°C and salinities estimated to be approximately 5 to 20 equivalent wt percent-NaCl. The $\delta^{18}O$ values for quartz range from +10.7 to +11.2 and for water calculated to be in equilibrium with quartz range from +4.7 to +5.3 per mil. The δD values of fluid inclusion water from quartz range from −121 to −83 per mil. Sulfide minerals analyzed for $\delta^{34}S$ range from +9.6 to +11.4 per mil. These preliminary data indicate that both deposits likely had ore fluids comprised of both meteoric and magmatic waters. Thompson Creek may have had as much as 60 to 90 percent magmatic water and Little Boulder Creek as much as 35 percent magmatic water. Sulfur in both deposits was likely derived from the surrounding Paleozoic rocks.

Oxygen isotope systematics of Basin and Range granites

The oxygen isotope composition of granitoid rocks of the Basin and Range province has been studied by D. E. Lee, I. Friedman, and J. D. Gleason. The $\delta^{18}O$ values determined for 115 randomly selected plutons range from 0.6 to 13.4 per mil. The average $\delta^{18}O$ value for 115 samples is 8.5, the mean, 8.6. These average and mean values are similar to those reported for other areas such as the Canadian Precambian shield (Shieh and Schwarcz, 1978), the Peninsular Ranges batholith of southern and Baja California (Taylor and Silver, 1978), and the New England batholith of Australia (O'Neil and others, 1977).

The Basin and Range results differ from those of most other regional studies in two respects, the extreme range of $\delta^{18}O$ values and the apparent lack of any systematic distribution of those values. The $\delta^{18}O$ values of the Peninsular Ranges batholith of California increase from west to east (Taylor and Silver, 1978). On the northeastern coast of Baffin Island, quartzofeldspathic rocks (20 samples) show higher $\delta^{18}O$ values (9.0) concentrated in the northwest and lower values (7.7) in the southeast over an area about 600 km long (Shieh and Schwarcz, 1978). In the large New England batholith of Australia, each of four different granite suites is characterized by a particular range of $\delta^{18}O$ values (O'Neil and others, 1977). The extreme range and haphazard geographic distribution of the $\delta^{18}O$ values of the Basin and Range area probably result from the complex history and tectonic framework of the area.

ADVANCES IN GEOCHRONOMETRY

Uranium series ages from western Missouri

Isotopic fractionation between ^{234}U and ^{238}U as great as 1,600 percent has been measured in spring waters, sediments, and fossils in the Pomme de Terre River Valley, Western Ozark Highland, Missouri. The activity ratio of $^{234}U/^{238}U$ in five springs ranges from 7 to 16. Analyses of two samples of organic sand at one of these springs, Trolinger Spring, have yielded $^{234}U/^{238}U$ ratios of about 13.6 and $^{230}Th/^{234}U$ uranium-series ages of 33,000 and 37,000 yr B.P. Clayey units overlying the organic sand are enriched in ^{230}Th relative to its parent ^{234}U; the excess ^{230}Th in these deposits is as great as 700 percent. Fossil bones in the clayey and sandy peats have yielded uranium-series ages between 15,000 and 76,000 yr B.P. The results indicate that ^{234}U-enriched uranium flux has been percolating through the sediment of Trolinger Spring during about the last 100,000 yr. The mechanism of uranium and thorium isotopic fractionation between the water phase and the solid phase appears to be governed by absorption of ^{230}Th, and the precursors of ^{234}U, ^{234}Th, and ^{234}Pa, on surfaces of

particulate matter at the interface. Beta decay of short-lived ^{234}Th and ^{234}Pa would leave some of their daughter ^{234}U atoms implanted on particulate matter. Given sufficient geologic time, this daughter-emplacement mechanism would result in solids that have $^{234}U/^{238}U$ and $^{230}Th/^{234}U$ activity ratios significantly higher than the equilibrium value.

Isotopic studies of the Sherman Granite

Z. E. Peterman completed a study of cores from the Sherman Granite in collaboration with R. A. Zielinski, J. N. Rosholt, J. S. Stuckless, and I. T. Nkomo. The granite is mineralogically fresh, relatively unstrained, and has been thermally undisturbed since its emplacement. Whole-rock Rb-Sr and Pb-Pb ages agree at 1.42 b.y. However, U-Pb systems show evidence of isotope mobility at ingress of water coincident with the Laramide orogeny. For the most part, uranium series data show equilibrium indicating that uranium mobility is occurring at a very slow rate.

Geochronology of Precambrian rocks, Hartville uplift, Wyoming

A detailed geochronologic study by Z. E. Peterman of Precambrian units in the Hartville uplift of eastern Wyoming is nearing completion. The results allow establishment of a provisional chronostratigraphy for comparison and correlation with adjacent regions in Wyoming, Colorado, and South Dakota. K-Ar and Rb-Sr mineral ages have been lowered as a result of an ill-defined thermal event in middle-Proterozoic time. Whole-rock Rb-Sr and U-Pb zircon ages define the following events: (1) emplacement of the granite of Haystack Range at 1.72 b.y. (2) intrusion of the diorite of Twin Hills at 1.74 b.y., (cut by granite of Haystack Range), (3) granite of Flattop Mountain, 1.97 b.y., and (4) granite of Raw Hide Butte, 2.60 b.y. A supracrustal sequence of dolomite, metagraywacke and pelitic schist, and pillow basalt is Archean in age as defined by intrusive relations with the granite of Raw Hide Butte. Samples from three outlying areas suggest the presence of older gneiss, perhaps about 2.9 b.y. old. The age for the granite of Flattop Mountain remains tentative. This intrusion is in proximity to the granite of Raw Hide Butte and intrudes the supracrustal sequence. The age is deduced from a five-point isochron with an unusually high strontium-isotope initial ratio. At present, the systematics could be inferred to indicate a metamorphic rotation of the isochron, but it is geologically more likely that the unit is crustally derived.

Thermal history of the Tejon Oil Field, California

N. D. Briggs and C. W. Naeser, in cooperation with T. H. McCulloh, have been studying the thermal history of the Tejon Oil Field area (southern San Joaquin Valley, Calif.), using fission-track dating. The Tejon area is divided by the seismically active White Wolf fault. Detrital apatite and zircon separated from Eocene to Miocene sandstones recovered from deep drill holes on both sides of the fault have been dated. The fission-track data show that apatite in the downthrown block immediately northwest of the fault is totally annealed at a maximum paleotemperature (reconstructed from laumontite geothermometry) of 135° to 140°C, suggesting heating of 1 m.y. duration. The higher paleotemperature (greater than 150°C) indicated for total annealing of apatite in the upthrown block shows that these samples could have been at the suggested maximum paleotemperatures for no more than 100,000 yr. These conclusions are consistent with the thermal history suggested by laumontite crystallization viewed in terms of stratigraphic and structural evidence.

Geochronology of southeastern New England

R. E. Zartman and R. S. Naylor (Northeastern University) summarized a decade of geochronologic work in southeastern New England. The U-Th-Pb zircon, Rb-Sr whole-rock, and K-Ar hornblende isotopic ages reveal two major episodes of igneous activity—one occuring in Proterozoic Z time (600–650 m.y. ago) and the other in Ordovician to Devonian time (445–375 m.y. ago). The dated rocks are from several individual structural provinces, which evolved more or less independently of each other prior to middle to late Paleozoic assembly. These provinces generally are bounded by major and (or) abrupt changes in metamorphic grade, and from east to west, include (1) the Boston platform, (2) The Putnam-Nashoba block, (3) the synclinorium, and (4) the Bronson Hill anticlinorium. From this and other recently published studies, reasonably accurate ages representative of the two major episodes can now be assigned to some of the igneous rocks.

K-Ar dating of clinker

Two potassium-bearing phases associated with clinker formation were analyzed by J. D. Obradovich, D. A. Coates, and J. R. Herring to determine the possibility of dating clinker by the K-Ar method. Several potential problems were identified: (1) incomplete degassing of feldspar crystals (either plagioclase or sanidine if formed), (2) incorporation of excess radiogenic argon, and (3) incorporation of extremely large amounts of air argon, which would make dating of young clinkers difficult. A sample of plagioclase recovered from clinker had an air argon-40 content of 1.4×10^{-10} moles/gm. Although high, this content is within the range of values

found for volcanic plagioclases. The radiogenic argon content per gram was determined to be 1.75×10^{-13} moles/gm (approx. 0.08 percent). Assuming a value of 0.3 potassium, it would be reasonable to say that the time of clinker formation is younger than 300,000 yr. A sample of buchite (similar to banded rhyolitic obsidian) from the Ferron Sandstone Member of Mancos Shale had an air argon-40 content of 2.4×10^{-11} moles/gm, well within the range found for obsidians and welded vitrophyres from Yellowstone National Park. No detectable radiogenic argon could be measured; and, in the extreme, it could be said that this sample is within the range of ^{14}C dating. The following conclusions, although based on only two samples, might be drawn: (1) Old feldspars (plagioclase) in the sediments are totally outgassed at the time of coal burning. (2) Excess radiogenic argon is not incorporated into the silicate melt (formation of buchite). (3) Reasonable levels of air argon-40 are associated with the samples 1×10^{-10} to 3×10^{-11} moles/gm. (4) Dating of plagioclase from clinker over 0.5 m.y. old is feasible. Dating of buchite over 0.1 m.y. old is feasible. (5) Sanidine formed during coal burn needs to be studied.

GEOTHERMAL SYSTEMS

Subsurface structure and geology of the Raft River geothermal area, Idaho

H. D. Ackermann and H. R. Covington interpreted five seismic reflection lines run in the area of the Raft River geothermal anomaly to better define the subsurface geology and structure of the KGRA. Reflectors within the Cenozoic basin fill indicate a complex depositional and structural history. In the area of the KGRA, beds dip steeply basinward, and abundant basinward-dipping faults can be seen. Near the center of the basin east of the KGRA, reflectors are nearly horizontal in the upper part and only gently dipping in the deeper part of the Cenozoic basin fill. Faults are sparse and apparently gently east dipping in the central and eastern parts of the basin. Precambrian basement surface that floors the Raft River basin slopes gently eastward and apparently is not offset by any of the faults mapped at the surface or indicated by reflectors. The seismic profiles suggest that the Bridge and Horse Well fault zones, on the western side of the basin, are clusters of sympathetic faults. These faults are steep ($> 60°$) in their upper parts and flatten with depth until they parallel the eastward-dipping basement surface where they come in contact with it. The geologic and structural implications that can be drawn from these profiles are (1) the Bridge and Horse Well fault zones are growth type faults resulting from movement along a detachment zone at the Precambrian-Cenozoic interface, and (2) the western part of the basin is much younger than the eastern part of the basin.

Geothermal potential of the San Francisco volcanic field, Arizona

Geologic studies of the San Francisco volcanic field by E. W. Wolfe and G. E. Ulrich have revealed several lines of evidence that focus interest on the central and eastern parts of the San Francisco volcanic field, Arizona, as a hot dry rock geothermal prospect. Ages of San Francisco field lavas in general range from about 6 m.y. to less than 1,000 yr B.P. However, combined data from field relations, magnetic polarity determinations, and K-Ar ages show that Brunhes-age (< 0.73 m.y.) volcanism is strongly concentrated in the central and eastern part of the volcanic field. This area includes San Francisco Mountain, an andesitic to dacitic stratovolcano (1.0 to 0.22 m.y.), the related O'Leary Peak silicic center (0.24 to 0.17 m.y.), and numerous basaltic vents to the north and east, the great majority of which are also of Brunhes age.

Analysis of P-wave residual data by D. A. Stauber (1980) shows a travel-time residual pattern suggesting a low-velocity body centered at 20 km under San Francisco Mountain, which may be caused by a magma conduit or reservoir for the surface volcanism. Magnetotelluric data (Ware, 1980) indicate possible conductors that may be related to hot or partly molten rock at depth in the vicinities of some of the younger basalt and basaltic andesite vents east of San Francisco Mountain.

First computer simulation of an evolving geothermal system

Computer simulation of the evolution of vapor-dominated geothermal systems using SHAFT 79 (simultaneous heat and fluid transport) was begun by A. H. Truesdell in collaboration with Karsten Preuss (Lawrence Berkeley Laboratory). In the simulation, a cylindrical system 10 km in diameter by 2.4 km deep in half section with 30 elements was heated by a 78.5 MW source. The system had the following parameters: A 10°C water-saturated surface; insulating, no flow sides and bottom; a 100-mD permeability reservoir; and a 1-mD caprock. The system reached a steady state after 148,000 yr with 250°C in the center and 195°C at the edges without boiling. Reducing the permeability of the caprock to 0.3 mD produced a steady state after an additional 107,000 yr with a vapor-dominated layer at the top of the reservoir.

The simulation shows several mechanisms operative at different stages in the evolution of the system: (1) initiation of intense reservoir-wide convection by means of a positive feedback between convective heat transport and reduction in fluid viscosity, and (2) the lateral

spreading of boiling by means of displacement of upward convection away from two-phase zones.

The steady state demonstrates many features inferred from natural systems, including (1) vertical counterflow of steam and liquid water with steam rising and condensate falling; (2) lateral movement of steam from the center toward the edges of the system; (3) condensation of steam due to upward conductive heat loss with condensate draining downwards to a liquid-dominated zone where it flows toward a central zone of boiling; (4) an interface between a shallow, liquid-saturated zone and the vapor-dominated zone that is at a temperature near the enthalpy maximum of saturated steam (236°C); and (5) boiling in the central part of the underlying liquid-dominated zone with boiling rates increasing with depth to a maximum close to the bottom of the two-phase zone.

Geomagnetic variations in the Cascades

Extensive observations of geomagnetic field variations were made by J. N. Towle over the Cascade Range on the Medicine Lake volcanic highlands–Mount Shasta region and in the vicinity of Mount St. Helens. Preliminary processing indicates that this data should outline the extent of an electrically conductive region that may be associated with a regional gravity low in the Medicine Lake-Mount Shasta region. An array of instruments was deployed to monitor geomagnetic activity on Mount St. Helens through the fall and winter (1980–81) to detect possible volcano-magnetic effects and anomalous telluric current channeling.

Electrical properties of basalt and granite

G. R. Olhoeft completed a series of measurements of the electrical properties of wet and dry basalt and granite. The only significant parameters controlling the electrical properties of silicates are water content and temperature. To produce a one order of magnitude change in the electrical resistivity of a dry silicate at 1,000°C, the oxygen fugacity must be changed by more than 6 orders of magnitude, or the dry hydrostatic pressure by 1300 MPa, or the temperature by 55°C, or the water content by 0.3 wt percent. At lower temperatures, the effects of water are even more pronounced. Further, the water must be present as free water, not structural water as in amphiboles, thus indicating the need for more water in the deep crust than is commonly accepted.

Crustal structure beneath the Kona coast of Hawaii

Combined analyses of gravity and seismic data from a 100-km-long profile of marine shots perpendicular to the Kona coast off Hawaii by J. J. Zucca and D. P. Hill suggest that the Moho is at a depth of nearly 20 km beneath the north flank of Mauna Loa. The depth decreases to about 14 km beneath the Kona coast and to about 10.5 km beneath the deep seafloor west of the Kona coast. The bulk of the crust along this profile is composed of high velocity (Vp about 7.0 km/s) and high density (2.9 g/cm^3) material. The gravity data suggest the presence of a high-density cylindrical structure trending roughly north-south along the Kona coast, possibly related to a buried rift zone of Hualalai volcano. Traveltime data from the profile of shots as well as relative delays from teleseismic sources are consistent with this interpretation.

Earthquake activity patterns in the Yellowstone–Hebgen Lake region, Wyoming and Idaho

The pattern of earthquake activity in the Yellowstone–Hebgen Lake region from 1973 to 1980 suggests that the seismicity is not simply part of an east-west trend extending into central Idaho. The north-trending Gallatin Range on the west side of Yellowstone has few earthquakes and no swarm-type activity. East of the Gallatin Range, seismicity is high, and swarm-type activity is common. The earthquakes appear to occur on north-to-northwest-trending faults observed north and south of the Yellowstone caldera, which probably extend across the caldera beneath volcanic flows. West of the Gallatin Range in the Hebgen Lake region, earthquakes occur along an east-west trend. Swarm-type activity is common. Fault-plane solutions in the Hebgen Lake region and further west indicate north-south extension. Within and east of the Gallatin Range, fault-plane solutions indicate northeast-southwest extension. This suggests an abrupt change in tectonic processes at the west edge of Yellowstone rather than a continuous east-west zone of earthquake activity.

Evolution of lava fields along the Great Rift, eastern Snake River Plain, Idaho

A multifaceted approach involving field, paleomagnetic, radiocarbon, and petrochemical studies by D. E. Champion, M. A. Kuntz, R. H. Lefebvre, and E. C. Spiker was used to investigate the evolution of three late Pleistocene to Holocene basalt lava fields that lie along the Great Rift in southern Idaho. The Great Rift is a volcanic rift zone from 1 to 9 km wide, consisting of a set of volcanic vents, eruptive fissures, and open cracks that extend 85 km across the eastern Snake River Plain. Three lava fields are aligned along the trend of the Great Rift.

The Craters of the Moon (COM) lava field is a composite feature; it consists of more than 40 lava flows that erupted from more than 25 cinder cones and fissure vents, most of which are located in Craters of the Moon National Monument. Stratigraphic, radiometric, and paleomagnetic data indicate that the lava flows of the

COM field were erupted in seven distinct intervals. The eruptions that formed the COM field began about 15,000 yr ago and ended 2,100 yr ago. Durations of eruptive intervals were as long as 1,000 yr or as short as about 100 yr and were separated by periods of dormancy that lasted from about 100 yr to 3,500 yr each. The petrochemical data indicate that COM lavas fractionated with time. The oldest lavas have SiO_2 contents of 44 to 47 percent; the youngest 47 to 63 percent.

The Kings Bowl lava field is made up of flows erupted during a single volcanic episode from fissures on the southern part of the Great Rift. The Wapi lava field is a broad shield volcano with a vent located at Pillar Butte on the southern part of the Great Rift. Paleomagnetic data indicate that the lava flows of the Wapi and Kings Bowl lava fields were erupted simultaneously in an interval of a few tens of years or, possibly, one as short as several weeks or months, about 2,100 yr ago.

Petrology and evolution of central Snake River Plain, Idaho, rhyolites

P. L. Williams and H. R. Covington found that calc-alkalic rhyolites make up the entire suite of silicic volcanic rocks from the central part of the Snake River Plain region that range in age from 7.0 to about 15 m.y. old. These rocks, which predate most of the basalts on the Snake River Plain, are predominantly densely welded ash-flow tuffs and subordinate lava flows. The rhyolites are from at least three eruptive centers, yet are quite uniform in chemical and modal composition. Average content of major oxides (calculated water free) is SiO_2, 73 percent; Al_2O_3, 13 percent; total iron as FeO, 3.5 percent; MgO, 0.4 percent; CaO, 1.5 percent; Na_2O, 2.9 percent; K_2O, 5.3 percent; and TiO_2, 0.5 percent. Phenocrysts, less than 15 percent of most rocks, are mostly plagioclase (An 32) and subordinate quartz; potash feldspar is rare. Mafic minerals are entirely clinopyroxenes and opaque oxides; biotite and hornblende are absent.

Rhyolites in the Jim Sage Mountains and the adjacent Raft River basin south of the Snake River Plain were emplaced mostly as lava flows, flow breccias, viscous plug domes, and small, shallow, concordant intrusive bodies that originated independently of any known ash-flow eruptive centers. These rocks differ chemically from the ash-flow tuffs of the central Snake River Plain region only by a lower K_2O content (averaging 4.4 percent vs. 5.3 percent for the ash flows) and by slightly greater amounts of the mafic oxides. Rhyolite ash flows on the Plain probably reflect underlying plutons; whereas, the rhyolite lava flows and related rocks south of the Plain probably indicate that their underlying magma sources either were much less voluminous or were deeper.

Geothermal studies in the Idaho batholith

In continuing geothermal studies in the Idaho batholith, H. W. Young and R. E. Lewis collected water samples from 57 thermal and 11 nonthermal springs in the Salmon River drainage basin. Water temperatures ranged from 20.5°C to 94°C. Chemical character of the water was varied; most of the waters are a sodium carbonate or bicarbonate type; however, some sodium sulfate and calcium carbonate waters occur locally. Reservoir temperatures, estimated using silica and sodium-potassium-calcium geothermometers, range from 30°C to 184°C, with a median temperature of about 74°C. With the exception of one spring, tritium in the thermal waters is zero or near zero, which indicates circulation times greater than about 30 yr. Stable-isotope analyses show a wide range in concentrations of oxygen-18 and deuterium in the thermal waters and indicate the absence of a single, hot-water reservoir, a source for hot springs in the drainage basin. Depletion of stable isotopes in thermal waters relative to local cold springs indicates a source of recharge from other than present-day meteoric water in the Salmon River drainage basin. Thermal-water discharge from inventoried springs was $2.6 \times 10^6 m^3$ in 1980; 110 MW of heat discharged convectively from the system.

SEDIMENTOLOGY

Sedimentology is the study of sediments and the processes by which they were formed and includes the detachment, entrainment, transportation, deposition, and consolidation of rock particles of all sizes. Usually these actions occur in water or air.

Sedimentological processes are of great economic importance to the Nation. For example, inorganic and organic particles can carry significant quantities of sorbed toxic metals, pesticides, herbicides, and other organic constituents, all of which can pollute the environment and accelerate the eutrophication of lakes and reservoirs. Sediment affects land conservation – rehabilitating strip-mined areas; flooding caused by channel aggradation; damage to urban areas (parks, homesites, streets); loss of topsoil; and silting of streams, lakes, reservoirs, canals, and navigational arteries.

USGS scientists study sedimentology in various ways, including basic research on pertinent physical principles, applied research directed toward site-specific problems, and instrumentation development. Many USGS projects involving sedimentology also apply to related topics, such as water-resource investigations, economic geology, marine geology, engineering geology, and regional stratigraphic studies.

Seasonal relations between streamflow and suspended-sediment discharge

Regression analyses of 5¼ yr of suspended-sediment records were done by T. R. Lazaro to define correlations between streamflow and suspended sediment discharge for Bay Creek, a 417 km² tributary of the Mississippi River in Pike County, Ill.

The best relations (correlation coefficients of 0.92 to 0.97) were between mean daily stream discharges and daily suspended sediment discharges, all arranged approximately by season, that is, October through December, January through March, April through June, and July through September.

Sedimentation in the upper Chesapeake Bay

The lower Susquehanna River has three reservoir empoundments between Harrisburg, Pa., and the mouth (Conowingo, Md.) at the head of the Chesapeake Bay. About 12 percent of the drainage area of the Susquehanna River lies downstream from Harrisburg, Pa. Sediment transport in the lower Susquehanna River increases rapidly above a threshold discharge of approximately 9,905 m³/s. Below this threshold value, sediment discharge is typically lower at the mouth than at Harrisburg. D. J. Lang and D. Grason noted that during a high-flow period in March 1980, with a peak discharge of 7,360 m³/s at the mouth, sediment discharge here was only 53 percent of that at Harrisburg. However, for a storm of approximately the same duration in March 1979, with a peak discharge of 14,200 m³/s, sediment discharge at the mouth was 45 percent higher than that at Harrisburg. The sediment discharged to the Bay for that one storm in March 1979, 1.25×10^6 Mg, was greater than the total sediment load from the Susquehanna River for the entire 1980 water year.

Sediment transport in the Tanana River near Fairbanks, Alaska

In 1977, the U.S. Army Corps of Engineers asked the USGS to study the sediment characteristics of the Tanana River between Moose Creek, near North Pole, Alaska, and the Chena River at Fairbanks. Engineering structures along the river that are part of the Chena Lakes flood project are affected by the river; and gravel extraction from the river bed, regulated by the Corps, is also affected by and may influence the fluvial processes. The USGS' study objectives are to determine the sediment transport characteristics and to identify significant changes over the study period, 1977-1982, or longer.

Analysis of data by R. L. Burrows and W. W. Emmett shows that for the site near Fairbanks, the average annual (1974–1979) load is 24 million Mg of suspended sediment and 321,000 Mg of bedload. Upstream, near the North Pole, the average annual load is 20.7 Mg of suspended sediment and 298,000 Mg of bedload. For both sites bedload is usually 1 to 1.5 percent of suspended-sediment load.

Particle-size distribution for suspended sediment is similar at Fairbanks and North Pole. Median particle size is generally in the silt range, but at some low-water discharges, it is in the very fine sand range.

Median particle size of bedload near the North Pole is generally in the gravel range, but at some low transport rates, it is in the medium sand range. In 1977, median bedload particle size was comparable at the two sites, but in 1978, the medium size was markedly smaller at Fairbanks. In 1979, generally coarser material was transported at both sites; the difference in bedload particle size was even greater between the sites. At both locations, suspended-load particles were significantly smaller than bedload particles for all water discharges and sediment-transport rates.

At North Pole in 1979, median bed-material particle size was in the coarse gravel range; at Fairbanks, it was in the medium gravel range in the main channel but in the fine sand range in the overflow part of the channel.

To facilitate application of the sediment data from this project, appropriate hydraulic data have also been gathered to allow empirical evaluation and interpretation of the sediment-transport data.

Sediment transport and water quality during urban development in Illinois

Analyses of streamflow and suspended-sediment discharge from the 7.28 km² Spring Creek rural drainage basin during the period June 13, 1979, to September 30, 1980, indicated that 65 mm of runoff per square kilometer carried 77 Mg of suspended sediment from the basin. Runoff during seven selected storms conveyed 46 Mg of suspended sediment, or 60 percent of the total suspended sediment transported within the period. Seasonal variations in suspended-sediment runoff were defined, with peak suspended-sediment concentrations tending to be 10 to 30 times higher in the late spring–early summer period compared to the late summer period.

CLIMATE

Research of the USGS Climate Program in 1980 was directed towards understanding the history of climate change. Studies documented records of past climates and determined correlation of climate change and sedimentary processes.

Quaternary reference core

Two continuous sediment cores 177 and 168 m long were taken in Clear Lake, Lake County, Calif., for multidisciplinary study of stratigraphy, chronology, and

paleoclimatic record of the sediments. The coring project was led by J. D. Sims. Core CL–80-1, 177 m long, was cored in 7.5 m of water with 66.5 percent recovery. The sediments are composed of sapropelic mud similar to that deposited in the lake today, interbedded with coarse sand and volcanic ash beds. The core ended in ccarse, rounded, gravel and cobbles of Franciscan lithology. Core CL–80-2 was taken in 9.1 m of water at a site between cores 1 and 4 of a 1973 drilling effort. Intervals between 53 and 77 m, and 99 and 168 m, were cored at site CL–80-2 with 80 percent recovery. Sediments in this core are similar to those in CL–80-1 and earlier cores.

Subsampling of core CL–80-1 is complete with sample sets suitable for 18 separate investigations ready for distribution. Paleomagnetic analysis shows only normal polarity after alternating-field demagnetization. The remanence in the upper 50 m is weak, but increases at least tenfold in the remainder of the core. Relative declination within and between each 3-m-long core segment is of no value because the core spun in response to rotation of the drill bit and core barrel during core recovery. Preliminary pollen data from core CL–80-1 (168 samples, 300 pollen counts/sample) reflect changes in the vegetation and climate of the northern Coast Range of California throughout deposition of the core. Comparison of the fossil pollen record and modern pollen data from 150 surface samples taken from north coastal California indicates an oscillation between pollen assemblages characteristic of oak woodland and pollen assemblages characteristic of conifer forest formations. An oak pollen assemblage similar to that found in the upper 13 m of core CL–80-1 occurs between 126 and 128 m depth in the core. This lower interval, preceded by an interval in which *Quercus* pollen is almost entirely absent, is much like the interval at the end of the last glaciation in which the pollen assemblage is dominated by conifer pollen. The pollen data confirm previous conclusions based on the 115-m-long core 4 taken in 1973. These preliminary data suggest that strata correlative with deep-sea oxygen isotope stage 6 were penetrated.

Chrysomonad cysts

Studies of sediment cores from California lakes by D. P. Adam show that there is a rich stratigraphic record of chrysomonad cysts in some localities. These siliceous cysts are the resting stages of chrysophyte algae and range in size between about 2.5 and 20 μm. They only rarely have been used as paleoenvironmental indicators, in part because their small size has made them difficult to observe. These observational difficulties now have been overcome largely by using both scanning electron microscopy and differential phase contrast microscopy. Our results thus far indicate that the study of chrysomonad cysts can be developed into an important new tool for both paleoecology and environmental monitoring. In order to evaluate fossil lake core material, about 300 modern chrysomonad samples from various localities (primarily in the Western United States) representing a variety of environments have been collected. Most samples contain cysts, and there are at least hundreds of distinct forms. They seem to be most common in fluctuating freshwater environments of low pH (acid conditions), which suggests that they may be useful in monitoring acid rain. Mountain lakes in California contain numerous cysts in their sediments, but lakes at low elevations, including Clear Lake, have few if any cysts; this is also true of Lake Atitlan in Guatemala.

The immediate goals in studying chrysomonad cysts are to document the various existing forms using scanning electron microscope photographs, to identify these forms whenever possible, and to establish the geographic distributions and environmental requirements of the various forms.

Central Valley Quaternary studies

Geologic mapping and stratigraphic studies by D. E. Marchand show that nonglacial fan and terrace alluvium flanking the entire San Joaquin–Sacramento Valley appears to have been deposited in brief pulses, separated by extended periods of stability and soil formation. Radiocarbon, uranium-trend, and thermoluminescence dating indicate that these pulses probably coincide in time with the rapid glacial-to-interglacial "terminations" of the marine isotope record. This conclusion is supported by the consistent observation of nonglacial alluvium overlying and interfingering with glacial outwash and associated eolian sand in deposits about 9,000–10,000 yr B.P., 40,000 yr B.P., 140,000 yr B.P., and 250,000 yr B.P. The interfingering of colluvium and alluvium of several different ages in the Sierra Nevada foothills indicates their contemporaneity and suggests that the cause of alluviation was hillslope denudation in the upper drainage basins.

Shallow auger holes in the west-central San Joaquin Valley reveal recurrent cycles of soils formed on mudflows underlain by alluvium. The deposition of mudflows extending many miles into the valley indicates a climate drier than that of the preceding alluvial episode but wetter than the present. Holocene mudflow and alluvial deposition in the same areas is restricted to areas close to present channels and to the range front. The relations between Quaternary facies in the alluvial system from the Sierra Nevada through the foothills to the Central Valley, Sacramento–San Joaquin delta, San Francisco Bay, and the coast, and systematic successions of facies in each of the contrasting environments

along this transect suggest a climatically induced cycle consisting of at least seven phases.

1. Onset of glaciation in the Sierra Nevada; beginning of lacustrine deposition in closed basins of the southern San Joaquin Valley; lowering of sea level and associated entrenchment of rivers; soil formation on exposed terraces and fans of the San Joaquin Valley and on marine terraces along the coast.
2. Glacial maximum in the Sierra Nevada; moraines constructed; glacial outwash deposited in the form of fine rock flour over fan surfaces during flood events; gravel and coarse outwash confined to channels; lacustrine deposition continues in basins.
3. Glacial retreat in Sierra Nevada; moraines breached by outwash; coarse outwash deposited on fans of glaciated basins during a brief period; coarse outwash fills closed basins and terminates lacustrine deposition.
4. Glacial retreat continues; volume of outwash decreases and rivers draining glaciated areas begin to incise, lowering the water table and permitting extensive eolian reworking of outwash deposits in the Central Valley, San Joaquin–Sacramento delta, and San Francisco Bay area; sea level begins to rise.
5. Glacial retreat nearly complete; warmer climate causes vegetational zones to rise, exposing soils formed under forest conditions to be stripped by colluviation; slope-derived debris overloads streams of unglaciated basins, causing widespread alluviation.
6. Climate becomes drier; alluviation changes to mudflow deposition on west side of San Joaquin Valley; soil formation begins on stable outwash surfaces; sea level rises and lower reaches of rivers begin to alluviate; upper reaches incise further as load decreases.
7. Full interglacial; sea level highest; marine shorelines cut; estuarine deposits laid down in San Francisco Bay; intertidal peats formed in the delta; soil formation on exposed fan and terrace surfaces; glaciers absent or confined to highest cirques.

San Joaquin Valley windstorm, December 20, 1977

Mapping completed by H. G. Wilshire indicates that more than 50 million t of soil was mobilized in the southern San Joaquin Valley by a severe windstorm of 24 h duration. A sediment plume was transported at least 650 km northward to the end of the Sacramento Valley, causing a dramatic increase in incidence of Valley Fever. As much as 60 cm of soil was eroded from natural surfaces; outcrops of granite were eroded to depths of 35 cm, and comparable depths of erosion were measured in weathered granitic rocks exhumed from the wind, and others to 2.5 cm in diameter were windborne to heights of at least 1.6 m. Deposits of eolian material include well-developed residual gravel pavements on gently sloping alluvial fan surfaces, coarse-to-fine gravel, granule and sand ripples, and sand dunes on lee sides of fences, vineyards, and orchards, and laminated sand sheets in alfalfa fields, drainage depressions, and on lee sides of hills. The principal factors contributing to the severity of the storm's impact were drought, overgrazing, and a general lack of windbreaks in the agricultural land. The windstorm was followed in early 1978 by heavy rainstorms. Previous denudation of the land by the windstorm contributed to severe gully erosion where this problem did not exist before, and to widespread, costly flooding.

Quaternary speleothem studies

Experiments completed to date by J. C. Tinsley show that modern calcite in some caves is in isotopic equilibrium with the depositing ground water. Oxygen isotope ratios are being measured presently at different sites along the same growth lamination in individual speleothems to check for variations due to nonequilibrium conditions. This isotopic technique provides an independent way of testing data on continental climates inferred from other sources.

Automated sediment traps

Part of a study of climatic records of lacustrine sediments by W. E. Dean and J. P. Bradbury included placing automated sediment traps in Soap Lake, Wash.; Lake Washington and Clear Lake, Calif.; Pyramid Lake, Nev.; Elk Lake, Minn.; and Green Lake, N.Y. The traps are designed to calibrate the collected sediment column at some specified time interval, usually 10 to 15 d. Traps have been placed in Spirit Lake on the northwest flank of Mount St. Helens and in Merrill Lake on the southwest flank. The sediment-trap studies of the lacustrine paleoclimate investigations are designed to measure the rates and timing of influx of sediment particles in lakes regardless of whether they are produced in the lake or are transported to the lake by wind or streams. The ash falls from the Mount St. Helens eruptions will provide an opportunity to document in detail the sediment record of fallout from a major volcanic eruption, and, particularly, to document the chemical, physical, and biological effects of the fallout on the lake and the lake ecosystem.

During July, collecting tubes were recovered from sediment traps in Merrill Lake and Soap Lake, Wash. Collecting tubes from both lakes contain 10-d time-calibrated records of ash fall from Mount St. Helens' eruptions, including spectacular graded ash sequences from the May 25 and June 12 eruptions. Samples from

these collecting tubes will be analyzed by researchers in regional geochemistry and paleontology and stratigraphy (USGS), University of Wisconsin, and University of New Mexico. At the time the collecting tubes were recovered, traps were placed in three additional lakes in Washington, northeast of Mount St. Helens. Consequently, fallout from Mount St. Helens is being monitored presently by time-calibrated traps in five lakes in Washington.

Late Pleistocene glaciation of the northwestern United States

Paleoclimatic studies by K. L. Pierce of late Pleistocene glaciation level (PGL) along an east-west transect extending from the Bighorn Mountains of Wyoming to the Pacific Ocean show a positive correlation between the PGL and modern snowpack. The PGL increases linearly about 700 m across each of the following major orographic barriers: the Cascade Mountains, the Salmon River Mountains, and the Yellowstone area. The PGL also descended where the prevailing westerly storm tracks traverse major lowlands – the most prominent being at the upper end of the Snake River Plain where the PGL descended 400 m from central Idaho to the Yellowstone area. Plots of the April 1 snowpack water content versus their altitude for areas along the same east-west transect show that, at a given altitude, snowpack varies by more than an order of magnitude, whereas adjacent ranges commonly differ by a factor of 5. The modern snowpack at the altitude of the PGL ranges from 170 cm at 1,900 m in the Cascades to 35 cm at 3,100 m in the Bighorn Mountains. The linear regression equation for 11 of these data pairs has a correlation coefficient; this value increases to 0.96 if two problematic sites are deleted. Thus, if the modern snowpack is known along this transect, the late Pleistocene glaciation level (PGL) can be predicted, or vice versa. Because the modern snowpack relates so closely to the PGL, the data suggest that late Pleistocene storm patterns along this transect did not differ from modern ones. Also, assuming that snowpack differences in the late Pleistocene between areas were comparable to modern differences, the activity of late Pleistocene glaciers differed greatly; those of the Oregon Cascades had an "activity" index five times larger than those to the east in the Bighorn Mountains.

Great Plains eolian processes

Stabilized sand dunes in the Nebraska Sand Hills, western Kansas, and eastern Colorado, were mapped by R. F. Madole using Landsat imagery, and field observations of soils formed in dunes were made along a 500-km transect from the Nebraska Sand Hills to the Front Range. Published ^{14}C ages indicate that the last major episode of sand movement in the Nebraska Sand Hills was in Altithermal time (about 8,000–5,000 yr B.P.). The radiometric age of the dune fields in Colorado is not known, as datable materials are not easily obtained. However, soils on dunes along the South Platte River in Colorado are similar to those on dunes in the Nebraska Sand Hills. These soils are either Ustipsamments or Torripsamments with A/AC/C profiles. Sola are thin (20–50 cm), have 10YR hues and low chromas, and contain less than 10 percent clay. Published soil surveys indicate that soils that developed in dune sand along the Arkansas and Cimarron Rivers in Kansas have similar weakly developed profiles. Collectively, the pedologic data suggest that dune activity was contemporaneous over much of western Nebraska, eastern Colorado, and western Kansas. This contemporaneity of dune formation can be extended to include the Ferris dune field of south-central Wyoming on the basis of the stratigraphy and reported ^{14}C ages. Older dunes also exist downwind of the younger dunes in eastern Colorado but are much less extensive than the younger dunes and were not studied. According to published surveys, they are characterized by A/BZt/CCa profiles.

Contemporaneous dune activity over such a large part of the central Great Plains implies prolonged regional aridity. Dune morphology and the occurrence of extensive dune deposits in Colorado and Kansas to the south of major drainages, which probably supplied much of the sand, imply transport by winds with a strong northwesterly component. This paleowind direction is in agreement with that determined for the Nebraska Sand Hills. Geomorphic, sedimentologic, and pedologic data suggest that during the Altithermal the westerlies may have been stronger than at present and that incursions of Arctic and Gulf air masses into the central Great Plains may have been less frequent.

Late Cenozoic sea levels

Biostratigraphic studies of sedimentary units in the Southern Atlantic Coastal Plain by T. A. Ager, T. M. Cronin, J. E. Hazel, J. P. Owens, and B. J. Szabo permit reconstruction of the history of sea-level changes and regional tectonic deformation during the past 5 m.y. Initial ecostratigraphic ostracode data, pollen analyses, and uranium series dates on coral indicate middle and late Pleistocene relative high stands of sea level and interglacial or near interglacial climates at about 500,000 to 400,000; 200,000 to 180,000; 125,000 and 80,000 to 70,000 yr B.P., which can tentatively be correlated to deep-sea oxygen isotope stages 13, 7, 5e, and 5a, respectively. Although these Coastal Plain high stands correspond to hemispheric warm periods when sea level was high relative to those of glacial times, deep-sea isotopic and faunal data and uranium series dates on coral ter-

races suggest that only at about 125,000 yr B.P. was sea level above (+2 to +10 m) that of the present mean sea level (MSL). For example, estimates of global sea level from 13 m to 43 m below present MSL at about 82,000 yr B.P. contrast sharply with preliminary Coastal Plain data, indicating correlative sea level about 2 to 6 m above present MSL at that time. Hence, to explain our preliminary findings, either our dating methods and climatic data are not accurate enough, current ideas of Quaternary sea levels need reassessment, or post-depositional uplift has altered the original position of upper Quaternary deposits. To resolve these problems, additional faunal and floral material and uranium series dates are being obtained, and both sets of conflicting data are being critically examined.

GROUND-WATER HYDROLOGY

Research and application of techniques in ground-water hydrology by the USGS covered a broad range of topics and geographical areas in the past year. Interest in ground water now has national awareness that is likely to continue in the coming years as more attention is given to the use and protection of ground water for water supplies and the use of underground space for the disposal of a wide variety of waste materials.

Development and application of digital modeling techniques continued during the year. A digital model that considers the transport of radionuclides was developed for ground-water flow at the Nevada Test Site. A three-dimensional finite-difference model of the "2,000-foot" sand in southern Louisiana was developed and used to predict water-level declines for selected withdrawal rates. The ground-water system of Long Island, N.Y., was simulated using a coupled coarse-scale regional model and fine-scale subregional model. Digital models were developed for ground-water flow in alluvial deposits in California and Arkansas.

Problems related to fluid injection of both freshwater and waste water continued to receive attention. The effects of recharge of large amounts of reclaimed water on the water-table aquifer and the upper part of the underlying Magothy aquifer are being studied in Nassau County, N.Y. Problems of well clogging and water migration are being considered in an injection-extraction well network near San Francisco Bay, Calif. Preliminary injection testing was conducted on two wells in the Arbuckle Group in Kansas as part of an investigation of liquid waste disposal.

Results of test drilling and model simulations indicated that aquifers that underlie St. Paul, Minn., have hydraulic properties for injection, storage, and retrieval of high-temperature water. The potential for storage and recovery of freshwater in saline aquifers is being studied in southern Florida to utilize surplus freshwater that is available during the rainy season; a three-dimensional finite-difference flow and transport model was used to evaluate recovery efficiency associated with the cyclic fresh-water injection.

Hydrologic effects of surface mining were reported in three studies. Local and regional ground-water flow systems have been affected by a strip mine in the southwestern part of the Eastern Interior coal basin. Local effects of coal strip mining on ground-water flow and water quality were studied in three small watersheds in eastern Ohio. The potential impact of lignite mining is being studied in Louisiana.

Other studies in FY 1980 included (1) use of "kriging" to generate water-table altitudes, (2) analysis of TCE contaminations in Michigan, (3) land subsidence in the Houston-Galveston area, and (4) interaquifer flow through well bores. Effects of geologic structures on ground-water flow were studied in West Virginia and Texas. Significant results were reported from hydrogeologic studies in parts of Missouri and North Dakota.

AQUIFER-MODEL STUDIES

Simulated steady-state flux in the Tertiary limestone aquifer system

The three-dimensional finite-difference model, developed by P. C. Trescott (1975) and S. P. Larson (Trescott and Larson, 1976) has been used by R. E. Krause and R. B. Randolph to simulate the pre-development flow system in the Tertiary limestone aquifer system in the eastern half of the Coastal Plain of Georgia and adjoining southern South Carolina and northeastern Florida. Initial simulation of the steady-state system was begun using recharge-discharge rates over the finite-difference grid. Calibration was accomplished by varying transmissivity and recharge rates until the pre-development potentiometric surface was approximately duplicated. The final calibrated model simulated a flux that was less than one-fifth of that originally estimated.

As a starting point for determining aquifer recharge and discharge, the general equation of rainfall minus runoff minus evapotranspiration was used. The model area was separated by basins, and streamflow records were used to calibrate the runoff for each basin. Rainfall was discretized by locating all rainfall stations on a regional base map and applying Thiessen polygons for distribution of the measured data. A method developed by Holdridge (1967) that incorporates temperature and precipitation was used to estimate evapotranspiration rates over the model area. Biotemperature, which is defined as the sum of hourly temperatures between 0°C

and 30°C divided by the number of hours in the year, is the central variable for the estimation of evapotranspiration by this method. A linear statistical relationship between the mean annual temperature and the biotemperature resulted in evapotranspiration values that were similar to those determined in some previous studies of the same areas.

With estimates of rainfall, runoff, and evapotranspiration available, the water-balance calculations were made for basins within the model area. Spring flow from the aquifer system was also included in the equations where applicable. The resulting values of interbasin-transfer and corresponding aquifer recharge (39.9 m^3/s) and discharge (26.6 m^3/s) were distributed among the finite-difference nodes and used as input to the model. These initial recharge and discharge values resulted in a massive build-up of potentiometric head in the model of more than 300 m over one-third of the model area. The final steady-state calibration of the model utilized a recharge of 14.8 m^3/s and a discharge of 12.2 m^3/s giving a net recharge to the aquifer of 2.5 m^3/s prior to development.

Alluvial-aquifer modeling, northeastern Arkansas

A digital model of the alluvial aquifer in northeastern Arkansas, constructed by M. E. Broom and F. P. Lyford (1981), showed that in 1978 pumping, mostly for rice irrigation, removed 660 hm^3 of water from storage and captured 530 hm^3 of streamflow. Streamflow was captured mostly from the Cache, L'Anguille, and St. Francis Rivers, and from Bayou DeView.

A projected annual pumping rate of 1,800 hm^3, based on 1978 irrigated acreage, would cause excessive drawdowns in parts of Poinsett, Craighead, and Cross Counties and would force a reduction in pumping in 1990 to 1,670 hm^3 per year. By the year 2000, the reduced amount of pumping would remove 604 hm^3 of water from aquifer storage and capture 1,060 hm^3 of streamflow per year.

Mathematical model for alluvial aquifer in Modesto, California

C. J. Londquist developed a digital mathematical model of the unconsolidated alluvial aquifer system in the Modesto area that can be used to determine the effects of increased pumping and water use on future water levels in the aquifer system. The model is divided into two units. The low unit is semiconfined by a clay bed in the western part of the study area; elsewhere in this unit the aquifer is unconfined. The upper unit represents an unconfined aquifer and lies above the clay bed or its extension. Where the clay bed is absent, the upper and lower units are considered as a single aquifer. The model, as calibrated, can estimate the effects of changing stresses on water levels only within the area of primary interest for the upper unit. In other areas of the upper unit and for the lower unit, predicted changes should be looked upon as representing only general trends.

Three-dimensional hydrologic model of the Piceance basin, Colorado

A layered three-dimensional mathematical model was prepared for the hydrologic system of aquifers and confining layers of the Green River and Uinta Formations in Piceance Basin, northwestern Colorado, by O. J. Taylor. These formations consist of marlstone, sandstone, and siltstone, and include large reserves of oil shale. Extensive fracturing and leaching of the formations have increased their permeability and resulted in aquifers that lie within, above, and below the oil shale deposits. Preliminary onsite evidence indicates that the oil shale aquifers have directional permeability. However, onsite data were inadequate for determining the directional permeability throughout the basin for incorporation in the model.

A technique was designed to evaluate the degree of error in various simulations of directional permeability under steady-state conditions. The potentiometric heads in 53 wells were compared with simulated potentiometric heads at the same sites and depths. The differences in the two values were tabulated and used to calculate the mean square error, the sum of the mean error squared, and the variance. Progressive changes in model parameters produced large progressive changes in the mean square error that conformed with onsite evidence. Apparently, the mean square error of potentiometric heads is a sensitive indicator for evaluating directional permeability.

Model study of the "2,000-foot" sand, Baton Rouge, Louisiana

A three-dimensional, finite-difference digital model of the "2,000-foot" sand of the Baton Rouge area was completed by L. J. Torak and C. D. Whiteman, Jr. The model will be used to predict the potential effects of development alternatives proposed by State and local officials on water levels to aid management of the ground-water resources of the greater Baton Rouge area. A computer model developed by the USGS was modified by Torak to include a transient clay-leakage routine by J. V. Tracy and to allow disk storage of all elements needed to make a continuation run under transient conditions. Analysis of the mode for the "2,000-foot" sand indicates that the computer program adequately accounts for transient leakage from the confining layers and for interaction between the modeled aquifer and overlying and underlying aquifers. The program is not only suitable for modeling the aquifers of the

Baton Rouge area but should be applicable in similar hydrogeologic settings.

Following calibration and verification of the model, prediction runs were made assuming increasing, steady, and decreasing pumpage from the "2,000-foot" sand. The most significant finding was that, after 65 yr of development, the "2,000-foot" sand still has not reached steady-state conditions. Reduction of pumpage at an average rate of 1 percent per year for the next 30 yr would result in a rise in water level near the pumping center, but declines in water levels would continue at distances beyond about 50 km from the pumping center.

This computer program is being used by Whiteman to develop a model of the "1,500-foot" and "1,700-foot" sands in the Baton Rouge area.

Ground-water-flow modeling in Las Vegas Valley, Nevada

Lithologic logs from 270 well-drillers' reports were interpreted in terms of standard USGS codes and put into the Ground-water Site Inventory file of WATSTORE. By using the Procedural Language Interface (PLI) with FORTRAN retrieval programs, these logs have been used to map and prepare for model input various hydrogeologic characteristics of the valley-fill reservoir, according to D. S. Morgan. Gravity data have been used to determine the combined thickness of sand, gravel, silt, and clay that constitutes the valley-fill deposits, and the shape of the underlying bedrock basin. According to R. W. Plume (USGS, unpub. data), the thickness of the valley-fill deposits along the axis of the basin varies from about 900 m in the vicinity of Las Vegas to over 1,500 m near the northern end. Poorly sorted sand and gravel form extensive alluvial fans along the valley margins, whereas silt and clay beds make up over 60 percent of the saturated thickness in the central parts of the valley. Regression analysis of transmissivity data and thickness of high-, medium-, and low-hydraulic-conductivity materials has yielded estimates of the range of hydraulic conductivities which may be expected for each class of materials. The ranges are 0.0003–0.0015 m/d for low-conductivity materials, 0.03–0.06 m/d for medium-conductivity materials, and 3.7–4.9 m/d for high-conductivity materials.

Modeling of ground-water flow and solute transport at Nevada Test Site

A model of ground-water flow in carbonate, tuffaceous, and alluvial rocks in southern Nevada was developed by R. K. Waddell as part of investigations of the feasibility of disposing of high-level nuclear waste at the Nevada Test Site. Inverse techniques developed by R. L. Cooley were modified to calculate sensitivities of flux to variations in the model parameters. Flux is most sensitive to variations in recharge rates and to transmissivities at the potential repository site and in a possible fracture zone, which may allow water to bypass the site.

A two-dimensional, finite-element solute-transport model program was developed by J. V. Tracy and R. K. Waddell. The model program simulates the transport of branching radionuclide chains in ground water and includes the effects of radioactive decay, linear sorption, and first-order dissolution. Matrices associated with members of the decay chain are stored on disks to minimize core storage.

Coupling coarse-scale regional and fine-scale subregional ground-water flow models, Long Island, New York

A complex three-dimensional model of the Long Island, N.Y. ground-water system was calibrated for steady-state and transient flow conditions by T. E. Reilly and H. T. Buxton. The model is composed of a coarse-scale regional model and two fine-scale subregional models. Stresses were simulated on the regional model. Boundary conditions for the two subregional models were then calculated from the regional model. The regional model, by extension of the model boundaries to the natural physical boundaries of the system, accurately simulates the extent and effects of applied stresses. The fine-scale subregional models give greater detail in the areas of primary concern. The use of coupled coarse-scale regional and fine-scale subregional models utilizes the advantages of scale gained from each.

Calibration of ground-water model using aquifer tests

A 25-day pumping test in the Sevier Desert near Lynndyl, Utah, conducted by W. F. Holmes and Michael Enright, provided valuable data to be used in the calibration of a ground-water digital-computer model. The test involved pumping an average of 340 L/s from a well completed in unconsolidated alluvial deposits. Thirty five observation wells within a 14-km radius were measured during the test which included 26 days of recovery measurements. Previous investigators have determined the presence of at least two artesian aquifers, separated by about 120 m of clay, sand, and gravel. The vertical hydraulic conductivity of the confining layer between the aquifers as well as the storage properties of the lower aquifer were needed to calibrate the ground-water model.

Preliminary results of the test indicated that the vertical hydraulic conductivity probably is about 0.3 m/d, and the storage coefficient of the lower aquifer ranges from about 1×10^{-4} to 1×10^{-5}. The observed drawdown in the lower aquifer after 25 days of pumping ranged from about 35.1 m at the pumped well to about 0.3 m at a distance of about 14 km. The maximum observed

drawdown in the upper aquifer after 25 days of pumping was about 0.09 in a well about 5 km from the pumped well. Transmissivities in the lower aquifer averaged about 900 m^2/d.

Model studies of the Northern Great Plains aquifer, North Dakota

A preliminary three-dimensional digital model of the Lower Cretaceous Dakota confined aquifer system developed by R. D. Butler indicated the need for transmissivity to be based on larger values of permeability (10 to 40 m/d) than previously determined. The average permeability, obtained from formation-factor analysis and onsite data, is multiplied by net sandstone-thickness values obtained from geophysical logs and corrected to formation water temperature to obtain transmissivity.

The model indicates that water in Paleozoic rocks in eastern North Dakota leaks to the Dakota, water from Dakota aquifer leaks to the overlying Cretaceous shale, and water from the overlying Cretaceous Shale leaks to the Dakota aquifer. Leakage appears significant along fracture zones. Coupling the Upper Cretaceous Fox Hills aquifer to the three-dimensional model indicated that the existing two-dimensional Fox Hills model is adequate. Calibration of the Dakota layer showed that leakage from the Fox Hills aquifer is small. Geochemical patterns in Lower Cretaceous aquifers in eastern North Dakota indicated upward leakage of water from Paleozoic aquifers to the Dakota aquifer and from the Dakota aquifer to overlying aquifers. Geochemical anomalies are present along major fractures and their intersections.

Regional variations in formation thickness, net sandstone thickness, and depositional facies (delta systems, for example) are present in Triassic to Tertiary rocks in the Williston basin. These trends supported a tectonic interpretation of deposition in subbasins bounded by major fracture zones.

RECHARGE STUDIES

Effects of recharging reclaimed water on ground-water quality, Nassau County, New York

The effects of large-scale recharge of reclaimed water on ground-water quality is being studied by E. J. Koszalka at East Meadow, Nassau County, N.Y. Water samples were collected from 48 wells that were screened in the upper glacial (water-table) aquifer and the upper part of the underlying Magothy (public-supply) aquifer in a 2.6-km^2 area around the recharge sites.

Preliminary results indicated that water from the upper glacial aquifer contained significant concentrations of nitrate and low-molecular-weight chlorinated hydrocarbons and detectable concentrations of organochlorine insecticides and polychlorinated biphenyls. At present, no fecal contamination was evident in either aquifer in the study area.

DISPOSAL AND STORAGE STUDIES

Sewage disposal by spray irrigation in Florida

The effects of spray irrigation with sewage effluent near Tallahassee, Florida are being investigated by M. C. Yurewicz. Routine spray irrigation of selected grasses and forage crops with secondarily treated municipal sewage began at the southeastern spray field in November 1980 on 440 ha of sandy soil.

Twenty-nine wells were drilled to monitor ground-water quality and levels. Lithologic samples and geophysical logs indicated that substrata comprise 4.6 to 30 m of sand underlain by limestone with a 0.3- to 1.6-m-thick clay layer separating the sand and limestone in most places. Three months after irrigation began, ground-water quality samples collected from wells open to the saturated part of the sand unit, and from others open to the limestone aquifer, indicated that sprayed effluent had not reached the zone of saturation. Chloride was used as a conservative tracer for effluent movement in the ground-water system. The natural quality of the water in the limestone aquifer was typical of carbonate formations. The water from the saturated sand layer exhibited low specific conductance, low pH, and low organic content.

Potential for storage and recovery of freshwater in saline aquifers, southern Florida

Aquifers in southern Florida containing brackish water are considered as possible reservoirs for the storage of freshwater. According to M. L. Merritt, an analysis of regional water use and disposition showed that some surplus freshwater was available for injection during the annual high-rainfall season. A three-dimensional, finite-difference flow and transport model was used to assess the recovery efficiency of cyclic freshwater injection associated with various management regimes and hydrologic conditions. An evaluation of freshwater injection and recovery tests indicated that the efficiency of cyclic injection of freshwater is highly dependent upon permeability and storage capacity of the aquifer and the salinity of the resident fluid.

Wastewater injection in Palo Alto, California

S. N. Hamlin reported that several months of low-level controlled injection of treated waste water produced no observable well-clogging in a well, which is a part of an injection-extraction well network in the Palo Alto baylands along the San Francisco Bay, Calif. The

Santa Clara Valley Water District injects treated waste water into the shallow aquifer system to reduce local hypersaline contamination that apparently has resulted from cyclic evaporation-concentration processes in the marshes near the bay. X-ray analysis of clay minerals in drill cuttings from wells showed a marked expansion of the mineral lattice when saline pore water was replaced with injection water. This expansion may have caused some localized clogging; but, because the aquifer is heterogenous, the effect was negligible, and injected water may have moved through relatively more permeable zones or through zones that had smaller amounts of clay minerals.

The density contrast between injected water and ground water—about 4 percent—produced an increased rate of water-level rise when the freshwater reached observation wells. When the freshwater replaced the saline water around the well, the rate of water-level rise returned to the rate that was observed before the freshwater arrived at the observation well. The pre-injection potentiometric gradient of the shallow aquifer system was very low compared to that of the post-injection potentiometric gradient. As a result, the pre-injection potentiometric gradient had virtually no effect on the migration of the injected water.

Aquifer suited for storage of high-temperature water

J. H. Guswa and R. T. Miller reported that the Franconia and Ironton-Galesville aquifers of Cambrian age that underlie St. Paul, Minn., have hydraulic properties suited for injection, storage, and retrieval of high-temperature water. A preliminary radial-flow and energy-transport model was constructed using data collected during the construction of test wells in the Franconia and Ironton-Galesville aquifers. Preliminary simulations involved 24-day, three-part cycles where 150°C water was injected at a rate of about 20 L/s for 8 days, stored for 8 days, and withdrawn for 8 days at a rate of 20 L/s. The location of the 40°C and 90°C temperature fronts after 8 days of injection are predicted to be 25 and 43 m from the injection well, respectively. The model indicated that approximately 50 percent of the injected heat could be recovered at the end of the 24-day cycle. Model calculations also indicated that hydraulic heads in the vicinity of the well bore may rise as much as 60 m during the injection phase and may be lowered as much as 76 m during the withdrawal phase.

SUMMARY APPRAISALS OF THE NATION'S GROUND-WATER RESOURCES

A series of assessments, initiated in 1970, to provide broad-scale analyses of the quantity and quality of ground water in each of the Nation's 21 water-resources regions (as defined by the Water Resources Council) is virtually complete. These assessments have demonstrated that ground water is a large, important, and manageable resource that should have a significant role in regional water development. The completed series of assessments will constitute a national ground-water compendium for the guidance of planning agencies and all others concerned with the Nation's water supply.

The analyses include appraisals of the significance of the ground-water resource to regional water supply, the quantities of ground water available, the quality of ground water, the present and potential problems associated with ground-water use, and additional information needed for planning and efficient development of ground water.

These summary appraisals are being published in the USGS Professional Paper 813 series, and the following 20 of the 21 regional appraisals are available: Bloyd, R. M., Jr., 1974, 1975; Price, Don, and Arnow, Ted, 1974; West, S. W., and Brondhurst, W. L., 1975; Thomas, A. E., and Phoenix, D. A., 1976; Baker, E. T., and Wall, J. R., 1976; Eakin, T. E., Price, Don, and Harrill, J. R., 1976; Bedinger, M. S., and Sniegocki, R. T., 1976; Sinnott, Allen, and Cushing, E. M., 1978; Weist, W. J., Jr., 1978; Reeder, H. O., 1978; Zurawski, Ann, 1978; Takasaki, K. J., 1978; Terry, J. E., Hosman, R. L., and Bryant, C. T., 1979; Cederstrom, D. J., Boswell, E. H., and Tarver, G. R., 1979; Taylor, O. J., 1978; Zenone, Chester, and Anderson, G. S., 1978; Davidson, E. S., 1979; Foxworthy, B. L., 1979; Gómez-Gómez, Fernando, and Heisel, J. E., 1980.

MISCELLANEOUS STUDIES

Kriging applied to water-table altitudes in the Ogallala aquifer, Kansas

Kriging, an interpolation method for autocorrelated, regionalized data, was applied by L. E. Dunlap and J. M. Spinazola to water-table altitude data in the Ogallala aquifer in west-central Kansas. The method generated interpolated water-table altitudes and error of estimate for the altitudes. Kriged water-table data were then combined with percentage change in saturated thickness. Maps of water-table altitude, saturated thickness, and percentage change compared favorably to maps manually contoured by the point-intersection method.

Injection testing of the Arbuckle Group, Kansas

J. B. Gillespie reported that injection tests were conducted on two test wells installed in the Arbuckle Group in southwestern and central Kansas. The tests were conducted using water previously pumped for each well and stored in a surface pit.

The first well, located in Labette County, was 554 m deep and was injected at a rate of 13.7 L/s. A transmissivity of 4.4 m^2/d was calculated from the recession data. The other well, located in Saline County, was 1,115 m deep and was injected for 5 hours at a rate of 9.2 L/s. The recession data for this well indicated a transmissivity of 3.2 m^2/d.

Interaquifer flow through well bores

According to M. F. Hult, flow through well bores open to more than one aquifer had major hydraulic and chemical effects on the ground-water-flow system in the St. Louis Park area, Minnesota. Ground water in near-surface aquifers has moved down the regional hydraulic gradient toward multiaquifer wells injecting contaminated water into the Prairie du Chien-Jordan aquifer. The contaminants consist of coal-tar derivatives that were produced by a wood-preserving plant from 1918 to 1972. Flow through the well bores of up to 10 L/s caused cones of depression and impression in the aquifers that were interconnected. Flow out of the St. Peter aquifer through one well affected water levels and the direction and rate of contaminant transport at a distance of at least 700 m. Flow into the Prairie du Chien-Jordan aquifer through another multiaquifer well caused a cone of impression of about 5 m at a single-aquifer well in which water levels have been recorded and published by the USGS since 1953. The Minnesota Department of Health has sealed or reconstructed wells found to be injecting contaminants into the Prairie du Chien-Jordan aquifer. This will reduce the amount of contaminants entering the aquifer, which is the region's major ground-water resource. However, in the near-surface aquifers, contaminants that previously were intercepted by multiaquifer wells will continue to migrate down the hydraulic gradient. Consequently, the area in which additional multiaquifer wells may affect the quality of water in the Prairie du Chien-Jordan aquifer will increase more rapidly than before the wells were sealed.

Aquifer tests in Northern Midwest RASA

The Northern Midwest Regional Aquifer-System Analysis (RASA) studied the Cambrian-Ordovician aquifer in Illinois, Indiana, Iowa, Minnesota, Missouri, and Wisconsin. This system consists of sandstone, dolomite, and shale formations with a wide range of aquifer properties and hydrologic heads, both areally and vertically. In order to obtain data for discrete layers as input to a three-dimensional ground-water flow model of the aquifer system, H. L. Young obtained a pump hoisting rig, inflatable packers, a submersible pump, and pressure transducers to test individual zones in multiaquifer wells.

Tests were made in nine wells within the study area. Transmissivity and hydraulic conductivity were determined for several aquifer units using the Jacob straight-line method with drawdown and (or) recovery data. Vertical head variation was documented in various geohydrologic settings – head decreasing with depth in recharge areas to head increasing with depth in discharge areas.

During testing of a 590-m deep test well at Zion, Ill., north of Chicago and near Lake Michigan, three intervals were packed off and pumped. The middle interval, containing the Ironton Member of the Franconia Sandstone and underlying Galesville Sandstone of Cambrian age, had the lowest head. Below this unit, the head was about 3.4 m higher, and above it the head was about 0.6 m higher. The Ironton-Galesville unit is the most transmissive of the Cambrian-Ordovician units and thus yields large quantities of water to deep wells in northeastern Illinois and southeastern Wisconsin. The lower head is likely a result of greater regional drawdown in this unit than in the other less transmissive units.

Effect of faults on ground-water circulation in the Edwards aquifer in the San Antonio, Texas, area

The Edwards Limestone in the Balcones fault zone of southern Texas forms a major productive confined aquifer. It consists predominantly of dense carbonate rocks but contains some very permeable and porous honeycombed rock leached from evaporitic, tidal flat, or reefal deposits. Fractures have hydraulically interconnected these layers at most places.

According to R. W. Maclay and T. A. Small, regional ground-water flow is toward major springs in the eastern part of the San Antonio area; however, circulation is locally diverted by vertical faults that have separated the aquifer and act as baffles that divert the flow to the northeast. The faults were mapped using electrical, geophysical, and drillers' logs from more than 500 wells.

Stress-relief fractures control ground-water flow

A hydrologic study made by G. G. Wyrick and J. W. Borchers (1980) in the Black Fork Valley at Twin Falls State Park, Wyoming County, W.Va., indicated that stress-relief fractures are the major controls on the storage and transmission of ground water.

Two sites about 3.6 km apart were selected for test drilling, pumping tests, and geophysical studies. Analysis of aquifer test data from test wells at both sites indicated that the primary permeabilities of the surficial sandstone, siltstone, and shale beds are very low. Ground water occurs mainly in bedding-plane separations and shear fractures under the valley floor and in nearly vertical and horizontal slump fractures along the

valley walls. Aquifer tests also indicated that the unfractured rocks beneath the hills flanking the valley act as impermeable boundaries to the flow of ground water. A hydrologic connection exists between the sites.

The fracture systems that constitute the transmissive part of the aquifer in the Black Fork Valley are like those described by other investigators as being formed by stress relief. The concept that stress-relief fractures are major controls on shallow ground-water-flow systems may have transfer value throughout the Appalachian coal region and may aid in the design of monitoring networks to assess the effects of deep and strip coal mining on ground water.

SURFACE-WATER HYDROLOGY

The objectives of research in surface-water hydrology are to develop improved techniques for estimating the magnitude and variability of streamflow in time and space, both under natural and man-modified conditions, to understand the flow process in stream channels and estuaries, and to define the rate of movement and the dissipation of pollutants in streams.

Applications of modeling

D. H. Conger used the USGS rainfall-runoff model to determine long-term synthetic flood-frequency characteristics at each of 20 rural small stream-gaging stations in Wisconsin. The standard error of estimate for the synthetic 100-yr floods was 23 percent compared to 31 percent for the observed 100-yr floods.

Research on the mechanisms of transport of both conservative and nonconservative solutes placed in small pool-and-riffle streams has led to the development of both conceptual and mathematical models to describe the movement of these added solutes. V. C. Kennedy, K. E. Bencala, A. P. Jackman, and G. W. Zellweger carried out field experiments and analyzed the physical and chemical data from these experiments that demonstrate the significant consequences of physical and chemical storage mechanisms on controlling solute transport. It has now been demonstrated that convection-dispersion is not the only mechanism required in describing solute transport in the two small streams that were studied.

R. J. Avanzino, in experiments at Uvas Creek, Calif., ($\approx$.02 m^3/sec discharge) with the conservative tracer, chloride, showed that percolation of water from pool to pool through stream gravels offers an explanation for the observed delay in the tracer transport down the stream channel.

A. P. Jackman and R. A. Walters showed that the transport of conservative chloride and nonconservative strontium in Uvas Creek can be simulated well mathematically by combining equations for the convection-dispersion mechanism with equations describing either diffusion into the bed, exchange between the stream and a well-mixed zone of interstitial water in the bed or exchange between bed and stream combined with transport of some stream water through stream gravels. They also showed that it is possible to use the models to determine realistic parameters for characterizing these mechanisms.

Bencala and Walters demonstrated the utility of a transient-storage model in simulating the form of the concentration-time curve for both conservative and nonconservative solute transport in Uvas Creek. The use of both finite-difference and finite-element formulations was investigated and the methods were found to be essentially equivalent for the analysis of these data. Documentation of the FORTRAN code described the use of the model, allowing for either numerical formulation without altering the user's input or output format. In a theoretical analysis, Bencala and Zellweger derived the mathematical relationships for estimating channel volume using a nonconservative tracer injection.

Further experiments were done with R. E. Rathbun at Little Lost Man Creek ($\approx$.01 m^3/sec discharge) in Redwood National Park, California, where chloride and rhodamine WT also showed that the departure from standard convection-dispersion transport is significant.

R. N. Oltmann applied an implicit branch-network flow-simulation model to 80 km of the Sacramento River from Sacramento to below Rio Vista and including the Sacramento Deep Water Channel, Delta Cross Channel, Sutter, Steamboat, Miner, Elk, Cache, Threemile, and Georgiana Sloughs. The model was divided into two separate models to simplify calibration. The upper-half model, which includes the Sacramento River from Sacramento to Walnut Grove, Sutter, Miner, Elk, and Steamboat Sloughs has been calibrated. The results of verification runs comparing measured and computed stage and discharge data were very impressive; computed stages and discharges were within 0.0305 m and 3 percent, respectively, of measured values. Calibration of the lower-half model has begun, but has not yet been completed.

An unsteady flow model for the Saginaw River, Mich., was developed by D. J. Holtschlag. The model provides a method of determining instantaneous discharge through the normal flow range of 225 to 340 m^3/s. The current slope-rating method can be used to compute discharge only under steady- and high-flow conditions. Unsteady flow on Saginaw River results from seiching action on Lake Huron and Saginaw Bay. Model computations are based on the solution of continuity and momentum flow equations, on hydraulic characteristics of Saginaw River, and on time-dependent boundary conditions. An

implicit, finite-difference technique is used to solve one-dimensional flow equations. Channel storage and conveyance characteristics were obtained from a 1979 field survey and through model calibration. Boundary conditions are specified by stage or discharge data at the model extremities. Optionally, wind velocity data may be incorporated in the model. For use in estimating flows larger than 340 m^3/s, the model was modified by increasing the flow-resistance coefficients on the basis of historic high-flow measurements.

A mathematical transient flow model was applied by R. D. Burnett to evaluate the aquifer-stream flow system between Webster Reservoir and Waconda Lake in the Solomon River Valley of north-central Kansas. The model was calibrated by comparing measured and simulated potentiometric surfaces and by comparing measured and simulated base flow in the South Fork beginning March 1970 and continuing through February 1979. Although ground-water development has been increasing since 1970, predictive-model analysis indicates that annual recharge from precipitation, and seasonal recharge from infiltration of surface water in canals and laterals and from the irrigated fields provide an adequate supply to sustain the area under its present development. However, if supplies of surface water for irrigation continue to decrease, then water levels, well yields, and base flows to the river will also decrease.

R. A. Barker used a simulation model of the stream-aquifer system along the Arkansas River Valley in southwestern Kansas to show that water levels and streamflow in the valley were more directly affected by reductions in incoming streamflow than by either below-normal precipitation or increased pumpage that occurred during the 1970's. The model indicated that the effects of increased pumpage were partly offset by increased recharge resulting from additional irrigation. The effects of reduced recharge from precipitation during the 1970's drought were offset by increased recharge during short periods when precipitation was much greater than the mean monthly amount.

D. A. Stedfast reported that a one-dimensional, implicit, transient-state flow-simulation model was calibrated and verified for a 122-km reach of the Hudson River Estuary between Albany and New Hamburg, N.Y. In the estuary, the direction of flow reverses four times daily as far north as Albany except during high spring flows, which override the tidal influence. Maximum upstream (−) and downstream (+) flows over a tidal cycle typically range from ± 570 m^3/s at Albany to $\pm 7{,}100$ m^3/s at New Hamburg. The study reach was treated as two separate subreaches to incorporate differences in channel conditions and to simplify model calibration. A total of 10 continuous tidal-cycle discharge measurements were used to calibrate and to verify both subreach models and the final model. These models can accurately simulate instantaneous stage, velocity, and discharge for any location in the study reach and can also calculate the net outflow or backflow between tide reversals.

Harvey Jobson reported that a computer program for simulating one-dimensional, unsteady temperature and solute transport in a river in Mississippi was developed and documented for general use. The solution approach to the convective-diffusion equation uses a moving reference frame (Lagrangian) which greatly simplifies the mathematics of the solution procedure and dramatically reduces errors caused by computing dispersion numerically. The solution procedure has further advantages, relative to conventional Eulerian solutions schemes, of being easy to understand in the physical sense, of being extremely stable numerically, and of providing an accounting system that is very useful for model calibration.

The model can be used either for making very accurate temperature estimates or for routing as many as 10 interacting constituents through a river reach. The mathematical description of the interaction between the constituents, which do not need to be linear, must be supplied by the user. An example problem was solved for a three-parameter system involving temperature, dissolved oxygen, and BOD. For simplicity, the model was developed and presented assuming steady non-uniform flow. Generalization to allow unsteady flow is extremely simple, involving the addition of no more than 18 cards to the program deck.

J. J. Vaccaro reported that unregulated streamflow for the Yakima River at Union Gap and Parker, Wash. was computed for 52 water years using a verified digital storage-routing model. Unregulated streamflow is an estimate of natural streamflow; that is, the streamflow that would have occurred had there been no storage reservoirs, diversion canals, and wasteways operating in the river basin. The unregulated streamflow was then compared to the regulated streamflow for the same period. The comparison showed that the mean annual regulated streamflow at Union Gap was about 36 percent smaller than the unregulated streamflow, and the regulated streamflow near Parker was about 74 percent smaller than the unregulated streamflow. The mean monthly regulated flows at Union Gap were smaller than the unregulated flows for all months except August and September, whereas the regulated flows near Parker were always smaller than the unregulated flows (80 percent smaller for August and September). Frequency analyses showed that regulated flows were less variable than unregulated flows at both Union Gap and Parker.

Computational hydraulics

Numerical schemes for simulating three types of transient flows in urban storm sewers in southern coastal areas were studied by Chintu Lai. The three types are full-pipe flow, open-channel flow, and mixed or two-phase flow. A computer model for full-pipe flow was applied to a storm sewer flow in South Miami, Fla., and the simulated discharge hydrograph generally agreed with the measured one (Lai, 1980).

While initial research emphasis was focused primarily on the development and testing of various numerical schemes, attention was later directed toward research and development leading to easily used, operational models. The principle attributes, which are the essences of a usable flow model, were identified as (1) the ability to simulate a wide range of flow conditions; (2) the adaptability to permit schematization of channels having diverse prototype geometry; (3) the ability to generate stable, accurate results repeatably; (4) the ability to provide a high degree of computational efficiency; and (5) the ability to facilitate function, user-oriented modeling (Lai, Baltzer, and Schaffranek, 1980). Validity, reliability, and predictability of a numerical model for unsteady open-channel flow simulation are dependent on how accurately and rationally certain key parameters are defined by calibration and how well the model is adjusted. Based on physical reasoning, procedures and techniques were set for adjusting primary, secondary, and special parameters with some concrete illustrations (Lai, 1981).

Low Flows

Low-flow investigations were made in Texas in five watersheds north of the Colorado River (Brushy Creek, South Fork San Gabriel River, North Fork San Gabriel River, Berry Creek, and Salado Creek) and in five watersheds south of the Colorado River (Barton Creek, Williamson Creek, Slaughter Creek, Onion Creek, and Bear Creek) to determine reaches having gains and losses in flow.

According to E. T. Baker, Jr., R. M. Slade, Jr., and M. E. Dorsey, the information gained from these studies will enable an accurate delineation to be made of the recharge zone of the Edwards aquifer system for much of the extent of the aquifer. This knowledge is useful for urban-development planning, for protection of the aquifer, and for long-range planning of water use and management.

R. H. Bingham used multiple-regression analyses to derive relations for estimating 7-d, 2-yr and 7-d, 10-yr low flows in natural streams. One equation for each recurrence interval applied statewide. The regression analyses indicated that baseflow recession rate, drainage area, and mean annual precipitation were the most significant basin characteristics affecting low flow. Baseflow recession rate was used to account for the effects of ground-water discharge on the rate of low flow. Standard errors of estimate using mapped values were 40 percent for 7-d, 2-yr and 44 percent for 7-d, 10-yr low flows.

R. J. Reynolds computed daily mean base flows for 1959-75 at 19 gaged streams on Long Island, N.Y. A hydrograph-separation technique was used. From these daily means, monthly and annual means were computed. Reynolds showed a close relation between annual mean base flow and the discharge at 55 percent on the annual flow-duration curve. This relation offers a rapid and reliable means of estimating annual mean base flows of Long Island streams using hydrograph-separation techniques if only the annual mean base flow is wanted.

Miscellaneous studies

D. M. Mades measured discharge on the Des Plaines River downstream from Brandon Road Dam near Joliet and on the Illinois River downstream from Dresden Island and Starved Rock Dams near Channahon and Utica, respectively. Measurements made downstream from Dresden Island Dam were used to define a stage-discharge rating for submerged orifice flow under an 18.3-m-wide tainter gate. The discharge through a 0.91 m gate opening from a normal upstream pool surface 4.27 m above the spillway crest will decrease from 98.8 to 65.1 m^3/s as the downstream pool surface rises from 1.37 to 3.20 m above the spillway crest. At Brandon Road Dam, measurements indicated that the discharge under one 15.2-m-wide tainter gate raised clear of an upstream pool surface 0.69 m above the spillway crest would be 15.8 m^3/s. Measurements made downstream from Starved Rock Dam indicated that the discharge under one 18.3-m-wide tainter gate clear of an upstream pool surface 5.18 m above the spillway crest would be 416 m^3/s.

In the fall of 1980, J. T. Krohelski made discharge measurements at approximately 1.6-km intervals on Duck Creek and the Suamico River in Wisconsin to determine if these streams were losing water into the ground. Duck Creek is located in eastern Outagamie and northwestern Brown Countries. The Suamico River is located in northwestern Brown County. The streams flow into Green Bay and are probably within a cone of ground-water depression caused by industrial pumping from the city of Green Bay and municipal and industrial pumping from surrounding communities.

The discharge measurements indicated that the streams have losing reaches. Maximum losses on Duck Creek occurred just north of the town of Oneida (0.34 m^3/s) and on the Suamica River near the town of Suamica (0.84 m^3/s). Flow durations, based on nearby

gaging stations, were 68 percent for Duck Creek (October 7) and 34 percent for the Suamico River (September 17) when discharge measurements were made. Discharges from upstream to downstream sites ranged from 1.37 to 3.61 m^3/s on Duck Creek and 0.92 to 7.06 m^3/s on the Suamico River. Specific conductance ranged from 770 to 1,030 μmhos/cm siemans on Duck Creek and 620 to 1,000 μhos/cm on the Suamico River.

M. E. Moss and E. J. Gilroy developed a procedure to analyze the cost-effectiveness of stream-gaging activities. The procedure requires as input (1) the uncertainty in a mean discharge—monthly or annual—as a function of the number of visits to a gage to service recording equipment and to make discharge measurements; (2) a definition of feasible routes which one can use to visit the gaging stations; (3) the unit costs of each route, the cost of a visit to an individual station, and the fixed cost of office work associated with each station. The procedure minimizes the uncertainties over all stations for a given budget. The uncertainty function was derived from an application of Kalman-filter theory to discharge-rating-curve analysis. The theoretical development and an application to 19 stations in the lower Colorado River system operated out of the Blythe field office were described by Moss and Gilroy (1980). The application was extended to 60 stations operated out of Blythe and the Yuma subdistrict office. The results of this extension indicated that the present level of uncertainty could be achieved at 47 percent of the present budget, or that the present budget could be expended to reduce the total uncertainty to 45 percent of its present level.

R. Lumia and R. B. Moore calculated daily inflows and outflows at eight lake sites and the daily discharges at three stream sites in the Oswego River basin, New York, for the period 1934-79, using available lake-stage and streamflow data.

Several computer programs and computational methods were needed for a consistent data base because of regulated lake outflows, diversions into and out of the basins, and the lack of lake-level and (or) outflow data for some periods. Daily mean inflows for periods without data were computed from regression analysis of discharges at a nearby streamflow station. The calculated data are being used in a basin model to evaluate the impacts of changes in the management of lake levels on outflow characteristics.

R. Lumia calibrated a rainfall-runoff model for each of ten stream sites in Rockland County, N.Y. using data from 1975-79. Initial results indicated that model simulations of the growing season were biased. After a seasonal adjustment was added to the model, the average difference between observed and simulated peak discharges was reduced from 42 to 28 percent. The calibrated models are being used to extend flood-peak records at the sites for use in regional flood-frequency relations.

A channel geometry study was conducted by R. J. Omang and Charles Parrett relating measured channel dimensions to mean annual flow and peak flow for streams in southeastern Montana. Data from 30 streamflow-gaging stations on perennial streams and 17 gaging stations on ephemeral streams were used in the mean annual-flow analyses. Data from 74 gaging stations were used in the peak-flow analyses. Estimating equations were developed to determine mean annual flow and peak flow for ungaged sites in southeastern Montana. Development of the channel-geometry method showed channel width to be the most significant parameter for estimating flow characteristics. Use of this method required that onsite measurement be made of channel width. Equations were defined from data on streams virtually unaffected by urbanization, regulation, or diversion.

PALEONTOLOGY

Research by USGS paleontologists involves biostratigraphic, paleoecologic, taxonomic, and phylogenetic studies of a wide variety of plant and animal groups. The results of this research are applied to specific problems related to the USGS program of geologic mapping, to resource investigation, and provision of a biostraigraphic framework for synthesis of the geologic history of North America and the surrounding oceans. Some of the significant results of paleontological research attained during the past year (many of them as yet unpublished) are summarized in this section by major geologic age and area. Many additional paleontologic studies are carried out by USGS paleontologists in cooperation with USGS colleagues. The results of these investigations ordinarily are reported under the section "Geological, Geophysical, and Mineral-Resource Investigations."

MESOZOIC AND CENOZOIC STUDIES

Paleoecology of the Alaska Range (Mt. McKinley National Park and vicinity) during late Quaternary time

Pollen analyses of lacustrine sediment cores and outcrop samples from Mt. McKinley National Park and adjacent areas of the Alaska Range are being used to reconstruct a detailed history of vegetation and climate during the late Quaternary by T. A. Ager. Radiocarbon dates obtained thus far indicate that the longest continuous record obtained from the Alaska Range and vicinity spans the past 15,000 yr. Pollen analyses indicate that the vegetation of unglaciated areas of the

Alaska Range was herbaceous tundra during the Wisconsinan glacial interval. About 13,000 yr ago, mesic shrub tundra with dwarf birch began to invade the northern foothills of the Alaska Range. Shrub tundra continued to spread in the region for several thousand years. By 10,000 years ago, *Populus* trees appeared in valleys of the Alaska Range. Spruce and alder appear to have invaded the Nenana Valley simultaneously about 7,500 yr ago, but probably later in the western region of Mt. McKinley National Park.

Quaternary history of climate, southwestern Alaska

Pollen and diatom studies of lake sediment cores from Mt. Michael Island (Norton Sound, western Alaska) and Yukon delta (southwestern Alaska) are contributing to a detailed reconstruction of climatic and environmental history of southwestern Alaska during the past 40,000 yr according to T. A. Ager. Samples analyzed thus far suggest that the regional vegetation of western Alaska between about 40,000 and 14,000 yr ago was herbaceous tundra. The middle Wisconsinan interstadial interval was a rather minor event in western Alaska, with some slight increases in low shrubs and a greater diversity of herbaceous taxa. The interstadial is not yet dated locally, but is probably about 30–35,000 yr B.P. About 14,000 yr ago climate changed to warmer, moister conditions; shrub tundra replaced herb tundra quickly. About 7,000 yr ago, alders spread through the Norton Sound–Yukon delta region. About 5,500 yr ago, spruce reached eastern Norton Sound.

Late Tertiary and Quaternary shoreline datum planes and tectonic deformation in the southeastern United States

T. A. Ager, T. M. Cronin, and B. W. Blackwelder report that biostratigraphic studies of sedimentary units in the southern Atlantic Coastal Plain are being used to reconstruct the history of sea-level changes and regional tectonic deformation during the past 5 m.y.

Regional ostracode, mollusk and pollen zonations were developed to distinguish Pliocene and Pleistocene marine sediments in North and South Carolina and Virginia. Average uplift rates from 1 to 3 cm/1,000 yr for the North Carolina/South Carolina border area were calculated by comparing the present elevations of ancient Pliocene and Pleistocene shorelines to correlative eustatic sea-level positions.

A major marine regression occurred approximately 3.0 m.y. ago, which probably corresponds with the initial buildup of Northern Hemisphere ice sheets and the closing of the Isthmus of Panama. Consequently, warmer climates have prevailed along the Atlantic coast during interglacials of the last 3.0 m.y. due to the influence of the Gulf Stream. Emerged marine deposits of the Coastal Plain have been correlated with deep-sea cores. Study of the emerged deposits is being extended to include correlation with Pliocene and Pleistocene sediments in submerged parts of the Atlantic continental margin. Resolution of variations identified in preliminary findings will include acquisition and dating of additional faunal and floral material and critical examination of published late Quaternary sea-level data.

Wood Rat Chronology of the Pliocene and Pleistocene

Wood rats, or pack rats, are a fairly conspicuous part of the mammalian fauna of the United States because of their habit of infesting manmade structures in rural areas and of raiding camp supplies not properly protected, according to C. A. Repenning. They have recently gained geologic attention because of the large nests they make by gathering sticks and nearly everything else that they can carry and placing them in a pile. These nests may endure for thousands of years and record changes in the elevation of vegetational zones that can be carbon dated, providing temporal control on past climatic variations, but they now also are becoming of value in older geologic situations.

During the study of fossil meadow mice, which now provide a biochronology for nonmarine deposits younger than 5 m.y. old that is comparable in precision to that which nannofossils provide marine deposits, it was noted that a considerable variety of wood rats (otherwise unidentifiable) were often associated with fossil meadow mice. This established temporal calibration for the various unknown wood rats and provided a means for their history to be reconstructed and biochronologically recognized. The wood rats have a history that is comparable in length of time to that of the meadow mice, and they are represented in the living fauna by a considerable variety; they obviously have diversified rapidly. Their biochronology could be as useful as that developed for the meadow mice.

Preliminary study of the wood rats was begun in 1980 to see if their history of development could be recognized and calibrated in K/Ar yr. Results so far clearly indicate that this is possible. In addition, as a group the wood rats have a more southerly distribution and are relatively abundant in deposits of the southern United States and in Mexico where meadow mice are rare in fossil faunas. Further, the majority of their diversification appears at present to have taken place in the last 1 m.y., largely during the Brunhes Normal Polarity Event when meadow mice faunas were increasingly characterized by the presence of living species with consequent uncertainty of age. To date, many faunas that are related to changing tectonic patterns have been significantly reevaluated, with respect to their interpreted age, on the basis of the wood rats they contain. Further study promises to be rewarding.

Lower Eocene paleosols and sedimentology, Willwood Formation, Bighorn basin, Wyoming

The Willwood Formation studied by T. M. Bown is a 770-m-thick accumulation of fluvial sandstones, mudstones, carbonaceous shales, and conglomerates. Nearly all of the mudstones and sandstones have undergone modifications by ancient soil-forming processes. Paleosols in the formation include gley, pseudogley, and gley-podzol variants of the Spodosol, Entisol, and possibly Ultisol groups. Evidence of soil formation is obtained from clearly observable features such as spodic and albic horizons, carbonaceous epipedons, Bca, Bg, Bt, and Box horizons, gley mottling, iron and manganese sesquioxide glaebules, abundant bioturbation, taproot pedotubules, *Ophiomorpha*-like decapod lebensspuren, illuviation cutans on skeleton grains, clay-lined vugs, pedodes, ped slickensides, possible gilgai structures, possible catenas, development of coloration with little regard to stratification type, widespread areal extent of colored lower solum horizons, and evidence from thin-section studies that $CaCO_3$ cement in many sandstones was introduced early and before significant packing due to deep burial. The Willwood Formation is divisible into several facies on the basis of intonguing paleosol suites; and, in general, the Willwood paleosols show a tendancy toward thicker, less mottled spodic horizons and greater abundances of $CaCO_3$ glaebules higher in the section, indicating conditions of increasing dryness. It is believed that the dry conditions are related to the progressive structural elevation of mountainous areas surrounding the basin on the south and southwest. Preliminary data indicate that stratigraphic points of origination and "extinction," changes in the geometries of carbonaceous shales and fluvial sandstones, and changes in the morphology of paleosol suites are, in a general way, related stratigraphically.

Paleontologic investigations of Paleocene to lower middle Eocene sediments of eastern Alabama and western Georgia

Detailed paleontologic investigations of Paleocene to lower middle Eocene sediments (from outcrops and cores) of eastern Alabama and western Georgia by G. A. Andrews, L. M. Bybell, L. E. Edwards, N. O. Frederiksen, T. G. Gibson, and L. W. Ward produced integrated biostratigraphic and paleoecologic syntheses of nonmarine, marginal marine, and marine deposits using calcareous nannofossils, dinoflagellates, foraminifers, mollusks, and sporomorphs. Comparison of these data with those from preliminary outcrop and core investigations in Virginia indicates that the two areas had significantly different regional tectonic patterns. In the Gulf Coastal Plain deposits, two significant unconformities occur: (1) between calcareous nannofossil Zones NP4 and NP7 (between Porters Creek Clay and Nanafalia Formation), and (2) between Zones NP10 and NP13 (between Hatchetigbee and Tallahatta Formations). However, in the mid-Atlantic Coastal Plain, the only significant unconformity is between Zones NP3 and NP5 (between Brightseat and Aquia Formations). Work on the surface and subsurface stratigraphy of the central Virginia Coastal Plain has revealed an unusually complete record of Tertiary sedimentary events. Units exposed along the Pamunkey River and its tributaries include the Aquia Formation (lower(?) and upper Paleocene), Nanjemoy Formation (lower and middle Eocene), a possibly unnamed middle Eocene unit, an unnamed upper Oligocene unit, the Calvert Formation (lower and middle Miocene), the Choptank Formation (middle middle Miocene), the Eastover Formation (upper Miocene), and the Yorktown Formation (lower and middle(?) Pliocene). This river section exposes numerous beds in a relatively short distance; several beds were previously known only in the subsurface.

California-Washington late Paleogene biostratigraphic zonations

Late Paleogene biostratigraphic zonations based on benthic foraminifers for California and Washington were developed independently, as reported by K. A. McDougall. These microfossil zonations were assumed to be properly alined, but correlations are difficult because of species endemism and because species common to these areas have different stratigraphic ranges. Problems such as these result in transgressive stage and zone boundaries, and ecologically or geographically (latitudinally) controlled units. Resolution of the chronostratigraphic and biostratigraphic problems is accomplished by careful examination of the ecology and the relation of the provincial framework to those of the planktic microfossil groups. With modification, the benthic foraminiferal sequence can be chronostratigraphically useful. Initial work has concentrated on several key sections in northwestern Oregon, southwestern Washington, and isolated sections in California. In all cases, evidence suggests that past correlations based on the provincial benthic zonations have missed features important to the interpretation of the geologic history and paleogeography. Among these features are synchronous but bathymetrically different assemblages, intervals of low-oxygen conditions, and regional correlations.

Tertiary global ice-volume history

A review of pertinent information concerning $\delta^{18}O$ record from Cenozoic marine calcite by R. Z. Poore indicates that the currently accepted concept of an ice-free world prior to middle Miocene time is erroneous. In fact, existing data from low-latitude areas are compatible

with significant global ice volume since the Eocene and perhaps throughout much of the Cretaceous.

Upper Cretaceous geological studies along Tombigee River, western Alabama and eastern Mississippi

Geological studies along the Tombigbee River in western Alabama and eastern Mississippi by C. C. Smith have documented significant variations in lithology, thickness, and contact relations for several Upper Cretaceous stratigraphic units. Geological field investigations have been completed along about 250 km of the river extending from near Gainesville, Ala., northwestward to Fulton, Miss. To date, 163 geological exposures have been measured and described, and 667 samples collected for sedimentologic and paleontologic investigations.

Within the southern portion of the area investigated, the Eutaw Formation consists principally of carbonaceous clay, whereas further north the Eutaw consists typically of crossbedded quartzose sand. The Tombigbee Sand, the upper member of the Eutaw Formation, varies dramatically in sedimentologic character as well as thickness. Near Pickensville, Ala., the Tombigbee consists of over 34 m of massive, extensively bioturbated, glauconitic quartzose sand. Where observed, the contact between the typical Eutaw and its Tombigbee is unconformable. The contact between the Eutaw Formation and the overlying Mooreville Chalk is generally disconformable, although at Plymouth Bluff near Columbus, Miss., the contact appears to be gradational. Within the areas studied, the Mooreville Chalk and its upper member, the Arcola Limestone, are each relatively uniform in lithological character – the Mooreville consisting of about 61 m of chalky marl and its Arcola consisting of between 0.6 to 2.2 m of indurated calcisphere-rich limestone with interbedded marl.

Mudstones as exploration guides to tabular sandstone-type uranium deposits

As part of continuing uranium mineralization studies, Fred Peterson proposed a lacustrine humate model that attempts to account for the presence of uranium in some of the tabular sandstone deposits in the Salt Wash Sandstone Member of the Morrison Formation of the Colorado Plateau. The present project of R. H. Tschudy and S. D. VanLoenen was designed to provide data on the amount and type of organic material in the sandstones and adjacent mudstones and thereby enable them to predetermine the favorability of a region for uranium mineralization. Preliminary results suggest a positive correlation between the presence of palynomorphs and some types of organic matter with uranium occurrence. A negative correlation is observed between the presence of the algae *Botryococcus* and uranium occurrence..

Tectonostratigraphic terranes of central Alaska Range

The central part of the Alaska Range near Mt. McKinley, as defined by D. L. Jones, N. J. Silberling, and P. J. Coney, is composed of eight separate tectonostratigraphic terranes that were accreted in southern Alaska during late Mesozoic time. These terranes now form long linear fault-bounded belts that are subparallel to the Denali fault on the north, but oblique to the fault on the south. Post-accretion right-lateral offset along the Denali fault system is about 220 km. From north to south, the major terranes are as follows:

1. Yukon-Tanana terrane: metasedimentary and metavolcanic rocks, mostly undated, but including rocks of known late Paleozoic age; polymetamorphosed with terminal events in the late Mesozoic.
2. Pingstone terrane: isoclinally folded Upper Triassic deep-water silty limestone, quartzite, and sooty slate, folded with upper Paleozoic phyllite, chert, tuff, and minor limestone.
3. McKinely terrane: upper Paleozoic flysch, chert, minor limestone; intruded by large gabbro sills and dikes, and overlain by thick piles of upper Mesozoic conglomerates, flysch, chert, and phyllite.
4. Dillinger terrane: very thick sequence of strongly folded lower Paleozoic micaceous sandstone (turbidites) and deep-water, poorly fossiliferous limestone; locally overlain unconformably by Jurassic fossiliferous sandstone or Triassic(?) pillow basalt.
5. Windy terrane: heterogeneous assemblage of serpentinite, basalt, tuff, and chert (=ophiolite?) with Paleozoic and Mesozoic flysch and blocks of Paleozoic and Mesozoic fossiliferous limestone.
6. Chulitna terrane: Upper Devonian ophiolite overlain by upper Paleozoic chert, volcanic conglomerate, limestone, and flysch, capped by Lower Triassic limestone and Upper Triassic red beds, basalt, and interbedded basalt and limestone; later Mesozoic rocks are sandstone, chert, and argillite.
7. West Fork terrane: Jurassic chert, sandstone, conglomerate, and Triassic(?) and Jurassic crystal tuff.
8. Broad Pass terrane: upper Paleozoic chert, tuff, and argillite, with blocks of Devonian and older limestone weakly associated with serpentinite. These diverse terranes, of mixed oceanic and continental affinities, are now juxtaposed in a complex sequence of folded, rootless nappes, with major suture zones marked by intensely deformed upper Mesozoic flysch.

Major post-Triassic tectonic juxtapositon in northwesternmost Nevada

Field studies in northwesternmost Nevada by N. J. Silberling during 1980, partly in collaboration with R. C. Speed and his students from Northwestern University, have clarified the geologic relations among tectonostratigraphic terranes suspected of having been tectonically accreted to the North American continent during Mesozoic time. This important sequence essentially spans the Norian Stage of the Upper Triassic in the Jackson Mountains and Pine Forest Range. As such, this sequence contrasts markedly with the adjacent, largely correlative nonvolcanic Norian strata of the Auld Lang Syne Group that represents part of the early Mesozoic miogeocline along the western margin of North America in northwestern Nevada. This relation demonstrates, for the first time, major tectonic juxtaposition of one or more accreted terranes against this part of the continental margin in post-Triassic time. This is of significance not only for understanding the tectonic evolution of the Pacific margin but also for delimiting metallogenic provinces in the region.

PALEOZOIC STUDIES

Paleoecology of Mississippian corals in western conterminous United States

In the Rocky Mountain and Great Basin regions of the United States, 46 coral genera and subgenera are associated with six lithofacies deposited in environments ranging from deep water to very shallow water in a study completed by W. J. Sando. Colonial Rugosa occur exclusively in shallow-water lithofacies. Tabulates occur in both deep- and shallow-water lithofacies. Among the solitary Rugosa, which occur in both deep- and shallow-water lithofacies, deep-water forms are predominately nondissepimented. The distribution patterns conform in a general way to the tripartite facies classification of coral morphotypes proposed by Dorothy Hill (1938) for the Early Carboniferous of Great Britain. Calculation of a shallow-water-habitat index (SWHI) numerically expresses the ecological occurrence of each taxon and permits ranking of the taxa in order of the approximate probability of their occurrence in shallow water. Most taxa that occur in both deep- and shallow-water lithofacies first appeared in deep water, then migrated to shallow water later in geologic time. Corals lived predominately in deep water during Kinderhookian (early and middle Tournaisian) time, despite the existence of large areas of shallow-water environments that took place in latest Kinderhookian (middle Tournaisian) time. In the Osagean (middle and later Tournaisian), Meramecian (early to late Viséan), and Chesterian (late Viséan and early Namurian), corals lived overwhelmingly in shallow water, although late Osagean (late Tournaisian) and early and middle Meramecian (early and middle Viséan) time was marked by the return of a significant number of Kinderhookian taxa and some younger taxa to deep water.

Newly discovered disconformity; lower Paleozoic, Bear River Range, Utah-Idaho

An integrated biostratigraphic and magnetostratigraphic study of the St. Charles and Garden City Formations in the Bear River Range, southeastern Idaho and northern Utah, was made in 1979 and 1980 by M. E. Taylor, S. Gillett, E. Landing, and J. E. Repetski. Results showed that (1) the Cambrian-Ordovician boundary is contained in the upper part of the St. Charles Formation, and (2) the sharp contact between coarse textured, secondary dolomites at the top of the St. Charles and the relatively unaltered lime mudstones and lime grainstones of the overlying Garden City Formation represents a disconformity. Presence of a disconformity is supported by petrographic evidence and the absence of several conodont subzones at the formational contact. In addition, trilobites from the basal Garden City correlate with the upper *Symphysurina* zone as developed in other parts of the Western United States—a correlation consistent with associated conodonts. Preliminary paleomagnetic data from the St. Charles indicate that the formation is dominantly and perhaps entirely of reversed polarity (declination 179°, inclination −31°), but with much scatter present. In contrast, data from the Garden City show normal polarity (declination 357°, inclination 31°) and are more tightly clustered. The directions obtained are not significantly different from being exactly antipodal and together yield a preliminary paleomagnetic pole at 65° N. 74° E. Age of magnetization is poorly known in detail. A "fold test" shows the magnetism to have been emplaced prior to Laramide folding of the Logan Peak syncline. The low inclination yields a paleolatitude of approximately 17°—a position consistent with independent sedimentological arguments for a low-latitude position of the early Paleozoic paleoequator. The change from reversed to normal polarity occurs abruptly at the disconformity between the St. Charles and Garden City Formations, a position within the Lower Ordovician *Symphysurina* zone. Because the paleomagnetic pole position is virtually the same in both formations, a hypothesis is suggested that the reversed-polarity magnetic signature was imposed on the St. Charles during a time of subareal exposure and diagenesis prior to Garden City deposition.

PLANT ECOLOGY

Longitudinal stream-dispersion measurements

J. B. Graf reported that measurements of travel time and longitudinal dispersion were made on Illinois streams ranging in drainage area from 326 km² to 3,926 km². Measurements were made at flows corresponding to about 20 percent, 50 percent and 80 percent on the flow-duration curve. Velocities of peak dye concentration ranged from 0.39 to 0.50 km/h for the low-flow measurements, and from 0.94 to 3.03 km/h for the high-flow measurements. Preliminary analyses indicate that section controls were more important than slope in controlling velocity of concentration peaks at low flows, and that slope increased in importance with increasing flow.

Reservoir storage requirements

Carryover storage requirements were defined by W. J. Carswell, Jr., using the probability-routing method and annual streamflows for unregulated Kansas streams with drainage areas of less than 780 km². Mass-curve analysis of flows for each year was used to define within-year storage requirements. Carryover and within-year storage requirements were combined to determine the total storage required to sustain gross reservoir outflow. From these results, regional draft-storage curves for 2-, 5-, and 10-precent chances of deficiency were developed and were presented as three-parameter plots of draft rate against average annual runoff for selected levels of storage. These curves can be used to estimate the storage required to sustain gross reservoir outflow at sites where continuous streamflow records are not available. A comparison of defined sustained gross outflow for a 2-percent chance of deficiency with gross outflow calculated from regional relations showed a root mean square error of 26.3 percent. Relations are included that can be used as a rough approximation to adjust draft-storage curves at ungaged sites for the effect of serial correlation.

Effects of flooding on vegetation and tree growth

Flood magnitude and frequency were shown to be important determinants of riparian vegetation distribution, and analysis of this distribution allows interpretation of hydrologic vegetation and geomorphic characteristics of a given reach of stream. In a study on parts of the Passage Creek flood plain, C. R. Hupp showed that changes in stream profile (gradual to steep) can affect the distribution of vegetation, flood frequency, and channel pattern. These changes are reflected in the vegetation types and various forest ecology parameters observed along different reaches of Passage Creek, Va. Discrete zones of vegetation may develop parallel to the stream channel where flood frequency is high. These zones may indicate the actual frequency of flooding and therefore can be useful in defining flood plains for a flood of any given magnitude.

Differences in ring widths for flood-plain trees along the Potomac River near Washington, D.C., appear in large part to be related to differences in flood-flow regimes. T. M. Yanosky found that trees exposed to the full forces of flood velocities are damaged more often than trees sheltered from high velocities, and thus have more variable ring-width patterns. The ring width variability of unsheltered trees was greatest at low flood-plain altitudes, which indicates that values are positively correlated with flood frequency. Sheltered trees, however, had less variable ring-width values that were approximately the same regardless of flood frequency. Unusually narrow rings formed in a vigorous tree during an otherwise favorable growth year may indicate severe flood-induced crown damage. Extremely wide rings may indicate that growth stimulation followed flood removal of parts of the adjacent forest. The rings of flood-plain trees can thus be used for reconstructing the occurrence and crest altitude of floods, and may aid in constructing risk-probability maps for potential flood-plain developments.

Tree-ring series provide proxy records of streamflow

Tree-ring series representing six tree species from seven sites were used by R. L. Phipps to reconstruct monthly summer flow in the Occoquan River basin of northern Virginia. Individual reconstructions were accomplished for the months April through August, from 1841 to 1975. Reconstructions for June, July, and August were judged more reliable than the months April and May. Major droughts of several years duration were indicated as having occurred in the early 1870's, the early 1930's and the mid 1960's. A greater frequency of extreme low flow during individual years is indicated for the entire record than for the most recent 50 yr.

Flood-plain tree distribution and forest litter-fall production

The tree distribution and wetland hydrology of the Apalachicola River flood plain in northwest Florida have been described by H. M. Leitman, J. E. Sohm, and M. A. Franklin. The flood plain supports 450 km² of bottomland hardwood and tupelo-cypress forests. The most common trees were five wet-site species, water tupelo (*Nyssa aquatica*), Ogeechee tupelo (*N. ogeche*), baldcypress (*Taxodium distichum*), Carolina ash (*Fraxinus caroliniana*), and swamp tupelo (*Nyssa sylvatica var. biflora*), comprising a relative basal area of 62 percent. Other common species were sweetgum (*Liquidambar styraciflua*), overcup oak (*Quercus lyrata*), planer-

tree (*Planera aquatica*), green ash (*Fraxinus pennsylvanica*), water hickory (*Carya aquatica*), sugarberry (*Celtis laevigata*), and diamond-leaf oak (*Quercus laurifolia*). Five forest types were defined based on dominance by basal area. Biomass increased downstream and was greatest in forests growing on permanently saturated soils. Water and tree relations varied with river location because range in water-level fluctuation and topographic relief in the flood plain diminished downstream. Height of natural riverbank levees and the size and distribution of breaks in the levees have a major controlling effect on flood-plain hydrology. Depth of water, duration of inundation and saturation, and river location, but not water velocity, were very highly correlated with forest types.

Litter fall from the same forest types was collected and described by J. F. Elder. Leaves from 42 species of trees and other plants accounted for 58 percent of total litter fall. The remaining 42 percent was non-leaf material. Average litter fall was 800 (g/m^2)/yr in the flood plain. Tupelo (*Nyssa*), baldcypress (*Taxodium*), and ash (*Fraxinus*), produce over 50 percent of the leaf fall. Common levee species such as sweetgum and diamond-leaf oak are also major contributors to total flood-plain litter fall. Flooding of the river annually transports portions of the litter-fall products to Apalachicola Bay.

Nutrient yield of the Apalachicola River, Florida

Four major gaging stations on the Apalachicola River in northwest Florida permitted subdivision of the 450 km^2 flood plain and river into three major input-output units, according to H. C. Mattraw and J. F. Elder. Extensive water-quality and flood-plain litter data were used to estimate flood-plain yields of nutrients and organic detritus. The gaged portion of the basin is 1,776 km^2, containing approximately 400 km^2 of bottom-land hardwoods. The net yield for the basin was 68,400 Mg of carbon, 1,070 Mg of nitrogen, and 237 Mg of phosphorus for the period June 1979 to June 1980. Flood-plain leaf studies by D. J. Cairns (unpublished data) indicated a rapid loss of nitrogen and phosphorus during decomposition. A large fraction of the residual carbon was transported by annual spring floods. Nitrogen and phosphorus solubilized from forest litter were retained on the flood plain and presumably recycled into the vegetative community.

Effects of flooding on Passage Creek, Virginia

A study by C. R. Hupp on parts of the Passage Creek flood plain showed that (1) flood magnitude and frequency is an important determinant of riparian vegetation distribution and that analysis of this distribution allows for inference on the hydrologic and geomorphic characteristics of a given reach of stream, and (2) increment core analysis of tree stem deformations along the stream allow for a 200-yr reconstruction of extension of peak flow.

Changes in stream profile (gradual to steep) can affect the distribution of vegetation, flood frequency, and channel pattern. These changes are reflected in the vegetation types and various forest ecology parameters observed along different reaches of Passage Creek, Va. Discrete zones of vegetation may develop parallel to the stream channel where flood frequency is high. These zones may indicate the actual frequency of flooding and therefore be useful in determination of the 2-5-10-etc.-yr flood plain. The extension of the peak-flow record should improve magnitude and frequency information, especially in recurrence-interval determinations.

Landslides, scars, and revegetation in western Virginia

A study by C. R. Hupp was expanded to show the generality of block-field movement in central Appalachia, particularly in the Massanutten mountain system in northwestern Virginia. Associated with block fields on steep slopes are slide tracks, where blocks and earth are repeatedly evacuated from block fields. These slide tracks are scars on the hillslope with a debris fan at their base. Revegetation studies on the slide tracks indicate a process adjustment by the plants growing here for repeated geomorphic disturbance. The dominant forest species (hemlock and sweet birch) germinate rapidly after block movement, thus maintaining the integrity of the forest composition.

CHEMICAL, PHYSICAL, AND BIOLOGICAL CHARACTERISTICS OF WATER

Trace metals in surface water on Healy and Lignite Creeks, Alaska

As part of a 2-yr study by D. E. Wilcox, four trips were made to Healy and Lignite Creek basins in the Nenana coal field in 1980 in an effort to determine the source, concentration, and distribution of 11 trace metals in surface waters and stream sediments. Samples were collected from three sites in each basin. Analytical results from the first year's samples showed that, of the 11 trace metals, iron, lead, manganese, nickel, and zinc were present in appreciable concentrations. Dissolved and suspended trace metals concentrations were higher in the Lignite Creek basin than in the Healy Creek basin; dissolved manganese consistently exceeded 100 $\mu g/L$ at each of the three sites in the Lignite Creek basin.

Tritium analyses for the Indiana Dunes National Lakeshore

Analysis of samples for tritium provided support for the hypothesis that the ground-water mound in Cowles Bog, Indiana Dunes National Lakeshore, Ind., is due to a discontinuity in the confining layer separating the shallow and deep aquifers, according to W. W. Lapham. Background tritium concentrations of 46 and 0.3 tritium units were found in samples from wells in the shallow unconfined and the deep confined aquifers, respectively. Ground-water samples taken from wells in the shallow aquifer in the mounded area of Cowles Bog were determined to have tritium concentrations approximately equal to those of the deep aquifer, ranging from 0.5 to 0.7 tritium units. Thus, low-tritium water from the confined aquifer is discharging upward into the unconfined aquifer through an apparent discontinuity in the confining layer beneath Cowles Bog.

Nutrient transport in a small agricultural watershed in New York

Preliminary calculations of nutrient-transport from the Switzer Creek basin, a small agricultural watershed in central New York, indicated that most phosphorous is transported during storm runoff, and most nitrogen is transported during base flow. According to D. A. Sherwood, 90 percent of the total phosphorous is transported during high flows because of the strong affinity of phosphate for particulate matter, which occurs in greatest concentrations during high flows. Approximately 80 percent of the total nitrogen is transported during base flow when nitrite plus nitrate are the major fraction. Organic nitrogen is the major fraction (85 percent) of the nitrogen transported during high flows.

Specific conductance and pH of precipitation in Oregon

Six sampling sites were established to monitor the quality of precipitation in northern and central Oregon. Samples were collected from June 1980 through March 1981. Specific conductance and pH were measured at the Portland laboratory within 48 hr after storm events. According to S. W. McKenzie and J. M. Laenen, analyses of 130 samples indicated that 90 percent of the samples had pH values of 5.6 or less, and 10 percent had pH values of 4.6 or less. The median pH value was 5.1 and the range was 4.0 to 6.2. ("Pure" rain is considered to have a pH of 5.6.) Of the 130 samples measured, 90 percent had specific conductances less than or equal to 31 μmhos/cm (at 25°C) and 10 percent had values less than or equal to 4 μmhos/cm. Specific conductances ranged from 2 to 81 μmhos/cm, with a median value of 9 μmhos/cm.

Ground-water quality in the Virginia Triassic

Chester Zenone and Alex Posner completed collection of ground-water-quality data from wells and springs in Triassic sedimentary rocks in the Culpeper basin in northern Virginia. Analysis of data indicates that most of the ground water is hard to very hard (from 120 to more than 180 mg/L $CaCO_3$), and that wells deeper than about 150 m in siltstone, and wells and springs located near the contact with diabase intrusions produce a highly mineralized calcium sulfate-type water. Wells completed in other rocks in the basin (sandstone and conglomerate) or at shallower depths in the siltstone yield a less mineralized, calcium bicarbonate water.

Calculation of pesticide values in water

A method of calculating the pesticide partition between sediment and water for environmental systems was devised by M. C. Goldberg. Pesticide values were calculated for natural systems in which the pesticides were partitioned between sediments and water. Two equations were evaluated that correlate the surface area, pesticide concentration on the sediment, and pesticide concentration in the water. The first, a linear equation, proved sufficiently accurate to calculate 45 of 48 data points to within one order of magnitude of the observed values. The second, a 7th degree polynominal, was used on the same data set and resulted in a calculation of 46 of 48 values within one order of magnitude. Comparisons of the relative accuracy of the two equations indicated that the linear equation was capable of reproducing the observed values to within 10 percent for 39 percent of the data set tested, whereas the 7th degree polynominal was capable of achieving this accuracy for 52 percent of the same data set. The correlations of surface area with pesticide partitioning illustrated the use of a readily measurable parameter (surface area) and pesticide concentration in the sediment to allow calculation of a non-measurable parameter (pesticide concentration in water). The results of this study can be used to make approximate calculations of the pesticide content of water at concentrations below measurable limits of present day analytical equipment.

Volatilization of organics from streams

R. E. Rathbun and D. Y. Tai developed several correlations relating the volatilization coefficients of slightly soluble organics to the hydraulic and geometric properties of streams. The multivariable correlation of volatilization coefficient with the energy dissipated per unit mass of water per unit time and the average depth

of flow resulted in the smallest root-mean-square error. Procedures for adjusting the volatilization coefficients for different organics were based on the molecular diffusion coefficient, molecular weight, or molecular diameter.

RELATION BETWEEN SURFACE WATER AND GROUND WATER

Stream-induced water-level changes, Chicot aquifer, southwestern Louisiana

A comparison of potentiometric maps for late February 1979 and 1981 showed that the major rivers in southwestern Louisiana have a significant effect on water levels in the Chicot aquifer. According to D. J. Nyman, water-level declines following a period of less-than-normal rainfall in 1980 through the spring of 1981 were greatest adjacent to major rivers partly because of decreases in river stages. Streams that originally were discharge boundaries have become sources of recharge to the Chicot aquifer because of intensive, long-term pumping for rice irrigation that has altered natural ground-water flow patterns.

In the northeastern part of the area where the aquifer is hydraulically connected to the Atchafalaya River, declines ranging from 1.5 to 3 m have occurred within 16 km of the river. Similarly, water-level declines within 16 km of the Sabine River in Beauregard Parish (at the northwestern boundary of the rice-growing area) ranged from 0.3 to 1.1 m. Water-level declines adjacent to the Calcasieu River in the natural recharge area of the Chicot aquifer ranged from 0.3 to 1.4 m.

In irrigated areas away from major rivers, water-level changes ranged from declines of about 0.3 m, or less, to rises of 0.1 to 1.5 m and averaged about 0.2 m.

Increased pumping may decrease lake levels and streamflow in parts of Minnesota.

R. T. Miller reported that an increase in the number of pumping wells in the Pelican River sand aquifer in northwestern Minnesota may cause nearby lake levels to be lowered. Two-dimensional ground-water-flow model simulations of hypothetical well locations and pumping rates indicated that, under current conditions of ground-water recharge, ground-water levels near Sallie, Mellisa, and Detroit Lakes may be lowered as much as 0.8 m. Long-term drought conditions may cause an additional 1.0-m decline of ground-water levels near the lakes, which, in turn, will cause increased seepage losses from the lakes. An analytical model used to simulate hypothetical pumping conditions along the Pelican River, from Pelican Rapids to Elizabeth, indicated that wells located near the river have the potential to decrease flow of the river by as much as 0.3 m^3/s.

Interrelations between lakes and ground water in Wisconsin

Hydrologic budget studies of two lakes in northern Wisconsin were begun by D. A. Wentz and W. J. Rose to examine potential responses to acid rain. Lake Clara in Lincoln County and Vandercook Lake in Vilas County have similar alkalinities (1 mg/L as $CaCO_3$), pH values (6), surface areas (0.34-0.39 km^2) and ratios of lake surface to contributing drainage area (27–30 percent); both lakes are surrounded by sandy soils. Neither lake receives channelized surface inflow. Although both lake surfaces are continuous with the local water table, preliminary data indicate that the two lakes are hydrologically dissimilar. Lake Clara appears to be a ground-water recharge lake (flow occurred away from the lake in all directions from October 1980 through March 1981), and Vandercook Lake appears to be a ground-water flow-through lake. The water table to the east is upgradient and discharged to the lake from November 1980 to March 1981; to the west the lake recharged the ground-water system.

Hydrologic effects of impoundment construction in Sherburne National Wildlife Refuge, Minnesota

Data collected by B. M. Wrege in a study of the potential effects of an impoundment system in the Sherburne Wildlife Refuge, south-central Minnesota, suggests a direct correlation between water levels in the surficial aquifer and the stage of the St. Francis River. The thin sand and gravel aquifer is underlain by till and reacts quickly to changes of river level. Water-quality data indicated that dissolved phosphorus may be retained by biota and that biological decomposition and ground-water discharge during the summer months may increase the dissolved-solids concentrations in surface water. Mass-transport calculations provided information on (1) the ability of the watershed to retain suspended sediment, (2) the amount of ground-water discharge, and (3) the retention of phosphorus in the wetlands due to biological activity. Preliminary data suggested that concentration of nitrite plus nitrate (as nitrogen) was inversely proportional to stream discharge, but sufficient data were lacking to define this relation well.

LIMNOLOGY AND POTAMOLOGY

Although the term "limnology" originally applied only to the study of lakes, its current usage also applies to the study of streams and rivers. The term "potamology" is more restrictive; it applies only to river investigations. Limnology is the study of the sources and nature of freshwaters, the motion and changing conditions of

freshwaters, and the organisms supported by freshwaters.

Nutrient Limitation in Arctic Tundra Lakes

Batch culture algal bioassays using *Selenastrum capricornutum* Prinz were used by G. A. McCoy to successfully predict the limiting nutrients in two small arctic tundra lakes near Umiat, Alaska. The lakes were fertilized with nitrogen and phosphorus to test the prediction developed from the results of bioassays. Phosphorus fertilizer caused the phytoplankton standing crop to increase 10-fold. The subsequent addition of nitrogen caused an additional 10-fold increase in phytoplankton and periphyton organisms. Nitrogen fertilizer alone did not stimulate algal growth.

Denitrification associated with algal communities in streams

The potential role of denitrification as a mechanism for nitrogen loss from streams was studied by F. J. Triska and R. S. Oremland. Laboratory and in situ experiments were conducted using the acetylene inhibition technique on samples of senescent algal mats of *Caldophora* from a small urban stream in California. In laboratory flasks, scrapings of decomposing algal mats produced nitrous oxide (N_2O) without a lag when incubated anaerobically with 15 percent acetylene. Denitrification (N_2O formation) was enhanced by addition of nitrate and was inhibited by autoclaving and by the presence of mercury (Hg^{+2}) or oxygen, and by the absence of acetylene. Chloramphenicol, an inhibitor of new protein synthesis, did not block N_2O formation, thereby indicating that the enzymes were present in the original stream microbial community. In situ incubations of periphyton scrapings in the light resulted in an inhibition of denitrification caused by algal photosynthetic oxygen production. In situ estimates of activity were 34 nanomols N_2-N per cubic centimeter of periphyton scrapings per day (40 micromols N_2-N per square meter of rock surface per day). These results indicated that denitrification is potentially a significant means of nitrogen removal from fluvial environments.

Effect of simulated canopy cover on algal nitrate uptake and primary production in small streams

Benthic algal communities in small pristine drainages may significantly affect the fluvial transport of inorganic nitrogen. The effect of canopy cover on algal nitrogen uptake and primary production was experimentally tested in plexiglass channels in a third to fourth order drainage in northwestern California. F. J. Triska, V. C. Kennedy, R. J. Avanzino (USGS) and B. N. Reilly (San Francisco State University) conducted the field experiments in which nutrient and shade combinations in the flowing-water channels were as follows (1) unshaded control with background concentrations of nutrients (40 μg/L NO_3-N, 10 μg/L PO_4-P); (2) shade treatments (0, 30, 66, and 92 percent shade) all of which were amended with approximately 100 μg/L NO_3-N and 25 μg/L PO_4-P. Algal biomass accumulation was similar in both of the fully lighted channels, but chlorophyll concentration was twice as great in the channel receiving nutrient additions. The biomass:chlorophyll ratio increased in the control channel but decreased by half or more in the treatment channels. Day-night differences were observed in nitrate concentration of water leaving the channels, but the magnitude of the fluctuations did not increase directly with biomass accumulation due to gradual algal senescence. Regression analysis indicated that nitrate uptake was significantly related to algal primary production. Consequently the impact of algae on nitrogen transport may be related to meteorological events which alter (or reset) the algal community.

Limnology of Lake Bruin, Louisiana

Limnological investigations of Lake Bruin, an oxbow lake in northeastern Louisiana, produced several significant findings during 1980, according to H. L. Leone, Jr. The lake was shown to be monomictic, remaining thermally stratified from approximately mid-March until November when fall overturn occurred. During the winter months when the lake was well mixed, dissolved oxygen was abundant (about 10 mg/L) throughout the water column. However, for the remainder of the year, anoxic conditions existed below the thermocline (at a depth of 5-8 m) in the lake, which has areas with a maximum depth of 16 m. An active phytoplankton population existed in the lake with peak densities occurring during the summer months. Nitrogen appeared to be the limiting nutrient, and bloom conditions did not occur. Nitrogen-fixing blue-green algae represented 99 percent of the algal population during the summer when inorganic nitrogen concentrations were less than 50 μg/L, but only 41 percent of the population during the winter when inorganic nitrogen concentrations were greater than 300 μg/L. Investigations of possible bacterial contamination of the lake showed extremely small concentrations of fecal-coliform and fecal-streptococci bacteria; 90 percent of the samples had zero counts.

Water quality of surface waters affected by a proposed flood-control project in Chaska, Minnesota

The water-quality characteristics of East Creek and Chaska Creek were determined by L. H. Tornes to be similar. Concentrations of dissolved solids, sulfate, chloride, and chromium in the creeks were found to

result primarily from ground-water discharge. The pesticides alachlor, atrazine, prometryne, and 2,4-D were found in samples from both creeks but were well below the lethal concentrations for fish.

Phytoplankton populations in Courthouse Lake, a 17.4-m deep-instream trout lake, varied seasonally with blue-green algae predominant in late summer. The algal-pollution index of the lake was highest in late summer, but it did not indicate high organic pollution. The apparently successful recovery of Courthouse Lake from total phosphorus concentrations as high as 0.66 mg/L caused by Minnesota River floodwaters suggests that the lake eventually will recover from runoff expected as a result of the proposed Chaska flood-control project. The runoff could temporarily raise the total-phosphorus concentration from 0.03 to 0.12 mg/L.

Limnological reconnaissance of reservoirs in eastern Montana

Several lakes and reservoirs in Phillips and Valley Counties, Mont., were sampled by R. F. Ferreira to determine their suitability for fish propagation, waterfowl habitat, livestock watering, and recreation. Surface areas range from 0.2 to 28 ha and depths range from 0.3 to 6.0 m.

Most of the reservoirs are enriched with plant nutrients and consequently can support large concentrations of phytoplankton and dense growths of aquatic plants. In late winter and late summer, this enrichment in shallow reservoirs results in dissolved-oxygen concentrations that are detrimental to fish. Of the 24 reservoirs studied, 6 generally contained water of good quality for fish propagation.

The reservoirs studied provide varying degrees of habitat for waterfowl. Some reservoirs had small dissolved-oxygen concentrations that may be critical if botulism were a concern. Toxic concentrations of water-quality variables were not detected.

Dissolved-solids concentrations of three reservoirs were critical to the protection of livestock. In addition, potentially toxic species of phytoplankton were collected from eight reservoirs. In general, most of the reservoirs serve well for livestock watering.

The reservoirs sampled generally would not be conducive to swimming. Visibility is poor in most reservoirs and eye irritation from high pH values would occur in late summer. In addition, leech populations and growths of submerged aquatic plants in most of the reservoirs would be a nuisance to swimmers.

Death of fish eggs in the Truckee River near Reno, Nevada

A cooperative United States Fish and Wildlife Service–USGS study to document cause-and-effect relations between observed mortality of Lahontan cutthroat trout eggs and various water-quality and streambed parameters was made in the Truckee River during the late winter and early spring of 1980. According to R. J. Hoffman, hatchery eggs were artifically planted in the river, both upstream from Reno where previous egg studies have shown good survival, and downstream from Reno where past studies have documented 100 percent mortality. After an incubation period of about 4 wk, virtually all eggs, including those at the upstream control sites, had died. The death of eggs at the control sites, of course, compounds the difficulty in determining what environmental factors contributed to the poor survival. The data suggest that the less hardy hatchery eggs used in this study, compared to wild stock, were not able to withstand prolonged low-water temperatures (less than 4°C) at the sites upstream from Reno. Downstream from Reno, where water temperatures were nearly optimal, intragravel dissolved-oxygen concentrations were well below the threshold level of 5 mg/L.

Water budget and nutrient sources of Pine Lake, Washington

A water budget was prepared for Pine Lake, Wash., a candidate for lake-quality restoration. Of the 1.02×10^6 m^3 (830 acre-feet) of water entering the lake in the 1980 water year, 42 percent was from precipitation, 55 percent was from surface inflow, and 3 percent was from ground-water seepage. An equal amount of water left the lake and, of this, 83 percent was by surface runoff, 17 percent was by evaporation, and less than 0.5 percent was by ground seepage. The theoretical water-renewal time of the lake, according to investigators N. P. Dion, S. S. Sumioka, and T. C. Winter, was calculated to be 2.0 yr. About 1,430 kg of nitrogen and 29 kg of phosphorus were contributed to the lake from combined sources of precipitation, and surface- and ground-water inflows.

One-dimensional limnological model

L. B. House reported that the Corps of Engineers "WESTEX" reservoir model was modified for use by the USGS to simulate temperature and dissolved oxygen in small lakes or impoundments in Wisconsin. In this one-dimensional model the body of water is divided into as many as 60 horizontal layers, each uniform in thickness and other properties. Temperature, dissolved oxygen (DO), biochemical oxygen demand (BOD), and the density effects of suspended sediment are simulated in each horizontal layer on a daily basis. Temperature, DO, and BOD of the average outflow water also is simulated when the position of the outlet (surface spillway, bottom draw, or combined outlet works) is specified by the user.

Sediments and nutrients in Steiner Branch, Wisconsin

Mean annual sediment yields from the Steiner Branch basin in Wisconsin were estimated to be 155 Mg/km^2 based on 2 yr of data according to S. J. Field and R. A. Lidwin. The majority of the nutrient load of the stream was transported during runoff: total organic nitrogen, 80 percent; ammonia nitrogen, 80 percent; total phosphorus, 84 percent; and total orthophosphorus, 77 percent. Transport of nitrite plus nitrate nitrogen and total nitrogen occurred primarily during base-flow conditions with 75 and 56 percent, respectively, of the total load for the study period being transported during these conditions. The time distribution of total phosphorus, total orthophosphorus, ammonia nitrogen, and total organic nitrogen transport was very similar to suspended-sediment transport.

NEW HYDROLOGIC INSTRUMENTS AND TECHNIQUES

Investigation into new acoustic velocity meter equipment showed improvement in the systems. According to A. Laenen, smaller, less-expensive (starting at $7,000) microprocessor systems are now available for use in streamflow measurement. These systems have the advantage of (1) using less electronics – thus less maintenance; (2) requiring relatively little power – battery operation; (3) using simplified test diagnostics; and (4) not requiring a temperature- and humidity-controlled environment. The only disadvantage over the existing minicomputer systems is the decreased flexibility of the microprocessor. Two microprocessor systems are now being tested on the Willamette River near Portland, Ore., to evaluate their performance, operational characteristics, and serviceability, and to make recommendations pertaining to system modifications and development.

J. V. Skinner, J. P. Beverage, and J. J. Szalona of the Interagency Sedimentation Project have conducted a number of methods development investigations for sediment data collection. In cooperation with D. W. Hubell and H. H. Stevens, Jr., they tested six different styles of Helley-Smith bedload samplers. Tests with 6.5-mm and 2-mm bed material were completed, and tests with 23-mm bed material were started. All bed materials have formed dunes through the tested range of flow depths and velocities.

A vibrating U-tube liquid-density gage was equipped with a custom-made precision timer and was calibrated for use as a continuously operating suspended-sediment concentration meter. Sources of measurement error were evaluated and; for some sources, methods of compensation were developed. A new bag-type sampler was tested for sampling suspended sediment over a wide range of water temperatures. For low temperatures, sampling-rate compensation methods were developed. In cooperation with R. F. Middleburg, Jr., Szalona designed a special bracket to meet needs in both biological sampling and sediment sampling. The bracket, which may be attached to a wading rod, supports a sampling-cap, a sampling-nozzle, and a variety of sample containers. Special pumping-type sediment samplers were constructed and laboratory tested for installation on Mount St. Helens. The samplers were designed to conserve battery power and to sample high-sediment concentrations.

Ulrich Schimschal developed a computer program to calculate hydraulic conductivities from volumetric-flow changes produced by losses into the borehole environment during fluid injection. Using an impeller flowmeter, losses into large fractures intersecting the borehole were detected during injection testing in fractured sedimentary rocks at the Raft River geothermal field in Idaho, and also in fractured and vuggy dolomites at the Brantley damsite in New Mexico. The purpose of the study is to aid in determining zones of fluid migration; applicability to liquid-waste management, geothermal production, or injection wells; and characterization of aquifers in water wells, (Schimschal, 1981).

Ulrich Schimschal also developed quantitative techniques for the interpretation of gamma-ray spectral data obtained in the borehole (Schimschal, 1981). Calibration techniques were developed for cylindrical detector crystals (Schimschal, 1980a). Furthermore, the effects of the borehole environment were tested both in the laboratory and the test pits at Grand Junction, Colo. (Schimschal, 1980b).

W. S. Keys and F. L. Paillet analyzed the effectiveness of various geophysical techniques for the identification and characterization of natural fractures intersecting a fluid-filled borehole. The physical techniques investigated include borehole-wall imaging (impression packers, downhole television, and acoustic televiewer), fracture resistivity (conventional single-point and laterolog resistivity, microresistivity, and microresisitivy dipmeter), and acoustic propagation and attenuation (conventional acoustic velocity, circumferential propagation, and waveform amplitude) (Paillet, 1981). Detailed comparison of these methods with core-fracture measurements at several sites in the United States and Canada showed that relatively inexpensive geophysical measurements can be used to extrapolate a limited set of core-fracture measurements to a large number of uncored boreholes. This represents a substantial savings when compared to the continuous coring of all boreholes, and a significant increase in number of potential data points for a given level of investment. The data also indicated that additional

fracture information can be extracted from log measurements not normally associated with individual fractures through the correlation of fracture frequency and aperture with lithologic responses. These correlations depend on factors such as hydrothermal alteration, migration of naturally occurring radioisotopes, or mineral leaching that are only indirectly related to fracture aperture, but which may contain important information about the ability of fractures to transmit ground water.

F. L. Paillet tested a previously formulated theory relating acoustic waveform amplitude to borehole wall permeability for analyzing acoustic waveforms obtained in several different rock types at various locations in the United States and Canada. The waveform analysis involves recognition of individual wave modes within the composite waveform by comparison with a theoretical model of wave propagation in impermeable and unfractured rock (Paillet, 1981). Data reduction algorithms were written to extract mean-square amplitudes associated with individual wave modes, such as the multiply reflected normal modes and wall-interact or tube waves that are known to be especially sensitive to wall permeability. Decreases of amplitude have been successfully correlated with wall permeability for porous sandstones with no fracture permeability, limestones with small vertical fractures and very small matrix porosity, and igneous and metamorphic rocks with a broad range of fracture permeability measured by packer studies, (Paillet, 1980). The greatest limitation on the permeability measurements based on acoustic attenuation is apparently imposed by the effects of minimal confining pressure on waveform amplitudes at shallow depths (less than 50 m for crystalline rocks). In these cases fracture permeability may still be estimated from the effects of open fracture on the transmission of compression and shear body waves. Initial results from two sites in Canada indicated that mode-conversion and mode-excitation effects may be related to fracture permeability even at very low shallow depths, but the relation involved is apparently much more complex than the relatively simple correlation between mode attenuation and permeability at depths greater than 50 m.

ANALYTICAL METHODS

ANALYSIS OF WATER

Selective concentration and isolation of ionogenic organ solutes from water

The subject research was performed by Harold Stuber for his Ph. D.thesis. Significant original findings of this study are (1) liquid-chromatographic concentration factors attainable for an ionogenic organic solute adsorbed in the neutral state and desorbed in the charged state depend on the ratio of the neutral to charge state capacity factors for an ideal column, (2) loss of concentration factors due to band spreading on a non-ideal liquid chromatographic column can be minimized by reverse elution of the solute in the charged state, and (3) sorbents with chargeable surface (weak acid and base exchange resins) can yield much larger ratios of solute-capacity factors because of the principle of ionic exclusion than can a neutral sorbent. The amphoteric resin, Duolite A-7, was found to yield very large concentration factors for the more hydrophobic aromatic amines. These original findings have wide applications to organic analyses of water, and have been specifically applied to analysis of the aromatic amine fraction in oil shale retort waste water.

Volatilization of ketones from water

Coefficients for the volatilization from water of acetone, 2-butanone, 2-pentanone, 3-pentanone, 4-methyl-2-pentanone, 2-heptanone, and 2-octanone were broken down into the liquid-film and gas-film coefficients of the two-film model by R. E. Rathbun and D. Y. Tai. The liquid-film coefficients varied with the 0.719 power of the molecular diffusion coefficient, in agreement with the literature. The coefficients showed a variable dependence on molecular weight, with the dependence ranging from the -0.263 power for acetone to the -0.378 power for 2-octanone. This is in contrast with the literature where a constant -0.500 power dependence is assumed. The gas-film coefficients showed no dependence on molecular weight, in contrast with the literature where a -0.500 power dependence is assumed.

Oil shale retort water organic analysis

Oil shale retort waters representing the process and gas condensate waters produced from the modified in situ retort 6 of Occidental Oil Corporation, Logan Wash. site near Grand Junction, Colo., were studied by J. A. Leenheer. Slightly more than 50 percent of the dissolved organic carbon was identified at the specific compound level of analysis in both of these retort waters. The gas-condensate organic solutes consisted almost exclusively of neutral and basic constituents that were steam volatile at pH 8.6 of the retort water. Organic compound groups that occurred at moderate to large concentrations in the gas condensate waters included aromatic amines, phenols, aliphatic nitriles, aliphatic alcohols, and aliphatic ketones. The process retort water (coproduced with shale oil as an emulsion) contained mainly acidic and polyfunctional constituents that were not steam-volatile at pH 8.6 of the retort water. Process

retort-water organic solutes induced fatty acids from C_2 to C_{10}, aliphatic dicarboxylic acids from C_2 to C_{11}, aliphatic hydroxy acids, aliphatic amides, and hydroxypyridines. Hydroxypyridines have not been previously reported in waste waters from synthetic fuels processing.

GEOLOGY AND HYDROLOGY APPLIED TO HAZARD ASSESSMENT AND ENVIRONMENT

EARTHQUAKE STUDIES

SEISMICITY

Operations and special investigations

The National Earthquake Information Service (NEIS) functions as a focus for the collection of worldwide seismic data and the location of earthquakes. The NEIS provides a valuable service for a wide variety of users in the scientific, government, and public sectors with the Earthquake Early Alerting Service (EEAS). The EEAS provided rapid and accurate information on M = 6½ or greater earthquakes worldwide, or M = 5 or greater in the United States.

In fiscal year 1980 (FY80), the NEIS determined the parameters (origin time, epicenter, focal depth, and magnitude) of 7,456 earthquakes from data supplied by seismic observatories located in nearly every country in the world. Of these, according to W. J. Person, 58 were considered significant because they had a magnitude of 6.5 or greater, were damaging, or caused fatalities or injuries. The worldwide total of fatalities caused by or resulting from earthquakes during FY80 was reported at 1,440. Sixty-six bulletins were issued by the EEAS on potentially damaging earthquakes worldwide and smaller U.S. earthquakes of significant interest. Person reported that these bulletins provided disaster relief agencies, public safety organizations, the press, and the public with the first factual and accurate information on potentially damaging earthquakes.

According to M. A. Carlson, a seismic network of 71 stations from coast to coast in the conterminous United States and Alaska was telemetered to the NEIS in Golden, Colo. The data from these stations and from the USGS observatories at Newport, Wash.; Cayey, P. R.; Agana, Guam; and Adak, Alaska, were used by the NEIS in rapidly locating earthquakes by the EEAS and in the computerized biweekly location of earthquakes.

J. N. Taggart reported that the South Pole Seismograph Station was operated throughout 1980 by two part-time observers from the National Mapping Service. They reported seismic data on a timely basis by radiotelegraph to the NEIS in Golden, Colo.

Eighty-one earthquakes in 19 states were canvassed by questionnaires during FY80. C. W. Stover reported that the information derived from the questionnaires was used to delineate the severity and extent of ground shaking and to draw isoseismal maps for the larger events. The most damaging earthquakes investigated in FY80 were in the Imperial Valley, Calif., area (lat 32.63° N., long 115.33° W., $M_L = 6.6$, maximum intensity IX), in the Livermore, Calif., area (lat 37.83° N., long 121.79° W., $M_L = 5.5$, maximum intensity VII), and in northern Kentucky (lat 38.17° N., long 83.190° W., $M_b = 5.2$, maximum intensity VII). The results of these and other investigations were published in a quarterly circular "United States Earthquakes."

Twelve state seismicity maps for the New England and the East Coast area were published at a scale of 1:1,000,000. According to Stover, each map displays the geographic distribution of the earthquakes to 0.1° and lists all recorded events through 1977.

J. W. Dewey and D. W. Gordon compared their revised hypocenters for eastern North America with results from regional microearthquake networks that were installed in the 1970's. In some regions, such as the regions near Attica, N.Y., Giles County, Va., and Charleston, S.C., their hypocenters of prenetwork earthquakes occur at or very near the same locations as small shocks recorded by the microearthquake networks. In much of New England and northeast New York, however, there is not a strong correlation between prenetwork hypocenters and recent network-recorded hypocenters.

J. W. Dewey has relocated the aftershock sequence of the Dulce, N. Mex., earthquake of January 23, 1966, as part of a study of that earthquake being conducted with R. B. Herrmann and S. K. Park of Saint Louis University. The focal mechanism of the earthquake determined by Herrmann and Park and the relocated epicenters point to the main shock, which occurred as additional movement on one of a family of north-northwest-striking normal faults that had their maximum activity in Miocene time. The distribution of aftershock epicenters suggests that the main shock triggered aftershock activity on adjacent faults.

W. J. Spence has shown that the 1974 Peru aftershock series occurred in two segments comprised of distinct space-time groups. Discussion of these findings is given later in this volume under the section on "International Cooperation in the Earth Sciences."

W. H. Bakun reported cumulative seismic moment, sum (Mo), for earthquakes on a 50-km-long creeping section of the Calaveras fault from near Mount Hamilton southeast to San Felipe Lake correlated with mapped fault-trace characteristics. In general, sum (Mo) is lower at the left-stepping offset in the trace at the south end of Anderson Lake and along linear segments of the fault than near right-stepping offsets and bends in the trace and intersections of the Calaveras with other faults. The correlations of seismic activity and fault-trace characteristics were similar to that for shocks along the creeping section of the San Andreas fault in central California. The rate of microearthquake occurrence along the 50-km-long section of the south half of the Calaveras fault zone increased beginning in May–June 1978. If this increase is viewed as a 15-mo-long large-scale precursor to the 1979 Coyote Lake sequence, the August 29, 1978, shocks at Halls Valley 30 km northwest of Coyote Lake and the $M_L = 4.5$ shock on May 8, 1979, are foreshocks, in a broad sense, to the Coyote Lake sequence. Details of the space-time pattern of microearthquake activity near Halls Valley and near San Felipe Lake are similar to those associated with moderate-sized shocks on the creeping section of the San Andreas fault, and this similarity suggests that they are contemporary, parallel examples of seismicity patterns that precede larger shocks. First, there is a deficit in sum (Mo) of several years along the section of the fault where the subsequent larger earthquakes are located. Second, the rate of microearthquake occurrence increases before the larger shocks along the fault near the section deficient in sum (Mo). Third, a cluster of microearthquakes at one end of the zone marks the start of the increased rate of microearthquakes.

The analysis by G. L. Choy of actual and synthetic seismograms, generated by using a spectral method (full wave theory) in conjunction with a causal rupture model, demonstrated that significant frequency dependent effects are incurred by body waves propagating through the Earth. These effects included diffraction, tunneling, and the system of rays that arise from a cusp or a caustic. It was demonstrated that the broad-band spectral information can be recovered from digital data of the Global Digital Seismic Network. These broad-band data were exploited to show that attenuation in the Earth is frequency dependent. The spectral peaks of normal modes may be split by a laterally heterogeneous Earth. These findings imply that studies of the seismic source would be imprecise without significant corrections for propagation effects in the raw data.

The Albuquerque Seismological Laboratory (ASL) provides technical and logistical support, which has kept the World Wide Standardized Seismograph Network (WWSSN) operational. Each station produced three components of short-period data and three components of long-period data. The records were forwarded periodically to the USGS for quality control. According to R. P. McCarthy, the operational quality and high standards of excellence of the WWSSN were demonstrated again in 1980. Timing accuracy of less than 50 ms error per 24-h period was evidenced at about 65 percent of the stations, and for the remainder, most were under 100 ms.

The Global Digital Seismograph Network (GDSN) as planned will consist of 37 observatories in 28 countries. N. A. Orsini reported that by the end of FY80, 21 had been installed. These are advanced seismological instrument systems, which provide high-quality digital short-period and long-period seismic data for use of the United States and foreign earthquake investigations and research. The network provided improved geographical coverage with highly sensitive short-period and long-period seismic sensors using analog and digital magnetic tape recordings. These digital station recordings are organized at ASL onto network-day tapes to provide seismic data in a convenient format ready for computer analysis. The network-day tapes contain a unique data base for the research analyst, as they provide the only global digital seismic data base available. In addition, each day tape contains all necessary parameters, time corrections, and complete calibration information for every station.

According to R. P. Buland, the portable software to extract data from network-day tapes nearly is completed. The refinement of software for interactive time series analysis has progressed to the point where it is usable. A method for automating focal mechanisms has been completed, and an initial study of the possibility of estimating magnitude from mantle waves has been successful.

As part of a task to document the Global Seismograph Network, J. R. Peterson reviewed the calibration of the WWSSN. Accurate transfer functions were derived and used to evaluate empirical calibration techniques. Systematic errors in calibration were found, but none exceeded 15 percent. In addition, noise spectra at the Seismic Research Observatories (SRO) and Abbreviated Seismic Research Observatories (ASRO) stations were computed for quiet periods from recorded data. As expected, short-period noise varied over a wide range as a function of station location, but long-period noise was relatively constant at all sites.

The ASL provided technical advice and assistance to seismograph stations of the USGS and cooperative observatories in the form of engineering support, equipment replacement, calibration, repair, and operational supplies. N. A. Orsini reported that all of these

observatories provided data to the NEIS routinely and rapidly when necessary.

Seismic network studies

R. Y. Koyanagi, F. W. Klein, and W. R. Tanigawa of the Hawaiian Volcano Observatory (HVO) reported that more than 150,000 earthquakes were instrumentally detected during 1980; most of them occurred beneath Kilauea and the southeastern flank of Mauna Loa. Microearthquakes associated with magmatic activity centered mainly in the summit and east rift zone of Kilauea. Independent daily counts of earthquakes in these areas ranged from less than a hundred to over a thousand. At least five significant swarms of shallow earthquakes occurred on the upper east rift zone. In all, nearly 4,000 earthquakes of about M=0.5 to 4.3 were processed for locations and magnitude.

R. A. White reported more than 40,000 shallow-focus earthquakes were recorded between August 1979 and May 1980 near Cerro Cruz Quemada in southeastern Guatemala. Discussion of these findings is given later in this volume under the section on "International Cooperation in the Earth Sciences."

D. H. Harlow located more than 700 shallow-focus earthquakes in western Nicaragua between March 1975 and December 1978, with data collected by a 16-station network of high-gain seismographs. Discussion of these findings is given later in this volume under the section on "International Cooperation in the Earth Sciences."

EARTHQUAKE MECHANICS AND PREDICTION STUDIES

Remote monitoring of source parameter for seismic precursors

It has been demonstrated that the digital data from the Global Digital Seismic Network have spectral information in an "intermediate" frequency band (several Hz to tens of seconds) that has not yet been exploited in earthquake source studies. Techniques were developed that used this broad-band data to extract earthquake source parameters and to describe the rupture process of earthquakes. The project succeeded in determining the complete rupture history for two deep earthquakes, including constraints on the dynamic and static stress drops, the rupture velocity, and the rupture complexity.

Having shown the appropriateness of broad-band digital data for detailed teleseismic source studies, the project began studies of the rupture characteristics of several large shallow earthquakes that preceded and encircled the seismic gap that was later ruptured by the Miyagi-oki earthquake. Preliminary indications were that dynamic stress drop, rupture duration, complexity, and the direction of rupture propagation changed systematically with time.

Seismic studies of earthquake prediction

Recent earthquake sequences in the San Francisco Bay area, along the eastern Sierra Nevada Mountain front and in the Imperial Valley indicate that California is emerging from a period of seismic quiescence, which began in the late 1950's. During the 1960's and the 1970's, only two earthquakes of M=6 or greater occurred per decade. From the 1850's through the 1950's, earthquakes of this magnitude occurred at an average rate of seven or eight per decade, based on data tabulated by the California Division of Mines and Geology. The seismic quiescence of the 1960's and 1970's is unprecedented in the available 130-yr record.

Parkfield prediction experiment

Using an adaptation of a crustal model developed by J. P. Eaton of the USGS, the project catalogs all microseismicity in the vicinity of the 1966 Parkfield, Calif., earthquake. South of the epicenter, but within the zone that broke in 1966 and also within the zone in which the creep rate decreases to the south from 3 cm/yr to <1 cm/yr, the recent pattern of earthquakes is spatially similar to the main aftershock pattern of the 1966 earthquake, outlining the main rupture zone. This pattern is consistent with the argument that the extent of the main 1966 rupture was controlled by two physical discontinuities: a small bend in the fault on Middle Mountain (point of initiation) and the offset in the fault south of Gold Hill (termination point).

Seismic studies of fault mechanics

The cyclic nature of strain accumulation and release in great earthquakes on the San Andreas fault leads to a quasi-periodic pattern of seismicity in the surrounding region. This recurrent pattern of seismicity has been identified in the work of Fedotov and Mogi as consisting of an extended period of quiesence after a major earthquake, followed by a period of increased activity that leads to the cycle-controlling earthquake and its foreshocks and aftershocks. Seismicity data from the region experiencing the 1906 San Francisco earthquake from both before and after that earthquake generally can be assigned to stages of the seismic cycle. The timing of the next great earthquake in this region cannot be forecast with precision at present, although it appears to be decades away. The recent occurrence of the two strongest earthquakes in the region since at least 1911, coupled with the reemergence of M=5 or greater earthquakes since 1955, after an extended period of quiescence following 1906, leads us to conclude that the region is entering the active stage of the cycle in which events as large as M=6, to perhaps M=7, can be expected. Geologic evidence and the historic seismicity

point to the Hayward fault, the Calaveras-Paicines fault, the Calaveras-Sunol fault, the Rodgers Creek fault, the portion of the San Andreas fault on the San Francisco peninsula, and possibly the San Gregorio fault as likely candidates for such earthquakes.

Coherent seismic wave analysis

A new family of computer programs was developed during FY80. It will digitize analog seismic tapes on the Eclipse minicomputer, transfer the digital data to 9-track archive tapes, and load the data from archive tapes onto the PDP-11/70 UNIX system. This facility provides the only path for rapid digital processing of data recorded on the certain field system. These programs were documented by Paul Reasenberg and Jeffrey Hobson (1980).

During FY 80, thorough investigation of seismic wave arrival-time measurement was made, which compared manual measurement systems with microprocessor-based automatic systems. The timing uncertainties, as well as other characteristics, of both manual and automatic systems was assessed by comparison of their performance on common data sets using over 3,200 wave arrivals. Despite the problems inherent in this kind of comparative approach, such as that of properly assigning error to one system or another when disagreements in arrival time are found, the following conclusions were reached: Expected errors of ± 0.07 s for the best quality arrivals and of ± 0.10 s for all arrivals are associated with the manual timing process for microearthquakes occurring in the central California seismic network. Corresponding expected errors of ± 0.02 s (best arrivals) and ± 0.06 s (all arrivals) are associated with the automatic timing system.

In addition to the random uncertainty, a secular error associated with the automatic system was detected. The automated system produces wave arrival times that are late by 0.01 to 0.02 s, and the error increases with decreasing signal-to-noise ratio. Corresponding secular errors associated with the manual process produce late estimates of wave arrival times of between 0.02 and 0.11 s; error increases with decreasing signal-to-noise ratio. Thus, the automated system routinely provides extremely dependable wave arrival times.

St. Elias, Alaska, earthquake studies

The St. Elias, Alaska, earthquake ($M_s = 7.1$ depth 20 km) of February 28, 1979, was produced by thrusting on a nearly horizontal fault zone within the tectonically complex northeastern corner of the Pacific–North American plate-boundary zone. Starting 18 mo prior to this earthquake, analysis of data from the USGS regional network of high-gain, short-period seismograph stations is uniformly complete above $M = 1.5$ for two 6-mo intervals. The first interval ended 11 mo before, and the second ended immediately preceding the St. Elias earthquake. During the 6 mo just prior to the main shock, there was a 34 percent increase in the number of events above $M = 1.5$ as compared to the earlier 6-mo period. The b values, calculated for four 3-mo intervals, decreased systematically with time from 1.36 to 0.78, while the b value for the aftershocks is 0.96. However, none of the preearthquake values differ significantly from the aftershock b value at the 95 percent confidence level. These observations, which suggest an increase in seismicity with time, and possibly a decrease in b value, need to be reviewed further to insure that there is no bias in the earthquake analysis that could have erroneously produced the effect.

The region between the aftershock zones of the St. Elias earthquake and the 1964 Alaska earthquake is being monitored currently for any changes in seismicity that might be precursory indicators of another large earthquake. This portion of the plate boundary has not broken since at least 1900. By analogy to the St. Elias earthquake, the rupture zone of such an earthquake might be expected to include the area of continued high seismicity northeast of Kayak Island, to be preceded by an increased level of seismicity (possibly caused by swarms along the future rupture boundary), and to follow a period with lower than average b value.

Minicomputer software development

During the first 15 mo that the current earthquake processing system has been operational, approximately 720 local earthquakes and 15 teleseisms from central California and Oregon have been processed. The locations, phase cards, and waveforms have been archived onto 95 digital tapes. The data comprise 345 events from the Coyote Lake aftershock sequence, 298 other events from central California, 75 local quakes, and 15 teleseisms from Oregon. Based on statistics provided by A. L. Rapport and C. A. McHugh of the USGS, processing of events takes from 48 min to 1.5 h, depending on the size and location of the event. Most of this time is spent in the interactive plot/pick program SISDS.

Because of the time required to process events, only events greater than $M = 2.5$ are being processed currently by the central California Network. Phase cards in HYPO71 format are transferred to the UNIX system via TAR tapes. A number of software and procedural bugs have been discovered and corrected during this period. Current problems relate to the speed and flexiblilty of the SELECT program, size and integrity of the Master History file, and to A/D hardware reliability.

Microprocessor-based seismic processing

A 250-station real-time processor is now operational with the central California seismic network. Its results are used routinely, in conjunction with results from hand analysis of film records, in the preparation of network catalogs. In the distance range of direct arrivals (<50 to 75 km), the seismic wave arrival times from the fully automatic system are at least as reliable as hand-picked times.

Southern California microearthquake network

A prototype version of a real-time digital data acquisition system was completed and put into operation at several universities during FY 1980. This software was put into operation at the University of Washington on March 1, 1980, several weeks before the onset of the events presaging the first eruption of Mount St. Helens. A preliminary version of the off-line analysis system was developed, distributed and is presently in use for the evaluation of the eruption hazard in Washington. A final version of the online data acquisition was developed and is in use collecting data from the southern California seismic network at California Institute of Technology.

Deterministic three-dimensional finite fault models of the 1971 San Fernando earthquake were constructed to explain the combined data sets of strong ground motions, teleseismic P and S waveforms, and static ground offsets. The modeling suggests that the San Fernando earthquake may have been a double event on two separate, subparallel thrust faults. The rupture apparently initiated at depth on the Sierra Madre fault and then progressed to within 3 to 5 km of the Earth's surface; and a second event, somewhat larger than the first, initiated 4 s after the initial event on the San Fernando fault zone and rupture, proceeded to the Earth's surface.

In response to the Mammoth Lakes earthquake sequence of May 1980, a temporary array of 7 accelerometers was installed on May 26, 1980 (the day following the two $M=6.25$ earthquakes). In the following 4 wk, a total of 270 accelerograms was obtained of which 169 could be correlated with specific aftershocks. This included six aftershocks with at least $M=4.8$ on at least four stations. The largest is the $M=6.3$ aftershock of May 27, 1980, for which six records were obtained. These six records were digitized and processed. The Convict Lake station, which lies at an epicentral distance of 10 km, showed a peak acceleration of 75 percent of the acceleration of gravity.

A system for the timely recognition of anomalous activity of southern California water wells was established recently. Requests were mailed to 500 southern California municipal and private water companies asking that any anomalous activity in the water well be immediately reported to the USGS field office at the California Institute of Technology where the data are logged and, if appropriate, further investigations are conducted.

Central California seismic studies

In the immediate vicinity of San Pablo Bay and Suisin Bay, north of San Francisco, Calif., earthquakes of $M\geq2.4$, that occurred from 1969 to 1978, were located. Most of these events fell along the Hayward and Concord faults south of the Bays and in a more diffuse zone extending mostly north of the Sacramento River, just east of Suisin Bay. Most focal mechanisms show north-northwest-trending, right-lateral, strike-slip motion.

EARTHQUAKE HAZARD STUDIES

TECTONIC FRAMEWORK AND FAULT INVESTIGATIONS

Structural controls for seismicity along the Ramapo seismic zone, New York

A preliminary tectonic map prepared by N. M. Ratcliffe showed the Ramapo seismic zone as it is defined by surface faults. In comparing seismic data with this map, Ratcliffe found that (1) Mesozoic faults, although more common than previously recognized, do not follow the trends shown by earthquake activity, (2) seismicity in the Ramapo seismic zone decreases north of 41.5° and west of the Green Pond syncline, although Mesozoic faults extend well beyond these boundaries, (3) phyllonitic shear zones of Proterozoic Y and Ordovician age traverse a broad area east of the Hudson River in the northern Reading Prong where seismic activity is significantly deeper than in nearby areas, and (4) a linear zone of earthquake activity east of the Hudson River in Westchester County, N.Y., extends to a depth of 11 km; this zone cannot be correlated with any known Mesozoic fault, but it may follow recognized ductile faults of Paleozoic age.

These relations lead Ratcliffe to reject the simple hypothesis that reactivated Mesozoic faults, such as the Ramapo, produce current seismicity in New York State. Instead, recurrent earthquakes in the Ramapo seismic zone appear to follow thick, exposed or near-surface bodies of penetratively faulted Proterozoic Y rocks; earthquakes appear to be absent where crystalline basement forms thin overthrust sheets. Thus current patterns of seismicity probably reflect the attitude and distribution of major through-going Paleozoic and older fault zones in basement rocks that extend from near the surface to depths of 15 km. Most of these faults are ancestral to Mesozoic border faults.

Possible seismogenic faults in the southeastern United States

Recent fieldwork by D. C. Prowell and others along the Belair fault zone near Augusta, Ga., showed that

this fault is a Paleozoic tear fault along an ancient overthrust—the Augusta fault—which has been reactivated by east-west compression during the Cretaceous and early Cenozoic. Evidence also indicates possible Cenozoic activity along the Paleozoic Towaliga fault in western Georgia.

The Wateree Creek fault near Columbia, S.C. displaces Paleozoic slates along brittle fracture zones similar to those found in the Belair fault zone. The Wateree Creek fault passes near-seismic activity at Monticello Reservoir, a relation that makes this fault a possible locus of renewed seismic activity in reponse to water impoundment. Multichannel and single-channel seismic-reflection data collected offshore of Charleston, S.C., in 1979 were interpreted by J. C. Behrendt, R. M. Hamilton, and H. D. Ackerman to define the following geologic structures:

1. The Helena Banks fault, a northeast-trending high-angle reverse fault at least 30 km long and about 12 km offshore, extends up to about 10 m from the sea floor. This fault is subparallel to the similar high-angle, reverse(?) Cooke fault on land in the epicentral area of the 1886 earthquake. Earliest movement on the Helena Banks fault was probably in Triassic time, and the fault was reactivated at least as recently as Miocene or Pliocene time. Other shallow Cenozoic faults were found also.
2. A subhorizontal surface, defined by diffractions at about 11.4 ± 1.5 km depth, is within the depth range of hypocenters calculated for Charleston area seismicity from 1973–1978 (Tarr and Rhea, unpublished data, 1980). A statistical analysis of aeromagnetic data identified sources of magnetic anomalies at about this depth.
3. Reflections from the Moho at 9 to 11 s correspond to about 29 to 35 km crustal thickness.
4. A series of west-dipping reflection surfaces or north-striking diffracting "edges" was identified beneath the decollement.

From these interpretations, Behrendt, Hamilton, and Ackerman hypothesize that the Charleston seismicity is related primarily to the décollement and that movement on the high-angle reverse faults is a second-order effect. Future corroboration of the décollement, or of reactivated shallow faults with seismicity, will be important in assessing the earthquake risk at Charleston and elsewhere in the Atlantic coastal and continental margin area.

Marvin Lanphere determined conventional K–Ar and Ar^{40}/Ar^{39} total fusion ages and conducted incremental heating experiments on three samples of basalt from Clubhouse Crossroads Corehole 2 near Charleston, S.C. Conventional K–Ar ages ranged from 162 m.y. to 204 m.y. and were not in the correct stratigraphic order. The Ar^{40}/Ar^{39} total fusion ages of the three samples of basalt range from 182 m.y. to 236 m.y. Only one of the total fusion ages agrees, within analytical uncertainty, with the conventional K–Ar ages of the same samples. Data from Ar^{40}/Ar^{39} incremental heating experiments indicate that only one sample meets the criteria for a reliable crystallization age. The Ar^{40}/Ar^{36} versus Ar^{39}/Ar^{36} isochron age for this basalt is 184 ± 3.3 m.y. This age agrees with reliable ages of diabase intrusive rocks in eastern North America and Liberia, and all of these data are consistent with an episode of central Atlantic rifting, which began about 190 m.y. ago.

Geophysical anomalies and seismicity patterns in the Eastern United States

Colored gravity and terrain maps prepared by Robert Simpson cover the northeastern and east-central United States at a scale of 1:2,500,000. These include free-air gravity, Bouguer gravity, gradient, and derivative and residual Bouguer anomaly maps. Simpson found that patterns of seismicity in the Eastern United States correlated with the gravity gradients. He also found that small Bouguer residual anomalies coincide with areas where the level of seismicity is significantly less than that which a random distribution of earthquakes would produce. Conversely, however, not all areas with high-gravity gradients and large-residual Bouguer anomalies exhibit high levels of seismicity. This may reflect either an incomplete earthquake record or that earthquakes are confined areally by structural grain or by the mechanical properties of rock.

Many of the gravity gradients and residual anomalies that correlate with seismicity patterns appear to represent fundamental crustal structures, which are being reactivated by the regional tectonic stress field.

Using newly completed gravity maps of New York and Pennsylvania, together with other geological and geophysical data, W. H. Diment concluded that some aseismic regions of the Eastern United States exhibit geologic conditions that tend to suppress shallow earthquake activity. These conditions include geopressured zones, bedded salt, and pre-existing bedding-plane thrusts. He cautions that the historical seismicity, based largely on felt reports, may not reflect adequately the stress regime at depth because of decoupling or aseismic slip near the surface.

Through his studies of basement relief and seismicity, M. F. Kane distinguished two levels of seismicity in the Eastern and Central United States. The rate of intraplate continental seismicity is relatively high where crystalline basement is either exposed or is at relatively

shallow depth. The rate of seismicity is lower over large curvilinear interior basins except where they are adjacent to active continental-scale tectonic structures. Seismic activity exhibits similar patterns in continental parts of France and Poland.

Geologic and geophysical results in the Mississippi Valley

D. P. Russ, A. J. Crone, and S. T. Harding used exploratory trenching and seismic-reflection profiles to interpret and model geologic structure and earthquake source zones in the New Madrid seismic region. From analysis of two-way traveltime data, they found that the buried Paleozoic surface had been uplifted 42 to 50 m in that part of northwestern Tennessee where surface warping defines the Lake County uplift. Synthetic cross sections made from the reflection profiles using ray- and wave-theory techniques showed that theoretical modeled structures, such as faults and intrusive bodies, closely mimic those seen on the profiles; this supports their interpretation of faulting and tabular intrusive rocks in the shallow subsurface.

Aeromagnetic and gravity data analysed by T. G. Hildenbrand delineate a prominent northeast-trending structure called the Mississippi Valley graben. The graben probably follows a pre-Late Cambrian rift, which formed on a Precambrian surface with structural relief of about 2 km. The graben evidently formed along a major midcontinental crustal flaw; and although the graben ends in western Kentucky, the crustal flaw continues northeastward into Illinois, Indiana, and Ohio.

The crustal flaw, expressed magnetically as a northeast-trending megalineament, parallels the midcontinent gravity and magnetic high and the New York-Alabama lineament. Hildenbrand also found evidence of several northwest-trending megalineaments in the midcontinent, and he proposes that these midcontinent megalineaments express major crustal flaws that formed in thin easily deformed Archean crust. Because the Mississippi Valley graben contains the most seismically active part of the Mississippi embayment, understanding its relation to the crustal flaw is important in evaluating intra-cratonic tectonics and earthquake hazards of the midcontinent.

Soil and fault investigations in the Great Basin

Soil properties commonly are used to date late movement on potentially hazardous faults. Investigations by R. R. Shroba in the eastern part of the Bonneville basin, near Salt Lake City, Utah, indicate that secondary $CaCO_3$ content can be used to identify and correlate buried soils and soil complexes, despite local variations in carbonate morphology and composition of the parent materials. At four widely spaced localities west of the Wasatch Range, buried soils and soil complexes, formed in the 100,000-yr interval between the last and penultimate high stands of Lake Bonneville, have about 55 to 60 g/cm^2 of secondary $CaCO_3$. However, a buried soil of equivalent age at the range front contains only about 25 g/cm^2. These values suggest average rates of secondary carbonate accumulation of about 0.6 and 0.3 g/cm^2/1,000 yr, respectively – rates about 1 to 3 times greater than those of nearby, but younger, post-Bonneville soils. The findings also suggest that (1) the type Promontory and Dimple Dell Soils of Morrison (1965a, 1965b), now considered to be stratigraphically equivalent (Scott and Shroba, 1980), contain similar amounts of secondary $CaCO_3$ (58 versus 56 g/cm^2, respectively), (2) the rapid rate of carbonate accumulation between high stands of the last two lake cycles may be due to greater influx of airborne carbonate from sediment deflation, and (3) the lower content of secondary $CaCO_3$ in soils near the range front may be attributable to leaching of carbonate from the profile.

R. C. Bucknam used data on the distribution and ages of late-Quaternary surface faulting in the Great Basin to define seismic source zones and to estimate long-term average rates of occurrence of damaging earthquakes. Several 10,000 km^2 or larger regions within the Great Basin display distinctive geomorphic evidence of faulting; the geomorphic evidence indicates the ages, and thus the rates, of late Quaternary surface faulting. Regions recognized thus far are (1) those within which unconsolidated deposits are undisturbed by fault scarps, (2) those with fault scarps of late Pleistocene age but without fault scarps of Holocene age, and (3) those with fault scarps of Holocene age.

Bucknam used the fault scarp data to calculate event rates for $M=7$ and greater earthquakes in each of the seismic source regions. These rates range from 0.7 events/104 yr/10^4 km^2 to 3.4 events/10^4 yr/10^4 km^2. The highest rate (Wallace, 1978) is for an area in north-central Nevada. The combination of rates and areas for each of the source regions gives an average recurrence interval of 240-yr event for the entire Great Basin. This value does not reflect the contribution of fault systems of possibly higher than average rates of activity such as the Wasatch fault in Utah.

Slip lineations on faults and fractures that cut widely scattered Miocene and older rocks in southwestern Utah showed important components of strike-slip motion, according to R. E. Anderson. His data, from abut 30 localities in Washington, Iron, Beaver, and Millard Counties, show that the different localities define three groups:

1. Those exhibiting normal slip; most of the slip surfaces exhibit modal north to north-northeast strikes, and most of the lineations are inferred to be of Pliocene and Quaternary age.

2. Those exhibiting predominantly strike slip. Most of the slip surfaces exhibit modal north to north-northeast strikes, but at some localities slip surfaces strike mainly northwest and east to west. At some localities the strikes of the vertical planes containing the slip lineations vary by only 15° to 25°; at others they vary by as much as 150°. Several localities that display predominantly strike-slip motion in rocks of Oligocene or Miocene age are near normally faulted Pliocene or Pleistocene strata in which the fault surfaces approximately parallel those with strike-slip displacement. If the strike-slip faults are older than the normal-slip faults, their failure to be reactivated may indicate that localized sources of extensional stress controlled the later episodes of faulting. If, on the other hand, the strike-slip and normal-slip faults are of the same age, they suggest local domains of strongly contrasting stress orientation and local sources of stress. Anderson favors the first, and simpler, option.
3. Those exhibiting mixed strike slip, oblique slip, and normal slip. Data from some of these localities are extremely variable and complex and are not understood, but at others the strike-slip component increases systematically as the strike of the slip surfaces deviates progressively from the strike of the strata. At such localities, slip surfaces parallel to bedding show dip-slip and those normal to bedding show large components of strike slip. Plots of slip lineations from slip surfaces of widely divergent strikes tend to be tightly concentrated in a field shared by the poles to bedding. Anderson considers these relations as proof that the stratal tilting and all modes of faulting formed during a single episode of deformation. The field occupied by the slip lineations and poles to bedding contains the tectonic transport direction. Its azimuth is generally southwest. The normal faults of such a system are probably listric, the deformation is extensional, and the vertical plane containing the model azimuth of the slip lineations also contains the least principal stress direction.

The May 3, 1887, Sonoran earthquake, located on a normal fault along the east side of San Bernardino Valley in extreme northeastern Sonora, Mexico, was one of the most severe in interior intermontane North America. The earthquake, probably of M=7+, nearly leveled the village of Bavispe, Sonora, and it damaged buildings throughout southeastern Arizona. D. G. Herd found that this earthquake broke nearly the entire length of one of three recently active faults in southern San Bernardino Valley. The 1887 faulting extends southward nearly 70 km from Arroyo Cajon Bonito (about 15 km south of the Mexican–U.S. border) to near the north end of Presa Angostura, on the Rio de Bavispe. The throw varies along the length of the scarp; it exceeds 4 m north of Cerro Pitaycachi, but averages about 2½ m. The fault, poorly exposesd, appears to dip about 60° to the west. About 5 to 10 km to the west of the 1887 fault, a second, parallel line of recently active faults extends southward approximately 25 km from Arroyo de los Embudos toward Arroyo de la Caballera. A third, 4-km-long set of eroded, east-facing fault scarps opposes the 1887 rupture, on the west side of San Bernardino Valley and just south of the Mexican–U.S. border.

Tectonic tilting shown by Alaskan lakes

The surfaces of large lakes provide a level reference surface to detect elevation changes of shoreline bench marks. Measurements are made by simultaneous operation of water-level recorders for several days at stations around a lake. The records are referenced twice to nearby bench marks by precise leveling. The noise level of repeated annual measurements of elevation change between two points is estimated conservatively at ±30 mm.

Twelve large lakes in southern Alaska occasionally are measured in order to detect and monitor tectonic tilt. According to S. H. Wood, a pair of stations 25 km apart on Kenai Lake, measured in the summers of 1964, 1966, 1979, and 1980, showed a 200 mm±30 mm component of down-to-southeast tilting (9±1 microradians) between 1966 and 1979. Tilt between 1979 and 1980 is marginally significant and of the opposite sense (30 mm±30 mm, or 1±1 microradian, down to northwest). The magnitude and timing of the 1966–79 tilt is consistent with the growth of a 0.5-m bulge since 1964, between Anchorage and Whittier, detected by Brown and others (1977) using data from repeated levelings. A 50-km triangular array of bedrock bench marks on eastern Iliamna Lake, measured in 1966 and 1979, showed no significant change in elevation differences (4 mm±30 mm, or 0.1±0.6 microradians) over the 13-yr interval.

Regional tilting and uplift in southern California

R. O. Castle analysed the 1978 releveling of southern California and found that, between 1974 and 1978, the southern California uplift sustained pervasive collapse characterized by a tilt to the north. Moreover, during the evolution of the uplift, and to the southeast of it, much of the Salton trough underwent northward-migrating collapse. Between 1977 and 1978 this collapse showed a major reversal of tilt and, in some places, ac-

celerating tectonic subsidence; for example, the area between El Centro and Ocotillo subsided as much as 0.35 m during the interval 1974–78.

J. C. Tinsely and L. D. McFadden discovered that the withdrawal of ground water from a shallow aquifer in Soledad Canyon between Saugus and Lang explained the local variance among the vertical positions of bench marks. Anomalies in the elevations of bench marks were detected by geodetic leveling, which was undertaken to define the southern California uplift centered near Palmdale. The geohydrologic model proposed by Tinsley and McFadden explains the strong correlation between residual signal and topography noted in this reach, a finding alleged by other researchers to be attributable to the surveyor's use of improperly calibrated or erroneously calibrated geodetic leveling rods.

Complex history of faulting on the Banning fault, San Gorgonia Pass area, California

D. M. Morton's and J. C. Matti's completed geologic mapping in the San Gorgonia Pass area extends the Banning fault zone from Whitewater on the east to the Calimesa area on the west. They found that the oldest structure in this zone, the Banning "A" strand, juxtaposes basement rocks of the southern San Bernardino Mountains against Tertiary sedimentary rocks. West of Cabazon, the Banning "A" strand exhibits no evidence of surface displacement during the last 500,000 to 1.0(?) m.y., and young undisturbed Quaternary alluvium overlap this strand north of Beaumont and west of the Calimesa area.

Faults west of Calimesa, in the lower San Timoteo–Live Oak Canyon area, previously assigned to the Banning fault zone, most likely are associated with the Crafton Hills tectonic block, a horstlike feature bounded by geomorphically expressed faults that break Holocene alluvium.

Throughout the Banning fault zone, a group of intermediate-age faults, here termed the Banning "B" group, offsets crystalline basement, Tertiary rocks, and some dissected alluvial units. The faulted alluvial units correlate with a soils chronosequence of Bull, Menges, and McFadden (1979), and are estimated to be as young as 5,000 yr. Faults of the Banning "B" group extend from Whitewater west to the vicinity of Live Oak Canyon. Faults comprising the Banning "C" group offset alluvium that is probably less than 1,000 yr old.

The faults of the Banning "B" and "C" groups are probably closely related thrust and reverse faults, and they resemble other faults found throughout the Transverse Ranges. The relation of these reverse faults in the Banning "B" and "C" groups to such right-lateral faults as the San Andreas and San Jacinto remains troublesome. At the eastern extent of the Banning "A", "B", and "C" groups, where the right-lateral segment of the Banning fault zone exits the Coachella Valley and enters San Gorgonio Pass, Morton and Matti identified at least 5 km of right-lateral displacement in the last 500,000 yr and at least 18 km of right-lateral displacement in the last 7 m.y.; all of this displacement is on the Banning "A" strand. Because the Banning "A" strand was inactive along its westward extent during the last 0.5 to 1.0(?) m.y., it was concluded that, during the late Quaternary, minor right-lateral displacements along the Banning "A" strand have been shunted northwestward to the south branch of the San Andreas fault via Potrero Canyon and Burro Flats.

GROUND-FAILURE INVESTIGATIONS

Improved methods of evaluating the potential for earthquake-induced ground failure

Shear modulus, a known strain-dependent (nonlinear) soil property, is sometimes determined in the laboratory by the use of a torsional pendulum testing device. However, the principles behind such a testing device are based essentially on linear elasticity. In a theoretical investigation, A. T. F. Chen (1980) identified the possible errors associated with the use of elastic theory and suggested the following improvements to minimize these errors: (1) using the concept of effective displacement, (2) determining vibration period, and (3) using acceleration amplitude for the logarithmic decrement in computing damping. Chen also showed that, in theory, the torsional pendulum test could be an effective tool for testing the Masing criterion and for determining the nonhysteretic damping component of soils.

Values of low-amplitude shear modulus and maximum shear stress, as determined in the laboratory, must be adjusted to accurately estimate in situ soil conditions for site response analyses during earthquakes. K. H. Stokoe and A. T. F. Chen (1980) discussed and compared the use of the five currently available methods for estimating in situ stress-strain curves of soils. Their main conclusions from that study are (1) the reference strain method is the most logical one to use, (2) failure to adjust the maximum shear stress value for the in situ condition could result in a 50 percent difference in the maximum surface acceleration; and (3) failure to adjust the low-amplitude shear modulus could result in a substantial shift in the frequency content of the surface response.

Liquefaction evidence in the Mississippi Valley

S. F. Obermier completed a 1:250,000-scale map showing the distribution of sandblows caused by the 1811–12 New Madrid earthquakes in the Mississippi alluvial valley. The map shows the percent of the land surface covered with extruded sand and is based on airphotos

taken in the late 1930's and on extensive field checks. Obermier analysed field engineering test data, including 500 Standard Penetration Tests and about 3,500 blow count data points, to determine the relative susceptibility of the Mississippi alluvial valley to liquefaction during the 1811–12 earthquakes. His maps show locations of Standard Penetration Tests and regional differences in liquefaction susceptibility during 1811–12.

Sandblows extended eastward and northward of the limits shown by Fuller (1912); they can be traced to the vicinity of Chickasaw Bluffs in western Tennessee.

Large areas of Mississippi River alluvium west of Sikeston's Ridge are only weakly susceptible to sandblow development because the alluvial sands are either coarse or relatively dense, as reflected by Standard Penetration Test blow counts. Alluvium further south is finer grained and less dense, and it produced more sandblows during 1811–12. The maps of sandblow extent and liquefaction susceptibility confirm the location of the New Madrid fault as determined from recent seismic-reflection profiles (Zoback and others, 1980).

Estimating seismic landslide potential, San Francisco Bay region, California

Regional zones of seismic landslide susceptibility in the San Francisco Bay area are shown on an experimental, 1:62,500, seismic slope stability map prepared by E. L. Harp for San Mateo County, Calif. Harp used dynamic numerical analysis to develop criteria for evaluating seismic slope stability. The analysis considered lithology, material strength, slope, and strong-motion records from several earthquakes. Failure criteria were derived as follows: (1) lithologic units were grouped into three general categories based on shear-strength parameters; (2) slopes were grouped into six categories identified on slope maps, and (3) for each combination of lithology and slope, the displacement of a potential landslide mass was then calculated by integrating that part of a strong-motion record that exceeded accelerations necessary to cause static slope failure. From these calculations, generalized criteria were established for each combination of slope and lithology, which were then incorporated with geologic and slope maps to construct a seismic slope stability map.

Liquefaction potential and geology are shown on maps of northern Monterery and southern Santa Cruz Counties, Calif., prepared by W. R. Dupre and J. C. Tinsley, III. The maps indicated that most of the cities of Salinas, Watsonville, and Castroville have a low-to-moderate potential for liquefaction during earthquakes. Areas of high-to-very-high liquefaction potential are confined mainly to farmlands along the Pajaro and Salinas Rivers and some of their tributaries, but a few urbanized and industrialized parts of Salinas and Watsonville also possess a high-to-very-high potential. The maps have helped evaluate (1) plans for a waste disposal system along the coast, (2) an environmental assessment of the Elkhorn slough area, and (3) geologic hazards to proposed housing developments. The geologic map, with 35 units, subdivides many previously undivided Quaternary units and provides new insight into Quaternary deformation along the San Andreas fault.

GROUND-MOTION INVESTIGATIONS

National and regional earthquake risk mapping

S. T. Algermissen and his colleagues completed probablistic ground acceleration and velocity maps for the United States. The maps, currently in review, are for an extreme probability of 90 percent for exposure times of 10, 50, and 250 yr.

Recurrence rates for Basin and Range earthquakes derived from historical seismicity agree with rates from geologic investigations of fault slip when the two rates are compared over broad areas of Holocene faulting. Probabilistic ground acceleration and velocity maps of the San Francisco Bay area prepared using recurrence rates of earthquakes obtained from historical seismicity also compare favorably with maps prepared using earthquake recurrence determined from fault-slip studies.

A major task in preparing probabilistic ground-motion maps of the United States is to map seismic source zones, incorporating the latest tectonic and seismologic information. To accomplish this task, five meetings of earth-science experts with regional expertise were convened. There were 24 experts from the academic and consultant communities and 54 from the USGS. Draft reports and maps for the five regions were prepared and used by the seismic risk group in synthesizing the information into a seismic source zone map for the entire United States.

GEOS–a versatile new system for recording seismic data

R. D. Borcherdt reported the successful completion, in 1980, of GEOS, a high dynamic range system for acquiring seismic data. GEOS can be adapted to record strong motion data, microearthquakes, local and regional seismic effects, aftershocks, and teleseisms as well as near-surface seismic exploration data. It uses a 16 bit A/D converter for high dynamic range without depending on gain ranging. Coupled with programmable preamplifiers and programmable prefiltering, almost any signal and sensor type can be accommodated. Efficient use of the memory bus and DMA allows the single CMOS microprocessor to operate the system at 1,200 samples/s. The system can be operated in an event-triggered mode for aftershocks or teleseismic signals

and can be programmed to turn on at preselected time intervals. The trigger algorithm operates on the basis of a Short Term Average (STA) and Long Term Average (LTA) ratio. The 100 db dynamic range of the input amplifier along with the 96 db range of the A/D converter yields a system with exceptional dynamic range for recording all types of seismic activity.

Recent earthquakes further understanding of strong ground motion

Recent earthquakes in California (1979 Coyote Lake, 1979 Imperial Valley, 1980 Mt. Diablo, 1980 Mammoth Lakes) provided invaluable new data on the character of near-source strong ground motion and source parameters over a wide range in magnitude and seismic moment.

Abundant near-source recordings of the 1979 Imperial Valley earthquake ($M_L = 6.6$), analysed by R. J. Archuleta and others, showed a complex interaction between propagating stress relaxation and wave propagation in a heterogeneous medium. From the seismic records, Archuleta infers that the sediment structure from 0 to 5.0 km depth significantly affects the generation and transmission of high-frequency waves.

Analysis of the spectral parameters of more than 70 aftershocks in the Mammoth Lakes sequence suggests that earthquakes with moments less than 2.0×10^{21} dyn-cm differ fundamentally from those with moments greater than 2.0×10^{21} dyn-cm. Stress drop is fairly constant (~ 100 bars) for the larger aftershocks. However, for aftershocks with moments less than 2.0×10^{21} dyn-cm, the stress drop depends on the seismic moment.

Paul Spudich qualitatively analysed seismograms from the main shock and aftershocks of the Coyote Lake earthquake. He found that the largest accelerations recorded in the main shock probably were caused by a wave that traveled in S mode from the source to the base of the Santa Clara Valley and converted to P mode in the valley sediments. His analysis also indicates both low velocities and low Q in the Calaveras fault zone.

Spudich also demonstrated the feasibility of calculating complete theoretical seismograms in a vertically varying medium, using separation of variables and a colocation method for solving coupled ordinary differential equations. This method is an alternative to the more usual normal-mode expansion.

T. C. Hanks and A. G. Brady successfully employed automatic trace-following laser equipment to digitize strong-motion film records from the 1979 Imperial Valley aftershocks.

Intensity distribution for 1906 San Francisco earthquake reinterpreted

Robert Nason reinterpreted seismic intensity data for the major 1906 earthquake, using newly obtained historic information. From this information he infers that the distribution of seismic intensity differed significantly from that shown on old maps (Lawson and others, 1908). Major differences include (1) the intensity levels in hill areas and valley areas were more similar than the old maps indicate, and (2) at a distance of 30 km from the earthquake fault the seismic intensity was approximately the same as at locations much closer to the fault.

Site transfer functions validated for Los Angeles

Underground nuclear explosions at the Nevada Test Site were recorded at 28 Los Angeles region strong-motion sites. Each of the sites also recorded the 1971 San Fernando earthquake, so that site transfer functions (STF) can be computed and tested by comparing computed STF's from the same station pair from both source types. A. M. Rogers grouped these stations geographically to compute spectral ratios (SR) because some earthquake SR's are contaminated by source and path effects when the azimuth or epicentral separation is too large. Rogers computed STF's and their mean values over several period bands for each recording site, using stations at California Insititute of Technology, Palos Verdes Estates, and Griffith Park Observatory as the base rock sites. He also computed some alluvium-to-alluvium spectral ratios, the ratios (R) of earthquake and nuclear STF's, and the correlation coefficients (r) for the scatter diagrams of mean nuclear and earthquake STF's. The hypothesis that r is drawn from a population with zero correlation can be rejected at the 1-percent significance level in every case. Confidence intervals (95 percent) for R indicate that 89–100 percent of the earthquake-nuclear STF ratios are statistically equal to 1. Thus, the nuclear and earthquake SR's are statistically equivalent with a few exceptions. These statistically significant results show that site transfer functions estimated in this way are valid.

NFS-funded strong-motion program

The strong-motion program operated by the USGS with funding from the National Science Foundation coordinates strong-motion data aquisition and analysis on a national scale. In 1980, the program, in affiliation with 13 other Federal, State, and local programs, coordinated maintenance of instruments at more than 700 sites. It also processed, archived, and interpreted the data obtained by these instruments. Examples of results from the program follow.

A 300-m-long array of six digital seismographs was installed at El Centro, Calif., in time to record the October 15, 1979, earthquake. The records were processed and

doubly integrated to give the first differential ground motions to be obtained in the United States. They should prove invaluable in the design of extended structures such as dams, bridges, pipelines, and nuclear power plants. From these data, G. N. Bycroft found that local inhomogeneity of the terrain contributes more to differential ground motion than does the traveling surface wave effect.

Christopher Rojahn gathered new earthquake response data from such instrumented structures as buildings, bridges, and dams for use in improving engineering design practice. Past studies of these data were aimed at developing and implementing instrumentation guidelines, and between 1973 and 1980 approximately 50 buildings, 9 bridges, and 4 dams were instrumented in accordance with these USGS guidelines. In 1980, however, effort was directed toward evaluating and interpretating strong-motion data from two instrumented structures: the severely damaged Imperial County Services Building at El Centro, Calif., and the undamaged Meloland Highway Overpass Bridge, Imperial County, Calif.; both structures were instrumented by the California Division of Mines and Geology.

The Imperial County Services Building was a recently designed 6-story reinforced-concrete structure located approximately 8 km from the October 15, 1979, Imperial fault rupture. The accelerograms recovered from this building provide critical information on forces, dynamic properties, and relative motions in the building during the entire history of shaking from the first nondamaging shaking until after collapse of the first-story columns. From these data Rojahn concluded that (1) damage initiation occurred when the lateral forces imposed on the building were approximately three to four times the design force, and (2) horizontal interstory motions between the second and ground floors were approximately 1 cm at damage initiation and 6 cm at column collapse.

SEISMICITY INVESTIGATIONS

National Earthquake Catalog

A 5-yr program to produce a National Earthquake Catalog began in 1980 under the direction of J. N. Taggart. Four principal elements of preparing the catalog are data preparation, related research, data base development, and publication. During July, August, and September 1980, about 5,400 listed earthquakes for Alaska, Hawaii, Puerto Rico, Guam, and American Samoa were checked against the original sources for errors.

Alaska seismic network

Since at least September 1974, when the regional seismic network east of Cordova reached approximately its present configuration, the level of seismic activity east of about 146° W has been low compared to that in the Prince William Sound–Kenai Peninsula–Cook Inlet region. Prior to the St. Elias earthquake in February 1979, most of the seismic activity in the eastern part of the network was concentrated in two broad zones, one near the aftershock zone of the St. Elias earthquake, and the other about 100 km northeast of Kayak Island. J. C. Lahr and C. D. Stephens reviewed seismic activity that preceded the 1979 St. Elias earthquake and found that, near the aftershock zone, earthquake activity increased for 6 mo before the main shock; they found a 45 percent increase in the number of events above $M = 1.8$ (the smallest magnitude at which all earthquakes in the network can be detected) and an apparent decrease in the regional b value (a measure of the frequency distribution of magnitude) relative to a comparable 6-mo period about 1 yr earlier. They also found that in the 6 mo preceding the main shock, many events clustered near the southeast corner of the aftershock zone. The record of seismic activity since 1974 is insufficient to determine how significant these short-term variations are.

Evaluating seismicity patterns in the Yakataga gap region, between the rupture zones of the 1964 Prince William Sound earthquake and the 1979 St. Elias earthquake, is even more difficult because the data there are less complete than data from near the St. Elias aftershock zone. But records from the gap region provide some evidence that the level of activity northeast of Kayak Island fluctuates with time; the rate of activity for events of $M = 2$ and above was lower between October 1979 and September 1980 than in the 6-mo period preceding the 1979 St. Elias earthquake. Offshore and southwest of Kayak Island, seismic activity increased between October 1979 and September 1980 and was higher than in the 6 mo preceding the St. Elias earthquake. On September 4, 1980, an earthquake with 5.2 m_b (PDE) occurred about 60 km southeast of Kayak Island; it was the largest earthquake within the gap region during the past year.

No strong-motion records have been obtained yet in the United States within 25 km of the causative fault of a $M = 7$ earthquake, or within 100 km of the causative fault of a $M = 8$ earthquake. Since the 1979 St. Elias earthquake, Lahr, Stephens, and their colleagues have installed several new strong-motion stations within or near the Yakataga seismic gap. Currently 10 USGS strong-motion instruments, including 3 new installations from the summer of 1980, are sited within the gap region between Kayak Island and Icy Bay. These and other nearby strong-motion instruments assure that a high-quality suite of accelerograms will be obtained for the major earthquakes expected in the next few decades.

POSTEARTHQUAKE INVESTIGATIONS

Fault displacements accompanying the October 1979 Imperial Valley earthquake

R. V. Sharp reported that the Imperial Valley earthquake of October 15, 1979, displaced the ground surface along the Imperial fault, the Brawley fault zone, parts of the Mesquite basin between these faults, and a minor structure here named the "Rico fault." The 30.5-km length of surface rupture on the Imperial fault included approximately the north half of the 1940 trace of surface faulting, which extended into Mexico. The first day after the earthquake, maximum right-lateral displacement on the Imperial fault was 55 to 60 cm and was located about 1.4 km from the south end of surface faulting and about 10.5 km northwest of the earthquake epicenter. Although the point of maximum right-lateral slip remained in the southernmost fifth of the surface rupture throughout the afterslip period, the point of maximum cumulative right-lateral slip shifted northward. At 160 d after the earthquake, the maximum measured cumulative horizontal slip was about 78 cm (29 cm of afterslip) at a point about 5.6 km from the south end of rupture. Average horizontal displacement on the Imperial fault grew from about 29 cm on the 4th d after the earthquake to about 43 cm on the 160th d.

Different segments of the Imperial fault varied considerably in the amount of horizontal afterslip. Sharp found that some segments revealed a simple inverse relation of horizontal afterslip to coseismic displacement; others with low initial slip increased only slightly in offset. At most localities on the fault, cumulative horizontal slip increased linearly as a function of the logarithm of postearthquake time, but a few localities displayed distinctly nonlinear growth of displacement.

The Brawley fault zone east of the northern section of the Imperial fault ruptured discontinuously along multiple strands over a length of 13.1 km. The faulting extended a kilometer or two beyond fault breaks that accompanied an earthquake swarm in 1975. Displacement was dominantly vertical, similar to but smaller than and opposite in sense to that on the northern section of the Imperial fault. The Mesquite basin block between the two faults dropped as much as 41 cm along the Imperial fault and no more than 15 cm along the Brawley fault zone. Horizontal right slip, detected locally on the westernmost breaks of the Brawley fault zone, was as much as 7 cm at Keystone and Harris Roads. Horizontal and vertical afterslips in the Brawley fault zone were insignificant compared to that on the Imperial fault.

The Rico fault, a newly recognized structure that broke along a 1-km length near Holtville, Calif., resembles the Brawley fault zone in orientation and sense of vertical displacement. It exhibits vertical offset no greater than 20 cm, no horizontal slip, and little or no afterslip.

Surface deformation accompanying the northern Mexico earthquake of June 9, 1980

The instrumental epicenter of the northern Mexico earthquake of June 9, 1980, was located near the Cerro Prieto fault about 55 km south of the international boundary. R. V. Sharp examined the Imperial fault (for triggered surface movement in the United States and Mexico) and the Cerro Prieto fault, where paved roads cross it in Mexico. He found surface deformation, some of which is possibly due to faulting, at the following locations:

- About 7 km northwest of the epicenter, en echelon cracks cross the pavement of BCN–4, 2.1 km east of its intersection with BCN–3. One crack showed about 1 cm of right-lateral offset; but because the fractures were confined to the road, the cracking is not considered to represent faulting.
- Cracks 3 km southeast of the epicenter and about 3.8 km southwest of Coahuila are also near the Cerro Prieto fault, but they are most likely secondary fractures associated with lateral spreading near a deep ditch that parallels the road.
- Left-stepping en echelon fractures with maximum observed right-lateral displacement of 16.5 cm delineate a 1-km zone just west of the settlement of Ejido Saltillo. Residents of Ejido Saltillo became aware of the surface ruptures shortly after the time of the earthquake in the evening of June 8. Sharp interprets these cracks as tectonic or possibly triggered faulting because he found no evidence of liquefaction or other secondary ground failure nearby. These surface breaks lie northeast of the Cerro Prieto fault and beyond the southeasternmost limit of the Imperial fault rupture that accompanied the 1940 Imperial Valley earthquake.

Concurrent displacement on conjugate Greenville and Las Positas faults, Livermore Valley, California

Surface faulting during the Livermore Valley, Calif., earthquakes of January 24 and January 26, 1980, as mapped by M. G. Bonilla, J. J. Lienkaemper, and J. C. Tinsley (1980), followed strands of the Greenville fault (Herd, 1977 and unpublished data). Tectonic displacement also followed parts of the Las Positas fault as mapped by Herd (1977). The principal surface break on the Greenville fault extended discontinuously for at least 4 km, and perhaps 6 km; this break exhibited about 25 mm of right-lateral displacement, including afterslip through January 28. Vertical components as large as 50

mm included large but unknown components of nontectonic gravity effects.

A right-stepping pattern of en echelon fractures on the Las Positas fault locally displayed less than 2 mm of left-lateral displacements. An alinement array surveyed by P. W. Harsh showed about 6 mm of left-lateral displacement between February 21 and March 26, 1980. These observations and the growth of some fractures confirm tectonic displacement along at least 1 km of the Las Positas fault. Concurrent displacement on conjugate faults, like the Greenville and Las Positas, also occurred in Japan in 1927 and 1930.

Faulting at Mammoth Lakes, California

A 17-km-long zone of intermittent surface ruptures, mapped by M. M. Clark and his colleagues, was associated with the Mammoth Lakes earthquakes of May 1980. The zone extended northwest from McGee Creek for 6 km along one strand of the Hilton Creek fault and then entered Long Valley caldera along 4 major splays of the fault in a zone of horsts and grabens as wide as 4 km. Displacement was extensional, roughly normal to the ruptures. At most places new ruptures, as single or multiple cracks in zones a few meters wide, followed older scarps. At these places new vertical slip was consistent with past slip and was roughly equal to new horizontal (opening) slip. Net slip was generally less than 50 mm on widely spaced cracks a few meters long, but locally slip exceeded 200 mm on ruptures tens of meters long. The faulting offset Quaternary lava in a few places in the caldera; but because most ruptures were on slopes near the boundaries of unconsolidated deposits, a component of slump obscured much of the tectonic displacement.

The four largest earthquakes in May were apparently not on the Hilton Creek fault, yet fault slip origin for the surface ruptures is indicated by offset of bedrock, the restriction of all ruptures to a discreet segment of the fault, and the fact that the ruptured fault segment was further from the main earthquakes than other unbroken fault segments.

Analysis of ground failure, Coyote Lake, California, earthquake of August 1979

The Coyote Lake earthquake (M = 5.9), located on the Calaveras fault in southern Santa Clara County, Calif., on August 6, 1979, produced numerous ground failures. One fissure, studied by R. C. Wilson, resulted when a preexisting landslide was reactivated by the Coyote Lake earthquake. The fissure, within 100 m of the Calaveras fault and near Lake Anderson, extended 20 m obliquely across an asphalt roadway and onto the dirt shoulders on both sides. It was 12 to 18 mm wide, with 5 to 10 mm of vertical displacement, down to the south. It appears to represent the scarp of an older slump landslide in weathered shales of the Cretaceous Berryessa Formation of Crittenden (1951). Wilson's measurements across the fissure indicate a seismically induced 20 mm displacement of the landslide mass.

Several accelerographs of the Coyote Lake earthquake are available from strong-motion instruments; and a USGS accelerometer, Gilroy Station No. 6, was located near the Calaveras fault in the epicentral area, about 10 km southeast of the landslide. The proximity of this slope failure to the strong-motion instruments provides a test of the method of analyzing seismic slope stability previously developed by Wilson. Using field measurements, standard slope stability measurements, and estimates of the strength of the shale, the critical acceleration (threshold of seismic-induced movement) of the landslide was estimated to be 15 to 25 percent gravity. Using the N. 50° E. component of the accelerogram from Gilroy Station No. 6 and these critical displacements, the dynamic analysis predicted displacements of 10 to 25 mm, in excellent agreement with the 20 mm displacement measured in the field. This result is especially significant because strong-motion records and well-documented slope failures so rarely coincide that few opportunities can be found to test the analytical techniques.

Tectonic deformation accompanying Tumaco, Colombia, earthquake of December 1979

Southwestern Colombia and northern Ecuador were shaken by a shallow-focus earthquake on December 12, 1979. The $M_s = 8$ shock, located near Tumaco, Colombia, was the largest in northwestern South America since 1942 and had been forecast to fill a seismic gap. Thrust faulting occurred along an east-dipping 280- by 130-km rectangular patch of subduction zone beneath the Pacific coast of Colombia.

A tsunami swept inland immediately after the earthquake, inundating a number of coastal villages. Many buildings collapsed during intensity VI to IX ground shaking, and sand fills in Holocene beach, lagoonal, and fluvial deposits liquefied. A field investigation in January 1980 by D. G. Herd, T. L. Youd, and members of the Colombian Instituto Nacional de Investigaciones Geologico-Mineras documented tectonic subsidence of as much as 1.6 m along a 200-km stretch of the Colombian coast and uplift offshore on the continental slope.

VOLCANO HAZARDS

VOLCANO HAZARDS PROGRAM

As a consequence of the devastating eruption of Mount St. Helens on May 18, 1980, the American public, particularly in the Pacific Northwest, has become acute-

ly aware that volcanic activity poses a real threat to human life, property, and natural resources in this country. Prior to that event the threat of volcanic hazards in the Cascades was not generally appreciated, and the forecast that Mount St. Helens would erupt again, "perhaps even before the end of this century" (Crandell and Mullineaux, 1975, 1978) was not taken seriously except by a handful of scientists.

Historical records show that Mount St. Helens was active intermittently for 23 yr during the mid-1800's, and that several other Cascade volcanoes (Mt. Baker, Mt. Ranier, Mt. Hood, and Lassen Cinder Cone) were also active during that same general period. Except for the eruption of Lassen Peak in 1914–1917, the Cascade volcanoes have been unusually quiet for nearly a century. During the past 6 yr, however, volcanic and seismic unrest has become increasingly evident. In 1975, increased heat flow at Mt. Baker caused intense steaming in the summit crater, resulting in massive melting of the glacial ice filling; although steaming has since decreased, melting of the ice continues at a greater than average rate. The current eruptions of Mount St. Helens, although apparently declining in intensity, may continue for decades. Brief seismic swarms occurred in 1978 and 1981 near Mt. Shasta and in 1980 at Mt. Hood, and although apparently of tectonic, not volcanic origin, their proximity to active volcanoes emphasizes that volcanism and tectonism in the region are not entirely unrelated. These events are reminders that the Cascade volcanoes are merely dormant, not extinct, and that more eruptions in the future are not an unrealistic expectation. Whether or not the recent events represent the return of activity comparable to that of the mid-1800's remains to be seen.

The responsibility of the USGS to provide timely and accurate warning of possible future eruptions, as mandated by the Natural Hazards Act of 1974 (P.L. 93–288), is of considerable concern in view of the present meager knowledge of most Cascade volcanoes and their past volcanic activity. In order to reduce the effects of hazards from possible future eruptions, the USGS has accelerated its efforts in volcano hazards mapping and risk assessment and in improved volcano monitoring. In 1980, with increased funding approved by Congress, the Volcano Hazards Program was reorganized and expanded; volcano monitoring, volcanic hazards mapping, and fundamental research elements of the program now are coordinated more closely, as are investigations in Hawaii, Alaska, and conterminous United States.

Accomplishments of the program in 1980–81 include (1) establishment of a volcano research center at Vancouver, Wash., to serve as a base for the continued monitoring of Mount St. Helens and for the study of other Cascade volcanoes; (2) initiation of new volcanic hazards mapping on Mt. Rainier, Wash.; Three Sisters, Oreg.; Lassen Peak and Mono-Inyo Craters, Calif.; and Hualalai, Hawaii; (3) installation of new monitoring equipment on Mt. Baker and Mt. Rainier, Wash.; Mt. Hood, Oreg.; and Mt. Shasta and Lassen Peak, Calif., and (4) publication of volcanic hazards assessment reports for Mt. Hood and for Mt. Shasta, Calif., (Crandell, 1980; Miller, 1980).

MOUNT ST. HELENS ERUPTIONS

Monitoring and hazards assessment

The 1980 eruptions of Mount St. Helens, although not the largest or most destructive of recent volcanic eruptions, were remarkable for the degree of national attention, public apprehension, and social and physical disruption they caused.

The renewal of activity at Mount St. Helens on March 20, 1980, was heralded by a swarm of shallow earthquakes beneath the volcano, which were felt on site and were instrumentally recorded by geophysicists of the University of Washington–USGS group in Seattle, Wash. As the unusual character of the increasing seismic activity became clear and the possibility of an eruption became evident, a warning of this possibility was conveyed to the U.S. Forest Service (USFS) staff at Clifford Pinchot National Forest, who are responsible for administration of the land surrounding the volcano. Advice was requested from volcanologists and other scientists of the USGS, including D. R. Crandell and D. R. Mullineaux, who, on the basis of previous studies of the volcano, had assessed that Mount St. Helens had been the most frequently active volcano in the Cascades, was potentially one of the most dangerous, and was likely to erupt again in the near future, "perhaps even before the end of this century." Recognition of these potential hazards prompted the USFS and State officials to restrict public access to the volcano and adjacent areas on March 26. At the same time a central office was established at USFS headquarters in Vancouver, Wash., for hazards evaluation, monitoring activity, press briefing, and public information.

On March 27, phreatic explosive activity began at the summit of Mount St. Helens, accompanied by cratering, ground fracturing, and growing of a topographic bulge on the upper north flank of the volcano. During the ensuing weeks in April and May, as the eruptive and seismic activity continued, the USGS developed an intensive program of geophysical monitoring and volcanic hazards analysis, drawing heavily on the equipment, staff, and experienced former staff from the USGS Hawaiian Volcano Observatory and on personnel of the Engineering Geology Branch. The ability to continuously measure and monitor the rapidly occurring changes

on the volcano provided information and justification for Federal and State officials to continue to limit access to the volcano and adjacent areas, despite heavy pressure to relax restrictions. Although it was hoped that the monitoring techniques being used would provide some warning of any major eruption, the catastrophic outburst of May 18 came with no precursory signs that were recognized in advance or by hindsight.

After May 18, studies began on the deposits and effects of the eruption: the debris avalanche, the blast deposit, the mudflows and pyroclastic flows, and the extensive pumice and ash falls. Continued monitoring during the ensuing months provided warnings of a few days to a few hours before the explosive eruptions of May 25, June 12, July 22, August 7, and October 16–18. Lava domes were extruded within the vent crater shortly after the June, August, and October eruptions, and the October dome was enlarged by growth of additional lobes of lava in December 1980, and in February, April, June, and September 1981. All of these latter extrusions were predicted with remarkable accuracy on the basis of ground deformation and seismic studies.

Effects of the eruption

Effects of the May 18 eruption were catastrophic near the volcano. To the north nearly 600 km^2 of heavily timbered land was totally devastated. More than 60 people, mostly within this area, were killed or are missing; but had public access not been restricted, the death toll might have been in the thousands.

The North Fork Toutle River valley, which was most severely affected, was inundated by the debris avalanche as far as 20 km downstream from the volcano and was filled to a maximum depth of nearly 200 m. Further downvalley, mud flows and floods spread over valley floors, which raised channel beds and destroyed or damaged countless homes and civil engineering works, including most roads and bridges. Sediment was carried even as far as the Columbia River, where it blocked the channel and prevented passage of shipping for several days before it could be dredged.

Downwind from the volcano to the northeast and east, falling ash produced darkness during daylight hours, halted highway traffic, damaged machinery – especially internal combustion engines – and caused shutdown of critical electronic equipment to avoid damage. Emergency conditions were in effect throughout eastern Washington, most of Montana, and part of Idaho. In the aftermath, the accumulation of ash severely hampered transportation, sewerage disposal, water supply, and storm drainage systems; and ash removal and disposal was a major problem in many communities. Locally, where the ash fall was heavier, agricultural crops were killed or severely damaged; but where the fall was lighter, the ash may have long-term beneficial effects because of the addition of new mineral nutrients and the improved moisture retention of the soils. However, the long-term effects of the eruption are not yet well known and are the subject of continuing study by Federal, State, and local agencies, as well as private interests. A comprehensive report of the 1980 activity has been published (Lipman and Mullineaux, 1981).

Analysis of hazards assessments

Many of the effects of the May 18th and subsequent eruptions were anticipated, but others were not; thus, the eruption emphasized some of the limitations of volcanic hazards assessments based on past eruptive records alone. Predictions of potential eruptions and assessments of volcanic hazards, based on the past activity of various volcanoes in the Cascade Range, have been made over the past 15 yr, mainly for the purposes of long-range land-use planning. These assessments describe kinds, locations, severity, frequency, and effects of future eruptions and suggest possible responses. Such an assessment for Mount St. Helens was completed in the mid-1970's, and the report was published in 1978. Because such assessments are for long-range planning they differ from short-term hazards assessments made during an active eruption, which consider, in addition to past activity, current information provided by daily monitoring. After the first phreatic eruptions of March 27, recommendations regarding hazards and appropriate responses were based not only on past eruptive records but also on day-to-day visual and instrumental monitoring. USGS hazards analysis coordinators described the range of expectable eruptions, possible responses, and expectable warnings to government officials, private interests, and the general public. In general these hazards forecasts were accurate, but the magnitude of the massive debris avalanche and laterally directed blast of May 18 exceeded expectations. Nevertheless, the experience of the 1980 eruptions emphasized the necessity of having (1) a volcanic hazards assessment completed before the eruption, (2) an extensive monitoring network and team available on short notice, (3) an onsite agency or organization capable of handling emergency situations, and (4) hazards assessments personnel familiar with the local geography and land use as well as with the past eruptive record.

Posteruption hazards of Spirit Lake

During the eruption of May 18, 1980, a massive (2.7 km^3) landslide off the north face of Mount St. Helens flowed into Spirit Lake and the North Fork of the Toutle River, raising the level of Spirit Lake 60 m and filling the Toutle valley with a tongue of debris up to 170 cm

thick extending 22 km downstream. The landslide and eruption caused a destructive flood of water, ash, and mud down the Toutle, Cowlitz, and Columbia Rivers. After the flood subsided on May 19, doubts were raised about the mechanical stability of the debris flow and the possibility that blockage on the Toutle River might suddenly breach and cause further flooding. A preliminary investigation of this potential hazard was conducted by R. C. Wilson and T. L. Youd on May 19–23, 1980. Three potential failure modes were investigated: (1) overtopping by impounded waters and resultant erosional failure, (2) slope failure of blockage, possibly under sesimic loading, and (3) failure by subsurface erosion (piping). It was found that about 60 m of the "freeboard" existed between the new level of Spirit Lake and the lowest point on the crest of the debris blockage, and that the level of lake was falling slowly, making overtopping unlikely before the 1981 spring thaw. Profiles drawn from point elevations (from helicopter altimeter) indicated that the overall slope of the debris blockage was only about 4 percent. Large-scale slope failures by either gravitational or seismic loading are unlikely on such gentle slopes, even in unconsolidated materials (factor or safety greater than or equal to 6). Failure by piping was considered unlikely because of the relatively low hydraulic gradient (425/L3700 m=3 percent) and because the material is well graded. T. L. Youd calculated a factor of safety against piping failure of greater than or equal to 3.6. It was concluded, therefore, that (under conditions existing on May 23) the Toutle River debris blockage was reasonably stable and that large-scale breaching and flooding was unlikely before the next spring thaw.

Computer program for ashfall trajectories

A computer graphics program was developed by W. Z. Savage, plotting predicted ashfall trajectories from Mount St. Helens, Wash. Raw forecast trajectory data were obtained from the NOAA computer in Suitland, Md., and transferred to the USGS Multics System in Denver, Colo. The plotting program then was executed from a remote terminal in Vancouver, Wash., to produce plots of expected ashfall patterns from an eruption occurring at any of several times that day. These plots are used by field personnel at Mount St. Helens for planning field operations and by emergency planning agencies for identifying danger zones on a day-to-day basis.

Physiographic diagrams of eruptive effects

In order to more clearly illustrate the sequence of events and effects of the 1980 Mount St. Helens eruptions, T. R. Alpha, collaborating with monitoring volcanologists, prepared several series of perspective drawings, using an oblique cartographic projection technique that he had previously used extensively to portray submarine geological features. These diagrammatic illustrations include (1) pre- and post-May 18 configurations of Mount St. Helens (Alpha and others, 1980), and (2) sequential changes during formation of the May 18 debris avalanche and lateral blast (Alpha and others, 1980). The illustrations are scale accurate and realistic in detail.

Effect of ash on wheat crops

The May 18, 1980, eruption of Mount St. Helens deposited varying amounts of ash over the Palouse region of eastern Washington, an area noted for production of soft white wheat. Between June 16 and 20, 1980, samples of grain heads (tops) from immature club wheat and wheat stems and leaves were collected by L. P. Gough and J. L. Peard at six locations along a 75-km transect south of Ritzville. Whole grain was sampled on July 14. The localities were edaphically, lithologically, and vegetationally similar, but differed in the thickness of ash received (40, 30, 20, 11, 7, and >0.1 mm).

The 50 mm of rainfall, received by the study area between the eruption and the sampling in mid-June, altered the chemical composition of soil extracts so that soil-chemical uniformity before the ashfall could not be definitely established. This amount of precipitation should replenish available water in the Ritzville Soil Series to a depth of about 25 cm.

Transect data for the concentration of 25 elements in plant materials revealed few strong trends related to ash deposition. A possible increase of aluminum and iron occurred in wheat stems and leaves at sites that received 20 mm or more of ash. Higher concentrations of sulfur were noted in samples of whole grain and grainhead material at sites that received large thicknesses of ash. The increased extractable levels of many elements measured in the soils, especially at the sites that received the thickest deposits of ash, may alter the levels of these metals in subsequent crops.

Studies of prehistoric activity

Studies by D. R. Mullineaux, R. P. Hoblitt, and D. R. Crandell showed that the eruptive history of Mount St. Helens began about 40,000 yr ago with dacitic volcanism, which continued intermittently until about 2,500 yr ago. This activity included many explosive eruptions over periods of a few thousand years, which were separated by apparent dormant intervals that ranged from a few hundred to 15,000 yr duration. Between 2,500 and 1,500 yr ago, eruptions of dacite alternated in quick succession with andesite and basalt. The sequence includes, from oldest to youngest, andesite, dacite, basalt, andesite, dacite, basalt. This eruptive

period marked the start of eruptions that built the modern volcano.

During the last 1,500 yr, Mount St. Helens repeatedly has erupted dacite domes, tephra, and pyroclastic flows as well as andesite lava flows, tephra, and pyroclastic flows. Two periods of activity, each decades in duration, were initiated by explosive eruptions of dacite, which were followed by andesite lava flows and pyroclastic flows and small amounts of tephra, then by the extrusion of dacite domes. During a third period of activity, a dacite dome was formed, accompanied by minor pyroclastic flows.

On the basis of the lengths of eruptive periods during the last 2,500 yr, the eruptive activity that began in March 1980, might be expected to continue for many years and perhaps, intermittently, for several decades. The volatile-rich dacite that was erupted during 1980 probably will eventually be followed by gas-poor magma, but it is not yet known whether a much more mafic magma will be extruded during the current eruptive period.

Tectonic influence on 1980 activity

Analysis of post-May 18, 1980 (date of the cataclysmic eruption), earthquakes by C. S. Weaver showed that Mount St. Helens is in a region dominated by horizontal compressional stress, and is located in a left-stepping offset between two right-lateral strike-slip seismic zones. North of Mount St. Helens, earthquake epicenters trend nearly north-south; whereas, southeast of the volcano, epicenters trend north-northwest. Earthquakes directly beneath the mountain have both strike-slip and thrust focal mechanisms and define a northeast-striking fault. All of the 1980 Mount St. Helens eruptions have been accompanied by earthquakes on this fault, suggesting that the fault serves as the zone of magma transport.

VOLCANIC HAZARDS IN HAWAII

Hazards near Hilo reevaluated

The northeast rift zone of Mauna Loa Volcano previously was thought to have been eruptively active only above about 2,440 m elevation for the past several thousand years. However, a young lava flow has been discovered by J. P. Lockwood far east of this point in dense rain forest east of Kulani Cone. The flow, named the Ola'a Uka flow, consists of distinctive plagioclase-rich basalt, is at least 10 km long, and was erupted from several vents extending from 1,220 to 1,525 m elevation, in a zone 11 to 15 km east of the previously considered eastern limit of the active northeast rift zone. Charred organic matter was collected beneath spatter at two localities for precise radiocarbon dating; fresh glass and a relatively youthful, though dense, forest cover suggest an age of 300 to 500 yr.

Discovery of this young flow has caused a reevaluation of volcanic hazards on the east side of Mauna Loa. The vents are much closer to Hilo than was previously thought possible and are upslope from the communities of Mountain View and Glenwood.

Ash beds increase earthquake induced hazards

As a result of geologic hazards studies in the Hilo quadrangle and parts of adjacent quadrangles, J. M. Buchanan-Banks recognized and mapped two separate saprolites developed on ancient lava flows from Mauna Kea. The younger saprolite, mapped in and north of the Wailuku River channel, is overlain by a variable-thickness ash bed, also believed to have erupted from Mauna Kea. Between the ash bed and the underlying saprolite is a locally thick bed of yellow-gray impermeable clay.

Carbon–14 dating of charcoal from beneath adjacent Mauna Loa lava flows indicates that the ash is older than 14,500 yr. USGS geotechnical tests indicate that this ash is more weathered, has a higher water content, and is more susceptible to flow than younger ash beds in the area.

These tests and geologic relations suggest that the relatively more permeable ash allows water to accumulate at its base, above the yellow-gray clay, where it acts as a lubricant, thereby creating a zone particularly susceptible to earthquake-induced flowage. Special precautions and practices are required in the construction of buildings and civil works in this area in order to reduce the risk of damage from earthquakes.

ENGINEERING GEOLOGY

ENGINEERING GEOLOGIC MAPPING

National engineering-environmental geology maps

Discussion and presentation of experimental engineering-environmental geologic maps was prepared by D. H. Radbruch-Hall, K. L. Edwards, and R. M. Batson at a scale of 1:7,500,000, as part of a program to compile a series of National Environmental Overview Maps of the United States. One map shows in color how generalized geologic units are related to the physical properties of the rocks and soils. On another map, computer-generated color patterns showing the intensity of geologic conditions and processes that might pose constraints to construction are overprinted on a black and white base consisting of the outlines of the geologic units; this method clearly indicates the relation of the constraints to the generalized geology. Other maps

show young faults, simplified drainage, and those areas where construction or land development may cause direct environmental damage by worsening existing restrictive geologic conditions or processes and where indirect effects may occur, for example, draining standing water may destroy wildlife habitats. The computer techniques used to compile the maps not only facilitated presentation of this information but also provided a method that can be used for rapid and economical black-and-white or color presentation of comparisons of overlays, maps, or other data. A review on the role of engineering geologic factors in the early settlement and expansion of the conterminous United States was prepared by D. H. Radbruch-Hall.

Port Townsend, Washington, sediment properties

As part of preparing a physical property map of the Port Townsend quadrangle, Washington, R. D. Miller collected samples of different surficial deposits and analyzed them for density, size, and plasticity. In addition, selected localities were sampled for testing the permeability of the glacial till and glaciolacustrine deposits. Results showed that the permeability of all samples ranged from low (1×10^{-3} cm/s) to practically impermeable (less than 1×10^{-9} cm/s). These figures quantify practical knowledge that most upland localities in the quadrangle are either marginal or unsatisfactory for standard design leaching fields.

Boston bedrock map

A new bedrock map of three Boston area quadrangles has been prepared by C. A. Kaye by remapping the central Boston area and incorporating much previously unused subsurface data. The lithologic rock types in the area exhibit a complex interfingering relation, expressing depositional facies in an unstable basin-range sedimentary environment. Volcanic intervals were numerous, and the lava types extruded were varied. Granitic intrusions are related to some of the volcanic outpourings. According to Kaye and Zartmann (1980), the age of the Boston Basin is given as probably late Proterozoic Z to Cambrian, rather than Carboniferous as heretofore thought. Rocks of the basin appear related directly to the Avalonian rocks of eastern Newfoundland and fit into the now well-established plate tectonic framework of the Appalachian system.

A new method of presentation for a geologic map of a structually and stratigraphically complicated area was devised using specially designed map symbols in order to make information available either on a lithologic, relative age, or formational basis and, therefore, particularly useful to engineers, planners, and other nongeologic users. The map units give primary emphasis to lithology rather than to stratigraphy (all granites are lumped together, all conglomerates, and so forth). The layered rocks (volcanic and sedimentary) are separated into eight relative ages. The relative ages for different map units are shown by means of small-size numerals, which are followed by large uppercase letters denoting lithology, which are followed by smaller size, lowercase designations for secondary characteristics—either stratigraphic, physical, or genetic.

New York City stratigraphy

Geologic study by C. A. Baskerville in the New York City area over a number of years has indicated that the east Bronx rocks are different from the New York City Group of Prucha (1956). Mapping by Baskerville during the 1980 field season has shown that the east Bronx rocks belong to the Hartland Formation. As mapped by Merrill (1898) and Merrill and others (1902) in the late 1800's, the east Bronx was shown as underlain by Manhattan Schist, which has different engineering characteristics than the Hartland Formation. The 1980 mapping has shown also that the Cameron's line suture, separating New England eugeosynclinal from miogeosynclinal rocks, traverses southwestward across Bronx County and down the East River between New York (Manhattan) and Queens Counties.

Young faults mapped in California

Geologic mapping in the Montara Mountain 7½-min quadrangle, San Mateo County, Calif., demonstrated the presence of previously unmapped faults juxtaposing Jurassic and Cretaceous Franciscan rocks with Pliocene and Pleistocene Merced and Colma Formations. According to E. H. Pampeyan, these faults, along the east edge of the San Andreas fault zone between San Bruno and Burlingame, dip westward to vertical with west side up. They appear to be part of a series of young faults on the San Francisco peninsula that include the Serra and Sargent-Berrocal faults. Geomorphic evidence for position and recency of activity of the faults, such as sag ponds and linear trenches, visible on 1946 aerial photographs has been obliterated largely by urban development, but in a few places there are bedrock exposures that verify the photointerpretive evidence.

RESEARCH IN ROCK MECHANICS

Barre Granite deformation studies

Experiments performed under a contract with the University of Colorado demonstrate that the assumptions required for application of the double-torsion compliance method to relaxation tests of the Westerly Granite contain major violations of theory. Erroneous values of crack velocity and stress intensity factor can

result because of (1) considerable frictional constraint along the previously fractured crack plane, (2) force relaxations due to time-dependent friction along the crack plane, and (3) an environmental dependence of the "elastic" properties throughout the entire specimen. Despite the complications with the double-torsion method, a clearer understanding of the process of fracture propagation is developed by using this technique.

A suite of constant strain rate deformation experiments was performed on samples of Barre Granite, at a confining pressure of 2.5 kbar, temperatures of 100°, 200°, 300°, 400°, and 500°C, and strain rates of 10^{-4}, 10^{-5}, and 10^{-6}/s. These experiments, performed at Brown University on contract, were designed to determine the fracture strength over this range of conditions, and additionally, to determine the influence of the fault that develops on sample deformation. As expected, the fracture strength is not a very sensitive function of either temperature or strain rate over this range of conditions, and ranges from 3 to 10 kbar. Controlled cooling and unloading experiments on Barre Granite show that stainless steel furnaces produce far fewer extension cracks than do the standard graphite furnaces.

In situ stresses, southeastern Maine

Stress-relief measurements made at depths to 8 m in the granite of the Mount Waldo pluton near Bucksport, Maine, by F. T. Lee indicated that stresses are affected by sheeting, tectonic jointing, topography, and temperature changes. Thermal expansion of the granite, which is being more extensively studied, is anisotropic and may be governed by the orientation of feldspar and quartz grains. Information collected to date strongly suggest that rock stresses determined in the "skin" (upper 1 m) of the rock mass are significantly affected by diurnal and annual temperature cycles. For example, an increase in rock temperature of 28°C—not unusual at depths to 0.3 m—results in a calculated increase in compression of 3.6 MPa, a major portion of the summer rock skin stresses.

The orientation of through-going, near-vertical, Mesozoic(?) dikes that cut the granite of the Devonian Mount Waldo pluton may be helpful in extrapolating between stress measurement sites in the granite. The maximum horizontal stress at 6.5 m (below significant temperature effects) is N. 75° E. Nearby dikes consistently trend N. 65–80° E., suggesting that the stress field existing in the granite when the dikes were intruded is still present in the rock mass.

Fault materials related to displacement

Observations of fault characteristics in rocks in mines of the Butte and Coeur d'Alene districts and at a number of surface exposures, as well as study of confined rock specimens sheared in the laboratory, lead to the tentative conclusion by E. C. Robertson that the displacement of a fault through the range from 1 mm to 1 km is approximately 100 times the thickness of its gouge and breccia (that is, comminuted rock), but not including adjacent jointed rock. Some factors may vary this relation; experiments indicate that confining pressure has an important effect but that water and temperature have only small effects. Twenty-four measurements of normal and reverse faults, taken in several different rocks, including quartzite, fit the relation between displacement and breccia thickness, showing some scatter on a log-log plot. The large displacements of strike-slip and low-angle overthrust faults are not well determined and their breccia thicknesses are widely varible, so the proposed fault relation cannot be applied to them.

RESEARCH IN GEOLOGIC HAZARDS

Utah landslide activity

The Manti landslide in Utah was reactivated in early June 1974 after debris flows inundated the head of the relatively "inactive" slide. By September 1975, reactivation had progressed to the toe of the slide and had caused widespread disruption of the forest cover. Tree-ring analysis by S. S. Agard of 105 tilted, uprooted, split, abraded, or partially buried trees that survived the slide movement revealed the following results:

1. In 90 percent of the trees sampled, one of the following abrupt internal growth changes occurred: (a) reaction wood (in conifers) or eccentric growth (in aspen), (b) severely suppressed growth, or (c) a combination of these. These growth responses were initiated within a growing season of the actual date of disturbance and, therefore, accurately date the event.
2. Debris flows inundated the head of the Manti landslide in 1912, 1928, 1936, 1942, 1947, 1952, 1954, 1957, 1963, 1965, 1968, 1970, and 1974. Prior to 1974, the most widespread events occurred in 1936, 1947, and 1968, and correspond to years of unusually heavy late winter/early spring (January–April) snowfall and late spring (April–May) snowpack.
3. Local reactivation of slide movement occurred in the upper two-thirds of the slide during the periods 1947–49 and 1968–70, possibly in response to the debris flow activity and climate conditions in 1947 and 1968. However, no previous slide events of the magnitude of the 1974 event have occurred within the lifespan of the trees (250–300 yr).

Possible active faults discovered in southwestern Wyoming

In southwestern Wyoming, D. D. Dickey and A. B. Gibbons identified recent faulting not recognized previously. Faults occur in two groups, one about 20 km southeast of Evanston, Wyo., the other about 15 km north of Evanston. In both areas faults locally displace alluvium. The faults generally trend northerly and are a few kilometers long; the downdropped side may be either to the west or east but most commonly is to the west. Very youthful landscape features such as scarps in Holocene alluvium and undrained depressions along a scarp (a sag pond if water were available) mark the traces of some faults. Total scarp heights are as much as 10 m, offsets in surficial materials as much as 2 m. Available records indicate seismicity has not been reported in the area. Although the latest movement of these faults has not been dated, the freshness of the scarps indicates that they may be part of an ongoing structural event and thus a potential geologic hazard. The area is in the Overthrust Belt hydrocarbon province that is undergoing active exploration and development, including drilling. A still speculative consideration is the possibly destabilizing effect of changing fluid pressures along these faults during extraction of gas and oil. Considering current population expansion and projected oil and gas development and refining facilities (including pipelines), the presence of "active" faults has increasingly practical significance.

Geologic problems of the Bighorn basin, Wyoming

Geologic field reconnaissance by R. M. Barker and C. M. Shifflett established that a variety of significant geologic conditions and problems affect all or parts of the Bighorn basin, Wyo. Examples include delineation of alinement and foundation conditions basinwide; local and basinwide availability of construction materials; large areas of steep, intricately dissected badland slopes, notably in the Eocene Willwood Formation; swell-shrink potential of bentonite layers in several formations and sediments derived from them; geologic considerations associated with widespread gypsiferous soils; basinwide slope stability conditions and severe landslide problems along the basin peripheries; and subsidence over small, mostly abandoned, underground coal mines and potential for subsidence over karst.

LANDSLIDES

Ground Failure Hazards Reduction Program

An interdivisional workshop to review and plan USGS research on ground failure hazards reduction was convened in Denver, Colo., on January 28–29, 1981. The 53 scientists and administrators, representing USGS units that are concerned with landslides, subsidence, swelling clay-shales, permafrost thaw, and construction-induced rock deformation found that the scope and rate of progress of present research is not commensurate with the scale of the nationwide problem (approximately $4 billion/yr in U.S. property losses, and an average of 25 U.S. deaths/yr). They concluded that effective mitigation of these staggering losses requires an accelerated program of earth-science research focused on rapid, comprehensive, and reliable assessment of the natural distribution and frequency of the potential hazards, and on the development of more precise measurements of engineering parameters and more reliable analytical models for quantitative slope stability evaluations. The workshop recommended major USGS participation in the further development of a coordinated National Program for Ground Failure Hazards Reduction. A comprehensive report on the conclusions and recommendations of the workshop is being prepared for publication.

Landslides near Pasco, Washington

According to studies by R. L. Schuster and W. H. Hays, most of the landslide activity in the White Bluffs area has occurred in the past 10 yr. The Pliocene Ringold Formation, comprised of lacustrine and alluvial sediments, forms steep bluffs, known as the White Bluffs, for about 50 km along the east bank of the Columbia River beginning about 25 km upstream from Pasco, Wash. These bluffs are the result of erosion by the Columbia River during Pleistocene flooding. Under the prevailing semiarid climate, they are stable at slopes of more than 30°. Prehistoric landsliding occurred along several miles of the bluffs, but aerial photographs dating back to 1948 indicate little historic landslide activity until the advent of irrigation from the Columbia Basin Project on the land immediately east of the bluffs. When irrigation water seeps through the Ringold Formation to the steep-faced bluffs, failure of the bluffs begins as slumping; individual slumps commonly change to mudflows as they move downslope, mix with water, and lose their integrity. Approximately 15 km of the bluffs are currently being affected by active landsliding. The remaining bluff area is susceptible to sliding, and much of this area will slide if irrigation is expanded.

Economic loss from landsliding in the White Bluffs area has not been large because there is little development along the east side of this part of the Columbia River. However, the potential effects of landsliding should be considered carefully in planning any future development in this area.

Landslides mapped in Seattle, Washington

During the course of detailed geologic mapping of deposits of the continental glacier in the Puget Lowland, numerous previously unreported landslides and slump

blocks were identified and mapped by J. P. Minard. The landslides range in size up to hundreds of meters across, and up to 1.6 km long, with vertical displacement as much as 30 m. Many of these features occur in areas where residential and commerical buildings have been completed on or adjacent to them; others occur in areas of intended development. Factors favorable to widespread sliding and slumping are the thick unconsolidated glacial sediments, and the deep valleys and steep slopes, which were eroded into the sediments by meltwater flowing from the receding glacier and ice-diverted rivers. Landslides were, and are, triggered by ground-waters sapping and by streams and waves undercutting the toes of the steep slopes.

UNESCO review of landslide zonation technology

A review of the principles and practice of landslide hazard zonation, with examples from the work in many countries was prepared by D. J. Varnes. This review was undertaken at the request of UNESCO by the Commission on Landslides and Other Mass Movements on Slopes of the International Association of Engineering Geology. It will be published by UNESCO in 1981 in English, French, and Spanish with the intent of providing wide distribution, particularly in developing countries.

Distribution of landslide types in southern California

An experimental field classification of landslide deposits was developed and applied to mapping in the Point Dume quadrangle, Los Angeles and Ventura Counties, Calif., by R. H. Campbell. The mapping identifies different dominant mechanisms and triggering factors that have distinctly different areal distributions. For example, the regional distribution of landslide deposits that result from rotational slumps is significantly different from the distribution of landslide deposits that result from translational movements on bedrock surfaces. If the results from the Point Dume quadrangle are applicable to a broader area, they could affect recommendations for zoning regulations, grading codes, defensive works, and hazard warnings.

Seasonal movements of landslides near Cincinnati, Ohio

Landslide problems in the vicinity of Cincinnati, Ohio, are among the most serious in the United States. A 1980 survey, by F. A. Taylor, of the cost of landslide damages in Hamilton County, including Cincinnati, covering the period 1943–78, identified annual per capita damages of $5.80/person/yr. One of the most common types of landsliding in the Cincinnati area involves sliding of colluvium on bedrock. Observations of the failures by R. W. Fleming revealed that most problems occur during the period of March to May and the failure surface follows the contact between the colluvium and bedrock. The landslides were studied by mapping on the surface and in trenches, and instruments with time recorders were installed to measure subsurface water levels, landslide movement, and precipitation.

Two ground-water regimes are important to landsliding in this area. The bedrock, consisting of about 80 percent shale and 20 percent limestone, contains water in the limestone units. The water levels in the limestone appear unaffected by precipitation from individual storms but vary seasonally by about 2 m. During September, at the end of the growing season, the water levels are coincident with the limestone layers. By late April, the water levels are 2 m above the limestone layers and exerting uplift pressures on the colluvium. A second water regime exists in the zone of contact of colluvium and bedrock. During most of the year, this zone does not contain measurable free water, but during the spring, water levels were measured that could be closely related to precipitation events. The highest water levels, which were nearly coincident with the ground surface, appear to trigger sliding of the colluvium.

Richard Durrell, University of Cincinnati, is preparing maps of the surficial geology of the Glendale and Cincinnati East quadrangles. These quadrangles contain large areas with severe landslide problems that are associated with glacial lake clays. Mapping is delineating areas containing lake clays as well as other surficial deposits. The distribution of the lake clays will influence the site selection for more detailed studies of the landslides.

Landslide studies in the Appalachian Plateaus

S. F. Obermeier, W. E. Davies, and associates made observations from trenches that were cut in selected landslides in West Virginia and Pennsylvania, which showed that the most widely distributed kinds are shallow, seldom extending more than 5 m in depth. In thinly bedded, flat-lying sequences of shale, sandstone, coal, and underclay, slides commonly start as wedges in earth and highly weathered rock. The zone at the base of these slides along which movement occurs is characterized by a layer of blue-gray clay up to 10 cm thick. This layer acts as an impermeable barrier, and the soil in the landslide above it is wet. The zone of movement is planar, and few circular failure surfaces have been observed. In colluvium derived from weathering of beds of shale, the landslides apparently move as slabs of clayey soil.

Triggering of the landslide results from lowering of shear resistance by progressive buildup of water in material above the zone of failure. Rapidity of movement appears to be related to the amount of water in the zone of failure at the base of the slide.

As the inventory of Appalachian Plateau landslides nears completion, indications are that unstable slopes in that region are among the most extensive in the United States. About 2 million slide areas have been identified, ranging from dimensions as small as 15 m on a side to one continuous area in northern West Virginia 40 km in length, along which there are multiple slides grading one into another. The incidence of landslides is about 3/km^2 throughout the plateau.

REACTOR HAZARDS

The USGS's program of research in geologic processes and tectonic features that are potential hazards to the siting of nuclear reactors supports about 40 research projects. The results from many of these are reported under other appropriate topical and areal headings elsewhere in this volume.

Inner Coastal Plain tectonics–Middle Atlantic States

Recent surface mapping and drilling near the Fall Line in Spotsylvania and Caroline Counties, Va., by R. B. Mixon have defined a previously unrecognized post-Cretaceous fault that displaces the crystalline Piedmont rocks and the overlying Coastal Plain strata of Early Cretaceous to late Tertiary age. The structure, here named the Arcadia fault, has been mapped from the inner margin of the Coastal Plain near Cedon, Va., north-northeastward about 10 km through parts of the Ladysmith, Spotsylvania, and Guinea 7½-min quadrangles. The strike of the fault varies from about N 15°E to 20°E. The crystalline rocks and Coastal Plain beds are upthrown, relatively, on the northwest side of the structure, suggesting a high-angle reverse fault similar to the main faults of the Stafford system to the north. Because of post-Cretaceous erosion, measurable vertical displacement of the basement-rock surface along the fault in the Arcadia area is only about 17 m; however, actual displacement is probably much greater. Further studies of displacement and time of fault movement will be made in the Po River drainage basin, where the sedimentary section is more complete and Potomac Formation beds are present on both sides of the structure. The discovery of the Arcadia fault raises interesting questions as to the extent and width of the Stafford fault zone and its relation to the Brandywine structural trend of Maryland and the Dutch Gap fault of the Hopewell, Va., area.

Tectonic studies, San Joaquin Valley–Sierran foothills, California

Preliminary study of Quaternary deposits in the west-central San Joaquin Valley and adjacent foothills of the Diablo Range indicates that at least six alluvial units postdate the Pliocene and Pleistocene Tulare Formation. The oldest unit is in part extensive foothill pediment that truncates Tulare sediments containing its Corcoran Clay Member and thus is younger than 600,000 yr. Preliminary thermoluminescence dating of pedogenic carbonate formed on the pediment suggests an age of approximately 200,000 to 300,000 yr B.P. The surface thus provides a broad datum from which the patterns, amounts, and rates of foothill deformation can be established. Surface reconstruction of the pediment shows late Quaternary northwest-trending faults and broad northeast-trending warps that coincide with major Diablo Range drainages. The pediment passes valleyward into alluvial terrace and fan deposits. The five postpediment units commonly are represented by strath terraces within the major stream valleys that merge downstream into nested depositional terraces and coalescing alluvial fans. The youngest of these terraces, which are not recognized in interfluve areas of the foothills, contains shell material 2,415 ± 190 ^{14}C yr old.

The stratigraphic sequence is recognized in the major drainages of the Diablo Range from Corral Hollow to Little Panoche Creek (1,500 km^2), suggesting regional climatic rather than local tectonic control. Buried soil profiles frequently separate units in the subsurface, suggesting alluviation in brief pulses separated by long intervals of surface stability, weathering, and soil formation. Radiocarbon, thermoluminescence, paleomagnetic, and tephrochronologic dating methods provide age control for the units and suggest correlation with the eastern San Joaquin Valley stratigraphy and with climatic changes evident in the marine isotope record.

Tectonic analysis, Washington

A recently completed study by K. F. Fox, Jr., and D. C. Engebretson may help understand the nature of the seismotectonic provinces of Washington. In western Washington, small- to medium-size earthquakes frequently occur within a north-trending linear belt coincident with the Puget Lowlands; in eastern Washington, earthquakes are much more rare. The difference in frequency of earthquakes within these regions parallels a corresponding difference in structural style; hence, the two regions probably constitute different seismotectonic provinces. The boundary between these provinces is a diffuse zone that seems to follow the axis of the Cascade Range in northern Washington.

Fox and Engebretson found that the stress patterns generated in photoelastic models of that part of the North American plate in contact with the adjacent Juan de Fuca and Pacific plates are very similar to the stress patterns in corresponding regions of Washington, Oregon, and northern California. That pattern, as deduced from the orientation of Miocene through

Pleistocene fold axes, basin and range structures, and volcanic alinements, is dominated by a set of principal compressive stress trajectories radiating horizontally outward to the north, east, and southeast from the contact of the North American plate with the Juan de Fuca plate. A second set, located farther to the east, sweeps out of the northeast and curves to a southward trend at the southern limit of the study area.

Judging from the photoelastic modeling, the observed stress pattern reflects a compressive force transmitted across the contact between the Juan de Fuca plate and the North American plate. Furthermore, this force must be applied in a direction at least roughly comparable to the direction of relative motion between these two plates, rather than that of the relative motion between the Pacific and North American plates. Application of this force results in the formation of an area of high shear stress, which is tentatively identified with the Puget Lowlands seismotectonic province. As the intensity of the shear stress and the principal horizontal stresses diminish going east and south out of the area of stress concentration, a zone apparently is reached where the minimum horizontal principal stress roughly equals that part of the lateral stress due solely to lithostatic load, causing a change in orientation of the stress ellipsoid and, hence, a change in structural style. This zone probably defines the boundary between the Puget Lowlands and the eastern Washington seismotectonic provinces.

Quaternary dating techniques

Studies by S. M. Colman of weathering rinds on volcanic clasts in Quaternary deposits in the Western United States are being conducted to improve age estimates derived from soils and weathering data, which are commonly used for assessment of hazards to nuclear reactors. These studies reveal that weathering rinds contain only very fine grained, poorly developed crystalline clay minerals. The clay-size fraction of the rinds is dominated by allophane and iron-oxide hydroxides. Clasts were sampled from soils in deposits about 100,000 yr old or more; these soils contain well-developed argillic B horizons. The clay-size fraction within the soil-matrix of the horizons clearly contains abundant, well-crystallized clay minerals. The contrast between the clay mineralogy of the weathering rinds and that of the associated soil matrices suggests a need to reassess assumptions concerning rates of clay mineral formation and source of clay minerals in argillic B horizons. This study shows that clay minerals form more slowly in weathering rinds than in the adjacent soil matrix. Dust-accumulation data suggest that aerosolic dust provides sufficient clay to explain the formation of many observed argillic B horizons, and may thus be a plausible alternative to weathering as a source of clay minerals in many soils.

Synthetic strong-motion seismograms

W. B. Joyner, D. M. Boore, and R. L. Porcella took advantage of the recent increase in strong-motion data at close distances to derive new attenuation relations for peak horizontal acceleration and velocity. Acceleration data from 183 recordings of 24 earthquakes and velocity data from 62 recordings of 10 earthquakes have been used. This new analysis uses a magnitude-independent shape for the attenuation curve based on geometrical spreading and anelastic attenuation. Although not required by the existing data, a magnitude-dependent shape can be accommodated by the method. In a process similar to Richter's original derivation of the local magnitude scale, the shape of the attenuation relation is determined by, in effect, translating the data from each event up or down until a best overall fit to a trial function is found. The trial function resulting in the least overall error gives the final shape of the attenuation curve, and the regression of the amount of relative translation for each earthquake against moment magnitude (Mw) gives the magnitude dependence. Comparison of prediction equations derived from data in the M = 5.0–7.7 range with those derived from data in M = 6.5–7.7 range shows small differences relative to the prediction uncertainty, especially for velocity, indicating that the data do not support a magnitude-dependent shape for the attenuation curve. The equations for the whole data set are

$$\log A = -1.52 + 0.316Mw - \log r - 0.00255r + 0.35P$$
$$r = SQRT(d*d + 7.3*7.3) \qquad 5.0 <= Mw <= 7.7$$
$$\log V = -1.30 + 0.581Mw - \log r - 0.00256r + 0.17S + 0.35P$$
$$r = SQRT(d*d + 4.0*4.0) \qquad 5.0 <= Mw <= 7.4$$

where A is peak horizontal acceleration in m/sec^2, V is peak horizontal velocity in cm/sec, d is the closest distance to the surface projection of the fault rupture in km, S takes on the value of zero at rock sites and one at soil sites, and P has the value zero for 50 percent exceedance probability and one for 84 percent.

NRC site seismicity

New information and data related to previously evaluated reactor sites were reviewed critically as part of a continuing effort to insure that earlier conclusions are consistent with such new material. Testimony related to licensing procedures was completed for the Diablo Canyon site (San Luis Obispo County, Calif.). The impact of the Charleston, S.C., earthquake upon the Summer site (Fairfield County, S.C.) was reviewed. A

report summarizing the conclusions reached during the review of the San Onofre site (San Diego County., Calif.) was completed, while preliminary questions related to the review of the Carroll County site (Carroll County, Ill.) were transmitted to the Nuclear Regulatory Commission for relaying to the power company applicant. A report detailing the results of an experiment investigating high-explosive blast effects upon the Limerick site (Montgomery County, Pa.) was completed.

HYDROLOGIC ASPECTS OF ENERGY

Effects of energy-production emissions on Colorado Lake

Samples from 15 lakes in the Flat Tops Wilderness area of northwestern Colorado, an area of coal and oil shale development, indicated an order-of-magnitude range in sensitivity to acidification, according to J. T. Turk. Buffering capacity, as indicated by field titration, ranged from no detectable bicarbonate to alkalinities sufficient to withstand moderate additions of acid to the watersheds. Lakes with the least buffering capacity were located on the flat-lying basalt caprock, and they probably receive most of their water as overland flow. Lakes with the greatest buffering capacity were located in the stream valleys that are incised in the basalt and are mantled with glacial debris and scree; these lakes probably receive a significant fraction of their water as ground-water seepage. Should precipitation in the area become as acidic as that of the northeastern United States, the least-buffered lakes would probably have pH values unsuitable for fisheries.

Samples of wetfall and of snowpack in northwestern Colorado yielded pH values from 5.0 to 6.9. It was not known whether the range is attributable to increased acid loading in the area of smallest pH or increased alkaline-dust loading in the area of largest pH.

Ground-water-flow effects from strip mining in Illinois

According to D. L. Galloway, preliminary results of a hydrologic investigation of a strip mine on the southwestern rim of the Eastern Interior coal basin indicated that the mine affects local and regional ground-water flow. Locally, in the vicinity of the advancing strip pit, potentiometric surfaces in aquifers above the coal underclay have lowered due to dewatering, and some nearby wells have gone dry. On a regional scale, lithologic units above the coal, which have been excavated and replaced as spoil in the mine, are in direct hydraulic connection with bedrock aquifers and saturated alluvial-sand deposits. The disruption of the hydrologic-flow system by the mine may affect the quantity and quality of ground water available to the users of this resource.

Water quality in the coal areas of Illinois

Dissolved solids and sulfate concentrations were two principal measurements used to indicate surface mine drainage in southern and western Illinois, according to E. E. Zuehls and G. L. Ryan. Specific conductance, which is commonly used to estimate the concentration of dissolved solids and sulfate, must be used with consideration of location relative to the mined areas and to geology. Multiplication factors for estimating dissolved solids from measurements of specific conductance ranged from 0.70 to 0.90 and were higher in southern Illinois at sites downstream from mining operations. The higher coefficients are apparently related to the proportionately higher concentrations of sulfate in water contributed from the mined areas.

Sludge-storage basins recharge ground water in Illinois

Ground-water levels synthesized for the period prior to the construction of four sludge-storage basins in strip-mine spoil in Fulton County, Ill., suggest that one basin extended 1.5 to 4.6 m below the water table. According to G. L. Patterson, a water-table contour map, prepared using data collected in June 1979, indicated that the water table near the basins has risen about 3.0 m since their construction, bringing the present water table to 6.1 to 7.6 m above the bottom of the basin. A two-dimensional ground-water flow model indicated that the water-table rise was due to leakage from the basin. The best fit between computed and observed data was obtained by using a value of hydraulic conductivity of 0.2 m/d, an areal recharge rate of 1.1×10^{-4} m/d, and a leakage rate of 1.5×10^{-3} m/d from the basin. Assuming the system is under steady-state conditions, the volume of water leaking from the basin is about 70,000 m^3/yr. The maximum flow velocities based on gradients calculated from the best-fit model were estimated to be from 6.4 to 7.0 m/yr.

Surface-mine hydrology, Illinois

Flow-duration curves of streams draining surface-mined basins had lower variability indexes than flow-duration curves of streams draining unmined basins, according to T. P. Brabets. By relating the percentage of basin surface mined to the percent reduction in variability index, existing techniques can be used to develop synthetic flow-duration curves for streams draining surface-mined basins.

Water-quality assessment of a reclaimed surface coal mine in Indiana

Active mining operations have temporarily altered local, shallow ground-water flow patterns, have created a cone of depression, and have caused water-elevation

fluctuations in a reclaimed surface-coal mine, according to S. E. Eikenberry and L. L. Bobo. Concentrations of dissolved solids, sulfate, and iron in ground water were highest in the middle of the reclaimed mine and were significantly higher in deep rather than in shallow cast overburden.

Water quality was variable in streams that intermittently received water pumped from active coal excavation pits. A settling pond, installed in upstream North Branch Honey Creek to receive water from the West Field excavation pit, significantly reduced concentrations of most dissolved constituents and reduced the variability of water quality in the stream.

During the 1978 coal miners' strike, pumping of water from the Southwest Field excavation pit into Stone Quarry Branch ceased. During this interim, concentrations of constituents returned to background levels and water type in the stream shifted from calcium and magnesium sulfate to calcium bicarbonate type.

Calcium and magnesium sulfate water types, high dissolved-sodium concentrations, and near neutral pH (6.0 to 8.9) were found in ground and surface waters affected by past and active surface-mining operations. Concentrations of aluminum, iron, manganese, boron, nickel, and zinc were significantly higher in both ground and surface water affected by surface coal mining.

Effects of surface coal mining on water quality in Indiana

The effects of surface coal mining on water quality of streams draining a mined area in Indiana are largely dependent upon geology, according to J. G. Peters. In southwestern Indiana, the calcareous clays and shales in the overburden tend to neutralize the acid formed by the mining process. In the study area, median concentrations of sulfate increased from 77 mg/L upstream from mining activity to 1,100 mg/L downstream owing to the oxidation of pyritic material in the overburden. However, a decrease in pH normally associated with oxidation of pyrite was not encountered. The mediam pH value downstream from mining was higher than that upstream (7.9 compared to 7.0), principally because of high buffering capacity in the calcareous overburden.

Metals transport in the coal-mining region of southwestern Indiana

C. G. Crawford reported that a continuous-flow-through supercentrifuge has been used successfully to distinguish between dissolved, colloidal, and particulate phases of metals transported in streams located in the coal-mining region of southwestern Indiana. The technique was used to compare the metal-phase distribution in streams draining forested, agricultural, and both reclaimed and unreclaimed surface-mined watersheds.

Most of the metals were transported in the dissolved phase regardless of land use. Metals associated with the suspended particulate and colloidal fractions usually amounted to only a small percentage of the total concentration in the stream. Concentrations of metals were generally highest in streams draining unreclaimed surface-mined watersheds. Concentrations of metals in streams draining reclaimed surface-mined watersheds were generally higher than those draining forested or agricultural watersheds, although substantially less than found in streams draining unreclaimed surface-mined watersheds.

Metals concentrations on the particles were found to be higher in the least disturbed watersheds. The highest concentrations were found on particles in streams draining forested watersheds and the lowest on particles in streams draining unreclaimed surface-mined watersheds.

Effects of coal fly-ash disposal on water quality at the Indiana Dunes National Lakeshore

M. A. Hardy reported that significant enrichment of dissolved Ca, F, K, SO_4, Al, As, B, Fe, Mn, Mo, Ni, Sr, and Zn was observed in surface and ground water downgradient from fly-ash settling ponds in and around the Indiana Dunes National Lakeshore (IDNL). Although the greatest enrichment of Ca, As, F, Mo, K, SO_4, and Sr in downgradient ground water occurred where settling pond seepage passed through an organic layer in the soil, the greatest enrichment of Al, Cu, Co, Pb, Ni, and Zn occurred where this organic layer was absent. Settling-pond seepage also seemed to be responsible for increased gross alpha and beta radioactivity in downgradient surface water.

Leachate from a landfill composed of leached ash removed from the settling ponds caused significant enrichment of boron, molybdenum, and potassium in the surface water of nearby IDNL wetlands.

Potential impact of lignite mining, De Soto Parish, Louisiana

The USGS is investigating the Dolet Hills aquifer, which immediately overlies the Chemard lake lignite lentil of the Naborton Formation (both of the Wilcox Group of Paleocene and Eocene age), in southeastern De Soto Parish and small parts of adjoining parishes. Planned surface mining of the lignite will involve dewatering and removing the aquifer at the sites to be mined. Data collected during the investigations have established premining conditions for measuring hydrologic changes that may be caused by mining of the lignite. According to J. L. Snider, geologic data indicated that the Dolet Hills aquifer is offset by several previously unmapped faults. The fault with the largest displacement trends

N. 39° E. in the southeastern corner of De Soto Parish and southeast of the area to be mined. The base of the Wilcox Group is downthrown 30 to 40 m on the southeast side of the fault, and geologic data indicated that the fault may serve as a boundary to the flow system of the Dolet Hills aquifer. Thus, if mining causes extensive water-level declines in the Dolet Hills aquifer, the effects may be largely limited to the northwest side of the fault.

Potential hydrologic effects of peat mining in the Glacial Lake Agassiz Peatlands, north-central Minnesota

Numerical models of ground-water flow along a north-south hydrogeologic section across the Glacial Lake Agassiz Peatlands of north-central Minnesota have been constructed using data from piezometers and test holes. D. I. Siegel reported that the major recharge zone for regional-flow systems in the peatlands is probably the Itasca Moraine and that upward head gradients occur in the peatlands. Preliminary results of the models suggested that (1) local flow systems, from 5 to 15 km in diameter, probably develop because of ground-water mounds under large bogs, (2) local flow systems discharge to mineraltrophic fens adjacent to the bogs, and (3) local flow systems are most sensitive to the height of the water-table mound. The models indicated that vertical head gradients may exist at depths of 40 m below the peat as a result of ground-water mounds only 0.5 m high, which suggest that ground-water flow in the Glacial Lake Agassiz Peatlands is probably a dynamic system that continuously evolves with seasonal and long-term changes in the water table and variations in the growth rate of *Sphagnum* on the raised bogs.

Hydrologic effects of surface mining in eastern Ohio

Flow- and water-quality characteristics of aquifers in three small (less than 20 hm^2) watersheds in eastern Ohio were studied by A. C. Razem to document the impact of surface mining.

The rate of postmining resaturation of spoils was unexpectedly slow and unsteady, indicating complex flow systems. Six of nine observation wells installed in the spoils after reclamation were initially dry. Water levels in the aquifer below the top underclay showed few effects of mining, except in two wells where water level rises of 1.5 m and 6.1 m have been observed. In one watershed, initial postmining water levels indicated that the top aquifer on the unmined side of the highwall has a saturated zone, while the spoils on the mined side of the highwall are unsaturated.

Comparison of premining and postmining water quality analyses from the spoils indicated that the water composition changed from a calcium bicarbonate to a magnesium sulfate type, with an increase in sulfate of up to 100 times. Dissolved iron and manganese also increased in water from the spoils. Dissolved sulfate, iron, and manganese were also higher after mining in the water from the aquifer below the top underclay.

Hydrology of coal-lease areas in eastern Oklahoma

As part of the Energy Minerals Rehabilitation Inventory and Analysis (EMRIA) Program in cooperation with the U.S. Bureau of Land Management, hydrologic data have been collected in the basins of Blue Creek (31.3 km^2), Taloka Creek (52.1 km^2), Brazil Creek (179.0 km^2), and James Fork (380.7 km^2) in the eastern Oklahoma coal field by M. V. Marcher, T. L. Huntzinger, J. D. Stoner, and S. P. Blumer. Coal has not been mined in Blue Creek basin for many years; Brazil Creek and Taloka Creek basins include active mines; James Fork basin includes both old and recent mines.

Bedrock in all four basins consists mainly of shale and siltstone with some sandstone. These rocks have low porosity and permeability and, therefore, have low yields and a limited capacity to accept or store large amounts of water. Alluvium along the streams is 4.6 m or less thick, consists of silt and clay, and does not contribute significantly to baseflow of streams.

Streamflow of Blue, Taloka, and Brazil Creeks consisted mostly of storm runoff lasting a few hours or days after precipitation. All three streams were dry about 30 percent of the time during the period of record. James Fork had no flow at times in late summer and early fall.

The chemical quality of ground water in all four basins was extremely variable, with dissolved-solids concentrations ranging from 63 to 2,100 mg/L. Water types were generally mixed but had a tendency toward sodium-calcium bicarbonate. The variability of ground-water quality did not have any apparent relation to geology, well depth, or geographic distribution.

The mean sediment loads were Blue Creek, 0.08; Taloka Creek, 1.55; Brazil Creek, 0.27; and James Fork, 0.14 $(Mg/km^2)/d$.

Of the toxic metals, total mercury exceeded 2 $\mu g/L$ in one sample from Blue Creek, and total lead exceeded 100 $\mu g/L$ in one sample from James Fork. Concentrations of dissolved and (or) suspended cadmium, lead, and mercury exceeded the maximum limits recommended for public water supply by the EPA in from one to four samples from both Taloka and Brazil Creeks.

Areas where mining has stopped have largely been reclaimed. However, the lack of rainfall since reclamation has precluded determining any residual effects on water quality.

Water quality of eastern Oklahoma coal mines

Water at 57 sites in 39 coal-mine ponds in eastern Oklahoma was sampled at least twice during June to November 1977–79 by L. J. Slack to determine specific conductance, pH, temperature, dissolved oxygen, sulfate, chloride, iron, and manganese. These determinations show that during June to November water in the ponds is stratified; temperature and dissolved oxygen usually decrease with depth, whereas specific conductance usually increases with depth. Specific conductance, which is a general measure of dissolved solids in the water, ranged from 93 to 7,070 μmhos/cm. The chemical and physical-chemical characteristics of the pond water are related to the coal bed in which the pond is located. Mean concentrations of dissolved iron, manganese, and chloride are greatest in the ponds associated with the mining of the Hartshorne coal. Dissolved sulfate is greatest in the water in ponds in the McAlester (Lehigh)-Stigler coal bed.

Hydrology of orphan coal lands, Haskell County, Oklahoma

Based on samples analyzed monthly for major constituents and quarterly for dissolved metals, the quality of the ground water obtained from two wells penetrating the local shallow alluvium and from four test holes drilled in abandoned spoil piles from strip mining in eastern Oklahoma is similar and relatively constant. The water is predominantly a sodium sulfate type and has a pH of 7.0 to 8.0 and a specific conductance of 2,000 to 3,500 μmhos/cm, according to L. J. Slack. The water from both the spoil piles and the native shallow aquifer is occasionally high in dissolved iron and manganese, exceeding the recommended secondary or aesthetic limits of 300 and 50 μg/L, respectively.

Water from two strip-mine ponds in the area is also a sodium sulfate type, has a pH of 7.9 to 8.4, and a specific conductance of 1,500 to 2,700 μmhos/cm.

Water collected at five sites on Mule Creek, which drains a partially reclaimed area, is also predominantly a sodium sulfate type but generally has a specific conductance of less than 1,000 μmhos/cm, primarily due to dilution effects.

Hydrology of the Cook Creek area, Ashland coal field, southeastern Montana

An investigation of the hydrology of the Cook Creek area near Ashland, Mont., was performed by M. R. Cannon for the purpose of defining existing hydrologic systems and assessing potential impacts of strip mining on the local water resources. Shallow aquifers of local importance include the Knobloch coal bed of the Tongue River Member of the Fort Union Formation, clinker formed by the burning of Knobloch coal along its outcrop, and alluvial deposits along stream channels. The aquifers are utilized primarily for the watering of livestock; several springs which discharge from alluvium and clinker have been diverted to stock tanks and several wells tap the Knobloch coal. Deeper aquifers occur within the Tullock Member of the Fort Union Formation and within the combined lower part of the Hell Creek Formation and the upper part of the Fox Hills Sandstone.

Mining of the Knobloch coal bed will remove several stock wells and springs. Some wells near the mine area may become dry or experience a reduction in yield during mining because of dewatering effects. Recharge to an alluvial aquifer in the downstream part of Cook Creek will be reduced during mining. Water in alluvial and clinker aquifers downgradient from the mine may show a long-term decrease in quality caused by the leaching of soluble salts from mine spoils. Supplies of stock water lost as a result of mining could be replaced by using the deeper aquifers that would not be affected by mining.

Hydrologic modeling of Coal Creek basin near Lehigh, Oklahoma

The USGS, in cooperation with the Bureau of Land Management, is conducting a study whose primary objectives are to collect and interpret hydrologic data to predict and assess the effects of surface mining for coal and subsequent reclamation efforts on hydrologic characteristics. The approach used includes the development, calibration, and verification of a watershed model in the Coal Creek basin in southeastern Oklahoma.

Since mining has not yet commenced, 1980 water-year activities were confined to collection and interpretation of baseline hydrologic data. These data include soil moisture, streamflow, water quality, ground-water levels, and meterological data.

Analyses of data by S. P. Blumer, showed good correlation of suspended iron, aluminum, and manganese with suspended sediment. Additional interpretation of sediment data indicated that suspended sediment load from just one runoff event per yr may completely dominate the total suspended-sediment load measures for the entire year. Rainfall-runoff models are being developed and calibrated with pre-mining data.

Modeled impacts of surface coal mining on dissolved solids in the Tongue River, southeastern Montana

A computer model was developed by P. F. Woods to simulate streamflow and dissolved solids in the Tongue River of southeastern Montana. Expected changes in dissolved-solids concentration due to increased irrigation and leaching of overburden from proposed surface

coal mines have been simulated with the model. Under a scenario of full mining development and mean streamflow, model results indicated that surface coal mining would increase the annual dissolved-solids concentration in the downstream reach by 4.8 percent over that expected with no mining. On a unit-area basis, irrigation withdrawal and return flow would increase dissolved-solids concentration more than leaching of overburden from surface coal mines.

Water resources in coal areas of Greene County, Pennsylvania

Well and spring inventory and test drilling have indicated that principal permeability of the bedrock aquifers in Greene County, Pa., are controlled by bedding plane and joint fractures, according to J. D. Stoner. The decrease of permeability with depth is tentatively attributed to the compression of fracture openings. Sustained specific capacities were typically less than 0.0001 (L/s)/m at depths greater than 70 m below land surface and averaged .006 (L/s)/m above that depth zone.

The low permeability of the bedrock aquifers at depth suggested that underground coal mining probably had little effect on the quantity of water resources within the area. However, a strong correlation was observed between water level decline in a well and active retreat-type mining (mine roof allowed to collapse) located 61 m away. Local dewatering might be expected where the effective aquifer permeability is increased by mining.

Abandoned deep-mine and surface-mine drainage have caused considerable surface water degradation in the eastern half of Greene County. Water-quality data collected below abandoned mine drainages during low-flow conditions showed pH values between 2.0 and 5.0, and high concentrations of sulfate, iron and manganese, all of which exceeded the safe drinking water recommended limits established by the EPA. The poor stream quality is attributed to unfavorable mine-reclamation practices of the past. Preliminary appraisals of water-quality data collected beneath an active surface mine and a deep mine in eastern Greene County indicated a much lower level of stream pollution.

Geochemical and water-quality modeling of coal areas in Virginia

Results of geochemical and water-quality modeling in the coal-mining area of southwestern Buchanan County by P. W. Hufschmidt and J. D. Powell indicated that drainage may be neutralized by alkaline material leached from dolomitic cement of prominent sandstone. Stream water in the upper Russell Fork basin is highly mineralized but is not acidic, with pH ranging from 6.1 to 9.1.

Water monitoring of coal-mining areas in Virginia

P. W. Hufschmidt and B. J. Prugh, Jr., reported results of water-quality streamflow monitoring in the coal-mining areas of southwestern Virginia that indicate mines and reclaimed basins sustain higher flows during low-flow periods than unmined basins. Highly mineralized and acidic water in headwater streams is diluted and neutralized by water draining from unmined basins. Nine synoptic sampling trips have been accomplished to date.

The dense network of 115 monitoring stations has been reduced to 45 stations representing differing land uses. Sampling resolution is thus enhanced to enable detection of specific sources of stream pollution.

Midnite Uranium Mine water-quality study, Washington

A reconnaissance of water-quality conditions downstream of Midnite Mine near Wellpinit, Wash., indicated that most of the discharges of water and chemicals occur by way of the surface-water system. The highest chemical concentrations, however, were observed in the ground water near a retaining dam at the downstream edge of the mine, according to S. S. Sumioka and N. P. Dion.

The net effect of the mine drainage on the chemical characteristics of the receiving stream, Blue Creek, was to raise the concentrations of almost all constituents above background levels to the point that drinking-water regulations were violated for manganese and sulfate. The quality of the mine drainage itself was within the limits set for uranium-mine effluents for the constituents tested.

Hydrologic effects of underground mining and mine collapse in northern West Virginia

W. A. Hobba, Jr., (1981) investigated the effects of underground mining and mine collapse on areal hydrology at one site where a mined bed of coal lies above major steams, and at two sites where the bed of coal lies below major streams. Subsidence cracks at land surface were generally parallel to predominant joint sets in the rocks. The mining and subsidence cracks increased hydraulic conductivity and interconnection of water-bearing rock units, which, in turn, caused increased infiltration of precipitation and surface water, decreased evapotranspiration, and higher base flows in some small streams. Water levels in observation wells in mined areas fluctuated as much as 30.5 m annually. Both gaining and losing streams were found in mined areas. Mine pumpage and drainage caused diversion of water underground from one basin to another. Areal and single-well aquifer tests indicated that near-surface rocks had higher transmissivity in a mine-subsided basin

than in unmined basins. Increased infiltration and circulation through shallow subsurface rocks increased dissolved mineral loads in streams as did treated and untreated contributions from mine pumpage and drainage. Subsidence cracks were not detectable by thermal imagery, but springs and seeps were detectable.

Abandoned coal mines as a source of water for public supply in Upshur County, West Virginia

Buckhannon is a growing city in Upshur County in central West Virginia that now uses the Buckhannon River as a source of public water supply. Current (1978) water use of 69 L/s exceeded the flow of the river measured during a drought period in 1930 by as much as 64 L/s. The purpose of the study was to determine if a source of mine water of adequate quantity and quality is available near Buchhannon for use by the city as a water supply in time of drought. Three flooded underground coal mines were located about 9.5 km south of Buckhannon at Adrian. They stored 1.44×10^6 m^3 of water. This stored water, plus an additional 31 L/s infiltration, is enough water to supply the current needs of the city (95 L/s) for 265 days, and projected needs of the city (158 L/s) for the yr 2018 for 135 days. Water from the flooded mines was moderately hard, slightly acidic, and generally contained excessive amounts of iron, manganese, and hydrogen sulfide. Dissolved solids were reported to increase 5-fold when pumped at a high rate for long periods of time. Thus, it may be too expensive to treat the water for public supply.

Water monitoring in coal-mining areas in West Virginia

T. A. Ehlke (1981) reported that water quality in the Kanawha River basin is generally good but is affected by increased concentrations of sulfate, iron, and manganese near coal-mining activities.

Hydrology is affected by topographic features as well as by the 469 underground and 255 surface coal mines presently operating within the Kanawha River basin. The steep land slopes and relatively low permeability of surface rocks increase surface runoff and the likelihood of flooding. Well yields are generally poor due to the low primary permeability of the rocks.

Water quality is affected by climate, surface geology, and the level of mining activity. Specific conductance of surface water ranged from less than 10 μmhos/cm to over 1,000 μmhos/cm. The concentration of sulfate ranged from less than 4 mg/L to over 800 mg/L. The highest sulfate concentrations were found in areas surrounded by long-established or abandoned mining operations. Manganese concentrations generally exceeded recommended limits in drinking water by about 3:1 and were highest in old mining areas. Iron concentrations averaged 1.7 mg/L in surface water throughout the basin but were highly variable between individual sites. About 95 percent of the iron was transported in the suspended phase.

GEOLOGY RELATED TO NATIONAL SECURITY

Geology of nuclear test sites, Nevada Test Site

The USGS, through interagency agreements with the DOE and the DOD, investigates the geological, geophysical, and hydrological environment of each site within the Nevada Test Site (NTS) where underground nuclear explosions are conducted. Geological and hydrological data are needed to assess the safety, engineering feasibility, and environmental effects of nuclear explosions. In addition, the USGS compiles geological and hydrological information pertaining to underground nuclear explosions conducted within the U.S.S.R. The USGS does research on specialized techniques needed to acquire geophysical and hydrological data at nuclear explosion sites; some of the results of this research are summarized below.

Containment of all underground nuclear tests (no release of radioactivity into the atmosphere) is a national commitment. Containment requires an expert apprasial of the geological, geophysical, and hydrological environment for each test site. The USGS, through the Special Projects Branch, provides this expertise with W. S. Twenhofel as the geologic consultant and A. T. Fernald as the alternate consultant. E. C. Jenkins advised the Containment Evaluation Panel, DOE, on matters relating to the stratigraphy, structure, media properties, and depth to the Paleozoic rocks for proposed nuclear events.

Geological and geophysical investigations at the NTS in support of the Los Alamos National Laboratory (LANL), the Lawrence Livermore National Laboratory (LLNL), the Sandia National Laboratories (SNL), and the Defense Nuclear Agency (DNA) have continued to develop a clearer understanding of Quaternary alluvuim, Tertiary volcanic rocks, and Paleozoic carbonate and clastic rocks and their structure in the Great Basin. Interdisciplinary communication within the USGS is the key to this clearer understanding. A. T. Fernald updated the isopach map of the surficial deposits of Yucca Flat with data obtained from the continued drilling program. Material-property data for shallow alluvium in part of Yucca Flat were reviewed (Spengler, 1980). Gravity data compiled, modeled, and interpreted by D. L. Healey, continue to be revised and updated to show the configuration of the Paleozoic surface below Cenozoic rocks in Yucca Flat. He also prepared, for proposed sites in Yucca Flat, profiles of the tuff-Paleozoic interfaces, Cenozoic isopach maps,

gravity station maps, and density contrast maps. The synthesis of material-properties data for additional areas of Yucca Flat was continued (Brethauer, Muller, and Kibler, 1980). This program is designed for use in predicting material properties by extrapolation and interpolation from the data base, thus effecting substantial savings by reducing exploratory drilling, coring, and geophysical logging for new sites.

Results of a vertical seismic profiling experiment at the NTS to determine depth and dip of the Paleozoic surface show that sufficient seismic energy can be generated at the ground surface to create a Paleozoic reflection (Balch, Lee, and Muller, 1980). It is also clear that velocity filtering is an extremely valuable tool for enhancing the Paleozoic reflection. Data suggest that seismic energy trapped in the near-surface zone is probably the reason for limited success of previous attempts to map the Paleozoic with surface seismic-reflection surveys.

Property changes in tuff from nuclear explosions

Core tests and in situ shear- and compressional-wave velocity measurements were made in horizontal holes and tunnels near a chimney, which resulted from the collapse of a cavity generated by a nuclear explosion in zeolitized tuff. Measurements were made in one tunnel that passed within 3 m of the chimney boundary. The data indicate that

1. The rock exposed in the tunnel by mining shows no visual evidence of extensive explosion effects other than a tendency for the tuff to disaggregate somewhat near the chimney.
2. Effects are observed chiefly in microfractures analyzed by SEM techniques.
3. Pronounced boundaries in in situ shear-wave velocity measurements and shear-wave velocities near the chimney have been reduced as much as 50 percent of the preshot value. Compressional-wave velocities are less sensitive, exhibiting a maximum reduction of 20 percent of the preshot value. The data strongly suggest that shear failure has been the principal failure mode arising from the explosion.
4. A boundary extending from the edge of the chimney to about 2 chimney radii from the detonation point is defined by both in situ and core-shear velocities as well as microcracking observed in samples. An additional zone, characterized only by significant reductions in in situ shear velocity, extends to a range in excess of three chimney radii from the explosion, the limit of measurement allowed by the tunnel geometry. The latter zone is believed due to macrodislocations along joints and bedding planes.
5. Because of sample size differences in sampling crack frequency, the in situ shear-velocity measurement in the zone of failure immediately adjacent to the cavity is 2½ times more sensitive to velocity changes than is the core velocity.

The USGS developed geophysical logging techniques for obtaining resistivity and velocity in deep horizontal holes (Carroll and Cunningham, 1980). These holes are used as a primary exploration tool for siting nuclear events in tunnels at NTS. A comprehensive report on geology, geophysics, gravity, and in situ stress regarding the Mighty Epic event, U12n.10 tunnel NTS, was released (USGS, 1980).

U.S.S.R. underground nuclear explosions

A number of areas in the U.S.S.R., where underground nuclear explosions have taken place, were studied in cooperation with the DOD and other U.S. Government agencies. Project members compiled geologic maps, stratigraphic sections, and other relevant geologic information in the areas of the U.S.S.R. tests, based on the published scientific literature. Using this basic data, together with information provided by the U.S.S.R. at international meetings and other materials, W. J. Dempsey, Selma Bonham, and Jack Rachlin analyzed the explosion sites and their regional geologic setting. This work included computational analyses and comparison with U.S. experience. Reports by J. W. Clarke and Jack Rachlin (1980a, 1980b) describe the geologic setting of a presumed nuclear explosion in an oil field in West Siberia and the possibility of the explosion being an attempt at stimulating production from a tight reservoir. Studies of U.S.S.R. deep seismic-sounding data for information on the structure and physical properties of the crust and upper mantle in relation to the propagation of seismic waves, especially in areas of nuclear explosions and monitoring stations, are continuing.

The USGS is responsible to the DOE for selecting and training a cadre of geologists for a Geology Verification Team as set forth in the Treaty on Underground Nuclear Explosions for Peaceful Purposes (PNE).

RELATION OF RADIOACTIVE WASTE TO THE GEOLOGIC ENVIRONMENT

Geomechanical characterization methods for potential radioactive waste storage sites

In support of the testing and the evaluation studies of geomechanical instruments (borehole type), a testing facility near Idaho Springs, Colo., and an evaluation test site near Golden, Colo., were established under the

leadership of H. S. Swolfs. The test facility is used to examine instrumental reponse to known boundary loads, whereas the evaluation test site is used to assess the effectiveness of these instruments in accurately characterizing a wide range of in-place rock-mechanical properties; that is, state of stress, displacement, modulus, and temperature.

These comparative studies are still in progress, but initial indications are that modulus determinations by borehole jacking underestimate the true deformation modulus of rock by a factor of three or more for reasons that are not yet understood. Similarly, side-by-side evaluations of two different methods of stress measurement yield results that are contradictory in sign and magnitude. These difficulties are primarily due to shortcomings in instrumental design and construction and, to a lesser degree, due to over-simplified assumptions concerning the behavioral properties of rock. A major goal of this research is to resolve these ambiguities and establish a methodology centered on efficient instrumental techniques for the characterization of potential sites for high-level nuclear waste repositories.

Benefits of interim storage of high-level nuclear waste

One major technical hurdle faced by designers of mined, geologic repositories for the Nation's commercially generated high-level radioactive wastes is that the fission products will generate considerable heat. The expected thermal-chemical, thermal-mechanical, and thermal-hydrological couplings are very complex and pose a major problem in the selection of media, sites, and waste and overpack design, as well as in the ability to predict future behavior of the repository system. These problems can be reduced if the waste has a sufficiently low power output so that the skin temperature of a modular waste canister will not exceed 70° C. This would be achieved if the waste were stored for about two half lives of the principal heat producers – ^{90}Sr and ^{137}Cs, or about 60 yr. E-an Zen suggested that the concept of interim storage in dedicated sites has enough merit on these grounds to warrant its incorporation in the overall system of waste management as as necessary intermediate step – not as a substitute, by regulation or neglect, of permanent isolation, but as a prelude to it. Other expected benefits include possible future retrieval of some isotopes as resources (not negligible) and the ability to design the final repository without making design compromises for retrievability. Interim storage sites need to be safe from molestation, but because of their expected short duration (possible 100 yr for the nuclear fuel episode of energy supply) and the likelihood of human surveillance during this time interval, the interim sites are expected to need less elaborate preparation than permanent sites and may be as simple as underground tunnels. Unreprocessed spent fuels are a flexible and conceivable interim waste form that should not be ignored.

STUDIES OF MEDIA

Crystalline rocks as possible sites for nuclear waste repositories

H. W. Smedes reviewed the rationale for geologic isolation of high-level radioactive waste and assessed the suitability of crystalline rocks as a waste-disposal medium (Smedes, 1980). This work was a continuation of a project funded initially by the DOE. The rationale presented for geologic isolation included an elaboration of why certain criteria have been ascribed and the consequences that might arise if the criterion should fail to be met. A number of lines of evidence strongly suggests that at least some crystalline rocks in some areas are not fractured at repository depths; therefore, the premise that fracture hydrology will be a significant problem in all crystalline rocks may not be valid.

A set of maps by D. J. Gable and C. T. Hatton depicting magnitudes of vertical movements of the crust of the conterminous United States during the last 10 m.y. provides a quantitative basis for determining relative tectonic stability of different regions of the country.

Brine migration in salt in radioactive waste repositories

A potential problem in the use of salt deposits for radioactive waste repositories arises from the presence of small amounts of water in most natural salt as fluid inclusions and in several other forms. When a thermal gradient is imposed on a fluid inclusion, as from radioactive heating by a waste canister, the fluid inclusion will move, generally up the gradient. There have been several theoretical studies of the migration rates within single crystals, but these have not evaluated all of the factors that are believed to influence the rates. E. W. Roedder and H. E. Belkin (1979) measured the rates of migration within single crystals of salt from several potential sites at appropriate temperatures and gradients. The rates were generally in the range of 1–5 cm/yr, up the gradient (that is, toward the canister).

Such data are needed in planning the engineering design of a repository, but since most salt is polycrystalline, with a grain size in the 1–2 cm range, a much more important question is the behavior of a migrating fluid inclusion when it intersects a grain boundary. Realistic simulation in the laboratory is difficult to achieve due to the complex and changing stress patterns on grain boundaries expected in actual repository operation; but Roedder and Belkin have established that, at least under some conditions, the fluid inclusions, on intersecting a grain boundary during migration up a thermal gradient, release most of their

fluid contents along the boundary and then reverse motion and move down the gradient. The possible paths that might be taken by the fluid released to the grain boundary are not known, but migration rates are expected to be considerably higher than those through single crystals.

Water content of rock salt

The in situ content of rock salt in beds or domes and the exact nature of its occurrence are of considerable importance in the design and operation of high-level nuclear-waste disposal facilities in salt. E. W. Roedder and R. L. Bassett (University of Texas) found that most published determinations of the "water" content of salt are not comparable. More important, many analyses contain serious and in part systematic errors, which are generally because of a combination of multiple sources of water in salt samples, sampling techniques, sample preparation, and analytical methods.

The total water present in a given small sample can be determined by various existing chemical methods. Such determinations may have high precision and may yield accurate results but are subject to two major shortcomings: (1) Their validity is limited seriously by the difficulty in obtaining a truly representative sample and by changes in this sample during sample preparation; and (2) Even if the sampling and analysis are both correct, an analysis for total water by itself is not very useful. Water is present in rock salt in a variety of forms; the amount of each form must be determined as each may behave differently under the possible conditions of a nuclear-waste disposal facility. Most water in rock salt in situ is present in (1) hydrous minerals (clays, hydrated salts, etc.), (2) intergranular pore fillings, and (3) intragranular fluid inclusions. In addition, water distribution in salt is generally erratic in the extreme.

As a result of such problems, there is no panacea permitting completely unambiguous and quantitative determinations of each of the three types of water in a given sample. However, Roedder and Bassett have developed a detailed sequence of steps in sample collection, preparation, and analysis that minimizes the major sources of error.

Monitoring and analysis of water in deep salt deposits by gamma-ray spectrometry

Domed and bedded salt formations are among the potential host rock being considered for radioactive waste disposal repositories. Though salt has been assumed to be essentially dry, water does occur along cracks or grain boundaries as inclusions in crystals and in hydrous minerals; the amount must be determined if its effects are to be assessed. A borehole probe was developed to measure water content of salt deposits by F. E. Senftle, J. L. Mikesell, and A. B. Tanner. Water is a good moderator for neutrons and will quickly reduce the neutron energy to thermal energy over short distances. Chlorine readily captures thermal neutrons and subsequently emits high-energy capture gamma rays. High-energy neutrons are scattered by sodium and also yield a characterisitic gamma ray. Preliminary laboratory tests showed that the ratio of the gamma rays due to scattering by sodium to those produced by neutron capture in chlorine provides a measure of the water concentration in the salt.

STUDIES OF POTENTIAL REPOSITORY SITES

Anhydrite as a possible host for high-level nuclear waste

All of the major anhydrite deposits within the conterminous United States are contained within 25 structural basins or geographic areas. These deposits were evaluated by W. E. Dean (USGS), K. E. Johnson (University of Oklahoma), and Serge Gonzales (Earth Science Associates) in terms of stratigraphic relations, and thickness and relative abundance of anhydrite. Anhydrite beds thicker than 30 m that occurred at moderate depths (greater than 300 m and less than 1,500 m) were identified; a total of 20 anhydrite deposits contained beds that met these criteria on the basis of available descriptions. These deposits were characterized in terms of their geologic age, stratigraphy, structure, thicknesses and distributions of individual anhydrite beds, depths to individual anhydrite beds, associated lithologies, and relative purity of anhydrite and its internal fabric. On the basis of these criteria, the most promising anhydrite deposits for use in nuclear waste isolation appear to be those in the Picacho basin of Arizona and the Castile Formation in the Delaware basin of Texas and New Mexico.

Test data on the following mechanical and thermal properties were compiled from the literature by S. F. Diehl and W. Z. Savage (USGS): density, porosity, thermal conductivity, sonic velocity, Young's modulus, Poisson's ratio, and shear modulii. Based on this compilation, anhydrite appears to have several advantages over halite for proposed nuclear waste isolation. Ductile deformation occurs at higher temperatures than for halite. Its ultimate strength at low confining pressures is two to three times that of halite, and it is less ductile under these conditions. However, this brittle behavior of anhydrite at low confining pressures could result in greater fracturing in the vicinity of the repository.

An inventory was prepared by William Thordarson from existing literature on the general hydrology, porosity, hydraulic conductivity, and transmissivity of

anhydrite that was obtained from outcrops, tunnels, mines, wells, and springs. The main hydrologic characteristic of anhydrite that makes it more favorable than halite as a medium for nuclear waste isolation is that it is about two orders of magnitude less soluble than halite. However, it is still relatively soluble compared to most rocks.

Data on the thermodynamics, crystallography, phase equilibria, solubility, kinetics of reactions, sorption characteristics for radionuclides, and radiation effects on anhydrite and related phases of calcium sulfate were evaluated by R. W. Potter and M. A. Clynne from the available literature. The initial chemical properties of anhydrite that suggested its use as a potential medium for nuclear waste isolation were its low solubility (relative to halite) and the retrograde nature of the solubility, that is, solubility decreases with increasing temperature. This combination of solubility characteristics means that fluids migrate slower in anhydrite than in halite and migrate away from a heat source rather than toward a heat source as they do in halite. The suitability of anhydrite as a waste disposal medium is enhanced further by the facts that is appears to have a higher sorptive capacity than halite for radionuclides, has a thermal conductivity about as high as that of halite, and like halite occurs in geologic environments that have been relatively stable for tens to hundreds of millions of years.

Electrical and electromagnetic studies of salt in the Paradox basin, Utah

Electrical and electromagnetic studies by R. D. Watts for the DOE in the Paradox basin of Utah are aimed at (1) defining those methods that can identify inhomogeneities in the sandstone environment of the Paradox basin, and (2) applying those methods to solve structural and hydrological problems related to identifying potential sites for a nuclear waste repository. Initial results indicated the usefulness of the very low frequency (VLF) method as a reconnaissace tool for finding or tracing faults covered with windblown sand deposits. Anomalies were detected at the southeast end of the Gibson dome (about 40 km south of Moab, Utah) using the dipole-dipole resistivity method. The surface rocks are heavily jointed, and the anomalies may be due to water in the joints. An airborne electromagnetic (EM) survey at Salt Valley detected long linear anomalies that probably represent splay faults on the flanks of the anticline, but further computer processing of these data is required.

Paradox basin remote-sensing studies

J. D. Friedman supervised the production of a series of remote-sensing data products and interpretations pertaining to the Paradox basin, Utah, for the DOE. The products are useful in the exploration of the basin for localities that might be used for a high-level nuclear waste repository. A preliminary uncontrolled slant-range X-band radar image mosaic of the northern Paradox basin with an accompanying report was completed. This mosaic product is suitable for geomorphic interpretations and identification of fracture traces; but because of lack of a ground-range data presentation, true azimuthal bearings are not available for the fracture traces mapped from the mosaic.

The present uncontrolled mosaic showed many previously unreported fracture traces and is a significant contribution to understanding the fracture pattern of the region. A 22-unit colored terrain map for three contiguous 2° quadrangles (Grand Junction, Moab, and Cortez) was produced from digitized topographic data, using a color Optronics system. The map units show the distribution of terrain above the specified hypsometric levels. The visual effect is to show the topographic grain very clearly. The Uncompahgre block, the La Sals domal uplift, the cross-axial breached anticlinal valleys, and the landforms of the Grand Valley of the Colorado are well demarcated. This map is an ideal terrain base for gravity and magnetic field data and for plotting the above-mentioned lineaments in relation to landforms.

Seismicity of the southern Great Basin

During the past year a seismograph network consisting of about 50 vertical component seismographs was operated at sites within a 150-km radius of the Nevada Test Site (NTS) for the DOE as a part of its evaluation of the NTS for sites for high-level nuclear waste repositories. The data from this network have been analyzed and processed to obtain the locations and magnitudes for about 400 earthquakes. The magnitude (based on duration) of the largest event recorded to date is $M = 4.0$. Earthquake epicenters have been plotted on geographic maps in order to determine the locations of currently active faults. These data have revealed that the following fault systems are active: Cane Springs, Rock Valley, Mine Mountain, Yucca fault, Pahute faults, faults in the Pharanagat Lakes area, and faults in the Grapevine Mountains. An area located in Death Valley 5 to 10 km west of the Furnace Creek fault zone is also active. No activity has yet been noted at Yucca Mountain, the site currently under consideration as a nuclear waste repository. Four mechanisms for several earthquakes in this region also have been determined and show that faulting and strike-slip faulting occur on faults having strikes varying east. The predominant orientation of the tension axis is northwest.

Use of vertical seismic profiles in salt formations

A. H. Balch and M. W. Lee used a new geophysical technique called vertical seismic profiling (VSP) at Salt Valley, Utah, (30 km north of Moab) to assist in the detection of thin shale interbeds in a salt formation and to estimate their strike and dip. The area is one of a number being investigated by the DOE as localities for storage of high-level nuclear waste in a mined geologic respository. The salt formation contains numerous "interbeds" of shale and anhydrite, which would probably have to be partially or completely avoided in constructing a repository. The VSP data obtained show several interbed reflections, and their dips and strikes can be estimated in the neighborhood of the test holes in which the VSP's were run.

Volcanic hazards of the Snake River Plain, Idaho

In an investigation conducted for the DOE, M. A. Kuntz and G. B. Dalrymple found that the chief volcanic hazard at the Radioactive Waste Managament Complex at the Idaho National Engineering Laboratory, located between Arco and Idaho Falls in southeastern Idaho, is potential inundation of the site by pahoehoe basalt lava flows from vents within the surrounding topographic basin. Stratigraphic, radiometric, and paleomagnetic studies showed that the waste storage site has been inundated by at least 18 lava flows and flow units erupted from 7 or more separate source vents in the last 500,000 yr. The lava flows and flow units were erupted in seven groups ranging from one to as many as five flows each.

Their data showed that each eruption event lasted less than 200 yr, that the groups of eruption events were separated by long intervals during which no lava flows entered the area, and that the eruptions were episodic rather than periodic. The radiometric data suggest that the groups of flows can be assigned to three major eruption episodes that occurred about 450,000, 225,000, and 75,000 yr ago. Thus the intervals between major eruption episodes are as long as 225,000 yr and as short as 150,000 yr. The last eruption of lava flows that covered the storage site occurred about 75,000 yr ago. Approximately one in every five volcanic eruptions within the topograhic basin in about the last 200,000 yr has produced lava flows that eventually reached the Radioactive Waste Management Complex site.

Borehole geophysical studies at the Nevada Test Site

Borehole geophysical studies at the NTS have included in situ physical properties measurements and hole-to-hole and hole-to-surface electrical measurements. These studies were also part of the DOE's search for a potential nuclear waste repository site. Analysis of magnetic susceptibility, induced polarization, gamma ray, neutron, resistivity, and density well logs characterized the gross lithologic changes interpreted from drill core at Yucca Mountain, Nev. However, welded tuffs are extremely complex lithologic units involving the superposition of several geologic factors and processes that cause detailed variations in the geophysical well logs. Magnetic susceptibility and resistivity anomalies were associated with crystal-rich zones of the welded tuffs and the induced polarization anomalies correlated with clay-rich zones. Qualitative interpretation of hole-to-surface DC-resistivity measurements made separately from four drill holes confirmed the presence of complex near-surface anomalies that could be caused by fracture zones.

RADIOACTIVE WASTES IN HYDROLOGIC ENVIRONMENTS

Radioactive waste-burial sites in Illinois

Tritium from the Palos Forest waste-burial site, one of the world's first low-level radioactive waste-burial sites, about 22 km southwest of Chicago, Ill., has migrated 40 m downward through glacial drift to a dolomite aquifer according to J. C. Olimpio. A tritium plume has formed in the drift and the center of the plume is presently 15 m beneath ground level at the site. Small portions of the plume extend northward (downgradient) in the drift, coinciding with lateral tritium movement and ground water along thin sand layers. The evidence suggested that the tritium plume moves as a single slug in ground water that originated from water infiltration into the open-burial site. Several factors control both the concentration level and extent of migration of tritium in the drift: (1) the limited amount of tritiated waste buried at the site, (2) the long elapsed period of waste burial (35 yr) relative to the radioactive half-life of tritium (12.3 yr), and (3) the great thickness and low permeability of the glacial drift at the site.

At another site near the town of Sheffield, flow paths in the underlying low-permeability glacial materials may provide avenues for migration of radionuclides, according to J. B. Foster, J. R. Erickson, and R. W. Healy. A flow path is generally all or part of a lithologic unit whose permeability is much greater than any of the associated sediments. One such body is the saturated portion of a pebbly sand unit which underlies almost 70 percent of the site. A ground-water-flow model of the area demonstrated that the pebbly sand transmitted most ground water from the site. Two other less extensive bodies of relatively permeable material have been identified. One is near the southeast corner of the site; tritium has been detected in water from observation

wells at this location. The second extends off site near the east-central boundary; tritium has been detected in water from a monitor well in this area. The tritiated ground water apparently moved to the well during a period of high-water levels in the spring of 1979.

Hydrologic investigations related to a radioactive-waste repository in salt in southeastern New Mexico

The hydrologic testing of test holes at the Nuclear Waste Isolation Pilot Plant near Carlsbad, N. Mex., by J. A. Basler, necessitated the use of inflatable packers and pressure transducers. A pressure-monitoring system was assembled that used commercially-available components. An inflatable packer equipped with a steel tube extending through the inflation element to the transducer permitted sensing formation pressures in the isolated test zones. Surface components of the monitoring system provided transducer excitation, signal conditioning for recording directly in engineering units, and analog and digital recording.

The transducer system was successfully used for monitoring recover from bailing, slug-injection tests, displacement tests, and pumping tests. Modification of the transducer assembly enabled monitoring of shut-in tests, slug tests, swabbing tests, and pressure-pulse tests. The monitoring system facilitated formation testing to determine transmissivities ranging from 10^{-7} to 10 m^2/d.

FLOODS

OUTSTANDING FLOODS

Tidal flooding of hurricane Frederic

H. H. Jeffcoat reported that hurricane Frederic was one of the most intense hurricanes of record to enter the United States. Significant tidal flooding and damage extended for approximately 185 km along the Gulf Coast. The maximum tide of 2.4 m, with an estimated recurrence interval of 25 to 30 years, occurred at the Alabama State Docks, Mobile, Ala. A series of 21 USGS maps delineating areas inundated as a result of the hurricane was published in 1980.

Major depression flooding in Florida

Tropical storms caused extensive depression flooding in northwestern Hillsborough and southern Pasco Counties, including north Tampa, on May 8 and in August and September 1979, according to W. R. Murphy. Because of the lengthly period of heavy rainfall in August and September, many homes in the Forest Hills subdivision in north Tampa were flooded for an extended period, resulting in several millions of dollars in damage. Part of the subdivision is in a large depression that has no surface outlet. Curiosity Creek, which drains several lakes to the north, flows into the depression and was a significant source of flooding. This same area also had flooding in 1959 and 1960 that covered an even larger area. Several lakes in north Tampa reached record high stages, including Lake Ellen near Sulphur Springs, which had stage record since 1946. Most lakes in the area between Tampa and Land-O-Lakes, some 30 km north, that had records since 1946, had maximum stages with 10- to 25-yr recurrence intervals.

Small-stream flood investigations in Minnesota

Indirect measurements were completed by T. A. Winterstein and G. H. Carlson to determine the peak flow of floods that occurred September 20, 1981, on two small adjacent watersheds, Big Trout Creek and Cedar Creek, in Winona County, Minn. The floods were caused when rain on September 19 was followed by an intense rainstorm on September 20 in which 180 to 190 mm of rain fell on the watersheds in less than 4 h. The peak discharge measured at the mouth of Cedar Creek, which has a long narrow watershed 45.8 km^2 in area, was 314 m^3/s. The peak discharge of Big Trout Creek, measured 2.2 km upstream from Pickwick, Minn., where the fan-shaped watershed has an area of 25.6 km^2, was 510 m^3/s. These measurements were made as part of an ongoing program for determining annual peak flows from small watersheds to document the occurrence of extreme flood events.

FLOOD-FREQUENCY STUDIES

Magnitude and frequency of floods of urban watersheds in Florida

Rainfall and runoff data from nine mixed land-use urban basins ranging in size from 0.9 to 8.9 km^2 were used to calibrate the USGS urban runoff model, RRURBAN 1. Annual maximum peak discharges from simulated runoff using historical rainfall records at the U.S. National Weather Service rain gage in Tampa, Fla., were used in log-Pearson frequency analysis at each watershed. Peak discharge was related to drainage area, a basin-development factor, and channel slope by multiple linear-regression analysis. Standard errors of regression ranged from ± 36 percent at the 10-yr recurrence intervals to ± 44 percent at the 2-yr recurrence interval.

Flood analysis of the Pearl River basin in Louisiana

F. N. Lee and G. J. Arcement used double-mass and trend curves to investigate causes of extreme flooding in the Pearl River basin in the Bogalusa and Slidell areas of Louisiana. Trend curves of annual precipitation and runoff, using a 10-yr moving average, showed a cyclic

pattern for all stations examined. Peaks for periods of sustained rainfall occurred about every 25 to 30 yr.

An in-depth study was made of a flood in April 1979 and in April 1980. Rainfall associated with the April 1979 flood was greatest in the northern part of the basin. The estimated peak inflow to Ross Barnett Reservoir was between 4,530 and 4,670 m^3/s. Peak outflow, measured at a streamflow-gaging station downstream from the dam, was about 3,620 m^3/s. This represents a reduction in peak discharge of about 20 percent, contrary to the theory that the reservoir increased the flood peak.

Rainfall associated with the April 1980 flood was fairly uniform throughout the basin. Extreme flooding in the Slidell area was caused by the uniform rainfall, significant antecedent rainfall, and the coincidence of peak-flows in the Pearl River and Bogue Chitto at their confluence downstream from Bogalusa.

Peak-flow analysis for Montana

A regional flood-frequency analysis for Montana was conducted by Charles Parrett and R. J. Omang. Regression equations were developed for determining flood magnitudes for recurrence intervals of 2, 5, 10, 25, 50, and 100 yr at ungaged sites using drainage basin parameters as independent variables. Eight sets of equations were developed for eight different geographic regions, and the standard errors of estimate for the 100-yr flood equation ranged from 39 percent to 83 percent. These standard errors represent a significant improvement in prediction accuracy over previous regional analyses.

Assessment of flood hazards at recreation sites on Lake Mohave, Nevada and Arizona

Most of the existing dikes at the Cottonwood Cove recreation site on Lake Mohave, Lake Mead National Recreation Area, Nevada and Arizona, are effective in diverting and routing floodflows (up to and including the 100-yr flood) away from people and facilities, according to Otto Moosburner. However, the extreme flood (a flood meteorologically and hydrologically possible but so rare as to preclude a frequency estimate) could cause great damage and possible loss of life. At Katherine Landing, potential flood hazards (as measured by the 100-yr flood) are considered to be minor, but the extreme flood poses hazards to life and property. The use areas at Telephone Cove are potentially hazardous. No improvements have been made at the site, and large floods could migrate between the confining bluffs.

Flood frequency in the Dallas-Fort Worth, Texas, area

The frequency and magnitude of flood-peak discharges from small ungaged basins in the Dallas-Fort Worth, Texas, metropolitan area can be estimated by the size of the basin and the degree of urbanization, according to L. F. Land, E. E. Schroeder, and B. B. Hampton. The best measure of urbanization was found to be the sum of an urbanization matrix, which is determined by estimating the relative level of development of three urbanization factors in each third of the basin and then adding the nine entries. The three factors include storm sewers, curbs and gutters, and channel rectification.

The study shows that as the recurrence interval increases, the effect of the urbanization decreases. Where a basin changes from rural to completely urban, the flood-peak discharge is increased by 183 percent for storms having a 5-yr recurrence interval and by 103 percent for storms having a 100-yr recurrence interval.

Technique for estimating magnitude and frequency of floods in West Virginia

A research project to develop flood-frequency curves for West Virginia was recently completed by G. S. Runner. Regression analysis using 12 basin characteristics indicated that the best estimate of the magnitude and frequency of floods in West Virginia could be obtained by dividing the State into 3 geographic regions (Runner, 1980).

All peak discharge-estimating equations developed by the study are of the form $Q_i = cA^b$, where Q_i is the peak discharge at a given recurrence interval $-i$; c is the regression constant; b is the regression coefficient; and A is the drainage area. Peak discharges may be estimated for streams with drainage areas of 0.8 to 5,200 km^2. The standard error of estimates for the equations ranged from 25 percent for Q_2 to 54 percent for the estimate Q_{500}.

EFFECTS OF POLLUTANTS ON WATER QUALITY

Subsurface contamination by gasoline in Death Valley National Monument, California

The extent of a pure gasoline layer overlying the water table at Stovepipe Wells Hotel, Calif., was delineated by Anthony Buono and E. M. Packard. Pure gasoline found in an unused well near the area's service station prompted test drilling and subsurface soil sampling, which resulted in finding the gasoline layer between 275 and 425 m downgradient from a leaky storage tank.

The area's water-supply wells, located about 0.64 km south of the source and almost perpendicular to the direction of ground-water movement, were determined to be outside the expected area of effect of both the gasoline layer and the soluble gasoline components in the aquifer.

No effect on local xerophytic vegetation was noted, but it was not determined what effect continued movement of gasoline vapors in the unsaturated zone may have. Phreatophytic vegetation, 3.2 km downgradient from the gasoline layer, is not expected to be affected by the contamination. Future migration of the layer is not expected to extend far enough to intersect these plants.

Occurrence and transport of PCB in the Housatonic River

K. P. Kulp completed an investigation of the distribution of PCB in the Housatonic River between Pittsfield, Mass., and Stevenson, Conn. Surficial or core samples of bed material were analyzed from 81 sites, and water samples were analyzed from 3 sites.

Concentrations of PCB in bed material ranged from 140,000 to 0 μg/kg. The highest concentrations were found in Woods Pond near Lenox, Mass. Core samples showed that PCB concentrations vary with depth in bed from one location to another, and that PCB exists to a depth of at least 0.9 m in bed at some locations. Concentrations of PCB in bed material generally decreased with distance downstream from Woods Pond.

Water samples had concentrations of PCB ranging from 0.4 to 0.0 μg/L in the total phase, and 0.1 to 0.0 μg/L in the dissolved phase. Concentrations decreased downstream with distance.

F. P. Haeni made seismic reflection surveys in the study area to determine the thickness of loose organic bottom sediments. Results demonstrated the presence of recent sediments up to 1.6 m thick in the larger impoundments, up to 2.2 m thick in small impoundments, and up to 0.6 m in thickness in non-impounded reaches surveyed.

Ground-water study of Wurtsmith Air Force Base, Michigan

The contamination of a shallow sand and gravel aquifer by trichloroethylene (TCE) at Wurtsmith Air Force Base, Mich., was studied by J. R. Stark, T. R. Cummings, and F. R. Twenter. Data from nearly 250 wells were compiled and analyzed to provide an understanding of the ground-water flow system, the extent of TCE contamination, and the directions and rates of movement of ground water and TCE. Mathematical models were used to aid in calculating average rates of ground-water flow. These rates vary from about 0.1 to 0.25 m/d.

TCE that leaked from a buried storage tank in the southeastern part of the Wurtsmith Air Force Base has moved northeastward at least 600 m under the influence of the natural ground-water gradient and induced ground-water gradient caused by the pumping of the Base water-supply wells. In the most highly contaminated part of the plume, concentrations are greater than 1,000 μg/L. Currently, purge pumping is removing some of the TCE, and it seems to have arrested its eastward movement.

TCE contamination has also been detected in the northern part of the Base. Here, a narrow plume of unknown source extends at least 1,350 m northeastward and off the Base. TCE has been identified in other areas on Base and is related to operations in those areas.

Coal-tar derivatives in ground water in the St. Louis Park area, Minnesota

M. F. Hult reported that operation of a coal-tar distillation and wood preserving plant in St. Louis Park, Minn., between 1917 and 1972, resulted in contamination of drift and bedrock aquifers. Polynuclear aromatic hydrocarbons from the plant have moved at least the following distances through the ground-water system: drift, 1,200 m; Platteville aquifer, 2,200 m; St. Peter aquifer, 1,100 m; and Prairie du Chien-Jordan aquifer, 3 km. The Prairie du Chien-Jordan aquifer is at a depth of 75 to 100 m in the area and provides about 75 percent of the ground water used in the St. Louis Park and Minneapolis–St. Paul Metropolitan area. The greatest mass of contaminants is in the drift and uppermost bedrock aquifer (Platteville) near the former plant site. Parts of the drift contain an undissolved liquid mixture of many individual coal-tar compounds. In June 1980, a sample of this liquid from a monitoring well completed in the drift 15 m below the water table contained 97,000 mg/L total organic carbon. The hydrocarbon fluid has moved vertically downward essentially perpendicular to the direction of ground-water flow because it is more dense than water. It is moving more slowly than the ground water because it is more viscous. Ground water entering the area of the plant site through the drift is contaminated by partial dissolution of the hydrocarbon fluids and by release of compounds sorbed on the drift materials. Coal-tar compounds with low molecular weight such as phenol and naphthalene are more soluble in water than compounds with a high molecular weight such as pyrene, fluoranthene, and benzo(a)pyrene. Because ground water flowing through the volume of drift containing hydrocarbon fluids is preferentially dissolving the more soluble constituents, the composition of the source is slowly changing. The proportion of compounds with low aqueous solubility is increasing relative to those with high solubility. Individual contaminant compounds have been identified that are (1) neither sorbed by the drift materials nor degraded biologically (sodium), (2) slightly sorbed and are not biologically degraded under anaerobic conditions (naphthalene), (3) strongly sorbed and are biologically non-reactive (benzo(a)pyrene), (4) not sorbed but are being converted to carbon dioxide and methane by anaerobic bacteria

(phenol), and (5) both sorbed and biologically reactive (ammonia).

Tertiary-treatment of water quality in Wilsons Creek and James River, Missouri

A network of streamflow-gaging stations was established to monitor the effects of sewage effluent from the Southwest Wastewater Plant near Springfield, Mo., on water quality in Wilsons Creek and the James River. After the gaging stations were established, a tertiary-treatment system was added to the wastewater plant. According to W. R. Berkas, the tertiary-treatment system significantly improved the dissolved-oxygen concentration in Wilsons Creek and the James River. Monthly water-quality samples indicated a decrease in the concentration of dissolved manganese and an increase in the concentration of total nitrate plus nitrite nitrogen due to the tertiary-treatment system.

Effects of petroleum-associated brine on the water resources of the Vamoosa-Ada aquifer, Oklahoma

A total of 353 water samples were collected and analyzed by R. B. Morton. Of these, 47 percent were surface-water, and 53 percent were ground-water samples. Logarithmic plots were made of sodium, chloride, bromide, lithium, and residue at 180°C. Interpretation of the plotted data showed four primary indexes of water degradation by petroleum-associated brine. These are chloride concentration, 400 mg/L, or greater; bromide concentration, 2 mg/L, or greater; sodium: lithium ratio, 0.01 or less, with chloride concentration, 400 mg/L, or more; and the ratio by weight of sodium plus chloride to residue at 180°C of 0.64, or more. Secondary indexes are sodium:chloride ratio by weight of about 0.46; sodium:bromide ratio by weight of about 92; and bromide: chloride ratio by weight of about 0.0048. Use of the general linear model and Duncan's multiple-range test in analysis of variance in a digital computer showed that the primary indexes are statistically significant at the 95-percent confidence level.

A qualitative study of 266 geophysical logs (133 pairs) showed that, in five instances, a rise in the fresh water–saltwater interface ranged from 27 to 76 m.

A total of about 83 sites showing mineralization by brine were disclosed by the study. When these sites were plotted on a map with outlines of oil and gas areas, a very close geographical relation was apparent.

PCB transport in the Hudson River, New York

Water-quality monitoring of the Hudson River showed that the level of contamination has not changed since 1977, according to R. A. Schroeder. Recent data confirmed a model developed during the first 2 yr of monitoring. The model, which relates PCB concentration to dischage, showed that higher concentrations occur at extreme flow. High concentrations at low discharge result because less water is available for dilution. High concentrations at high discharge result from resuspension of contaminated bottom material into the water column.

Transport of PCB from highly contaminated reaches of the upper Hudson River to the Hudson River estuary remained about 5 kg/d, except during periods of peak discharge such as the spring snowmelt. The proportion of total annual load transported during spring snowmelt ranged from about 10 percent in 1978 and 1980 to about 33 percent in 1977 and 1979.

Migration of contaminated ground water near hazardous chemical dumps in New York

According to preliminary results obtained by H. R. Anderson and T. S. Miller as part of a study of chemical dump sites in Oswego County, N. Y., leachate movement may be occurring near two of the sites.

At one site, underlain by silt, fine sand, and clay over bedrock, conductance and heavy-metals concentrations showed that leachate may have migrated a short distance (less than 100 m) from the site. At another site, underlain by sand and gravel, conductance and heavy-metals concentrations showed that leachate may have migrated a moderate distance (100 to 200 m) toward a nearby stream. Some of the EPA organic priority pollutants also have been found in samples within the dump sites and, in one sample, down-gradient from the dump sites.

ENVIRONMENTAL GEOCHEMISTRY

Quaternary framework for earthquake studies, Los Angeles basin

Changes in pedogenic iron oxyhydroxide with time in soils formed in lithic arkosic alluvium provide a valuable tool for correlation among Quaternary strata deposited during the past 0.5 m.y., according to J. C. Tinsley and L. D. McFadden. Maximum ratios (0.2–0.6) of ferrihydrites NH_4 oxalate-soluble to total secondary free iron oxyhydroxides (dithionite soluble) characterize late Pleistocene and Holocene soils forming under xeric and aridic hyperthermic climates. Minimum ratios (0.01–0.08) characterize old soils whose ages are at least 0.5 m.y.

Soil correlation and dating, western region

A new soil development index applied to chronosequences formed under different climates demonstrated that (1) many field properties change systematically over time, (2) moisture regime is reflected in the depth functions of indexed properties, and (3) volume (or area) of soil development is strikingly similar in different

climates. Many field properties of soils are quantified and combined in the index to assess soil development. However, quantified field properties also can be compared separately.

Jennifer Harden and Emily Taylor examined four chronosequences in California, New Mexico, and Pennsylvania that have similar parent material and slope but four different soil moisture regimes: xeric-inland, xeric-coastal, aridic, and udic.

Some soil characteristics reflect development processes only in certain age ranges, and a steady state is eventually reached. These characteristics include soil structure (develops systematically over 300,000–600,000 yr), hardening or changes in dry and moist consistence (develops over about 100,000 yr), and melanization (develops over less than 1,000 yr). Other soil characteristics do not reach steady states; soils as old as 600,000 yr and even 3 m.y. are still undergoing rubification (expressed by chroma and hue), acidification, and development of texture and clay films. Some soil characteristics reflect age development only in certain climates. Rubification develops with soil age in all regimes except the aridic. Strong colors of aridic soils do not reflect soil age. Clay films and acidification are useful age indicators only in xeric-inland and humic regimes. Depth of maximum texture varies with moisture regime: xeric coastal greater than xeric-inland, udic greater than aridic-regime soils. Greatest color development is often deepest in xeric and humic soils but is shallowest in aridic soils.

When development of individual horizons of similar-aged soils is compared, the data displayed many trends evident in the field; for example, textures and colors are strong in aridic soils relative to other areas. However, if horizon thickness is multiplied by the index and summed through the profile, a striking similarity is found among soils of a given age for all moisture regimes. Profile texture, structure, clay films, and color are impressively similar for any given age of soil, regardless of moisture regime. Such normalization for climatic differences may allow direct age correlation of soils on a regional basis.

Soil geochemistry in Powder River basin, Wyoming

R. R. Tidball analysed data from 93 composite soil samples collected from the Recluse, Wyo., 1:100,000 quadrangle by *Q*-mode (interrelations among samples) and *R*-mode (interrelations among chemical variables) factor analysis. *Q*-mode analysis identified five extreme sample types, four of which occur on stratigraphic members of the Fort Union Formation–Tullock, Lebo, and Tongue River–and the fifth type on the Wasatch Formation. *R*-mode analysis identified four extreme element assemblages that are defined as follows: (1) trace element-heavy metal, (2) manganese oxide, (3) silica, and (4) silica-sodium. All four of the latter occur on the Fort Union Formation.

Contour maps of factor loadings were compiled by kriging estimators. The composition of a sample from any location on the map can be estimated by mixing proportions of each end member as determined from each factor map. The factor maps drastically reduce the number of maps that would otherwise be needed to display the element distributions.

Extractable metals in topsoil and coal spoil materials, Western United States

Data on the composition of extractable metals were obtained for topsoil and spoil samples from rehabilitated areas of the following coal strip mines in the Western United States: Dave Johnston, Seminoe No. 2, and Jim Bridger (Wyo.); Seneca No. 2 and Energy Fuels (Colo.); South Beulah, Velva, and Huskey (N. Dak.); Big Sky, Absaloka, and Decker (Mont.); San Juan (N. Mex.); and Usibelli (Alaska). R. C. Severson, M. L. Tuttle, J. L. Peard, and J. G. Crock reported that differences in the levels of many DTPA-extractable metals could not be consistently related to regions or mines. For some metals, the range of concentration measured within a small rehabilitated area at a single mine was nearly as large as the range measured at all mines. Generally, topsoil and spoil material appeared uniform in physical properties between sample sites at any single mine; extractable metals, however, did not show similar uniformity.

Broad-scale regulations for "suspect" or "toxic" levels of these metals, based on DTPA-soil extracts, may be inappropriate because these data indicate that large differences can be expected to occur between regions, between mines, and even between small areas within a single mine. Rather than specific "suspect" or "toxic" levels for a metal based on DTPA extracts of a few samples, it may be more realistic to evaluate areas using multiple prediction equations that include measurements of soil pH, organic matter, and coal content, combined with other physical and chemical properties of soils.

Chemistry of native plants at strip-mine sites, San Juan basin, New Mexico

L. P. Gough and R. C. Severson investigated the variability in the biogeochemistry of native plant species at strip-mine and undisturbed sites, San Juan basin, N. Mex. Three studies are involved in this investigation: Study (1) the biogeochemical variability of native species found at sites throughout that part of the basin underlain by economically recoverable coal; Study (2) the biogeochemical variability of native species growing on soils considered favorable for use in the topsoiling of spoil areas; and Study (3) the biogeochemical variability

of native species on rehabilitated sites at the San Juan coal mine.

The studies showed the following results: Study (1) Concentrations of Mn, Mo, Ni, and U (and possibly Fe and Se) in galleta grass showed regional patterns, with the highest values generally found in the south-central region and western edge of the basin; Study (2) Significant regional (greater than 10 km) variation for Al, Fe, S, V, and Zr in galleta grass was found. However, for most elements, a significant proportion of the variation in the data was measured locally (less than 0.1 km); Study (3) Comparisons of the chemistry of plants on rehabilitation plots with control samples of similar material from native sites showed that concentrations of Al, As, B, Co, Cu, F, Fe, Pb, Mn, Na, and U in samples of saltbush growing over spoil generally exceed the levels of these elements in control samples. Concentrations of Na in saltbush were 100 times higher in mine samples than in control samples. This high concentration reflects a corresponding 100-fold increase in the extractable Na levels in spoil material as compared to C horizon control samples. Study (3) data indicate that topsoiling rehabilitation sites to a depth of 20 cm does little to ameliorate the uptake of elements from spoil by saltbush.

Extractable element composition of soils from the northern Great Plains

The mode of occurrence of extractable elements (major elements Ca, K, Mg, Na; trace elements Cd, Co, Cu, Fe, Mn, Ni, Pb, Zn) in soils of the northern Great Plains using a variety of extractants (DTPA, EDTA, HCl, hydroquinone, magnesium nitrate, ammonium oxalate) was examined by Jim McNeal using *R*-mode factor analysis. Four factors (clay, organic, Fe-Mn oxide, extractable Na) explained nearly 75 percent of the total variance for A horizon variables. Seven factors (carbonate, clay, cation exchange capacity, extractable Na, organic, total Fe and Mn, plagioclase) explained about 77 percent of the total variance for the 79 C horizon variables.

A and C horizon extractable trace elements are related most generally to Fe and Mn oxides, as indicated by positive loadings on the Fe-Mn oxide factor and negative loadings on the carbonate factor for the A and C horizons, respectively. The mode of occurrence of each major element is dominated by the same factor for all extractants. A horizon Ca and Mg and C horizon K and Mg are strongly related to a clay factor. C horizon Ca and A horizon K are related strongly to the CEC and organic factors, respectively. A and C horizon extractable Na are related very strongly to the extractable Na factor. These results suggest that extractable major elements are water soluble and are associated with the constituents that are responsible for that factor. Consequently, any extractant should provide essentially the same information for any of these extractable major elements.

Two A and two C horizon soils from this sample suite were treated with extractants (DTPA, EDTA ammonium oxalate) for varying lengths of time to determine an optimum length of time for performing soil extractions. The extraction of the major elements (Ca, K, Mg, Na) was completed in less than 15 min for all extractants, and the extraction of the trace elements by oxalate (Cu, Fe, Mn, Zn) also was completed in less than 15 min. The kinetics of the extraction of the trace elements by DTPA and EDTA can be described best by a geometric equation of the form:

$$\log C = \log A + B \log t$$

where C is concentration, t is time, and A and B are empirical constants. This equation was found to be useful in describing the dissolution kinetics involving ion exchange and readily soluble minerals and in adequately describing other soil, mineral, and rock dissolution data reported in the literature.

Potential Cu-Mo problem in oil shale revegetation

Low Cu-Mo ratios were found by B. M. Anderson in samples of saltbush (a winter browse species for livestock) grown on spent oil shale revegetation test plots in the Piceance basin. Five plant samples were collected in 1978 from each of five test plots constructed by Colorado State University in 1977. A sixth plot consisted of seeding spent oil shale directly with no top soil interface. No samples were collected from this plot since only a few very fine seedlings were present – none more than 3 cm in height.

Test Plots	Samples	Cu ppm	Mo ppm	Ratio
1.	30.5 cm topsoil over oil shale	77	100	.77
2.	91.5 cm topsoil over oil shale	77	25	3
3.	Control, no shale	59	9.9	5.96
4.	61 cm topsoil over shale	75	78	.96
5.	61 cm topsoil with gravel interface over shale	71	62	1.1

Low Cu-Mo ratios were reported in sweetclover grown on coal mine spoil materials in the northern Great Plains by J. A. Erdman, R. J. Ebens, and A. A. Case (1978). The literature states a ratio less than 5 can cause swayback in sheep and (or) hypocuprosis in cattle. As shown in the above data, a Cu-Mo ratio less than 5 resulted in the plant samples regardless of depth of topsoil

over the oil shale. It is interesting to note that the greater the depth to the oil shale, the higher the ratio.

Geochemistry of clinker

A large freshly exposed clinker outcrop in the Powder River basin reveals a petrology that ranges from slightly heated Fort Union Formation rock to the same parent rock, but which has been melted and fused to form a magmatic slag. Temperatures of alteration for these latter rocks exceed 1,500°C. Typical (very) high temperature minerals that are produced during this alteration include cristobalite, mullite, indialite (Fe-cordierite) and hercynite (Fe-spinel). The altered rocks are perhaps most interesting for their highly variable iron content due to the differences to which they have been heated. Thus a highly developed understanding of iron geochemistry in the altered rocks will contribute to the development of inexpensive surface techniques to detect clinker at active or prospective coal mine sites.

LAND SUBSIDENCE

Fissuring subsidence research

A complex system of man-induced earth fissures or tension cracks in unconsolidated alluvium on the east side of the Casa Grande Mountains, located 80 km south-southeast of Phoenix, Ariz., is associated with relief on the buried bedrock surface that defines the base of the alluvium. The fissure system, which has a cumulative length of more than 8.7 km, has been slowly evolving since 1949 in response to ground-water withdrawal from alluvium. On the basis of precise regional gravity surveys, the fissures occur along the loci of points of convex-upward curvature in the bedrock surface.

The mechanism of earth-fissure formation in the study area was concluded to be localized flexing or bending of the strata above the bedrock irregularity. The bending is caused by differential vertical displacements related to differential compaction beneath the base of the strata above the irregularity. Differential compaction is caused by ground-water withdrawal. Modeling of the field conditions suggests that tensile strain at failure ranged approximately from 0.02 to 0.2 percent. The inferred surface deformation is similar to that measured across fissures in other areas (Holzer and Pampeyan, 1980).

Solution subsidence and collapse

Knowledge gained from the ongoing investigation of subsidence related to mining and dissolution of salt beds has been applied to two national programs. A subsidence-measuring procedure was submitted to the DOE for monitoring any possible subsidence above the proposed Waste Isolation Pilot Plant (WIPP) site near Carlsbad, N. Mex. Recommendations and review of mine-closure procedures for potash mines, located on Federal lands in the Carlsbad area, were made and given to a U.S. Government advisory committee studying safe mine-abandonment methods.

Possible salt movement hazards, central Utah

Upwelling or removal of the salt could cause major stability problems to major installations constructed in an area of central Utah, according to I. J. Witkind. Plans are currently underway for the construction of a series of coal-fired power plants in central Utah; one site under consideration for such a power plant is near Axtell, midway between Gunnison and Salina. Although surface geologic relations near Axtell suggest that the area is free of major geologic hazards, recent geologic work has indicated that much of this part of central Utah is underlain by salt, either in beds or as diapirs. In the past this salt has moved repeatedly, welling upward and arching the overlying strata. Removal of the intruded salt, either through lateral flowage or solution, has resulted in widespread subsidence. A geologic map of the Redmond quadrangle, the area surrounding Axtell, is now in preparation; the map emphasizes the possibility that the underlying salt may be a geologic hazard, and that it should be considered in any plans to construct a power plant in the area.

Mining, geologic, and hydrologic controls on coal mine subsidence

Subsidence and engineering geologic studies in the Somerset coal mining area of western Colorado showed that subsidence equals as much as 70 percent of the thickness of coal mined above room-and-pillar mines, where the pillars are extracted and the lengths and widths of the mining areas (panels) are greater than 1.2 to 1.4 times the overburden thickness (Dunrud and Osterwald, 1980). In the United Kingdom and in the Netherlands, however, maximum subsidence commonly equals about 90 and 96 percent of the mining thickness respectively (National Coal Board, 1975, p. 9; Pöttgens, 1979).

Coal mine subsidence might be greater in Europe than in the Somerset area because (1) mining methods used in Europe may increase the amount of subsidence, (2) the overburden in Europe is more likely to be weakened by past mining of another coal bed in the same area, (3) the mine roof rocks in Europe may consist of a higher percentage of soft shales and mudstones and other weak rocks, and (4) the amount of ground water and surface water in Europe commonly is greater.

Longwall mining, which is common in Europe but only beginning in the Somerset area, can increase subsidence because a larger percentage of coal commonly is removed by longwall methods than by room-and-pillar methods. Subsidence also might be reduced in room-and-pillar mining areas because the height of breaking and caving of the mine roof rocks also can be greater in room-and-pillar mining areas than in longwall mining areas. The mine roof rocks break, cave, and undergo a volumetric increase where the coal is extracted and backfilling (stowing) is not practiced. Breaking and caving commonly is higher in mine roofs composed of laminated shales, mudstones, and other soft weak rocks than in massive sandstones, limestones, and other hard strong rocks.

The caved rocks also undergo compaction where they are loaded by the weight of the subsiding overburden. Compaction is greater in caved areas consisting of thinly laminated soft weak rocks than in caved areas consisting of massive strong hard rocks. Caved fragments composed of thinly laminated soft weak rocks also break down and compact more readily, where immersed in water, than do massive hard strong rocks.

Factors controlling coal mine subsidence, therefore, include thickness of the coal mined, the methods of mining, the lithology and structure of the overburden rocks, and the behavior of the caved rocks when loaded and (or) exposed to water.

Subsidence investigations above coal mines

Tentative guidelines for surface subsidence instrumentation and monitoring were developed, under contract with the Colorado School of Mines, that recommend the layout of subsidence monuments in relation to mining panels (workings) at various depths, including spacing of the monuments, surveying frequency with respect to mining of the panels, and drilling and logging to obtain the lithology of the overlying rocks. The purpose of the program is to develop uniform monitoring and reporting procedures that will obtain enough data to help analyze, predict, and control subsidence. The same surface subsidence instrumentation and monitoring procedures are recommended for both longwall and room-and-pillar mining operations. One mining panel should be instrumented for each mine if only longwall or room-and-pillar mining is employed. Where both mining methods are employed, one panel for each method should be instrumented.

Coal mine deformation studies, Powder River basin

Studies by C. R. Dunrud of subsidence and fires above abandoned underground coal mines near Sheridan, Wyo., indicate that the removal of coal remaining in these mines probably would have fewer environmental impacts and would have significant economic return if mined by surface methods before further subsidence and fires occur. As much as 80 to 90 percent of the total resource still remains in these mines, and surface mining is economic because the overburden thickness is less than about 10 times the thickness of the beds mined. The fires, which commonly start by spontaneous ignition where air and water enter the mine workings through subsidence cracks, pits, or mine portals and shafts, already have burned an estimated 25 to 50 million t of low-sulfur subbituminous coal within and adjacent to the abandoned coal mines. Once ignition occurs, the fires can spread by ventilating through subsidence cracks and pits or mine portals and shafts. The fires often create more cavities, more subsidence pits and cracks, and more ventilation, which accelerates the burning process. Surface mining, with proper restoration procedures, would (1) prevent the loss of coal resources by mine fire; (2) virtually eliminate further subsidence and fire hazards to people, property, and animals; and (3) eliminate air and water pollution by subsidence and fires.

Land-surface subsidence in the Texas Gulf Coast area

The shift of ground-water withdrawals from the eastern to the western part of the Houston-Galveston area continued during 1980 according to R. K. Gabrysch. The population growth caused additional needs for water, which were met by pumping ground water from the western part of the area. The increased pumping continued to cause accelerated declines in water levels and accelerated subsidence. An extensometer in the western part of Harris County showed that 35 mm of subsidence occurred during 1977, 39 mm during 1978, 40 mm during 1979, and 63 mm during 1980.

Subsidence in the eastern and southern parts of the area continued at a decreased rate because surface water was brought into the area from Lake Livingston during 1976 as a substitute for ground water. As a result, ground-water pumping was reduced by about 4.9 m^3/s, and water-level rises by the end of 1980 were as much as 40 m in part of the Evangeline aquifer and 34 m in the lower part of the shallower Chicot aquifer. Analysis of the data is complicated by the wide range of stress changes, by the compressibility of clay in a vertical direction, by the effect on the extensometer records of the shrinking and swelling of the near-surface clays, and by the pressure increase in the Chicot aquifer due to a ruptured gas well affecting an area of about 520 km^2.

HAZARDS INFORMATION AND WARNING

Since 1977, information from USGS scientists on hazardous conditions or processes has been used in a program for Hazards Warning, Preparedness, and Technical Assistance. The Governors of all States and U.S. territories were informed of this program and asked to designate representatives to work with the USGS to develop procedures for communicating information on hazards and to develop information on hazards preparedness and mitigation. Contacts also were made with about 75 Federal agencies that have facilities, programs, or activities that may be affected by geologic-related hazards.

Late in 1979, the USGS notified representatives of the Governor of Texas, public officials of metropolitan Houston, and appropriate Federal agencies of hazards posed by surface faults in the southeastern Houston metropolitan area. This information was developed by E. R. Verbeek (USGS) and U. S. Clanton (NASA) (1978) and E. R. Verbeek and others (1979). Public officials are sent additional information as it is documented.

The USGS and University of Washington scientists, working together, first detected and monitored seismic activity at Mount St. Helens in March 1980. Analysis of this and other data led the USGS to issue a formal warning of an eruption to government officials in Washington, Oregon, and Idaho. Earlier work by D. R. Crandell and D. R. Mullineaux (1978) describing potential hazards from eruptions of Mount St. Helens was provided to officials and the news media. The USGS temporarily reassigned over 40 scientists and support staff to Vancouver, Wash., to monitor the volcano and provide continual technical assistance to responsible officials. A permanent staff was subsequently assigned in Vancouver and is continuing to monitor volcanic activity and provide hazard assessments and technical assistance to public officials.

In response to seismic activity near Mount Hood, an active volcano in Oregon, the USGS increased the monitoring of seismic and other geologic activity in the area and advised State and local officials of the potential hazards of an eruption. These potential hazards were described in a recent USGS publication by D. R. Crandell (1980) which was sent with the official USGS hazard announcement. From the increased monitoring and further analysis of data, researchers determined that the seismic activity was not associated with volcanism. In August 1980, the USGS downgraded its hazard assessment and reduced the level of its monitoring.

The USGS volcano hazard research in the Cascade Mountains continues to serve as a source of technical information and advice for State and local jurisdictions. A field office for the volcano research program was established in Vancouver, Wash., and will serve as an emergency command center for the Pacific Northwest until a permanent Cascade volcano facility is established.

A report by M. F. Meier and others (1980) indicates that the rate of retreat of the Columbia Glacier, near Valdez, Alaska, will significantly accelerate during the next 2 to 3 yr. As a result, the discharge of icebergs will increase, and this may pose a hazard to shipping activities. In mid-1980, this information was forwarded to the State Geologist of Alaska, who is the Governor's representative for receiving USGS information on hazards, and to other State and Federal officials. The USGS will continue to monitor changes in the Columbia Glacier and keep appropriate officials informed of any significant developments.

ASTROGEOLOGY

PLANETARY STUDIES

VOYAGER OBSERVATIONS OF THE SATURNIAN SATELLITES

GENERAL GEOLOGY

On November 12, 1980, the NASA spacecraft *Voyager 1* flew past Saturn, acquiring numerous television images of the giant ringed planet and many of its moons. *Voyager 1* obtained high-quality images of most of the previously known satellites. Mimas and Dione were imaged at a range of less than 200,000 km with typical resolutions of a few kilometers. Rhea was observed at a range of only 59,000 km with a resolution of 1.3 km/line pair. Enceladus, Tethys, Iapetus, and Hyperion were observed at much lower resolution. On August 25, 1981, the *Voyager 2* spacecraft encountered the saturnian system and acquired much higher resolution images of Enceladus, Tethys, Iapetus, and Hyperion.

The preliminary geologic analysis of these icy satellites, dominantly by USGS scientists L. A. Soderblom, M. H. Carr, Harold Masursky, and E. M. Shoemaker, yielded discovery of a complex suite of heavily cratered surfaces, a considerable variation in density (1.0 to 1.9 g/cm^3), albedo (0.3 to 1.0), and surface morphology and substantial evidence for endogenic surface modifications (Smith and others, 1981). Trends in density and crater characteristics were found to be quite unlike those of the Galilean satellites of Jupiter.

The most striking feature on Mimas, a body only 350 km in diameter, is a giant 130-km crater centered on the leading hemisphere. Mimas is heavily cratered, but few craters with diameters larger than 50 km are seen. The Voyager team suggested that the dense population of 20- to 50-km-diameter craters likely represents secondary craters produced by collisions of larger objects with the satellite.

Tethys (1,050-km diameter) was found to be heavily cratered, much like Mimas; but, in addition, it displays an enormous trenchlike groove more than 1 km deep, 100 km wide, and more than 1,000 km long. Dione is only slightly larger (1,120-km diameter) than Tethys; it has a higher density (1.4 versus 1.0 g/cm^3) and has a different global appearance. Dione showed large regional variations in albedo, including a complex network of bright, wispy, linear markings that divide the dark trailing hemisphere into polygons. Like Mimas, Dione has a paucity of craters larger than about 30 km in diameter; but unlike Mimas, its overall crater population is lower. Dione consists of at least two terrains of contrasting topography and relative age. The younger terrain has been clearly resurfaced with a layer of material sufficiently thick to mantle preexisting cratered terrain.

Voyager 1's passage over the north polar region of Rhea provided our closest view of any of the icy satellites. Its surface was observed to be highly variable in albedo. Like Dione, Rhea's leading hemisphere was found to be generally bland; the darker trailing hemisphere displays bright wispy streaks similar to those seen on the trailing hemisphere of Dione. Rhea is extremely cratered; surfaces resemble the rolling cratered highlands of the Moon and Mercury.

Notably absent on the saturnian satellites are the flattened crater forms common on the icy Galilean satellites, Ganymede and Callisto. According to Shoemaker, the lower gravity and smaller diameters of the saturnian satellites permitted them to cool rapidly and freeze, enabling their crusts to rapidly support craters from an early period in their history.

CARTOGRAPHY-NOMENCLATURE

R. M. Batson reported that maps of albedo markings and surface topographic features on the saturnian satellites Dione, Rhea, Tethys, and Mimas already have been published. Harold Masursky reported that the Committee on Planetary Nomenclature of the International Astronomical Union decided, during the past year, to name features on the satellites of Saturn for characters made famous in epics and sagas of various cultures. The Arthurian legend will be the theme for Mimas, the Aeneid for Dione, and the Iliad and Odyssey for Tethys. Rhea is the exception to this plan, as its names will be those of characters in creation myths from worldwide ethnic groups. Additional names are being presently applied to Hyperion, Enceladus, and Iapetus.

GALILEAN SATELLITES

GENERAL GEOLOGY

Io, Europa, Ganymede, and Callisto

Preliminary terrain and geologic maps were completed for Io, Europa, and Ganymede during 1981 by B. K. Lucchitta, L. A. Soderblom, G. G. Schaber, E. M. Shoemaker, E. W. Wolfe, and others (USGS). A variety of topical studies on the three satellites has been under-

taken, and the results have been published (Batson and others, 1980; Schaber, 1980; Soderblom, 1980; Soderblom and others, 1980; Clow and Carr, 1980; Lucchitta, 1980; and Shoemaker, 1981).

Schaber (1980) compiled a preliminary geologic map of Io on which nine volcanic units and six types of structural features are identified and mapped. Photogeologic evidence indicates dominantly silicate composition for the mountain material, which supports heights of at least 9 ± 1 km. Sulfur flows of diverse viscosity and sulfur-silicate mixtures (only a few percent silicates) are thought by Schaber to compose the pervasive plains. Pit-crater and shield-crater vent-wall scarps reach heights of more than 2 km, and layered-plains scarps have estimated heights of as much as 1700 m; such scarps were reported by G. D. Clow and M. H. Carr (USGS) (1980) to indicate a material with considerable strength.

Lucchitta and Soderblom concluded that Europa's surface geology is dominated by intrusive processes related to crustal fracturing, and by infilling and progressive replacement of the surface by vertical diapirs of ice, unlike the dominantly stratigraphic geology characteristic of nearly all other bodies in the Solar System studied so far. Complex tectonic episodes with varied stress fields were identified and separated into time units.

Q. R. Passey and E. M. Shoemaker (USGS; 1980, 1981) reported that during the period of heavy impact bombardment, the icy lithospheres of Ganymede and Callisto were sufficiently soft to allow relatively rapid viscous relaxation of individual craters, smothering of the groups of flattened craters beneath ejecta deposits, and regional disruption of the crust by multiring structures. The oldest retained craters, they report, are relatively small (less than 10 km in diameter), and they occur near the antapex of motion on both Ganymede and Callisto. Passey and Shoemaker suggest that the observed gradients in crater-retention ages from the leading to trailing hemisphere, noted by Shoemaker, J. B. Plescia (Jet Propulsion Laboratory), and J. M. Boyce (NASA Headquarters), may provide clues to the primordial pattern of the heating of each satellite body during the late stages of accretion.

Shoemaker and Wolfe have developed an evolutionary time scale for the Galilean satellites based on observation of active and extinct comet nuclei. Because of the high orbital velocities of the satellites, the present cratering rate at the apex of motion is 5 to 15 times that at the antapex. They conclude that Europa's surface may be as young as $\sim 10^8$ years. Lucchitta has completed a preliminary analysis of the tectonic systems on Ganymede and has suggested that the evidence for extension and spreading in some places, and shear in others, supports the hypothesis that the grooved and smooth terrains on Ganymede reflect active tectonic processes that result in the addition of new material, the breakup and consumption of the cratered terrain, and an extensive reworking of the crust of the satellite.

PROJECT GALILEO

Solid-state imaging experiment

L. A. Soderblom, Harold Masursky, M. H. Carr, and H. H. Kieffer (USGS) reported that operations plans for the NASA Galileo mission to Jupiter are progressing toward a 1985 launch and a 1988 encounter. Plans were completed during the past year for the development of a high spatial- and spectral-resolution planetary camera/spectrometer that uses solid-state detectors; the instrument is currently being tested. Designing of the Galilean satellite tour part of the Galileo mission and of specific imaging sequences will continue during the coming year.

PIONEER-VENUS RADAR

GENERAL GEOLOGY

Geology from radar images and altimetry

Harold Masursky and G. G. Schaber (Masursky and others, 1980) reported that altimetry and radar-image data obtained by the Pioneer-Venus spacecraft and Earth-based radars have provided a first look at the global distribution of topographic relief, regional morphology, and surface-roughness characteristics of Venus. Venus displays a narrow, distinctly unimodal distribution of relief. The planet was divided arbitrarily into three provinces: upland rolling plains (elevation 6,051 to 6,053 km, 65 percent of the surface) highlands (6,053 to 6,062 km, 8 percent) and lowlands (6,049 to 6,051 km, 27 percent). A granitic composition for the rolling plains is indicated by gamma-ray spectrometry from the U.S.S.R. *Venera 8* lander; this province may represent most of the planet's ancient crustal material, according to Masursky and Schaber. The two highest points in the highland province stand 11 km and 5.7 km above planetary datum, which is the mean radius, 6,051.5 km. One, Maxwell Montes, appears to be a great volcanic construct. Gravity and altimetry data indicate that the highlands are compensated isostatically. The lowland province of Venus includes several crudely circular low areas that are apparently smooth.

Schaber and Masursky (1981) also reported that regions in the southern hemisphere display well-developed ridge-and-trough topography. The best terrestrial analogs for the troughs are large continental rifts such as the East African rift valleys. The ridges and troughs make up only small sections of large linear surface disruptions postulated by Schaber to extend

halfway around Venus for a distance of 21,000 km; they rival in scale some of the midoceanic structures on Earth.

CARTOGRAPHY-NOMENCLATURE

R. M. Batson and Harold Masursky reported the publication during 1981 of a topographic map of Venus compiled (in color elevation intervals of 500 m) from altimetric data from Pioneer-Venus radar (USGS, 1981), in addition to completion of a 16-inch globe featuring the same topographic contour data in color. The published topographic map of Venus is the first in a series of six Atlases of Venus that are in various stages of formal publication. Other maps in the series will portray Pioneer-Venus radar-image data and Earth-based radar images from the Goldstone, Calif., and Arecibo, P.R., radar stations.

Masursky reported that the Committee for Planetary Nomenclature of the International Astronomical Union has chosen to use names of goddesses, heroines, and famous women for Venus' surface features. At present only Maxwell Montes, the highest topographic feature on Venus, retains the name of its discoverer.

MARTIAN GEOLOGIC INVESTIGATIONS FROM VIKING DATA

Using a new application of impact-crater dating methods based on buried craters, D. H. Scott has recognized nine periods of major volcanism in the Tharsis region (Scott and Tanaka, 1980, 1981a). Most of the lava flows mapped by Scott and Tanaka originated from Olympus Mons and the three large shield volcanoes alined along the crest of the Tharsis Montes ridge. They reported that volcanism diminished after the earlier eruptions from Tharsis Montes but continued with surges of activity until late in the history of the planet. Faults and fractures radiate outward from the central part of the Tharsis region and form complex patterns in the basement terra units. Scott and Tanaka (written commun.) also recognized a series of rock units thought to represent ignimbrites covering an area of more than 2 million km^2. In places, individual ash flows can be distinguished by erosional patterns developed along fractures and joint systems in the more indurated units.

Many origins have been proposed for the aureole of grooved terrain that surrounds Olympus Mons, the giant shield volcano on Mars, including glacial processes suggested by R. Williams and B. K. Lucchitta and volcano-glacial processes suggested by C. A. Hodges and H. J. Moore. E. C. Morris suggested that a pure pyroclastic origin can explain most observed conditions and relations of the aureole deposits. The deposits consist of several thick overlapping sheets of great areal extent similar to those on Earth, have a ridge-and-valley structure characteristic of pressure ridges that form on flowing viscous material, and are composed of easily eroded material. The aureole deposits dip inward to a basin that surrounds Olympus Mons, suggesting the basin to be a subsidence structure resulting from the extrusion of the great quantity of volcanic material that formed Olympus Mons.

Mass-wasting and periglacial results on Mars

B. K. Lucchitta and K. L. Kaufman reported detailed studies of seven large landslides and their surroundings in the Vallis Marinaris area. The slides apparently traveled across the valley floors at high velocities. A minimum speed was derived in one location, where a slide deposit lapped up onto a ridge to a height of 1 km. By equating the potential energy of the slide mass, a speed of about 300 km per hour was calculated for this slide at a distance of 50 km from its origin. This speed is slightly higher than that of most terrestrial catastrophic landslides, but near the speed (close to 400 km per hour) determined for the upper reaches of the Huascaran slide in Peru. Locally, faults scarps appear to cut the slide deposits, indicating that tectonic activity persisted into post-slide time.

Lucchitta also reported that a survey of terrestrial glacial terrain and areas formerly covered by ice in Pleistocene time was conducted on Landsat images in order to locate geomorphic analogs to some martian channels. She has found fluted ground in valleys as much as 20 km wide in northern Iceland; in the Anchorage basin of Alaska where the Chulitna-Susitna and Yenta valleys merge to form a vast grooved region 80 km wide, and in the Northwest Territories of Canada where fluted ground similar to that seen on Mars extends 180 km south of the Great Bear Lake. Lucchitta notes that the widths are comparable to the grooved terrain on the floor of Kasei Vallis, although many grooves on Mars are much deeper and wider than presently exposed terrestrial counterparts, suggesting that the grooves on the martian channel floors record the passage of several ice sheets. Lucchitta concluded that the morphologic resemblance of glacially fluted terrain on Earth to grooves on the floors of martian outflow channels is striking; sculpturing by ice may well have been a dominant mechanism.

Eolian features of the north polar region on Mars

J. F. McCauley, C. S. Breed, and M. J. Grolier reported that the Gilf Kebir region of Western Egypt, in the center of the largest hyperarid region on Earth, provides clues as to how ergs (sand seas) on Mars may have originated from fluvial source materials transported by

the wind. Along the northern margin of the cratered highlands of Mars is an arc of major channel outlets and fretted terrain that closely resembles the highlands, dry wadis, and inselbergs of the Gilf Kebir plateau region. The martian valleys, like those in Egypt, debouch into smooth plains where little or no trace of fluvial activity can now be seen. These workers reported that in Egypt, sand blown from the wadi sediments is in transit, via "eolian thoroughfares", to the ergs of the east-central Sahara. On Mars, at some time after a fluviatile interval, sand deposited on the northern plains by streams that issued from the highlands was deflated and carried to the polar lowlands by north-blowing winds.

Mars thermal data analysis

H. H. Kieffer reported that study of the thermal properties of Mars using Viking data revealed a wavelength dependence of infrared emissivity (7 to 20 μm) that can be used to recognize inhomogeneity of the surface at scales below the spatial resolution of the data (Palluconi and Kieffer, 1981). Kieffer suggested that the major variation in thermal inertia is related to the nature of the soil rather than to a large variation in the abundance of rocks on the surface.

Mars consortium

H. H. Kieffer reported that the consortium, a research coalition of scientists from throughout the world who are studying the surface and atmosphere of Mars primarily by remote sensing, is well on the way to producing standardized data of a wide category of global Viking data sets. Thus far, standard data arrays have been generated for color observations, gravity, thermal inertia, broad-band albedo, and predawn residual temperatures from the Viking approach; topography and geology based on *Mariner 9* observations; windstreak patterns and channels based on Viking imaging; and some Earth-based radar and albedo observations.

New geologic map of Mars

D. H. Scott reported that compiled geologic data for Mars, derived from the extensive Viking image data set, is being transfered from uncontrolled to controlled base maps covering three subdivisions of the planet: western hemisphere, eastern hemisphere, and north and south polar regions. The combination of larger map scale (1:15 million) and superior quality of the Viking images compared to *Mariner 9* pictures will allow three to four times more detail to be shown on the new geologic map of Mars. Scott reported that in some areas, materials previously mapped as individual units at 1:25 million scale have been subdivided into six or more rock units.

Martian crater-forming processes

D. J. Roddy, L. A. Soderblom, and R. J. Pike, Jr., reported that comparison of flat-floored martian impact craters bearing central peaks with terrestrial analogs, such as the Flynn Creek impact crater in Tennessee, and explosion craters tends to confirm the likelihood of major ring-fault zones at the bases of the terraced and nonterraced crater walls. These studies also indicate that structural uplift in the central peaks is on the order of 10 to 15 percent of the apparent crater diameter. Theoretical calculations indicate that 20 percent or more may not be unreasonable if the martian crust is temporarily fluidized by impact melting of permafrost layers. Roddy reported that the result expected is significant uplift of large parts of the martian crust beneath the actual crater.

LUNAR INVESTIGATIONS

Petrology and geochemistry of lunar highlands breccias

O. B. James reported that review and evaluation of currently available data on the nature and history of the early lunar crust showed that the endogenous plutonic rocks of the lunar highlands comprise two distinct mineralogic trends. In one trend, the rocks are mostly anorthosites (generally termed ferroan anorthosites); as a group, these rocks contain relatively calcic plagioclase having a small compositional range and relatively iron-rich mafic minerals having a large compositional range. In the other trend, the rocks are norites, troctolites, dunite, spinel troctolites, and spinel anorthosites (generally termed magnesium-rich plutonic rocks); as a group, these rocks contain mafic minerals relatively high in magnesium, and their plagioclase and mafic minerals have large ranges of compositions and strongly correlated compositional variations. The mineralogic variations in highly evolved endogenous igneous highlands rocks–felsites, quartz monzodiorite, and KREEP basalts–indicate that these rocks are related genetically to the magnesium-rich plutonic rocks. Granulitic breccias and fragment-laden impact-melt rocks are the two most important types of impact-generated rocks formed during early lunar history. The granulitic breccias represent aggregates of fragments of plutonic rocks (derived from both the ferroan anorthosite and magnesium-rich suites) that were reheated to temperatures near or above their solidus and recrystallized and (or) partly melted. James reported that isotopic data suggest that this reheating took place early in highlands history, before 4.15 b.y. ago. The fragment-laden melt rocks formed by mechanical

mixing of super-heated impact melt with relatively cold granulated bedrock. The mineralogies of the impact-melt fractions of these rocks suggest that the precursors of the melts were magnesium-suite rocks. Isotopic data suggest that most of the fragment-laden melt rocks formed between 4.05 b.y. and 3.85 b.y. ago. James suggested a model for the early evolution of the lunar crust, as follows: during the final stages of accretion, about 4.5 b.y. ago, the outer part of the Moon melted to form a magma ocean about 300 km deep. This ocean fractionated to form mafic and ultramafic cumulates at depth and an overlying anorthositic crust, consisting of ferroan anorthosites. Subsequent partial melting in the primitive mantle underlying the crystallized magma ocean produced melts that segregated, moved upward, intruded the primordial crust, and crystallized to form layered plutons of magnesium-rich rocks. Intense impact bombardment of the lunar surface between about 4.5 and 4.0 b.y. ago mixed and melted the rocks of the two suites, forming a thick layer of granulated debris, granulitic breccias, and impact-melt rocks. A period of bombardment by large objects between about 4.0 and about 3.9 b.y. ago formed the fragment-laden melt rocks, according to James.

TERRESTRIAL STUDIES

IMPACT CRATERING

Strangways Crater, Australia

D. J. Milton reported that Goat Paddock, a 5-km-wide impact crater in western Australia, was mapped geologically and geophysically by Milton, John Ferguson and A. L. Jaques (Bureau of Mineral Resources, Australia), and R. F. Fudali (Smithsonian Institution). The crater, of early Eocene age, is a transitional type that shows features of both smaller, simple, bowlshaped craters and larger, complex craters. Goat Paddock is being studied, according to Milton, particularly for the information it may yield on the nature of the transition between simple and complex craters that occurs at different critical diameters on each terrestrial planet.

Crater mechanics

D. J. Roddy reported that a deep drilling program has been completed at Flynn Creek impact crater in Tennessee, created 360 m.y. ago in a shallow-water, constant plain environment. Contrary to the traditional interpretation, the new drilling program reveals that the initial cavity was not a bowlshaped depression but a broad, flat-floored cavity with a deep central zone of intensly disrupted and uplifted strata. This configuration is presently interpreted as the approximate shape of the maximum transient cavity; however, additional experimental and calculational studies are necessary to determine cratering sequences that can lead to such final morphologies and structures. This new drilling information combined with earlier detailed surface and laboratory studies, provides the most complete data base on surface morphologies and subsurface structural deformation yet assembled for flat-floored craters with central uplifts. The combined data, moreover, have been critical in the formulation of the generalized sequence of cratering that has produced these types of craters. In collaboration with S. Shuster and K. Kreyenhagen (California Research and Technology, Inc., Woodland Hills, Calif.), Roddy has completed a series of detailed calculations to model the formation of the largest and best preserved terrestrial meteorite impact crater (Meteor Crater, Ariz.). Sets of initial impact conditions and initial material properties were earlier determined, estimated, and calculated by Roddy and were used in computer-code simulations. The code studies, conducted by Roddy in contractual conjunction with California Research and Technology, Inc., involved adaptations of the highly advanced formulations presently in use in large-scale explosion-cratering research. Roddy reported that the results of the first calculations indicate a number of critical aspects, including the fact that the impact energy that produced Meteor Crater was 10 to 20 Mt, a factor of four to five times larger than earlier calculations published in the literature. The results suggest a lower impact velocity (20 km/sec) than previously expected.

REMOTE SENSING AND ADVANCED TECHNIQUES

EARTH RESOURCES OBSERVATION SYSTEMS OFFICE

The Earth Resources Observation Systems (EROS) Office supports and coordinates research in applications of remote sensing technology and conducts demonstrations of those applications within bureaus and offices of the DOI. Research in the applications of remotely sensed data is conducted by scientists in the EROS Office headquarters in Reston, Va., the EROS Data Center (EDC) in Sioux Falls, S. Dak., and the EROS field offices in Anchorage, Alaska, and Flagstaff, Ariz.

The EROS Data Center is the principal archive for and distributor of data collected by the USGS and the NASA research aircraft and by Landsat, Skylab, Apollo, and Gemini spacecraft. The Center's other major functions are assistance and training in the use of remotely sensed data and development, demonstration, and transfer of remote sensing technology.

Scientists from each of the EROS offices cooperate with Federal and State user agencies in projects that apply remote sensing techniques to resource management problems. The cost effectiveness and usefulness of the techniques are assessed and documented, and the user agencies gain experience in applications.

GEOLOGIC APPLICATIONS

Lineament detection in the Wind River Range, Wyoming

Scott Southworth analyzed Landsat multispectral scanner (MSS) and return beam vidicon (RBV) data and Seasat synthetic aperture radar (SAR) images to detect lineaments in the Wind River Range, a highly faulted and fractured uplift in west-central Wyoming. This northwest-trending, asymmetric, and anticlinal structure is composed of a Precambrian crystalline core that is flanked on the west by Tertiary sedimentary units and Quaternary glacial and alluvial deposits. To the east, the mountains are flanked by Paleozoic, Mesozoic, and Tertiary sedimentary rock units that dip uniformly toward the Wind River basin. The Wind River Range area is perhaps one of the largest in the conterminous United States for which geologic mapping and studies are incomplete.

Landsat MSS band 7 (0.8–1.1 μm) and RBV (0.505–0.750 μm) data with Sun elevation angles varying from 18° to 35° were analyzed at scales of 1:500,000 and 1:250,000. Seasat SAR images (23.5-cm wavelength), which were acquired on the ascending (south to north) satellite node with a look direction of N. 67.5° E., and on the descending (north to south) node with a look direction of N. 67.5° W., were analyzed at a scale of approximately 1:500,000.

Some of the lineaments were identified consistently on all image types, but others were highlighted or obscured by differences in illumination (Sun elevation angle, Sun azimuth, radar look direction or angle, and radar depression). The greater resolution of Landsat RBV data (3 m vs. 80 m for MSS data) increased the number and accuracy of lineaments delineated. Although the deeply dissected crest of the range caused some foreshortening and layover distortion in the Seasat SAR images, lineaments were identified, especially on the west flank of the core, that were not discernible on Landsat images because of high Sun illumination. Most previously mapped faults in the Wind River Range were identified on the images, and many new lineaments were also observed.

The large-scale features in the Wind River Range are difficult to map from field observations because of their great extent and because of the rugged, inaccessible terrain in the area. The synoptic and temporal coverage of Earth-imaging satellites thus made a significant contribution to completion of geologic mapping and studies in the Wind River Range area.

A multistage image investigation of Des Moines Lobe glacial deposits

C. A. Sheehan and J. R. Lucas (Technicolor Graphic Services, Inc.) conducted a multiscale image investigation of the late Wisconsinan-Age glacial deposits of the upper Midwest. Curvilinear trends in drainage, vegetation, and soil tone patterns related to the depositional and recessional history of the glacial deposits of the Des Moines lobe were delineated on a mosaic of Landsat MSS images. The 1:1,000,000-scale mosaic covering approximately 1,036,000 km^2 is centered over Minneapolis, Minn., and includes portions of seven States. The 47 Landsat MSS scenes that comprise the mosaic were acquired during the springtime when soil tone variations in the area are most apparent. On a Landsat 1:250,000-scale RBV image over the seven-county intensive-study area in northern Iowa, the higher resolution of the RBV cameras permitted differentiation of the minor or washboard moraines, which are small, subtle, landform features not visible on the MSS images.

A 1:82,000-scale mosaic of the Iowa portion of the Des Moines lobe was compiled from approximately 500 high-altitude aerial photographs. Interpretation of this mosaic allowed a more detailed breakdown of image patterns in the seven-county study area into ground moraine, washboard moraine, circular disintegration ring terrain, hummocky terrain, and terrace and outwash landforms. Comparison of the higher resolution aircraft photographs with the Landsat images provided information on the sources of the Landsat tonal patterns. An analysis of drainage on a low-altitude 1:20,000-scale black-and-white photographic stereopair from the Iowa area illustrated the differences in topography.

The four scales of data provided regional to local levels of observation. The Landsat MSS mosaic supplied a view of the entire U.S. portion of the glacial deposits of the Des Moines lobe. It permitted the tracing of landform and morainal trends for hundreds of kilometers and perception of the lobe as a single, integrated unit. The high resolution of the aircraft mosaic allowed detailed mapping of these trends along a portion of the lobe. The RBV image and the low-altitude aircraft stereopair provided a more detailed look at selected areas of interest. The information derived from these interpretations can be used in investigations of the glacial history of the area.

Soda ash deposits, Lake Magadi, Kenya

A computer-compatible tape of a Landsat image (E-2386-07032) acquired February 2, 1976, of the Lake Magadi area was analyzed by W. D. Carter (USGS) and Melanie Morgen (Technicolor Graphic Services, Inc.) in preparation for a workshop on remote sensing and mineral exploration held in 1980 in Nairobi, Kenya, at the Regional Center for Remote Sensing. They found that the natron ($Na_2CO_3 \cdot 10H_2O$) deposits that encrust the surface of the lake, which is fed by CO_2 springs, have a signature that is distinct and separable from other white salt surfaces such as the Salar of Uyuni in Bolivia. In subsequent field examinations the surface differences observed on the Landsat images were correlated with chemical characteristics, bladed crystal structure (monoclinic), associated fracture patterns, and an abundance of algae.

Sand and gravel deposits of Budapest, Hungary

Using computer algorithms designed by G. K. Moore to enhance lineaments, W. D. Carter analyzed a Landsat scene (E-30557-08573) of Budapest, Hungary, acquired September 13, 1979. Northwest- and northeast-trending lineaments dominate the scene and correlate with many of the paleochannels of the ancient Danube River. The oldest channel flowed southeasterly along fracture-controlled valleys; where it emerged on the Central Plain of Hungary, the channel formed large deposits of sand and gravel that are now being mined in commercial quantities.

Landsat-based mineral exploration

An approach to improve the U.S. position on strategic mineral resources employs a lineament map of the conterminous United States, compiled by W. D. Carter in 1974 (Fischer and others, 1976) and the USGS's Computerized Resource Inventory Base (CRIB) file on mineral resources. Mineral deposits are plotted by commodity on a separate lineament map base, and the locations are compared to local lineament trends to define possible exploration targets. Landsat images of selected target areas in the Nation are then subsequently analyzed at larger scales by visual and manual methods, and, later, via computer-compatible tapes to determine if spectral measurements, ratioing, and other methods provide any additional information on prospecting possibilities in each area. These procedures provide an orderly progression of data application from a national to a local level. These data can be supplemented by other digital data bases that allow presentation of aeromagnetic, gravity, and geochemical surveys in stereoscopic image format. The stereoscopic image then can be superimposed on the Landsat image base to define areas where additional exploration may be warranted.

Analogous drainage processes in gobi terrain and on Mars

A. S. Walker compared drainage patterns in the black gobi terrain of the People's Republic of China (PRC) with drainage patterns on Mars. The gobi consists of unsorted loose subangular to subrounded quartzite gravels, predominantly of pebble size but with occasional cobbles. The terrain is located on the outer fringes of the Turpan Depression, a 50,000-km² fault-formed interior drainage basin in Xinjiang Autonomous Region, PRC. The depression is named after Turpan County (43° N., 89° E.) and is surrounded by the Tian Shan (Sky Mountains), a permanently glaciated range that was uplifted during the Cenozoic. The glaciers of the Tian Shan are the primary source of streamwater in the gobi.

The anastomosing stream pattern in the gobi is a product of two environments—a mountain drainage system with well-defined channels and an alluvium drainage system with high infiltration. The velocity and volume of flow coming from the mountain drainage system initially control the behavior of the stream when it reaches the gobi, and thus the stream channels are not in equilibrium with the gobi terrain in which one would expect immediate anastomosing. Analysis of temporal Landsat data acquired on October 4, 1972, October 28,

1976, and November 21, 1980, indicates that the channel patterns remain consistent for at least 8 yr, and that the streams maintain their integrity for up to 15 km into the gobi before they begin to anastomose.

One of the major surprises of NASA's *Mariner* and *Viking* explorations of Mars was the detection of channel patterns that resemble abandoned streambeds. Many investigators (most recently Pieri, 1980) argue that channels on Mars were formed by running water, but not necessarily water from rain. Images returned from the *Viking 1* and *2* landing sites on Mars show features that bear striking resemblances to those of the gobi terrain.

Channel patterns at the mouth of the Maja Vallis on Mars, for example, have a morphology similar to those of the gobi channels. They appear to debouche from cratered highlands onto plains. The water that formed some of the channels on Mars may have originated in an area in which the channels were in a state of quasi-equilibrium with the martian surface environment. This state may not have continued through the entire length of the channels, however, and some features near the mouths of the channels may reflect relic equilibrium states upstream, just as some reaches of the channels in the gobi are controlled by glacial runoff from nearby mountains.

Fraunhofer line discriminator experiments

The Fraunhofer line discriminator (FLD) is an electro-optical device that detects solar-stimulated luminescence several orders of magnitude below the intensity detectable by the human eye. R. D. Watson and A. F. Theisen analyzed FLD images of rock luminescence in Big Indian Valley, near Moab, Utah. Field and laboratory studies confirmed that high luminescence was associated with areas of uranium-vanadium mineralization. Rock and soil samples from five sites were analyzed for 11 major elements and 8 trace elements. Measurements of luminescence and results of the elemental analyses correlated in a positive multiple linear regression analysis. The analysis showed a positive correlation between uranium content and luminescence. Other elements that indicated a positive correlation with luminescence were nickel, lanthanum, and vanadium. Zinc, cobalt, and chromium were found to have a negative correlation with luminescence.

The Santa Margarita Formation north of Sespe Creek in western Ventura County, Calif., about 40 km northeast of Santa Barbara, is a phosphatic formation of late Miocene age. Laboratory spectral measurements confirmed that samples of phosphatic rock and associated gypsum from this area luminesce within the sensitivity range of the Fraunhofer line discriminator. FLD images acquired at the 486.1-nm Fraunhofer line showed luminescence that correlated well with phosphatic outcrops of the formation. Intermediate-level luminescence south of the Santa Margarita Formation is believed to be associated with detrital material washed downslope from that formation. Luminescence is insignificant in the area south of Sespe Creek.

Watson, Theisen, and D. J. Roddy conducted a series of laboratory spectral measurements on shocked sandstone and dolomite from Meteor Crater, Ariz. These measurements showed that shocked rocks may exhibit solar-stimulated luminescence and that a direct correlation exists between luminescence intensity and the level of impact metamorphism. Aerial measurements, made at Meteor Crater with the FLD, indicate that the airborne FLD system also is capable of detecting direct solar-stimulated luminescence in the most highly shocked rocks. Solar and thermal-stimulated luminescence in shocked rocks appears related to certain types of shock-produced internal defects that are sensitive to activation by electromagnetic energy. For example, studies at Meteor Crater and other impact sites have shown that shocked sandstone, limestone, and dolomite respond to thermal excitation by releasing thermoluminescent energy. Luminescence stimulated by direct solar radiation has not been found with the FLD in the same shocked rocks at Meteor Crater. Without exception, the most highly shocked Coconino Sandstone from the southern ejecta blanket exhibits a luminescence 10 to 65 times greater than that of unshocked Coconino. The FLD appears to have potential for detecting areas of exposed, shocked rocks in isolated meteorite impact sites.

In collaboration with the Geosat committee's remote sensing test site program, luminescence images were acquired of parts of the Patrick Draw–Brady oil and gas test site in Wyoming. The FLD was operated at the 486.1-nm, 589.0-nm, and 656.3-nm Fraunhofer lines. Most of the luminescence highs were observed in the transition zone between the Wasatch and Fort Union Formations and are probably caused by outcrops of coal and gypsum. Geochemical and mineral data, which were available for a limited number of the image areas, showed that the most luminescent elements at the Patrick Draw–Brady test site are P, B, Be, Ba, V, and Ni.

In collaboration with R. D. Jackson (USDA), Watson and Theisen also used the FLD to monitor alfalfa fields in which irrigation treatments were applied to induce several degrees of moisture stress. The FLD was carried on a truck-mounted boom, and measurements were made over test areas several meters long within the alfalfa plots. Solar-reflected and thermal-infrared radiation also were measured over the same areas using hand-held radiometers. Plant water potential

measurements were made at several times during the day using the pressure bomb technique on plant stems. The most highly stressed test plot showed luminescence only slightly less than that of the well-watered plot, contrary to expectations of increasing luminescence with increasing stress. Because of wilting, however, the stressed plot had less biomass and less chlorophyll. The ratio of the broad-band shortwave infrared to the visible red radiance was used to adjust the luminescence values because this ratio is proportional to the green biomass viewed by a radiometer. With this correction, luminescence was shown to increase with increasing stress.

Seasat and GOES-3 radar altimetry evaluation

In cooperation with the USGS National Mapping Division, Water Resources Division, and the NASA Wallops Island Station, the EROS Office funded a contract with GeoScience Research Corporation of Salisbury, Md., to evaluate Seasat and GOES-3 radar altimetry data in applications over several types of land surfaces. Because the radar altimeter was designed specifically to measure sea surface variations such as wave heights, it failed to "lock" onto land surfaces having abrupt changes in topography. The altimeter worked very well, however, when crossing the Salar of Uyuni, a large salt lake in the southern Altiplano of Bolivia. The altimeter measurements agreed within 10 cm of previously established surface elevations, and the microtopography of this very flat to slightly rough surface was accurately portrayed. The Salar surface was found to be ideal for these studies and for corrections of waveforms.

Similar tests were conducted over an area of known surface subsidence in the Casa Grande–Eloy area between Phoenix and Tucson, Ariz. Subsidence caused by ground-water withdrawal was found to have increased up to 2.0 m since the most recent topographic maps of the area were published in 1965. Where ground tracks of Seasat and GOES orbits intersect, the subsidence estimates of the same area agreed within 0.2 m. Seven land-leveling surveys have been conducted in the Eloy area since 1905, and each survey recorded an increase in subsidence. The most recent leveling survey, in 1977, conducted by the USGS recorded a maximum of 3.29 m of subsidence between Eloy and Picacho, located to the southeast.

Because of reports of recent uplift in Yellowstone National Park's Pitchstone Plateau area, an attempt was made to analyze Seasat altimetry data (revolution 574) of the area. Although the altimeter appeared to "lock" onto the rugged surface momentarily, the data were too discontinuous to produce a reliable profile. A shorter and more frequent gate interval, a larger time sample, and a faster response system would be required to track the surface accurately.

Tests of the Seasat altimeter over the Great Salt Lake and the Salt Lake Desert, Utah, revealed that the water level of the lake was 1.4 to 1.6 m higher than it was when mapped in 1969. The higher water levels correspond to official lake-level fluctuation charts recorded from 1847 to 1977. Studies of waveforms showed that water, water/land transition zones, mud flats, and highly specular desert surfaces are each distinct and cause separable responses on the altimeter. Thus, waveform analysis of altimetry data can provide additional information on surface roughness and corresponding materials that may not be clearly visible in the supporting radar images.

Petroleum exploration in the People's Republic of China

Cooperative research on the application of remote sensing to petroleum exploration, involving geologists at the EROS Data Center and scientists from the Scientific Research Institute for Petroleum Exploration and Development, Ministry of Petroleum Industry, People's Republic of China, continued in 1980.

G. B. Bailey (USGS) and P. D. Anderson (Technicolor Graphic Services, Inc.) conducted detailed image analysis and interpretation studies of the western Qaidam basin.[1] Their interpretation of the structural geology of the Qaidam basin compared very favorably, in terms of the identification and location of major structural folds, thrust faults, high angle faults, and fracture systems, with data compiled in the field by Chinese scientists since the mid 1950's. Bailey and Anderson identified several potential hydrocarbon traps and other features that are associated with petroleum occurrences in the basin. They also designed a model, based on their findings and on Asian plate-tectonic theory, to predict the types and trends of structural features that occur in the eastern part of the Qaidam basin where rock exposures have been generally obscured by surficial cover.

Geological investigations in West Africa

D. A. Hastings (Technicolor Graphic Services, Inc.) is investigating Magsat anomaly data for their significance in increasing understanding of regional crustal structure. His initial work has consisted of the interpretation of ancillary geophysical data, Landsat data, and the preliminary Magsat scalar (total field) $2° \times 2°$ anomaly map, which was produced in 1980 by the NASA Goddard Space Flight Center, for investigation of regional crustal structure and metallogenesis in West Africa. The West African shield is characterized by a thick cover of lateritic soil, by rapid weathering rates,

[1] Qaidam is the currently accepted Pinyin transliteration for the name of this basin, which in previous transliterations appeared as Tsaidam or Chaidamu.

and by a vegetative cover comprised of plants possessing generally shallow root systems. Each of these characteristics is an obstacle to geological remote sensing in the area because the underlying rock is spatially, chemically, and biologically divorced from the surface. In addition, severe cloud or haze cover often prevents full Landsat coverage of the area.

A synthesis of investigations of the geological framework of West African mineral deposits (Hastings, 1980) suggests that Precambrian rifting and metamorphism and subsequent geomorphologic activity may have led to the genesis of central West African mineral deposits through the middle Mesozoic. These processes can be correlated with hypotheses on the formation of the Atlantic Ocean and of petroliferous coastal sedimentary basins in the area (Hastings and Bacon, 1979).

Contrast-enhanced Landsat images of parts of western Upper Volta showed a strong near-infrared response over greenstones. The strong response originally was attributed to the vegetation that is generally healthier over the greenstones than over neighboring granitoids or metasediments. The areas of stronger infrared response correspond well to mapped exposures of greenstones. One area of high-infrared response was interpreted to be a possible (but previously unmapped) greenstone belt. This correlation is significant, as the flanks of greenstone belts are associated with occurrences of gold, manganese, and other minerals.

The initial interpretation of the preliminary Magsat anomaly map showed the expected preference for east-west versus north-south orientations. North of the magnetic Equator, lower Precambrian shields tend to form negative total field Magsat anomalies, while sedimentary basins tend to form positive anomalies. The reverse is true south of the magnetic Equator. Of particular note is the excellent correspondence of the famous "Bangui negative anomaly," discovered by the Polar Orbiting Geophysical Observatory (POGO) satellites (Regan and others, 1975), to the exposure of lower Precambrian shield and the positive anomalies corresponding to the Benue trough and Congo basin. An as-yet unexplained feature of the anomaly map is the change in polarity of Magsat anomalies at 5° to 15° S. latitude, even though the geomagnetic Equator crosses Africa at about 11° N. latitude.

Enhancement, analysis, and interpretation research for geosciences

Rock fractures commonly are indicated by edge and line segments that form lineaments on remotely sensed images. Manual methods of mapping lineaments are subjective, and the results are frequently controversial. A long-term research goal at the EROS Data Center is to develop automated objective procedures for lineament mapping. In support of this goal, G. K. Moore (USGS) and F. A. Waltz (Technicolor Graphic Services, Inc.) designed a five-step digital convolution procedure to directionally enhance images; the resultant images contain few artifacts and little noise. The main limitation of this procedure is that little enhancement of lineaments occurs in dissected terrain, in shadowed areas, and in flat areas with a uniform land cover.

The directional enhancement procedure can be modified to extract edge/line segments from an image. Any of various decision rules then can be used to connect the line segments for a final lineament map. The result is an interpretive map based on an objective method of extracting lineament components.

D. K. Scholz (Technicolor Graphic Services, Inc.) completed the first phase of a digital study for ratioing Landsat spectral bands to enhance differences in rock lithologies (Rowan and others, 1976; Swain and King, 1973). This work was conducted using images of exposed rock materials from eight geologic units in the Uinta basin area, northwestern Colorado and northeastern Utah. The basin geology consists of sequences of shale, sandstone, and limestone, which were deposited in a nonmarine lacustrine environment during the Cretaceous and Tertiary Periods.

Thirty different ratios of brightness values of the original four Landsat bands were generated. These ratios were calculated for linear combinations of Landsat bands as well as for single bands and inverses of those same bands. Results were evaluated by statistical comparison of the ability to separate the reflectance values for the individual rock units on the basis of means and covariances of their pixel brightness values. Initial quantitative results for the lithologies in this study suggest that Landsat bands 4, 5, and 7 allow maximum rock identification when ratioed in such a way that band 7 brightness values are divided by the sum of the values for the two visible bands. The three ratios that allow best discrimination have been selected to facilitate generation of a ratio color composite for qualitative evaluation by image interpretation techniques. These three band radios were 4/6, 6/(4+5+6+7), and 4/(6+7).

Digital geologic data base of Nabesna quadrangle, Alaska

In preparation for an advanced course in geologic remote sensing techniques given at the EROS Data Center in November 1980, a digital geologic data base was developed for a portion of the Nabesna quadrangle, Alaska. The data base incorporated Landsat MSS data, Defense Mapping Agency (DMA) topographic data, and data sets from the Alaska Mineral Resource Assessment Program (AMRAP), including residual aeromagnetic, Bouguer gravity, stream sediment geochemical (for Cu,

Pb, Au, Cr, and Co), geologic, mineral occurrence, and land status data. All map data were digitized, interpolated to generate continuous data arrays, resampled to a 50-m cell size, and geographically registered to a Universal Transverse Mercator (UTM) grid.

The Nabesna quadrangle was selected because of the diverse types of geologic data available for the area, the known mineral-resource potential of the area, and the DOI mission to evaluate mineral resource potential under AMRAP.

The objectives in designing the data base were to demonstrate the usefulness of digital processing techniques for analyzing, merging, and integrating diverse types of data in mineral-resource investigations, and to provide workshop participants with a case example of geologic data base planning, implementation, interaction, and management.

The data base was used to develop and test a geologic model for evaluating potential porphyry copper resources in the area. Interim products generated to define the model included image raw data and derivatives; stereoscopic merges of Landsat MSS data with gravity, aeromagnetic, and geochemical copper data; and integrated ratios of aeromagnetic and gravity data and geochemical copper and chromium data. The final product was an image that incorporated all of the regional model parameters to show the most likely areas of porphyry copper occurrence.

Evaluation of new satellite imaging systems for geologic applications

W. D. Carter and Scott Southworth conducted an investigation to assess the usefulness of Landsat 3 MSS band 8, HCMM (Heat Capacity Mapping Mission), CZCS (Coastal Zone Color Scanner), Seasat SAR (Synthetic Aperture Radar) and airborne SAR data for geologic applications.

A Landsat 3 MSS band 8 (10.4–12.6 μm) thermal image acquired on May 31, 1978, of the Wind River Range in Wyoming was analyzed for lineaments and surficial materials. Although operation of band 8 was termed "unsuccessful," sufficient information was extractable from transparencies of the daytime thermal data for discrimination of rock and soil types, mapping of glacial and alluvial deposits, and mapping of lineaments based on evapotranspiration of collected moisture along fractures and faults.

Lineaments and drainage patterns in snow-covered terrain of the Wind River Range were identified by Southworth and Carter on day-thermal data on the basis of temperature differences in moisture-related phenomena. These features were not observed in the visible Landsat wavelengths because high saturation of bright snow obscured their details. Further applications of Landsat band 8 data may be possible in Arctic regions where snow, ice, and cloud cover create interpretation problems.

HCMM day-visible (0.55–1.10 μm) and day-infrared (10.5–12.5 μm) images of the West Coast, Rocky Mountain, and Alaska regions also were obtained and analyzed. Differences in surface materials, specifically vegetation, soil moisture, rock types, and thermal effluents, were observed in both the visible and infrared response regions. Thus, HCMM images can provide scientists with an additional tool for small-scale regional studies.

Standard HCMM products (day-visible and day- and night-thermal infrared images) and special products (temperature difference and thermal inertia images) acquired on September 26, 1978, of the Valley and Ridge province in Pennsylvania were analyzed by H. A. Pohn, Scott Southworth, and W. D. Carter. Negatives at 1:4,000,000-scale were enlarged photographically to 1:250,000-scale glossy and matte contact prints to fit the new Pennsylvania State geologic map. Tonal differences observed in the thermal inertia and temperature difference data showed distinct boundaries of lithologic units.

The Nimbus 7 CZCS provides repetitive coverage (every 6 d) of coastal, oceanographic, and atmospheric phenomena. CZCS images are composed of six bands of data ranging in wavelength from 0.43 μm to 12.5 μm. Standard CZCS images are approximately 1:4,000,000-scale with a 1,800-km swath width and a resolution of 825 m. CZCS images obtained on April 21, 1979, of the eastern seaboard region provided information not previously revealed on other types of imagery of the Valley and Ridge province of Pennsylvania. Bands 1, 5, and 6, centered at 0.44, 0.75, and 11.50 μm respectively, showed contrasting tones that may reflect differences in ground water, surface materials, and (or) rock composition in the folded Appalachian Mountains.

The Seasat SAR provides geologists with unique images for geologic applications even though the primary objective of the Seasat SAR mission was oceanographic monitoring. This alltime, all-weather system is advantageous because of its varying look directions (N. 67.5° E. or N. 67.5° W.) and consistent look angle (20.5°). The Seasat SAR, which operates in the L-Band (23.5-cm wavelength) with a 25-m resolution, is most useful for enhancing subtle topographic and morphologic features. Lineaments, which provide keys to occurrence of minerals and ground water, are easily identified on SAR images. SAR data are especially useful in areas where year-round cloud cover prohibits clear views of the land surface.

Goodyear SAR mosaics, obtained by Litton Aeroservice, were assessed for geometric accuracy and

usefulness as geologic mapping tools. The airborne Goodyear SAR system, GEMS, operates in the X-Band wavelength (3 cm) with 30-m resolution. Images of the "Overthrust Belt Area," which corresponds to the 1:250,000-scale quadrangle sheets of Choteau, Dillon, Butte, and Wallace, Mont., and Richfield, Utah, were analyzed. The mosaics were compared to USGS topographic maps (all UTM projections) for geometric accuracy. Although internal geometry created some misregistration of land features, the SAR images were found to be a useful mapping tool for the field geologist. For example, certain rock types may be discriminated by tonal and textural differences in the radar images; the differences result from the variation in moisture-and composition-controlled dielectric constants of surface materials.

Classification of geologic hazards of Iceland

Few, if any, areas on Earth have the diversity and frequency of occurrence of geologic hazards as Iceland, an island republic in the North Atlantic with an area about the same as that of Virginia. R. S. Williams, Jr., has been studying the natural hazards of Iceland in order to develop a more widely applicable hazards classification scheme. He defined a "natural hazard" as any naturally occurring environmental phenomenon that potentially can cause injury, illness, or death to humans, animals, or plants, or that can damage or destroy property.

R. S. Williams found that the natural hazards of Iceland can be grouped into six primary classes: geologic, hydrologic, glaciologic, meteorologic, oceanographic, and biologic. He also determined that the most significant class is geologic, accounting for 15 of the 38 discrete potential natural hazards in Iceland in the six primary classes (Williams, 1980). The geologic class can be further divided into four subclasses: geomorphic, geothermic, seismic, and volcanic. Geologic hazards defined as geomorphic include solifluction, debris avalanches, and floods; as geothermic: hot springs, geysers, solfataras, and jökulhlaup (glacier outburst flood); as seismic: earthquake shaking and rifting; and as volcanic: lava flows, tephra falls, volcanic gases, maars (explosion craters), jökulhlaup, and floods. Many of these geologic hazards, as with the jökulhlaup phenomena, are interrelated. Historically, the principal geologic hazard in Iceland has been of the volcanic subclass (Thorarinsson, 1977), but, as with the hazards of all the primary classes and subclasses, enormous variability exists in its potential magnitude and effect.

In order to assess the potential adverse effects of a geologic hazard, the following factors must be evaluated: (1) the anticipated magnitude or intensity of the natural event; (2) the size of the area that may be affected; (3) the proximity to, and density of, populated or cultivated areas; (4) the recurrence interval of the event (frequency of occurrence); and (5) the exactness of the event's predictability in time and space. Each of these five factors is relevant to the subclasses of geologic hazards in Iceland, particularly the seismic and the volcanic subclasses.

HYDROLOGIC APPLICATIONS

Lineament analysis for ground-water applications

W. D. Carter and Scott Southworth analyzed lineaments on a Seasat SAR image to assess the potential usefulness of this type of imagery for ground-water applications. Although the Seasat mission was primarily designed for oceanographic monitoring, the SAR imagery was found to be useful for geologic investigations because its view angle enhances subtle morphological features. The SAR is an L-Band (23.5-cm wavelength) system with 25-m resolution.

A Seasat SAR image (revolution 558) of the Culpeper basin, Va., acquired on August 5, 1978, was analyzed. The 100-km wide image swath was produced on a north-to-south descending satellite node with a look direction of N. 67.5° W. The look direction and look angle (20.5°) enhanced the N. 15° E. regional trend. Lineaments were mapped and correlated to well data obtained from the Fairfax County Water Resources Division. Wells with significant yields were located near lineaments mapped on the image; however, other areas with high fracture concentrations were not associated with productive wells. These results indicate that the SAR data must be supplemented with field data, such as data on specific capacity and transmissivity of the aquifer, or data obtained from seismic profiles and subsurface drilling, to effectively identify ground-water exploration targets.

The usefulness of lineament enhancement of Landsat digital data for interpreting ground-water occurrence in Rock County, Minn., was investigated by L. G. Batten (Technicolor Graphic Services, Inc.). Lineaments were extracted through a five-step digital convolution procedure (See "Enhancement, analysis, and interpretation research for geosciences") that creates directionally enhanced images. The primary goal of the extraction was to identify fracture zones within the thick quartzite bedrock. All ground water in the area is produced from fractures because the quartzite is impermeable. Lineament trends on the Landsat images closely matched previously mapped fracture trends, and a series of experimental lineament maps was prepared to aid in ground-water exploration in the county.

Speed of flow of terminus of Pine Island Glacier, West Antarctica

Successive Landsat images of Pine Island Glacier, a tidal outlet glacier in West Antarctica at approximate latitude 75° S., and longitude 101° W., taken on January 24, 1973 (Landsat 1 image 1185-13530), and on February 13, 1975 (Landsat 2 image 2022-13582), were used to measure the speed of flow of the terminus of the glacier. On January 24, 1973, a tidal crevasse had just begun to form transverse to the axis of the glacier. On February 13, 1975, 750 days later, the tidal crevasse had widened, but the geometry of the island side of the tidal crevasse had been retained. By superimposing the Landsat images and using several nunataks for registration, 4.5 km of forward movement was measured over the 750-d period, giving an average daily speed of 6 m.

The 6 m/d average velocity of the terminus of the Pine Island Glacier compares to the 1.8 m/d average velocity (also determined from Landsat images) of the terminus of Skeidarárjökull, an outlet glacier near Vatnajökull, Iceland (Williams and others, 1975) and to the 6 m/d average velocity, determined from field measurements, for Columbia, a tidal glacier in Alaska (R. M. Krimmel, USGS, oral communication). The Pine Island Glacier moves at 30 percent of the 20 m/d velocity of flow of the Jakobshavn Isbrae, a tidal outlet glacier in western Greenland (T. J. Hughes, University of Maine, written communication), the fastest continuously flowing glacier yet measured.

Extent of sea ice in the harbors and bays of Cape Cod

At 9:45 a.m. e.s.t. on February 15, 1979, the Landsat 3 MSS acquired a unique image (30347-14450) of Cape Cod, Mass., and environs, showing the enormous areal extent of sea ice in the harbors and bays of Cape Cod. The extreme sea ice conditions were caused by weeklong northwesterly winds and subfreezing temperatures from an Arctic air mass. These meteorological conditions produced especially heavy concentrations of pack ice in the southeastern Cape Cod Bay.

Although field observations are necessary to measure the actual sea ice thicknesses, the Landsat image was indispensible in showing the true areal extent of the sea ice in the harbors and coastal waters of Cape Cod; a pictorial view of probable conditions in past years of heavy sea ice (such as 1857, 1918, and 1937); and a record indicating those areas on Cape Cod that may require special coastal engineering structures in the future because of heavy sea ice accumulation.

Evaluation of Landsat images of Antarctica

Preparation of the USGS "Satellite Image Atlas of Glaciers" has involved compilation of several specialized Landsat index maps of the glaciated areas of the world. A 1:5,000,000-scale Landsat index map of Antarctica was completed in manuscript form. On this map, each of the Landsat nominal scene centers is represented by a symbol showing the suitability of the best available Landsat images for the preparation of planimetric image maps (and for glaciological studies). From the coastline of Antarctica to approximately 82° S. latitude, 2,470 nominal scene centers were plotted including all 251 paths (orbits) and all or parts of rows 102 to 119.

Landsat images from 1972 through 1980 for each of the 2,470 nominal scene centers were evaluated to identify the best available image. All images were assessed with a preference for low percentage of cloud cover, minimum snow cover in areas of exposed bedrock, and low Sun elevation angle (to maximize morphologic details on the ice sheet surfaces). Results for all nominal scenes were as follows: excellent, 41 percent; good (that is, up to 10 percent cloud cover), 12 percent; fair to poor (that is, 10-90 percent cloud cover), 30 percent; unusable, 5 percent, and no images acquired, 12 percent.

Taking into account both sidelap and image suitability, 70 percent of the Antarctic continent, from the coast to about 82° S. latitude, is represented on high-quality Landsat MSS images that can be used for the preparation of 1:250,000-scale planimetric image maps. Maps of Antarctica at scales of 1:250,000 or larger already exist for 20 percent of the 14 million-km^2 contintent of Antarctica (Swithinbank, 1980).

Irrigation water use in the Columbia River basin

G. E. Johnson, T. R. Loveland, and W. H. Anderson (Technicolor Graphic Services, Inc.), in cooperation with the U.S. Army Corps of Engineers, Portland District, developed and tested techniques for using Landsat and related geographic data to evaluate irrigation agriculture in portions of the Columbia River basin. The methods were applied to the 650,000-ha Umatilla River basin of north-central Oregon. Landsat data were manually interpreted to map increases in irrigation from 1973 to 1979 and then digitally analyzed to identify crop types under irrigation in 1979. The crop-type data then were used in conjunction with historical agricultural data and digital topographic and hydrographic data to estimate water and power use for the 1979 irrigation season. The final project task involved production of a composite map of land suitability for irrigation development based on land cover (from Landsat), landownership, soil irrigability, slope gradient, and potential energy-cost data.

The analyses identified an annual irrigation expansion of over 4,000 ha/yr. Also, for 1979, irrigation water use was estimated at 258,930,000 m^3 for the 50,600 ha of irrigated land, and irrigation power use was estimated at approximatey 300 million kWh of electricty. These

results provided the Corps of Engineers with a quantified assessment of the impact of irrigation on regional resources. In addition, the water and power estimates, along with the composite map of land suitability for future irrigation development, provided the Corps of Engineers with a sound basis for evaluating the expanding irrigation agriculture while monitoring the impact of that development on other essential uses of land and water resources in the Columbia River basin.

LAND-RESOURCE APPLICATIONS

Digital data base for BLM resource planning and management

The Federal Land Policy and Management Act of 1976 requires the BLM to maintain an inventory of resources on public lands. In this regard, BLM requires a low-cost, quick, and accurate means of inventorying vegetation on millions of acres of arid public land in the Southwest.

W. G. Rohde (USGS), W. A. Miller and others (Technicolor Graphic Services, Inc.), and BLM personnel completed a cooperative demonstration project in Mohave County, Ariz. The objective of the project was to determine the usefulness of Landsat data, combined with conventional aerial photographs and data from ground surveys, for mapping and inventorying wildland vegetation. To achieve this objective, project investigators sought to determine the accuracy with which vegetation classes could be mapped from Landsat data using a vegetation classification system supplied by BLM, and to evaluate the utility of a digital data base as an input to the BLM planning process.

The digital data base was comprised of terrain, road network, ownership, Landsat-derived vegetation, and other disparate data. To map the vegetation, Landsat digital data were used to classify 1,000,900 ha of land into 76 classes according to the spectral response of the vegetation cover. When digital terrain data for the area (elevation, slope, and aspect) were combined with the Landsat data, the vegetation map accuracy was improved from 54 to 73 percent. The overall cost for conducting this project was $0.17 per hectare (Miller and others, 1980).

Combining the terrain data with the Landsat data produced a digital data base that could be used to produce map overlays showing suitable areas for different types of grazing, areas of mule deer summer and winter ranges, desert Bighorn sheep and antelope habitats, and pinyon-juniper areas that could be cleared to improve grazing potential. The map overlays were geometrically correct so that they could be used with standard BLM maps to locate areas of interest. After evaluating these preliminary map products, BLM field personnel suggested improvements that would allow the maps to be directly incorporated into the BLM planning process. The BLM personnel needed a more detailed vegetation map, map products at the same scale as their base map (1:126,720), separate maps for the Grand Wash Planning Unit within Mohave County, and more refined overlays to meet specific management objectives.

EDC and BLM completed a cooperative effort to demonstrate the flexibility of manipulating the digital data base to satisfy the needs mentioned. With the assistance of BLM Arizona Strip District personnel, W. A. Miller and D. O. Ohlen (Technicolor Graphic Services, Inc.) developed a new vegetation map and more meaningful management overlays. The BLM was able to replace an existing vegetation map with the one produced digitally and is using the new overlays to locate areas for firewood collection, wildlife re-establishment (Bighorn desert sheep and antelope) and range improvement (Ramey and others, 1981).

EDC and BLM also cooperated in evaluating the level II vegetation map developed for the Mohave County, Ariz., project. This evaluation was initiated in order to determine the accuracy with which Landsat data can be used to map vegetation classes.

John Szajgin and D. S. Linden (Technicolor Graphic Services, Inc.) developed a cost-effective sampling design to meet the objectives set forth for evaluating the map product. The sample design was based on a stratified cluster sampling technique in which there were equal probabilities of selection within strata (Cochran, 1977). The strata were defined by the eight level II vegetation classes represented in the final map product. Ground data were collected for 10 sample clusters within each stratum. In order to assure accurate location of each sample cluster, a detailed field procedure was developed. All pixels in each sample cluster were interpreted to level II on the basis of a vegetation classification framework developed for the Mohave County project.

Overall accuracy of the final map was estimated to be 66 percent with a standard error of 7 percent. Although accuracies ranged from 9 to 90 percent for individual classes, 95 percent of the mapped area included vegetation classes that were greater than 55-percent correct.

Digital data base for mapping forest fuels over broad areas

M. B. Shasby and G. R. Johnson (Technicolor Graphic Services, Inc.) and R. E. Burgan (USFS) investigated methods for producing a digital data base of spatially registered forest fuels and terrain information derived from Landsat MSS data and USGS digital elevation model data. The fuels and terrain data base was developed for a study site in the Lolo National Forest in western Montana and was designed for input to a USFS mathematical fire simulation model that provides site-specific prediction of wildland fire behavior. Applica-

tions of this model range from real-time, site-specific predictions of the rate of spread of a flaming front, to broad-scale regional planning.

The digital analysis techniques, which were used to map six different fuel types and two nonfuel classes, employed both the Landsat MSS brightness values and the digital elevation model data in a "layered" spectral-terrain classification approach. The first level of the layered classifier assigned brightness values of the four Landsat data bands into 48 spectral classes using controlled clustering procedures. After the spectral data were classified, a fuel-type terrain distribution model was designed using discriminant analysis techniques to provide a quantitative characterization of the topographic distribution of fuel types within the spectral classes. A second classification was then performed on a four-band terrain image (elevation, slope, tangent of the slope multiplied by the cosine of the aspect, and tangent of the slope multiplied by the sine of the aspect) to produce the final fuel-type map. The principal road network from USFS engineering maps was digitized and added to this image. The fuels-road network data base was then merged with the elevation, slope, and aspect data to provide the USFS with the necessary data base to drive the fire behavior model.

On the basis of a stratified random sample of 205 pixels, the accuracy of the fuel map classification was estimated to be 68.2 percent (standard error = 3.6 percent). A fuels map based solely on classification of Landsat spectral data was only 52.2-percent accurate and showed only four of the six fuel types present in the study site. The layered classifier, which incorporated both spectral and terrain data, provided a more accurate and representative map of the fuel types.

Digital data base for city- and county-level planning in Sioux Falls area

J. A. Sturdevant (Technicolor Graphic Services, Inc.), in a cooperative demonstration project with the Sioux Falls City and Minnehaha and Lincoln County Planning and Zoning Offices, S. Dak., investigated the usefulness of aerial photographic interpretation and geobased information system techniques for providing city- and county-level planning information. Primary objectives were to conduct a rural land use inventory through aerial photograph interpretation, to determine rural areas suitable for urban development, and to monitor urban tree cover changes through the interpretation of two dates of conventional aerial photographs. Results of the project were maps and statistics useful in the routine planning processes and a greater familiarity, on the part of the cooperating planners, with remote sensing and geographic data analysis.

Color-infrared 1:24,000-scale aerial photographs acquired in July 1979, were used to interpret USGS level II and certain level III land use classes in the immediate Sioux Falls area. The interpretations were digitized and rastorized at the EROS Data Center for inclusion in a digital data base. Overall accuracy of the digital land use data was 86 percent ±5 percent at the 90-percent confidence level. This accuracy was influenced by an interpretation error of 10 percent and a digitizing/rastorizing error of 8 percent.

The digital land use data are being merged with DMA digital terrain data, soils data, and other digital planning information to determine which rural areas are most suitable for urban development. As part of this analysis, the accuracy of the digital terrain data was assessed. Less than 50 percent (at the 90-percent confidence level) of the sampled digital terrain tape elevation values were within one-half the width of the contour interval of a 1:24,000-scale quadrangle. However, 85 percent of the samples were within four confidence intervals, and the slope classification derived from the terrain data was representative of the study area.

The 1:24,000-scale color-infrared and black-and-white aerial photographs were unsuitable as a source of urban tree cover information at the level required by the city planners. Impervious ground surfaces, however, were interpreted satisfactorily from the two dates of photographs, entered into a digital data base, and analyzed for change. These data were found to be useful as surrogate tree cover data in a change-detection analysis of stable residential areas.

Although additional studies are necessary to explore other formats of photography and other methods of accuracy assessment in digital data base applications, these results suggest that geographic information systems and aerial photographic interpretation can be used effectively to provide city- and county-level planning information.

Use of Landsat data to evaluate lesser prairie chicken habitats in western Oklahoma

L. R. Pettinger (Technicolor Graphic Services, Inc.), R. W. Cannon (FWS), and F. L. Knopf (Oklahoma State University) used Landsat digital data to evaluate lesser prairie chicken (*Tympanuchus pallidicinctus*) habitats in western Oklahoma. Field-collected data on the chicken populations and Landsat-derived land cover data were analyzed for four study areas in shinnery oak (*Quercus havardii*) and three study areas in sand sagebush (*Artemisia filifolia*) rangeland using the Interactive Digital Image Manipulation System (IDIMS) at the EROS Data Center. In the shinnery oak rangeland, the density of the prairie chicken population was correlated

positively (r = 0.89) with the proportion of the study area in grassland classes and negatively (r = 0.95) with the proportion in brushland classes. In sand sagebrush rangeland, the population density also was correlated negatively (r = 0.75) with the proportion of the study area in grassland classes and positively (r = 0.76) with the proportion in brushland classes. The relations between the prairie chicken population densities and the land cover classes derived from Landsat data closely parallel relations observed during on-site field measurements of percentage grass and brush. Analysis of Landsat digital data is an effective tool for monitoring vegetative parameters that correlate significantly with lesser prairie chicken numbers over large areas.

CARTOGRAPHIC APPLICATIONS

Landsat image maps of Cape Cod

Four Landsat 3 RBV images of Cape Cod and environs were mosaicked to serve as a 1:100,000-scale base for the "Geologic Map of Cape Cod," compiled by Robert N. Oldale (USGS), and as a prototype 1:100,000-scale image of the northeast quadrant (New Bedford quadrangle) of the 1:250,000-scale Providence, R.I., 1°×2° National Topographic Map Series quadrangle map. Careful geometric control was maintained during the assembly of the mosaic by registering the image mosaic to a control base. The control base was created by optically transferring known ground control points identified on vertical aerial photographs to the Landsat 3 RBV images of the same area. Photogrammetric measurements of the control points on the four Landsat 3 RBV images established that the root mean square error (RMSE) from true geographic position of the control points was 34 m. An RMSE of 33 m is the maximum permissible for image maps at a scale of 1:100,000 under existing National Map Accuracy Standards of the United States.

DIGITAL IMAGE PROCESSING

Multidimensional histogramming

Software to perform multidimensional histogramming has been implemented and documented for the Interactive Digital Image Manipulation System (IDIMS) in the EROS Data Center Data Analysis Laboratory by Sue Jenson (Technicolor Graphic Services, Inc.). The software was completed as part of a contract with Dr. Jack Bryant (Texas A&M University).

A multidimensional histogram is a valuable tool for investigating the spectral structure of a data set. Histogram tables also reduce the volume of computer storage because they represent spectral information more compactly, thus reducing time required to process the data. The histogramming technique, which is based on an efficient hashing scheme, fills a histogram table that is wholly contained in the computer's main memory. The resultant histogram table is then accessible to other programs that process spectral data, such as clustering algorithms and classifiers. In addition, an analyst can determine some characteristics of the data set, such as the number of histogram bins in the data, the number of bins that have a count of one or two, which bins have many members, and if the bins correspond to the centers of classes of interest. Multidimensional histograms contribute to the understanding of spectral dimensions and relations in data sets.

Remote image processing systems

H. L. Wagner, L. Nady, and G. R. Hansen (Technicolor Graphic Services, Inc.) are engaged in an ongoing study to develop hardware and software techniques necessary for the construction and deployment of microprocessor-controlled remote-site image analysis hardware systems. The use of these systems will permit cheaper and more widespread access to digital Landsat data analysis techniques via telecommunications networks. Significant results in 1980 were

1. Design and construction of a low-cost image processing terminal device based on commercially available microprocessor modules.
2. Demonstration of the feasibility of image transmission using standard voice-grade telephone systems and acoustically coupled modems.
3. Development (in conjunction with Jack Bryant of Texas A&M University) of an efficient data compression technique that permits a data transmission rate for Landsat nearly twice as high as that provided by regular transmission equipment.
4. Development of a standard rides information exchange protocol that permits remote processing sites to be efficiently controlled by a centralized information network.
5. Development of FORTRAN language software that allows a wide range of image analysis tasks to be performed on a low-cost microprocessor.

Registration using fast fourier transform

J. M. Thormodsgard (USGS) and Kenneth Crouse (Technicolor Graphic Services, Inc.) developed an automatic method for locating control points in a production environment. This method was developed in response to the need for products that require image-to-image registration and because experience has shown that relying entirely on the manual location of control points on an interactive display system is not always

cost-effective or accurate. The automatic method is especially applicable to projects requiring temporarily registered MSS or RBV data, to MSS-to-RBV registration, and to locating ground control points overlapping areas of images to be mosaicked.

This method of locating control points is based on a correlation of radiometric values. Given an initial approximate location in both images, a window is formed around these locations. The technique involves computing the fast fourier transform (FFT) for each window, multiplying the values together, and then computing the inverse FFT of this product. A search of the resultant window for the location of a maximum correlation is performed to determine the refined control point. Use of this method has greatly enhanced the ability to register different data sets.

Film recorder response contouring

H. E. Lockwood, J. E. Boyd, and W. J. Happel (Technicolor Graphic Services, Inc.) extended the applicability and usefulness of the radiometric lookup tables used to control the system transfer function of the EROS Data Center laser beam film recorder. Formerly, the lookup table implemented a transfer response common to all four Landsat MSS bands of a complete scene, a response curve tailored to emphasize a selected portion of the total brightness range. As a result of this research, the lookup table function in the preprocessing of image data was recognized as having additional versatility and power. More effective application of the lookup table required that the transfer function be specified for each band, with different apparent gammas, film speeds, and maximum densities. To determine the individual transfer functions, it was only necessary to obtain tricolor density measurements of the stepwedge in the reference images. Then the test transfer functions, implemented in three lookup tables, were modified empirically on the basis of visual comparison of reference and test image.

A solution was found for a specific color problem that could not be eliminated by manipulation of the three transfer functions. The difficulty was that orange-red features on the reference images appeared to have a magenta hue on the test scenes. The desired orange-red hue was obtained on the test images by exposing the band 7 (red) positive separation to band 5 (green) light for approximately one-eighth of the normal band 5 exposure time.

Analysis showed remarkable similarity between the test and the reference images, although the latter were produced on a different type of film having substantially higher gamma, different processing chemistry, and different developing rates.

APPLICATIONS TO GEOLOGIC STUDIES

Analysis from thermal-satellite data

Analysis was made of a nighttime thermal image from the experimental satellite HCMM (Heat Capacity Mapping Mission) with a detailed map of hydrothermal features of Yellowstone National Park by R. L. Smith and R. L. Christiansen using a zoom transferscope. The analysis indicates that nighttime thermal satellite data at this resolution (500 m) are unlikely to be useful for detecting and mapping hydrothermal features due to the dominating effects of other factors, for example, elevation, slope, exposure, rock type. Of greater interest was the general correlation between the caldera outline and some thermal anomaly lows and a pronounced thermal anomaly that coincides with that part of the gravity field map that bounds the southwestern side of the caldera. This latter feature has no obvious counterpart in the Landsat images and occurs in the general vicinity of one of the two low-velocity zones discovered recently with extensive seismic profiling. New developments included a new thermal-inertia mapping algorithm, a new method to derive regional meteorologic parameters solely from remotely sensed data, an algorithm for determining the sensible heat flux from ground-station data, and a fast topographic correction algorithm, which can be used in conjunction with DMA digital terrain tapes to correct thermal images for simple topographic effects.

Thermal-inertia mapping

A method based solely on remote-sensing data has been developed to estimate those meteorological effects that are required for thermal-inertia mapping. It assumes that the atmospheric fluxes are spatially invariant and that the solar, sky, and sensible heat fluxes can be approximated by a simple mathematical form. Coefficients are determined from least squares method by fitting observational data to our thermal model. A comparison between field measurements and the model-derived flux shows that good agreement can be achieved under clear sky conditions.

Thermal energy at Mount St. Helens

J. D. Friedman reported that qualitative (and some calibrated) infrared images in the 8 and 11.5 and 8–14 micrometer spectral region were obtained over Mount St. Helens by forward-looking and vertical-mount aerial scanning systems on May 31, June 3, 6, 7, 8, and 19, July 15, and August 11, 12, 13, and 20, 1980. These images depict the spatial pattern of high thermal emission associated with the crater and vent area on June 7 and 8. The images of June 19 showed a concentric and an-

nular distribution of thermal emission associated with the emergent dome. On June 19 the emergent dome, the rampart, and southeast-striking fracture controlling alinement of fumaroles within the crater floor area were recorded in detail, using three different scanning systems. Infrared images of July 15 showed the annular and radial fracture pattern of the dome prior to its partial destruction on July 22. An en echelon set of northwest-striking fractures in the crater and amphitheater region, discernible on the July 15 image, appeared to control the location of the first and subsequent lava domes and at least two of three smaller hot spots. The calibrated surveys of August 13–17 gave the temperature of the rind or partly cooled carapace of the August dome and the day-night temperature differences of an array of pyroclastic flow deposits, as well as the temperature of Spirit Lake, several secondary or phreatic fumaroles, and surrounding terrain.

The heat content per unit mass of the June dome was estimated from laboratory measurements of thermophysical properties of fragments ejected from the dome or protodome, supplemented by recently published data on latent heat of fusion. The bulk density (ρ), thermal conductivity (k), thermal diffusivity (α), specific heat (C), thermal inertia (β), and other physical properties of the dacite were determined or calculated in the laboratory. Dry-melt temperatures and magnetite-ilmenite geothermometry permitted a crystallization temperature of 970–990° C to be inferred. The volume of the visible part of the June dome was estimated from vertical aerial photographs made on July 1 and observed uplift after June 15.

The heat content of the solid-phase dacite lava was estimated at 1385 J gm^{-1}. The ancillary heat content of associated volatiles was 140 J gm^{-1}. The thermal energy equivalent of the visible part of the dome is 1.5×10^{16} J, indicating that the evolution of the dome in itself was comparable to an eruption of intermediate magnitude, of intensity IV on the Hédervári scale.

The total thermal energy released at Mount St. Helens between May and October 1980 was estimated conservatively at 1.2×10^{25} ergs, about 93 percent of the total volcanic energy released.

Limonitic rocks in the Richfield quadrangle, Utah

The remaining 15 percent of the Richfield $1° \times 2°$ quadrangle have been classified using Landsat data to identify limonitic rocks. Approximately 70 percent of the large limonite anomalies in the quadrangle have been field checked. Of those checked, about 50 percent proved to be related to hydrothermal alteration; these were predominantly in the strongly limonitic category as determined by the classification procedure. Other areas having strong limonitic signatures are related to hematitic residual soils (terra rosa?) on carbonates, unaltered pink volcanic tuffs, maroon argillites and quartzites, and oxidized B horizons in valley-fill materials. Several small areas of weak limonite, predominantly in vegetated terranes where outcrops were small (generally < 160 m across), proved to be hydrothermally altered. Some mineralized areas were not classified due to the adverse effects of shadows in rugged terrane, small outcrop area (< 80 m), lack of a limonitic signature, or the masking effect of vegetation. Vegetation cover greater than 40 to 50 percent effectively masks the limonitic signature. Limonitic stains due to surface weathering of black shales also showed characteristic weak limonitic signatures.

Lineaments in the Lewiston–Sherbrooke quadrangle, Maine

Lineament mapping of Landsat images of the Lewiston-Sherbrooke 2° quadrangle has revealed several large (.5–1.5 km wide and 50–100 km long) lineaments trending northwest to west-northwest. These trends are normal to the structural grain of the region and may represent the presence of some structures such as strike-slip faults.

Structural studies in the Pennsylvania Appalachian Mountains

Lineament analysis of Landsat RBV (Return-Beam Vidieon), MSS (Multispectral Scanner), and HCMM (Heat Capacity Mapping Mission) images of Pennsylvania has been used to locate target areas of possible structural complexities in the Allegheny Plateau, the Valley and Ridge, and the transition zone between these two provinces. Coordinated field studies have succeeded in locating megascopic and mesoscopic structures and in recognizing several types of structural disruptions, some which are probably undescribed in the geologic literature. These studies reveal that there are a limited number of types of structural disruptions in the Appalachians of Pennsylvania and that these disruptions (faults, folded faults, faulted folds) exist in all sizes from centimeters to kilometers. The repetition and symmetry of the positions of the mapped disruptions with relation to the Appalachian and Allegheny folds suggest that in many cases the type and location of disruption can be predicted.

Studies in a vegetated terrane

Differences in geologic environments are long term and may be perpetrated in the vegetation as patterns of species distribution. Analysis of forest types that have a restricted distribution and can be mapped by the presence or absence of a single species seems to be the most workable for correlation with the underlying geology. The problem with distinguishing forest types

by remote sensing is that forest composition is highly variable and many species in the middle of their growth range tend to be ubiquitous. Furthermore, the distinguishing spectral properties of a forest type are difficult to predict.

The advantage of principal component analysis is that it presents optimally the subtle variation in the data set. Forest categories were defined by their location on the enhanced image and their spectral characteristics were determined from the image data set. A forest was distinguished in eastern Virginia using principal component analysis of a winter Landsat scene. Study of a late November Landsat scene suggested that small differences between MSS band 4 and MSS band 5 may be responsible for the separation of a chestnut-oak forest unit on the principal component image. The forest is characterized by the presence of chestnut-oak (*Quercus prinus*), but also includes many of the more common northern hardwood trees such as white oak (*Q. alba*) and black oak (*Q. velutina*). Investigations have focused on an area west of Richmond, Va., where the chestnut-oak forest seems to correlate with highly weathered upland gravel deposits near the James River. Chestnut-oak is known to favor elevated, well-drained sites, and soils maps confirm its occurrence on gravelly soil types.

Present work with the Landsat Multispectral Scanner (MSS) data is forming the basis for future multichannel radar-image processing. The ultimate goal is to understand the application of microwave systems to the geology in forested areas. Radar is sensitive to the topography of the forest canopy and to the number, size, and shapes of the volume scatters, the leaves and limbs. Only the diffuse component of the microwave radiation reaches the ground in a dense forest. Research in microwave backscatter has been impeded by the lack of a radar image with adequate gray level response and geometric fidelity. A digital Seasat L-band (25 cm) image, received from the Jet Propulsion Laboratory in February, when enhanced to extend the gray level range and reduce the speckle, showed that variations in the radar correspond more to topography than to forest type in the test area west of Richmond, Va. The correlation to topography on a forested slope was not as obvious as on a nonforested slope. Since trees are nearly vertical with respect to slope, slope differences represent slight thinning of the canopy layer with increasing slope toward the radar. Present theoretical models are not adequate to explain this phenomenon. Examination of the Seasat image revealed that conifers have a higher backscatter than most deciduous forests in a summer image and that two common pine species, Virginia pine (*Pinus virginiana*) and loblolly pine (*P. taeda*) can be distinguished. Although these observations have unknown geologic significance, they may lead to a better understanding of the microwave backscatter process from forested areas.

LAND USE AND ENVIRONMENTAL IMPACT

MULTIDISCIPLINARY STUDIES IN SUPPORT OF LAND-USE PLANNING AND DECISIONMAKING

In recent years, planners, developers, and public officials have begun to appreciate more fully the use and predictive power of earth-science information in day-to-day decisionmaking. Costly blunders such as placing homes in floodplains, hospitals on earthquake faults, and waste-disposal facilities where they contaminate water supplies can be avoided by appropriate application of this information.

Much of the earth-science information required to evaluate impacts of alternative uses of the land and to facilitate related planning and decisionmaking is derived from more than one of the USGS core disciplines—geology, hydrology, cartography, and geography. During the last few years, increased emphasis has been given to multidisciplinary studies that provide specialized and interpretive data that can be understood and used by planners and decisionmakers who may have little or no training in the earth sciences. The research described in the following sections is indicative of the broad range and variety of earth-science information applicable to land-use planning.

Earth-Sciences Data Applications Workshops

Local land-use planners frequently find themselves without necessary data on earth-science factors important to the land-use decisionmaking process. Furthermore, local scientists are not always cognizant of the potential problems facing the planner. Therefore, an Earth-Sciences Data Applications Workshop series was designed to unite these two groups in short courses comprised of lectures, field trips, and a hypothetical but realistic planning exercise.

During fiscal year 1980, applications workshops were conducted in the following cities: Atlanta, Ga.; Houston, Tex.; Orlando, Fla.; St. Louis, Mo.; Columbus, Ohio; and Minneapolis, Minn. Local planning and earth-science problems determined the lecture topics, field trips, and planning exercises. Typical discussions at the workshops included the following topics: (1) the influence of development on water quantity and quality, (2) karst terrain as a constraint for development, (3) slope stability as it affects grading, (4) physical siting criteria for waste-disposal facilities, (5) ground-water models as planning tools for development patterns and waste-disposal facility location, (6) seismicity concerns for various construction designs, and (7) low streamflow conditions and their physical determinants.

The applications workshops require cooperation between the Earth Sciences Assistance Office and the local or State chapter of the American Planning Association, the State Geologist, the WRD District Office, the closest university or college department of planning, and other university departments.

Mineral resources of the Culpeper basin in northern Virginia

The Culpeper geologic basin, a structural trough filled with sedimentary and igneous rocks of Mesozoic age, borders the eastern front of the Blue Ridge some 50 km west-southwest of Washington, D.C. This hitherto rural area is undergoing rapid suburban development in response to urban growth radiating from the Nation's Capital. A mineral-resources map showing current and historic data helpful in making land-use planning decisions has been published (Froelich and Leavy, 1981) as part of a basin-wide series of earth-science maps showing geologic and hydrologic resources.

Commercial mineral extraction began in the Culpeper basin in the mid-1840's after barite was first discovered in the central basin in Fauquier County. For a short time thereafter, Virginia was the leading producer of barium in the United States (Edmundson, 1938). Diabase and basalt, widespread rock resources of the Culpeper basin, are being quarried actively and are used extensively for construction material, highway fill, and building stone according to A. J. Froelich and B. D. Leavy (1981). The abundant red shales in the basin have long been used as a source of clay for brick and tile manufacture. In addition, the study has shown that lesser-known deposits of gray shale apparently have characteristics of lightweight aggregate.

Effect of land use on phosphorus content of lakes, Puget Sound, Washington

R. J. Gilliom developed a quantitative method for assessing the relation between present phosphorus content of lake water, land-use history in the lake's drainage basin, and probable phosphorus loading of the lake under natural (predevelopment) conditions. This method provides a useful and relatively inexpensive means for judging (for lakes in the Puget Sound region and probably for other lakes in similar settings) the phosphorus loading that has accompanied different

types of land development. From this information, the most effective measures for reducing phosphorus loading can be determined.

Some probable effects of major oil spills on various coastal settings, Puget Sound, Washington

R. F. Keuler found that the coastal settings near certain major petroleum spills around the world closely resembled various coastal types in the Puget Sound region, Wash., with reference to geomorphic setting, sediment texture, wave energy, tidal range, and water temperature. Observations of petroleum deposition, storage, and persistence from these previous spills allowed Puget Sound coastal settings to be ranked according to the probable effects of a major spill.

ENVIRONMENTAL IMPACT STUDIES

The Environmental Affairs Office (EAO) provides an integrated USGS response to the requirements of the National Environmental Policy Act (NEPA). The office develops NEPA-related policy and guidance for the USGS; manages USGS technical staffs assigned to other agency environmental impact statements (EIS's); furnishes technical information and expertise to support the preparation of USGS EIS's and other environmental documents; provides technical analysis, review, and comment on environmental documents prepared by other bureaus and agencies; performs specialized studies in support of environmental analyses; and conducts research and training to improve the NEPA process.

ENVIRONMENTAL IMPACT STATEMENTS AND RELATED DOCUMENTS

During fiscal year 1980, USGS had lead or joint-lead responsibility with State or other Federal agencies in the preparation of 10 EIS's. Of the 10, 6 concerned coal mining, 2 petroleum exploration, 1 phosphate mining, and 1 copper-molybdenum mining. The EIS's completed during the year involved potential oil and gas exploration and development in the National Petroleum Reserve, Alaska, and regional impacts of coal development in the northern Powder River Basin, Mont.

The USGS participated in the preparation of 20 additional EIS's under the lead of other bureaus and Federal agencies – the Bureau of Land Management (BLM), the Bureau of Indian Affairs (BIA), the U.S. Forest Service (USFS), the Tennessee Valley Authority (TVA), the U.S. Air Force (USAF), and the U.S. Environmental Protection Agency (EPA). Sixteen of these statements were energy related; two dealt with critical minerals; one dealt with potential forest land management planning; and one concerned the siting of the Air Force Strategic MX Missile.

The USGS also provided technical information to the USFS for one EIS on geothermal energy resources and to BLM for 10 EIS's on oil and gas leasing in the Outer Continental Shelf (OCS).

Environmental impacts emphasized in the environmental statements prepared in fiscal year 1980 under USGS or joint lead included the following:

- Disruption of aquifers.
- Reduction of air quality caused by dust from mining operations and temporarily devegetated ground surfaces.
- Degradation of livestock and wildlife grazing, recreational hunting, and open-space qualities until reclamation is completed.
- Disruption of the existing land surfaces, vegetation, and soils.
- Reduction of future productivity of the disturbed ground.
- Modification of socioeconomic patterns, including permanent increases in population, traffic, roads, powerlines, and buildings; and impacts on public services and recreational facilities.
- Increase of tax and royalty income to the affected States and (or) counties.

In addition, EAO staff members provided technical reviews and comments on more than 1,800 EIS's and related documents to support in-house environmental studies and to assist other agencies in areas of USGS jurisdiction and expertise.

SOCIOECONOMIC ASSESSMENT

Study of change and disorganization in energy-development communities of the Great Plains

R. R. Reynolds, Jr. (USGS), J. G. Thompson (University of Wyoming), L. M. Ostresh (University of Wyoming), and K. P. Wilkinson (Pennsylvania State University) assessed the validity of existing assumptions and hypotheses concerning the effects of rapid community change associated with energy development. An analysis of the literature reveals many conceptual inconsistencies and a lack of empirical support for the general assumption that energy-related "boom" growth produces personal and social disruption. A preliminary analysis of a commonly used disruption indicator (divorce) for the 1970–75 period indicates a weak and indirect relation between the alleged impact and "boom" growth.

Socioeconomic assessment of Cache Creek drilling site

J. G. Thompson (Wyoming Research Corporation) assessed the socioeconomic impacts of oil and gas exploration and production on Teton County, Wyo., and the service base community of Jackson Hole, Wyo. The assessment provides the basic social and economic description and analysis necessary for writing a site-specific EIS and includes a description of the environment; an evaluation of the impacts of the proposed mining activity on the social and economic environment, including the recreational and agricultural industries; specification of unavoidable adverse effects; and specification of irreversible social and economic effects. In contrast to previous EIS-related socioeconomic studies, a social disorganization perspective of the energy-impacted base community was not assumed. Instead, a social change theoretical perspective was applied to the analysis of various data sets to reveal both positive and negative impacts on the well-being of various segments of the population at different points in time. The assessment includes a discussion of potential measures for mitigating negative consequences of development.

Socioeconomic assessment of the Rojo Caballos Mine

J. G. Thompson (Wyoming Research Corporation) assessed the socioeconomic impacts of coal production on Campbell County, Wyo., and the service base community of Gillette, Wyo. The assessment provides the basic social and economic description and analysis necessary for writing a site-specific EIS. The results of the assessment indicate that because the Rojo Caballos mine is but 1 of 8 to 12 major developments occurring simultaneously in Campbell County, potential negative impacts attributable to it are minimal. Some of these impacts are (1) the mine, if developed, will have a negative impact on the fiscal position of the city of Gillette through fiscal year 1985; and (2) the mine will lead to an increase in population, making it difficult to insure an adequate supply of housing. In addition, the mine will contribute indirectly to two cumulative problems affecting the region. One is that the increasing size of the region's population will require a greater complement of medical specialists than are presently found in the region. If this deficiency continues to grow, it could become a major social and political problem in the region. The second is that occupational groups in the region, such as some agricultural operators, retired persons, and low-income groups, are affected more negatively by coal development than other groups. The results of this study are published by the Wyoming Research Corporation (1980).

ASSISTANCE TO ACHIEVE NEPA COMPLIANCE

As the result of a cooperative effort involving input from all USGS Divisions, EAO completed an interim handbook on the NEPA process for USGS program initiatives and permit and regulatory functions. The handbook, which will be used on a trial basis, identifies responsible officials in the USGS and current procedural requirements, including an explanation of Federal and DOI NEPA requirements.

OILSPILL RISK ANALYSES

Oilspill risk analyses (OSTA's) are conducted to determine the relative environmental hazards of developing oil in different regions of the U.S. Outer Continental Shelf (OCS). These studies employ a large mathematical model to analyze the probability of spill occurrences, likely movement of spilled oil, and locations of resources vulnerable to spilled oil. The analyses include estimates of oil degradation rates and slick dispersion paths and indicate the possibilities of mitigating effects by cleanup efforts. The combined results yield estimates of the overall oilspill risks associated with development of proposed lease areas.

OCS lease area

W. B. Samuels and K. J. Lanfear (1980a) conducted an oilspill risk analysis for the South Atlantic (Proposed Sale 56) OCS lease area. The leasing and development of the 286 tracts proposed for Sale 56 will result in an expected 3.0 oilspills over the 30-yr life of the leases. The estimated probability that land will be contacted by one or more spills that have been at sea less than 30 d is 0.50.

Oilspill risk analysis for the mid-Atlantic (Proposed Sale 59) OCS lease area

W. B. Samuels and K. J. Lanfear (1980b) conducted an oilspill risk analysis for the mid-Atlantic (Proposed Sale 59) OCS lease area. If oil is found, the leasing and development of the 253 tracts proposed for Sale 59 will result in an expected 14 to 19 oilspills over the 30-yr life of the leases, depending on the routes chosen to transport the oil to shore. The estimated probability that land will be contacted by one or more spills that have been at sea less than 30 d is 0.39 to 0.64, depending on the chosen transportation method.

Oilspill risk analysis for the Cook Inlet and Shelikof Strait, Alaska, (Proposed Sale 60) OCS lease area

R. P. LaBelle, W. B. Samuels, and K. J. Lanfear (1980) conducted an oilspill risk analysis for the Cook Inlet and Shelikof Strait (Proposed Sale 60) OCS lease

area. If oil is found, the leasing and development of the 153 tracts proposed for Sale 60 will result in an expected 4.0 oilspills over the 30-yr life of the leases, depending on the routes chosen to transport the oil to shore. The estimated probability that land will be contacted by one or more spills that have been at sea less than 30 d is 0.96.

INTERNATIONAL ACTIVITIES IN THE EARTH SCIENCES

The year 1980 marked the 40th year that the USGS has been actively involved with earth-science studies in other countries. The early investigations were concerned with strategic mineral supplies, and this activity grew into programs designed to provide technical assistance to developing countries. In the last few years there has been a significant shift in interest to scientific cooperation and research agreements as extensions of the USGS domestic activities. The USGS presently has 30 cooperative research agreements, including 2 regional, in addition to 27 technical assistance programs, including 4 regional. The USGS also undertakes energy-resource studies on behalf of the DOE and the AID. Representational duties at international congresses, unions, and symposia round out the foreign program of the USGS.

Technical assistance and training programs are undertaken at the request of other U.S. agencies, other governments, or international organizations, as authorized by the Foreign Assistance Act. Scientific and technical cooperation generally results from mutual interest in specific research, from governmental initiatives, scientist-to-scientist correspondence, or combinations of these. Table 1 shows the personnel assigned to other countries during the fiscal year. Participation and representation in international organizations, commissions, and congresses generally grow out of U.S. foreign policy interests.

Decisions to undertake international assistance, exchange, or other activities are based in part on (1) whether the work provides opportunities for studying and obtaining information about geologic and resources phenomena of interest to the USGS; (2) whether the work will broaden the knowledge, understanding, expertise, and international reputation of the USGS staff; and (3) how the work supports political, economic, or strategic interests of the United States as defined by the Department of State.

Thus it can be seen that a large part of the USGS international work is actually an extension of its domestic program and is important to U.S.-foreign policy objectives.

TECHNICAL ASSISTANCE AND PARTICIPANT TRAINING

All USGS technical assistance projects are undertaken basically in support of U.S. foreign policy and on a reimbursable basis under authority of the Foreign Assistance Act. Current projects range from multidisciplinary activities involving nearly 40 man-years of work per year to small single-discipline projects involving only a few man-months per year.

Projects providing some type of technical assistance to developing countries currently are active (fiscal 1980) in 20 countries and 4 regional organizations. Some are described in the section "Summary by country or region." Much of the work is concerned with identifying and assessing natural resources, geologic hazards prediction and mitigation, and strengthening of indigenous earth-science agencies or institutions. Since 1940 more than 2,944 technical and administrative documents describing USGS international work have been authored or closely supervised by USGS personnel. During fiscal 1980, 30 administrative reports were issued and 54 map/reports were published (table 2).

Conventional energy resources of selected developing countries were assessed by the USGS under two programs supported by other Federal agencies: (1) the Department of Energy (DOE) and (2) the Agency for International Development (AID). The programs are coordinated by M. J. Bergin.

For the DOE program, which is authorized under Title V of the Nuclear Non-Proliferation Act of 1978, the USGS assesses the resources of fossil fuels (oil, gas, coal, oil shale, and tar sands), nuclear raw materials, geothermal energy, water, and energy-related minerals that are indigenous to a particular country. Country assessments are accomplished by first compiling and evaluating the available published information on the country's energy resources (commonly referred to as phase I studies). As phase II, a team of five to eight specialists, generally recruited from the USGS domestic program, visits the country to work with counterparts in collecting additional unpublished information, examining deposits and field localities, and preparing an assessment of the resources. This assessment is incorporated into a report by DOE that, on the basis of a supply-demand analysis of all potential energy sources, evaluates the energy options open to the country and forms a basis for the country to make policy decisions on its energy production and development. During FY 1980, phase I and II studies were conducted for Argentina, Portugal, and South Korea; more specific information is reported in the section on selected activities by

TABLE 3.—*Technical assistance to other countries provided by the USGS during FY 1980*

Country	USGS personnel assigned to other countries			Scientists from other countries trained in U.S.	
	Number	Title	Type of Program[1]	Number	Field of Training
Latin America					
Argentina	3	Geologist	A, B	1	Uranium geology
	1	Geophysicist	B	1	Geological interpr.
	1	Physical scientist	A	1	Remote sensing
Brazil	1	Geologist	C	1	Radioactive tracers
				1	Hydrometry
				1	Geochronology
				1*	Geophysics
				1*	Geology
Chile	--			1	Aerial radiometric prosp.
				2	Remote sensing
				1	Explor. data processing
Costa Rica	--			1	Remote sensing
Guatemala	1	Hydrologist	B		
Guyana	--			1	Mineralogy
Mexico	1	Hydrologist	B	1	Digital image processing
	3	Geologist	C	4	Remote sensing
Nicaragua	--			1	Geology & geophysics
				2	Seismology
Peru	3	Geologist	C		
	1	Geophysicist	C		
Venezuela	1	Geophysicist	C		
Africa					
Benin	1	Physical scientist	C		
Cameroon	--			1	Remote sensing
Congo	--			2	Remote sensing
Egypt	2	Geophysicist	C	1	Field geologic mapping
	3	Geologist	C	5	Remote sensing
				1	Geochemical lab. tech.
				1	Geologic interpr.
				2	Analytical chem. tech.
				1	Geophysical elect. meth.
Gambia	--			3	Hydrology
Kenya	1	Geologist	C		
Morocco	--			2	Remote sensing
Nigeria	--			1	Cartography
				5	Remote sensing
Togo	--			1	Geomagnetic methods
Tunisia	1	Cartographer	C	3	Remote sensing
	1	Photo. technician	C		
	2	Remote sensing spec.	C		
Near East and South Asia					
Bangladesh	--			1	Ground water & admin.
				1	Hydrologic management
				2	Hydrogeology
				1	Geochemistry
				1	Geochemical explor.
India	--			1	Mathematical modeling
				3	Remote sensing
				3	Ground water
				1	Geophysics
				3	Uranium geology
				1	Microearthquake
				1	Geochemical
Israel	--			2	Remote sensing
Jordan	2	Geophysicist	C	1	Mineral development
	1	Hydrologist	B	3	Hydrology
Oman	1	Geologist	C		
Pakistan	--			5	Hydrologic equipment
				1	Uranium exploration

See footnote at end of table.

TABLE 3.—*Technical assistance to other countries provided by the USGS during FY 1980*—Continued

Country	USGS personnel assigned to other countries			Scientists from other countries trained in U.S.	
	Number	Title	Type of Program[1]	Number	Field of Training
Near East and South Asia—Continued					
Saudi Arabia	16	Geologist	A, B, C	6	English
	7	Geophysicist	A, C	1	Geo. administration
	1	Supply specialist	C	2	Academic
	1	Supply assistant	C	3	Business administration
	1	Mathematician	C	2	Administration
	1	Chemist	C	1	Computers
	7	Technical advisor	A, B, C	1	Health physics
	3	Computer specialist	C	1	Spectroscopy
	1	Cartographer	C	1	Computer sciences
	2	Hydrologist	C	1	Computer techniques
	1	Physicist	A	1	Seismology
				1	Fission track studies
				2	Cartography
				1	Management training
				1	Computer programming
				1	Geologic interpret.
				1	Geophysical tech.
				2	Industrial spectroscopy
Syria	--	--	--	3	Remote sensing
				1	Exploration geophysics
				1	Aerial photo-mapping
Turkey	1	Geologist	A	2	Remote sensing
				1	Ground water
				1	Well design & const.
				1	Data base mang. stst.
				1	Uranium exploration
				1	Copper deposits
				1	Stratiform chromites
Yemen	1	Hydrologist	B	2	Remote sensing
Far East and Pacific					
Australia	--	--	--	1	Remote sensing
				1*	Spectrochemical tech.
				1*	Sand dunes
				1*	Geochemistry
China					
Mainland	--	--	--	2, 1*	Geophysics/seismology
				1*	Impact metamorphism
				1*	Coal petrology
				1*	Geothermal research
				1*	Earthquake prediction
				2*	Seismology
				1*	Tectonics
Taiwan	--	--	--	1	Remote sensing
				1	Ground water hydrology
Indonesia	3	Geophysicist	C	1	Geophysics
	6	Geologist	C		
	1	Physical sci. tech.	C		
	1	Environmental scient.	C		
Japan	--	--	--	4	Remote sensing
				1	Water quality
				1*	Geophysics
				1*	Electromagnetism/geomag.
				1	Geologic interpr.
				1*	Landslides
Korea	5	Geologist	A, C		
	1	Geophysicist	A		
	2	Physical scientist	A		
	1	Mining Engineer	A		
	1	Hydrologist	A		
Malaysia	6	Geologist	A, C	1	Remote sensing
	1	Engineer	C		
	1	Petroleum engr. tech.	C		

See footnote at end of table.

TABLE 3.—*Technical assistance to other countries provided by the USGS during FY 1980*—Continued

Country	USGS personnel assigned to other countries			Scientists from other countries trained in U.S.	
	Number	Title	Type of Program[1]	Number	Field of Training
Far East and Pacific—Continued					
New Zealand	--	----------	----------	1*	Engineering geology
				1*	Digital image processing
				1*	Crustal movements
Oceania	1	Geologist	C		
Philippines	6	Geologist	A, C	2	Remote sensing
				1	Geologic interpretation
Singapore	3	Geologist	A, C		
Sri Lanka	1	Geophysicist	C	1	Remote sensing
Thailand	8	Geologist	A, C	1	Remote sensing
	1	Geophysicist	A	1	Data processing
Europe					
Austria	1	Geologist	C		
France	2	Geologist	C	1*	Seismology
				1*	Tectonophysics
				1*	Geophysics
				1	Digital image processing
				1	Marine geology
Germany	--	----------	----------	1*	Geothermal energy
				1*	Study networks mont. faults
Greece	--	----------	----------	1	Seismotechnics
Hungary	--	----------	----------	1*	Sedimentation
				1*	Seismic risk
				1*	Electromagnetic meth.
				1*	Seismic modeling
				1*	Geophysics
Italy	1	Research forester	C	1*	Geothermal research
	1	Geophysicist	C	1	Remote sensing
				1*	Geochemistry
				1*	Seismology
Netherlands	--	----------	----------	1	Digital image processing
Poland	3	Geologist	A, C		
Portugal	5	Geologist	A		
	3	Geophysicist	A, C		
	2	Hydrologist	B		
Spain	1	Geologist	C	1	Principles of data proc.
Sweden	1	Hydrologist	C		
Switzerland	1	Geologist	C		
United Kingdom	2	Geologist	C	1*	Astrogeology
				2*	Petrochemistry
Yugoslavia	1	Geophysicist	C	1	Data processing
Other					
Canada	1	Geologist	C	1	Tectonophysics
Iceland	--	----------	----------	1*	Geochemistry
				1*	Data processing
Jamaica	--	----------	----------	1	Organic petrology

*Visiting scientist.

[1] A, Geologic mapping and resource appraisal; B, Studies of hydrologic phenomena; C, Other assistance in developing or strengthening earth-science institutions.

country or region. Preliminary phase I investigations also were made for the Philippines and Venezuela.

As part of an effort to identify and evaluate the energy resources, reserves, and range of energy production capabilities of countries throughout the world, DOE requested that the USGS, collaborating with the DOE personnel, conduct a program aimed at collecting and analyzing appropriate geological information. The ultimate objective of this interagency agreement is a quantified evaluation of world energy resources. The scope of the Foreign Energy Supply Assessment Program (FESAP) is to assess only the oil and natural gas resources of selected countries. Should it be deemed desirable, substitute countries may be selected by the USGS and the DOE. In subsequent years, additional countries may be included in the FESAP studies.

TABLE 4.—*Technical and administrative documents issued during FY 1980 as a result of USGS technical and scientific cooperation programs.*

Country or region	Reports or maps prepared			
	Project and administrative reports	Approved for publication by counterpart agencies or USGS	Published	
			In technical journals	By USGS
Australia	1	--	--	--
Africa	--	--	--	1
Brazil	--	1	--	2
CENTO	--	--	1	--
Chile	--	1	--	--
China	--	2	--	1
Circum Pacific	--	1	--	1
Colombia	--	1	--	1
Costa Rica	--	1	--	--
Egypt	4	2	--	1
Greece	--	--	--	1
Indonesia	5	--	1	1
Jordan	1	1	--	1
Kenya	--	--	--	1
Liberia	--	--	--	1
Morocco	1	1	--	1
Pakistan	--	2	--	3
Peru	--	--	1	--
Philippines	--	--	--	1
Poland	--	--	2	--
Saudi Arabia	14	17	10	16
Spain	--	--	1	--
Tunisia	1	--	--	--
Turkey	--	--	--	1
Venezuela	1	1	--	1
Yemen	--	1	--	1
General	2	5	--	2
Total	30	37	16	38

Countries for which work has been done in FY 1980 include Brunei-Malaysia, China, Indonesia, Iraq, Kuwait-Neutral Zone, Mexico, Nigeria, Oman-Dubai, Saudi Arabia, UAE-Abu Dhabi-Qatar-Bahrain, Venezuela, and Trinidad.

The USGS is in the forefront of the rapidly developing field of resource data systems and resource investigations. There are increasingly numerous requests, mostly through the Department of State, from foreign governments and regional and international organizations for help in evaluating their resource data system needs and in devising and implementing data systems to meet their needs. At the request of and sponsored by the Committee for Coordination for Joint Prospecting in Asian Offshore Areas, and in cooperation with the International Union of Geological Sciences, the USGS also assisted Indonesia, Korea, Malaysia, Philippines, and Thailand.

In September 1980, the USGS entered into an agreement with the AID to assess by literature surveys the conventional energy resources (principally, but not restricted to, oil, gas, and coal) for some 60 developing countries. Along with the assessment of known and potential energy resources, assessment also is to be made of educational and training needs, technical assistance in program planning and implementation of exploration and development techniques, and cooperative work on projects providing on-the-job training.

Training activities related to international work commonly stem from, or are an integral part of, projects carried out under one of the major international programs. The training is provided in a variety of forms: (1) as formal regularly scheduled special classes at the USGS facilities in the United States; (2) as formal courses in foreign countries presented by the USGS instructors under the auspices of international organizations or other U.S. Government agencies; (3) as on-the-job training at the USGS facilities in the United States in which the trainee works essentially as a member of a USGS project; (4) as on-the-job training in which USGS scientists and foreign scientists work together as counterparts on a technical assistance project; and (5) as formal courses at colleges and universities in which the USGS provides guidance and assistance in selection of schools and courses and provides administrative and logistical support for the trainee. Table 3 lists the USGS courses.

Training offered at Flagstaff, Ariz., represented new courses in advanced work. To augment training already available in digital image analysis, the USGS now has a course scheduled in the "Principles of Data Processing for Earth Scientists," which was first offered in 1980. Although training programs continue to involve the largest number of foreign nationals, exchange of scientists under the terms of the Exchange Visitor Program continues to grow in size and scope (see table 1). Exchange activities during Fiscal Year 1980 with scientists from 11 countries included research in geophysics, seismology, marine geology, engineering geology, geothermal studies, and petrology. During fiscal 1980, 189 earth scientists from 46 countries pursued academic, observation, or interim training in the United States.

All technical assistance programs of the USGS have institutional development as one of the major goals; such institutional development is essential to effective transfer of technology and to achieving long-range benefits from such programs. Close ties that develop between the USGS staff and foreign counterparts, though intangible, are significant benefits that accrue to the USGS, and the field training programs in foreign countries provide many significant direct benefits to the USGS instructors; such courses also provide opportunities to study geologic phenomena that relate to domestic activities under environmental conditions that may not be present in the United States.

TABLE 5.—*USGS training courses presented during FY 1980*

Course title	Course dates	Course location	No. of attendees	Countries and areas represented
13th International Remote Sensing Workshop–Introductory	Sept. 10–Oct. 5, 1979	EROS Data Center Sioux Falls, S. Dak.	20	Australia, Cameroon, Congo (2), Egypt, India, Japan (3), Philippines, Saudi Arabia, Sri Lanka, Syria (3), Thailand, Turkey, Yemen (2)
14th International Remote Sensing Workshop–Introductory	May 5–May 30, 1980	EROS Data Center Sioux Falls, S. Dak.	9	Chile (2), Egypt (2), Mexico (2), Syria, Taiwan, Tunisia
Land Use Planning and Environmental Applications	Oct. 8–Nov. 9, 1979	USGS Flagstaff, Ariz.	3	Thailand, Yemen (2)
Digital Image Processing	Feb. 11–Mar. 7, 1980	USGS Flagstaff, Ariz.	2	Mexico, Netherlands
Geologic Interpretation	June 3–July 3, 1980	USGS Flagstaff, Ariz.	6	Argentina, Egypt, Japan Philippines, Saudi Arabia, Tunisia
Principles of Data Processing for Earth Scientists	Feb. 2–Feb. 4, 1980	USGS Reston, Va.	4	France, Spain, Thailand, Yugoslavia

SCIENTIFIC AND TECHNICAL COOPERATION AND RESEARCH

Activities in the category of scientific cooperation and research range from informal scientist-to-scientist exchange by means of discussion and correspondence, through formal, jointly funded, jointly staffed cooperative research projects, to multinational projects focused on a particular problem or topic and coordinated internationally. The majority of such activities are funded on the basis that each side pays its own expenses.

International cooperation in scientific research plays an important role in the USGS in broadening the base of experience of individual scientists, in providing for exchange of ideas and information that is essential to healthy scientific research, and in providing opportunities to study relevant geologic phenomena in a variety of geologic settings and different climatic conditions.

All activities under the category of scientific cooperation and research are regarded primarily as extending or enhancing elements of the domestic program. The program includes a wide range of topical research carried out under the sponsorship or coordination of international and regional organization and under bilateral agreements with 19 countries.

EARTHQUAKE HAZARDS REDUCTION PROGRAM

The Earthquake Hazards Reduction Act of 1977 (P.L. 95–124), in authorizing the National Earthquake Hazards Reduction Program, stated that "The research elements of the program shall include . . . studies of foreign experience with all aspects of earthquakes." Given this authority, the USGS developed cooperative agreements for earthquake research with the Soviet Union and China, and sponsors earthquake research efforts in Mexico, Australia, Iceland, and Venezuela. Most of these research projects are carried out by non-USGS personnel under contract through universities.

A cooperative program with the Soviet Union is carried out under the U.S./U.S.S.R. Joint Committee on Cooperation in the Field of Environmental Protection. This agreement is administered by the EPA; the USGS works closely with that agency in the conduct of the program. A joint agreement for cooperation in earthquake research between the National Science Foundation, the USGS, and the State Seismological Bureau of the People's Republic of China was signed late in January 1980; in 1980 the USGS had primary responsibility for two specific projects dealing with earthquake predictions and geologic studies of active faults. In addition, the USGS maintains a network of some 120 seismographs at various cooperating institutions throughout the world. These networks originally were established by the Defense Department as the Worldwide Standard Seismograph Network (WWSSN) and the Global Digital Seismograph Network (GDSN). The equipment at these stations was given to the cooperating institutions with the understanding that the local institution will operate the station and the USGS will provide supplies, spare parts, and maintenance visits. Data from these stations are sent to the USGS for copying and are returned to the cooperating country.

Through its Disaster Assistance Office, the AID sponsors USGS disaster-related programs. One in Guatemala is designed to study the relation between tectonic movements and caldera formation based on data col-

lected from four caldera lake bottoms. Also sponsored by AID, a planning study by the Office of Earthquake Studies was made of a proposal for Earthquake Hazard Mitigation in Southeast Asia.

CIRCUM-PACIFIC MAP PROJECT

The Circum-Pacific Map Project intends to show, in a set of eight map series at a common scale (1:10,000,000) and projection (equal-area), coordinated geologic and resource data for the Pacific basin and the peripheral continental areas that were affected by geological phenomena in the development of the basin during the Mesozoic and Cenozoic. The project's original objective to compile available factual data was modified to permit the derivation of new data sets (such as magnetic lineations and surficial sediments on the sea floor). Five panels, one for each quadrant of the Pacific region and one for Antarctica, are compiling the thematic maps of their respective quadrants (1:10,000,000); and they also contribute data for composite Pacific basin maps at a scale of 1:20,000,000. The chairman of these panels are Chikao Nishiwaki of Japan (Northwest), Fred Doutch of Australia (Southwest), Campbell Craddock of the United States (Antarctica), José Corvalan of Chile (Southeast), and Kenneth Drummond of Canada (Northeast). The USGS participation involves the overall coordination of the project, as well as expert consultation and final cartographic work; the USGS also hosts an annual Panel Chairmen's Meeting. The set of maps will comprise the following thematic series: plate-tectonic, geologic, tectonic, geodynamic, mineral resources, and hydrocarbon resources. In 1980, six geographic maps and six base (plotting) maps were published.

During the year, color proofs of the 1:10,000,000-scale Northeast Quadrant Plate Tectonic Map, which is the pilot map in the plate tectonic series, were completed. Preliminary maps of the other three quadrants and Antarctica showing plate boundaries and plate motion vectors were completed by G. W. Moore. The plate tectonic series, which will be the first thematic series to be published, depicts active plate boundaries, major intraplate faults, plate-motion vectors, seismicity, Holocene volcanic activity, and magnetic lineation on the sea floor.

BILATERAL PROGRAMS

Bilateral projects of technical cooperation and research, which range widely in scope, are carried out under a variety of funding arrangements. In several countries in which the United States has excess foreign currency, cooperative research programs are funded out of joint deposits into a Special Foreign Currency Program (SFCP) fund. Poland is funded under the SFCP, and Yugoslavia is funded jointly by the United States and Yugoslavia under the SFCP. A 5-yr extension has been approved.

A variety of contacts, both informal and formal, contributed to the drafting of two agreements with the People's Republic of China (PRC). The growing relation between the U.S. and PRC geoscience communities has included mutual exchange visits; in the fields of general geology, paleontology, marine geology, coal geology, and seismology, 31 Chinese were hosted by the USGS and 23 USGS personnel visited the PRC. The exchanges included substantive discussions on possible future project work and culminated in Director Menard's visiting Beijing in January 1980 and signing two Protocols—one in earthquake studies (See Earthquake Hazard Reduction Program) and one in earth sciences. The joint working group stipulated by the Earth-Sciences protocol met in Beijing during June and began negotiation on specific project proposals.

The USGS and the National Environment Research Council (NERC) of the United Kingdom have undertaken 5 yr of bilateral cooperation in the geological, geophysical, and oceanographic sciences and related technology.

The USGS and the Service Géologique National (SGN) of the Bureau des Recherches Géologique et Minières (BRGM) of France entered into an agreement in January 1979 for cooperation in the field of geophysical sciences. The agreement provides for technological exchange in geophysics applied to regional geologic studies, exploration for and evaluation of mineral and energy resources, seismo-tectonics, geologic hazards, engineering, and underground storage. Activity under the agreement has consisted of short-term visits between the two parties and a 10-mo assignment of a USGS geophysicist (M. F. Kane) to BRGM in Orleans. The agreement terminates in 3 yr unless extended by mutual agreement.

For many decades there has been frequent and significant scientific and technical cooperation between scientists of the USGS and scientists in counterpart scientific organizations in Iceland. A Memorandum of Understanding (MOU) between the USGS and Iceland is currently in the review stage. The MOU is directed at the strengthening of technical exchange of scientists and scientific information between Iceland and the USGS, especially in the following subdisciplines of geology having particular relevance to the USGS: geothermal, volcanology, seismology, structural geology and tectonics of a rift zone, glaciology, hydrology, geologic hazards, geochemistry, geophysics, astrogeology, petrology and mineralogy, paleomagnetism, gravity, and aerial and satellite remote sensing. Iceland occupies a unique location with respect to the evolution and

testing of modern geological concepts, is a major geological laboratory for scientists from many nations, and provides an especially good opportunity for cooperative scientific research of mutual benefit to the USGS and Icelandic scientists.

Since 1966, the USGS has been involved in an aerial and satellite remote sensing study of dynamic geological phenomena and geologic hazards of Iceland, especially in the study of volcanism, geothermal activity, and glaciology. During the course of this project, 44 scientific papers and maps were published, and at least four major publications will result from the current geological remote sensing research.

The USGS has a long history of active cooperative exchange with U.S.S.R. counterparts in the field of earthquake studies, in which there currently are four major projects. A variety of other geoscientific contacts is maintained by attendance at meetings in the U.S.S.R. or by individual invitations. A U.S. panel was organized to review ideas for a more formal cooperative program in the earth sciences; R. G. Coleman and Harold Masursky represent the USGS on this panel.

INTERNATIONAL COMMISSIONS AND REPRESENTATION

Many intergovernmental meetings, especially meetings of international organization committees and commissions, are concerned with natural resources and earth sciences. The Department of State frequently requests the USGS to send representatives to such meetings. In a typical year, between 20 and 25 scientists from the USGS are involved in such activities for periods of a few days to several weeks. In 1979, for example, V. E. McKelvey participated in meetings of the United Nations Seabeds Commission; J. A. Reinemund was on the U.S. delegation to the United Nations Committee on Natural Resources and to the annual meeting of the Committee for Coordination of Joint Prospecting for Mineral Resources in Asian Offshore Areas (CCOP); M. J. Terman and J. I. Tracy represented the United States at meetings of the Coordinating Committee for the South Pacific (CCOP/SOPAC) and D. F. Davidson was a delegate to the meeting of the Committee on Natural Resources of the U.N. Economic and Social Council for Asia and the Pacific. Such activities generally involve the preparation or review of position papers in advance of the meeting, participation in the discussions and work of the meetings, as appropriate and in the U.S. interest, and preparation of a report to the Department of State.

Apart from participation in intergovernmental meetings, the USGS also participates in the work of international organizations by detailing or assigning scientists to work with such organizations on specified tasks or projects. For many years, for example, the USGS has detailed a scientist to work with the International Atomic Energy Agency. Frank Wang was assigned to CCOP to assist in developing a seabed mapping and a marine environmental program; M. J. Cruikshank completed an assignment in cooperation with the United Nations to explore and evaluate alluvial tin deposits at Tenasserim, Burma.

In recent years, the USGS has been increasingly involved in representational activities connected with the negotiation and monitoring of bilateral scientific exchange agreements. U.S. Government policy has been to develop such agreements especially with those countries in which scientific cooperation could be mutually beneficial. To the extent that such agreements include subjects of concern to the USGS, scientists from the USGS generally have been included in the negotiating teams or in the working groups responsible for follow-on program development. In fiscal 1980, USGS scientists served on teams negotiating with China, Venezuela, Brazil, Peru, and the Andean Pact.

International unions and commissions are important mechanisms whereby international cooperation is promoted and coordinated. Representation on the councils and on standing and ad hoc committees of these bodies and participation in international scientific meetings are valuable adjuncts to the programs of the USGS although the activities are generally limited to a few days per year.

Members of the USGS participate in councils and in standing committees of several international unions and commissions, in international meetings, and represent the Department of State and other governmental agencies on international forums. Examples of such activities are as follows:

L. A. Braconnier and A. H. Watkins represented the Department of the Interior in Argentina at the Landsat Ground Station Operations Working Group. The Director of the USGS was represented at the Austria Conference of the International Institute for Applied Systems by B. M. Miller. J. B. Robertson represented the USGS at the Advisory Group Meeting of the International Atomic Energy Agency, also in Austria. D. H. Mason and R. E. Sylwester participated in the U.S. Antarctic Research Program. R. B. Southard presented the keynote address at the fourth Australian Cartographic Conference in November 1980, and Roy Mullen went to Ivory Coast as a representative to the United Nations Cartographic Conference.

Philip Cohen, R. H. Langford, and Della Laura were delegates at the Third Session of the Intergovernment Council of the International Hydrological Program, which met in France, and H. C. Briggs participated in

the working group, Water Resources of Arid Regions Seminar in Brazil. J. R. Anderson was an official delegate to the 24th International Geographical Congress in Japan; R. P. Sheldon served as a member of the American Delegation to a meeting of the Fertilizer Commission of the Food and Agriculture Organization of the United Nations in Italy; H. H. Barnes, Jr., and O. M. Hackett were U.S. delegates to the World Meteorological Organization (WMO) in Spain; Thomas Maddock, Jr., was a member of UNESCO Hydrological Program Working Group of WMO; H. H. Barnes, Jr., and E. D. Cobb represented the United States on the National Committee, International Organization for Standarization, which met in France.

PARTICIPATION IN IUGS COMMISSIONS AND AFFILIATED BODIES

The International Union of Geological Sciences (IUGS), now 20 yr old, has more than 80 member countries, including the United States; its ongoing activities, conducted by various commissions and committees, are focused on fostering international cooperation in research, improving the international exchange of scientific information, and establishing international standards for geologic measurements, nomenclature, and data systems.

The USGS has been deeply involved in IUGS activities for years. T. B. Nolan was a founder and vice president of the Union, and J. A. Reinemund now serves as its treasurer. The USGS has budget authority to support the U.S. National Committee on Geology (the U.S. adhering body to IUGS) and provides staff assistance to the committee. The IUGS Commission on Stratigraphy and its various subcommissions have at least six USGS geologists (Mackensie Gordon, Jr., H. L. James, R. M. Kosanke, W. A. Oliver, Jr., R. J. Ross, and P. K. Sims) as members, and two others (A. L. Clark and D. F. Davidson) serve on the Committee on Geological Data. D. M. Kinney has been the long-term North American vice president for the Commission for the Geological Map of the World, and P. W. Guild is president of the Metallogenic Map Subcommission. The USGS Director is an ex-officio member of the U.S. National Committee on Geology, and he or his designated representative (V. E. McKelvey for 1980) heads the U.S. delegation to the quadrennial meeting of the IUGS Council.

In many other IUGS member countries the national geological survey is the adhering body. The United States, however, has chosen to divide this function between the USGS and the National Academy of Sciences, both of which are sponsors of the U.S. National Committee on Geology. Nevertheless, the USGS as an organization and individual USGS staff members have important responsibilities in helping direct IUGS affairs, which leads to an increased awareness of international geological activities and problems and the betterment of geological research at home.

International Geological Correlation Program

The International Geological Correlation Program (IGCP) is a multinational geological research program sponsored by the IUGS and UNESCO. Established in its present form in 1973, IGCP now consists of 51 projects, each assigned to one of the following four research categories: (1) time and stratigraphy, (2) major geological events in time and space, (3) distribution of mineral deposits in time and space, and (4) quantitative methods and data processing in geological correlation. Twelve additional IGCP projects have been completed. Money to support the organizational, planning, and administrative aspects of IGCP is provided by the sponsoring organizations; project research funds, on the other hand, have to be generated by the participating countries.

The United States is one of 67 countries that conduct IGCP-related research. U.S. participation consists of working groups for 24 projects, including 9 for which the U.S. working group chairman also is the international project leader. The U.S. National Committee for IGCP provides coordination and oversight for the U.S. effort and liaison with the IGCP board.

Since the beginning of the Program, the USGS has had a predominant role in IGCP. T. B. Nolan was instrumental in organizing it; and J. A. Reinemund was, until recently, a member of the IGCP Board. P. W. Guild served as a member of the Scientific Advisory Committee. The U.S. National Committee for IGCP, with a total membership of 12, includes 3 USGS geologists; 4 others have had terms on the Committee. Four IGCP projects were organized and are led by USGS representatives: (1) Circum-Pacific plutonism, by P. L. Bateman; (2) Standards for computer applications in resource studies, by A. L. Clark; (3) Siliceous deposits in the Pacific region, by J. R. Hein; and (4) Remote sensing and mineral exploration, by W. D. Carter. W. O. Addicott, R. G. Coleman, G. K. Czamanski, J. E. Gair, R. B. Neuman, G. M. Richmond, and R. P. Sheldon are U.S. working group chairmen for projects that originated in other countries. Including those who are designated as members of the various U.S. working groups for IGCP projects, about 60 scientists from the USGS are associated with the Program.

IGCP Project No. 60, the Correlation of Caledonian Stratabound Sulfides, has as its objective the correlation of data on the geological environments and characteristics of the Precambrian and lower Paleozoic stratabound base-metal sulfide deposits in the Caledonian Appalachian orogenic belt, with a view to elucidating their

genesis, predicting further mineral resources, and facilitating the exploration and development of individual prospects. Participating countries are Norway, Sweden, Denmark, United Kingdom (Scotland), Ireland, Canada, and the United States, each with its own national working group. The U.S. working group is a loosely knit unit, communicating principally by correspondence and telephone. The chairman of the U.S. working group is J. E. Gair; V. F. Slack is also involved. The participation of the two USGS members has been an inherent part of their principal USGS domestic research assignments dealing with stratabound sulfide deposits of the Appalachians.

The principal accomplishments have been (1) completion of national bibliographies dealing with Appalachian-Caledonian stratabound sulfides, (2) preparation of a review volume on the stratabound sulfide deposits of the respective countries, and (3) compilation of a map at a scale of 1:1,000,000 of the geology and stratabound massive sulfide deposits of the Appalachian-Caledonian belt from Alabama to northern Norway. The U.S. map compilation shows 103 deposits and a table listing as many as 17 attributes for each deposit. The existence and activities of the project have stimulated a number of research projects in universities, the results of which have been and will continue to be of help to the USGS projects on Appalachian stratabound sulfides. Field conferences and (or) symposia have been held in Norway-Sweden, Ireland, and Virginia, U.S.A., attended by 40 to 60 geologists each.

IGCP Project No. 98, Standards for Computer Application in Resource Studies, has as its objectives establishing guidelines for (1) general principles and specific details for the application of computer-based information systems to the study and assessment of resources; (2) to determine the most advantageous levels of financial and technological commitment to such computer applications for a given country; and (3) methods of data collection, storage, retrieval, and display of resource data. The chairman of the international working group and several other members of the U.S. working group are members of the USGS.

The project has had several annual meetings-symposia (in Norway, Kenya, Mexico, Thailand). In Colombia, resource data have been collected from one province, and geochemical maps are being drawn using computerized analytical techniques. In Turkey, data from a chromite district have been entered in a computer and are being used to develop an occurrence model. Data for 13 commodities have been collected in Israel preparatory to being entered into computer storage.

IGCP Project No. 161, Sulfide Deposits in Mafic and Ultramafic Rocks, has as its objectives (1) the acquisition and compilation of systematic data sets on magmatic ore deposits from a wide variety of tectonic environments and host rock types in order to understand the best ore-forming environments and (2) the promotion of field conferences and symposia to stimulate interest in the subject, to increase familiarity with and understanding of these rocks and deposits, and to assist in the data compilation mentioned in (1).

G. K. Czamanske, M. P. Foose, and N. J. Page are participating as members of the U.S. working group. The IGCP project activities are directly related to and in support of the domestic responsibilities of two participants as the nickel and platinum-metal commodity specialists of the USGS.

Participation in IUGG activities

The International Union of Geodesy and Geophysics (IUGG) is a counterpart organization to IUGS. It is about 40 yr older than the geological union and is concerned primarily with geophysical phenomena, including physical oceanography, meteorology, and space physics. Because its interests are largely outside the area of the USGS activities, the USGS has only a few representatives in IUGG. They include the chairman of the Commissions on Earthquake Prediction and on Strong Motion Seismology and members of the Working Group on the World Volcanic Map and on Radiogenic Isotopes. A few USGS geologists and geophysicists customarily attend the quadrennial scientific assemblies of IUGG and its subsidiary associations, particularly the International Association of Volcanology and the Chemistry of the Earth's Interior and the International Association of Seismology. Dallas Peck, USGS Chief Geologist, was a member of the U.S. National Committee for IUGG.

Other international representation activities

Four USGS geologists serve on the following U.S. National Committees: International Association of Geochemistry and Cosmochemistry, International Union for Quaternary Research, International Association of Hydrogeology, and International Association for the History of Geology.

J. N. Jordan, U.S. Member of the Commission on Geophysics of the Pan American Institute of Geography and History (PAIGH), a specialized agency of the Organization of American States (OAS), was co-organizer of a project to relocate earthquakes in and about South America for the International Seismological Month. Seismographic station data are being reinterpreted for South American facilities and adjacent regions. Wherever possible, calibration events are being used to improve locations. This project, a multinational project of the PAIGH also includes Dr. Edgar Kausel (Chile), Dr. Jesus Ramirez, S. J. (Colombia), Dr. Leo

Ocola (Peru), and Dr. Jose Antonio Rial (Venezuela). The International Geodynamics Project, a joint activity of IUGG/IUGS, which was carried out from 1970 to 1980, attracted the participation of some USGS scientists, one of whom is a member of the U.S. Geodynamics Committee. There is also USGS representation in the Special Committee for Antarctic Research, the Special Committee for Oceanic Research, and the Committee for Space Research, all of which operate under the aegis of the International Council of Scientific Unions. Finally, the USGS has some involvement in the International Phase of Ocean Drilling (IPOD) and its proposed follow-on program of continental margin drilling.

Resource Attache Program

The USGS and the Bureau of Mines continue to cooperate with the Department of State in supporting the Resources Attache and Reporting Program. During 1980 regional resources attaches were on duty in eight countries: Australia, Belgium, Brazil, India, Japan, Peru, South Africa, and Venezuela, and mineral reporting officers were assigned to many other countries.

Information supplied by the attaches and mineral reporting officers is used in the Department of the Interior and other agencies that use information on mineral supplies and mineral development and production in other countries. Increased awareness of the mineral availability problems that the United States faces will doubtless result in an improved and expanded mineral reporting program for the forseeable future.

Centennial Symposium

In connection with its centennial celebration, the USGS convened the International Centennial Symposium, "Resources for the 21st Century," from October 14–19, 1979, at the National Center in Reston, Va. Outstanding earth-science leaders from around the world presented invited papers in the fields of resource exploration and development; problems of energy and mineral resources; water; geologic hazards; geology and man's environment; surveying, mapping, and cartography; and cartography and printing of colored geologic maps. H. W. Menard gave the opening paper on world mineral interdependence. The symposium was attended by representatives from 41 countries and 13 international organizations; a total of 109 foreign scientists attended, of whom 41 were invited speakers; 359 USGS members representing all the divisions were involved in some way with organizing and running the symposium.

SUMMARY OF SELECTED ACTIVITIES BY COUNTRY OR REGION

ANTIGUA

J. W. Dewey and S. T. Harding, working with Lamont-Doherty Geological Observatory, have found that the large (magnitude 7.1) Antigua earthquake of October 8, 1974, occurred in the overriding wedge of the Caribbean plate. The focal-mechanism solution and aftershock locations imply that the earthquake occurred on a southeast-dipping normal fault oriented transverse to the regional strike of the northern Lesser Antilles arc. The position of the 1974 earthquake above the Benioff Zone and its normal-fault focal mechanism indicate that the shock has not released the elastic strain thought to have been accumulating along the thrust boundary of this segment of the Lesser Antilles arc since the great earthquake of 1843.

ARGENTINA

Under a Memorandum of Understanding (MOU) between the USGS and the Argentina Commission Nacional de Investigaciones Especiales, a project implementation plan is being developed for a study of Argentina's possible lithium resources.

Energy assessment

Members of the USGS energy resources assessment team that visited Argentina during November–December 1979 include R. E. Mattick and K. A. Yenne, petroleum; E. R. Landis, coal; E. A. Noble, uranium; T. J. Casadevall, geothermal; A. R. Taylor, minerals related to energy production; and S. L. Schoff, water.

The Republic of Argentina, one of the most industrialized nations in South America, has significant resources of the energy-producing materials water, petroleum, natural gas, coal, uranium, oil shale, and pyrobituminous asphalt. During the 1960's, energy production in Argentina lagged behind an increasing consumption that caused recurrent shortages. These problems partly were overcome during the 1970's by increased production of petroleum and natural gas to supply thermoelectric power plants and by construction of new hydroelectric and nuclear power generating stations. However, development and use of its indigenous energy resources have not kept pace with industrialization; therefore, Argentina still must import petroleum, natural gas, and coal.

The vast hydroelectric potential of the rivers of the western mountains and in the northeastern part of

Argentina has undergone significant development only during the past decade. About 17 percent of the electricity used in Argentina is generated at hydroelectric stations; 83 percent is supplied by thermoelectric plants burning oil, coal, and natural gas. By 1985, hydroelectric power will contribute 36 percent of the total electric energy supply. Argentina's water resources appear to be ample for development to meet foreseeable needs for hydroelectric power.

Argentina is one of the oldest oil-producing countries in the Western Hemisphere—production dating from 1907. Total oil resources in Argentina are estimated as $1{,}052.957 \times 10^6$ m^3 ($6{,}623.1 \times 10^6$ bbl); of that amount, 49 percent is classed as reserves; 1979 production was reportedly 172.8×10^6 bbl, which represents nearly 95 percent self-sufficiency. No production of crude oil is foreseen from offshore areas before 1985, but 50 exploratory offshore wells are to be drilled during the intervening period. Total resources of natural gas in Argentina are estimated as $1{,}581{,}278 \times 10^6$ m^3; about 45 percent of that is classed as reserves. Approximately $12{,}565 \times 10^6$ m^3 of gas was produced in 1979, almost 80 percent self-sufficiency.

Argentina's greatest potential for increased energy production appears to be in petroleum and natural gas. Argentina has a large petroleum resources base; known occurrences onshore have not been explored and developed to their potential, and possibilities for petroleum and natural gas exist on the Argentina continental shelf. Two of the five sedimentary basins identified on the shelf are seaward continuations of important onshore petroleum-producing basins.

Most of Argentina's significant resources of coal, estimated at $7{,}805 \times 10^6$ t, are in rocks of early Tertiary (Paleogene) age in Santa Cruz Province and the Territory of Tierra del Fuego in the southern part of the country. Coal produced in 1979 was reported to be 732,000 t, mostly from the Rio Turbio field and was used to supply thermoelectric power plants. Rio Turbio, in extreme southern Argentina, is far away from consumption centers; the lack of transportation and transmission facilities probably limit the production of coal.

Argentina's uranium reserves are mainly in sandstone beds of Mesozoic age and are mined both by surface operations and by underground methods to depths of 200 m; grade of the ore ranges from 0.025 to 0.119 percent uranium. Uranium resources ($50/lb U_3O_8) are estimated at 283,500 t in all categories ranging from reserve to speculative. The U_3O_8 content of uranium mined in Argentina during 1979 was estimated as 190 t.

Much more exploration and evaluation need to be done to determine the geothermal resources of Argentina. The Argentine Federal Government undertook a 5-yr program of exploration to identify and develop geothermal resources that began in 1980. Two areas are recommended for study: (1) the area of recent volcanic activity in the Andean Cordillera where potential for development of high-temperature (more than 150°C) geothermal systems is good, and (2) the seismically active belt east of the Andes where natural hot springs (temperatures of 40°–90°C) are known. Potential capacity or "resources" of the systems cannot be estimated accurately because of lack of information, but capacities for electrical power generation ranging from 20 to 1000 MW are inferred. Water from natural hot springs could be used now with available technologies for heating and industrial and agricultural processing.

Recovery of oil from shale and asphalt rock probably has little potential for development in Argentina because of the small amount of resources identified and the low potential for locating new deposits. Past production has been less than 6,000 t/yr.

AUSTRALIA

In May 1980, A. R. Ludwig began a 1-yr detail to the University of Adelaide, Department of Geology and Mineralogy, studying lead/uranium isotopes of specific uranium deposits in Australia. An Australian copper commodity specialist, J. H. C. Bain, is spending a year at our California facility to study assessment techniques and visit a variety of copper deposits. Four geologists spent July 1980 in the East Alligator uranium district participating in cooperative research with their counterparts in the Commonwealth Scientific and Industrial Research Organization. In August, D. S. Milton studied Goat Paddock Crater in Western Australia as part of a NASA cooperative on impact crater research.

BANGLADESH

R. L. Miller reviewed drill-hole data and made recommendations for new drilling to the Geological Survey of Bangladesh to adequately assess the coal resources of Bangladesh.

BOLIVIA

S. T. Algermissen and J. N. Jordan, with the assistance of Ed Medina (Albuquerque Seismological Center), have ordered equipment for Phase II of the Cochabamba project. The Cochabamba Valley has had earthquake damage in the past; and in light of expected regional development, the project has been locating earthquakes on a limited basis in order to regionalize seismic data. Phase II will bring the network up to eight stations centrally recorded for more effective operation and analysis. The new stations will be installed as soon as permitted in Bolivia.

BRAZIL

The USGS cooperated with the Government of Brazil in providing a month-long work-study course on processing and printing side-looking airborne radar imagery and in designing a cartographic-photographic laboratory. It also provided assistance to the State of Sao Paulo's Instituto de Pesquisas Technologicas in developing a petroleum exploration program. Funds were provided by Brazil. Results of previous cooperative studies of structure in Gois and Minas Gerais were published as professional paper chapters (Drake, 1980; Drake and Morgan, 1980).

BURMA

M. J. Cruikshank completed an assignment in cooperation with the United Nations to explore and evaluate alluvial tin deposits at Tenasserim, southern Burma.

CENTO

The last CENTO annual workshop on applications of remote sensing data and methods was held in Istanbul, Turkey, in October 1976 under the sponsorship of the CENTO Economic Program. The USGS assisted CENTO in publishing the proceedings of the last meeting by preparing camera copy, contracting for printing with funds provided by AID, and managing the distribution of copies to the member countries and interested parties.

CHINA

The USGS began to evolve a cooperative research program with its counterpart in China (People's Republic of China (PRC)) when Director Menard, as a member of a U.S. Government delegation of senior science administrators, visited Beijing in June 1978. These efforts were enhanced considerably by normalization of relations between the PRC and the United States on January 1, 1979, and particularly after the Science and Technological Cooperation Agreement was signed on January 31, 1979. An exchange of initial drafts of two Protocols took place during the 1979 visit by a PRC delegation from what is now China's Ministry of Geology. The Earthquake Studies Protocol was signed in January 1980 by the Directors of the USGS, the National Science Foundation (NSF), and the State Seismological Bureau of the PRC. At the same time, seven annexes establishing specific projects under this were signed. Of these, the USGS is principally responsible for two; the remaining five annexes are primarily the responsibility of the NSF and the NOAA. The Second Protocol, also signed by the USGS Director in January 1980, provided for earth-science studies.

USGS/China activities in geoscience evolved initially in support of U.S. foreign policy, as determined by the Department of State and the Office of Science and Technology Policy, but have since developed, additionally, as extensions of the USGS's international responsibilities, such as studies of global seismicity and world energy supplies. In developing these activities with China, three requirements must be met: (1) Work done under the exchanges must show a clear benefit to the United States. (2) Work done under the exchanges must strengthen our ability to achieve the objectives of our domestic programs and not represent a diversion of resources from them. (3) Exchanges must be financed from funds currently available.

Earthquake Studies Protocol

China has a very active earthquake prediction program due to the large number of damaging earthquakes there and the consequent great loss of life and property. Several earthquakes have been predicted successfully in China – most notably the Haicheng event of 1975; that prediction caused officials to evacuate the city, saving many thousands of lives. Because of the large-scale support for prediction in China and a rate of seismicity for large earthquakes much higher than in the United States, cooperation with the Chinese in earthquake studies serves the goals of those U.S. agencies charged with earthquake hazards mitigation. Specifically, such cooperation gives the United States access to data on large earthquakes more rapidly than would be the case through an exclusively domestic program.

Annex 1—Premonitory phenomena and techniques for earthquake prediction

Activities under this annex involve field observations of earthquake precursors and analysis of such observations for the purpose of earthquake prediction. The initial efforts concentrated on areas near Beijing and in Western Yunnan Province. Current activities are

- Beijing seismic network support: A computer system was purchased and is being assembled at facilities for testing prior to shipment to China. Plans have been made for several Chinese scientists to be trained in the United States in the operation of the system and in the use of special routines and techniques used by the USGS to locate earthquakes and analyze data. Current plans call for the computer to be installed in Beijing in late 1981 or early 1982, to be used for virtually real time, location, and analysis of the many earthquakes in the Beijing area.

- Magnetic precursors: A program to measure precursory changes in the geomagnetic field in seismic areas near Beijing and in Western Yunnan Province was initiated by USGS fieldwork in the fall of 1980. Recording magnetometers are being constructed for shipment to China in the fall of 1981. Plans have been made for a USGS delegation to return to Yunnan in the fall of 1981 to resurvey the magnetic network and discuss Chinese measurements made over the past year.
- Deformation observation: USGS observations of crustal deformation near active faults began in 1981. A laser distance meter has been purchased for shipment to China in late 1981 for increased surveillance of motion on active faults. A resurvey of this network will be done in the fall 1981 by USGS and Chinese personnel.
- A USGS delegation traveled to Yunnan province in October 1980 to discuss installation of additional seismometers in the existing Chinese network. Agreement was reached on the type of instrument, and six of the systems have been ordered, with additional systems to be ordered in the fall of 1981.
- Analysis of strain data: Strain data from Chinese observatories were analyzed during 1981 by Chinese and U.S. university scientists, the latter supported by the USGS and the NAS. Analysis techniques were developed to permit removal of noise from strain records, and strain events apparently precursory to the disastrous Tangshan earthquake were identified. Plans have been made to continue such analysis.
- Analysis of the Haicheng earthquake: A university group with USGS support has established a cooperative effort with Chinese scientists to analyze foreshocks and aftershocks of the Haicheng earthquake of 1975. This event was predicted, and Haicheng evacuated, due to unusual foreshock activity. The analysis of these events and following aftershocks suggested that different faults were involved in the foreshock sequence than in the main shock and aftershocks. Plans have been made to continue study of this sequence to determine the fault geometry and the implications for prediction studies on other faults.

Annex 2—Intraplate active faults and earthquakes

Activities under this annex are related to studies of earthquake recurrence on active faults, principally by geological techniques and analysis of remote imagery.

- Tanlu fault studies: A USGS delegation visited China in October 1980 to examine exposures of the Tanlu fault and to find appropriate sites for detailed geologic investigations of fault recurrence. In February 1981, a Chinese delegation visited the United States to continue discussions of the joint program and to visit field sites in the United States where similar work is underway. It was agreed that further efforts were needed to isolate sites on the Tanlu fault for detailed field studies. Aerial and satellite photographs are being examined by both sides in an effort to find such sites, which are not readily apparent because cultural activities have obliterated much of the surface expression of the fault. In addition, shallow test boring will be done in China to determine fault location.
- Red River fault studies: A delegation of university geologists, supported by the USGS, visited Yunnan Province in March 1981 to examine exposures of the Red River fault. This effort succeeded in identifying several likely locations for further detailed studies that may determine the frequency of earthquakes on this fault. A delegation of geologists from Yunnan Province visited the United States in February 1981 to examine related work on the San Andreas fault. A joint paper on the fieldwork in China is being written, and plans have been made to discuss further work.

Earth Sciences Protocol

Activities under the Earth Sciences Protocol are just now being fully negotiated. The negotiators generally have agreed on the title and scope of 20 mutually beneficial projects that, during the next few years, could involve exchanges of approximately 78 scientists for 125 man months. These initial exchanges will concern such topics as exploration and analysis of uranium deposits, coal basins, and petroleum basins; relations of volcanism to metallogeny; the general nature and occurrence of petroleum in carbonate rocks; geologic and tectonic framework of the circum-Pacific region; and karst phenomena. Generally, the broader the geographic study of geoscience phenomena, the greater the understanding that scientists can gain of their genesis, classification, and economic appraisal. For U.S. geoscientists, the large land area of China has unique examples of many of these phenomena.

Within the framework of the USGS/NSF/PRC Protocol on Earthquake Studies, Annex 7, it is required that the U.S. Government and PRC exchange seismic data and films of seismograms. Under this project, a joint effort between NOAA/NGSDC and the USGS, the capability was provided to the State Seismological Bureau of the PRC to film seismograms from the Chinese network and provide these film copies to the U.S. Government and the seismological community.

NOAA provided a 70-mm panoramic camera for filming the seismograms, installed the camera, and trained

Chinese personnel in its use. The USGS provided logistic support (peripheral equipment, photographic supplies, shipment of equipment, and spare parts) for NOAA personnel in carrying out this effort.

The filming capability was established at the Central Seismic Station at Beijing, China. Initially, current records from selected stations of their 17-station network will be photographed and film copies provided to USGS scientists. If time permits, selected past records may be included.

CCOP

F. H. Wang, senior technical advisor, has continued to assist the United Nations Committee for Coordination of Joint Prospecting for Mineral Resources in Asian Offshore Areas (CCOP), which is an inter-governmental body composed of 13 countries in east and southeast Asia. At the request of the Commission for the Geological Map of the World (CGMW) and in cooperation with the Circum-Pacific Map Project, geological maps of the sea floor and continental margin of eastern Asia at the scale of 1:5 million are being compiled. These maps will constitute parts of the third edition of the Geological Map of South and East Asia to be published by CGMW. Wang also initiated a program on marine environment relations to offshore exploration and exploitation for CCOP in cooperation with the U.N. Environment Program (UNEP) and the Association of Southeast Asian Nations (ASEAN) Council on Petroleum.

At the request of CCOP, USGS scientists R. L. Rioux, N. T. Edgar, and F. H. Wang organized a CCOP ad hoc group meeting on the marine environment held in March 1980 in Bangkok, Thailand. Subsequently they made an on-the-spot evaluation of the interest and long-term needs of the five countries in southeast Asia (Indonesia, Malaysia, Singapore, Philippines, and Thailand) and proposed programs to cope with the potential environmental problems of offshore exploration and exploitation. During the year, A. L. Clark and J. L. Cook served on the IUGS/COGEODATA group that provided consultation to CCOP on petroleum-data systems. They organized and conducted workshops on hydrocarbon assessments at Kuala Lumpur in March 1980; standardization of terminology and formats for energy data at Manila in July 1980; and resource-data handling at Bangkok in October 1980. Also, Cook prepared a bilateral study of preliminary recommendations for a data handling and management system for the Thailand Department of Mineral Resources.

CCOP/SOPAC

In 1979, the USGS provided two technical advisors (M. J. Terman and J. I. Tracey, Jr.) for short terms to participate in the annual program review for the U.N. Committee for Coordination of Joint Prospecting for Minerals Resources in South Pacific Offshore Areas (CCOP/SOPAC). S. J. Gawarecki, remote-sensing specialist, compiled a satellite imagery index and has made, insofar as possible, a reconnaissance analysis of natural resource potential. A computer applications expert, A. L. Clark, provided consultation for both CCOP/SOPAC and New Zealand, the only member nation that has a major computer capacity.

COLOMBIA

Prior seismicity and aftershocks of the Colombian earthquake of December 12, 1979, (M=8) have been relocated. Seismicity prior to the earthquake may be viewed as only partly consistent with a pattern recognized by others before other great thrust-fault earthquakes. Prior seismicity was concentrated near several edges of the 1979 fault rupture, but the region within 50 km of the main shock hypocenter experienced no recorded prior earthquakes of $>M=4.8$ in the years 1964–1979. It is noteworthy that the 1979 main shock epicenter lay in a zone of intense aftershock activity of a previous great earthquake on January 19, 1958. It is possible that this part of the 1958 aftershock sequence was, in effect, the "prior seismicity" near the 1979 mainshock hypocenter that was not found in 1964–1979.

EAST AFRICA REGION

Under a participating agency services agreement with AID, (June 1, 1978–December 31, 1980) the USGS provides assistance to the East Africa Region Remote Sensing Center, Nairobi, Kenya, in conducting short courses in applications of remote sensing to earth-resources investigations. USGS specialists in cartography, water, and agriculture taught two courses in calendar 1979.

EGYPT

A program of technical assistance to the Egyptian Geological Survey and Mining Authority (GSE) is in its third year. Funding is provided by AID. Objectives are to enhance capabilities of GSE to compile and publish maps and to investigate Egypt's mineral resources. Activities include technical advice in the design, construction, and implementation of a photographic-cartographic laboratory, and training in Egypt and the United States in cartographic and publication methods, in geological data management, in remote sensing, and in mineral-resource field and laboratory methods, instrumentation, and practice. Roger Shaff is in charge of the project in Cairo and has trained five Egyptian cartographers who are preparing a 1:2,000,000-scale map

of Egypt, two 1:250,000-scale geologic maps, and a metallogenic map at 1:500,000 scale.

During November and December 1979, G. E. Andreasen visited Egypt to evaluate the capabilities of the Egyptian government to use geophysical methods in its mineral-resource assessment program. The quality of data already collected was also evaluated, as well as the present equipment, staff, and facilities. R. L. Reynolds helped design a paleomagnetics laboratory and conducted a seminar on paleomagnetism.

Evaporites

The Miocene section of the Gulf of Suez and Red Sea area contains one of the world's thickest accumulations of evaporites (more than 3000 m). R. J. Hite made a quick review of the data available regarding them for the Geological Survey of Egypt in late 1979. He recommended further study of the data combined with geophysical techniques to determine the potential for potassium salts and other valuable evaporite minerals.

Bibliography

C. R. Glenn and J. M. Denman (1980) compiled a bibliography entitled Geologic literature on Egypt, 1933 to 1978, which has been released in open file. This library compilation includes published works only. Items are cross indexed under subject headings; subheadings under Areal Studies provide a rapid survey of literature pertaining to a particular geographic area.

EL SALVADOR

El Salvador is a populous and industrialized country and with its high seismicity permits informative studies relevant to the U.S. Earthquake Hazards Reduction Program. J. N. Jordan has continued to consult with colleagues in El Salvador for the purpose of establishing a centrally recorded radiotelemetric network for a joint program of earthquake hazards reduction. Instrument specifications, network design, spare parts, test equipment, and strong-motion and portable aftershock equipment were identified in sessions with personnel of the Geotechnical Research Center of the Ministry of Public Works. The instrumentation for the network has been purchased, but installation has been deferred. This work was sponsored by AID.

GERMANY (WEST)

A cooperative agreement between the USGS and the Bundesanstalt für Geowissenschaften und Rohstoffe (BGR) was implemented in July 1975 and in January 1979 was extended for an additional 5 yr. The agreement provides for cooperation in mineral-resource investigations, resource-data systems, energy resources, water and soil investigations, environmental geology, geological applications to food production and underground disposal of waste, and stratabound sediment-associated sulfide deposits. Under the agreement there have been many exchange visits concerned largely with such topics as resource-data bases, computer-assisted exploration, mineral-resource evaluation, calculation of ore reserves and resources, remote sensing, and digital processing of Landsat data.

BGR and USGS entered into a cooperative project to develop techniques for evaluating the potential for base-metal deposits in black shales in the Appalachian region and similar deposits elsewhere. The initial phase of the project was done by Helmuth Wedow and by Wolfgang Klau and Duncan Large of BGR, who brought to the project large data bases on German, Australian, and Canadian deposits and a deposit model as the basis for carrying out characteristic analysis. Preliminary analysis of about five deposit attributes by manual operations has demonstrated the feasibility of performing similar operations by computer on 50 or more attributes.

In marine geology, a cooperative project with Carl Hinz of the BGR began on August 11, 1979, with a cruise by the West German geophysics vessel *Explorer* off the U.S. Atlantic continental margin. The purposes of the program are

- The collection of a 4900-km grid of geophysical data (multichannel seismic-reflection profiles, magnetic and gravity profiles, and sonobuoys) over the outer continental shelf, slope, and rise, between Virginia and the eastern end of Georges Bank, to extend the existing USGS grid of geophysical data. This new closer grid of data (line spacing 10–25 km) will allow more detailed mapping of the buried carbonate platform front, larger folds and faults, and possible hydrocarbon anomalies and correlation of key reflectors penetrated in the COST B–2 and B–3 holes.
- A cooperative USGS–BGR effort to compare the tectonic framework and pattern of rifting for the eastern North American margin with the conjugate West African margin where BGR has 20,000 km of multichannel seismic-reflection profiles.
- A preliminary survey for future IPOD (International Program of Ocean Drilling) sites of the U.S. Atlantic slope and rise (*Explorer* Program).

GUATEMALA

In cooperation with Dartmouth College, Hanover, N.H., and Guatemala's Instituto Geográfico Nacional, and partly supported by AID, a project was undertaken

to determine the tectonism and hazards associated with stresses near a subduction zone by geophysical studies of caldera lakes and to determine the same factors associated with a transcurrent plate boundary on the North American–Caribbean plate boundary in eastern Guatemala. C. K. Paull, G. V. McCarthy, K. F. Parolski, D. H. Mason, D. W. Folger, and W. P. Dillon were involved in data gathering.

R. A. White reported that more than 40,000 shallow-focus earthquakes have been recorded between August 1979 and May 1980 near Cerro Cruz Quemada in southeastern Guatemala. No previous events had been detected in this section of the Central American volcanic chain since the local network of high-gain seismographs began operation in March 1975. The seismicity increased for a month, both in number of events and maximum magnitudes generated. The largest event of the swarm ($m_b = 5.0$) occurred on October 9, injuring 40 persons and destroying over 140 adobe houses. Fluctuating activity continued for another 7 mo. Such earthquake swarms are typical of volcanic seismicity and may result from movement of magma within the crust. The Tertiary age of the Cerro Cruz Quemada and a history of similar swarms every 20 to 40 yr, however, argue against the likelihood of a volcanic eruption. The alinement of epicenters and a composite focal mechanism indicate that the swarm probably originated along a normal fault that strikes N. 10° W. This area has in the past had events as large as magnitude 6, typically preceded by a dramatic increase in seismicity; and therefore, careful monitoring of activity levels in the Cerro Cruz Quemada region may provide early warning for damaging earthquakes of this type.

HUNGARY

Under a science and technology agreement for cooperation in culture, education, science, and technology entered into on May 21, 1979, between the Governments of the United States and Hungary, the USGS and the Central Office of Geology (COG), People's Republic of Hungary, are in the process of concluding a bilateral agreement for calendar years 1980–1981. The purpose of the program is to exchange scientific and technical knowledge and personnel in the geological and geophysical sciences and to conduct joint research studies of mutual interest. The program plan for 1980 consisted of exchanging personnel as follows:

- To Hungary: The USGS sent four scientists for a total duration of 4 mo to work in the Geological Institute and the Geophysical Institute in areas pertaining to data management, coal geochemistry, induced polarization, and electromagnetic methods.
- To the United States: COG is to send six scientists for a total duration of 10 mo to work in the USGS in areas pertaining to sedimentation models, petroleum resources assessment, induced polarization methods, electromagnetic methods, coal data banking, seismic signal processing, and seismic-risk assessment.

The program implementation plan for this exchange is presently under review by the State Department.

INDONESIA

The USGS is in the midst of a 4½-yr program of technical assistance designed to increase Indonesia's ability to collect and interpret data regarding mineral resources, the geologic environment, and geologic hazards (especially mitigation of volcanic hazards). W. W. Olive, Chief, and D. B. Tatlock, are stationed in Bandung in support of the project. Daniel Dzurisin and Kenneth Yamashita visited Indonesia in late 1979 to test the feasibility of introducing a radiotelemetered seismic network by measuring dry-tilt sites at Merapi and Kelut, two volcanoes that erupt frequently and threaten nearby populated areas. Indonesia counterparts were trained in installing and operating the devices and interpreting the measurements. The team was able to recommend ways to improve the existing equipment and results. A later study by D. W. Crandall resulted in more definitive recommendation for volcanic hazards zonation studies. By January 1980, nine USGS experts had made feasibility analyses of environmental geology, volcano monitoring, volcanic hazard mapping, computer applications, and seismicity. Under the DOE's Energy Resources Assessment Program, V. E. Swanson and E. R. Landis made a 6-wk study of Indonesia's coal resources program and supporting laboratories.

E. R. Force initiated environmental geologic studies in the southeastern Kalimantan transmigration area in April 1980 by preparing a 1:100,000-scale map and a report on the Samarinda area, describing the resources and geologic hazards. He was succeeded in this subproject in August by P. F. Norton, who provided guidelines for the preservation of the environment, particularly the soils and slope, through the use of types of vegetation and erosion control practice.

W. E. Davies, engineering geologist, arrived in Indonesia in July 1980 and together with his counterparts completed an inspection of readily accessible landslides in southeastern Java. Davies then developed a formal plan for conducting future landslide studies in Java.

Age of *Homo erectus* from Java

At Sangiran Dome in central Java numerous finds of *Homo erectus* have been made in the Kobah beds of Pleistocene age. Current age estimates range from 0.5

to 1.4 m.y. A sample of dacitic pumice collected approximately 12 m above the site of *H. erectus* VIII was dated by the K-Ar and fission-tracking methods by J. D. Obradovich and C. W. Naeser. The results are 1.05+, −0.1 m.y. and 1.6+, −0.7 m.y. (both +, 2 sigma), respectively.

JORDAN

Under the auspices of AID, G. E. Andreasen provided technical advice to the Kingdom of Jordan, National Resources Authority (NRA), in the preparation of project specifications for airborne geophysical surveys and in the evaluation of results.

R. N. Eicher made a study of the Jordanian Natural Resources Authority's needs for acquiring an in-house computer facility and of the types of specific applications of computer-processing techniques that would be useful to NRA. A variety of applications was determined to be feasible for interpreting or storing existing data and for the management of new data resulting from NRA's exploration programs.

KOREA, SOUTH

Members of the USGS energy resources assessment team that visited South Korea during March and April 1980 included R. L. Miller (USGS) and L. V. Wade (USBM), coal; M. A. Fisher and K. A. Yenne, petroleum; V. E. Swanson, uranium; N. G. Banks, geothermal; R. B. Hall, thorium and minerals related to energy production; and G. F. Worts, Jr., water.

The Republic of Korea does not produce sufficient energy from indigenous resources to meet its energy demands. More than 50 percent of the energy used in the Republic is produced from petroleum that is imported as crude and is refined in-country; domestically produced coal supplies about 32 percent of the energy demand and hydroelectric power about 4 percent. Other sources include the recently completed Kori-I nuclear power plant and small amounts from firewood, charcoal, and dung. South Korea's government program stresses construction of additional hydroelectric power generators, increased production of coal, energy production by additional atomic reactors, and energy savings through conservation as immediate measures to offset the use of imported petroleum. Onshore and offshore exploration for petroleum and natural gas, development of geothermal potential, and generation of energy by tidal power are stressed as long-range measures.

Coal is South Korea's most plentiful energy-mineral resource. Most of the coal is anthracite in rank and occurs in Carboniferous and Jurassic strata; an unexplored and unestimated amount of lignite is present in Miocene strata near the east coast of the peninsula. Anthracite production in 1980 was about 20 million t; the 5-yr energy plan projects 1981 production at 24 million t, but the anticipated demand at that time may be as much as 31 million t. Practically all anthracite produced in South Korea is used domestically, primarily for space heating. The anthracite as mined is high in ash (20–65 percent) and low in heating value (4,400–10,000 Btu); washed and cleaned samples of anthracite, however, may have ash contents as low as 14 percent and Btu values as high as 11,800.

Korean government officials have committed the Republic to generation of electricity by nuclear power. The Kori-I plant began operation in 1978 and the Kori-II plant is nearly completed; four other plants should be operational by 1985. Approximately 40 nuclear power plants are to be operating by year 2000. South Korea plans to extract the uranium contained in the Ockcheon black slate as the domestic source for nuclear fuel. If technology is developed to substitute thorium as the fuel, that element may be extracted from the abundant monazite deposits in the Republic.

The energy potential from petroleum, natural gas, geothermal, and tidal sources in Korea is now being investigated. South Korea does not produce petroleum or natural gas, but the Mesozoic and Tertiary strata in sedimentary basins where "shows" have been encountered are being explored both onshore and offshore. Areas having low- to intermediate-temperature waters on the islands of Cheju-do and Ulleyng-do are recommended for additional studies for geothermal energy potential. The harnessing of tidal power in seven bays on the west coast of South Korea, such as at Wolmi-do off Inchon where tides reach as high as 9 m, is being considered as an alternative source of energy; one tidal plant may be operable in 1986.

MALAYSIA

B. C. Ray, supervisory petroleum engineering technician, assisted PETRONAS, the Malaysian national oil company, in the implementation procedures for the supervision of petroleum regulations. In particular, Ray assisted and advised on the proposed procedures for drilling operations, and developed the details for drilling and plugging and abandonment field inspection and reporting procedures by foreign oil companies in Malaysia.

A. L. Clark and J. L. Cook, data processing geologists, helped Carigoli, the operating arm of PETRONAS, to develop archiving procedures, data files, and a data handling system for exploration and development functions of offshore oil exploration.

MEXICO

A formal Scientific and Technical Cooperation Agreement between Mexico and the United States was signed in June 1972. Pursuant to terms of that Agreement, the USGS cooperated with various agencies of the Mexican Government under Memoranda of Understanding (MOU). Seven MOU are pending and two MOU are presently in force: The Cerro Prieto Geothermal Studies Program has been in force since 1979 under the auspices of the DOE. The program, Research on Techniques of Geochemical, Geophysical, and Geological Exploration in the Sonoran environment, also has been in force since 1979 with the Consejo de Recursos Minerales. The USGS cooperates with that agency through the NSF.

As a byproduct of the Mexico investigations, a new uranium mineral, cesium-rich analog of carnotite, was recently discovered and named margaritasite by K. J. Wenrich-Verbeek. The margaritasite is part of the ore at the Margaritas deposit in the Pena Blanca uranium district near Chihauhau, Mexico. It occurs as disseminated pore filling and relict phenocrysts within a rhyodacitic tuff breccia of the lower part of the Escuadra Formation (Oligocene). Margaritasite is fine grained, yellow and optically indistinguishable from carnotite; it is most easily recognized by X-ray diffraction through a shift in the (001) reflection representing an increase, relative to carnotite, in the *c* dimension due to the large cesium atom in sites normally occupied by potassium in the carnotite structure.

The crystallography and chemistry of margaritasite have been determined by P. J. Modreski, R. A. Zielinski, and J. L. Seeley. This cesium-potassium uranyl vanadate, with cesium-potassium about 5, is the natural equivalent of the compound $Cs_2(UO_2)_2(VO_4)_2$ synthesized by Paul Barton (1958) by fusion. Chemical analyses of the mineral have resulted in the formula

$$(Cs_{1.38}(H_3O)_{0.35}K_{0.29})_{\Sigma}2.02(UO_2)_{1.99}(VO_4)_{2.00}\cdot 1.07H_2O$$

corresponding to the generalized formula

$$(Cs,H_3O,K)_2(UO)_2(VO_4)_2\cdot nH_2O \text{ where } Cs\nabla H_3O,K \text{ and } n\cong 1.$$

Cell parameters are $a=10.51$, $b=8.41$, and $c=7.25$, $\beta=105.9^{9}$ (P_2/a, $Z=2$). Microprobe analyses suggest that there may be a solid solution between carnotite and margaritasite, but X-ray powder patterns reveal that two discrete *c* dimensions exist with no transitions between them. The margaritasite has an (001) reflection at 12.7° (2θ) whereas that of carnotite lies at 13.8° (2θ); these peaks do not shift.

The discovery of cesium-rich carnotite in the Pena Blanca uranium district provides important evidence for local hydrothermal or pneumatolitic activity during or after uranium mineralization. Data from the geochemical literature indicate that the high concentrations of dissolved cesium required to produce cesium-rich minerals can be generated and sustained only by high-temperature environments. Synthesis experiments from this study have shown that margaritasite can form at 200°C but does not appear to do so at 80°C. Consequently, it is improbable that margaritasite is part of the ore in any sedimentary uranium deposit. In contrast, carnotite from uranium deposits of probable hydrothermal origin are good candidates for new localities of margaritasite.

Petrology of organic matter in sedimentary rocks

The Cerro Prieto geothermal field consists of a liquid-dominated hydrothermal convection system contained within faulted Pliocene to Holocene sediments of the Colorado Delta and adjacent Cerro de La Cucapas. The field is located 35 km south-southeast of Mexicali, B.C., Mexico, and 8 km southeast of the Cerro Prieto Volcano from which it derives its name. The geothermal reservoir consists of an alternating sequence of nonmarine shale and sandstone sealed by a shallow impermeable mudstone, which acts as an aquitard. The producing zone appears to be partially bounded by or cut from numerous northwest-trending faults, which may also act as conduits for the rise of thermal fluids.

Measurements of vitrinite reflectance (percent R(o)=reflectance at random orientation under immersion oil) on particulate organic matter (phytoclasts) extracted from chip samples have now been completed on 15 wells at Cerro Prieto. The organic matter is Type III kerogen consisting of terrestrial plant remains. Recycled organic matter and some "cavings" in the chip samples required the measurement of the modal vitrinite population rather than the conventional least altered vitrinite population. In Well M-84, for example, the phytoclasts persist at 1700 m. This corresponds to an increase in temperature from 30°-60° to 325°C. The percent R(o) measurements fall on smooth curves that correlate with the measured temperature logs. A least square exponential curve fit on the mean percent R(o) and temperature data give correlation coefficients typically in excess of 0.8. These relations, based on reflectance data, allow prediction of stable reservoir temperatures in new wells in the Cerro Prieto system without waiting for thermal equilibrium.

In another application, the measured percent R(o) (rank) profiles and well temperatures from logs and mineral studies allow use of time-temperature-rank models to estimate the duration of thermal activity. Thermal alteration of phytoclasts is essentially a devolatilization reaction and is an irreversible process. Therefore, vitrinite reflectance indicates the maximum temperature reached in the burial history of the

sediment—which may not be the existent temperature of the geothermal system. Time-temperature-rank models presume that the temperature observed in the reservoir is presently at a maximum. If temperatures have retrograded, heating duration will be overestimated. The approximate equivalence of temperatures from well measurements, and from fluid inclusion and oxygen isotope geothermometry, and the absence of retrograde mineral assemblages indicate that the sediments penetrated are now at the highest temperature they have yet experienced.

Reservoir processes at Cerro Prieto geothermal field, Mexico

Analyses of noble gas from Cerro Prieto drill-hole samples made by A. H. Truesdell in collaboration with Emanuel Mazor (Weizmann Institute of Science, Israel) indicate that most cooling at Cerro Prieto is by mixture with cold dilute water rather than by boiling and steam loss. Less than 5 percent of the water has been lost as steam as indicated by very limited depletion of atmospheric noble gases (introduced in the recharge) and helium (introduced at depth from radioactive decay). Cold water containing atmospheric noble gases, but no helium or chloride, mixes with more-or-less gas-depleted thermal water at the margins and in the area of drawdown. One sample showed depletion in atmospheric gases and enrichment in radiogenic gases (helium and argon-40) due to long storage after boiling. The lack of extensive boiling and steam loss at Cerro Prieto is remarkable because the brines are everywhere at the boiling point and have a temperature range of 340° to 260°C. This suggests that there is no permeability barrier at the hot water–cold water boundary.

Studies of extensive physical and chemical measurements by Truesdell in collaboration with Malcolm Grant (DSIR, New Zealand) and Alfredo Manon (CFE, Mexico) show that dilution with cold water is the dominant cooling process at Cerro Prieto—both naturally and under exploitation. This behavior contrasts with that at Wairakei, New Zealand, where boiling has been the major cooling process, with an extensive two-phase zone formed upon exploitation.

Although general boiling and production of an extensive two-phase zone has not occurred at Cerro Prieto, local near-well boiling is common. This near-well boiling causes enthalpy excesses that decrease or disappear with time and silica deficiencies that decrease but do not disappear.

These and earlier studies suggest that the Cerro Prieto reservoir is bounded below by low-permeability hydrothermally cemented rocks, and above by an interface with relatively cold water. There is no permeability barrier immediately above the reservoir. Permeability within the reservoir is intergranular rather than formed by fractures. Mixture with cold water rather than boiling is the dominant cooling process in the natural state, and production causes displacement of hot water by cold water rather than by vapor. This may drastically limit the useful life of the field.

Analyses of Cerro Prieto geothermal gases

Calculations of gas equilibria were made by N. L. Nehring in collaboration with Franco D'Armore (Consiglio Navionale delle Richerche, Pisa, Italy) in the system $(C-H_2-O_2N_2-S(-Fe)$ for dissolved gas compositions of the Cerro Prieto aquifer fluid. Results show that methane is apparently in equilibrium at $326 \pm 11°C$; hydrogen at $295 = \pm 9°C$; ammonia at $293 = \pm 17°C$, and $283 = \pm 18°C$, respectively. Each geothermometer indicates temperatures at a different depth due to different rates of reequilibration. Methane is the slowest to reequilibrate and indicates temperatures close to the maximum observed at Cerro Prieto (340°C); hydrogen sulfide is the most rapid and gives the same temperatures as the sodium-potassium-calcium geothermometer. All temperatures appear to be real for Cerro Prieto and should be useful in guiding exploitation.

Analyses of gases from the higher temperature eastern wells are in progress, and their gas temperatures may suggest the maximum temperature of the system. The present calculations show that oxygen fugacity in the sampled reservoir is near 10^{-35} and is apparently controlled by carbon-CO_2 reaction near 290°C; sulfur fugacity is near 10^{-13} and is apparently controlled by pyrite-pyrrhotite reaction near 280°C; and all reactive gases considered appear to be in equilibrium within the temperature range observed at Cerro Prieto.

Gases	The Geysers	Steamboat Springs	Cerro Prieto
CO_2	−12.7	− 8.5	− 5.6
Methane (C–1)	−30.5	−35.5	−30.9
Ethane (C–2)	−24.8	--	−20.6
Propane (C–3)	−21.8	--	−21.8
Butanes (C–4)	−20.5	−30.8	−22.2
Pentanes (C–5)	--	−28.4	−24.2
Hexanes (C–6)	--	−25.2	−24.1
Benzene (C–6)	−21.1	−25.2	−23.6

The relatively low carbon-13 content of chlorine in these hydrocarbons suggest their formation by thermocatalytic breakdown of higher molecular weight organic matter. The isotope composition of carbon in coal from Cerro Prieto drill cuttings (del carbon-13 = −24.3 permil) is similar to that in C–5 and C–6 gases from that field. Parallel isotopic relations occur during thermal decomposition of organic matter in experiments and in the genesis of petroleum-related gases. Present data from The Geysers and Steamboat Springs show a positive correlation between carbon number and carbon-13 content. This correlation is the simplest expres-

sion of the kinetic isotope effect during thermal decomposition. Cerro Prieto C–2 through C–6 hydrocarbons display a negative correlation. Experimental hexane decomposition under uniform conditions (time and temperature) cannot reproduce such a pattern. Perhaps Cerro Prieto gases are a mixture of hydrocarbons produced under low intensity (low temperature and (or) short times yielding lower carbon–13 and more of the higher hydrocarbon gases and high intensity (higher carbon–13, more chlorine and C–2) conditions.

NICARAGUA

D. H. Harlow located more than 700 shallow-focus earthquakes in western Nicaragua between March 1975 and December 1978, using data collected by a 16-station network of high-gain seismographs. These events occurred at depths of 0 to 20 km and, in cross section, lie above and are separate from seismic activity associated with plate subduction along Nicaragua's Pacific coast. Magnitudes range from approximately 1.0 to 3.7. Most events fall in a 10- to 20-km-wide belt along the chain of active volcanoes, and a few events are scattered as far as 25 km inland from the northeast edge of the Nicaraguan Depression.

Composite focal mechanisms of several of the larger earthquakes along the volcanic chain indicate strike-slip faulting with either N. 25° E., left-lateral motion, consistent with fault movement during the 1972 Managua, Nicaragua, earthquake, or N. 65° E. right-lateral motion, parallel to the strike of the volcanic line. The north-south maximum horizontal-stress axis indicated by these data is consistent with Quaternary geologic features but inconsistent with a maximum compressive-stress axis of N. 30° E., expected from the direction of plate convergence.

PAKISTAN

A report stemming from a cooperative program undertaken by the Geological Survey of Pakistan (GSP) and the USGS from 1956 to 1970 (Calkins and others, 1981) was completed and advance copies forwarded to GSP. The area described is in the remote Hindu Kush Mountains in Chitral State. Copper, lead, antimony, arsenic, mica, and beryl are known from the area, and some mining has been done. The analytical results reveal the presence of several metals, including gold, silver, copper, and tin, that have not been previously reported. The region would benefit by systematic sampling and analysis.

PERU

W. J. Spence showed that the 1974 Peru aftershock series occurred in two segments. The main shock (MS = 7.8) occurred on October 3, 1974, near the end of the offshore, parallel-to-coast segment. Aftershocks in this segment occurred 10 to 25 km in focal depth and had P–wave first-motion distributions consistent with the shallow-dipping thrust focal mechanism of the main shock. The second segment was perpendicular to the first at its approximate midpoint and extends downdip to a depth of about 60 km beneath the Peruvian coast. This aftershock segment may represent internal deformation produced by subduction of the Nazca Ridge. Each of the aftershock segments contained one primary cluster of activity. The cluster in the parallel-to-coast segment lies between the main shock and the November 9, 1974, aftershock, which is about 30 km to the south-southeast. The cluster in the perpendicular-to-coast segment lies at the segment's eastern terminus. The aftershock series comprised distinct space-time groups. The primary space-time phenomenon is that a given segment tends to be active for a period of 2 to 2½ days, while the other segment is lacking in activity; then the situation reverses.

PHILIPPINES

In continuing support of the Philippine Bureau of Mines and Geosciences, J. L. Cook formatted and developed a chromite data base, and D. L. Rossman completed his field research on chromite deposits and associated ultramafic rocks of the Zambales Range.

POLAND

The cooperative research program with Poland funded by the Special Foreign Currency Program includes projects on mining hydrology, base metals, coal geology and geochemistry, native sulfur, copper in black shale, and fission-track dating of intrusive rocks.

The "base metals in carbonate rocks" project is completed. This program, embracing a wide range of topical studies ranged from stratigraphy, petrology, fluid inclusions, and lead isotopes to paleohydrology, focused on the genesis of lead-zinc deposits in Upper Silesia. Several topical papers were published in the course of the project (Karkowski and others, 1979) (Zartman and others, 1979). The final report, in the form of a symposium volume of six papers in English, was published at the end of 1979. The consensus of the authors is that the deposits were formed by four main periods of influx of highly saline paleobrines in a sequence that extended from the Triassic through the Quaternary.

The coal geology and geochemistry of coal projects focus on the geologic characteristics of coal basins, and on the geochemistry of coal and the computerization of coal data. Data gathering and data analysis scheduled under the current agreement have been completed, and

preparation of final reports, to be published in English, is underway. Topical studies include prediction of quality and quantity of water in underground coal mines, geochemical sampling and analysis, coal data methodologies, calculation of coal resources, geophysical methods applied to coal exploration and evaluation, coal petrography, coalification and rank of coal, facies relations and depositional environments, and correlation between coal basins and between continents.

The native sulfur project was initiated in late 1979. Geologic and isotopic studies will compare native sulfur deposits in Poland with similar occurrences in the United States. The studies focus on the structural and hydrochemical conditions that controlled the metasomatic alteration of evaporite deposits to native sulfur and the geologic and structural characteristics that will aid in prospecting.

The project on copper in black shale, also begun in late 1979, applies geologic, geochemical, and geophysical techniques to the study of copper deposits in black shales in the vicinity of Wroclaw and uses computer techniques of mathematical modeling and characteristic analysis to analyze the data and develop regional models to guide exploration.

The project on fission-track dating of intrusive rocks involves research on and applies techniques of fission-track dating of several appropriately chosen minerals in an intrusive-rock body and the surrounding rocks, and applies that information to understanding the tectonic and erosional history of the region. The project was initiated in late 1979.

PORTUGAL

Members of the USGS energy resources assessment team that visited Portugal during November–December 1979 included M. M. Ball and R. D. Carter (petroleum); F. D. Spencer (coal); E. A. Noble (uranium); D. A. Johnston (geothermal); and J. W. Allingham (minerals related to energy production).

Portugal lacks sufficient indigenous supplies of organic fuels to meet its energy demands and must import large quantities of petroleum and coal. Approximately 80 percent of Portugal's electric energy is produced by hydroelectric stations; thermal stations produce the other 20 percent.

Portugal has produced no crude oil, natural gas, or condensate. Exploratory wells were drilled offshore to test for oil and gas along the western and southern coasts of Portugal; all wells were abandoned as commercially unsuccessful, although some were reported to have had oil shows. No significant onshore petroleum exploration was done in Portugal between 1963 and 1980. It is unreasonable to suppose that future exploration successes will solve Portugal's energy needs of approximately 8×10^6 m^3 of oil per year; to produce this amount yearly would require reserves of about 80×10^6 m^3. Although there are untested structures in the Portugese offshore that are capable of trapping hydrocarbons in quantities of this order of magnitude, past experience in the drilling of 22 dry offshore tests has indicated that some combination of inadequate reservoirs, seals, or source beds has inhibited accumulation of commercial quantities of oil. Efforts need to be intensified and expanded to interpret the more than 25,000 km of reflection seismic data now available for Portugal.

Portugal's coal production has declined steadily to the present annual yield of about 200,000 t. On the basis of estimates in only three coal fields, resources of coal of all ranks in Portugal total at least 76 million t. Only one mine produced coal in 1979, and 90 percent of that coal was used for generating electric power at one thermal plant.

Uranium is mined near Viseu and Guarda in the northern part of Portugal; the Nisa mine in east-central Portugal will begin producing uranium ore in 1985 after installation of a processing plant. Portugal produced 100 to 120 t of uranium oxide (U_3O_8) per year from 1975 through 1979.

Geothermal energy has not been developed in mainland Portugal; however, hot springs that may have geothermal energy potential are known in northern, western, and southwestern Portugal. Exploration to determine if high-temperature reservoirs exist in these areas is recommended. Geothermal energy resources exist in the Azores, and a program of evaluation and exploration with technical assistance from the USGS is presently in progress there.

Exploration of known mineral resource areas, rather than exploration for new mineral districts, appears to be the mining industry's policy in Portugal. Mining, which provides less than 1 percent of both the gross national product and the employment, significantly influences local economy but only slightly influences national economy.

SAUDI ARABIA

The USGS cooperated with the NSF in a project to provide guidance in the design of a Saudi Arabian Center for Science and Technology. Activities included the preparation of concepts of an Institute for Natural Resources and Environmental Research and participation in a workshop at Riyadh where U.S. and Saudi scientists considered the concept papers and modified them to fit Saudi specific conditions.

Miscellaneous shield studies

W. R. Greenwood, D. B. Stoeser, R. J. Fleck, and J. S. Stacey completed their report, "Late Proterozoic complexes and tectonic belts in the southern part of the Arabian Shield."

Study of Phanerozoic rocks

R. G. Coleman, R. T. Gregory, and H. R. Taylor on temporary duty assignments (TDY) mapped and sampled the Cenozoic volcanic rocks of Harrats Rahat, Kishib, and Nawasif during FY 1980. After returning to the United States, Coleman and Gregory began laboratory studies of the samples collected.

Coleman, Taylor, and Gregory completed several weeks of fieldwork on the Jabal Tirf subvolcanic rift zone and the surrounding region. Coleman and Taylor, the former being responsible for petrologic studies and the latter for an oxygen isotope study, are conducting laboratory studies of samples collected.

Geochronology and isotope studies

R. J. Fleck on TDY with W. C. Prinz, also on TDY, collected 110 samples of volcanic and plutonic rocks in the Al Lith–Jiddah–Khulays and Al Banah–Jabal Shada–Al Aqiq areas to determine the ages and relations of stratigraphic units in these areas. Fleck is conducting Rb/Sr studies of these rocks at the USGS geochronology laboratory in Menlo Park.

Fleck also completed a study of the Rb/Sr isochron of dioritic to granitic plutons of the Jiddah–Makkah area. The results showed that the age of the plutonic rocks ranges from 700 m.y. to 820 m.y., the age of most being between 760 m.y. to 790 m.y. Low $^{87}Sr/^{86}Sr$ ratios suggest that orthogenesis occurred during or shortly after the forming of plutons within a low Rb/Sr crust, probably at an intraoceanic convergent plate margin. In relation to evolution of the Arabian Shield, the results are consistent with models indicative of early development in an island-arc environment.

C. E. Hedge continued with laboratory studies, both Rb/Sr and U/Pb zircon methods, on samples that he and W. E. Davies collected from the Waji area, northeastern Hijaz. Hedge and Davies are undertaking this study as a collaborative work project.

J. S. Stacey completed zircon dating of a sample from a quartz diorite in the Wadi Wassat region. The results gave an age of 642 m.y. for this intrusive body, which was determined previously to be 815 m.y. by R. J. Fleck, using the Rb/Sr dating method. The latest determination, which resulted in a younger age, suggests that the layered rocks of the Wadi Wassat region are of Halaban age. Stacey also collected samples in the Halaban–Al Amar region with D. B. Stoeser and in the Ranyah–Jabal as Sukkah region with M. R. Brock and R. C. Greene to determine zircon/common-lead ages and to establish the common-lead distribution pattern in those regions. He also collected samples of felsic intrusive rock near Mahd adh Dhahab for U/Pb zircon dating and, galena samples from the ore deposit at Mahd adh Dhahab for common-lead study.

J. N. Aleinikoff is conducting laboratory studies on peralhaline granite samples from the Wadi Wassat– Najran region, from Jabal Dibbigh in northwestern Hijaz, and from the west-central and east-central Shield. Zircon dating of the Jabal Dibbigh granite samples gave a date of 570 m.y.

Studies of geomorphology

J. W. Whitney conducted field investigations in the southern shield region of Saudi Arabia, studying and collecting samples of surficial deposits associated with major and minor drainage systems. Fluvially redeposited eolian silts were examined at Badr, Hamdah, Wadi Habawnah, and As Subaykah.

A preliminary petrographic study of silt grains from loessal deposits found on the Arabian Shield revealed a relatively high proportion of minerals not normally found in eolian deposits. The presence of easily weathered minerals seems to indicate local sources of exposed and weathered bedrock for the primary components of the silt deposits.

Fieldwork at the western edge of the Rub al Khali produced evidence that the majority of dune forms in this region have been largely stabilized for at least several thousand years.

Whitney also investigated several major drainage basins in the southern escarpment region, studying and collecting samples of terrace deposits and basalt flows that are present in places found on erosion surfaces in the scarp mountains. It is anticipated that a series of K-Ar dates on basalts from these surfaces will indicate late Tertiary and Quaternary uplift of the Arabian Shield.

Whitney and D. J. Faulkender discovered the remnants of an erosion surface of probable Tertiary age at the edge of and beneath the sands of the An Nafud. This surface was developed largely on Paleozoic sandstones and is a likely source for the sands of the sand sea when the region became distinctly arid in the Quaternary. Highly altered sandstone, possibly a laterite-saprolite sequence, also was discovered on Jabal Irnan and Jabal al Misma. This sequence was developed on the Tabuk Formation on surfaces that are at least 60 m above the present general erosion surface on the south side of the An Nafud.

Whitney and G. M. Fairer examined saprolite deposits in the Asir region and concluded that there are at least two episodes of saprolite-laterite formation in the area.

The older and less intense period is pre-Wajid sandstone in age and is best developed in the Suq al Ithnayn area and at Jabal Sawdah; the second is probably Eocene in age. Fragments of the underlying saprolite can be found in the lower 4 m of exposed Wajid sandstone at places concentrated along former erosional surfaces in the sandstone. The saprolite appears to be preserved only in areas of low topographic relief and ranges in thickness from less than 1–8 m, depending on location and rock type. Pre-Wajid saprolite definitely was affected during the better known episode of laterite formation of probable Eocene age in which thin laterite with classic pisolitic structure developed on the Wajid in the region of the Asir volcanics. It is underlain by essentially unaltered sandstone that has been recemented by silica solutions probably related to the Tertiary weathering episode. Below the sandstone, pre-Wajid saprolite can extend as deep as 6 m in the metamorphic and igneous basement complex and is generally altered to a greater degree than in areas where no effects of the Tertiary episode are present.

Preliminary results of research on pollen by E. Schulz, University of Marseille–Luminy, France, and Whitney indicate that pollen is present in most surficial deposits in Saudi Arabia and that concentrations are apparently greater than those normally found in the Sahara. Deposits interpreted to be the product of moister climates contain vegetation that is considered to be normal for arid to semi-arid climates. This seems to indicate that climatic changes in the later Quaternary in Saudi Arabia were not very great.

Studies of Red Sea coastal areas

D. L. Schmidt studied the Tertiary sedimentary and volcanic rocks of the Red Sea coastal plain between Jizan and Qunfudhah. The work included mapping and measuring sections of the Baid Formation and volcanic rocks of the Wadi Dhamad Group. Fossils collected from the Baid Formation included fish, freshwater clams, and gastropods. Shell fossils from the Khums sandstone and vertebrate fossils from the Amran limestone were also collected.

Mineral-resources investigations

I. M. Naqvi and M. A. Hussein completed geologic mapping and rock sampling for trace-metal analyses in two adjoining electromagnetic anomalous zones. This study is the last of a number of ground followup investigations of airborne anomalies in the Wadi Bidah district.

Naqvi reported that the area seems to be part of a north-trending eroded anticlinorium composed of predominantly north-striking, steeply dipping metasedimentary rocks. Much of the stratigraphic section consists of silty mudstone and chemical precipitates, including massive chert locally containing pyrite and minor copper staining. Cherty iron manganese rocks are a major feature. In places manganiferous zones grade into goethite-hematitic gossans that are copper stained. These beds closely resemble the strata in Wadi Bidah proper. Analytical results to date indicate an association of gold, silver, zinc, copper, and high manganese.

On work completed earlier in the year in the Al Qunfudhah area, M. M. Mawad reported that base-metal sulfides were intersected by drill holes UAR–1 and UAR–2. UAR–1 intersected a sulfide zone from 48.7 m to 52.0 m, and a 1–m interval within this zone assayed 70 g/t silver and 1.07 percent copper. UAR–2 intersected sulfides from 111.7 m to 118.3 m, and the highest assays obtained within this interval were 40.3 g/t silver and 1.25 percent copper from 115.8 m to 116.3 m. Mawad states that the fine sulfide mineral can be identified only after the drill core is split. Chalcopyrite and bornite were the principle base-metal minerals recognized.

M. D. Fenton completed investigation of the Wadi Habawnah and Najran quadrangles. Analyses of samples from 22 gossans and associated stream sediments did not give promising results and suggest that the potential for stratabound sulfides in the layered volcanic rocks in these areas is poor. The results for several local areas in granitic rocks gave slightly higher values that are worthy of reconnaissance Wadi sediment geochemistry surveys.

Studies of felsic volcanic rocks

Analytical results of E. A. du Bray's reconnaissance sampling of the felsic plutonic rocks in the eastern Arabian Shield suggest the existence of a province of S-type granites in the eastern Shield that are potential hosts of Sn, W, or Mo mineralization. These small plutons are characterized by F content greater than 1,500 ppm, Li greater than 100 ppm, a Rb/Sr ratio greater than 1, and higher than normal content of any of the following: Bi, Ag, Pb, Rb, Y, Zr, and Nb.

Du Bray's reconnaissance geochemical study of the At Taif–Al Baha area identified a copper anomaly associated with a porphyritic monzogranite pluton; and a low-grade tin and rare-earth anomaly associated with a monzogranite was located southwest at At Taif. Work will continue on these anomalies and on a tungsten anomaly south of At Taif.

J. C. Cole, C. W. Smith, and M. D. Fenton reported that significant tungsten mineralization in the Baid al Jimalah tungsten deposit is present within and marginal to a small irregular cupola and dike network of late Proterozoic, porphyritic, biotite-bearing microcline-albite

granite in the Al Jurdhawiyah quadrangle (sheet 25/42 D). The granite is highly enriched in Li, F, Be, W, and Sn, and has been heavily veined and greisenized, probably during an intense hydrothermal event related to the emplacement of the granite. Mineralization consists principally of very coarse crystals of wolframite, lesser cassiterite, and minor scheelite in stockworks and in dense, subvertical zones of vuggy quartz veins. Greisenized granite and country-rock hornfels contain some disseminated cassiterite, wolframite, and lesser pyrite. Composite outcrop samples of vein material, greisen, and relatively fresh granite contain up to 6,400 ppm tungsten and 300 ppm tin. The outcrop extent of the mineralized area exceeds 700 m by 800 m and encloses four subparallel zones of closely spaced quartz veins. The southernmost of these zones is somewhat distinct, containing higher median concentrations of lithium, fluorine, tin, beryllium, and sulfides, and may have been formed at slightly lower temperatures.

The granite and veins were emplaced into fine-grained clastic rocks of the Murdama Group, just below the subhorizontal unconformity that marks the base of the younger Al Jurdhawiyah Group of continental andesitic volcanic and volcaniclastic rocks. Tungsten mineralization is most likely younger than the Al Jurdhawiyah Group and may be cogenetic with a vein- and fracture-controlled lead-zinc-silver deposit 2 km to the east.

Analyzed samples of Wadi sediments from the vicinity of the tungsten deposit showed that the ore minerals have not been widely dispersed by surficial processes. Anomalous concentrations of tungsten and tin are present only within a radius of about 2 km of the mineralized area and, therefore, similar deposits easily could escape detection in geochemical surveys of low sample density.

In followup investigations, J. E. Elliott (TDY), J. C. Cole, and Rashid Samater completed detailed mapping at 1:1,000 scale and sampling of the Baid al Jimalah prospect. The samples were collected along both walls of 11 bulldozed trenches. Assay results have not yet been received.

R. G. Worl reported that numerous samples collected from quartz veins in the old mine workings and dumps of the Aqiq Ghamid area gave high values for gold.

Commodity investigations

C. L. Smith collected samples of salt and brine from two known salt deposits and two sabkhahs in the Eastern Province for bromine analyses. The assay results obtained for these samples are being used in computer programs specifically developed to manipulate the assay data for future exploration purposes.

Studies at the Mahd adh Dhahab mine

USGS TDY personnel visited the Mahd adh Dhahab mining area to undertake various studies. The team was as follows (research area in parentheses): R. G. Worl, team leader (geochemistry); R. J. Ebens (geochemistry); Abdul Afifi (mapping, petrography, stable isotopes, and fluid inclusions); R. O. Rye (stable isotopes); C. G. Cunningham (fluid inclusions); J. S. Stacey (U/Pb geochronology, common Pb isotopes); and W. E. Hall (ore petrography). From field examination, the team felt that the mineralization is associated with an hypabyssal rhyolite mass that intruded its own volcanic ejecta. The later stages of intrusion were dominated by forceful emplacement that domed the overlying country rocks. A metamorphic aureole (or hornfels) was formed, and xenoliths were incorporated in the stock. Pervasive silicification and sericitization grade locally into chlorite and potassium-feldspar alteration as the dominant assemblage.

Pressure gradients at the margin of the stock resulted in the formation of a crackle breccia by hydrofracturing. The breccia is pervasive and extends into the country rock. At the highest levels of the dome, the spalling off of slabs of country rock and solidified rhyolite produced cracks that filled with clastic debris.

Ore deposition was largely controlled by the pressure gradients and by attendant thermal, physical, and chemical changes at the margin of the stock. In the course of going from a lithostatically dominated rhyolite magma system to a hydrostatically dominated system in the adjacent country rocks, the fluids would be expected to boil, and cool, losing H_2O and CO_2, and to undergo resulting pH changes.

Continued extensional tectonism produced regional north-striking fractures that cut the rhyolite. Some vein systems in these fractures are mineralized at the surface and others are barren. Some veins may result from continued activity during waning stages of the hydrothermal systems or may be related to an undiscovered younger system at depth.

In a separate study, L. S. Hilpert and R. J. Roberts (both TDY) remapped an area approximately 450 m by 300 m around the old mine workings at Mahd adh Dhahab at 1:800 scale. The purpose of this work was to correlate surface and underground geology and to obtain a better understanding of the ore controls.

Andrew Griscom completed the interpretation of 11 of the 1:250,000-scale aeromagnetic maps in the southern Najd and part of the southern Tuwayq quadrangles. Significant contributions included the delineation of zones of reversely polarized versus normally polarized

rock and the determination of dips of major structural boundaries such as the Al Amar fault zone.

H. Sadek and H. R. Blank obtained spectral energy plots of anomalies on 240 of the 20-km profile increments (complete Fourier transform method), most of which showed a clear separation of volcanic and basement sources. Interpretation is continuing.

THAILAND

J. C. Wynn found that potash deposits in northeastern Thailand appear to be controlled by basin-margin structures. Gravity data appear to outline these structures in a broad regional sense, and electrical geophysical methods may help resolve local structural complications that currently bedevil the exploration drilling program. Landsat image analysis already has proven effective in partially outlining regional structural interrelations.

V. E. Swanson visited Thailand from July 27 to August 8, 1980, reviewed existing lignite data, and recommended an 18-m drilling program for the Mae Sot–Mae Ramad coal exploration project.

TURKEY

The USGS maintains an active project in Turkey that is part of the Earthquake Prediction Network.

Results of part of a former assistance program with the Maden Tetkik ve Arama Institusu were published as Bulletin 1461 (Krushensky and others, 1980). The Karalar–Yesiller area was mapped to demonstrate the value of quadrangle mapping in delineating mineralized areas, in defining stratigraphic and structurally significant relations, and in defining controls for base-metal mineralization.

W. J. Moore, economic geologist, and D. G. Rogick of the Bureau of Mines and under AID sponsorship visited the Cayeli copper project in the eastern Black Sea region of Turkey and assessed the development potential of this volcanogenic copper deposit. Moore determined that the development potential is good and that limited AID involvement through funding of a prefeasibility/feasibility study is warranted.

UNITED KINGDOM

The first project undertaken by the USGS and the National Environment Research Council (NERC), the joint USGS–IOS (Institute of Oceanographic Sciences) geophysical oceanographic survey in September 1979 to map the morphologic characteristics of the sea floor and to identify areas of sea floor instability, was accomplished by using the IOS side-scan sonar Geological Long Range Inclined Asdic (GLORIA) whose swath of approximately 40 km allowed rapid mapping of the continental slope between Georges Bank and the Bahamas. The project is sponsored by the USGS and the DOE. Chief scientists were David Roberts of IOS and P. G. Teleki of the USGS.

Other USGS personnel included D. C. Twichell, Jr., K. M. Scanlon, K. V. Cashman, Patricia Collins, K. M. Kent, F. R. Musialowski, A. O. Goodman, and F. R. Keer.

Remaining commitments include the digital correlation of raw sonar signal data recorded by the USGS onboard ship; the application of various image correction and processing methods to the data; generation of sea floor mosaics; technical/scientific information exchange and joint reports with IOS.

VENEZUELA

Through the DOE, the USGS conferred with the Ministry of Mines and Energy and Simon Bolivar University of Venezuela in designing a program for evaluation of energy demands and supplies for the future; R. W. Fary (1980) reviewed the geology of petroleum in Venezuela.

YUGOSLAVIA

Four projects, karstic terrain, rare metals, crustal structure, and geologic factors affecting urban development, are included in the USGS cooperative research program that uses the Special Foreign Currency Fund. Each of these projects essentially has completed scheduled fieldwork. Each project has a USGS project monitor who spends about 1 man-month/year in monitoring the project. A fifth project on ground motion during earthquakes has been approved.

- Karstic terrain: Research on geophysical methods for determining permeability and for tracing underground caverns and streams uses seismic detection of bombs exploded at timed intervals in underground streams and repeated measurements of electrical resistivity along an established network of stations. Through continued monitoring of the electrical resistivity network, the project expects to detect changes in permeability with time and with variations in water level, with the object of being able to predict possibly disastrous collapse and flooding.
- Rare metals: The project has studied the relations between different types of granite intrusions and the associated Sn, Ta, Nb, Li, Be, and rare-earth minerals in order to identify geologic associations that will aid in exploration of an arcuate mineral belt in eastern and northern Yugoslavia.
- Crustal structure: The project has completed four two-way seismic profiles and half of a fifth profile;

seven profiles are included in long-range plans. Analysis of data from the completed profiles, incorporated with gravity data, has led to a proposal of dynamic isostasy for the Dinaride region.

- Geologic factors affecting urban development: The project has made detailed geologic, engineering-geology, tectonic, and physiographic studies in the Bosanska Krajina near Sarajevo and has prepared a series of derivative maps applying these studies to problems of urban development in an earthquake-prone area.

ANTARCTIC PROGRAMS

Geology of the Orville coast

During the 1977–78 field season, the Orville coast and parts of eastern Ellsworth Land, Antarctica, were geologically mapped in reconnaissance (P. D. Rowley, 1978). At that time 14 stocks and 1 batholith were discovered intruding folded fine-grained sedimentary rocks of the Latady Formation (Middle and Upper Jurassic) and folded volcanic rocks that intertongue with the Latady. Five of the plutons, considered representative of all plutons, were recently dated using potassium-argon methods by Edward Farrar (Queen's University, Kingston, Ontario) and P. D. Rowley (Farrar and Rowley, 1980). Most are of quartz diorite and granodiorite composition. Ages from the Haggerty stock, southeast Sweeney Mountains, range from 105 m.y. to 116 m.y. Ages from the Witte stock, Witte Nunataks, range from 108 m.y. to 112 m.y. Ages from the Smart stock, southwest Sweeney Mountains, range from 103 m.y. to 111 m.y. Ages from the Sky-Hi stock, Sky-Hi Nunataks range from 121 m.y. to 123 m.y. This pluton is altered and weakly mineralized and may represent the barren upper part of a porphyry copper-molybdenum deposit. Ages from the west Behrendt batholith, west of the Behrendt Mountains, range from 105 m.y. to 109 m.y. The ages of the plutons indicate a Late Cretaceous magmatic event. Ages and rock types of the plutons are similar to those reported elsewhere in the southern Antarctic Peninsula.

CARTOGRAPHIC AND GEOGRAPHIC RESEARCH

PHOTOGRAMMETRY

Online Aerotriangulation Data Collection and Editing System

The Online Aerotriangulation Data Collection and Editing System is being developed to collect and edit coordinate data while aerial photographic plate measurements are being made. The system will detect mensuration blunders by performing interior orientation on a single photograph and relative orientation between successive photographs. Microcomputers will be interfaced to manual comparators and stereoplotters and to peripherals such as flexible disk drives. The communication between each computer and its comparator/plotter will be through an Altek digitizer.

Pass point marking system

Aerotriangulation is used in the process of making maps from aerial photographs to establish control for each stereoscopic model. Model control points—pass points—are marked on photographic plates or film by drilling minute holes in the emulsion. Pass point data are generally stored in the USGS computer system using the Photogrammetric Archival Storage System (PASS) program.

New copies of original aerial photographs need to have the pass points marked on them. The hardware for marking them consists of a Kern CPM-1 monocomparator/stereoscopic point marker interfaced to an Altek AC-74 digitizer. The left stage of the CPM-1 is equipped with linear encoders and serves as a monocomparator. A Hewlett-Packard HP-9835 desktop computer is interfaced to the digitizer and a nine-track 1600-bpi Dylon magnetic tape unit.

The original pass point coordinates from PASS are transformed to the stage coordinate system of the CPM-1 using a six-parameter affine transformation. Transformation parameters are based on measurements of four to eight fiducial marks. The operator manually moves the stages to the desired coordinates and drills the left photographic plate. The right photographic plate is marked by stereoscopic transfer.

Early tests of the software indicate that this system also can improve the efficiency of normal aerotriangulation work by allowing the operator to mark and measure points in one setup, instead of the usual two-step process.

Glacier movement

Photogrammetric techniques were used to measure the surface and terminus movement of the Columbia Glacier, Alaska. The unusually rapid surface movement and the recession of the terminus have been of recent concern to glaciologists and users of nearby shipping lanes to the oil port of Valdez. Analytical aerotriangulation techniques were used to track and digitize an array of points on over 20 successive dates of aerial photography. Some unique control and point transfer techniques were required to achieve desired accuracy of the study. Surface velocity, ice volume, and terminus recession data were computed from coordinate changes between successive dates of photography.

SATELLITE APPLICATIONS

MAPSAT

Results of a feasibility study indicate that the Mapsat concept is within the state of the art and encompasses features that could make an operational satellite system an economic and practical possibility. This system uses many Landsat mission characteristics, but features improved resolution, stereocoverage, and epipolar plane scanning geometry. Multicolor image maps at scales as large as 1:50,000 with 20-m contour intervals are envisioned as products of the system.

The epipolar plane concept is a totally new approach to remote sensing of the Earth from space. Each sensor is composed of several thousand linear array detectors sensing in epipolar planes and, therefore, providing the potential for correlation of stereoimagery in a one-dimensional sense. One-dimensional data correlation is expected to reduce the computational workload required in the stereocorrelation process.

MULTISPATIAL DATA ACQUISITION AND PROCESSING

Data rate limits are a primary design parameter in any electro-optical system, and they tend to counter multispectral high-resolution requirements. It generally is acknowledged that when more than one spectral band is involved, considerable redundancy exists in acquired data. Since the same boundaries (spectral signature dif-

ferences) are recorded in more than one spectral band, it should be possible to record one dominant band at high resolution and others at a lower resolution with a decrease in data rate but without a corresponding loss in information.

The multispatial principal can apply to digital image data as well as to analog data. Reconstruction of two lower resolution bands based on the boundaries resolved in a higher resolution band yields significant improvement in radiometric quality and, by inference, information content. This has far-reaching significance with respect to the design of an operational Earth-sensing system, and it indicates that for any general-purpose multispectral system on which a maximum data rate is imposed, the multispatial concept must be applied if the system is to produce a maximum of information.

IMAGE MAPS

Landsat data are useful in expediting the preparation of image maps in poorly mapped and inaccessible areas. Since the USGS has successfully demonstrated unique new methods and techniques that are necessary to compile image maps of optimum detail, many requests for assistance have been received from various parts of the world.

In response to these requests a number of Landsat color or infrared image maps have been produced. They include:

- Pakistan – 1:500,000 scale.
- Parts of Ethiopia, Kenya, Sudan, Tanzania, and Uganda – 1:500,000 scale.
- Saudi Arabia – 1:250,000 scale and smaller.

The Pakistan image maps were printed in an atlas format by the three-color halftone process in Karachi. The East Africa image maps were prepared using the same process during a technical training program held in Kenya.

In addition, Landsat image data have been used to compile a 1:100,000-scale return-beam-vidicon (RBV) image map of Cape Cod, Mass., and vicinity. Four RBV images were mosaicked and fitted to a control base. This image base map will be used in preparing a geologic map of Cape Cod and in preparing an intermediate-scale planimetric map.

Landsat multispectral scanner (MSS) images of the Berry Islands, Bahamas, were digitally and photographically enhanced to emphasize underwater detail. Bands 4, 5, and 7 were combined to form a color composite, while Band 4 alone was combined with bathymetric details. The two resulting maps were printed on one sheet.

RADAR STUDIES

The USGS is participating in the evaluation of the utility of side-looking airborne radar (SLAR) imagery. Existing real- and synthetic-aperture SLAR data of areas within the contiguous United States have been purchased, and new SLAR data in two areas of Alaska have been acquired.

SLAR imagery compared with computer-generated imagery

Three adjacent 15-min quadrangles – Garrison, Avon, and Ellison – all in the Butte, Mont., 1:250,000-scale quadrangle have been selected for comparison of SLAR imagery with computer-generated shaded-relief imagery. For these quadrangles shaded-relief imagery was generated by mosaicking the 1:24,000-scale digital elevation models (DEM) within the computer. A Sun elevation angle of 30° and Sun azimuth angle of 90° were chosen so as to closely correspond to the illumination of the radar beam. The radar imagery is west looking. In addition, Sun azimuth angles of 45° (southwest look) and 270° (east look) were used to generate shaded-relief images. Each 15-min quadrangle, therefore, has three shaded-relief images.

While the shaded-relief imagery does not depict surface features such as streams, roads, and towns that appear on radar imagery, this may not be a drawback in that this additional detail may be distracting when analyzing geologic structural detail. Radar imagery must have at least two orthogonal "looks" in order to detect all ground structure. However, this entails reflying each area at a considerable increase in cost. It is simple and economical to produce multiple-look shaded-relief images once the DEM's are available.

The shaded-relief image has the added advantage of not being subject to radar shadowing, which can be detrimental to interpretation. A more geometrically correct product also results from the shaded-relief image, because radar layover is absent, and the DEM collection procedures are more precise than is radar data collection.

Determining base mapping categories from SLAR images

Synthetic-aperture SLAR image mosaics of the Butte and Wallace, Mont., 1:250,000-scale quadrangles were chosen for analysis of base mapping categories. Both of these topographic quadrangles have the five principal base categories:

1. Hydrography – Drainage, rivers, wetlands, reservoirs, shorelines.
2. Landforms – Hypsography (terrain), non-vegetative or geologic features.

3. Transportation–Roads, railroads, pipelines, bridges, tunnels.
4. Boundaries–Artificial, military reservations, forests.
5. Culture–Manmade structures, buildings.

The evaluation of these five categories has shown that natural features such as hydrography and landforms are easiest to detect and identify without the need of the corresponding line map as a guide. Transportation features are difficult to trace because they intermittently disappear in the imagery.

Urban areas image as white patches, and road patterns within urban areas cannot be easily detected. Images of airports also appear as bright spots, caused by the returns from metallic and concrete objects. The urban patterns and airports lose sharp form because of low resolution and backscatter.

Screenless printing of SLAR imagery

Experimental maps of real- and synthetic-aperture SLAR imagery have been printed in different hues and colors of ink by the screenless printing process. This process results in a duotone effect without the cost and time of making two impressions with two inks on the press. In addition the screenless process provides improved resolution of detail due to structuring the image as random dots equivalent to the very fine chemical grain structure of the aluminum pressplate.

An inherent problem of SLAR imagery is the image loss in shadowed areas created by a lack of radar beam return. A SLAR image "illuminated" from the opposite direction partially fills this void. After reproduction by screenless printing, combinations of synthetic- and real-aperture images are being evaluated.

A 1:250,000–scale mosaicked radar quadrangle of Seattle, Wash., has been printed in experimental map form using the screenless process and a mixed black-brown ink. A collar was designed that gives the pertinent data concerning the radar image and diagrams the flight strips that comprise the mosaic. A fitted UTM (Universal Transverse Mercator) grid was generated by measuring control points on the mosaic and on the corresponding line maps.

The Hoquiam, Wash.-Oreg., quadrangle, which includes Mount St. Helens, has been printed in a black-green ink as a comparison to the black-brown ink of the Seattle quadrangle. No grid or collar was made for Hoquiam. Both a screenless and a halftone version were printed.

Fitted grids for the radar quadrangles studied produced root-mean-square errors of approximately 250 m, which is comparable to results found for 1:250,000–scale Landsat MSS image quads. Control points for radar imagery must be chosen so as to lie on the same elevation, otherwise radar layover produces horizontal discrepancies of up to a kilometer in mountainous terrain.

GEOGRAPHIC RESEARCH

Land-use and land-cover map accuracy

An operational technique for testing the accuracy of land-use and land-cover maps was developed and tested. Both the minium sample size needed to validate the accuracy for each category and the critical level to test whether a category met a specified accuracy are developed from the cumulative binomial distribution. The algorithm for selecting a sample for testing is based on sampling from two frames. The sampling algorithm and computer program were tested using the Tampa, Fla., land-use and land-cover map, and the results were compared with a previous accuracy evaluation using a manual sample selection. In the manual sample only 6 of the 26 categories were represented adequately, and 9 were not represented at all. In the operational test, all 26 categories were represented, and an optimum number of points were selected as a minimum unless there were too few polygons in the category to achieve the optimum number. The accuracy of the manual sample was 93 percent, with a one-tailed 95–percent lower confidence limit of 91 percent. The accuracy of the operational test was 97.6 percent, with a lower one-tailed 95–percent confidence limit of 97 percent.

Further research established a methodology for analyzing area data acquired in land-use and land-cover mapping experiments. Some techniques of nonparametric statistics are applicable to the analysis of area data in thematic mapping experiments. A two-test procedure is used that is analogous to testing the shape of two curves and the distance between them in order to determine if they are statistically identical. A multiple-sample experiment of land-use and land-cover classification at three scales was conducted. In this experiment the land-use and land-cover classification at the scale of 1:250,000 was determined by area to be significantly different from the two other scales (1:100,000 and 1:24,000). In a paired-sample experiment of the land-use and land-cover classification at 1:24,000 scale from both high-altitude aerial photographs and Skylab S–190B imagery, no significant difference was determined by area.

Evaluation of variables of thematic mapping experiments that affect classification by thematic categories (such as scales, images, or algorithms) was undertaken by the use of the analysis of variance technique. Data from an experiment using three scales of land-use and land-cover mapping have been analyzed. There is evidence of significant differences among the

three scales (1:24,000, 1:100,000, and 1:250,000). Multirange tests showed that all three scales are different.

Land-cover pattern analysis

Some success was achieved in discriminating flooded wetland forest from other surrounding forest using imagery from Seasat L-band radar. Analysis of this imagery was most effective in the nearly level sections of the Atlantic and Gulf coastal plains. However, in rugged terrain, distortion introduced during the conversion of the reflected radar energy to an image as well as saturation of various parts of the image due to topographic roughness hinders wetland delineation.

Experimentation with the satellite-borne L-band radar continued in the pursuit of better delineation of snow and ice features. The critical gap revealed during the research was the need to have simultaneous field data collection coordinated with the radar overflight, since the boundaries of the snow and ice features are so variable during the season of minimum extent.

Land-use change in Allegheny County, Pennsylvania

In 1980, the USGS published a one-sheet color-lithographed land-use and land-cover map of the six-country Greater Pittsburgh region at 1:125,000 scale, USGS Miscellaneous Investigations Map I-1248. The map was compiled from aerial photographs acquired in 1969 and 1973–just before and after the 1970 Census. This new map contains several aids on its margins for analyzing and interpreting the land use and land cover in the Pittsburgh metropolitan area, including a unique analysis of land-use change in Allegheny County. Between 1969 and 1973, land use and land cover of 1.57 percent of the Allegheny County total land and water area was converted from one class to another, or was undergoing change. Besides urban expansion, other significant changes were the result of interstate highway construction and the resurgence in strip mining for coal.

Issued just after the 1980 Census, the Pittsburgh land-use map and data thus offer area planners a bench mark for correlating and interpreting a decade of land-use change with corresponding changes in population and housing. The changes observed attest to the dynamic nature of land use and land cover and to the value of remotely sensed data in monitoring change phenomena. They also demonstrate the need for geographic information systems to update earth-science data and to relate them to population and to resource management problems.

Cropland/pasture area delineation

High-altitude color-infrared photographs used to prepare Level II land-use and land-cover maps were studied to determine whether they could be used to differentiate cropland from pasture in three Louisiana parishes–Ascension, Cameron, and East Carroll. Photointerpretation and field verification suggest that the USGS should not, as a standard practice, delineate cropland from pasture from high-altitude photographs, particularly when the photographs have been obtained at times other than the growing season. The low interpretive accuracy level (74 percent) of the test fell short of the USGS requirement of 85 percent.

Estimating irrigated land area using Landsat imagery

To aid computer-modeling studies of the ground-water hydrology of the High Plains aquifer, the USGS is compiling maps and data of irrigated cropland and pasture obtained from analyzing multitemporal Landsat digital data. Such data can be used to help estimate yearly water withdrawals from the aquifer.

More than one billion pixels from nearly 100 Landsat scenes are being analyzed and aggregated into a digital data base of 200,000 grid cells directly compatible with the hydrologic model. Lessons learned from this operational test will be used to specify techniques for efficiently using Landsat data for other hydrologic applications in the western United States.

Use of Landsat and terrain data in Alaska

To help inventory land resources contained within lease areas of the National Petroleum Reserve in Alaska (NPRA), the USGS has interpreted land-cover data for NPRA from digital Landsat data. The BLM is combining the digital land-cover data with digital 1:250,000-scale terrain data from USGS for the inventory. The NPRA land-cover data base currently is being extended with work to include the Prudhoe Bay area and the Arctic National Wildlife Refuge in support of needs of the U.S. Army Corps of Engineers and the U.S. Fish and Wildlife Service.

DIGITAL CARTOGRAPHY

Sci-Tex map scanning and digitizing system

Feasibility testing of various product applications of the Sci-Tex map scanning and digitizing system has been started. The system has been found to be an efficient tool for updating and revising maps and in producing high-quality map color-separation films.

The Sci-Tex is a color raster system that permits an operator to scan and edit multicolor graphics and to generate map color separations. A map is input to the system from a variable-resolution scanner that can distinguish up to 12 colors or shades. Using the editing station with its interactive color-graphics terminal and display, changes to the map can be made manually by stylus and tablet or automatically by system commands from the keyboard. A large-format high-resolution laser plotter produces film positives and negatives. The central processing unit coordinates the peripherals and controls file storage, processing, and modification.

Gestalt Photo Mapper II

Integration of a real-time disk operating system (RDOS) and USGS photogrammetric routines into an upgraded Gestalt Photo Mapper II (GPM2) operating system is now in its final stages. Orthophotographs and digital elevation models (DEM) have been produced from test models using the RDOS. These products have demonstrated that the RDOS provides algorithms for improved interior and exterior orientation, for scanning in a unified reference system on one, two, or n-models, and for prevention of redundant scanning of any portion of the scanned domain.

Major remaining tasks for the successful completion of this project are the final debugging of all software and system enhancements based on feedback from operating personnel. When completed, this project will result in significant improvements in GPM2 productivity. Resampling of elevation data, which is presently required to combine several models into a single DEM, will be simplified.

Voice data entry systems

Five voice data entry systems have been purchased, tested, and accepted for use in map-digitizing work. Each system is composed of a microcomputer with an interactive terminal having 40-character alpha-numeric display, line printer, voice-recognition module, and speaker. The floppy-disk storage can be reformatted and copied by the use of software routines. The two disk drives of each system optimize file space.

The major advantage of the system is the ability of the user to make voiced data entries with no interruption to his cartographic task. The operator of a digitzer, for example, is not required to enter attribute code changes by hand. He simply speaks the appropriate word, the voice-recognition module recognizes the speech by comparing it to a pretrained vocabulary reference pattern for that user, and the proper code is entered. To verify that the word was properly interpreted, a voice synthesizer may be used to speak the word for the entered code.

Kongsberg symbol plotter

Research has continued toward the development of an automatic map-symbol placement system by testing an Altek angle-measuring data acquisition system driving a Kongsberg automatic plotter. The plotter positions and exposes topographic and geologic symbols on a photographic lettering separate during the mapmaking process. The map symbols are placed at precise x and y coordinates and rotated to specific angles using commands stored on magnetic tapes that direct the plotter movements.

Digital elevation models from stereomodel digital data

The Digital Cartographic Software System (DCASS) collects and uses digital data obtained directly from the stereoplotter. DCASS is modular in design, and supports basic cartographic manipulations such as automatic feature-join between photogrammetric models, batch or interactive editing, vector or raster graphic output, and production of high-accuracy digital elevation models (DEM).

The software package produces DEM's from stereomodel digital data. The process involves a specialized conversion in which elevation-tagged digitized contour lines are software-scanned and gridded by bilinear interpolation. The scanning process copes with certain peculiarities of a contour data set, such as banded, feathered, and discontinuous (supplemental) contour lines. Provisions also were made for correct treatment of grid intersections falling inside a top or depression. In addition, the method employs extensive checks for logical errors (miscoded line attributes or elevations) and physical errors (missing or extra contour lines, join faults) in the contour files. Graphical error depiction, in the form of contour overlays coupled with statistical error-line analysis, provides for identification of the error-causing vectors.

Production of high-accuracy DEM's is feasible due to the density of useful information available from a digital contour file. The degradation of relative vertical accuracy when going from the contour (vector) representation to the DEM (raster) representation is less than one-tenth the contour interval for a medium-density quadrangle. While currently being used for the production of DEM's, the method has applications in gridding any surface represented by isoline vectors.

Digital landlines for orthophoto production

Manual preparation of the public land survey printing separates is expensive, and the cost to extract the information from 1:48,000-scale source material is even greater. A computer program was developed to use

standard digital line graph (DLG) data to prepare the landline plate for orthophoto production. In addition to satisfying the orthophoto production requirement, using the DLG data provides an additional check on its attribute coding.

Cartographic plot and map projection software

The original Cartographic Automatic Mapping (CAM) program employed by the USGS could be used only to plot small-scale maps and was limited to IBM computers. To overcome these limitations and to increase the application range, a double-precision version of the CAM program was converted to all-FORTRAN language. A general cartographic transformation package replaced the original map projection routines in the original CAM by including additional projections and both forward and inverse computations. The new composite program was renamed "GS-CAM" and will be distributed by the National Cartographic Information Center.

Interactive editing of digital elevation models

When the GPM2 is scanning over large water bodies, the system cannot properly correlate the left and right images. This results in elevation errors in the DEM; and if the errors are not corrected, the DEM will not pass the accuracy requirements for entry into the digital cartographic data base.

To overcome this problem, a procedure is being developed by which the boundaries of the water bodies are digitized on an interactive computer graphics system, tagged with their true surface elevations, and cross-correlated with the unedited DEM's by a "polygon fill" program. This procedure will handle multiple water bodies and islands simultaneously.

Traverse adjustment, transformation, and plotting program

A computer program has been developed to generate x-y coordinates and plots from boundary descriptions. Up to 2,000 bearings (or azimuths) and distances may be input. Options include a first-order transformation to State plane coordinates, traverse adjustment using the compass rule, calculations of closure error and enclosed area, and inverse calculations. Plots of both the adjusted and unadjusted coordinates can be drawn at any scale, with optional grid overlay.

CARTOGRAPHIC DESIGN

In anticipation of the second edition of the "National Atlas of the United States," the design of the 1:2,000,000-scale reference maps has been scrutinized. Each class of point, line, and area symbol used in the first edition has been analyzed by using the principles of cartographic communications. The analysis indicates that the symbolization in the first edition may have been unnecessarily complex.

Several proofs using the digital files of the 1:2,000,000-scale reference maps have been produced employing the suggested revised symbolization. The number of road categories and number of populated place categories have been reduced. The hierarchy of the colors used for the various categories of Federal lands has been redesigned. The proofs presently are being evaluated prior to the specification of the final design.

SYSTEMS DESIGN

Aerial Profiling of Terrain

The Aerial Profiling of Terrain (APT) system is to execute accurate surveys of the terrain from low-flying aircraft using laser-ranging and inertial-guidance technology. The airborne instruments include a laser profiler, TV camera, inertial measuring unit, laser tracker, computer, and magnetic tape recorder. The computer interacts continually with the sensors by directing their actions and performing the necessary computations for initial alinement and calibration, for navigation to the survey site, and for execution of the surveys. The laser tracker provides correction data by measuring distances and directions to ground reflectors whose positions and elevations are known. Error analyses indicate that correction data are needed at 3-min time intervals to maintain the desired survey accuracy of 15 cm vertically and 61 cm horizontally.

Initial component fabrication is nearing completion and will be followed by a 2-yr contract to complete the prototype system, including component integration, installation of the system in the aircraft, performance of shakedown flights, and complete performance evaluation.

Orthophotoprojector clean room

A soft-walled clean room and filtration system was designed, fabricated, and installed over USGS orthophotoprojection equipment. This enclosure keeps the instrument's projector diapositive and orthonegative particulate-free during scanning operations. A steel frame supports the 14-mil matte-black nylon-reinforced vinyl tent. A vestibule permits the instrument operators to change from street apparel to lint-free clothing. A housekeeping vacuum was installed in the vestibule with an extension to carry the exhaust from the room.

To eliminate shadows during set-up, ceiling lights were installed on each side of the instrument. A third light is directed at the control console. Safe lights are used during scanning.

The film exposed during the 1- to 5-h scanning operation remains uncovered and vulnerable to the ambient air. To limit the particulates in this air, a laminar-flow module containing a high-efficiency particulate air (HEPA) filter was installed in the ceiling to provide positive pressure within the room. An HEPA filter is 99.97 percent efficient (by volume) in trapping 0.3 μ particles. A hot-air exhaust ventilation system was provided for the control console to remove the heat it generates.

Measurements of the airborne dust particles within the room will be taken during the year to assess the system's benefits.

Roll film transport

A 35-mm roll film transport system has been developed, fabricated, and installed on a printer originally designed to reproduce maps at original scale from computer cards with 35-mm film frame inserts.

The roll film transport eliminates the need to cut 350 film frames per roll and mount each frame in a computer card, resulting in a 25-percent timesaving in processing a customer's map order. A photoelectric digital counter is preset to advance selected film frames for printing. The transport and counter system can be operated at speeds up to 600 frames per minute.

Stereoplotter map revision module

To expedite map revision, the USGS has purchased a prototype map-revision module for Kern PG2-AT stereoplotters. The module superimposes the map manuscript image on the stereoimage of the stereoplotter using a TV camera and high-contrast TV monitor, a beam splitter, and auxiliary optics. The prototype module has met the basic functional requirements; however, some of the components are being modified to increase efficiency and ease of operation.

Sheet-film viewer

The USGS has developed a new sheet-film carrier to allow complete viewing of a 9.5×11-inch film without rotating or moving the film in the carrier. The carrier supports two glass plates. The bottom glass, upon which the film is placed, is held stationary on the carrier, which can be moved in both the x and y directions by precision sliding mechanisms. The top glass is mounted to a hinge that lifts it automatically when the carrier is moved to the extreme forward position in the viewer. This feature enables the operator to install or remove the film quickly. The modified viewer presents clear and highly detailed imagery, due primarily to the nonglare screen, multiple selection of light drawers, and numerous magnification lenses.

COMPUTER RESOURCES AND TECHNOLOGY

During 1980, the Computer Center Division (CCD) continued to receive requests from USGS scientists for additional data processing and data communication facilities. Data storage requirements continued to increase. Many USGS users increased their use of distributed systems, batch systems, interactive systems, graphics, and word processing equipment.

To provide improved service to the USGS's divisions and offices, the CCD expanded and upgraded its computational facilities during 1981. The following paragraphs outline the major actions taken to provide computing service to USGS scientists. Four areas are discussed: data communications, batch computing, interactive computing, and microcomputers.

DATA COMMUNICATIONS

Trends within the USGS's data processing community provided impetus to the growth of data communications. With the growing acceptance of distributed systems and word processing, users continued to request increased data communications capabilities. Scientists continued to increase the use of data processing techniques in their scientific research. Much of this research required computerized data to be transferred between geographically dispersed locations. These trends are expected to continue.

The CCD continued to expand and upgrade the data communications access facilities for all USGS users. Numerous requests for dedicated lines, modems, and multiplexers were processed. Other CCD actions that support the growing data communications requirements include

- continuation of the Value-Added Network TYMNET. Usage increased approximately 25 percent over that of 1980.
- efforts to install the ARPANET network delayed due to manufacturing problems. However, the equipment was to be delivered to each site by February 1981, and an operational date of June 1981 was planned.
- contract awarded in September 1980 for port sharing devices (PSD) for Reston, Va., Denver, Colo., and Menlo Park, Calif. This equipment will permit better use of existing computer ports by eliminating port dedication. All asynchronous users then will contend equally for the host computing resources. Installation was planned for first quarter 1981.
- plans in conjunction with the PSD's initiated to install a USGS backbone network providing high-speed linkage in a ring configuration involving Reston, Va., Denver, Colo., and Menlo Park, Calif. Installation was planned for April 1981. This will initially be for asynchronous communications.
- the absorption of the Washington Computer Center (WCC) into the USGS CCD. Plans for communications connecting WCC to the existing USGS computers were initiated.
- plans initiated to improve the quality of communication between Alaska and the General Purpose Computer Center (GPCC). This plan includes replacement of dialup facilities with a dedicated circuit. Also, TYMNET is upgrading its facilities in Alaska to provide better asynchronous service.

BATCH COMPUTING

An IBM-compatible processing system, Amdahl V/7, was procured and installed during 1980. The workload from the old central processing units (CPU's) of RE–1 and RE–2 was moved to this new system. Current plans include transferring a portion of the computing workload from RE–3 to the Amdahl System. The Amdahl V/7 will provide much of the processing capability that is required for the growing batch processing workload at the USGS.

Batch processing continues to dominate the USGS computer workload. During 1980, the batch workload increased approximately 23 percent. Numerous users installed inexpensive terminals such as the Intertec Data Systems Superbrain Q.D. The Superbrain Q.D. can function as a remote batch terminal as well as an interactive terminal.

It is anticipated that the batch workload will continue to grow as additional multifunction terminals are installed at the remote locations of the USGS. The CCD continues to use the American Management Systems contract to provide for overload processing.

INTERACTIVE COMPUTING

Various hardware components to supplement the interactive computing systems of the USGS were pro-

cured and installed in 1980. An additional CPU and an additional one million bytes of memory were added to each of the three large scale MULTICS computing facilities at Reston, Va., Denver, Colo., and Menlo Park, Calif. These hardware-component enhancements were added to provide the users of the USGS computing systems with improved interactive response time.

During 1980, the scientific community increased its usage of large interactive computing systems. Computer systems like the Digital Equipment Corporation VAX 11/780 (large minicomputer) were installed at various USGS locations. These minicomputer systems, along with the MULTICS computing system, are being used to process the growing interactive workload of the USGS.

MICROCOMPUTERS

During 1980, the CCD began evaluating the potential application of microcomputers in the various data processing activities throughout the USGS. This new technology is important to the USGS because many data processing functions can be directly supported on today's microcomputer in a very cost-effective manner. When mainframes are relieved of the more mundane processing chores such as editing data as it is being entered by a user, they are more available to perform tasks that demand mainframe power, such as number crunching, large data base processing, and global telecommunications support.

Present-day microcomputers offer a lengthy menu of capabilities. Such things as intelligent data entry, word processing, communications support, application software development (including FORTRAN, COBOL, PL/1, PASCAL, and other high-level languages), data base management, and management modeling are all currently available on a variety of microcomputer systems.

The CCD began evaluating a microcomputer system, manufactured by the Intertec Data Systems Corporation, known as the "SuperBrain." This device is a desktop microcomputer integrating a keyboard, CRT, twin Z80A microprocessors, 64K bytes of RAM and a pair of mini-floppy disk drives providing 676K bytes (formatted) of removable storage. The SuperBrain employs the CP/M 2.2 operating system from Digital Research, which is fast becoming the defacto standard for 8080-, 8085-, and Z80-based microcomputers. The device has two programmable serial RS–232C I/O ports for interfacing to a modem and a printer.

The microcomputer is expected to play an ever-increasing role in data processing activities at the USGS. However, the sheer number of products in the marketplace makes any selection process a rather overwhelming task. Therefore, the CCD is taking an active role in this technology in an effort to assist potential users in making intelligent, well-informed decisions.

U.S. GEOLOGICAL SURVEY PUBLICATIONS

PUBLICATIONS PROGRAM

Books and maps

Results of research and investigations conducted by the USGS are made available to the public through professional papers, bulletins, water-supply papers, circulars, miscellaneous reports, and several map and atlas series, most of which are published by the USGS. Books are printed by the Government Printing Office, and maps are printed by the USGS. Both books and maps are sold by the USGS.

All books, maps other than topographic quadrangle maps, and related USGS publications are listed in the catalogs: "Publications of the Geological Survey, 1879–1961" and "Publications of the Geological Survey, 1962–1970," available at nominal cost, and in yearly supplements, available free on request, that keep the catalogs up to date.

New publications, including topographic quadrangle maps, are announced monthly in "New Publications of the Geological Survey." A free subscription to this list can be obtained on application to the *U.S. Geological Survey, 582 National Center, Reston, VA 22092.*

State list of publications on hydrology and geology

"Geologic and Water-Supply Reports and Maps, [State]," a series of booklets, provides a ready reference to these publications on a State basis. The booklets also list libraries in the subject State where USGS reports and maps can be consulted; these booklets are available free on request to the USGS.

Surface-water, quality-of-water, and ground-water-level records

Surface-water records through water year 1970 were published in a series of water-supply papers titled "Surface-Water Supply of the United States"; through water year 1960, each volume covered a single year, but the period from 1961 to 1970 was covered by two 5-yr volumes (1961–65 and 1966–70).

Quality-of-water records through water year 1970 were published in an annual series of water-supply papers titled "Quality of Surface Waters of the United States."

Both surface-water and quality-of-water records for water years 1971 to 1974 were published in a series of annual reports titled "Water Resources Data for [State]." Some of these reports contained both types of data in the same volume, but others were separated into two parts, "Part 1: Surface-Water Records" and "Part 2: Water-Quality Records." Limited numbers of these reports were printed, as they were intended for local distribution only. Since the data in these reports will not be republished in the water-supply paper series, reports are sold by the National Technical Information Service.

Records of ground-water levels in selected observation wells through calendar year 1974 were published in the series of water-supply papers titled "Ground-Water Levels in the United States." Through 1955, each volume covered a single year, but, during the period from 1956 to 1974, most volumes covered 5 yr.

Starting with water year 1975, records for surface water, quality of water, and levels of ground-water observation wells are all published under one cover in a series of annual reports issued on a State-boundary basis. Reports for water year 1975 and subsequent water years appear in a series of reports titled "Water-Resources Data for [State]"; these reports are sold by the *National Technical Information Service, U.S. Department of Commerce, Springfield, VA 22161.*

State hydrologic unit maps

State hydrologic unit maps, which are overprints of the 1:500,000-scale State base maps, show culture in black, hydrography in blue, hydrologic subdivision boundaries and codes in red, and political (FIPS county) codes in green. The Alaska State map is at 1:2,500,000 scale, and the Puerto Rico map is at 1:240,000 scale. All river basins having drainage areas greater than 700 mi^2 (except for Alaska) are delineated on the maps. The hydrologic boundaries depict (1) water-resources regions, (2) water-resources subregions, (3) National Water-Data Network accounting units, and (4) cataloging units of the USGS "Catalog of Information on Water Data." These maps are available for every State and Puerto Rico.

State water-resources investigations folders

A series of folders titled "Water-Resources Investigations in [State]" is a project of the Water Resources Division to inform the public about its current programs in

the 50 States and Puerto Rico, the U.S. Virgin Islands, Guam, and American Samoa. As the programs change, the folders are revised. The folders are free on request as follows: for areas east of the Mississippi River, including Minnesota, Puerto Rico, and the Virgin Islands–*Eastern Distribution Branch, U.S. Geological Survey, 1200 South Eads Street, Arlington, VA 22202,* and for areas west of the Mississippi, including Alaska, Hawaii, Louisiana, Guam, and American Samoa–*Western Distribution Branch, U.S. Geological Survey, Box 25286, Federal Center, Denver, CO 80225.*

Open-file reports

Open-file reports, which consist of manuscript reports, maps, and other preliminary material, are made available for public consultation and use. Reports and maps released only in the open files are listed monthly in "New Publications of the Geological Survey," which also lists places of availability for consultation. Most open-file reports are placed in one or more of the three USGS libraries: Room 4A100, National Center, 12201 Sunrise Valley Drive, Reston, VA 22092; 1526 Cole Boulevard at West Colfax Avenue, Golden, Colo. (mailing address: Stop 914, Box 25046, Federal Center, Denver, CO 80225); and 345 Middlefield Road, Menlo Park, CA 94025. Other depositories may include one or more of the USGS offices listed on p 308 and interested State agencies. Some open-file reports are superseded later by formally printed publications. Effective October 1, 1981, the Government Printing Office began distributing open-file reports to requesting depository libraries.

Microfiche and (or) paper copies of most open-file reports can be purchased from the *Open-File Services Section, Western Distribution Branch, U.S. Geological Survey, Box 25425, Federal Center, Denver, CO 80225.*

Earthquake publications

The "Earthquake Information Bulletin" is published bimonthly by the USGS to provide information on earthquakes and seismological activities of interest to both general and specialized readers. Each issue also lists a worldwide summary of felt earthquakes.

The USGS National Earthquake Information Service locates most earthquakes above magnitude 5.0 on a worldwide basis. A chronological summary of location and magnitude data for each located earthquake is published in the monthly listing "Preliminary Determination of Epicenters." The "Earthquake Data Report," a bimonthly publication, provides a chronological summary of location and magnitude data for each located earthquake and contains station arrival times, individual distances, azimuths, and traveltime residuals. "Earthquakes in the United States" is published quarterly as a USGS circular. The circulars supplement the information given in the monthly listing "Preliminary Determination of Epicenters" to the extent of providing detailed felt and intensity data as well as isoseismal maps for U.S. earthquakes.

"United States Earthquakes [year]" is published jointly by the USGS and the NOAA. This annual sourcebook on earthquakes occurring in the United States gives location, magnitude, and intensity data. Other information such as strong-motion data fluctations in well-water levels, tsunami data, and a list of principal earthquakes of the world also is given.

PUBLICATIONS ISSUED

During fiscal year 1981, the USGS published 6,838 maps.

Kind of map printed	*Number*
Topographic	5,628
Geologic and hydrologic	731
Maps for inclusions in book reports	47
Miscellaneous (including maps for other agencies)	432
Total	6,838

In addition, six issues of the "Earthquake Information Bulletin," 176 technical book reports, and 338 leaflets and maps of flood-prone areas were published.

At the beginning of fiscal year 1981, more than 104.6 million copies of maps and 2.1 million copies of book reports were on hand in the USGS distribution centers. During the year 9,388,682 copies of maps, including 493,118 index maps, were distributed. Approximately 6.1 million maps were sold, and $5,079,879 was deposited to Miscellaneous Receipts in the U.S. Treasury.

The USGS also distributed 175,159 copies of technical book reports, without charge and for official use, and 1,581,663 copies of booklets, free of charge, chiefly to the general public; 384,000 copies of the monthly publications announcements and 600,000 copies of a sheet showing topographic map symbols were sent out.

The following table compares USGS map and book distribution (including map indexes and booklets, but excluding map-symbol sheets and monthly announcements) during fiscal years 1980 and 1981:

Number of maps and books distributed

Publication	Fiscal year 1980	Fiscal year 1981	Change (percent)
Maps	9,806,694	9,388,682	.04
Books	436,817	208,307	.52
Popular publications	1,319,115	1,581,663	.17
Total	11,562,626	11,178,652	.03

HOW TO OBTAIN PUBLICATIONS

OVER THE COUNTER

Book reports

Book reports (professional papers, bulletins, water-supply papers, "Techniques of Water-Resources Investigations," and some miscellaneous reports) can be purchased from the *Eastern Distribution Branch, U.S. Geological Survey, 604 South Pickett Street, Alexandria, VA 22304,* and from the USGS Public Inquiries Offices listed below under "Maps and Charts" (authorized agents of the Superintendent of Documents).

Some book publications that can no longer be obtained from the Superintendent of Documents are available for purchase from authorized agents of the Superintendent of Documents.

Maps and charts

Maps and charts can be purchased at the following USGS offices:

Distribution Branch:

1200 South Eads St.,
Arlington, Va.

Building 41, Federal Center,
Denver, Colo.

Alaska Distribution Section:

New Federal Bldg.,
101 Twelfth Ave.,
Fairbanks, Alaska

National Cartographic Information Center:

1400 Independence Rd.,
Rolla, Mo.

Public Inquiries Offices:

Rm. 108, Skyline Bldg.,
508 2d Ave.,
Anchorage, Alaska

Rm. 7638, Federal Bldg.,
300 North Los Angeles St.,
Los Angeles, Calif.

Rm. 122, Bldg. 3,
345 Middlefield Rd.,
Menlo Park, Calif.

Rm. 504, Customhouse,
555 Battery St.,
San Francisco, Calif.

Rm. 169, Federal Bldg.,
1961 Stout St.,
Denver, Colo.

Rm. 1028, General Services Bldg.,
19th and F Sts., NW.,
Washington, D.C.

Rm. 1C45, Federal Bldg.,
1100 Commerce St.,
Dallas, Tex.

Rm. 8105, Federal Bldg.,
125 South State St.,
Salt Lake City, Utah

Rm. 1C402, National Center
12201 Sunrise Valley Dr.,
Reston, Va.

Rm. 678, U.S. Courthouse,
West 920 Riverside Ave.,
Spokane, Wash.

USGS maps are also sold by some 1,950 commercial dealers throughout the United States. Prices charged are generally higher than those charged by USGS offices.

Indexes showing topographic maps published for each State, Puerto Rico, the U.S. Virgin Islands, Guam, American Samoa, and Antarctica are available free on request. Publication of revised indexes to topographic mapping is announced in the monthly "New Publications of the Geological Survey." Each index also lists special and U.S. maps, as well as USGS offices and commercial dealers from which maps can be purchased.

Maps, charts, folios, and atlases that are out of print can no longer be obtained from any official source. They may be consulted at many libraries, and some can be purchased from second-hand book dealers.

BY MAIL

Book reports

Technical book reports and some miscellaneous reports can be ordered from the *Eastern Distribution Branch, U.S. Geological Survey, 604 South Pickett Street, Alexandria, VA 22304.* Prepayment is required and should be made by check or money order in U.S. funds payable to the U.S. Geological Survey. Postage stamps are not accepted; please do not send cash. On orders of 100 copies or more of the same report sent to the same address, a 25-percent discount is allowed. Circulars, publications of general interest (such as leaflets,

pamphlets, and booklets), and some miscellaneous reports can be obtained free from the Distribution Branch.

Maps and charts

Maps and charts, including folios and hydrologic atlases, are sold by the USGS. Address orders for maps of areas east of the Mississippi River, including Minnesota, Puerto Rico, and the U.S. Virgin Islands, to *Eastern Distribution Branch, U.S. Geological Survey, 1200 South Eads Street, Arlington, VA 22202,* and for maps of areas west of the Mississippi River, including Alaska, Hawaii, Louisiana, Guam, and American Samoa, to *Western Distribution Branch, U.S. Geological Survey, Box 25286, Federal Center, Denver, CO 80225.* Residents of Alaska also may order maps of their State from the *Alaska Distribution Section, U.S. Geological Survey, New Federal Building–Box 12, 101 Twelfth Avenue, Fairbanks, AK 99701.*

Prepayment is required. Remittances should be by check or money order in U.S. funds payable to the U.S. Geological Survey. On an order amounting to $500 or more at the list price, a 50-percent discount is allowed. Prices are quoted in lists of publications and in indexes to topographic mapping for individual States. Prices include the cost of surface transportation.

Earthquake Information Bulletin

Subscriptions to the "Earthquake Information Bulletin" and the "Preliminary Determination of Epicenters" are by application to the *Superintendent of Documents, Government Printing Office, Washington, DC 20402.* Payment is by check payable to the Superintendent of Documents or by charge to your deposit account number. Single issues can be purchased from the *Eastern Distribution Branch, U.S. Geological Survey, 604 South Pickett Street, Alexandria, VA 22304.*

National Technical Information Service

Some USGS reports, including computer programs, data and information supplemental to map or book publications, and data files, are released through the National Technical Information Service (NTIS). These reports, available either in paper copies or microfiche or sometimes on magnetic tapes, can be purchased only from the *National Technical Information Service, U.S. Department of Commerce, Springfield, VA 22161.* USGS reports that are released through NTIS, together with their NTIS order numbers and prices, are announced in the monthly "New Publications of the Geological Survey."

REFERENCES CITED

Allmendinger, R. W., 1981, Structural geometry of Meade Thrust plate in northern Blackfoot Mountains, southeastern Idaho: Amer. Assoc. Petro. Geol. Bull., v. 65, no. 3, 509–525.

Alpha, T. R., Moore, J. R., and Jones, D. R., 1980, Sequential physiographic diagrams of Mount St. Helens Washington, 1979–1980: U.S. Geol. Survey Open-File Rept. 80–792.

Alpha, T. R., Moore, J. G., Morley, J. M., and Jones, D. R., 1980, Physiographic diagrams of Mount St. Helens and vicinity, Washington: U.S. Geol. Survey Open-File Rept. 80–920.

American Association of Petroleum Geologists–U.S. Geological Survey, 1976, Geothermal gradient map of North America: U.S. GPO, Washington, D.C., 1:5,000,000.

Anderson, T. H., and Silver, L. T., 1981, The role of the Mojave-Sonora megashear in the tectonic evolution of Sonora, Mexico [abs.]: Geol. Soc. of Amer. Abs. with Programs, v. 13, no. 2, p. 42.

Bader, J. S., Chisholm, J. L., Downs, S. C., and Bragg, R. L., 1977, Hydrologic data for the Guyandotte River basin, West Virginia: W. Va. Geol. and Econ. Survey Basic Data Rept. 7, 550 p.

Balch, A. H., Lee, M. W., and Muller, D. C., 1980, A vertical seismic profiling experiment to determine depth and dip of the Paleozoic surface at drill hole U10bd, Nevada Test Site, Nevada: U.S. Geol. Survey Open-File Rept. 80–847, 25 p.

Banks, P. O., and Rebello, D. P., 1969, Zircon age of a Precambrian rhyolite, northeastern Wisconsin: Geol. Soc. Amer. Bull., v. 80, n. 5, p. 907–910.

Barnes, C. G., 1981, Petrology of the Wooley Creek batholith, Klamath Mountains, Northern California: Geol. Soc. of Amer., Abs. with Programs 1981, v. 13, no. 7, September 1981, p. 403.

Barton, P. B., Jr., 1958, Synthesis and properties of carnotite and its alkali analogues: Am. Mineralogist, v. 43, nos. 9–10, p. 799–817, illus., Sept.–Oct. 1958.

Batson, R. M., Bridges, P. M., Inge, J. L., Isbell, C. E., Masursky, Harold, Strobell, M. E., and Tyner, R. L., 1980, Mapping the Galilean satellites of Jupiter with Voyager data: Photogrammetric Engineering and Remote Sensing, v. 46, no. 10, p. 1301–1312.

Berg, H. C., 1979, Significance of geotectonics in the metallogenesis and resource appraisal of southeastern Alaska–a progress report: in Johnson, K. M., and Williams, J. R., eds., The U.S. Geol. Survey in Alaska–accomplishments during 1978: U.S. Geol. Survey Circ. 804–B, p. B115–118.

Berg, H. C., Elliott, R. L., Smith, J. G., and Koch, R. D., 1978a, Geologic map of the Ketchikan and Prince Rupert quadrangles, Alaska: U.S. Geol. Survey Open-File Rept. 78–73A, scale 1:250,000, 1 sheet.

Berg, H. C., Jones, D. L., and Coneyu, P. J., 1978b, Map showing pre-Cenozoic tectonostratigraphic terranes of southeastern Alaska and adjacent areas: U.S. Geol. Survey Open-File Rept. 78–1085, scale 1:1,000,000, 2 sheets.

Bissell, H. J., 1960, Eastern Great Basin Permo-Pennsylvanian strata–Preliminary statement: Amer. Assoc. of Petro. Geol. Bull., v. 44, no. 8, p. 1424–1435.

Bonilla, M. G., Lienkaemper, J. J., and Tinsley, J. C., 1980, Surface faulting near Livermore, California associated with the January 1980 earthquakes: U.S. Geol. Survey Open-File Rept. 80–523, 35 p., 1 sheet, scale 1:24,000.

Bowdre, J. H., and Krieg, N. R., 1974, Water quality monitoring bacteria as indicators: Va. Polytech. Inst., State Univ. Water Research Ctr., Bull. 69.

Brethauer, G. E., Muller, D. C., and Kibler, J. E., 1980, Preliminary analysis of physical-properties data characteristics of tunnel beds 3 and 4 in a part of Areas 4 and 7, Nevada Test Site: U.S. Geol. Survey Report USGS–474–310 (Special Projects–44), 77 p.; available *only* from U.S. Department of Commerce, National Technical Information Service, Springfield, VA 22161.

Broom, M. E., and Lyford, F. P., 1981, Alluvial aquifer of the Cache and St. Francis River basins, northeastern Arkansas: U.S. Geol. Survey Open-File Rept. 81–476.

Brown, L. D., Reilinger, R. D., Holdahl, S. R., and Balazs, E. I., 1977, Postseismic crustal uplift near Anchorage, Alaska: J. Geophys. Res., v. 82, no. 23, p. 3369–3378.

Bull, W. B., Menges, C. M., and McFadden, L. D., 1979, Stream terraces of the San Gabriel Mountains, Calif., Contract Report 14–08 0001–G–394, Office of Earthquake Studies, U.S. Geol. Survey, Menlo Park, Calif.

Calkins, J. A., S. Jamiluddin, Kamaluddin Bhuyan, and Ahrad Hussain, 1981, Geology and mineral resources of the Chitral-Partsan area, Hindu Kush Range, northern Pakistan: U.S. Geol. Survey Prof. Paper 716–G, 73 p.

Carroll, R. D., and Cunningham, M. J., 1980, Geophysical investigations in deep horizontal holes drilled ahead of tunneling: International Jour. of Rock Mechanics and Mining Sciences, v. 17, no. 2, p. 89–107.

Cathcart, J. B., and Tooker, E. W., 1979, Preliminary map of phosphorous provinces in the conterminous United States: U.S. Geol. Survey Open-File Rept. 79–576A, 1 pl., scale 1:5,000,000.

Chapman, R. M., and Patton, W. W., Jr., 1979, Two upper paleozoic sedimentary rock units identified in southwestern part of the Ruby quadrangle, *in* Johnson, K. M., and Williams, J. R., eds., The U.S. Geol. Survey in Alaska–Accomplishments during 1978: U.S. Geol. Survey Circ. 804–B, p. B59–B61.

Chen, A. T. F., 1980, The torsional pendulum test for soils: a theoretical investigation: Rept. No. U.S. Geol. Survey–GD–80–003, NTIS No. PB80–154115, January, 37 pages.

Chenoweth, W. L., 1957, Radioactive titaniferous heavy-mineral deposits in the San Juan Basin, New Mexico and Colorado: New Mexico Geol. Society, 8th Field Conference, p. 212–217.

Chou, I. M., 1978, Calibration of oxygen buffers at elevated P and T using the hydrogen fugacity sensor. Am. Mineralogist 63, p. 690–703.

Clarke, J. W., and Rachlin, Jack, 1980, Salym–Potential giant oil field in West Siberia; Possible reservoir stimulation experiment using a nuclear explosion: U.S. Geol. Survey Open-File Rept. 80–145, 14 p.

———1980, Salym: Potential W. [sic] Siberian oil giant: Oil and Gas Jour., v. 78, no. 24, p. 132–135.

Claassen, Hans C., 1981, Estimation of calcium sulfate solution rate and effective aquifer surface area in a ground-water system near Carlsbad, New Mexico: *Ground Water,* May–June v. 19, p. 287–297.

Clow, G. D., and Carr, M. H., 1980, The stability of sulfur slopes on Io: Icarus, v. 44, p. 268–279.

Cochran, W. G., 1977, Sampling techniques (3rd ed.): New York, John Wiley and Sons, 330 p.

Coskren, T. D., and Rice, C. L., 1979, Contour map of the base map of the Pennsylvanian system in eastern Kentucky: U.S. Geol. Survey Misc. Field Studies Map, MF-1100.

Crandell, D. R., 1980, Recent eruptive history of Mount Hood, Oregon, and potential hazards from future eruptions: U.S. Geol. Survey Bull. 1492, 81 p.

Crandell, D. R., and Mullineaux, D. R., 1978, Potential hazards from future eruptions of Mount St. Helens volcano, Washington: U.S. Geol. Survey Bull. 1383-C, 26 p.

Crandell, D. R., Mullineaux, D. R., and Rubin, Meyer, 1975, (Volcano Hazards Program Expanded-Bailey) Mount St. Helens volcano; recent and future behavior: Science, v. 187, p. 438-441.

Crittenden, M. D., Jr., 1951, Geology of the San Jose-Hamilton area, California: California Division of Mines Bull. 157, 74 p.

Crowell, J. C., 1952, Geology of the Lebec quadrangle: California Division of Mines Special Report 24, 23 p.

Dearborn, L. L., and Schaefer, D. H., 1980, Surface geophysical investigations at two cross-valley lines in the middle Eagle River valley: U.S. Geol. Survey Open-File Rept. 80-2000, 14 pages.

Doherty, D. J., McBroome, L. A., Kuntz, M. A., 1979, Preliminary Geological Interpretation and lithologic log of the Exploratory Geothermal Test well (INEL-1), Idaho National Engineering Laboratory, Eastern Snake River Plain, Idaho: U.S. Geol. Survey Open-File Rept. 79-1248.

Dolton, G. L., and others, 1981, Estimates of undiscovered recoverable resources of conventionally producible oil and gas in the United States, a summary: U.S. Geol. Survey Open-File Rept. 81-192, 17 p.

Dott, R. H., Jr., 1971, Geology of the southwestern Oregon coast west of the 124th meridian: Oregon Department of Geology and Mineral Industries Bull. 69, 63 p.

Douglass, R. C., (1979), The distribution of fusulinids and their correlation between the Illinois Basin and the Appalachian Basin, *in* Palmer, J. E., and Dutcher, R. R., eds., Depositional and structural history of the Pennsylvanian System of the Illinois basin. Part 2, Invited papers: Ninth International Congress of Carboniferous Stratigraphy and Geology, Urbana, Ill., 1979, Field Trip 9, pt. 2: Illinois State Geol. Survey Guidebook Series 15a, p. 15-20.

Drake, A. A., Jr., 1978, The Lyon Station-Paulin Kill nappe: frontal structure of the Musconetom Nappe system in eastern Pennsylvania and New Jersey: U.S. Geol. Survey, Prof. Paper 1023, 20 p.

———1980, Chapter A, The Serra de Caldas window, Goias: U.S. Geol. Survey Prof. Paper 1119-A, 11 p., 9 figs.

Drake, A. A., Jr., and Morgan, B. A., 1980, Precambrian plate tectonics in the Brazilian shield - Evidence from the pre-Minas rocks of the Quadrilatero Ferrifero, Minas Gerais: U.S. Geol. Survey Prof. Paper 1119-B, 19 p. 8 figs., 3 tables.

Dunrud, C. R., and Osterwald, F. W., 1980, Effects of coal mine subsidence in the Sheridan, Wyoming, area: U.S. Geol. Survey Prof. Paper 1164, 49 p.

Earhart, R. L.; Grimes, D. J.; Leinz, R. W.; and Kleinkopf, M. D., 1981, The Conterminous United States Mineral Resource Appraisal Program: background information to accompany folio of geologic, geochemical, geophysical and mineral resource maps of the Choteau 1°×2° quadrangle, Montana: U.S. Geol. Survey Circ. 849, 9 p.

Edmundson, R. S., 1938, Barite deposits of Virginia: Virginia Geol. Survey Bull. 53, 85 p.

Ehlke, T. A., 1981, Hydrology of Area 9, Eastern Coal Province, West Virginia: U.S. Geol. Survey Open-File Rept. 81-803, 154 p.

Ehlke, T. A., Bader, J. S., Puente, Celso, and Runner, G. S., 1981, Hydrology of Area 12, Eastern Coal Province, West Virginia: U.S. Geol. Survey Open-File Rept. 81-902, 164 p.

Emmons, W. E., and Calkins, F. C., 1913, Geology and ore deposits of the Philipsburg quadrangle, Montana: U.S. Geol. Survey Prof. Paper 78, 271 p.

Erdman, J. A., Ebens, R. J., and Case, A. A., 1978, Molydbenosis A potential problem in ruminants grazing on coal mine spoils: Jour. of Range Management v. 31, p. 34-36.

Eugster, H. P., and G. B. Skippen, 1967, Igneous and metamorphic reactions involving gas equilibria, in Abelson, P. H., eds., Researches in geochemistry, 2, p. 492-521, New York: John Wiley.

Eugster, H. P., Albee, A. L., Bence, A. E., Thompson, J. B., Jr., and Waldbaum, D. R., 1972, The two-phase region and excess mixing properties of paragonite-muscovite crystalline solutions: Jour. of Petrology, v. 13, p. 147-179.

Evans, J. G., and Ketner, K. B., 1971, Geologic map of the Swales Mountain quadrangle and part of the Adobe Summit quadrangle, Elko County, Nevada: U.S. Geol. Survey Misc. Geol. Inv. Map I-667.

Farrar, Edward, and Rowley, P. D., 1980, Potassium-argon ages of Upper Cretaceous plutonic rocks of Orville Coast and eastern Ellsworth Land: Antarctic Jour. of the U.S. v. 15, no. 5, p. 26-28.

Fary, R. F., Jr., 1980, A review of the geology of petroleum in Venezuela: U.S. Geol. Survey Open-File Rept. 80-782, 49 p., 21 figs., 2 tables.

Finch, W. I., Granger, H. C., Lupe, Robert, and McCammon, R. B., 1980, Genetic-geologic models - A systematic approach to evaluate geologic favorability for undiscovered uranium resources, Part I, Research on uranium resource models, A progress report: U.S. Geol. Survey Open-File Rept. 80-2018-A, 55 p.

Fischer, W. A., Anguswathana, Prayong, Carter, W. D., Hoshino, Kazuo, Lathram, E. H., Albert, N. R., and Rich, E. I., 1976, Surveying Earth and its environment from space, *in* Circum Pacific Energy and Mineral Resources: Amer. Assoc. of Petro. Geology, Memoir 25, p. 63-72.

Foose, M. P. and McQueen, D. R., 1979, Preliminary map of cobalt occurrences in the conterminous United States: U.S. Geol. Survey Open-File Rept. 79-576J, 1 over-size scale 1:5,000,000.

Foster, H. L., Albert, N. R. D., Griscom, Andrew, Hessin, T. D., Menzie, W. D., Turner, D. L., and Wilson, F. H., 1979, The Alaska Mineral Resource Assessment Program: Background information to accompany folio of geologic and mineral resource maps of Big Delta quadrangle, Alaska: U.S. Geol. Survey Circ. 783, 19 p.

Friedman, Irving, Smith, G. I., and Hardcastle, K. G., 1976, Studies of Quaternary saline lakes-II. Isotopic and compositional changes during desiccation of the brines in Owens Lake, California, 1969-1971: Geochim. et Cosmochim. Acta, v. 40, p. 501-511.

Froelich, A. J., and Leavy, B. D., 1981, Map showing mineral resources of the Culpeper Basin, Va.-Md.: availability and planning for future needs: U.S. Geol. Survey Misc. Inv. Map 1-1313-B, scale 1:125,000.

Fuller, M. L., 1912, The New Madrid earthquake: U.S. Geol. Survey Bull. 494, 119 p.

Furcron, A. S., 1939, Geology and mineral resources of the Warrenton quadrangle, Va.: Virginia Geol. Survey Bull. 54, 94 p.

Gillespie, W. H., and Pfefferkorn, H. W., 1979, Distribution of commonly occurring plant megafossils in the proposed Pennsylvanian System stratotype, Virginia and West Virginia, ed. by Englund, K. J., Arndt, H. H., and Henry, T. W.: American Geological Institute AGI Selected Guidebook Series No. 1, Ninth International Congress of Carboniferous Stratigraphy and Geology, p. 87-96.

Glancy, P.A., 1981, Geohydrology of the basalt and unconsolidated sedimentary aquifers in the Fallom area, Churchill County, Nevada: U.S. Geol. Survey Open-File Rept. 80-2042, 110 p.

Glenn, C. R., and Denman, J. M., 1980 Geological literature on Egypt, 1900 to 1978: U.S. Geol. Survey Open-File Rept. 80-930 ((IR)EG-11), 218 p.

Granger, H. C., Finch, W. I., Kirk, A. R., and Thaden, R. E., 1980, Genetic-geologic model for tabular humate uranium deposits, Grants Mineral Belt, San Juan Basin, New Mexico, Part III, Research on uranium resource models, A progress report: U.S. Geol. Survey Open-File Rept. 80-2018-C, 58 p.

Grimes, D. J., and Leinz, R. W., 1980a, Geochemical and generalized geologic maps showing the distribution and abundance of copper in the Choteau 1° × 2° quadrangle, Montana: U.S. Geol. Survey Misc. Field Studies Map MF-858B, scale 1:250,000.

———1980b, Geochemical and generalized geologic maps showing the distribution and abundance of silver in the Choteau 1° × 2° quadrangle, Montana: U.S. Geol. Survey Misc. Field Studies Map MF-858C, scale 1:250,000.

Hack, J. T., 1965, Post glacial drainage evolution and stream geometry in the Ontonagon area, Michigan: U.S. Geol. Survey Prof. Paper 504-B, 39 p.

Hait, M. H., Jr., and Scott, W. E., 1978, Holocene faulting, Lost River Range, Idaho: Geol. Soc. Amer. Abs. with Programs, v. 10, no. 5, p. 217.

Hall, W. E., Rye, R. O., and Doe, B. R., 1978, Wood River mining district, Idaho – Intrusion-related lead-silver deposits derived from country rock source: U.S. Geol. Survey Jour. of Research, v. 6, no. 5, p. 579-592.

Harrison, J. E., and Peterman, Z. E., 1980, Note 52 – A preliminary proposal for a chronometric time scale for the Precambrian of the United States and Mexico: Geol. Soc. of Amer. Bull., Part I, v. 91, no. 6, p. 377-380.

Harvey, E. J., 1980, Ground water in the Springfield-Salem Plateaus of southern Missouri and northern Arkansas: U.S. Geol. Survey Water-Resources Inv. 80-101, 66 p.

Hastings, D. A., 1980, On the tectonics and metallogenesis of West Africa: a model influenced by new geophysical data (abs.): International Geological Congress, 26th, Paris, Proceedings, v. 2, p. 726.

Hastings, D. A., and Bacon, M., 1979, Geologic structure and evolution of Keta Basin, West Africa: discussion: Geol. Society of Amer. Bull., v. 90, p. 889-892.

Hawley, K. T. 1975, The Racetrack pluton – a newly defined Flint Creek pluton: Northwest Geology, v. 4, p. 1-8.

Herd, D. G., 1977, Geologic map of the Las Positas, Greenville, and Verona faults, eastern Alameda County, California: U.S. Geol. Survey Open-File Rept. 77-689, 25 p., 1 pl., 6 figs., scale 1:24,000.

———1978, Intracontinental plate boundary east of Cape Mendocino, Ca.: Geology, v. 6, no. 12, p. 721-725.

Hewitt, C. H., 1959, Geology and mineral deposits of the northern Big Burro Mountains-Redrock area, Grant County, New Mexico: N. Mex. Bureau of Mines and Mineral Resources Bull. 60, 151 p.

Hietanen, A. M., 1967, On the facies series in various types of metamorphism: Jour. of Geology, v. 75, p. 187-214.

Hill, Dorothy, 1939, A monograph on the Carboniferous rugose corals of Scotland, pt. 1: London, Palaeontographical Society, p. 1-109.

Hobba, W. A., Jr., 1980, Locating ground-water supplies in Randolph County, West Virginia: U.S. Geol. Survey Open-File Rept. 80-973, 67 p.

———1981, Effects of underground mining and mine collapse on the hydrology of selected basins, West Virginia: W. Va. Geol. and Econ. Survey Rept. of Investigation RI-33, 88 p.

Hobbs, S. W., and Tooker, E. W., 1979, Preliminary map of tungsten provinces in the conterminous United States: U.S. Geol. Survey Open-File Rept. 79-576C, 1 pl., scale 1:5,000,000.

Hodge, D. W., Owen, L. B., and Smithson, S. B., 1973, Gravity interpretation of the Laramie Anorthosite Complex, Wyoming: Geol. Society of Amer. Bull., v. 84, no. 4, p. 1451-1464.

Holdridge, L. R., 1967, Life zone ecology: Tropical Science Center, San Jose, Costa Rica.

Holzer, T. L., and Pampeyan, E. H., 1980, Earth fissures and localized differential subsidence: Water Resources Research, v. 17, no. 1, p. 223-227.

Hopkins, H. T., Bower, R. F., Abe, J. M., and Harch, J. F., 1981, Potentiometric surface map for the Cretaceous aquifer, Virginia Coastal Plain, 1978: U.S. Geol. Survey Open-File Rept. 80-965.

Hoskins, J. H., and Cross, A. T., 1952, The petrifaction flora of the Devonian-Mississippian black shale: The Palaeobotanist, v. 1, p. 215-238, fig. 7.

Houston, R. S., and Murphy, J. F., 1977, Depositional environment of Upper Cretaceous black sandstones of the Western interior: U.S. Geol. Survey Prof. Paper 994-f, 29 p.

Hunt, G. R., 1980, Electromagnetic Radiation: The communication link in Remote Sensing. Chapter 2 in Book *Remote Sensing in Geology* eds: Gillespie and Siegel, John Wiley & Sons, p. 5-47.

Hunt, John M., 1967, The origin of petroleum in carbonate rocks, *in* Chilingar, G. V.; Bissell, H. J., and Fairbridge, R. W., Carbonate rocks: Elsevier, Pub. Co. New York, p. 225-251.

Hussey, A. M., II, 1971, Geologic Map of Portland, Maine: Maine Geol. Survey, GM-1.

Irwin, W. P., 1972, Terranes of the western Paleozoic and Triassic belt in the southern Klamath mountains, California: U.S. Geol. Survey Prof. Paper 800C, p. 103-111.

Jackson, E. D., Stevens, R. E., and Bowen, R. W., 1967, A computer-based procedure for deriving mineral formulas from mineral analyses, in Geological Survey research 1967: U.S. Geol. Survey Prof. Paper 575C, p. C23-C31.

Jones, T. H., and Cate, A. S., 1957, Preliminary report on a regional stratigraphic study of Devonian rocks of Pennsylvania: Pennsylvania Geol. Survey, 4th Series, Special Bull. 8, 5 p.

Karkowski, Lukasy, Kozlowski, Andrezej, and Roedder, Edwin, 1979, Gas-liquid inclusions in minerals of ores of zinc and lead from the Silesia-Crakow region [Poland] *in* Research on the genesis of zinc-lead deposits of Upper Silesia, Poland: Prace Instytutu Geologicznego, v. XCV, p. 87-94.

Katz, F. J., 1917, Stratigraphy in southwestern Maine and southeastern New Hampshire: U.S. Geol. Survey Prof. Paper 108, p. 165-177.

Kaye, C. A., and Zartmann, R. E., 1980, A Proterozoic Z to Cambrian age for the stratified rocks of Boston Basin, Massachusetts, *in* Wones, D. R., ed., The Calidonides in U.S.A.: Virginia Polytechnic Institute and State University, Dept. Geol. Sci. Memoir 2, p. 257-264.

Kelley, V. C., and Northrop, S. A., 1975, Geology of Sandia Mountains and vicinity, New Mexico: New Mexico Bureau of Mines and Mineral Resources Memoir 29, 135 p.

Ketner, K. B., and Smith, J. F., Jr., 1981, Mid-Paleozoic age of the Roberts Thrust unsettled by new data from northern Nevada [abs.]: Geol. Soc. of Amer. Abs. with Programs, v. 13, no. 2, p. 64.

Kikuchi, T., 1965, Some aspects of hyper-hydrogen sulfide producing activity and copper resistance in yeast: Memoir of the College of Science, Univ. of Kyoto, B., v. 31, p. 113-124.

Klemic, Harry, and Tooker, E. W., 1979, Preliminary map of iron provinces in the conterminous United States: U.S. Geol. Survey Open-File Rept. 79-576H, 1 over-size sheet.

———1979, Vanadium provinces in the conterminous United States: U.S. Geol. Survey Open-File Rept. 79-576I, 1 over-size sheet.

Klevtsov, P. V., and Lemmlein, G. G., 1959, Determination of the minimum pressure of quartz formation as exemplified by crystals from the Pamir. Zap. Vses. Miner. Obshch. 85(6), p. 661–666 (in Russian).

Kosanke, R. M., and Harrison, J. A., 1957, Microscopy of the resin rodlets of Illinois coal: Illinois State Geol. Survey Circ. 234, 14 p.

Krumhardt, A. P., 1979 (1980), Arsenic, nitrate, iron, and hardness in ground water, Chena Ridge vicinity, Fairbanks, Alaska: U.S. Geol. Survey Open-File Rept. 80–49, 2 sheets.

Krushensky, R. D., Akcay, Yavuz, and Karaege, Erdogan, 1980, Geology of the Karalar-Yesiller area, northwest Anatolia, Turkey: U.S. Geol. Survey Bull. 1471, 126 p., 1 fig., 1 table, 1 plate.

LaBelle, R. P., Samuels, W. B., and Lanfear, K. J., 1980, An oilspill risk analysis for the Cook Inlet and Shelikof Strait (Proposed Sale 60) Outer Continental Shelf lease area: U.S. Geol. Survey Open-File Rept. 80–863, 83 p.

Lai, C., 1980, Urban storm sewer flows in coastal areas: Proc. of National Symp. on Urban Stormwater Management in Coastal Areas, ASCE, Virginia Polytech. Inst. and State Univ., Blacksburg, Va., June 19–20, 1980, pp. 244–254.

———1981, Procedures and techniques for a rational model adjustment in numerical simulation of transient open-channel flow: Proc. of Internat'l Conf. on Numerical Simulation of River, Channel and Overland Flow for Water Resources and Environmental Applications, Bratislava, Czechoslavakia, May 4–8, 1981.

Lai, C., Baltzer, R. A., and Schaffranek, R. W., 1980, Techniques and experiences in the utilization of unsteady open-channel flow models: Proc. of ASCE Hydraulics Div., 28th Annual Hydraulics Specialty Conf., Illinois Inst. of Tech., Chicago, Ill., Aug. 6–8, 1980, pp. 177–191.

Lajoie, K. R., Kern, J. P., Wehmiller, J. P., and others, 1979, Quaternary marine shorelines and crustal deformation, San Diego to Santa Barbara, California, *in* Abbott, P. L., ed., Geologic Excursions in the Southern California Area, San Diego State Univ., San Diego, Calif., p. 3–16.

Lawson, A. C., and others, 1908, The California earthquake of April 18, 1906: Report of the California Earthquake Investigation Committee: Carnegie Inst., Washington, publ. 87, 451 pages.

Klitgord, K. D. and Grow, J. A., 1980, Jurassic seismic stratigraphy and basement structure of western Atlantic magnetic quiet zone: Am. Assoc. Petrol. Geol. Bull., v. 64, no. 10, p. 1658–1680.

Leake, B. E., 1978, Nomenclature of amphiboles: Min. Mag., 42, 533–563.

Leinz, R. W., and Grimes, D. J., 1980a, Geochemical and generalized geologic maps showing the distribution and abundance of lead in the Choteau 1°×2° quadrangle, Montana: U.S. Geol. Survey Misc. Field Studies Map MF–858D, scale 1:250,000.

———1980b, Geochemical and generalized geologic maps showing the distribution and abundance of zinc in the Choteau 1°×2° quadrangle, Montana: U.S. Geol. Survey Misc. Field Studies Map MF–858E, scale 1:250,000.

———1980c, Geochemical and generalized geologic maps showing the distribution and abundance of mercury, arsenic, and molybdenum in the Choteau 1°×2° quadrangle, Montana: U.S. Geol. Survey Misc. Field Studies Map MF–858F, 2 sheets, scale 1:250,000.

Leonard, B. F., 1973, Thunder Mountain District *in* Cater, F. W., and others, 1973, Mineral Resources of the Idaho Primitive Area and vicinity, Idaho: U.S. Geol. Survey Bull. 1304, 431 p.

Lineback, J. A., 1970, Stratigraphy of the New Albany Shale in Indiana: Indiana Geol. Survey Bull. 44, y3 p., 1 pl.

Lipman, P. W. and Mullineaux, D. R., eds., 1981, The 1980 eruptions of Mount St. Helens, Washington: U.S. Geol. Survey Prof. Paper 1250, 405 p.

Lucchitta, B. K., 1980, Grooved terrain on Ganymede: Icarus, v. 44, p. 481–501.

Lyakhov, Y. V., 1973, Errors in determining pressure of mineralization from gas-liquid inclusions with halite, their causes and ways of eliminating them. Zap. Vses. Miner. Obshch. 102(4), p. 385–393 (in Russian).

McCammon, R. B., 1980, Geologic decision analysis and its application to genetic-geologic models, Part II, Research on uranium resource models, A progress report: U.S. Geol. Survey Open-File Rept. 80–2018–B, 30 p.

McIntyre, D. H., and Foster, Fess, 1981, Pre-Tertiary volcanic rocks in central Idaho – a reappraisal: Isochron/west, no. 30, p. 3.

McIntyre, D. H., Marvin, R. F., Mehnert, H. H., Naeser, C. W., and Futa, K., 1978, Pre-Tertiary volcanic rocks in central Idaho: Isochron/west no. 23, p. 29–31.

Masursky, Harold, Eliason, Eric, Ford, P. G., McGill, G. E., Pettengill, G. H., Schaber, G. G., and Schubert, Gerald, 1980, Pioneer-Venus radar results: Geology from images and altimetry: Jour. Geophys. Research, v. 85, no. A13, p. 8232–8260.

Maughan, E. K., and Roberts, A. E., 1967, Big Snowy and Amsden Groups and the Mississippian-Pennsylvanian boundary in Montana: U.S. Geol. Survey Prof. Paper 554–B, p. B1–B27.

Meier, M. F., Rasmussen, L. A., Post, A., Brown, C. S., Sikonia, W. G., Bindschadler, R. A., Mayo, L. R., and Trabant, D. C., 1980, Predicted timing of the disintegration of the lower reach of Columbia Glacier, Alaska: U.S. Geol. Survey Open-File Rept. 80–582, 58 p.

Merrill, F. J. H., 1898, The geology of the crystalline rocks of southeastern New York: New York State Museum Ann. Rept. 50, v. 1, p. 21–31.

Merrill, F. J. H., Darton, N. H., Hollick, Arthur, Sailsbury, R. D., Dodge, R. E., Willis, Bailey, and Pressey, H. A., 1902, Description of the New York City District: U.S. Geol. Survey Geol. Atlas, Folio 83, 19 p., 2 sheets.

Mickelson, D. M., and McCartney, M. C., 1980, History of the Green Bay lobe, eastern Wisconsin, between 13,000 and 11,000 years B.P.: Geol. Soc. of Amer., Abs. with programs, north-central section, 14th annual meeting.

Miesch, A. T., and Reed, B. L., 1979, Compositional structures in two batholiths of circumpacific North America: U.S. Geol. Survey Prof. Paper 574–H, 31 p.

Miller, B. M., and others, 1975, Geological estimates of undiscovered recoverable oil and gas resources in the United States: U.S. Geol. Survey Circ. 725, 78 p.

Miller, C. D., 1980, Potential hazards from future eruptions in the vicinity of Mount Shasta volcano, northern California: U.S. Geol. Survey Bull. 1503, 43 p.

Miller, W A., Bonner, W. G., Rohde, W. G., and Schwartz, L. P., 1980, Digital Landsat and terrain data applied to an arid land resource inventory, *in* Proceedings of Arid Land Resource Inventory Conference, December 1980, La Paz, Mexico, 3 p.

Moench, R. H., and Erickson, M. S., 1980, Occurrence of tungsten in the Sangre de Cristo Range near Santa Fe, New Mexico: Possible stratabound scheelite peripheral to favorable settings for volcanogenic massive-sulfide deposits: U.S. Geol. Survey Open-File Rept. 80–1162.

Morrison, R. B., 1965a, New evidence on Lake Bonneville stra tigraphy and history from southern Promontory Point: Utah, U.S. Geol. Survey Prof. Paper 525–C, p. C110–C119.

———1965b, Lake Bonneville; Quaternary stratigraphy of the eastern Jordan Valley south of Salt Lake City, Utah: U.S. Geol. Survey Prof. Paper 477, 80 p.

Moss, M. E., and Gilroy, E. J., 1980, Cost effective stream-gaging strategies for the Lower Colorado River Basin; the Blythe field operations: U.S. Geol. Survey Open-File Rept. 80–1048, 112 p.

Myers, J., and W. D. Gunter, 1979, Measurement of the oxygen fugacity of the cobalt-cobalt oxide buffer assemblage. Am. Mineralogist 64, p. 224–228.

Nacken, R., 1921, Welche Folgerungen ergeben sich aus dem Auftreten von Flüssigkeitsein-schlüssen in Mineralien? Zentralblatt Mineralogie, p. 12–20, 35–43.

Nash, J. T., 1979, Uranium and thorium in granitic rocks of northeastern Washington and northern Idaho, with comments on uranium resource potential: U.S. Geol. Survey Open-File Rept. 79–233, 39 p.

National Coal Board, 1975, Subsidence engineers' handbook: National Coal Board [United Kingdom], Mining Department, 111 p.

Naumov, V. B. and Malinin, S. D., 1968, A new method for determining pressure by means of gas-liquid inclusions. Geochem. Int. 5, p. 382–391 (English translation).

Nelson, G. L., 1981, Hydrologic reconnaissance near Fourth of July Creek, Seward, Alaska: U.S. Geol. Survey Water-Resources Inv. 81–21, 14 pages.

Nieuwoudt, H. H., Ambrosio, R. E., and DeKlerk, H. C., 1980, Heavy metal resistance and the effects of antibiotics and metals on pigmentation in *Serratia marcescens*: South Africa Jour. of Sci., v. 76, p. 379–380.

Nilsen, T. H., and Stewart, J. H., 1980, The Antler orogeny Mid-Paleozoic tectonism in western North America: Geology, v. 8, no. 6, p. 298–302.

Noll, J. H., 1981, Geology of the Picacho Colorado area, northern Sierra de Cobachi, central Sonora, Mexico [abs.]: Geol. Soc. of Amer. Abs. with Programs, v. 13, no. 2, p. 99.

Obradovich, J. D., and Cobban, W. A., 1975, A time-scale for the Late Cretaceous of the Western Interior of North America: Geol. Assoc. of Canada Spec. Paper 13, p. 31–54.

Olhoeft, G. R., 1980, Electrical properties of the crust: EOS, v. 61, p. 1150–1151.

Olhoeft, G. R. and J. H. Scott, 1980, Nonlinear complex resistivity logging, pp. T1–T18 in Proc. of the 21st Annual SPWLA Logging Symposium, Lafayette, LA, July, 1980.

O'Neil, J. R., Shaw, S. E., and Flood, R. H., 1977, Oxygen and hydrogen isotope compositions as indicators of granite genesis in the New England batholith, Australia. Contr. Mineralogy and Petrology, v. 62, p. 313–328.

Oriel, S. S., and Platt, L. B., 1979, Younger-over-older thrust plates in southeastern Idaho: Geol. Soc. Amer. Abstracts with Programs, v. 11, no. 6, p. 298.

Oversby, Brian, 1972, Thrust sequences in the Windermere Hills, northeastern Elko County, Nevada: Geol. Soc. Amer. Bull., v. 83, no. 9, p. 2677–2688.

———1973, New Mississippian formation in northeastern Nevada and its possible significance: Amer. Assoc. of Petro. Geol. Bull., v. 57, no. 9, p. 1779–1783.

Page, N. J., and Tooker, E. W., 1979, Preliminary map of platinum and platinum-group metal provinces in the conterminous United States: U.S. Geol. Survey Open-File Rept. 79–576B, 1 over-size sheet, scale 1:5,000,000.

Paillet, F. L., 1980, Acoustic propagation in the vicinity of fractures which intersect a fluid-filled borehole: Society of Professional Well Log Analysts, 21st Annual Logging Symposium, Lafayette, La, Proceedings, p. DD1–DD33.

———1981, A comparison of fracture characterization techniques applied to near-vertical fractures in a limestone reservoir: Society of Professional Well Log Analysts, 22nd Annual Logging Symposium, Mexico City, Mexico, Proceedings.

———1981, Predicting the frequency content of acoustic waveforms obtained in boreholes: Society of Professional Well Log Analysts, 22nd Annual Logging Symposium, Mexico City, Mexico, Proceedings.

Palluconi, F. D., and Kieffer, H. H., 1981, Thermal inertia mapping of Mars from 60°S to 60°N: Icarus, v. 45, p. 415–426.

Passey, Q. R., and Shoemaker, E. M., 1980, Global distribution of craters and multiring structures on Callisto [abs.]: Bull. of the Amer. Astronomical Society, v. 12, p. 712.

———1981, Ganymedian thermal gradients from studies of crater relaxation: American Geophysical Union Bulletin EOS (Baltimore, Md., meeting, May 25-29, 1981), EOS, v. 62, no. 17, p. 317.

Patton, W. W., Jr., 1978, Juxtaposed continental and oceanic-island are terranes in the Medfra quadrangle, west-central Alaska, in Johnson, K. M., ed., The United States Geological Survey in Alaska Accomplishments during 1977: U.S. Geol. Survey Circ. 772B, p. B38–B39.

Patton, W. W., Jr., Moll, E. J., Dutro, J. T., Jr., Silberman, M. L., and Chapman, R. M., 1980, Preliminary geologic map of the Medfra quadrangle, Alaska: U.S. Geol. Survey Open-File Rept. 80–811A, scale 1:250,000, 1 sheet.

Pavlides, Louis, 1979, Piedmont tectonic features in Virginia: U.S. Geol. Survey Prof. Paper 1150, p. 258.

Pfeiffer-Rangin, Francoise, 1979, Les zones isopiques du Paléozoïque inférieur du nord-ouest Mexicain, témoins du relais entre Appalaches et la Cordillère ouest-Américaine: C. R. Acad. Sc. Paris, v. 288, no. 20, Série D, p. 1517–1519.

———1981, Early Paleozoic paleogeographic zonation of Sonora [abs.]: Geol Soc. of Amer. Abs. with Programs, v. 13, no. 2, p. 100.

Peyru, G., and Novick, R. P., 1968, Streptomycin suppression of plasmid-linked mutations in *Staphylococcus aureus*: Jour. of Bacteriology, v. 96, p. 1863–1866.

Pieri, David, 1980, Formation of martian valley network (abs.): EOS Transactions of the American Geophysical Union, v. 61, p. 1020.

Piotrowski, R. G., and Harper, J. A., 1979, Black shale and sandstone facies of the Devonian "Catskill" clastic wedge in the subsurface of western Pennsylvania: U.S. Dept. of Energy, Morgantown Energy Tech. Ctr., EGSP Series, no. 13, p. 33–34, pl. 6.

Poole, F. G., and Christiansen, R. L., 1980, Allochthonous lower and middle Paleozoic eugeosynclinal rocks in the El Paso Mountains, northwestern Mojave Desert, California [abs.]: Geol. Soc. of Amer. Abs. with Programs, v. 12, no. 3, p. 147.

Pöttgens, J. J. E., 1979, Ground movements by coal mining in the Netherlands, *in* Saxena, S. K., ed., Evaluation and prediction of subsidence, International Engineering Foundation Conferences, Pensacola Beach, Florida, 1978: Amer. Soc. of Civil Engineers, p. 267–282.

Pratt, W. P., ed., 1981, Metallic mineral-resource potential of the Rolla 1°×2° quadrangle, Missouri, as appraised in September, 1980; U.S. Geol. Survey Open-File Rept. 81–518, 82 p., 3 pl.

Pregger, B. H., 1981, A recently discovered Devonian bedded barite deposit in central Sonora, Mexico [abs.]: Geol. Soc. of Amer. Abs. with Programs, v. 13, no. 2, p. 101.

Provo, L. J., Kepferle, R. C., and Potter, P. E., 1978, Division of black Ohio Shale in eastern Kentucky: Amer. Assoc. of Petro. Geol. Bull., v. 62, no. 9, 1703–1713.

Prucha, J. J., 1956, Stratigraphic relationships of the metamorphic rocks in southeastern New York: Amer. Jour. Sci., v. 254, no. 11, p. 672–684.

Ramey, George, More, Kenneth, Walker, L. D., and Wolfe, R. C., 1981, Executive Summary: Arizona vegetation resource inventory and mapping project final report: BLM Arizona State Office, Phoenix, Ariz., February 1981, 17 p.

Reasenberg, Paul, and Hobson, Jeffrey, 1980, Digitizing five-day recorder tapes on the Eclipse and PDP-11/70 UNIX systems, U.S. Geol. Survey Open-File Rept. 80–610, 94 p.

Regan, R. D., Cain, J. C., and Davis, W. M., 1975, A global magnetic anomaly map: Jour. of Geophysical Research, v. 80, p. 794–802.

Riva, J. P., Jr., 1980, Sulfur in crude oil - A troubling factor for domestic refineries: Library of Congress Congressional Research Service Rept. 80–129 SPR, 25 p.

Robertson, J. M., and Moench, R. H., 1979, The Pecos greenstone belt; a Proterozoic volcano-sedimentary sequence in the southern Sangre de Cristo Mountains, New Mexico: N. Mex. Geol. Society Guidebook, 30th Field Conference, Santa Fe country, p. 165–173.

Roedder, E. W. and Belkin, H. E., 1979, Application of studies of fluid inclusions in Permian Salado salt, N.M., to problems of siting the Waste Isolation Pilot Plant: Scientific Basis for Nuclear Waste Management, v. 1, p. 313–321.

Roedder, E. W., and Bodnar, R. J., 1980, Geologic pressure determinations from fluid inclusion studies: Ann. Rev. Earth Planet. Sci., v. 8, p. 263–301.

Roen, J. B., Wallace, L. G., and deWitt, W., Jr., 1978a, Preliminary stratigraphic cross section showing radioactive zones of the Devonian black shale in eastern Ohio and west-central Pennsylvania: U.S. Geol. Survey Oil and Gas Inv. Chart OC–82.

———1978b, Preliminary stratigraphic cross section showing radioactive zones in the Devonian black shale in the central part of the Appalachian Basin: U.S. Geol. Survey Oil and Gas Inv. Chart OC–87.

Ross, C. P., 1934, Geology and ore deposits of the Casto quadrangle, Idaho: U.S. Geol. Survey Bull. 854, 135 p.

Rowan, L. C., Wetlaufer, P. H., Goetz, A. F. H., Billingsly, F. C., and Stewart, J. H., 1976, Discrimination of rock types and detection of hydrothermally altered areas in south-central Nevada by the use of computer-enhanced ERTS images: U.S. Geol. Survey Prof. Paper 883, p. 35.

Rowley, P. D., 1978, Geologic studies in Orville Coast and eastern Ellsworth Land, Antarctic Peninsula: Antarctic Jour. of the U.S., v. 13, no. 4, p. 7–9.

Runner, G. S., 1980, West Virginia Department of Highways Research Project 16 "Runoff studies on small drainage areas" (Technique for estimating magnitude and frequency of floods in West Virginia): U.S. Geol. Survey Open-File Rept., 44 p.

Rutherford, M. J., 1969, An experimental determination of iron biotite–alkali feldspar equilibria. J. Petrology, 10, p. 381–408.

Ryer, T. A., Phillips, R. E., Bohor, B. F., and Pollastro, R. M., 1980, Use of altered volcanic ash falls in stratigraphic studies of coal-bearing sequences: an example from the Upper Cretaceous Ferron Sandstone Member of the Mancos shale, central Utah: Geol. Soc. Amer., pt. 1, v. 91, p. 579–586.

Samuels, W. B., and Lanfear, K. J., 1980b, An oilspill risk analysis for the Mid-Atlantic (Proposed Sale 59) Outer Continental Shelf lease area: U.S. Geol. Survey Open-File Rept., 80–2026, 82 p.

Samuels, W. B., and Lanfear, K. J., 1980a, An oilspill risk analysis for the South Atlantic (Proposed Sale 56) Outer Continental Shelf lease area: U.S. Geol. Survey Open-File Rept. 80–650, 76 p.

Sando, W. J., Sandberg, C. A., and Gutschick, R. C., 1981, Stratigraphic and economic significance of Mississippian sequence at North Georgetown Canyon, Idaho: Amer. Assoc. of Petro. Geol. Bull., v. 65, no. 8, p. .

Sass, J. H., Blackwell, D. D., Chapman, D. S., Costain, J. K., Decker, E. R., Lawver, L. A., and Swanberg, C. A., 1981, Heat flow from the crust of the United States *in* Physical Properties of Rocks and Minerals, Touloukin, Y. S., Judd, W. R., and Roy, R. F., eds., McGraw-Hill Book Company, p. 503–548.

Schaber, G. G., 1980, The surface of Io: Geologic units, morphology and tectonics: Icarus, v. 43, p. 302–333.

Schaber, G. G., and Masursky, Harold, 1981, Large-scale equatorial and midlatitude surface disruptions on Venus: preliminary geologic assessment [abs.]: Proceedings, Lunar and Planetary Science Conference, 12th Lunar and Planetary Science Instit., Houston, Tex., p. 928–931.

Schimschal, Ulrich, 1980a, Scintillation detectors in gamma spectral logging: geometry, absorption and calibration: U.S. Geol. Survey Open-File Rept. 80–688, 29 p.

———1980b, Quantitative effects of lithology, borehole environment, and probe design in gamma spectral logging in scintillation crystals: The Log Analyst, v. XX1, no. 5, p. 3–10.

———1981, Flowmeter analysis at Raft River, Idaho: Ground Water, v. 19, no. 1, p. 93–97.

———1981, Mathematical model of gamma-ray spectrometry borehole logging for quantitative analysis: U.S. Geol. Survey Open-File Rept. 81–402.

Schmoll, H. R., Dobrovolny, Earnest, and Gardner, C. A., 1980: Preliminary geologic map of the middle part of the Eagle River valley, Municipality of Anchorage, Alaska: U.S. Geol. Survey Open-File Rept. 80–890, 1 sheet, 11 pages.

Scott, D. H., and Tanaka, K. L., 1980, Mars Tharsis region: Volcanotectonic events in the stratigraphic record: Proceedings, Lunar and Planetary Science Conference, 11th, Geochim. et Cosmochim. Acta, v. 3, p. 2403–2421.

———1981a, Mars: paleostratigraphic restoration of buried surfaces in Tharsis Montes: Icarus, v. 45, p. 304–319.

Scott, W. E., and Shroba, R. R., 1980, Stratigraphic significance and variability of soils buried by deposits of the last cycle of Lake Bonneville: Geol. Soc. of Amer. Abs. with Programs, v. 12, no. 6, p. 304.

Seeland, D. A., 1976, Sedimentology and stratigraphy of the Lower Eocene Wind River Formation, central Wyoming: *in* Guidebook Wyo. Geol. Assoc. Resources of the Wind River Basin, 30th Annual Field Conference, p. 181–198.

Shieh, Y.N., and Schwarcz, H. P., 1978, The oxygen isotope composition of the surface crystalline rocks of the Canadian Shield: Canadian Jour. of Earth Sci., v. 15, p. 1773–1782.

Shoemaker, E. M., 1981, Collision of solid bodies with the planets and satellites, *in* The new Solar System: Cambridge, Mass., Sky Publishing Corp., Bealty, J. K., O'Leary, Brian, and Chaikin, Andrew, eds., p. 33–44.

Siegel, D. I., 1981, The effect of snowmelt on the water quality of Filson Creek and Omaday Lake, northeastern Minnesota: Water-Resources Research, v. 17, p. 238–242.

Silver, L. T., and Anderson, T. H., 1974, Possible left-lateral early to middle Mesozoic disruption of the southwestern North American craton margin [abs.]: Geol. Soc. of Amer. Abs. with Programs, v. 6, no. 7, p. 955–956.

Singer, D. A., Menzie, W. D., DeYoung, J. H., Jr., Sander, M., and Lott, A., 1980, Grade and Tonnage Data Used to Construct Models for the Regional Alaskan Mineral Resource Assessment Program; U.S. Geol. Survey Open-File Rept. 80–199, 58 p.

Singer, D. A., and Mosier, D. L., 1980, Review of Methods of Resource Assessment: 109th AMIE Annual Meeting, February 24–28, 1980, Las Vegas, Nev.

Skipp, Betty, and Hait, M. H., Jr., 1977, Allochthons along the northwest margin of the Snake River Plain, Idaho: Twenty-ninth Annual Field Conference, Wyo. Geol Assoc. Guidebook, p. 499–515.

Smedes, H. W., 1980, Rationale for geologic isolation of high-level radioactive waste, and assessment of the suitability of crystalline rocks, U.S. Geol. Survey Open-File Rept. 80–1065, 57 p.

Smith, B. A., and 26 others (including scientists M. H. Carr, Harold Masursky, E. M. Shoemaker, and L. A. Soderblom), 1981, Encounter with Saturn: Imaging Science Results: Science, v. 212, p. 159–191.

Smith, G. I., and Ketner, K. B., 1970, Lateral displacement on the Garlock Fault, southeastern California, suggested by offset sec-

tions of similar metasedimentary rocks: U.S. Geol. Survey Prof. Paper 700-D, p. D1-D9.

Smith, J. F., Jr., and Ketner, K. B., 1968, Devonian and Mississippian rocks and the date of the Roberts Mountains Thrust in the Carlin-Piñon Range area, Nevada: U.S. Geol. Survey Bull. 1251-I, p. I1-I18.

Smith, T. E., and Turner, D. L., 1973, Geochronology of the Maclaren metamorphic belt, south-central Alaska - a progress report: Isochron/West, no. 7, p. 21-25.

Snyder, G. L., 1979, Archean and Proterozoic structural and stratigraphic details of the Hartville uplift in Wyoming: *in* Geol. Survey Research 1979, U.S. Geol. Survey Prof. Paper 1150, p. 69.

———1980, Map of Precambrian and adjacent Phanerozoic rocks of the Hartville uplift, Goshen, Niobrara, and Platte counties, Wyoming: U.S. Geol. Survey Open-File Rept. 80-779, 2 sheets.

Soderblom, L. A., 1980, The Galilean satellites of Jupiter: Scientific American, v. 242, no. 1, p. 88-100.

Soderblom, L. A., Johnson, T. V., Morrison, David, Danielson, E., Smith, B. A., Veverka, Joseph, Cook, A., Sagan, Carl, Kupferman, P., Pieri, David, Mosher, J., Avis, C., Gradie, J., and Clancy, T., 1980, Spectrophotometry of Io: Preliminary Voyager 1 results: Geophysical Research Letters, v. 7, p. 963-966.

Soukup, W. G., 1980, Ground-water appraisal in northwestern Big Stone County, west-central Minnesota: U.S. Geol. Survey Water-Resources Inv. 80-568, 41 p.

Souza, W. R., 1981, Ground-water status report, Lahaina District, Maui, Hawaii 1980: U.S. Geol. Survey Water-Resources Inv. 81-549, 2 sheets.

Spengler, R. W., and Glanzman, V. M., 1980, Review of geology and material property data in shallow alluvium, eastern Area 2, Nevada Test Site: U.S. Geol. Survey Report USGS-474-266 (NTS-262), 20 p.; available *only* from U.S. Department of Commerce, National Technical Information Service, Springfield, VA 22161.

Stauber, D. A., 1980, Short-period teleseismic P residual study of San Francisco volcanic field: EOS, v. 61, p. 1025.

Stewart, J. H., 1981, Early and middle Paleozoic margin of the North American Continent in the southwestern United States and northern Mexico, *in* Howard, K. A., Carr, M. D., and Miller, D. M., eds., Tectonic framework of the Mojave and Sonoran Deserts, California and Arizona: U.S. Geol. Survey Open-File Rept. 81-503, p. 101-103.

Stokoe, K. H., II., and Chen, A. T. F., 1980, Effects on site response of methods of estimating in situ nonlinear soil behavior: Proceedings of the 7th World Conference on Earthquake Engineering, Istanbul, Turkey, v. 3, p. 395-402.

Stormer, J. C., Jr., 1975, A practical two-feldspar geothermometer: Am. Mineralogist 60, 667-674.

Stuckless, J. S., 1979, Uranium and thorium concentrations in Precambrian granites as indicators of a uranium province in central Wyoming: Contributions to Geology, v. 17, no. 2, p. 173-178.

Swain, P. H., King, R. C., 1973, Two effective feature selection criteria for multispectral remote sensing: Laboratory for Applications of Remote Sensing, Purdue University, LARS Information Note 042673, p. 5.

Swanson, D. A., Wright, T. L., Hooper, P. R., and Bentley, R. D., 1979, Revisions in stratigraphic nomenclature of the Columbia River Basalt Group: U.S. Geol. Survey Bull. 1457-G, 59 p.

Swithinbank, Charles, 1980, The problem of a glacier inventory of Antarctica: World Glacier Inventory, Proceedings of the Reideralp (Switzerland) Workshop, IAHS-AISH Publication No. 126, p. 229-236.

Tabet, D. E., and Frost, F. J., 1979, Environmental Characteristics of Menefee coals in the Torreon Wash area, New Mexico: New Mexico Bureau of Mines and Min. Res. Open-File Rept. 102, 134 p.

Taylor, H. P., and Silver, L. T., 1978, Oxygen isotope relationships in plutonic igneous rocks of the Peninsular Ranges batholith, southern and Baja California, in Short papers of the Fourth International Conference, Geochronology, Cosmochronology, Isotope Geology, 1978: U.S. Geol. Survey Open-File Rept. 78-701, p. 423-426.

Thayer, T. P. and Lipin, B. R., 1979, Preliminary map of chromite provinces in the conterminous United States: U.S. Geol. Survey Open-File Rept. 79-576R, 1 over-size sheet, scale 1:5,000,000.

Thomasson, M. R., 1959, Late Paleozoic stratigraphy and paleotectonics of central and eastern Idaho: abstract *in* Dissertation Abstracts, v. 20, no. 3, p. 999; and Geol. Society of Amer. Bull., v. 70, no. 12, p. 1687.

Thorarinsson, Sigurdur, 1977, At leve pa en Volkan (Living on a volcano): Geografisk Tidsskrift, v. 76, p. 1-13.

Tilling, R. I., 1973, Boulder batholith, Montana: A product of two contemporaneous but chemically distinct magma series: Geol. Soc. Amer. Bull., v. 84, p. 3879-3900.

Tooker, E. W., 1980, Background information to accompany the atlas of some metal and nonmetal minerals provinces in the conterminous United States: U.S. Geol. Survey Circ. 792, 15 p.

Tooker, E. W., 1979, Preliminary map of aluminum provinces in the conterminous United States: U.S. Geol. Survey Open-File Rept. 79-576M, 1 over-size sheet, scale 1:5,000,000.

——— 1979, Preliminary map of copper provinces in the conterminous United States: U.S. Geol. Survey Open-File Rept. 79-576D, 1 over-size sheet, scale 1:5,000,000.

——— 1979, Preliminary map of fluorine provinces in the conterminous United States: U.S. Geol. Survey Open-File Rept. 79-576F, 1 over-size sheet.

Tooker, E. W., and Cannon, W. F., 1979, Preliminary map of manganese provinces in the conterminous United States: U.S. Geol. Survey Open-File Rept. 79-576O, 1 over-size sheet, scale 1:5,000,000.

Tooker, E. W., and Force, E. R., 1979, Preliminary map of tin occurrence areas in the conterminous United States: U.S. Geol. Survey Open-File Rept. 79-576K, 1 over-size sheet, scale 1:5,000,000.

Tooker, E. W., and Johnson, M. G., 1979, Preliminary map of gold provinces in the conterminous United States: U.S. Geol. Survey Open-File Rept. 79-576S, 1 over-size sheet, scale 1:5,000,000.

Tooker, E. W., and Morris, H. T., 1979, Preliminary map of lead provinces in the conterminous United States: U.S. Geol. Survey Open-File Rept. 79-576P, 1 over-size sheet, scale 1:5,000,000.

Tooker, E. W., and Parker, R. L., 1979, Preliminary map of columbium (niobium) and tantalum provinces in the conterminous United States: U.S. Geol. Survey Open-File Rept. 79-576N, 1 over-size sheet, scale 1:5,000,000.

Tooker, E. W., and Reed, B. L., 1979, Preliminary map of aluminum provinces in the conterminous United States: U.S. Geol. Survey Open-File Rept. 79-576L, 1 over-size sheet.

Tooker, E. W., and Wedow, Helmuth, Jr., 1979, Preliminary map of zinc provinces in the conterminous United States: U.S. Geol. Survey Open-File Rept. 79-576Q, 1 over-size sheet, scale 1:5,000,000.

Tooker, E. W. and Wong, G., 1980, CRIB-UTAH: Metal and Nonmetal Resources Information Available in the U.S. Geological Survey Computerized Resource Information Bank; U.S. Geol. Survey Open-File Rept. 80-845, p. 8.

Trescott, P. C., 1975, Documentation of finite-difference model for simulation of three-dimensional ground-water flow: U.S. Geol. Survey Open-File Rept. 75-438, 32 p.

Trescott, P. C., and Larson, S. P., 1976, Supplement to Open-File Report 75-438, Documentation of finite-difference model for simulation of three-dimensional ground-water flow: U.S. Geol. Survey Open-File Rept. 76-591, 21 p.

U.S. Geological Survey, 1980, U.S. Geological Survey investigations in connection with the Mighty Epic Event, *with a section on* Geologic investigations by G. M. Fairer and D. R. Townsend, *a section on* Geophysical logging and seismic investigations by R. D. Carroll, M. J. Cunningham, and D. C. Muller, *a section on* Gravity survey Rainier Mesa and U12n.10 tunnel by D. L. Healey, *and a section on* In situ stress investigations by W. L. Ellis: U.S. Geol. Survey report USGS-474-228, 191 p.; available *only* from U.S. Department of Commerce, National Technical Information Service, Springfield, VA 22161.

U.S. Geological Survey, 1981, Altimetric and shaded relief map of Venus: U.S. Geol. Survey Misc. Map Series, Atlas of Venus, 1:50,000,000 scale, I-1324.

Van Alstine, R. E., and Tooker, E. W., 1979, Preliminary map of flourine provinces in the conterminous United States: U.S. Geol. Survey Open-File Rept. 79-576G, 1 over-size sheet.

Verbeek, E. R., and Clanton, U. S., 1978, Map showing surface faults in the southeastern Houston metropolitan area, Texas: U.S. Geol. Survey Open-File Rept. 78-797, scale 1:24,000.

Verbeek, E. R., Ratzlaff, K. W., and Clanton, U. S., 1979, Faults in parts of north-central and western Houston metropolitan area, Texas: U.S. Geol. Survey Misc. Field Studies Map MF-1136, scale 1:24,000.

Wagener, H. D., 1977, The granitic stone resources of South Carolina: South Carolina Geological Survey, State Development Board Mineral Resources, Series 5, p. 1-65.

Wallace, L. G., Roen, J. B., and deWitt, W., Jr., 1977, Preliminary stratigraphic cross section showing radioactive zones in the Devonian black shale in the western part of the Appalachian Basin: U.S. Geol. Survey Oil and Gas Inv. Chart OC-82.

Wallace, R. E., 1978, Patterns of faulting and seismic gaps in the Great Basin Province: Proceedings of Conference VI, Methodology for identifying seismic gaps and soon-to-break gaps, U.S. Geol. Survey Open-File Rept., 78-943, p. 857-868.

Ware, R. H., 1980, Magnetotelluric survey of the San Francisco volcanic field, Arizona: U.S. Geol. Survey Open-File Rept. 80-1163.

Wenrich-Verbeek, K. J., 1977a, Uranium and co-existing element behavior in surface waters and associated sediments with varied sampling techniques used for uranium exploration: Jour. of Geochem. Exploration, v. 8, p. 337-355.

———1977b, Anomalous uranium in waters of the Rio Oho Caliente, New Mexico, *in* Campbell, J. A., ed., Short papers of the U.S. Geological Survey uranium-thorium symposium, 1977: U.S. Geol. Survey Circ. 753, p. 73-75.

Wentworth, C. K., 1938, Ash formations of the Island Hawaii: Hawaiian Volcano Observatory, 3d Special Report, 183 p.

White, David, 1900, The stratigraphic succession of the fossil floras of the Pottsville Formation in the southern anthracite field, Pennsylvania: U.S. Geol. Survey, 20th Annual Report, Part II, p. 749-953.

Williams, Howel, 1942, The geology of Crater Lake National Park, Oregon, with a reconnaissance of the Cascade Range southward to Mount Shasta: Carnegie Inst. of Wash. Pub. 540, 162 p.

Williams, R. S., Jr., 1980, Geologic hazards of Iceland: a classification (abs.), *in* Abstracts with Programs, 1980 Annual Meetings: Geol. Society of Amer., Boulder, Colo., v. 12, no. 7, p. 550.

Williams, R. S., Jr., Bödvarsson, Ágúst, Rist, Sigurjon, Saemundsson, Kristján, and Thorarinsson, Sigurdur, 1975, Glaciological studies in Iceland with ERTS-1 imagery (abs.): Jour. of Glaciology, v. 15, no. 73, p. 465-466.

Witkind, I. J., 1974, A possible concealed pluton in Beaverhead and Madison Counties, Montana and Clark County, Idaho: U.S. Geol. Survey Open-File Rept. 74-312.

Wright, N. A., 1973, Subsurface Tully limestone, New York and northern Pennsylvania: N.Y. State Museum and Science Service, Map and Chart Series No. 14.

Wyoming Research Corporation, 1980, A socioeconomic assessment of the Rojo Caballos Mine: Laramie, Wyo., 238 p.

Wyrick, G. G., and Borchers, J. W., 1980, Hydrologic effects of stress-relief fracturing in an Appalachian Valley: U.S. Geol. Survey Water-Supply Paper 2177, 51 p.

Zartman, R. E., Pawlowska, Jadwiga, and Rubinowski, Zbigniew, 1979, Lead isotopic composition of ore deposits from the Silesia-Crakow Mining District, *in* Research on the genesis of zinc-lead deposits of Upper Silesia, Poland: Prace Instytutu Geologicznego, v. XCV, p. 133-149.

Zielinski, R. A., 1979, Uranium mobility during interaction of rhyolite obsedian, perlite and felsite with alkaline carbonate solutions: T=120°C, P=210 kg/cm^3: Chemical Geology, v. 27, p. 47-63.

Zoback, M. D., Hamilton, R. M., Crone, A. M., Russ, D. P., McKeown, F. A., and Brockman, S. R., 1980, Recurrent intraplate tectonism in the New Madrid seismic zone: Science, v. 209, p. 971-976.

Zohdy, A. A. R., 1973, A computer program for the automatic interpretation of Schlumberger sounding curves over horizontal stratified media: available only from U.S. Dept. of Commerce, National Technical Information Service (N.T.I.S.), Springfield, VA 22161; as USGS report, GD-74-017; PB-232702.

INVESTIGATIONS IN PROGRESS IN THE GEOLOGICAL SURVEY

Investigations in progress during fiscal year 1981 are listed below together with the names and headquarters of the individuals in charge of each. Headquarters at main centers are indicated by NC for the National Center in Reston, Va., D for Denver, Colo., and M for Menlo Park, Calif. The lowercase letter after the name of the project leader shows the Division technical responsibility: c, Conservation Division; o, Office of Earth Sciences Applications; w, Water Resources Division; no letter, Geologic Division.

The projects are classified by principal topic. Most geologic-mapping projects involve special studies of stratigraphy, petrology, geologic structure, or mineral deposits but are listed only under "Geologic mapping" unless a special topic or commodity is the primary justification for the project. A reader interested in investigations of volcanology, for example, should look under the heading "Geologic Mapping" for projects in areas of volcanic rocks, as well as under the heading "Volcanology." Likewise, most water-resource investigations involve special studies of several aspects of hydrology and geology but are listed only under "Water Resources" unless a special topic—such as floods or sedimentation—is the primary justification for the project.

Areal geologic mapping is subdivided into mapping at scales smaller than 1:62,500 (for example, 1:250,000) and mapping at scales of 1:62,500 or larger (for example, 1:24,000).

Abstracts. *See* Bibliographies and abstracts.
Aluminum:
Resources of the United States (S. H. Patterson, NC)
Analytical chemistry:
Activation analysis (J. J. Rowe, NC)
Analytical methods:
Textural automatic image analyzer research (M. B. Sawyer, D)
Water chemistry (M. J. Fishman, w, D)
Analytical services and research (J. I. Dinnin, NC; Claude Huffman, Jr., D; C. O. Ingamells, M)
Mineral deposits, characteristic analysis (J. M. Botbol, NC)
Organic geochemistry and infrared analysis (I. A. Berger, NC)
Organic polyelectrolytes in water (R. L. Wershaw, w, D)
Plant laboratory (T. F. Harms, D)
Radioactivation and radiochemistry (H. T. Millard, D)
Rock chemical analysis:
General (D. R. Norton, D)
Rapid (Leonard Shapiro, NC)
Services (L. B. Riley, D)
Trace analysis methods, research (F. N. Ward, D)
Ultratrace analysis (H. T. Millard, D)
X-ray spectrometer for Viking lander (Priestley Toulmin III, NC)
See also Spectroscopy.
Arctic engineering geology (Reuben Kachadoorian, M)
Artificial recharge:
Artificial recharge (G. J. Leonard, w, Pueblo, Colo.)
Chemical reactions, mineral surfaces (J. D. Hem, w, M)
Columbia River basalt recharge (M. R. Karlinger, w, Tacoma, Wash.)
Deepwell waste injection (R. W. Hull, w, Tallahassee, Fla.)
Fort Allen recharge (J. R. Diaz, w, Fort Buchanan, P.R.)
Fresh water storage, saline aquifers (J. N. Fischer, w, Miami, Fla.)
Injection wells, Santa Rosa County (R. W. Hull, w, Tallahassee, Fla.)
Lee County freshwater injection (F. A. Watkins, w, Fort Myers, Fla.)
Nassau County recharge (D. A. Aronson, w, Syosset, N.Y.)
Salina hydrology (R. M. Waller, w, Ithaca, N.Y.)
Salt-Gila recharge (P. B. Rohne, w, Phoenix, Ariz.)
Supplemental recharge by storm basins (D. A. Aronson, w, Syosset, N.Y.)
Automated cartography:
Datamap (Cooperative Mapping Program) (D. Peuquet, o, NC)
Raster Mode Geoprocessing (D. Peuquet, l, NC)
Barite:
Geology, geochemistry, and resources of barite (D. A. Brobst, NC)
Base metals. *See* base-metal names.
Bibliographies and abstracts:
Luna bibliography (J. H. Freeberg, M)
Borates:
California (N):
Furnace Creek area (J. F. McAllister)
Searles Lake area (G. I. Smith)
Chromite. *See* Ferro-alloy metals.
Clays:
Georgia, Kaolin investigations (S. H. Patterson, NC)
Climate:
Tree ring analysis (S. Agard, D)
Climatic changes:
California, Quaternary (D. P. Adam, M)
Lakes, Holocene (W. E. Dean, D)
Rocky Mountain area, Quaternary deposits (K. L. Pierce, D)
Coal:
Appalachia, Safe mine waste disposal (W. E. Davies, NC)
Coal petrochemistry and related investigations (E. C. T. Chao, NC)
Geochemistry of United States coal (V. E. Swanson, D)
Geotechnical research in western energy lands (F. W. Osterwald, D)
National Coal Resources Data System (M. D. Carter, NC)
Natural combustion and metamorphism of overlying rocks (J. R. Herring, D)
Regional geotechnical studies, Powder River Basin (S. P. Kanizay, D)
States:
Alaska:
Bering River coal field (C, Anchorage)
Nenana (Clyde Wahrhaftig, M)
Regional engineering geology of Cook Inlet coal lands (H. R. Schmoll and L. A. Yehle, D)
Shallow geophysical logging for coal-National Petroleum Reserve in Alaska (J. E. Callahan, c, Anchorage)

Coal—Continued

States—Continued

Arizona, Collection of coal samples for analysis (R. T. Moore, Tucson; V. E. Swanson, D)

Colorado (c, D, except as otherwise noted):
- Citadel Plateau (G. A. Izett)
- Collection of coal samples and coal resource data in Colorado and entry of data into the USGS National Coal Resources Data System (D. K. Murray; M. D. Carter, NC)
- Disappointment Valley, eastern (D. E. Ward, D)
- Douglas Creek Arch area (B. E. Barnum)
- Geology and energy resources of the Book Cliffs coal field (R. S. Garrigues)
- Geology and energy resources of the Danforth Hills area (J. R. Smith)
- Geology and energy resources of the Grand Hogback and adjacent areas (D. H. Madden)
- Geology and energy resources of the Grand Mesa coal field (S. L. Covington)
- Geology and energy resources of the Paonia and Crested Butte coal fields (D. L. Gaskill)
- Geology and energy resources of the Rawlins coal field, Wyoming-Colorado (C. S. V. Barclay)
- Geology and energy resources of the Trinidad coal field (G. W. Rice)
- Geology and energy resources of the Yampa coal field (M. E. Brownfield)
- North Park area (D. J. Madden)
- Smizer Gulch and Rough Gulch quadrangles (W. J. Hail, D)

Idaho, Collection of coal samples in Idaho (C. R. Knowles, Moscow; V. E. Swanson, D)

Illinois, Preparation of Illinois coal resource and chemical data for entry into the USGS National Coal Resources Data System (H. J. Gluskoter, Urbana; M. D. Carter, NC)

Kentucky (D):
- Adams quadrangle (D. E. Ward)
- Blaine quadrangle (C. L. Pillmore)
- Louisa quadrangle (R. M. Flores)
- Richardson quadrangle (P. T. Hayes)
- Sitka quadrangle (P. T. Hayes)

Missouri, Coal data collection and transfer to the National Coal Resources Data System (C. E. Robertson, Rolla; M. D. Carter, NC)

Montana:
- Birney coal area (V. D. Niermeier, c, Casper, Wyo.)
- Collection of coal samples in Montana (R. E. Matson, Butte; V. E. Swanson, D)
- Geology and energy resources of the Williston Basin, North Dakota, South Dakota, and Montana (J. S. Hines, c, Billings)

Nevada, Collection of coal samples in Nevada (J. A. Schilling, Reno; V. E. Swanson, D)

New Mexico:
- Collection of coal samples in New Mexico (F. E. Kottlowski, Socorro; V. E. Swanson, D)
- Gallup East quadrangle (E. D. Patterson, c, Roswell)
- Manuelito quadrangle (J. E. Fassett, c, Farmington)
- Twin Butte quadrangle (M. L. Millgate, c, Farmington)
- Western Raton field (C. L. Pillmore, D)

North Dakota (c, Billings, Mont., except as otherwise noted):
- Adams, Bowman, and Slope Counties—lignite resources (R. C. Lewis)
- Clark Butte 15-minute quadrangle (G. D. Mowat)

Coal—Continued

States—Continued

North Dakota—Continued
- West-central North Dakota lignite resources (E. A. Rehbein)
- Williston area lignite resources (J. M. Spencer)

Oklahoma (c, Tulsa, except as otherwise noted):
- Blocker quadrangle (E. H. Hare, Jr.)
- Collection of coal samples in Oklahoma (S. A. Friedman, Norman; V. E. Swanson, D)
- Hackett quadrangle (E. H. Hare, Jr.)
- Panama quadrangle (E. H. Hare, Jr.)
- Spiro quadrangle (E. H. Hare, Jr.)

Pennsylvania (NC, except as otherwise noted):
- Collection of coal samples for analysis (W. E. Edmunds, Pennsylvania State Geological Survey, Harrisburg; M. J. Bergin)
- Northern anthracite field (M. J. Bergin)
- Southern anthracite field (G. H. Wood, Jr.)

Utah (c, D, except as otherwise noted):
- Basin Canyon quadrangle (Fred Peterson)
- Blackburn Canyon quadrangle (Fred Peterson)
- Engineering geologic studies, east-central Utah (E. E. McGregor, D)
- Geology and coal resources of Wasatch Plateau coal field (L. F. Blanchard)
- Geology and energy resources of the Henry Mountains coal basin (W. E. Bowers)
- Geology and energy resources of the Emery coal field (L. F. Blanchard)

Virginia and West Virginia, Central Appalachian Basin (K. J. Englund, NC)

Washington, Collection of coal samples for analysis (V. E. Livingston, Jr., Olympia; V. E. Swanson, D)

West Virginia:
- Formatting coal data for National Coal Resources Data System (M. C. Behling, Morgantown; M. D. Carter, NC)
- Louisa quadrangle (C. W. Connor, D)

Wyoming (c, D, except as otherwise noted:
- Coal mine deformation studies, Powder River Basin (C. R. Dunrud, D)
- Engineering geologic mapping, Sheriden-Buffalo area, Wyoming (E. N. Hinrichs, D)
- Engineering geologic studies, Kemmerer 1:100,000 sheet (D. D. Dickey, D)
- Geology and coal resources of the Rock Springs Uplift (D. H. Madden)
- Geology and energy resources of the Powder River Basin (L. H. Jefferis, c, Casper)
- Geology and energy resources of the Rawlins coal field, Wyoming-Colorado (C. V. S. Barclay)
- Hilight coal area (L. H. Jeffries, c, Casper)
- Weston SW quadrangle (R. A. Katock c, Casper)

Construction and terrain problems:

Areal slope stability analysis, San Francisco Bay region (S. D. Ellen, M)

Damsite investigations (F. N. Houser, D)

Electronics instrumentation research for engineering geology (J. B. Bennetti, D)

Engineering geologic map of United States (D. H. Radbruch-Hall, M)

Fissuring-subsidence research (T. L. Holzer, M)

Geophysical studies for engineering geology (C. H. Miller, D)

Geotechnical measurements and services (H. W. Olsen, D)

Geotechnical research in western energy lands (F. W. Osterwald, D)

Construction and terrain problems—Continued
- Landslide overview map of the conterminous U.S. (D. H. Radbruch-Hall, M)
- Potential volcanic hazards to nuclear facilities, Washington, Oregon, and northern California (M. H. Hait, Jr.; W. H. Hays, D)
- Reactor hazards research (W. H. Hays, D)
- Reactor site investigations (M. H. Hait, Jr. D)
- Regional geotechnical studies, Powder River Basin (S. P. Kanizay, D)
- Research in rock mechanics (F. T. Lee, D)
- Safe mine waste disposal, Appalachia (W. E. Davies, NC)
- Sino-Soviet terrain (L. D. Bonham, I, NC)
- Solution subsidence and collapse (J. R. Ege, D)
- Special intelligence (L. D. Bonham, I, NC)
- Tephra hazards from Cascade Range volcanoes (D. R. Mullineaux, D)
- Volcanic hazards (D. R. Crandell, D)
- *States:*
- Alaska, Regional engineering geology of Cook Inlet coal lands (H. R. Schmoll and L. A. Yehle, D)
- California (M, except as otherwise noted):
  - Geology and slope stability, western Santa Monica Mountains (R. H. Campbell)
  - Pacific Palisades landslide area, Los Angeles (J. T. McGill, D)
  - Palo Alto, San Mateo, and Montara Mountain quadrangles (E. H. Pampeyan)
- Colorado, Coal mine deformation studies, Somerset mining district (C. R. Dunrud, D)
- Hawaii, Seismic hazards of the island of Hawaii with special emphasis on the Hilo 7½ min. quad. (J. Buchanan-Banks, Hawaii)
- Nevada:
  - Seismic engineering program (K. W. King, Las Vegas)
  - Surface effects of nuclear explosions (R. P. Snyder, D)
- Utah, Engineering geologic studies, east-central Utah (E. E. McGregor, D)
- Wyoming:
  - Coal mine deformation studies, Powder River Basin (C. R. Dunrud, D)
  - Engineering geologic mapping, Sheridan-Buffalo area (E. N. Hinrichs, D)
  - Engineering geologic studies, Kemmerer 1:100,000 sheet (D. D. Dickey, D)
  - Geologic environmental maps for land-use planning (D. D. Dickey, D)
  - Weathering effects on geotechnical properties, Sheridan and Buffalo 1° × 1/2° quadrangles (A. F. Chleborad, D)
- *See also* Urban geology; Land use and environmental impact; Urban hydrology.

Copper:
- New England massive sulfides (J. F. Slack, NC)
- United States and world resources (D. P. Cox, NC)
- *States:*
- Alaska, Southwest Brooks Range (I. L. Tailleur, M)
- Arizona, Ray porphyry copper (H. M. Cornwall, M)
- Colorado, Precambrian sulfide deposits (D. M. Sheridan, D)
- Maine-New Hampshire, Porphyry with molybdenum (R. G. Schmidt, NC)
- Michigan (NC):
  - Greenland and Rockland quadrangles (J. W. Whitlow)
  - Michigan copper district (W. S. White)
- Virginia, Massive sulfides (J. E. Gair, NC)

Crustal studies. *See* Earthquake studies; Geophysics, regional.

Drought studies:
- Drought in Colorado (T. R. Dosch, w, D)
- Low-flow characteristics of South Carolina streams (W. M. Bloxham, w, Columbia, S. C.)
- Northwest Iowa (M. R. Bukart, w, Iowa City)
- Tree rings and drought (R. L. Phipps, w, NC)

Earthquake studies:
- Active fault analysis (R. E. Wallace, M)
- Comparative elevation studies (R. O. Castle, M)
- Computer fault modeling (J. H. Dieterich, M)
- Computer operations and maintenance (T. C. Jackson, M)
- Crustal evolution studies and isotopic measurements (J. S. Stacey, D)
- Crustal inhomogeneity in seismically active areas (S. W. Stewart, M)
- Crustal strain (J. C. Savage, M)
- Crustal studies (ARPA) (Isidore Zietz, NC)
- Dynamic soil behavior (A. T. F. Chen, M)
- Earth structure studies (J. H. Healy, M)
- Earthquake field studies (W. J. Spence, C. J. Langer, J. N. Jordan, M)
- Earthquake-induced landslides (E. L. Harp, M)
- Earthquake-induced sedimentary structures (J. D. Sims, M)
- Earthquake recurrence and history (R. D. Nason, M)
- Eastern United States (R. K. McGuire, D)
- Experimental liquefaction potential mapping (T. L. Youd, M)
- Fault-zone tectonics (J. C. Savage, M)
- Fluid injection, laboratory investigations (J. D. Byerlee, Louis Peselnick, M)
- Geologic parameters of seismic source areas (F. A. McKeown, D)
- Ground failure related to the 1811–12 New Madrid earthquakes (S. F. Obermeier, NC)
- Ground failures caused by historic earthquakes (D. K. Keefer, M)
- Ground-motion modeling and prediction (W. B. Joyner, M)
- Ground-motion studies (R. D. Borcherdt, R. P. Maley, M)
- Interaction of ground motion and ground failure (R. C. Wilson, M)
- Microearthquake data analysis (W. H. K. Lee, M)
- National Earthquake Information Service (A. C. Tarr, D)
- National Strong-Motion Instrumentation Network (R. B. Matthiesen, M)
- New seismic instrumentation for geothermal surveys (P. A. Reasenberg, M)
- Nicaragua, Central America, technical assistance in establishing center for earthquake hazard reduction (P. L. Ward, M)
- Precursory phenomena (P. L. Ward, M)
- Prediction, animal behavior studies (P. A. Reasenberg, M)
- Prediction monitoring and evaluation (R. N. Hunter, D)
- Quaternary dating and neotectonics (K. L. Pierce, D)
- Recurrence intervals along Quaternary faults (K. L. Pierce, D)
- Reduction of noise in precursor signals (J. A. Steppe, M)
- Reservoir-induced seismicity, statistical approach, (D. E. Stuart-Alexander, M)
- Seismic-risk studies (S. T. Algermissen, D)
- Seismic-source studies (W. R. Thatcher, M)
- Seismic studies for earthquake prediction (C. G. Bufe, M)
- Seismicity and Earth structure (J. N. Taggart, D)
- Seismological research observatories (J. R. Peterson, Albuquerque, N. Mex.)
- Spectral and time domain analysis of near field recordings of earthquakes (J. B. Fletcher, M)
- Stress studies (C. B. Raleigh, M)
- Surface faulting studies (M. G. Bonilla, M)

Earthquake studies—Continued
- Synthetic strong-motion seismograms (W. B. Joyner, M)
- Tectonic studies (W. B. Hamilton, D)
- Teleseismic search for earthquake precursors (J. W. Dewey, D)
- Theoretical seismology (A. F. Espinosa, D)
- Worldwide Network of Standard Seismographs (J. R. Peterson, Albuquerque, N. Mex.)
- *States and territories:*
- Alaska:
  - Earthquake hazards:
    - Anchorage (H. R. Schmoll, D)
    - Southern part (George Plafker, M)
  - Microearthquake studies (R. A. Page, M)
  - Turnagain Arm sediments (A. T. Ovenshine, M)
- California (M, except as otherwise noted):
  - Basement rock studies along San Andreas fault (D. C. Ross)
  - Depth of bedrock in the San Francisco Bay region (R. M. Hazlewood)
  - Earthquake hazards:
    - San Francisco Bay region (E. E. Brabb)
    - Southern part (D. M. Morton, Los Angeles)
  - Foothills fault system (D. E. Stuart-Alexander, M)
  - Geodetic strain (W. H. Prescott)
  - Geophysical studies, San Andreas fault (J. H. Healy)
  - Measurement of seismic velocities for seismic zonation (J. F. Gibbs, R. D. Borcherdt, T. E. Fumal)
  - Microearthquake studies:
    - Central part (J. H. Pfluke)
    - New Melones (J. C. Roller)
    - Southern part (D. P. Hill)
  - Recency of faulting, eastern Mojave Desert (W. J. Carr)
  - Tectonics:
    - Central and northern part (W. P. Irwin)
    - Central San Andreas fault (D. B. Burke, T. W. Dibblee, Jr.)
    - Salton Trough tectonics (R. V. Sharp)
    - Southern part (M. M. Clark)
  - Theory of wave propagation in anelastic media (R. D. Borcherdt)
- Colorado:
  - Neotectonic map of Colorado (S. M. Colman, D)
  - Rangely (C. B. Raleigh, M)
- Hawaii, Seismic hazards of the island of Hawaii with special emphasis on the Hilo 7½ min. quad. (J. Buchanan-Banks, Hawaii)
- Idaho, Active faults, Snake River Plain (S. S. Oriel, M. H. Hoit, W. E. Scott, D)
- Massachusetts, Fault definition, northeastern Massachusetts (A. F. Shride, D)
- Missouri:
  - Ground failure related to the New Madrid earthquake (S. F. Obermeier, NC)
  - New Madrid fault-zone geophysics (M. F. Kane, D)
- Montana, Yellowstone National Park, microearthquake studies (A. M. Pitt, M)
- New Mexico:
  - Neotectonic maps of New Mexico and the Rio Grande Rift (M. N. Machette, D)
  - Seismotectonic analysis, Rio Grande rift (E. H. Baltz, Jr., D)
- Puerto Rico, Preliminary assessment of liquefaction potential in and near San Juan (T. L. Youd, M)
- South Carolina, microearthquake studies (A. C. Tarr, D)

Earthquake studies—Continued
- *States and territories—Continued*
- Utah:
  - Soil dating of faulting, Wasatch Front (R. R. Shroba, D)
  - Wasatch Front geology (R. D. Miller, D)
- Washington (M):
  - Earthquake hazards, Puget Sound region (J. C. Yount, P. D. Snavely, Jr.)
  - Hanford microearthquake studies (J. H. Pfluke)

Ecology:
- Estuarine plankton dynamics (J. E. Cloern, w, M)

Engineering geologic studies. *See* Construction and terrain problems; Urban geology.

Environmental assessment:
- Analysis of digitized maps of NASQAN water basins (K. J. Lanfear, o, NC)
- Analysis of alternative and synthetic fuel development (P. F. Narton, C. T. Schoen, L. A. Yost IV, o, NC)
- Chaco Energy Company, Star Lake Mine environmental impact statement (C. M. Albrecht, o, D)
- Comparative study of change and disorganization in energy development communities of the Great Plains (R. R. Reynolds, Jr., o, NC)
- Guidance and training for NEPA compliance (J. R. Burns, o, NC)
- Holocene climatic trends with respect to atmospheric changes in CO_2 concentrations (C. Larsen; D. Hoglund, o, NC)
- Ideal Basic Industries, LaVentana Mine environmental impact statement (M. Busby, o. D)
- Improvement in analyzing impacts in environmental impact statements (P. Cheney; D. Schleicher, o, D)
- Kerr-McGee East Gillette mine (W. G. Weist, Jr., l, D)
- Mobil Oil Company Rojo Caballos coal mining (L. G. Marcus, o, NC)
- Mode of deformation of Rosebud coal, Colstrip, Montana—Room temperature, 102.0, MPa (J. M. White, c, Billings)
- Northern Coal Company, Meeker area mines environmental impact statement (C. M. Albrecht, o, D)
- North Fork of the Gunnison River regional environmental baseline study, Colorado (C. M. Albrecht, o, D)
- Off-site movement of radioactive materials, La Bajada mine, New Mexico (P. F. Narten, E. L. Meyer, o, NC)
- Oilspill trajectory analysis (K. J. Lanfear, o, NC)
- Physical effects of off-road vehicles (H. G. Wilshire and J. K. Nakata, M)
- Powder River Basin, uranium (E. S. Santos, D)
- Reclamation potentials for western coal mines (P. F. Narten, o, NC)
- Review of environmental impact statements (L. D. Bonham, o, NC)
- Social disruption and rapid community growth and examination of the western "boomtown" hypotheses (R. R. Reynolds, o, NC)
- South Florida environment (B. F. McPherson, w, Miami)
- Supplemental socioeconomic assessment of the East Gillette mine and a socioeconomic assessment of the North Antelope mine (R. Reynolds, Jr., o, NC)
- Tracking of environmental laws and regulations (H. C. McWreath, o, NC)
- Volatile elements from natural coal burning (J. R. Herring, D)

Environmental geology:
- Quaternary dating applications—overview map (K. L. Pierce, D)
- *States:*
- Alaska:
  - Peterburg quadrangle (D. A. Brew, M)
  - Regional engineering geology of Cook Inlet coal lands (H. R. Schmoll and L. A. Yehle, D)
- Montana, Land resources, Helena region (R. G. Schmidt, NC; G. D. Robinson, M)
- Utah:
  - Cedar City 2° quadrangle (K. A. Sargent, D)
  - Central Utah energy lands (I. J. Witkind, D)
  - Kaiparowits Plateau coal basin (K. A. Sargent, D)
- Wyoming:
  - Bighorn Basin (R. M. Barker, NC)
  - Hams Fork coal basin (A. B. Gibbons, D)
- *See also* Construction and terrain problems; Land use and environmental impact; Urban geology.

Evapotranspiration:
- Evaporation, Colorado lakes (N. E. Spahr, w, D)
- Evapotranspiration data analyses (T. E. A. van Hylckama, w, Lubbock, Tex.)
- Mechanics of evaporation (G. E. Koberg, w, D)
- Pecos evapotranspiration studies (E. P. Weeks, w, D)
- Vegetation ecohydrology (R. M. Turner, w, Tucson, Ariz.)

Extraterrestrial studies:
- Lunar analog studies, explosion craters (D. J. Roddy, Flagstaff, Ariz.)
- Lunar data synthesis:
  - Imbrium and Serenitatis Basins (J. F. McCauley, Flagstaff, Ariz.)
  - Synoptic lunar geology (D. E. Wilhelms, M)
- Lunar microwave (G. R. Olhoeft, Denver)
- Lunar sample investigations:
  - Chemical and X-ray fluorescence analysis (H. J. Rose, Jr., NC)
  - Lunar igneous-textured rocks (O. B. James, NC)
  - Major lunar breccia types (E. C. T. Chao, NC)
  - Mineralogical analyses (R. B. Finkelman, NC)
  - Oxygen fugacities and crystallization sequence (Motoaki Sato, NC)
  - Petrologic studies (Edwin Roedder, NC)
  - Pyroxenes (J. S. Huebner, NC)
- Planetary analog studies, mass movements (E. C. Morris, Flagstaff, Ariz.)
- Planetary investigations:
  - Geologic mapping of Mars (D. H. Scott, J. F. McCauley, Flagstaff, Ariz.)
  - Geologic synthesis of Mars (Harold Masursky, Flagstaff, Ariz.)
  - Image-processing studies (L. A. Soderblom, Flagstaff, Ariz.)
  - Mariner Jupiter-Saturn (L. A. Soderblom, Flagstaff, Ariz.)
  - Mariner Venus-Mercury TV (N. J. Trask, NC)
  - Mars mineralogy and chemistry, Viking lander (Priestley Toulmin III, H. J. Rose, Jr., NC)
  - Mars topographic synthesis (S. S. C. Wu, Flagstaff, Ariz.)
  - Planetary cartography (R. M. Batson, Flagstaff, Ariz.)
  - Radar applications (G. G. Schaber, Flagstaff, Ariz.)
  - Viking mission:
    - Lander (E. C. Morris, Flagstaff, Ariz.)
    - Orbiter TV (M. H. Carr, M)
    - Physical properties of Mars (H. J. Moore, M)
    - Site analysis (Harold Masursky, Flagstaff, Ariz.)

Ferro-alloy metals:
- Chromium:
  - Geochemistry (B. A. Morgan III, NC)
  - Resource studies (T. P. Thayer, NC)
- Molybdenum-rhenium resource studies (R. U. King, D)
- *States:*
- North Carolina, Tungsten in Hamme district (J. E. Gair, NC)
- Oregon, John Day area (T. P. Thayer, NC)
- Pennsylvania, State Line district (B. A. Morgan III, NC)

Flood-hazard mapping:
- Alabama (C. O. Ming, w, Montgomery)
- Arkansas (R. C. Gilstrap, w, Little Rock)
- California (J. R. Crippen, w, M)
- Colorado (T. R. Dosch, w, D)
- Connecticut (M. A. Cervione, Jr., w, Hartford)
- Georgia (P. McGlone, w, Atlanta)
- Idaho (W. A. Harenberg, w, Boise)
- Indiana (J. B. Swing, w, Indianapolis)
- Iowa (O. G. Lara, w, Iowa City)
- Kansas (D. B. Richards, w, Lawrence)
- Kentucky (C. H. Hannum, w, Louisville)
- Louisiana (A. S. Lowe, w, Baton Rouge)
- Maine (R. A. Morrill, w, Augusta)
- Michigan (R. L. Knutilla, w, Lansing)
- Minnesota (G. H. Carlson, w, St. Paul)
- Montana (R. J. Omang, w. Helena)
- North Dakota (O. A. Crosby, w, Bismarck)
- Ohio (D. K. Roth, w, Columbus)
- Pennsylvania (Andrew Voytik, w, Harrisburg)
- Puerto Rico (C. B. Bentley w, San Juan)
- South Carolina (W. T. Utter, w, Columbia)
- South Dakota (H. L. Dixson, w, Huron)
- Texas (E. E. Schroeder, w, Austin)
- United States (G. W. Edelen, w, NC)
- Washington (C. H. Swift, w, Tacoma)
- West Virginia (G. S. Runner, w, Charleston)
- Wisconsin (C. L. Lawrence, w, Madison)

Flood-insurance studies:
- Arizona (P. L. Stiehr, w, Tucson)
- Connecticut (M. A. Cervione, Jr., w, Hartford)
- Florida (S. D. Leach, w, Tallahassee)
- Illinois (G. W. Curtis, w, Champaign)
- Kansas (K. D. Medina, w, Lawrence)
- Louisiana (G. J. Wiche, w, Baton Rouge)
- Minnesota (G. H. Carlson, w, St. Paul)
- Montana (R. J. Omang, w, Helena)
- Nevada (R. R. Squires, w, Carson City)
- New Jersey (R. D. Schopp, w, Trenton)
- New Mexico (L. P. Denis w, Albuquerque)
- New York (R. T. Mycyk, w, Albany)
- Oregon (D. D. Harris, w, Portland)
- Puerto Rico (K. S. Johnson, w, San Juan)
- United States (E. J. Kennedy, w, NC)
- Virginia (E. H. Mohler, w, Fairfax)
- Washington (C. H. Swift, w, Tacoma)

Flood investigations:
- Dating infrequent floods (R. A. Sigafoos, w, NC)
- Documentation of extreme floods (H. H. Barnes, Jr., w, NC)
- Floods Big Sandy-Tug Fork (A. G. Scott, w, NC)
- Flow frequency analysis (W. O. Thomas, w, NC)
- Hydraulics laboratory studies (V. R. Schneider, w, Bay St. Louis, Miss.)
- Nationwide flood-frequency (A. G. Scott, w, NC)
- Stream channel behavior (J. C. Brice, w. M)

Flood investigations—Continued
States and territories:
Alabama, Flood studies (C. O. Ming, w, Montgomery)
Arkansas (T. E. Lamb, w, Little Rock)
Arizona:
Flood-warning network (F. C. Boner, w, Tucson)
1977–78 flood report (B. N. Aldridge, w, Tucson)
1978–79 flood report (B. N. Aldridge, w, Tucson)
California:
Flood hydrology, Butte basin (J. C. Blodgett, w, Sacramento)
Floods-small drainage areas (A. O. Waananen, w, M)
Hydraulic studies at bridge sites (J. C. Blodgett, w, Sacramento)
Park and monument flood risk (J. R. Crippen, w, M)
Colorado (w, D):
Floods, Elbert County (T. R. Dosch)
Foothill floods (R. D. Jarrett)
Connecticut, Small stream flood characteristics (L. A. Weiss, w, Hartford)
Florida (w, Tampa):
Flood assessment (W. C. Bridges, w, Tallahassee)
Regional lake stage evaluation (R. F. Giovannelli, w, Tampa)
Georgia:
Atlanta flood characteristics (E. J. Inman, w, Doraville)
Flood and bridge site studies (McGlone Price, w, Doraville)
Urban flood-frequency (E. J. Inman, w, Doraville)
Hawaii, Special flood-data collection (R. H. Nakahara, w, Honolulu)
Idaho (W. A. Harenburg, w, Boise)
Illinois, Urban floods in northeastern Illinois (H. E. Allen, Jr., w, Dekalb)
Indiana, Flood frequency (R. L. Gold, w, Indianapolis)
Iowa (w, Iowa City):
Flood data for selected bridge sites (O. G. Lara)
Flood profiles, of Iowa streams (O. G. Lara)
Kentucky (w, Louisville):
Floods, Big Sandy-Tug Fork (C. E. Schoppenhorst, w, Louisville)
Flood studies—statewide (L. E. Schoppenhorst)
Small-area flood hydrology (C. E. Schoppenhorst, w, Louisville)
Louisiana, Roughness coefficients (G. J. Arcement, w, Baton Rouge)
Maryland, Floods—small drainage areas (D. H. Carpenter, w, Towson)
Minnesota:
Flood-plain coordination (G. H. Carlson, w, St. Paul)
1979 flood—Red River (D. W. Ericson, w, Grand Rapids)
Mississippi:
Flood, April 1979, Pearl River, (L. E. Carroon, w, Jackson)
Multiple-bridge hydraulics (B. E. Colson, w, Jackson)
Montana:
Willow Creek modeling (C. Parrett, w, Helena)
Nevada (w, Carson City):
Environmental study (P. A. Glancy)
Flood investigations (R. R. Squires)
New Jersey:
Flood peaks and flood plains (R. O. Schopp, w, Trenton)
Somerset County (J. B. Campbell, w, Trenton)
New Mexico, Flood analysis (R. P. Thomas, w, Santa Fe)

Flood investigations—Continued
States and territories—Continued
New York:
Flood investigations (T. J. Zembrzuski, w, Albany)
Schoharie Creek runoff-rainfall model (T. J. Zembrzuski, w, Albany)
North Dakota:
Red River hydrologic response (J. E. Miller, w, Bismarck)
Oklahoma:
Flood mapping of Cherokee lands (T. L. Huntzinger, w, Oklahoma City)
Small watersheds (T. J. Huntzinger, Jr., w, Oklahoma City)
Pennsylvania, Bridge waterways analysis (J. O. Shearman, w, Harrisburg)
Puerto Rico:
Eloise floods (K. G. Johnson, w, San Juan)
St. Croix flood of October 7–8, 1977 (K. G. Johnson, w, San Juan)
South Carolina:
Hydraulic site reports (B. H. Whetstone) w, Columbia)
Savannah streamflow simulation (G. E. Lonon, w, Columbia)
Tennessee (W. J. Randolph, w, Nashville)
Virginia:
Floods in Tug Fork (P. M. Frye, w, Richmond)
Hydrology, Wytheville fish hatchery (J. R. Hendrick, w, Marion)
Statewide (B. J. Prugh, w, Richmond)
Washington:
Flood profiles (J. E. Cummans, w, Tacoma)
St. Helens monitoring (E. H. McGavock, w, Tacoma)
West Virginia:
Floods in Tug Fork (R. L. Bragg, w, Charleston)
Wisconsin (w, Madison):
Digital model-flood flow Rock River (W. R. Krug, w, Madison)
Flood-control effects on Trout Creek (D. A. Wentz)
Flood documentation in Wisconsin (P. E. Hughes)
Flood-frequency, urban and rural (D. H. Conger, w, Madison)
St. Croix scenic river waste study (C. L. Laurence)
Wyoming, Flood investigations (G. S. Craig, w, Cheyenne)

Fluorspar:
Cenozoic lacustrine deposits of the United States (R. A. Sheppard, D)
Colorado, Bonanza and Poncha Springs quadrangles (R. E. Van Alstine, NC)
Illinois-Kentucky district, regional structure and ore controls (D. M. Pinckney, D)

Foreign nations, geologic investigations:
Africa, Advisory services relative to facilities for reception and processing of satellite data for earth resources information, West Africa remote sensing center, Ouagadougou (S. R. Addess)
Brazil, Mineral, resources and geologic training (S. A. Stanin, Rio de Janeiro)
Burma, Technical assistance in offshore tin deposits (M. Cruikshank)
China, People's Republic of:
Cooperative studies in earth sciences (M. J. Terman)
Cooperative earthquake studies (R. M. Stewart)
Egypt, Mineral resources exploration methods and map production techniques; technology transfer (R. W. Schaff, Cairo)

Geochemistry and petrology, field studies—Continued
- Western coal regions:
  - Geochemical survey of rocks (R. J. Ebens, D)
  - Geochemical survey of soils (R. R. Tidball, D)
  - Geochemical survey of vegetation (J. A. Erdman, D)
  - Geochemistry of clinker (J. R. Herring, D)
- Western energy regions:
  - Element availability—plants (L. P. Gough, D)
  - Element availability—rocks (J. M. McNeal, D)
  - Element availability—soils (R. C. Severson, D)
  - Geochemistry of clinker (J. R. Herring, D)
- *States:*
- Alaska (M):
  - La Perouse layered intrusion (R. A. Loney)
  - Metasedimentary and metaigneous rocks, southwestern Brooks Range (I. L. Tailleur)
  - Petersburg quadrangle (D. A. Brew)
  - Petrographic studies, Yukon-Tanana Upland (C. Dusel-Bacon)
- Arizona (M):
  - Ray program:
    - Mineral Mountain (T. G. Theodore)
    - Silicate mineralogy, geochemistry (N. G. Banks)
  - Stocks (S. C. Creasey)
- California:
  - Geochemistry of sediments, San Francisco Bay (D. S. McCulloch, M)
  - Granitic rocks of Yosemite National Park (D. L. Peck, NC)
  - Kings Canyon National Park (J. G. Moore, M)
  - Long Valley Caldera-Mono Craters volcanic rocks (R. A. Bailey, NC)
  - Sierra Nevada xenoliths (J. P. Lockwood, M)
- Colorado:
  - Geochemistry of clinker (J. R. Herring, D)
  - Petrology of Mt. Princeton igneous complex (Priestley Toulmin III, NC)
  - Tertiary-Laramide intrusives (E. J. Young, D)
- Hawaii, Ankaramites (M. H. Beeson, M)
- Idaho, Wood River district (W. E. Hall, M)
- Montana:
  - Diatremes, Missouri River Breaks (B. C. Hearn, Jr., NC)
  - Geochemistry of clinker (J. R. Herring, D)
  - Geochronology, north-central Montana (B. C. Hearn, Jr., NC; R. F. Marvin, R. E. Zartman, D)
  - Pioneer batholith (E-an Zen; J. M. Hammarstrom, NC)
  - Wolf Creek area, petrology (R. G. Schmidt, NC)
- Nevada, Igneous rocks and related ore deposits (M. L. Silberman, M)
- New Mexico, Geochemistry of clinker (J. R. Herring, D)
- Pennsylvania, Geochemistry of Pittsburgh urban area (H. A. Tourtelot, D)
- South Dakota, Keystone pegmatite area (J. J. Norton, Rapid City)
- Wyoming, Geochemistry of clinker (J. R. Herring, D)

Geochronological investigations:
- Archean terranes in the Wyoming age province and in the Lake Superior region (Z. E. Peterman, D)
- Carbon-14 method (Meyer Rubin, NC)
- Geochronology and rock magnetism (G. B. Dalrymple, M)
- Geochronology of uranium ores and their host rocks (K. R. Ludig, D)
- Geothermal (M. A. Lanphere, M)
- Igneous rocks and deformational periods (R. W. Kistler, M)
- Lead-uranium, lead-thorium, and lead-alpha methods (T. W. Stern, NC)

Geochronological investigations—Continued
- Magnetic chronology, Colorado Plateau and environs (D. P. Elston, E. M. Shoemaker, Flagstaff, Ariz.)
- Quaternary dating techniques, numerical and relative-age (K. L. Pierce, D)
- Radioactive-disequilibrium studies (J. N. Rosholt, D)
- San Francisco volcanic field (P. E. Damon, University of Arizona)
- *States:*
- Alaska, K-Ar dates, southwest Brooks Range (I. L. Tailleur, M; R. B. Forbes, D. L. Turner, Fairbanks)
- Colorado, Geochronology of Denver area (C. E. Hedge, D)
- *See also* Isotope and nuclear studies.

Geologic mapping:
- Map scale smaller than 1:62,500:
  - Antarctica, Dufek Massif and Forrestal Range, Pensacola Mountains (A. B. Ford, M)
  - Belt basin study (J. E. Harrison, D)
  - Columbia River basalt (D. A. Swanson, M)
  - Engineering geology map of the U.S. (D. H. Radbruch-Hall, M)
  - Ouachita Mountains, Arkansas-Oklahoma (B. R. Haley, Little Rock, Ark.)
  - *States:*
  - Alaska (M):
    - Ambler River and Baird Mountains quadrangles (I. L. Tailleur)
    - Charley River quadrangle (E. E. Brabb)
    - Circle quadrangle (H. L. Foster; F. R. Weber)
    - Craig quadrangle (G. D. Eberlein, Michael Churkin, Jr.)
    - Delong Mountains quadrangle (I. L. Tailleur)
    - Geologic map (H. M. Beikman)
    - Glacier Bay National Monument (D. A. Brew)
    - Hughes-Shungnak area (W. W. Patton, Jr.)
    - Iliamna quadrangle (R. L. Detterman)
    - Juneau and Taku River quadrangles (D. A. Brew)
    - Metamorphic facies map (D. A. Brew)
    - Natural landmarks investigation (R. L. Detterman)
    - Petersburg quadrangle (D. A. Brew)
    - St. Lawrence Island (W. W. Patton, Jr.)
    - Yukon-Tanana Upland (H. L. Foster, F. R. Weber; Cynthia Dusel-Bacon)
  - Arizona (Flagstaff):
    - North-central part (D. P. Elston)
    - Phoenix 2° quadrangle (T. N. V. Karlstrom)
  - California:
    - Tectonic studies, Great Valley area (J. A. Bartow, D. E. Marchand)
    - Yosemite National Park (N. K. Huber)
  - Colorado (D):
    - Colorado Plateau geologic map (D. D. Haynes)
    - Denver 2° quadrangle (B. H. Bryant)
    - Geologic map (O. L. Tweto)
    - Greeley 2° quadrangle, western half (W. A. Braddock)
    - Leadville 2° quadrangle (O. L. Tweto)
    - Neotectonic map of Colorado (S. M. Colman)
    - Pueblo 2° quadrangle (G. R. Scott)
    - Sterling 2° quadrangle (G. R. Scott)
  - Connecticut, Cooperative mapping program (J. P. Schafer, NC)
  - Idaho (D):
    - Challis Volcanics (D. H. McIntyre)
    - Dubois 2° quadrangle (M. H. Hait and B. A. Skipp)
    - Idaho Falls 2° quadrangle (M. A. Kuntz)

Geologic mapping—Continued
Map scale smaller than 1:62,500—Continued
States—Continued
Idaho—Continued
Preston 2° quadrangle (S. S. Oriel)
Snake River Plain, central part, volcanic petrology (H. E. Malde)
Snake River Plain region, eastern part (S. S. Oriel)
Missouri, Rolla 2° quadrangle, mineral-resource appraisal (W. P. Pratt, D)
Montana, White Sulphur Springs 2° quadrangle (M. W. Reynolds, D)
Nevada:
Elko County:
Central (K. B. Ketner, D)
Countywide (R. A. Hope, M)
Western (R. R. Coats, M)
Geologic map (J. H. Stewart, M)
New Jersey, Pennsylvania, New York, Newark 2° quadrangle (A. A. Drake, Jr., NC)
New Mexico (D):
Neotectonic map of New Mexico M. N. Machette)
Neotectonic map of the Rio Grande Rift (M. N. Machete)
North Church Rock area (A. R. Kirk)
Sanostee (A. C. Huffman, Jr.)
Santa Fe 2° quadrangle, western half (E. H. Baltz, Jr.)
Socorro 2° quadrangle, (G. O. Bachman)
Tusas Mountains (Kim Manley)
North Carolina, Charlotte 2° sheet (Richard Goldsmith, NC)
South Carolina, Charlotte 2° sheet (Richard Goldsmith, NC)
South Carolina, Georgia, North Carolina, Greenville 2° quadrangle (A. E. Nelson, NC)
Utah (M), except as otherwise noted:
Delta 2° quadrangle (H. T. Morris)
Price 2° quadrangle (I. J. Witkind)
Richfield 2° quadrangle (T. A. Steven, P. D. Rowley)
Tooele 2° quadrangle (W. J. Moore)
Wasatch Front surficial geology (R. D. Miller, D)
Wasatch-Uinta Tectonics, Salt Lake City and Ogden 2° quadrangles (B. H. Bryant, D)
Washington, Wenatchee 2° sheet (R. W. Tabor, R. B. Waitt, Jr., V. A. Frizzell, Jr., M)
Washington, Idaho, and Montana, Sandpoint 2° sheet (F. K. Miller)
Washington-Oregon, NW Olympic land-sea transect (P. D. Snavely, Jr., M)
Wyoming:
Geologic map (J. D. Love, Laramie)
Preston 2° quadrangle (S. S. Oriel, D)
Wasatch-Uinta Tectonics, Ogden 2° quadrangle (B. H. Bryant, D)
Teton Wilderness (J. D. Love, Laramie)
Map scale 1:62,500 and larger:
States and territories:
Alaska:
Anatuvuk Pass (G. B. Shearer, c, Anchorage)
Anchorage area (H. R. Schnioll, D)
Bering River coal field (R. B. Sanders, c, Anchorage)
Geology and mineral resources of the Ketchikan quadrangle (H. C. Berg, M)
Nelchina area, Mesozoic investigations (Arthur Grantz, M)

Geologic mapping—Continued
Map scale 1:62,500 and larger—Continued
States and territories—Continued
Alaska—Continued
Nenana coal investigations (Clyde Wahrhaftig, M)
Nome area (C. L. Hummel, M)
Regional engineering geology of Cook Inlet coal lands (H. R. Schmoll and L. A. Yehle, D)
West Chichagof-Yakobi Islands (B. R. Johnson, M)
Yukon-Tanana Upland (F. R. Weber)
Arizona:
Bagdad, vicinity of Old Dick and Bruce mines (C. M. Conway, M)
Cumminge Mesas quadrangle (Fred Peterson, D)
Hackberry Mountain area (D. P. Elston, Flagstaff)
Mazatzal Wilderness (C. M. Conway and C. T. Wrucke, M)
Mt. Wrightson quadrangle (H. D. Drewes, D)
Ray district, porphyry copper (H. R. Cornwall, M)
Sedona area (D. P. Elston, Flagetaff)
Western Arizona, tectonic studies (Ivo Lucchitta, Flagetaff)
California (M, except as otherwise noted):
Coast Range, ultramafic rocks (E. H. Bailey)
Condrey Mountain and Hornbrook quadrangles (P. E. Hotz)
Elk Creek-Black Butte areas (R. J. McLaughlin)
El Paso Mountains and Pilot Knob Valley areas (M. D. Carr)
King Range-Chemise area (R. J. McLaughlin)
California (M, except as otherwise noted)—Continued
Long Valley caldera (R. A. Bailey, NC)
Merced Peak quadrangle (D. L. Peck, NC)
Northern Coast Ranges (K. F. Fox, Jr.)
Pacific Palisades landslide area, Los Angeles (J. T. McGill, D)
Palo Alto, San Mateo, and Montara Mountain quadrangles (E. H. Pampeyan)
Peninsular Ranges (V. R. Todd, La Jolla)
Regional fault studies (E. J. Helley, D. G. Herd, B. F. Atwater)
Ryan quadrangle (J. F. McAllister)
Santa Lucia Range (V. M. Seiders)
Searles Lake area (G. I. Smith)
Sierra Nevada batholith (P. C. Bateman)
The Geysers-Clear Lake area (R. J. McLaughlin)
Western Santa Monica Mountains (R. H. Campbell)
Colorado (D, except as otherwise noted):
Barcus Creek quadrangle (W. J. Hail)
Barcus Creek SE quadrangle (W. J. Hail)
Bonanza quadrangle (R. E. Van Alstine, NC)
Central City area (R. B. Taylor)
Citadel Plateau (G. A. Izett)
Coal mine deformation studies, Somerset mining district (C. R. Dunrud)
Cochetopa area (J. C. Olson)
Denver metropolitan area (R. M. Lindvall)
Desert Gulch quadrangle (R. C. Johnson)
Disappointment Valley, geology and coal resources (D. E. Ward)
Middle Dry Fork quadrangle (R. C. Johnson)
Northern Park Range (G. L. Snyder)
Poncha Springs quadrangle (R. E. Van Alstine, NC)
Rocky Mountain National Park (W. A. Braddock)
Rustic quadrangle (K. L. Shaver)
Ward and Gold Hill quadrangles (D. J. Gable)

Geologic mapping—Continued
Map scale 1:62,500 and larger—Continued
States and territories—Continued
Connecticut, Cooperative mapping program (J. P. Schafer, NC)
Georgia, Macon-Gordon district (S. H. Patterson, NC)
Idaho (D, except as otherwise noted):
Bayhorse area (S. W. Hobbs)
Black Pine Mountains (J. F. Smith, Jr.)
Boulder Mountains (C. M. Tschanz)
Goat Mountain quadrangle (M. H. Staatz)
Grouse quadrangle (B. A. Skipp)
Hawley Mountain quadrangle (W. J. Mapel)
Malad SE quadrangle (S. S. Oriel)
Montour quadrangle (H. E. Malde)
Patterson quadrangle (E. T. Ruppel)
Strevell quadrangle (J. F. Smith)
Wood River district (W. E. Hall, M)
Yellow Pine quadrangle (B. F. Leonard)
Kentucky, Cooperative mapping program (E. R. Cressman, Lexington)
Maine:
Blue Hill quadrangle (D. B. Stewart, NC)
Castine quadrangle (D. B. Stewart, NC)
Orland quadrangle (D. R. Wones, NC)
Rumford quadrangle (R. H. Moench, D)
The Forks quadrangle (F. C. Canney, D)
Maryland (NC):
Delmarva Peninsula (J. P. Owens)
Northern Coastal Plain (J. P. Minard)
Western Maryland Piedmont (M. W. Higgins)
Massachusetts:
Boston and vicinity (C. A. Kaye, Boston)
Cooperative mapping program (J. O. Peper, NC)
Michigan, Gogebic Range, western part (R. G. Schmidt, NC)
Minnesota, Vermilion greenstone belt (P. K. Sims, D)
Montana:
Cooke City quadrangle (J. E. Elliott, D)
Craig quadrangle (R. G. Schmidt, NC)
Crazy Mountains Basin (B. A. Skipp, D)
Elk Park quadrangle (H. W. Smedes, D)
Lemhi Pass quadrangle (M. H. Staatz, D)
Melrose quadrangle (H. W. Smedes and G. D. Fraser, D)
Northern Pioneer Range, geologic environment (E-an Zen, NC)
Wolf Creck area, petrology (R. G. Schmidt, NC)
Nebraska, McCook 2° quadrangle (G. E. Prichard, D)
Nevada:
Austin quadrangle (E. H. McKee, M)
Bellevue Peak quadrangle (T. B. Nolan, NC)
Carlin region (J. F. Smith, Jr., D)
Jordan Meadow and Disaster Peak quadrangles (R. C. Greene, M)
Kobeh Valley (T. B. Nolan, NC)
Midas-Jarbridge area (R. R. Coats, M)
Round Mountain and Manhattan quadrangles (D. R. Shawe, D)
New Mexico:
Acoma area (C. H. Maxwell, D)
Alma quadrangle (J. C. Rattë, D)
Bull Basin quadrangle (J. C. Rattë, D)
Church Rock-Smith Lake (C. T. Pierson, D)
Cretaceous stratigraphy, San Juan Basin (E. R. Landis, D)

Geologic mapping—Continued
Map scale 1:62,500 and larger—Continued
States and territories—Continued
New Mexico—Continued
Dillon Mountain quadrangle (J. C. Rattë, D)
Glenwood quadrangle (J. C. Rattë, D)
Hillsboro quadrangle (D. C. Hedlund, D)
Holt Mountain quadrangle (J. C. Rattë, D)
Iron Mountain (A. V. Heyl, Jr., D)
Laguna Peak (J. L. Ridgley, D)
Manzano Mountains (D. A. Myers, D)
Mongollon quadrangle (J. C. Rattë, D)
O-Block Canyon quadrangle (J. C. Rattë, D)
Pinos Altos Range (T. L. Finnell, D)
Raton coal basin, western part (C. L. Pillmore, D)
Reserve quadrangle (J. C. Rattë, D)
Saliz Pass quadrangle (J. C. Rattë, D)
Tusas Mountains (Kim Manley, D)
Valles Mountains, petrology (R. L. Smith, NC)
New York, Geologic correlations and mineral resources in Precambrian rocks of St. Lawrence lowlands (C. E. Brown, NC)
North Carolina, Central Piedmont (A. A. Stromquist, D)
Pennsylvania (NC):
Northern anthracite field (M. J. Bergin)
Southern anthracite field (G. H. Wood, Jr.)
Wind Gap and adjacent quadrangles (J. B. Epstein)
Puerto Rico (R. D. Krushensky, NC)
South Dakota:
Black Hills Precambrian (J. A. Redden, Hill City)
Keystone pegmatite area (J. J. Norton, Rapid City)
Medicine Mountain quadrangle (J. C. Rattë, D)
Texas:
Agency Draw NE quadrangle (G. N. Pipiringos, D)
Bates Knolls quadrangle (G. N. Pipiringos, D)
Tilden-Loma Alta area (K. A. Dickinson, D)
Utah (c, D, unless otherwise noted):
Basin Canyon quadrangle (Fred Peterson)
Blackburn Canyon quadrangle (Fred Peterson)
Confusion Range (R. K. Hose, M)
Matlin Mountains (V. R. Todd, M)
Ogden 4 NW quadrangle (R. J. Hite)
Redmond quadrangle (I. J. Witkind)
Salt Lake City and vicinity (Richard VanHorn, D)
Sheeprock Mountains, West Tintic district (H. T. Morris, M)
Sunset Flat quadrangle (Fred Peterson)
Wah Wah Summit quadrangle (L. F. Hintze, Salt Lake City)
Wasatch Front surficial geology (R. D. Miller, D)
Willard Peak area (M. D. Crittenden, Jr., M)
Virginia (NC):
Culpeper Basin (K. Y. Lee)
Delmarva Peninsula (J. P. Owens)
Northern Blue Ridge (G. H. Espenshade)
Rapidan-Rappahannock (Louis Pavlides)
Rose Land district (Norman Herz; E. R. Force)
Washington:
Glacier Park area (F. W. Cater, Jr., D)
Northern Okanogan Highlands (C. D. Rinehart, M)
Olympic Peninsula, eastern part (W. M. Cady, D)
Togo Mountain quadrangle (R. C. Pearson, D)
Wisconsin, Black River Falls and Hatfield quadrangles (Harry Klemic, NC)
Wyoming (c, D, unless otherwise noted):
Albany and Keystone quadrangles (M. E. McCallum, D)
Alkali Butte quadrangle (M. W. Reynolds, D)

Geologic mapping—Continued
Map scale 1:62,500 and larger—Continued
States and territories—Continued
Wyoming—Continued
Badwater Creek (R. E. Thaden, D)
Banner quadrangle (E. N. Hinrichs, D)
Devils Tooth quadrangle (W. G. Pierce, M)
Eagle Peak quadrangle (H. W. Smedes and H. J. Prostka, D)
Fortin Draw quadrangle (B. E. Law)
Gillette East quadrangle (B. E. Law)
Grand Teton National Park (J. D. Love, Laramie)
Gros Ventre Range (F. S. Simons)
Moyer Springs quadrangle (B. E. Law)
Oriva quadrangle (B. E. Law)
Story quadrangle (E. N. Hinrichs, D)
Two Ocean Pass quadrangle (H. W. Smedes, D)
Wapiti quadrangle (W. G. Pierce, M)

Geologic-related hazards:
Hazards warning, preparedness, and technical assistance (J. C. Stephens, o, NC)
Techniques for reducing landslide hazards (D. Erley; W. J. Kockelman, M)

Geomagnetism:
External geomagnetic-field variations (W. H. Campbell, D)
Geomagnetic-data analysis (C. O. Stearns, D)
Geomagnetic observatories (J. D. Wood, D)
Geomagnetic secular variation (L. R. Alldredge, D)
Magnetic-field analysis and U.S. charts (E. B. Fabiano, D)
World magnetic charts and analysis (E. B. Fabiano, D)

Geomorphology:
Morphology, provenance, and movement of desert sand (E. D. McKee, D)
Quaternary landforms and deposits interpreted from Landsat 1 imagery, Midwest and Great Plains (R. B. Morrison, D)
Surface processes in arid lands (H. G. Wilshire, M)
States:
Arizona, Post-1890 A.D. erosion features interpreted from Landsat 1 imagery (R. B. Morrison, D)
Colorado, Hydraulics of stream channels (E. D. Andrews, w, D)
Florida, Geohydrology of sinkholes (W. C. Sinclair, w, Tampa)
Idaho, Surficial geology of eastern Snake River Plain (W. E. Scott, M. D. Hait, Jr., D)
New Mexico, Chaco Canyon National Monument (H. E. Malde, D)
Utah, Quaternary geology (W. E. Scott, D)
Wyoming (D):
Wind River Mountains, Quaternary geology (G. M. Richmond)
Yellowstone National Park, glacial and postglacial geology (G. M. Richmond)
See also Sedimentology; Geochronological investigations.

Geophysics, regional:
Airborne and satellite research:
Aeromagnetic studies (M. F. Kane, D)
Electromagnetic research (F. C. Frischknecht, D)
Gamma-ray research (J. S. Duval, D)
Regional studies (Isidore Zietz, NC)
Antarctic, Pensacola Mountains, geophysical studies (J. C. Behrendt, Woods Hole, Mass.)
Basin and Range geophysical studies (W. E. Davis, M)
Crust and upper mantle:
Aeromagnetic interpretation of metamorphic rocks (Isidore Zietz, NC)

Geophysics, regional—Continued
Aeromagnetic studies of the United States (Isidore Zietz, NC)
Analysis of traveltime data (J. C. Roller, M)
Seismicity and Earth structure (J. N. Taggart, D)
Seismologic studies (J. P. Eaton, M)
Engineering geophysics (H. D. Ackermann, D)
Florida Continental Shelf, gravity studies (H. L. Krivoy, NC)
Gravity surveys:
Maryland cooperative (D. L. Daniels, NC)
Ground-water geophysics (W. D. Stanley, D)
Magnetic chronology, Colorado Plateau and environs (D. P. Elston, E. M. Shoemaker, Flagstaff, Ariz.)
Mobile magnetometer profiles, Eastern United States (M. F. Kane, D)
New England, magnetic properties of rocks (Andrew Griscom, M)
Program and systems development (G. I. Evenden, W. L. Anderson, D)
Rainier Mesa (J. R. Ege)
Rocky Mountains, northern (D. L. Peterson, M. D. Kleinkopf, D)
Southeastern States geophysical studies (Peter Popenoe, NC)
Southwestern States geophysical studies (D. L. Peterson, NC)
Thermal modeling investigations (Kenneth Watson, D)
Ultramafic rocks, geophysical studies, intrusions (G. A. Thompson, M)
United States, aeromagnetic surveys (E. R. King, NC)
States and territories:
Alaska:
Ambler River and Baird Mountains quadrangles, gravity studies (D. F. Barnes, M)
Gravity and magnetic interpretations (J. W. Cady. D)
Uranium geophysics (J. W. Cady, D)
California, Sierra Nevada, geophysical studies (H. W. Oliver, M)
Idaho, Snake River Plain (D. L. Peterson, D)
Massachusetts, Geophysical studies (M. F. Kane, NC)
Minnesota (NC):
Keweenawan rocks, magnetic studies (K. G. Books)
Southern part, aeromagnetic survey (E. R. King)
Nevada, Engineering geophysics, Nevada Test Site (R. D. Carroll, D)
New Mexico, Rio Grande graben (L. E. Cordell, D)
Pennsylvania, Magnetic properties of rocks (Andrew Griscom, M)
Puerto Rico, Seismicity of Puerto Rico (A. C. Tarr, D)

Geophysics, theoretical and experimental:
Borehole electrical techniques in uranium exploration (J. J. Daniels, D)
Borehole geophysical research in uranium exploration (J. H. Scott, D)
Earthquakes, local seismic studies (J. P. Eaton, M)
Elastic and inelastic properties of Earth materials (Louis Peselnick, M)
Electrical properties of rocks (R. D. Carroll, D)
Electrical resistivity studies (A. A. R. Zohdy, D)
ERDA/DOE geothermal petrophysics (G. R. Olhoeft, D)
Experimental rock mechanics (C. B. Raleigh, M)
Gamma-ray spectrometry in uranium (J. S. Duval, D)
Gamma-ray spectrometry for uranium exploration in crystalline terranes (J. A. Pitkin, D)
Geophysical data, interpretation using electronic computers (R. G. Henderson, NC)
Geophysical studies for engineering geology (C. H. Miller, D)
Geophysical studies relating to uranium deposits in crystalline terranes (D. L. Campbell, D)

Geophysics, theoretical and experimental—Continued
- Ground-motion studies (J. H. Healy, M)
- Infrared and ultraviolet radiation studies (R. M. Moxham, NC)
- Magnetic and luminescent properties (F. E. Senftle, NC)
- Magnetic Properties Laboratory (M. E. Beck, Jr., Bellingham, Wash.)
- Microwave studies (A. W. England, D)
- Mineral Research Petrophysics (G. R. Olhoeft, D)
- NASA, electrical properties for the detection and mapping of waters on Mars (G. R. Olhoeft, D)
- NASA, laboratory microwave-, radar-, and thermal-emission-studies of basalt soil in vacuum (G.R. Olhoeft, D)
- Paleomagnetism, Precambrian and Tertiary chronology (D. P. Elston, Flagstaff, Ariz.)
- Petrophysics-geothermal (G. R. Olhoeft, D)
- Remanent magnetization of rocks (C. S. Grommé, M)
- Resistivity interpretation (A. A. R. Zohdy, D)
- Rock behavior at high temperature and pressure (E. C. Robertson, NC)
- Seismicity patterns in time and space (C. G. Bufe, M)
- Stress studies (C. B. Raleigh, M)
- Theory of gamma rays for geological applications (J. S. Duval, D)
- Thermal modeling investigations (Kenneth Watson, D)
- Thermodynamic properties of rocks (R. A. Robie, NC)
- Ultramafic intrusions, geophysical studies (G. A. Thompson, M)
- Uranium geophysics in frontier areas (J. W. Cady, D)
- Uranium petrophysics (G. R. Olhoeft, D)
- Volcano geophysics (E. T. Endo, M)
- *States:*
- California, Mass properties of oil-field rocks (L. A. Beyer, M)
- Nevada (D):
  - Nevada Test Site:
  - Interpretation of geophysical logs (R. D. Carroll)
  - Seismic velocity measuring techniques (R. D. Carroll)

Geotechnical investigations:
- Computer modeling research for engineering geology (W. Z. Savage, D)
- Dynamic soil behavior (A. T. F. Chen, M)
- Earthquake-induced landslides (E. L. Harp, M)
- Electronics instrumentation research for engineering geology (J. B. Bennetti, Jr., D)
- Experimental liquefaction potential mapping (T. L. Youd, M)
- Fissuring-subsidence research (T. L. Holzer, M)
- Geomechanics of radioactive waste storage (H. S. Swolfs, D)
- Geotechnical measurements and services (H. W. Olsen, D)
- Ground failure related to the New Madrid earthquake (S. F. Obermeier, NC)
- In-situ stress in shales (T. C. Nichols, Jr., D)
- Interaction of ground motion and ground failure (R. C. Wilson, M)
- Marine geotechnique (H. W. Olsen, D)
- In-situ stress (T. C. Nichols, Jr., D)
- Miscellaneous landslide investigations (R. W. Fleming, D)
- Open-pit slope stability (W. K. Smith, D)
- Research in rock mechanics (F. T. Lee, D)
- Solution subsidence and collapse (J. R. Ege, D)
- *States:*
- Alaska, Regional engineering geology of Cook Inlet coal lands, Alaska (H. R. Schmoll and L. A. Yehle, D)
- Colorado, Coal mine deformation at Somerset (C. R. Dunrud, D)
- Montana-Wyoming, Regional geotechnical studies, Powder River Basin (S. P. Kanizay, D)
- Virginia, Reston (S. F. Obermeir, NC)

Geotechnical investigations—Continued
- Wyoming, Coal mine deformation studies, Powder River Basin (C. R. Dunrud, D)

Geothermal investigations:
- Broad-band electrical surveys (Mark Landisman, University of Texas)
- Colorado Plateau, potential field methods (R. R. Wahl, D)
- Convection and thermoelastic effects in narrow vertical fracture spaces:
  - Analytical techniques (Gunnar Bodvarsson, Oregon State University)
  - Numerical techniques (R. P. Lowell, Georgia Institute of Technology)
- Development of first-motion holography for exploration (Keiiti Aki, Massachusetts Institute of Technology)
- Electrical and electromagnetic methods in geothermal areas (D. B. Jackson, D)
- Evaluation of intermediate-period seismic waves as an exploration tool (D. M. Boore, Stanford University)
- Evaluation of noble gas studies in exploration (Emanuel Mazor, Weizmann Institute of Science, Rehovot, Israel)
- Exploration and characterization from seismic activity (E. A. Page, ENSCO, Inc.)
- Geochemical exploration (M. E. Hinkle, D)
- Geochemical indicators (A. H. Truesdell, M)
- Geochemistry of geopressured systems (Y. K. Kharaka, w, M)
- Geophysical characterization of young silicic volcanic centers, eastern Sierran Front (W. F. Isherwood, D)
- Geothermal, Coachella Valley (J. H. Robison, w, M)
- Geothermal coordination (F. H. Olmsted, w, M)
- Geothermal geophysics (D. R. Mabey, D)
- Geothermal helium sniffing (Irving Friedman, D)
- Geothermal hydrologic reconnaissance (F. H. Olmsted, w, M)
- Geothermal investigations (H. W. Young, w, Boise, Idaho)
- Geothermal petrophysics (G. R. Olhoeft, D)
- Geothermal reservoirs (Manuel Nathenson, M)
- Geothermal resource assessment (L. J. P. Muffler, M)
- Geothermal resources file (J. R. Swanson; J. D. Bliss, M)
- Geothermal studies (A. H. Lachenbruch, M)
- Gravity variations as a monitor of water levels (J. M. Goodkind, University of California, San Diego)
- Heat flow (J. H. Sass, A. H. Lachenbruch, M)
- Isotopic and chemical studies of geothermal gases (Harmon Craig, University of California, San Diego)
- Low-frequency electromagnetic prospecting system (J. Clarke and H. F. Morrison, University of California, Berkeley)
- Mercury geochemistry as a tool for geothermal exploration (P. R. Buseck, Arizona State University)
- Oxygen isotopes (J. R. O'Neil, M)
- Physics of geothermal systems (W. H. Diment, M)
- Radioactivity series isotopic disequilibrium (J. K. Osmond and J. B. Cowart, Florida State University)
- Regional geoelectromagnetic traverse (J. F. Hermance, Brown University)
- Regional volcanology (R. L. Smith, NC)
- Remote sensing (Kenneth Watson, D)
- Rock-water interactions (R. O. Fournier, M)
- Seismic exploration (P. L. Ward, M)
- Signal processing methods for magnetotellurics (W. C. Hernandez, ENSCO, Inc.)
- Statistical characteristics of geothermal resources, Basin and Range province (W. F. Isherwood, D)
- Thermal waters (D. E. White, M)
- Western United States—geothermal waters (R. H. Mariner, w, M)

Heavy metals—Continued
- Solution transport (G. K. Czamanske, M)
- Southeastern States, geochemical studies (Henry Bell III, NC)
- *States:*
- Alaska (M):
  - Gulf of Alaska, nearshore placers (Erk Reimnitz)
  - Hogatza trend (T. P. Miller)
  - Southeastern part (D. A. Brew)
  - Southern Alaska Range (B. L. Reed)
  - Southwestern part (J. M. Hoare)
  - Yukon-Tanana Upland (H. L. Foster)
- Idaho, Washington Peak quadrangle (D. A. Seeland, D)
- Nevada:
  - Aurora and Bodie districts, Nevada-California (F. J. Kleinhampl, M)
  - Basin and Range (D. R. Shawe, D)

Hydrologic data collection and processing:
- Automatic data processing, ground-water site inventory consulting services (C. H. Baker, w, Lawrence, Kan.)
- Automatic processing hydrologic data (R. E. Hammond, w, Concord, N.H.)
- Data file for well records (K. L. Hunt, w, Madison, Wis.)
- Data verification (C. W. Alexander, w, Portland, Ore.)
- Distributed information systems (S. M. Longwill, w, NC)
- Distributed systems, Kansas (J. M. McNellis, w, Lawrence, Kan.)
- Hydrologic probability models (W. H. Kirby, w, NC)
- New Mexico data bank (E. V. Thomas, w, Albuquerque, N. Mex.)
- Northwest water resources data center (N. A. Kallio, w, Portland, Oreg.)
- Peaks above base, Delaware River basin (A. A. Vickers, w, Trenton, N.J.)
- Store-retrieve hydrologic data (G. W. Hawkins, w, Mineola, N.Y.)
- *See also* Hydrologic instrumentation.

Hydrologic instrumentation:
- Acoustic velocity meter feasibility study (A. Laenen, w, Portland, Oreg.)
- Acoustic velocity meter progress report (A. Laenen, w, Portland, Oreg.)
- Chipps Island acoustic flowmeter (S. H. Hoffard, w, M)
- COMSAT General Pilot Program (F. C. Boner, w, Tucson, Ariz.)
- COMSAT General Pilot Program, Colorado (L. L. Jones, w, D)
- Drilling techniques (Eugene Shuter, w, D)
- Ground-water Site Inventory Data Base (L. J. Topinka, w, Tacoma, Wash.)
- Instrumentation and environmental studies (G. E. Ghering, w, D)
- Instrumentation coordination (R. W. Paulson, w, NC)
- Instrumentation research, water (F. C. Koopman, w, Bay St. Louis, Miss.)
- Interagency sedimentation project (J. V. Skinner, w, Minneapolis, Minn.)
- Laser spectroscopy (M. C. Goldberg, w, D)
- Remote video streamgaging (L. L. Jones, w, D)
- Satellite data relay project (W. G. Slope, w, NC)
- Sensor development (C. R. Wagner, w, Bay St. Louis, Miss.)
- Suspended solids sensors (J. V. Skinner, w, Minneapolis, Minn.)
- Techniques of flood-plain mapping (R. H. Brown, w, Bay St. Louis, Miss.)
- Telemetry evaluation program (W. M. Woodham, w, Tampa, Fla.)
- *See also* Hydrologic data collection and processing.

Hydrology, ground water:
- Analysis of ground-water systems (S. S. Papadopulos, w, NC)
- Appalachian Basin, waste storage (P. M. Brown, w, Raleigh, N. C.)
- Borehole geophysics (W. S. Keys, w, D)
- Central midwest regional aquifer system analyses (D. G. Jorgensen, w, Lawrence, Kan.)
- Climax heater experiment (R. K. Waddell, w, D)
- Consultation and research (C. V. Theis, w, Albuquerque, N. Mex.)
- Energy transport in ground water (A. F. Moench, w, M)
- Fate of organisms in ground water (G. G. Ehrlich, w, M)
- Fissuring-substance research (T. L. Holzer, M)
- Fractured hydrogeologic systems (C. R. Faust, w, NC)
- Geopressured-geothermal resources (R. H. Wallace, w, Bay St. Louis, Miss.)
- Ground-water geophysics research (A. A. R. Zohdy, w, D)
- Ground-water staff functions (S. W. Lohman, w, D)
- Hydro characteristics of anhydrite (William Thordarson, w, D)
- Hydrologic analysis of petrofabrics (R. T. Getzen, w, M)
- Hydrology of the Madison aquifer (E. M. Cushing, w, D)
- Limestone hydraulic permeability (V. T. Stringfield, w, NC)
- Missouri River basin study (H. H. Hudson, w, D)
- Modeling of geothermal systems (M. L. Sorey, w, M)
- North Atlantic Coast regional aquifer system analysis (H. Meisler, w, Trenton, N.J.)
- Northern Great Plains aquifer study (G. A. Dinwiddle, w, D)
- Northern midwest regional aquifer study (W. L. Steinhilber, w, Madison, Wis.)
- Paradox basin hydrology (F. F. Rush, w, D)
- Planning, northern coastal plain (H. Meisler, w, Trenton, N.J.)
- Role of confining clays (R. G. Wolff, w, NC)
- Southeast limestone aquifer study (R. H. Johnston, w, Atlanta, Ga.)
- Transport phenomena in porous media (J. W. Mercer, w, NC)
- Tropical carbonate aquifers (William Back, w, NC)
- Unsaturated zone field studies (E. P. Weeks, w, D)
- Yucca Flat hydrology (G. C. Doty, w, Mercury, Nev.)
- *States and territories:*
- Alabama, Environmental hydrogeology highways (J. C. Scott, w, Montgomery)
- Alaska (w, Anchorage):
  - Capps Creek coal study (G. L. Nelson, w, Anchorage)
  - Eagle River Valley ground water (L. L. Dearborn)
  - Hydrologic data (L. L. Dearborn)
  - Kenai Borough project (G. L. Nelson)
  - Mendenhall hydrology (G. O. Balding, w, Fairbanks)
- Arizona:
  - Aqua Fria water resources (R. P. Wilson, w, Tucson)
  - Ground water to Colorado River (S. A. Leake, w, Yuma)
  - Ground water, Vekol Valley, Arizona (L. J. Mann, w, Tucson)
  - Southern Apache County (T. W. Anderson, w, Flagstaff)
  - Special site studies (R. D. MacNish, w, Tucson)
  - Water supply, Lake Mead area (R. L. Laney, w, Phoenix)
- Arkansas, Hydrology of Claiborne and Wilcox (M. E. Broom, w, Little Rock)
- California:
  - Artificial recharge, San Joaquin County (H. T. Mitten, w, Sacramento)
  - Artificial recharge, southern California (J. H. Koehler, w, Laguna Niguel)
  - Central Valley aquifers (G. L. Bertoldi, w, Sacramento)
  - City of Merced ground-water appraisal (C. L. Londquist w, Sacramento)

Hydrology, ground water—Continued
States and territories—Continued
Idaho—Continued
- Snake River Plain regional aquifer system analyses (G. F. Lindholm, w, Boise)
- Water resources of the Camas Prairie (H. W. Young, w, Boise)
- Water resources, Rockland Valley (H. W. Young, w, Boise)

Illinois:
- Regional aquifer study in Illinois (M. G. Sherrill, w, Champaign)
- Shallow ground water, McHenry County (J. T. Krohelski, w, DeKalb)

Indiana (w, Indianapolis):
- Decatur County (T. K. Greenman)
- Elkhart ground-water study (T. E. Imbrigiotta)
- Ground-water model, Outwash aquifer (B. S. Smith, w, Indianapolis)
- Ground water, Upper West Fork of the River basin (W. W. Lapham)
- Indiana dunes ground-water study (D. C. Gillies)
- Jennings County fracture trace (T. G. Greeman)
- Johnson-Morgan ground-water study (D. C. Gillies)
- Newton Jasper, ground water (M. F. Bergeron)
- Regional aquifer study in Indiana (R. J. Shedlock)
- Southeast Indiana lineaments (T. K. Greeman)

Iowa (w, Iowa City):
- Carbonate terrane hydrology (Phase 1) (K. D. Wahl)
- North-central Iowa (Gary Galliot)
- Pennsylvanian aquifers, coal region (J. C. Cagle)
- Regional aquifer study in Iowa (M. R. Burkart)
- Water resources, west central Iowa (G. Gaillot, w, Iowa City)

Kansas:
- Aquifer test evaluation (R. D. Burnett, w, Lawrence)
- Chemical quality, deep aquifers (J. Kume, w, Garden City)
- Geohydrologic maps, southwestern Kansas (E. D. Gutentag, w, Garden City)
- Geohydrology for planning in western Kansas (Jack Hume, w, Garden City)
- Geohydrology Wellington, Salina area (J. Gillespie, w, Lawrence)
- Ground-water depletion maps, west-central Kansas (L. E. Dunlap, w, Garden City)
- Hydrologic data base, Ground Water Management District 3 (H. F. Grubb, w, Garden City)
- Hydrologic data base, Western Kansas Ground Water Management District 1 (J. M. Spinazola, w, Garden City)
- Liquid waste, Arbuckle Group (A. J. Gogel, w, Lawrence)
- Models North and South Fork Solomon (J. B. Gillespie, w, Lawrence)
- Sandstone aquifer, southwest Kansas (Jack Hume, w, Garden City)
- Water resources of Ford County (J. Spinazola, w, Garden City)
- Wellington aquifer parameters (J. B. Gillespie, w, Lawrence)

Kentucky:
- Hydrogeology, eastern Kentucky coal field (P. A. Emery, w, Louisville)
- Mississippi Plateau potentiometric map (T. W. Lambert, w, Louisville)

Hydrology, ground water—Continued
States and territories—Continued
Louisiana (w, Baton Rouge):
- Geohydrologic mapping in south Arkansas (R. L. Hosman, w, Baton Rouge)
- Red River waterway study (J. E. Rogers, w, Alexandria)
- Southwestern Louisiana (D. J. Nyman)

Maine (w, Augusta):
- Androscoggin, ground water (G. C. Prescott, Jr.)
- Little Andy Valley aquifer (D. J. Morrissey, w, Augusta)
- Maine sand and gravel aquifers (G. C. Prescott)

Maryland (w, Towson):
- Baltimore industrial area ground water (F. H. Chapelle, w, Towson)
- Definition of Maryland aquifers (E. G. Otton, w, Towson)
- Garrett County, well inventory (L. J. Nutter)
- Hydrologic impacts of power plants (F. K. Mack, w, Annapolis)
- Hydrology of water-table aquifer (L. L. Bachman)
- Maryland Aquifer Studies III (F. K. Mack)
- Western Montgomery County ground-water study (E. G. Otton)

Massachusetts (w, Boston):
- Connecticut River aquifer study (D. F. Delaney, w, Boston)
- Estimating maximum ground-water levels (M. H. Frimpter)
- Ground water, Cape Cod (D. R. LeBlanc)
- Monitoring Cape Cod's ground water (B. J. Ryan)
- Northeastern Massachusetts river basins (R. A. Brackley)
- Water resources, Blackstone River basin (E. H. Walker)

Michigan:
- Ground water of coal deposits, Bay County, Michigan (J. R. Stark, w, Lansing)
- Hydrology of Sands plain area (N. G. Grannemann, w, Lansing)

Minnesota (w, St. Paul):
- Aquifer thermal-energy storage (J. H. Guswa, w, St. Paul)
- Carlton, Pine, and Kanebec Counties (C. F. Myette, w, St. Paul)
- Ground-water appraisal, Pelican River sand plain (R. T. Miller)
- Ground water:
  - Southwestern Minnesota (D. G. Adolphson)
  - Todd, Cass, Morrison Counties (C. F. Myette)
- Hydrology of peatlands (D. I. Siegel, w, St. Paul)
- Hydrology of Red Lake peatlands (D. I. Siegel)
- Lake Williams—water balance (D. I. Siegel)
- Pomme de Terre-Chippewa ground water (W. G. Soukup, w, St. Paul)
- Reconnaissance of sand-plain aquifers (H. W. Anderson)
- Regional aquifer study in Minnesota (D. G. Woodward)
- Underground injection control (D. G. Adolphson, w. St. Paul)
- Water resources, Buffalo River (R. J. Wolf)

Mississippi (w, Jackson):
- Aquifers as drinking water sources (L. A. Gandl, w. Jackson)
- Eutaw-McShan aquifer model (J. M. Kernodle, w, Jackson)
- Hydrologic impact lignite mining in alluvium (J. K. Arthur, w, Jackson)
- Hydrology-Tennessee-Tombigbee (A. G. Lamonds)
- Potentiometric mapping (B. E. Wasson)
- Tupelo model (J. M. Kernodle, w, Jackson)

Hydrology, ground water—Continued
States and territories—Continued
Oklahoma:
- Arbuckle aquifer (R. W. Fairchild, w, Oklahoma City)
- Central midwest regional aquifer system analysis (J. H. Irwin, w, Oklahoma City)
- Roubidoux aquifer (R. W. Fairchild, w, Oklahoma City)

Oregon (w, Portland):
- Bend-Redmond ground water (J. B. Gonthier)
- Dalles-Monmouth ground-water study (J. B. Gonthier)
- Ground water, Clackamas County (A. R. Leonard)
- Ground water, Hood basin (S. J. Grady)
- Ground water, Rouge River basin (J. B. Gonthier, w, Portland)
- Underground injection (D. D. Harris, w, Portland)

Pennsylvania (w, Harrisburg, except as otherwise noted):
- Ground water, central Columbia County (J. H. Williams)
- Ground-water resources of Pike County (D. K. Davis, w, Harrisburg)
- Hydrogeology:
  - Erie County (J. T. Gallaher w, Meadville)
  - Great Valley (A. E. Becher)
- Hydrology of Gettysburg Formation (C. R. Wood)
- Lower Susquehanna ground water (J. M. Gerhart)
- Major fracture systems, western Pennsylvania (J. D. Stoner, w, Pittsburgh)
- Philadelphia ground water (C. R. Wood, w, Malvern)
- Water levels and quality monitoring (W. C. Roth)
- Water resources of anthracite region (A. E. Becher, w, Harrisburg)

Puerto Rico:
- Ground water, Canovanas-Rio Grande area (A. E. Torres-Gonzalez, w, Ft. Buchanan)
- Ground water in critical areas (E. Colon-Dieppa, w, Ft. Buchanan)
- Manati water resources (Fernando Gomez-Gomez, w, Ft. Buchanan)
- Water for North Coast rice (J. R. Diaz, w, San Juan)
- Water-resources appraisal of St. Croix, Virgin Islands (H. J. McCoy, w, San Juan)
- Water resources of Rio Guanajibo basin (Eloy Colon, w, Ft. Buchanan)
- Water resources, Rio Cibuco area (A. E. Torres-Gonzalez, w, Ft. Buchanan)

Rhode Island, Ground water in Pawcatuck River basin (H. E. Johnston, w, Providence)

South Carolina (w, Columbia, except as otherwise noted):
- Assessment of ground-water resources (A. D. Park)
- Ground-water resources in northeast South Carolina (G. K. Speiran, w, Columbia)
- Subsurface samples repository (N. K. Olson, w, Columbia)
- Water-resources evaluation—Horry, Georgetown (A. L. Zack)

South Dakota:
- High Plains aquifer study (H. L. Case, w, Rapid City)
- Hydrology of the Madison Group (L. W. Howells, w, Huron)
- Northern Great Plains aquifer study (H. L. Case, w, Rapid City)
- Water resources, Walworth County (E. P. LeRoux, w, Huron)

Tennessee (w, Nashville):
- Ground-water study for lignite (W. S. Parks, w, Memphis)
- Hydrology of hard rock aquifers (E. F. Hollyday)
- Memphis aquifer studies (W. S. Parks, w, Memphis)
- Paleozoic rocks, Highland Rim (E. F. Hollyday, w, Nashville)

Hydrology, ground water—Continued
States and territories—Continued
Tennessee—Continued
- Tennessee aquifer delineation (J. V. Brahana, w, Nashville)

Texas:
- Limestone County ground water (P. L. Rettman, w, San Antonio)
- Limestone hydrology study (R. W. Maclay, w, San Antonio)
- Mississippi embayment west Gulf Coast regional aquifer system analyses (H. F. Grubb, w, Austin)
- Rusk County ground water (S. J. Halasz, w, Houston)
- Salinity control, Brazos and Red Rivers (S. Garza, w, Austin)
- Salt dome hydrology (phase I) (J. E. Carr, w, Houston)
- Trinity River alluvium (S. Garza, w, Austin)

Utah (w, Salt Lake City):
- Great Basin aquifer systems (J. S. Gates, w, Salt Lake City)
- Ground water in Sevier Desert (R. W. Mower)
- Hydrology, Tooele Valley area (A.G. Razem)
- Morgan Valley (J. S. Gates)
- Navajo Sandstone, Southwestern Utah (R. M. Cordova)
- Northern Utah Valley ground water (D. W. Clark, w, Salt Lake City)
- Reconnaissance, Fish Springs Flat (E. L. Bolke)

Vermont, Ground water in Rutland area (R. E. Willey, w, Montpelier)

Virginia:
- Culpeper Basin study (Chester Zenone, w, Fairfax)
- Fairfax County urban-area study (Chester Zenone, w, Fairfax)
- Ground-water resources, Blue Ridge Parkway (H. T. Hopkins, w, Richmond)

Washington (w, Tacoma, except as otherwise noted):
- Clallam County water resources (B. W. Drost)
- Gig Harbor water resources (B. W. Drost)
- Horse Heaven Hills ground water (F. A. Packard, w, Tacoma)
- Hydrologic basin analysis (K. L. Walters)
- Island County ground water (D. R. Cline, w, Tacoma)
- Lower Yakima summary (B. W. Drost)
- Muckleshoot ground water (Dee Molenaar)
- Nisqually ground water (W. E. Lum)
- Shoalwater water resources (W. E. Lum)
- Spokane ground-water quality (E. L. Bolke)
- Spokane planners' summary (D. Molenaar, w, Tacoma)
- Tulalip ground water (W. E. Lum, II, w, Tacoma)
- Washington non-potable aquifers (W. E. Lum, w, Tacoma)
- Water data for coal mining (F. A. Packard)
- Water, Yakima Reservation (E. A. Prych)

West Virginia (w, Charleston):
- Ecology and underground coal mining (W. A. Hobba)
- Elk River basin study (G. T. Tarver)
- Ground-water atlases (C. Puente, w, Charleston)
- Hydrology of stress-relief fracturing (J. W. Borchers, w, Charleston)
- Remotely sensed ground water (W. A. Hobba, w, Morgantown)
- Water resources of Tug Fork basin (J. S. Bader)

Wisconsin (w, Madison):
- Ground water, Dodge County (R. W. Devaul)
- Ground-water level fluctuations (R. M. Erickson, w, Madison)

Hydrology, ground water—Continued
States and territories—Continued
Wisconsin—Continued
Ground-water quality (P. A. Kammerer, Jr.)
Regional aquifer study in Wisconsin (P. J. Emmons)
Iron River hatchery study (S. M. Hindall)
Water resources of Forest County (R. A. Lidevin)
Water resources of Vilas County (E. H. Reinen, w, Madison)
Wyoming (w, Cheyenne):
Bighorn Basin aquifers (M. E. Cooley)
Hanna basin water resources (P. B. Freudenthal)
High Plains aquifer study (C. F. Avery)
Madison limestone (C. R. Joy)
Model of Bates Hole (K. C. Glover)
Northern Great Plains aquifer study (D. T. Hoxie)
Saratoga Valley (L. W. Lenfest, w, Cheyenne)
Southern Powder uranium (M. E. Lowry, w, Cheyenne)
Wheatland Flats model (M. A. Crist)
White Mountain oil shale (W. J. Head, w, Charleston)

Hydrology, surface water:
Circulation, San Francisco Bay (T. T. Conomos, w, M)
Hydrologic estimating techniques (D. G. Frickel, w. D)
Hydrology defined by rainfall simulation (G. C. Lusby, w, D)
Isotope fractionation (T. B. Coplen, w, NC)
Numerical simulation (R. A. Baltzer, w, NC)
Platte River hydrology (R. F. Hadley)
States and territories:
Alabama (w, Tuscaloosa):
Flow characteristics of streams (C. O. Ming, w, Montgomery)
Mobile River study (J. E. Bowie, w, Montgomery)
Small-stream studies (D. A. Olin)
Alaska;
Hydrology near Craig (G. O. Balding, w, Juneau)
Kenai morphology (K. M. Scott, w, Anchorage)
Arizona, Flood hydrology of Arizona (B. N. Aldridge, w, Tucson)
Arkansas (w, Little Rock):
Arkansas basin flows (G. G. Ducret)
Duration and frequency of streams (T. E. Lamb)
California (w, Sacramento, except as otherwise noted):
Alameda Creek surface-water quality (L. E. Lopp, w, M)
California lakes and reservoirs (W. L. Bradford, w, M)
Tidal River discharge computation (R. N. Oltmann)
Colorado (w, D):
Arkansas River Compact (J. F. Blakey)
Instream flow evaluation (D. P. Bauer)
Inventory of water resources on Ft. Carson (G. J. Leonard)
Mannings "N" value study (R. D. Jarrett)
Peak discharge small watershed (D. R. Minges)
Reconnaissance of strip-mine site (R. S. Williams, Jr., w, D)
Streamflow analysis, Piceance Basin (N. E. Spahr, w, D)
Connecticut, Water quality of Lake Waramang (K. P. Kulp, w, Hartford)
Delaware, Delaware River master activity (F. T. Schaefer, w, Milford, Pa.)
Florida:
Golden Gate study (M. L. Merritt, w, Miami)
Hillsborough River basin water supply (J. F. Turner, w, Tampa)
Hydrology Area B, Sarasota County (H. R. Sutcliffe, w, Sarasota)
Hydrology of lakes (G. H. Hughes, w, Tallahassee)

Hydrology, surface water—Continued
States and territories—Continued
Florida—Continued
St. Johns River deepening study (R. B. Stone, w, Jacksonville)
Small stream flood frequencies (W. C. Bridges, w, Tallahassee)
Georgia (w, Doraville):
Computation of dynamic streamflow (M. E. Blalock, w, Doraville)
Seasonal low flow (T. R. Dyar)
Storage requirements for Georgia streams (R. F. Carter)
Time-of-travel, Georgia streams (J. L. Pearman)
Hawaii, Surface-water data summary (I. Matsuoka, w, Honolulu)
Idaho:
Skew mapping (L. C. Kjelstrom, w, Boise)
Water quality, Spokane River (H. R. Seitz, w, Boise)
Illinois:
Dam ratings (D. M. Mades, w, DeKalb)
Hydrologic information service (D. G. Glysson, w, Champaign)
Stream dispersion (J. B. Graf, w, Champaign)
T and K studies on Illinois streams (J. B. Graf, w, Champaign)
Indiana:
Mapping of Big Long Lake (R. R. Contreras, w, Indianapolis)
River mileage (G. E. Nell, w, Indianapolis)
Streamflow characteristics (D. W. Blevins, w, Indianapolis)
Kansas (w, Lawrence):
Channel geometry, coal areas (E. E. Hedman)
Channel geometry, Kansas River (W. R. Osterkamp)
Channel geometry, regulated streams (W. R. Osterkamp)
Flood investigations (H. R. Hejl, Jr.)
Flood volume, western Kansas (C. O. Perry, w, Lawrence)
Gains and losses, Neosho River (W. J. Carswell, Jr., w, Lawrence)
High-flow volume (P. R. Jordan, w, Lawrence)
Sediment-active channel geometry (W. R. Osterkamp)
Soldier Creek (W. J. Carswell)
Streamflow characteristics (P. R. Jordan)
Water yield, Kansas (W. J. Carswell)
Louisiana: Characteristics of streams (M. J. Forbes, Jr., w, Baton Rouge)
Maine (w, Augusta):
Drainage areas (R. A. Fontaine)
Flow and water quality character, Maine streams (G. W. Parker)
Maryland:
Flow characteristics of Maryland streams (D. H. Carpenter, w, Towson)
Low-flow studies in Maryland (R. W. James, w, Towson)
Massachusetts, Drainage areas (S. S. Wandle, w, Boston)
Michigan, Flow model of Saginaw River (D. J. Holtschlag, w, Lansing)
Minnesota:
Big Marine Lake (G. E. Groschen, w, St. Paul)
Small streams program (K. T. Gunard, w, St. Paul)
Mississippi:
Drainage areas, Mississippi streams (J. W. Hudson, w, Jackson)
Flow characteristics of Tombigbee River (B. E. Colson, w, Jackson)

Hydrology, surface water—Continued
States and territories—Continued
Missouri:
Flow duration, Missouri streams (L. D. Hauth, w, Rolla)
Small streams analysis (L. D. Hauth, w, Rolla)
Montana (w, Helena, unless otherwise noted):
Bridge-site investigations (R. J. Omang)
Limnology of lakes in eastern Montana (R. F. Ferreira)
Peak flow, small drainage areas (R. J. Omang)
Runoff characteristics, eastern Montana (R. J. Omang, w, Helena)
Watershed model (L. E. Cary, w, Billings)
Nevada, Lake Mead recreation area flood hazards (Otto Moosburner, w, Carson City)
New Jersey:
Base flow studies (R. D. Schopp, w, Trenton)
Drainage areas of streams (A. J. Velnich, w, Trenton)
Low-flow regionalization (B. D. Gillespie, w, Trenton)
New Mexico:
Precipitation-runoff modeling (H. R. Hejl, w, Albuquerque)
Runoff from channel geometry (J. P. Borland, w, Albuquerque)
New York (w, Albany):
Acid lakes (N. E. Peters)
Discharges Oswego River basin studies (R. Lumia, w, Albany)
Headwaters locations (B. B. Eissler, w, Albany)
Low-flow study (B. B. Eissler)
Rockland County rainfall-runofff (R. Lumia, w, Albany)
Stream gazetteer (L. A. Wagner)
North Carolina (w, Raleigh):
Channelization effects, Chicod Creek (C. E. Simmons)
Data site information for 208 study (C. E. Simmons)
Ohio (w, Columbus):
Floods versus channel geometry (E. E. Webber)
Hydraulics of bridge sites (R. I. Mayo)
Low-flow frequency analyses (D. P. Johnson)
Low flow of Ohio streams (R. I. Mayo)
Reaeration (J. Hren w, Columbus)
Rural hydrology (E. E. Webber)
Rush Creek water quality (Janet Hren)
Time-of-travel studies of Ohio streams (A. O. Westfall)
Oklahoma:
Coal field hydrology (A. W. Smart, w, Oklahoma City)
Effects of control on discharge (T. L. Huntzinger, w, Oklahoma City)
Pennsylvania (w, Harrisburg):
Coal hydrology, Greene County (D. R. Williams, w, Pittsburgh)
Low-flow regionalization (H. N. Flippo)
Mean discharge (W. J. Herb)
Regionalization of streamflow data (J. M. Bettandorff, w, Harrisburg)
Time of travel, Lehigh River (C. D. Kaufman)
Puerto Rico, Islandwide 208 assistance study (A. E. Torres , w, San Juan)
South Carolina (w, Columbia):
Drainage basin inventory (G. G. Patterson, w, Columbia)
Non-point discharges, Reedy River (D. I. Cahal)
South Dakota (w, Huron):
Flood-frequency study (L. D. Beeker)
Small-stream flood frequency (L. D. Becker)
Tennessee (w, Nashville, except as otherwise noted):
Miscellaneous data services (V. J. May)
Tennessee bridge scour (W. J. Randolph)

Hydrology, surface water—Continued
States and territories—Continued
Texas: Small watersheds (B. O. Massey, w, Austin)
Utah, Mined lands rehabilitation (G. W. Sandberg, w, Cedar City)
Virginia:
Historic streamflow record—Occoquan (B. J. Prugh, w, Richmond)
Low flows (B. J. Prugh, w, Richmond)
Washington (w, Tacoma):
Low flow of Washington streams (E. H. McGavok)
Newaukum basin study (E. R. Prych)
Okanogan River streamflow modeling (J. J. Vaccaro, w, Tacoma)
Rating of new St. Helens stations (M. B. Miles, w, Tacoma)
Streamflow statistics, southwestern and eastern Washington (L. M. Nelson, w, Tacoma)
Unregulated flow at Union Gap (J. J. Vaccaro)
Water resources of the Hoh Indian Reservation (W. E. Lum)
West Virginia:
Small drainage areas (G. S. Runner, w, Charleston)
Time of travel on the New River (D. H. Appel, w, Charleston)
Wisconsin (w, Madison):
Bridge Creek hydrology (B. K. Holmstrom)
Drainage area determination (E. W. Henrich)
Flood-frequency study (D. H. Conger)
Low-flow study (B. K. Holmstrom)
Nonpoint source pollution (S. J. Field)
Pheasant Branch study (W. R. Krug)
Water-quality control (B. K. Holstrom)
Water resources of Apostle Islands (W. J. Rose, w, Madison)
Wyoming:
Infiltration model (J. G. Rankl, w, Cheyenne)
Streamflow in energy areas (H. W. Lowham, w, Cheyenne)
See also Evapotranspiration; Flood investigations; Marine hydrology; Plant ecology; Urbanization, hydrologic effects.

Industrial minerals. *See specific minerals.*

Iron:
Resource studies, United States (Harry Klemic, NC)
States:
Michigan, Gogebic County, western part (G. G. Schmidt, NC)
Wisconsin, Black River Falls (Harry Klemic)

Isotope and nuclear studies:
Atmospheric carbon dioxide (Irving Friedman, D)
Carbon isotopes and the global carbon cycle (M. A. Arthur, D)
CUSMAP (Carl E. Hedge, D)
CUSMAP (T. W. Stern, NC)
CUSMAP (Ronald W. Kistler, M)
Data bank (R. F. Marvin, D)
Geochronology (B. R. Doe, D)
Geochronology (C. W. Naeser, D)
Geochronology (T. W. Stern, NC)
Geochronology (R. E. Zartman, D)
Hard-rock waste disposal (Z. E. Peterman, D)
Instrument development (F. J. Jurcska, J. D. Obradovich, Ernest Wilson, D)
Isotope ratios in rocks and minerals (Irving Friedman, D)
Lead isotopes and ore deposits (B. R. Doe, R. E. Zartman, D)
Light stable isotopes (Irving Friedman, D)
Magnetic properties of coal (F. E. Senftle, NC)
Mass spectrometry and isotopic measurements (J. S. Stacey, D)
Mineral separation (G. T. Cebula, D)
Neutron activation (F. E. Senftle, NC)

Limnology—Continued
States and territories:
Massachusetts, Hager Pond nutrient study (W. D. Silvey; w, Boston)
Montana, Limnology of Valley County lakes (R. F. Ferreira, w, Helena)
Ohio:
Limnology of selected lakes (C. G. Angelo w, Columbus)
Urban impact on instream biology (W. P. Bartlett, w, Columbus)
Pennsylvania, Biological monitoring, Chester County (C. R. Moore, w, Malvern)
Puerto Rico, Quality of Water, Lago Carraizo (Ferdinand Quinones-Marquez, w, San Juan)
Wisconsin, Hydrology of lakes (D. A. Wentz, w, Madison)
Wyoming, Stream habitats (D. A. Peterson, w, Cheyenne)
See also Quality of water.

Lithium:
Cenozic deposit history (J. R. Davis, D)
Exploration for and resource appraisal of nonpegmatite deposits (J. D. Vine, D)
Geochemistry of lithium clays (R. K. Glanzman, D)
Regional distribution (E. F. Brenner-Tourtelot, D)

Lunar geology. *See* Extraterrestrial studies.

Manganese. *See* Ferro-alloy metals.

Marine geology:
Atlantic Continental Shelf:
Coastal Plain estuaries (E. A. Martin, Corpus Christi, TX)
Environmental impact of petroleum exploration and production (H. J. Knebel, Woods Hole, Mass.)
Geophysics studies (J. C. Behrendt, Woods Hole, Mass.)
Magnetic chronology (E. M. Shoemaker, D. P. Elston, Flagstaff, Ariz.)
New England coastal zone (R. N. Oldale, Woods Hole, Mass.)
Organic geochemistry of Atlantic Continental Shelf and nearshore environments (R. E. Miller, NC)
Site surveys (W. P. Dillon, Woods Hole, Mass.)
Stratigraphy (J. C. Hathaway, Woods Hole, Mass.)
Stratigraphy and structure (J. S. Schlee, Woods Hole Mass.)
Caribbean and Gulf of Mexico:
Biogenic methane in modern marine sediments (L. E. Garrison, Corpus Christi, TX)
Coastal environments (H. L. Berryhill, C. W. Holmes, Corpus Christi, Tex.)
Continental Slope (A. H. Bouma, Corpus Christi, TX)
Estuaries (C. W. Holmes, Corpus Christi, Tex.)
Mississippi delta studies (L. E. Garrison, Corpus Christi, Tex.)
Natural resources and tectonic features (R. G. Martin, Jr., Corpus Christi, Tex.)
Nepheloid layer development (G. L. Shideler)
Oil migration and diagenesis of sediments (C. W. Holmes, Corpus Christi, Tex.)
Quaternary history and sea floor stability (H. Berryhill Corpus Christi, TX)
Sand resources of the Virgin Islands (C. W. Holmes, Corpus Christi, TX)
Texas Barrier Island stratigraphy (G. L. Shideler)
Tectonics, Caribbean (J. E. Case, Corpus Christi, Tex.)
Tectonics, Gulf (L. E. Garrison, Corpus Christi, Tex.)
West Florida Continental Shelf (C. W. Holmes, Corpus Christi, TX)

Marine geology—Continued
Geotechnical investigations (D. A. Sangrey, D)
Marine mineral resources, worldwide (F. H. Wang, M)
Pacific-Arctic Oceans (M, except as otherwise noted):
Acoustic measurement of in situ physical properties of shelf sediments (G. Boucher)
Advanced geopotential data (collection, processing, modeling) (A. K. Cooper)
Advanced seismic systems (D. H. Tompkins)
Alaskan marine micropaleontology (P. J. Quinterno)
Benthic processes in San Francisco Bay (F. H. Nichols)
Biogenic sedimentary processes (G. W. Hill)
Comparative sedimentology of continental margin environments for exploration and recovery of energy resources (C. H. Nelson)
Computer systems analyses and applications programming (G. A. McHendrie)
Continental margin petroleum resources framework (T. H. McCulloh)
Continental margin processes (J. V. Gardner)
Continental margin sediment dynamics (D. A. Cacchione)
Deep-sea fan studies (W. R. Normark)
Depositional processes and facies coastal embayments (R. L. Phillips)
Dynamics of sediment bedforms (D. M. Rubin)
Eastern Gulf of Alaska resource assessment (G. Plafker)
Environmental geologic studies, Beaufort and Chukchi Seas (P. W. Barnes; E. Reimnitz)
Environmental geologic studies, eastern Gulf of Alaska (B. F. Molnia)
Environmental geologic studies, northern and central California continental shelf and margin (D. S. McCulloch)
Environmetal geologic studies, southern California borderland (H. G. Greene)
Environmental geologic studies, western Gulf of Alaska (M. A. Hampton)
Geochemistry of sediments (W. E. Dean, D)
Geologic and resource assessment, northern Bering Sea (M. A. Fisher)
Geologic framework and resource assessment, Aleutian-Bering Sea area (M. S. Marlow)
Geologic framework and resource assessment, Gulf of Alaska (R. E. von Huene)
Geologic framework and resource assessment, northern and central California continental shelf and margin (D. S. McCulloch)
Geologic framework and resource assessment, of Oregon-Washington continental margin (P. D. Snavely, Jr.)
Geologic framework and resource assessment, southern California borderland (J. G. Vedder)
Geologic framework and resource, Beaufort and Chukchi Seas (A. Grantz)
Geologic hazards in Navarin Basin province (P. R. Carlson)
Linear island chains, tectonic movsments of the Pacific crust (D. A. Clague)
Marine geotechnical studies (M. A. Hampton)
Marine organic geochemistry (K. A. Kvenvolden)
Metallic deposits in the oceanic crust (R. A. Koski)
Nearshore sediment dynamics (A. H. Sallenger, Jr.)
Ocean floor mineralization studies (J. L. Bischoff)
Ocean floor mineral resources (D. Z. Piper)
Oceanic Micropaleontology (J. D. Bukry)
Open-coast sedimentary lithogenesis (R. E. Hunter)

Marine geology—Continued
Pacific-Arctic Oceans—Continued
Pacific Ocean, biostratigraphy, oceanic (J. D. Bukry, La Jolla, Calif.)
Pacific reef studies (J. I. Tracey, Jr., NC)
Petroleum geology of Cook Inlet-Shelikof Strait (L. B. Magoon)
Properties of submarine volcanic rocks (J. G. Moore)
Resource and geo-environmental assessment, Aleutian ridge and shelf (D. W. Scholl)
Sediment processes and facies in the shelf-slope transition zone (M. E. Field)
Sediment transport and diffusion in abyssal benthic boundary layer (S. L. Eittreim)
Sedimentary processes of submarine canyon heads (J. R. Dingler)
Silica and clay mineral distributions and diagenesis in deep sea (J. R. Hein)
Small Boat Surveys (Harley J. Knebel, Woods Hole, Mass.)
Spanish continental margin (Almeria Province) (P. D. Snavely, Jr., H. G. Greene, H. F. Clifton, W. P. Dillon, J. M. Robb, M)
Volcanic geology, Mariana and Caroline Islands (Gilbert Corwin, NC)
States and territories:
California (M), La Jolla marine geology laboratory (J. D. Bukry)
Oregon-Washington, Geologic framework (P. D. Snavely, Jr., M)
Puerto Rico, Coooperative program (J. V. A. Trumbull, Santurce)
Texas, Barrier islands (R. E. Hunter, Corpus Christi)

Marine geotechnique:
Marine geotechnical investigations (H. W. Olsen, D)

Marine hydrology. *See* Hydrology, surface water; Quality of water; Geochemistry, water; Marine geology.

Mercury:
Geochemistry (A. P. Pierce, D)
Mercury deposits and resources (E. H. Bailey, M)
State:
California, Coast Range ultramafic rocks (E. H. Bailey, M)

Metamorphism:
Combustion, high temperature minerals (J. R. Herring, D)

Meteorites. *See* Extraterrestrial studies.

Mine drainage and hydrology:
Water monitoring-coal mining, Northeastern region (J. F. Bailey)
Water monitoring—coal mining, Southeastern region (C. A. Pascale, w, Atlanta, Ga.)
States:
Alabama, Hydrologic assesment—coal areas (J. R. Harkins, w, University)
Alaska, Placer mine study (R. J. Madison, w, Anchorage)
Colorado, Hydrology of coal spoils piles (R. S. Williams, w, D)
Georgia, Water monitoring—coal mining (W. H. Norris, w, Doraville)
Illinois (w, Champaign):
Mine reclamation hydrology (M. F. Deneen)
Strip mine modeling (D. L. Galloway, w, Champaign)
Water monitoring-coal mining (E. E. Zuehls)
State:
Indiana (w, Indianapolis):
Effects of strip mining and reclamation (J. C. Peters)
Effects of strip mining on ground water and surface water (R. J. Shedlock, w, Indianapolis)
Hydrology of coal mine area (J. S. Zogorski)

Mine drainage and hydrology—Continued
States—Continued
Indana—Continued
Uranium, remote sensing for uranium exploration (G. L. Raines, D)
Water monitoring—coal mining (W. G. Wilber)
Kansas, Coal hydrology of east-central Kansas (C. D. Albert, w, Lawrence)
Kentucky (w, Louisville):
Downstream effects of coal mining (J. E. Dysart)
Hydrologic data monitoring—coal areas (Ferninand Quinones)
Water from coal mines (D. S. Mull)
Maine, Hydrologic effects, northern Maine mining (R. A. Fontaine, w, Augusta)
Maryland:
Hydrologic effects of coal mining (M. T. Duigon, w, Towson)
Water monitoring—coal mining (W. W. Staubitz, w, Towson)
Montana, Surface water-quality water analysis, eastern Montana (J. J. Knapton, w, Helena)
Chaco Canyon, New Mexico hydrology (H. R. Hejl, w, Albuquerque)
New Mexico:
Individual coal mine effects (C. L. Goetz, w, Albuquerque)
San Juan coal monitoring (J. D. Dewey, w, Albuquerque)
North Dakota, Knife River evaluation (J. E. Miller, w, Bismarck)
Ohio:
Acid mine drainage characterization (C. G. Angelo, w, Columbus)
Mine reclamation, Lake Hope Basin (V. E. Nichols, w, Columbus)
Water monitoring—coal mining (D. K. Roth, w, Columbus)
Oklahoma:
Abandoned zinc mines (C. J. Hill, w, Oklahoma City)
Hydrogeology orphan lands, eastern Oklahoma (L. J. Slack, w, Oklahoma City)
Pennsylvania (w, Harrisburg):
Coal hydrology of Big Sandy Creek (D. E. Stump)
Daylighting—hydrology of Babb Creek (L. A. Reed)
Mine-site application for Office of Surface Mining (W. J. Herb)
Water monitoring—coal mining (W. J. Herb)
Western Middle anthracite hydrology (D. J. Growitz)
Tennessee:
Landsat basin characteristics (E. F. Hollyday, w, Nashville)
Water monitoring, coal mining (V. J. May, w, Nashville)
Utah (w, Salt Lake City):
Ferron sandstone, Castle Valley (G. C. Lines)
Huntington coal hydrology (T. W. Danielson)
Price River basin (K. M. Waddell)
Water monitoring—coal mining (G. C. Lines)
Virginia:
Geochemistry of mine drainage (P. W. Hufschmidt, w, Richmond)
Ground-water coal mining (H. T. Hopkins, w, Richmond)
Water monitoring—coal mining (P. M. Frye, w, Richmond)
Washington:
Midnite mine quality water (N. P. Dion, w, Tacoma)
Western Washington coal network (L. A. Fuste, w, Tacoma)
West Virginia (w, Charleston):
Deep-mine collapse hydrology (W. H. Hobba)
Effects of deep mining in West Virginia (J. W. Borchers, w, Charleston)
Quantitative mine-water studies (G. G. Wyrick)
Water monitoring—coal mining (T. A. Elke)
Wyoming, water monitoring coal mining (J. R. Schuetz w, Cheyenne)

Mineral and fuel resources—compilations and topical studies:
- Acid-altered volcanogenic mineral deposits, Eastern United States (R. W. Luce, NC)
- Application massive sulfides, Virginia deposits (J. E. Gair, NC)
- Arctic mineral-resource investigations (R. M. Chapman, M)
- Basin and Range, geologic studies (F. G. Poole, D)
- Colorado Plateau (R. P. Fischer, D)
- Geochemistry of Central Region Wilderness Study Areas (J. C. Antweiler, D)
- Geology and resources of zirconium and hafnium (M. E. Paidakovich, NC)
- Information bank, computerized (J. A. Calkins, NC)
- Mineral-resource surveys:
  - Mineral resource estimation (W. D. Menzie, M)
  - Mineral resources of Precambrian rocks in St. Lawrence County, New York (C. E. Brown, NC)
  - Minerals for energy production (L. F. Rooney, NC)
  - Primitive, Wilderness, and RARE II Areas:
    - Arnold Mesa, Arizona (E. W. Wolfe, Flagstaff)
    - Beaver Creek, Kentucky (K. J. Englund, NC)
    - Beaver Creek Wilderness and Troublesome RARE II, Kentucky (K. J. Englund, NC)
    - Big Sandy-W. Elliotts Creek RARE II, Alabama (S. H. Patterson, NC)
    - Bob Marshall Wilderness Area, Montana (R. L. Earhart, D)
    - Caney Creek Wilderness, Arkansas (G. E. Erickson, NC)
    - Cheat Mountain RARE II, West Virginia (K. J. Englund, NC)
    - Cohutta Wilderness, Georgia-Tennessee (J. E. Gair, NC)
    - Cornplanter RARE II, Pennsylvania (F. G. Lesure, NC)
    - Devils Fork RARE II, Virginia (K. J. Englund, NC)
    - Dolly Ann RARE II, Virginia (F. G. Lesure, NC)
    - Eagle Rock Study Area (RARE II), Washington (R. W. Tabor; V. A. Frizzell, Jr., M)
    - Elk Creek-Black-Butte RARE II, California (R. J. McLaughlin, M)
    - Elkhorn Wilderness Study Area, Montana (W. R. Greenwood, D)
    - Ellicott Rock Wilderness, South Carolina-North Carolina-Georgia (R. W. Luce, NC)
    - Florida RARE II (S. H. Patterson, NC)
    - Fossil Springs, Arizona (G. W. Weir, Flagstaff)
    - Gates of the Mountains Wilderness Area, Montana (M. W. Reynolds, D)
    - Gee Creek Wilderness, Tennessee (J. E. Epstein, NC)
    - Glacier Bay National Monument Wilderness Area, Alaska (D. A. Brew, M)
    - Illinois RARE II (J. S. Klasner, Macomb, Ill.)
    - James River Face Wilderness Area, Virginia (C. E. Brown, NC)
    - John Muir Wilderness, California (N. K. Huber, M)
    - King Range—Chemise Mountains, California (R. J. McLaughlin, M)
    - Linville Gorge Wilderness, North Carolina (J. P. D'Agostino, NC)
    - Little Frog RARE II, Tennessee (E. R. Force, NC)
    - Los Padres Study Areas RARE II, California (V. A. Frizzell, Jr., M)
    - Madison—Gallatin Study Area, Montana (F. S. Simons, D)
    - Mazatzal Wilderness, Arizona (C. T. Wrucke and C. M. Conway, M)

Mineral and fuel resources—compilations and topical studies—Continued
- Mineral-resource survey—Continued
  - Primitive, Wilderness, and RARE II Areas—Continued
    - Monte Cristo Study Area RARE II, Washington (R. W. Tabor; V. A. Frizzell, Jr., M)
    - Mount Hood and Zigzag Wilderness Areas, Oregon (T. E. C. Keith M)
    - Mount Raymond RARE II Wilderness Study Area, California (N. K. Huber, M)
    - North Georgia RARE II (A. E. Nelson, NC)
    - Otter Creek Wilderness, West Virginia (K. J. Englund, NC)
    - Pecos Wilderness, New Mexico (R. H. Moench, D)
    - Pennsylvania RARE II (S. P. Schweinfurth, NC)
    - Polvadera and Caballo proposed Wilderness Areas (Kim Manley, D)
    - Rawah Wilderness Area and nearby study areas, Colorado (R. C. Pearson, D)
    - Sandy Creek RARE II, Mississippi (E. G. A. Weed, NC)
    - Selway-Bitterroot Wilderness, Idaho and Montana (W. R. Greenwood, D)
    - Shinbone-Adams Creek RARE II, Alabama (G. E. Tolbert, NC)
    - Shining Rock Wilderness, North Carolina (F. G. Lesure, NC)
    - Sipsey River, Alabama (S. P. Schweinfurth, NC)
    - Sipsey River Wilderness and RARE II Additions, Alabama (S. P. Schweinfurth, NC)
    - Snow Mountain Wilderness Area, California (D. Grimes, D)
    - Snowy Range Wilderness Study Area, Wyoming (R. S. Houston, D)
    - Southern Massanutten RARE II, Virginia (F. G. Lesure, NC)
    - Superstition Wilderness, Arizona (D. W. Peterson, D)
    - Teton Wilderness, Wyoming (J. C. Antweiler, D)
    - Vermont Wilderness and RARE II (J. F. Slack, NC)
    - Washakie Wilderness, Wyoming (J. C. Antwiler, D)
    - West Chichagof-Yakobi Wilderness Study Area, Alaska (B. R. Johnson, M)
    - West Clear Creek, Arizona (G. E. Ulrich, Flagstaff)
    - Williams Fork RARE II, Colorado (P. K. Theobald, D)
    - Wonder Mountain Study Area RARE II, Washington (R. W. Tabor, M)
- Nonmetallic deposits, mineralogy (B. M. Madsen, M)
- Oil and gas resources:
  - Central and northern California Continental Shelf (C. W. Spencer, D)
  - Outer Continental Shelf (R. B. Powers, E. W. Scott, D)
  - Permian Basin (G. L. Dolton, S. E. Frezon, Keith Robinson, A. B. Coury, K. L. Varnes, D)
  - Petroleum potential of southern California borderland appraised (C. W. Spencer, D)
- Resources and geology of nickel and cobalt (M. P. Foose, NC)
- Sand and gravel availability studies (W. H. Langer; D. L. Belval, NC)
- Wilderness Program:
  - Geochemical services (D. J. Grimes, D)
  - Geophysical services (M. F. Kane, D)

States:

Alaska (M):
- AMRAP Circle (H. L. Foster; W. D. Menzie)
- AMRAP Program (J. E. Case)
- Mineral resources (E. H. Cobb)

Mineral and fuel resources—compilations and topical studies—Continued
States—Continued
Alaska—Continued
Petersburg quadrangle (D. A. Brew)
Southwestern Brooks Range (I. L. Tailleur)
Arizona, Geochemical exploration, Ajo 2° quadrangle (P. K. Theobald, D)
Colorado:
Precambrian sulfide deposits (D. M. Sheridan, D)
Summitville district, alteration study (R. E. Van Loenen, D)
Missouri, Rolla 2° quadrangle, mineral-resource appraisal (W. P. Pratt, D)
Montana, Butte 1°×2° quadrangle, geochemistry (J. C. Antweiler, D)
Nevada, igneous rocks and related ore deposits (M. L. Silberman, M)
United States:
Central States, mineral-deposit controls (A. V. Heyl, Jr., D)
Iron-resources studies (Harry Klemic, NC)
Lightweight-aggregate resources (A. L. Bush, D)
Metallogenic maps (P. W. Guild, NC)
Northeastern States, peat resources (C. C. Cameron, NC)
Southeastern States, mineral-resource surveys (R. A. Laurence, Knoxville, Tenn.)
Wisconsin, northern, mineral-resource survey (C. E. Dutton, Madison)
See also specific minerals or fuels.

Mineral resource investigations—resource information systems and analysis:
Computer-based mineral and energy resource system for the Navajo Tribe (J. D. Bliss, M)
Computerized coal resource assessments (A. L. Medlin, NC)
CUSMAP Program (W. D. Grundy, D)
Economics of mineral resources (J. H. DeYoung, Jr., NC)
Energy resource studies (R. F. Meyer, NC)
Geologic database management (R. W. Bowen, NC)
Metallogenic map of North America (P. W. Guild, NC)
Mineral Data System (MDS) (J. A. Calkins, NC)
Mineral scarcity model development (S. M. Cargill, NC)
Petroleum resource appraisal and discovery process modeling (L. J. Drew, NC)
Resource analysis (E. D. Attanasi, NC)
Resource assessment (D. W. Menzie, M)
Resource assessment methods (D. A. Singer, M)
Statistical analysis of mineral assessment data (J. T. Hanley, NC)
United States and world mineral resource assessments, physical factors that could restrict mineral supply (J. H. DeYoung, Jr., NC)
Uranium resource analysis (R. B. McCammon, NC)

Mineralogy and crystallography, experimental:
Crystal chemistry (Malcolm Ross, NC)
Crystal structure, sulfides (H. T. Evans, Jr., NC)
Electrochemistry of minerals (Motoaki Sato, NC)
Mineralogic services and research (R. C. Erd, M)
Mineralogical crystal chemistry (J. R. Clark, M)
Mineralogy of heavy metals (F. A. Hildebrand, D)
Planetary mineralogical studies (Priestley Toulmin III, NC)
Research on ore minerals (B. F. Leonard, D)
See also Geochemistry, experimental.
Geochemistry (George Phair, NC)
Niobium:
Colorado, Wet Mountains (R. L. Parker, D)
Niobium and tantalum, distribution in igneous rocks (David Gottfried, NC)

Mineralogy and crystallography, experimental—Continued
Niobium—Continued
Phosphoria Formation, stratigraphy and resources (R. A. Gulbrandsen, M)
Nonpegmatic lithium resources (J. D. Vine, D)
Rare-earth elements, resources and geochemistry (J. W. Adams, D)
Trace-analysis methods, research (F. N. Ward, D)

Model studies, geologic and geophysical:
Computer modeling:
Research for engineering geology (W. Z. Savage, D)
Rock-water interactions (J. L. Haas, Jr., NC)
Tectonic deformation (J. H. Dieterich, M)
Ice Ages (D. P. Adam, M)

Model studies, hydrologic:
Alluvial fan deposition (W. E. Price, w, D)
Atchafalaya River basin model (M. E. Jennings, w, Bay St. Louis, Miss.)
Chattahoochee intensive river quality (R. N. Cherry, w, Atlanta, Ga.)
Deterministic surface water models (M. E. Jennings, w, Bay St. Louis, Miss.)
High Plains aquifer study (J. B. Weeks, w, D)
Hydrodynamics of a tidal estuary (R. T. Cheng, w, M)
Information on planning models (I. C. James, w, NC)
Modeling of hydrodynamic systems (R. W. Schaffranek, w, NC)
Nevada Test Site hydrologic model (R. K. Waddell, w, D)
Numerical simulation (V. C. Lai, w, NC)
Physical modeling (V. R. Schneider, w, Bay St. Louis, Miss.)
Potomac estuary hydrodynamics (R. W. Schaffranek, w, NC)
Rainfall-runoff modeling (G. H. Leavesley, w, D)
Regional Studies Coordination (G. D. Bennett, w, NC)
Simulation of hydrogeologic systems (R. L. Cooley, w, D)
Surface-water-quality modeling (S. M. Zand, w, M)
Systems Analysis Laboratory (I. C. James, w, NC)
Transient flow (C. E. Mongan, w, Cambridge, Mass.)
Transport in fluid flow (Akio Ogata, w, M)
Water-quality modeling (D. B. Grove, w, D)
States:
Alabama, Southeast regional aquifer study (M. E. Davis, w, Tuscaloosa)
Arizona:
Coconino aquifer—Apache County, Arizona (P. P. Ross, w, Phoenix)
Southwest alluvial basins (T. W. Anderson, w, Tucson)
Arkansas (w, Little Rock):
Illinois River model (C. T. Bryant)
Quachita River model (C. T. Bryant, w, Little Rock)
Stream water-quality modeling (C. T. Bryant, w, Little Rock)
California:
Develop ground-water models, Salinas Valley (M. J. Johnson, w, M)
Digital model of Carmel Valley (M. J. Johnson, w, M)
Ground water, Model Fresno County (H. T. Mitten, w, Sacramento)
Impact of Marble Cone Fire (K. W. Lee, w, M)
Sacramento Valley ground water (S. K. Sorenson, w, Sacramento)
Colorado:
Black Squirrel model (J. L. Hughes, w, Pueblo)
Closed basin (G. J. Leonard, w, Pueblo)
Geochemical investigation (R. L. Tobin, w, D)
Rocky Mountain Arsenal DIMP contamination (S. G. Robson, w, D)

Model studies, hydrologic—Continued
States—Continued
Colorado—Continued
San Luis Valley modeling (G. J. Leonard, w, Pueblo)
Streamflow simulation (R. S. Parker, w, D)
Traveltime and transit losses (P. O. Abbott, w, Pueblo)
Water management—High Plains (R. G. Borman, w, D)
Delaware:
Coastal aquifers study (A. L. Hodges, Jr., w, Dover)
Delaware Potomac aquifer study (M. M. Martin, w, Dover)
Florida:
Estuarine hydrology Tampa Bay model (C. R. Goodwin, w, Tampa)
Ground water, Ft. Lauderdale (Ellis Donsky, w, Miami)
Hydrologic effects, west-central Florida (D. M. Johnson, w, Tampa)
Hydrology of mining areas southwest Florida (W. R. Murphy, Jr., w, Tampa)
Low flow in southwest Florida (K. M. Hammett, w, Tampa)
North Tampa regional model (C. B. Hutchinson, w, Tampa)
Southeast limestone, east-central Florida (C. H. Tibbals, w, Orlando)
Southeast limestone, west-central Florida (P. D. Ryder, w, Tampa)
Water resources, Ft. Walton Beach area (L. R. Hayes w, Tallahassee)
Georgia (w, Doraville):
Coastal Plain sand aquifer study (R. E. Faye, w, Doraville)
Cretaceous-Tertiary Aquifer (L. D. Pollard)
Ground water models (H. E. Gill)
Principal artesian aquifer (L. R. Hayes)
Idaho, Rathdrum Prairie aquifer (H. R. Seitz, w, Boise)
Indiana (w, Indianapolis), Logansport ground-water study (D. C. Gillies)
Kansas:
Central Midwest aquifer study (C. H. Baker, w, Lawrence)
Ground water-surface water, north-central Kansas (L. E. Stullken, w, Garden City)
Ground water pumping effect on Arkansas River (R. A. Barker, w, Garden City)
High Plains aquifer study (J. S. Rosenshein, w, Lawrence)
Streamflow models (P. R. Jordon, w, Lawrence)
Louisiana, Hydrology of Pearl River basin (F. N. Lee, w, Baton Rouge)
Maine, Surface water network (R. A. Morrill, w, Augusta)
Maryland (w, Towson):
Aquia-Piney Point-Nanjemoy aquifers (F. H. Chapelle)
Coastal Plain aquifers, Maryland-Delaware (W. B. Fleck, w, Towson)
Ground water from Maryland coastal plain (W. B. Fleck)
Potomac Reservoir release routing (D. H. Carpenter, w, Towson)
Small basin modeling (R. E. Wiley)
Massachusetts:
De-icing chemicals, ground water (L. R. Frost, w, Boston)
Mattapoisett aquifer study (M. H. Frimpter, w, Boston)
Otis plume model (D. R. LeBlanc, w, Boston)
Minnesota, Evaluation of quality-of-water, data for management (M. S. McBride, w, St. Paul)
Mississippi:
Ground water model—Yazoo River navigation (J. M. Kernodle, w, Jackson)
Modeling of Tupelo ground-water system (J. M. Kernodle w, Jackson)

Model studies, hydrologic—Continued
States—Continued
Mississippi—Continued
Southeast regional aquifer study, Mississippi-Alabama (L. E. Carroon, w, Jackson)
Montana, Tongue River salinity model (P. F. Woods, w, Helena)
Nebraska, High Plains aquifer study (R. A. Pettijohn, w, Lincoln)
Nevada (w, Carson City):
Eagle Valley ground-water model (F. E. Artega)
Jones-Galena Creek water resources (T. L. Katzer)
Las Vegas Valley ground-water models (David Morgan)
New Jersey (w, Trenton), Regional aquifer study, (O. S. Zapecza, w, Trenton)
New Mexico:
High Plains aquifer study (D. R. Hart, w, Albuquerque)
High Plains study, Lea County (D. P. McAda, w, Albuquerque)
New York:
Chemical weathering model (N. E. Peters, w, Albany)
Flow routing—Upper Susquehanna (T. J. Zembrzuski, w, Albany)
Ground water models, Long Island (T. E. Reilly, w, Syosset)
Ground water-surface water interaction (M. P. Bergeron, w, Ithaca)
Hudson River estuary flow model (D. A. Stedfast, w, Albany)
Impact and mitigation of sewering (Bronius Nemickas, w, Syosset)
Regional aquifer study, Long Island (M. S. Garber, w, Syosset)
Tioughnioga River ground water (O. J. Cosner, w, Albany)
North Carolina, Coastal Plain aquifer study (R. W. Coble, w, Raleigh)
North Dakota, Surface water modeling, Fort Union coal region (D. G. Emerson, w, Bismarck)
Ohio:
Franklin County digital model (A. C. Razem, w, Columbus)
Ground water evaluation of Geauga County (A. C. Razem, w, Columbus)
Ground-water hydrology, strip-mining areas (A. C. Razem, w, Columbus)
Oklahoma (w, Oklahoma City):
Coal Creek basin, (S. P. Blumer)
Great Salt Plains study (J. E. Reed)
High Plains aquifer study (J. S. Havens)
North Canadian hydrology (R. E. Davis)
North Canadian hydrology, phase 2 (S. C. Christenson, w, Oklahoma City)
Oregon:
Portland Well Field Model (J. E. Luzier, w, Portland)
Umatilla structural basin model (A. Zurawski, w, Portland)
Pennsylvania (w, Harrisburg):
Delaware River streamflow model (J. O. Shearman)
Laurel Run Dam failure (J. R. Armbruster)
West Branch Brandywine Creek stormwater model (R. A. Sloto, w, Malvern)
West Branch flow-routing (S. A. Brua, w, Harrisburg)
South Carolina, Coastal Plain sand aquifer study (R. N. Cherry, w, Columbia)
South Dakota:
Digital model, James River basin (L. K. Kuiper, w, Huron)
Digital model, Minnehaha County (N. C. Koch, w, Huron)
Water resources of Big Sioux Valley (N. C. Koch, w, Huron)

Model studies, hydrologic—Continued
States—Continued
Tennessee:
Hydrologic process model, coal basins (W. P. Carey, w, Nashville)
Memphis ground-water model (J. V. Brahana, w, Nashville)
Texas:
High Plains Aquifer Study (I. D. Yost, w, Austin)
Miocene aquifer study (E. T. Baker, Jr., w, Austin)
Utah, Hydrology of Beryl-Enterprise area (R. W. Mower, w, Salt Lake City)
Virginia, Coastal Plain aquifers, (J. F. Harsh, w, Richmond)
Washington (w, Tacoma):
Columbia River basalt model (D. B. Sapik)
Spokane drainfield study (E. L. Bolke)
Wisconsin (w, Madison):
Lake Winnebago digital model (W. R. Krug)
Land-use changes, southwest Wisconsin, (W. R. Krug)
Nonpoint pollution in Fox basin (P. E. Hughes)
Wyoming, Digital model, La Grange area (W. B. Borchert, w, Cheyenne)

Molybdenum. *See* Ferro-alloy metals.

Moon studies. *See* Extraterrestrial studies.

Nickle. *See* Ferro-alloy metals.

Nuclear explosions, geology, Engineering geophysics, Nevada Test Site (R. D. Carroll, D)

Oil shale:
East-central Uinta Basin (G. N. Pipiringos, D)
Organic geochemistry (R. E. Miller, D)
Petrology (J. R. Dyni, D)
Regional geochemistry (W. E. Dean, Jr., D)
Stratigraphic studies, eastern Uinta Basin (W. B. Cashion, Jr., D)
Trace elements (W. E. Dean, Jr., D)
States:
Colorado (D):
Central Roan Cliffs area (W. J. Hall)
Lower Yellow Creek area (W. J. Hall)
Piceance Creek basin:
East-central (R. B. O'Sullivan)
General (J. R. Donnell)
Northwestern (G. N. Pipiringos)
Stratigraphy of the Green River Formation (R. C. Johnson, D)
Colorado-Utah-Wyoming, geochemistry (W. E. Dean, Jr., D)
Colorado-Wyoming, Eocene rocks (H. W. Roehler, D)
Nevada, Investigations of oil shale of Tertiary age (B. Solomon, c, M)
Utah, South ½ Nutters Hole quadrangle (W. B. Cashion, Jr., D)

Paleobotany, systematic:
Diatom studies (G. W. Andrews, NC)
Floras:
Cenozoic:
Pacific Northwest (J. A. Wolfe, M)
Western United States and Alaska (J. A. Wolfe, M)
Devonian (J. M. Schopf, Columbus, Ohio)
Paleozoic (S. H. Mamay, NC)
Fossil wood and general paleobotany (R. A. Scott, D)
Modern seeds, California (J. A. Wolfe, D. P. Adam, M)
Plant microfossils:
Mesozoic (R. H. Tschudy, D)
Paleozoic (R. M. Kosanke, D)

Paleoclimatology:
California, Southwestern Great Basin (G. I. Smith, M)

Paleoecology:
Faunas, Late Pleistocene, Pacific coast (W. O. Addicott, M)
Fish, Quaternary, California (R. Casteel, D. P. Adam)
Foraminifera, ecology (M. R. Todd, NC)
Insects, Quaternary, Alaska (R. E. Nelson, Seattle)
Ostracodes, Recent, North Atlantic (J. E. Hazel, NC)
Paleoenvironmental studies, Miocene, Atlantic Coastal Plains (T. G. Gibson, NC)
Pollen, Quaternary, Alaska (R. E. Nelson, Seattle)
Pollen, Quaternary, California (D. P. Adam, M)
Tempskya, Southwestern United States (C. B. Read, Albuquerque, N. Mex.)
Vertebrate faunas, Ryukyu Islands, biogeography (F. C. Whitmore, Jr., NC)

Paleontology, invertebrate, systematic:
Brachiopods:
Carboniferous (Mackenzie Gordon, Jr., NC)
Ordovician (R. B. Neuman, NC; R. J. Ross, Jr., D)
Upper Paleozoic (J. T. Dutro, Jr., NC)
Bryozoans, Ordovician (O. L. Karklins, NC)
Cephalopods:
Cretaceous (D. L. Jones, M)
Jurassic (R. W. Imlay, NC)
Upper Cretaceous (W. A. Cobban, D)
Upper Paleozoic (Mackenzie Gordon, Jr., NC)
Chitinozoans, Lower Paleozoic (J. M. Schopf, Columbus, Ohio)
Conodonts, Devonian and Mississippian (C. A. Sandberg, D)
Corals, rugose:
Mississippian (W. J. Sando, NC)
Silurian-Devonian (W. A. Oliver, Jr., NC)
Foraminifera:
Fusuline and orbitoline (R. C. Douglass, NC)
Cenozoic (M. R. Todd, NC)
Cenozoic, California and Alaska (P. J. Smith, M)
Mississippian (B. A. Skipp, D)
Recent, Atlantic shelf (T. G. Gibson, NC)
Gastropods:
Mesozoic (N. F. Sohl, NC)
Miocene-Pliocene, Atlantic coast (T. G. Gibson, NC)
Paleozoic (E. L. Yochelson, NC)
Graptolites, Ordovician-Silurian (R. J. Ross, Jr., D)
Mollusks, Cenozoic, Pacific coast (W. A. Addicott, M)
Ostracodes:
Lower Paleozoic (J. M. Berdan, NC)
Upper Cretaceous and Tertiary (J. E. Hazel, NC)
Upper Paleozoic (I. G. Sohn, NC)
Pelecypods:
Inoceramids (D. L. Jones, M)
Jurassic (R. W. Imlay, NC)
Paleozoic (John Pojeta, Jr., NC)
Triassic (N. J. Silberling, M)
Trilobites, Ordovician (R. J. Ross, Jr., D)

Paleontology, stratigraphic:
Cenozoic:
Diatoms, Great Plains, nonmarine (G. W. Andrews, NC)
Foraminifera, smaller, Pacific Ocean and islands (M. R. Todd, NC)
Mollusks:
Atlantic coast, Miocene (T. G. Gibson, NC)
Pacific coast, Miocene (W. O. Addicott, M)
Pollen and spores, Kentucky (R. H. Tschudy, D)

Paleontology, stratigraphic—Continued
Cenozoic—Continued
Vertebrates:
Atlantic coast (F. C. Whitmore, Jr., NC)
Pacific coast (C. A. Repenning, M)
Panama Canal Zone (F. C. Whitmore, Jr., NC)
Pleistocene (G. E. Lewis, D)
Mesozoic:
Pacific coast and Alaska (D. L. Jones, M)
Cretaceous:
Alaska (D. L. Jones, M)
Foraminifera:
Alaska (H. R. Bergquist, NC)
Atlantic and Gulf Coastal Plains (H. R. Bergquist, NC)
Pacific coast (R. L. Pierce, M)
Gulf coast and Caribbean (N. F. Sohl, NC)
Molluscan faunas, Caribbean (N. F. Sohl, NC)
Western Interior United States (W. A. Cobban, D)
Jurassic, North America (R. W. Imlay, NC)
Triassic, marine faunas and stratigraphy (N. J. Silberling, M)
Paleozoic:
Devonian and Mississippian conodonts, Western United States (C. A. Sandberg, D)
Fusuline Foraminifera, Nevada (R. C. Douglass, NC)
Mississippian:
Stratigraphy and brachiopods, northern Rocky Mountains and Alaska (J. T. Dutro, Jr., NC)
Stratigraphy and corals, northern Rocky Mountains (W. J. Sando, NC)
Mississippian biostratigraphy, Alaska (A. K. Armstrong, M)
Onesquethaw Stage (Devonian), stratigraphy and rugose corals (W. A. Oliver, NC)
Ordovician:
Bryozoans, Kentucky (O. L. Karklins, NC)
Stratigraphy and brachiopods, Eastern United States (R. B. Neuman, NC), Western United States (R. J. Roxx, Jr., D)
Paleobotany and coal studies, Antarctica (J. M. Schopf, Columbus, Ohio)
Palynology of cores from Naval Petroleum Reserve No. 4 (R. A. Scott, D)
Pennsylvanian:
Fusulinidae:
Alaska (R. C. Douglass, NC)
North-central Texas (D. A. Myers, D)
Spores and pollen, Kentucky (R. M. Kosanke, D)
Permian, floras, Southwestern United States (S. H. Mamay, NC)
Silurian-Devonian:
Corals, Northeastern United States (W. A. Oliver, Jr., NC)
Upper Silurian-Lower Devonian, Eastern United States (J. M. Berdan, NC)
Subsurface rocks, Florida (J. M. Berdan, NC)
Upper Paleozoic, Western States (Mackenzie Gordon, Jr., NC)

Paleontology, vertebrate, systematic:
Artiodactyls, primitive (F. C. Whitmore, Jr., NC)
Pinnipedia (C. A. Repenning, M)
Pleistocene fauna, Big Bone Lick, Kentucky (F. C. Whitmore, Jr., NC)
Tritylodonts, American (G. E. Lewis, D)

Paleotectonic maps. *See* Regional studies and compilations.

Petroleum and natural gas:
Automatic data-processing system for field and reservoir estimates (K. A. Yenne, c, Los Angeles, Calif.)
Borehole gravimetry, application to oil exploration (J. W. Schmoker, D)
Catagenesis of organic matter and generation of petroleum (N. H. Bostick, D)
Devonian black shale, Appalachian Basin:
Borehole gravity study (J. W. Schmoker, D)
Clay mineralogy (J. W. Hosterman, NC)
Conodont maturation (A. G. Harris, NC)
Data storage and retrieval system
Geochemical study (G. E. Claypool, D)
Stratigraphy (J. B. Roen, NC)
Structural studies (L. D. Harris, NC)
Uranium and trace-element study (J. S. Leventhal, D)
Geology of the Volga-Ural petroleum province (J. A. Peterson; J. W. Clarke)
Gulf of Mexico, oil and gas resources of the Gulf of Mexico (B. M. Miller, D)
Hydrocarbon source rocks and paleoceanography (M. A. Arthur, D)
Methods of recovery (F. W. Stead, D)
Oil and gas map, North America (W. W. Mallory, D)
Oil and gas resource appraisal methodology and procedures (B. M. Miller, D)
Organic geochemistry (J. G. Palacas, D)
Origin and distribution of natural gases (D. D. Rice, D)
Origin, migration, and accumulation of petroleum (L. C. Price, D)
Petroleum geology and resource appraisal, Southern Mexico and Guatemala (J. A. Peterson)
Petroleum geology of Permian Phosphoria and Park City Formations (J. A. Peterson)
Petroleum prospecting with helium detector (A. A. Roberts, D)
Petrology of organic matter in sedimentary rocks (N. H. Bostick, D)
Rocky Mountain States, seismic detection of stratigraphic traps (R. T. Ryder, D)
Tight gas sands (D. D. Rice, D)
Western Interior Cretaceous studies (C. W. Spencer, D)
Western United States:
Devonian and Mississippian (C. A. Sandberg, D)
Devonian and Mississippian flysch source-rock studies (F. G. Poole, D)
Properties of reservoir rocks (R. F. Mast, D)
Source rocks of Permian age (E. K. Maughan, D)
States:
Alaska (M):
Cook Inlet (L. B. Magoon III)
Northeastern Arctic Slope Federal-State field project (I. F. Palmer, c, Anchorage)
NPRA (National Petroleum Reserve Alaska) Oil and Gas Source Rock Study (L. B. Magoon III, M)
Petroleum assessment geology, North Slope provinces (K. J. Bird, M)
Arkansas, Sandstone reservoirs (B. R. Haley, Little Rock)
California:
Carpenteria and Hondo-Santa Ynez field reserves, OCS (D. G. Griggs, c, Los Angeles)
Eastern Los Angeles basin (T. H. McCulloh, Seattle, Wash.)
Salinas Valley (D. L. Durham, M)
Southern San Joaquin Valley, subsurface geology (J. C. Maher, M)

Quality of water—Continued
- Radioanalytical methods (L. L. Thatcher, w, D)
- Radiohydrology of explosion sites (W. E. Wilson, w, D)
- Radionuclide migration at Nevada Test Site (H. C. Claassen, w, D)
- Radionuclides on sediments (D. D. Gonzalez, w, D)
- Standard reference water sample program (M. J. Fishman, w, D)
- Techniques of water resources investigations support (M. J. Fishman, w, D)
- Thermal modeling (H. E. Jobson, w, Bay St. Louis, Miss.)
- Thermal pollution (G. E. Harbeck, Jr., w, D)
- Toxic substances in aquatic ecosystems (H. V. Leland, w, M)
- Trace-element availability in sediments (S. N. Luoma, w, M)
- Transition metal hydrogeochemistry (Edward Callender, w, NC)
- Transport in ground water (L. F. Konikow, w, D)
- Transport modeling, saturated zone (L. F. Konikow, w, NC)
- Transuranium research (J. M. Cleveland, w, D)
- Turbulent diffusion and thermal loading (Nobuhiro Yotsukura, w, NC)
- Waste management off Nevada Test site (J. E. Weir, w, D)
- Water quality analysis—other federal agencies (J. P. Monis, w, D)
- Water quality and health (G. L. Feder, w, D)
- Water-quality-data evaluation (W. H. Doyle, Jr., w, D)
- *States and territories:*
- Alaska:
  - Arctic lakes (G. A. McCoy, w, Anchorage)
  - Healy trace metals (D. R. Wilcox, w, Fairbanks)
- Arizona:
  - Ground-water, Little Colorado basin (S. G. Brown, w, Tucson)
  - Papago-arsenic in drinking water (L. J. Mann, w, Tucson)
- Arkansas (w, Little Rock), Soil Conservation Service watershed studies (J. C. Petersen)
- California:
  - Ground-Water Quality Inventory (G. L. Faulkner, w, M)
  - Ground-water quality, Livermore-Amador Valley (M. A. Sylvester, w, M)
  - New River water quality (J. G. Setmire, w, Laguna Niguel)
  - Nitrogen isotope study (P. Martin, w, Laguna Niguel)
  - Quality of water, California streams (W. L. Bradford, w, M)
  - San Francisco Bay urban study (R. D. Brown, M)
  - Santa Barbara ground water (Peter Martin, w, Laguna Niguel)
  - Stovepipe wells contamination (A. Buono, w, Laguna Niguel)
  - Water quality studies design-National Park Service (W. L. Bradford, w, M)
  - Water resources Upper Coachella (Anthony Buono, w, Laguna Niguel)
- Colorado (w, D, except as otherwise noted):
  - Acid-rain study (J. T. Turk, w, D)
  - Aquatic biology of Piceance Creek (K. J. Covay, w, Meeker)
  - Colorado landfills (J. T. Turk)
  - Colorado River salinity (K. E. Goddard, w, Grand Junction)
  - Effects of sludge basins on ground water (S. G. Robson)
  - Energy development, stream quality (L. J. Britton, w, D)
  - Hayden powerplant study (R. L. Tobin, w, Meeker)
  - In-situ uranium mining (J. W. Warner)
  - Nitrogen levels, San Luis Valley (P. F. Edelmann, w, Pueblo)
  - Northwestern Colorado, water quality (T. R. Ford, w, Meeker)
  - Oil shale methods development (D. J. Ackermann, w, Grand Junction)
  - Pueblo County 208 (D. L. Cain, w, Pueblo)

Quality of water—Continued
- *States and territories—Continued*
- Colorado—Continued
  - Quality of water characteristics of Colorado streams (M. W. Gaydos)
  - Sediment chemistry (J. T. Turk)
  - Upper Colorado energy impacts (T. D. Steele)
  - Water quality, Jefferson County (D. C. Hall)
- Connecticut:
  - Changes in ground-water quality (E. H. Handman, w, Hartford)
  - PCB in the Housatonic River (K. P. Kulp, w, Hartford)
- Delaware, Thermal regimen, water-table aquifer (A. L. Hodges, Dover)
- Florida:
  - Apalachicola River quality (H. C. Mattraw, w, Tallahassee)
  - Aquifer pollution, Lake County (G. F. Taylor, w, Orlando)
  - Bay-aquifer interconnection (C. B. Hutchinson, w, Tampa)
  - Bridge runoff quality of water assessment (D. McKenzie, w, Miami)
  - Geohydrology of drainage wells (G. R. Schiner, w, Orlando)
  - Ground-water quality, Dade County (D. J. McKenzie w, Miami)
  - Hydrogeochemistry, Florida phosphate (P. R. Seaber, w, Tallahassee)
  - Intensive quality of water surveys (J. E. Coffin, w, Tallahassee)
  - Lakes Faith, Hope, and Charity (E. R. German, w, Orlando)
  - Long-term trend analysis surface water (F. A. Watkins, w, Fort Myers)
  - Radionuclides in ground water (Horace Sutcliffe, Jr., w, Sarasota)
  - Salt water interface, southwest Florida (K. W. Causseaux, w, Tampa)
  - Salt water intrusion, Cape Coral (D. J. Fitzpatrick, w, Fort Myers)
  - Southeast spray field, Tallahassee (M. C. Yurewicz, w, Tallahassee)
  - Subsurface waste storage (John Vecchiolis, w, Tallahassee)
  - Traffic related contaminants (H. C. Mattraw, w, Miami)
  - Wastewater impact on ground water (B. J. Franks, w, Tallahassee)
- Georgia (w, Doraville):
  - Ground water irrigation, southwest Georgia (R. G. Grantham)
  - Quality of water, West Point reservoir (D. B. Radtke)
- Hawaii, monitoring of critical ground-water areas (K. J. Takasaki, w, Honolulu)
- Idaho (w, Boise):
  - Ground water, Michaud Flats (N. D. Jacobson, w, Idaho Falls)
  - Ground-water-quality assessment (H. R. Seitz)
  - Idaho phosphate radiation study (W. H. Low)
  - Water quality of irrigation flows (H. R. Seitz, w, Boise)
- Illinois (w, Champaign):
  - Coal hydrology (G. G. Glysson,w, Champaign)
  - Palos Hills waste burial site (J. C. Olimpio, w, Champaign)
  - Sludge irrigation hydrology (R. F. Fuentes)
  - Sludge storage in strip-mine land (G. L. Patterson)
  - Strip mine hydrology (T. P. Brabets)
- Indiana (w, Indianapolis):
  - Landfill monitoring, Marion County (J. R. Marie)
  - Metals transport in mining areas (W. G. Wilber, w, Indianapolis)
  - Surface-water quality study (M. A. Hardy)

Quality of water—Continued
States and territories—Continued
Puerto Rico (w, San Juan):
Freshening, Cano Tiburones area (A. L. Zack, w, Ft. Buchanan)
Surface impoundents, (J. R. Diaz)
Well monitoring (J. R. Gonzalez, w, Ft. Buchanan)
Rhode Island, Quality of Rhode Island streams (H. E. Johnston, w, Boston, Mass.)
South Carolina (w, Columbia):
Fluoride in ground water, coastal plain (J. M. Rhett)
Ground water data definition at radwaste site (J. M. Cahill)
South Dakota, Geochemical survey Big Sioux aquifer (N. F. Leibbrand, w, Huron)
Tennessee:
Burial-ground studies at Oak Ridge National Laboratory (D. A. Webster, w, Knoxville)
Chemical character of shallow ground water (W. S. Parks, w, Memphis)
Solute transport, Memphis Sand (J. V. Brahana, w, Nashville)
Texas, Colorado River salinity (Jack Rawson, w, Austin)
Utah (w, Salt Lake City):
Jordan River quality study (R. C. Christensen, w, Salt Lake City)
Reconnaissance of Utah coal fields (K. M. Waddell)
Surface-water quality, Dirty Devil River basin (J. C. Mundorff)
Trace-element transport (B. A. Kimball, w, Salt Lake City)
Water quality, San Rafael River basin (J. C. Mundorff)
Weber River basin water quality (K. R. Thompson)
Vermont, Ground-water quality (R. E. Willey, w, Montpelier)
Virginia:
Coastal plain salt water (J. D. Larson, w, Richmond)
Dredge spoil disposal (J. F. Harsh, w, Richmond)
Washington (w, Tacoma):
Columbia basin demonstration project (P. R. Boucher)
Ground-water-quality network (J. C. Ebbert)
Hydrology of Pine Lake (N. P. Dion)
Quinault ground-water quality (B. W. Dost)
Salt-water intrusion (N. P. Dion)
Spokane ground water quality (E. L. Bolke)
Sulphur Creek program (P. R. Boucher)
Wisconsin (w, Madison):
Bench mark water quality (D. A. Wentz, w, Madison)
Chemical loading to Lake Michigan (C. C. Harr)
Forest County potawatonic (R. A. Lidwin, w, Madison)
Ground-water quality, Waukesha County (J. J. Schiller)
Nederlo Creek biota (P. A. Kammerer, Jr.)
Stream reaeration (L. B. House)
Wyoming (w, Cheyenne):
Herbicides Wyoming streams (J. R. Schuetz)
North Platte reservoirs (S. J. Rucker IV)
Nutrient release, Lake DeSmet (D. J. Wangsness)
Water quality small streams (L. L. Delong, w, Cheyenne)
See also Geochemistry; Hydrologic instrumentation; Hydrology, surface water; Limnology; Marine hydrology; Sedimentology; Water resources.

Quicksilver. *See* Mercury.

Radioactive materials, transport in water. *See* Geochemistry, water.

Radioactive waste disposal:
Favorable radioactive waste disposal areas (W. E. Hale, w, Albuquerque, N. Mex.)
Geomechanics of radioactive waste storage (H. S. Swolfs, D)
Hydrology of nuclear landfill (D. E. Prudic, w, Albany, N.Y.)

Radioactive waste disposal—Continued
Hydrology of salt domes (G. N. Ryals, w, Baton Rouge, La.)
Implications of long-term climate changes (D. P. Adam)
In-situ stress in shales (T. C. Nichols, Jr., D)
Interim storage policy (E-an Zen, NC)
Natural radionuclide systems in crystalline rocks (Z. E. Peterman, D)
Nevada waste coordination (W. S. Twenhofel, D)
Pierre Shale (G. W. Shurr, D)
Radioactive byproducts in salt (J. W. Mercer, w, Albuquerque, N. Mex.)
Radioactive-waste burial (George Debuchananne, w, NC)
Radioactive-waste-burial study (J. M. Cahill, w, Columbia, S. C.)
Radiohydrology technical coordination (George Debuchananne, w, NC)
Radwaste coordination (A. M. Lasala, w, Columbus, Ohio)
Sheffield site investigation (J. B. Foster, w, Champaign, Ill.)
Waste emplacement crystalline rocks in conterminous United States (H. W. Smedes, D)
States:
Idaho, Hydrology of subsurface waste disposal (J. T. Barraclough, w, Idaho Falls)
Illinois:
Ground-water flow Sheffield site (J. B. Foster, w, Champaign)
Sheffield unsaturated flow (J. B. Foster, w, Champaign)
Kentucky, Maxey Flats investigation (R. J. Faust, w, Louisville)
Nevada:
Geologic investigations (G. L. Dixon, D)
Southern Great Basin tectonics and volcanism (W. J. Carr, D)
New Mexico (D):
Eddy and Lea counties, exploratory drilling (C. L. Jones)
Southeastern, waste emplacement (C. L. Jones)
New York, West Valley nuclear storage study (W. M. Kappel, w, Ithaca)
South Carolina, Hydrology study of unsaturated zone (J. M. Cahill, w, Columbia)
See also Geochemistry, water.

Rare-earth metals. *See* Minor elements.

Regional studies and compilations, large areas of the United States:
Appalachians-Caledonides synthesis analysis (R. B. Neuman, Washington, D.C.)
Characterization of crystalline rock terrane (H. W. Smedes and D. J. Gable, D)
Paleotectonic map folios:
Devonian System (E. G. Sable, D)
Mississippian System (L. C. Craig, D)
Pennsylvanian System (E. D. McKee, D)
Physiography of Southeastern United States (J. T. Hack, NC)
Volcanic rocks of the Appalachians (D. W. Rankin, NC)

Remote sensing:
Cartographic applications:
Composite mapping and topographic analysis (D. D. Greenlee, Technicolor Graphics Services, Inc., Sioux Falls, S. Dak.)
Landsat image maps of Cape Cod (R. S. Williams, Jr., I, NC)
Geologic applications:
Airborne and satellite research:
Aeromagnetic studies (M. F. Kane, D)
Bibliography and index of the geological literature of Iceland: 1777-1980 R. S. Williams, Jr., NC)

Remote sensing—Continued
States—Continued
Florida:
Integration of Landsat data and hydrologic data for water management of the Everglades National Park (D. T. Lauer, James Lucas, Technicolor Graphic Services, Inc., l, Sioux Falls, S. Dak.)
Southern, Landsat (A. L. Higer, w, Miami)
Kansas, Mined land hydrology, southeast Kansas (A. M. Diaz, w, Lawrence)
Pennsylvania, COMSAT General Pilot Program (C. D. Kauffman, w, Harrisburg)
Maine, COMSAT Pilot project (J. T. Armbruster, w, Augusta)
Washington, GOES telemetry (E. H. McGavock, w, Tacoma)
Wisconsin, Streamflow estimates using LANDSAT (G. J. Allord, W, Madison)
Land-resource applications:
Application of Landsat albedo change images to arid lands in Mexico (C. J. Robinove, NC)
Application of Landsat to mapping of diversity of archeological sites on NPS lands (C. J. Robinove, NC)
Colorado River natural resources and land use data inventory (H. D. Newkirk, Bureau of Reclamation, Denver, Colo.)
Comparison of Landsat and Seasat data of Yellowstone National Park (A. S. Walker, NC)
Deserts and arid land reclamation in the People's Republic of China (A. S. Walker, NC)
Development of a vegetation terrain shadowing model for correction of Landsat data (J. Otterman, NC)
Development of automatic techniques for land use mapping from remote-sensor data (J. R. Wray, l, NC)
Drought and desertification indicators from Landsat imagery (C. J. Robinove, l, NC)
Forest fire fuels mapping (Mark Shasby, Technicolor Graphic Services, Inc., o, Sioux Falls, S. Dak.)
Land resource analysis using airborne scanner data (R. L. Hanoen, Bureau of Reclamation, D)
Reclamation land use analysis R. L. Hansen, Bureau of Reclamation, D)
Land resource analysis using airborne scanner data (R. L. Hansen, Bureau of Reclamation, D)
Reclamation land use analysis (R. L. Hansen, Bureau of Reclamation, D)
States:
Alaska:
Environmental impact statements for the NPRA (D. Carneggie, Anchorage, Alaska)
Radar evaluation (G. Moore, Sioux Fall, S. Dak.)
Resource assessment in Wrangell—St. Elias National Monument (David Carneggie, l, Anchorage)
Arizona:
Application of Landsat albedo change images to BLM lands in northern Arizona (C. J. Robinove, NC)
Wildland vegetation inventory (W. G. Rohde, Technicolor Graphic Services, Inc., Sioux Falls, S. Dak.)
California, Large-scale photographs for range-trend analysis (D. M. Carneggie, l, Sioux Falls, S. Dak.)
Minnesota, Lineament analysis of imagery of the Mesabi Range, Minnesota (A. S. Walker, NC)
Michigan, Vegetation mapping in the Pictured Rocks National Lakeshore (William Anderson, Technicolor Graphic Services, Inc., l, Sioux Falls, S. Dak.)

Remote sensing—Continued
States—Continued
Washington, Department of Natural Resources forest classification (G. R. Johnson, Technicolor Graphic Services, Inc., l, Sioux Falls, S. Dak.)
Techniques in processing Landsat image data:
Data Analysis Laboratory activity (F. A. Waltz, Technicolor Graphic Services, Inc., Sioux Falls, S. Dak.)
Reservoirs. *See* Evapotranspiration; Sedimentology.
Resource planning analysis:
Designing local water conservation plans workshops (K. A. Fitzpatrick-Lins, o, NC)
Environmental conditions and trends report (K. A. Fitzpatrick-Lins, o, NC)
Environmental conflict management and collaborative problem-solving activities (K. A. Fitzpatrick-Lins; P. A. Marcus; E. T. Smith, o, NC)
Inventory of computer software for spatial data handling (O. Kays, o, NC)
Long-range planning and future research studies (E. T. Smith, o, NC)
Natural resource data management system for water and related land resources planning (O. Kays, o, NC)
Western Coal Planning Assistance Project (W. J. Ulman, o, NC)
States:
All States except Hawaii, Guidebooks on State permit requirements for development of energy and other selected natural resources (W. J. Ulman, o, NC)
Illinois Coal Basin Planning Assistance Project (W. J. Ulman, o, NC)
Rhenium. *See* Minor elements; Ferro-alloy metals.
Saline minerals:
Mineralogy (B. M. Madsen, M)
States:
California, Continental evaporites (G. I. Smith, M)
Colorado and Utah, Paradox Basin (O. B. Raup, D)
New Mexico, Carlsbad potash and other saline deposits (C. L. Jones, M)
Wyoming, Sweetwater County, Green River Formation (W. C. Culbertson, D)
Saltwater intrusion. *See* Marine hydrology; Quality of water.
Sedimentology:
Arctic fluvial processes, landforms (K. M. Scott, w, Laguna Niguel, Calif.)
Bedload-transport research (W. W. Emmett, w, D)
Coon Creek morphology (S. W. Trimble, w, Los Angeles, Calif.)
Estuarine intertidal environments (J. L. Glenn, w, D)
Estuary sedimentation and eutrophication (J. L. Glenn, w, D)
Forest geomorphology, Pacific coast (R. J. Janda, w, M)
Measurement of sediment-laden flows (A. G. Scott, w, NC)
Petrology Laboratory (L. G. Schultz, D)
Potomac estuary transport (J. P. Bennett, w, NC)
Sediment-hillside morphology (G. P. William, w, D)
Sediment impacts from coal mining (W. R. Osterkamp, w, NC)
Sediment movement in rivers (R. H. Meade, Jr., w, D)
Sediment transport model (W. W. Sayre, w, D)
Sediment transport phenomena (D. W. Hubbell, w, D)
States:
Alabama, Hydrology of Warrior coal field (Celso Puento, w, Tuscaloosa)
Alaska:
Coastal environments (A. T. Ovenshine, M)
Hydrology and quality of water of Keta River basin (G. O. Balding, w, Juneau)

Stratigraphy and sedimentation—Continued
States—Continued
Oregon-California black sands (M):
Geologic investigations (H. E. Clifton)
Hydrologic investigations (P. D. Snavely, Jr.)
Utah, Promontory Point (R. B. Morrison, D)
Wyoming, Lamont-Baroil area (M. W. Reynolds, D)
See also Paleontology, stratigraphic; *specific areas under* Geologic mapping.
Structural geology and tectonics:
Central Appalachian tectonics (A. A. Drake, Jr., NC)
Contemporary coastal deformation (R. O. Castle, M)
Rock behavior at high temperature and pressure (E. C. Robertson, NC)
Structural studies, Basin and Range (F. G. Poole, D)
States:
Arizona:
Western tectonics (I. Lucchitta, Flagstaff)
Southeastern tectonics (Harold Drewes, D)
California-Nevada, transcurrent fault analysis, western Great Basin (R. E. Anderson, D)
See also specific areas under Geologic mapping.
Talc:
New York, Pope Mills and Richville quadrangles (C. E. Brown, NC)
Tantalum. *See* Minor elements.
Thorium:
Analytical support (C. M. Bunker, D)
Investigations of thorium in igneous rocks (M. H. Staatz, D)
States:
Colorado (D):
Cochetopa area (J. C. Olson)
Wet Mountains, thorium resources appraisal (T. J. Armbrustmacher)
Wyoming, Bear Lodge Mountains (M. H. Staatz, D)
Titanium:
Rutile in porphyry copper deposits (E. R. Force, NC)
Tungsten. *See* Ferro-alloy metals.
Uranium:
Applied uranium geochemistry (J. N. Rosholt, D)
Exploration techniques:
Geochemical techniques (R. A. Cadigan, D)
Geochemical techniques of halo uranium (J. K. Otton, D)
Morrison Formation (L. C. Craig, D)
Uranium in streams as an exploration technique (K. J. Wenrich-Verbeek, D)
Genesis of a uranium orbody near Crownspoint, New Mexico (R. L. Reynolds; N. S. Fishman, D)
Genesis of tabular uranium deposits on the Colorado Plateau (R. A. Brooks, D)
Geophysics:
Borehole electrical techniques in uranium exploration (J. J. Daniels, D)
Borehole geophysical research in uranium exploration (J. H. Scott, D)
Gamma-ray spectrometry in uranium (J. S. Duval, D)
Gamma-ray spectroscopy for uranium exploration in crystalline terranes (J. A. Pitkin, D)
Geophysical studies relating to uranium deposits in crystalline terranes (D. L. Campbell, D)
Hydrogenochemistry of uranium deposits (C. G. Bowles, D)
Magnetic and mineralogic studies of uranium deposits (R. L. Reynolds, D)
Ore-forming processes (H. C. Granger, D)
Petrophysics (G. R. Olhoeft, D)

Uranium—Continued
Precambrian sedimentary and metasedimentary rocks (F. A. Hills, D)
Radium and other isotopic disintegration products in springs and subsurface water (R. A. Cadigan, J. K. Felmlee, D)
Remote sensing for uranium exploration (G. L. Raines, D)
Remote sensing, Richfield, Utah, 2° sheet (M. H. Podwysocki, NC)
Resources of radioactive minerals (A. P. Butler, Jr., D)
Resources of United States and world (W. I. Finch, D)
Southern High Plains (W. I. Finch, D)
United States:
Eastern:
Appalachian Basin Paleozoic rocks (A. F. Jacob, D)
Basin analysis as related to uranium potential in Triassic sedimentary rocks (C. E. Turner, D)
Uranium vein deposits (R. I. Grauch, D)
Southwestern, basin analysis related to uranium potential in Permian rocks (J. A. Campbell, D)
Western:
Relation of diagenesis and uranium deposits (M. B. Goldhaber, D)
Vein and disseminated deposits of uranium (J. T. Nash, D)
Uranium daughter products in modern decaying plant remains, in soils, and in stream sediments (K. J. Wenrich-Verbeek, D)
Volcanic source rocks (R. A. Zielinski, D)
States:
Alaska, uranium geophysics (J. W. Cady, D)
Arizona-Colorado-New Mexico-Utah, Colorado Plateau (D):
Basin analysis of uranium-bearing Jurassic rocks (Fred Peterson)
Tabular deposits (R. A. Brooks)
Arizona-Nevada-Utah, Uranium potential of Basin and Range province (J. E. Peterson, D)
Colorado (D):
Cochetopa Creek uranium-thorium area (J. C. Olson)
Colorado Plateau (Summary) Report (R. P. Fischer)
Marshall Pass uranium (J. C. Olson)
Schwartzwalder mine (E. J. Young)
Uranium-bearing Triassic rocks (R. D. Lupe)
Colorado-New Mexico-Texas-Utah-Wyoming, Organic chemistry of uranium (J. S. Leventhal, D)
New Mexico (D):
Acoma area (C. H. Maxwell)
Church Rock-Smith Lake (C. T. Pierson)
Crownpoint uranium studies (J. F. Robertson)
North Church Rock (A. R. Kirk)
San Juan Basin uranium (M. W. Green)
Sanostee (A. C. Huffman, Jr.)
Thoreau uranium studies, New Mexico (J. F. Robertson)
South Dakota-Wyoming, Uranium-bearing pipes (C. G. Bowles, D)
Texas:
Coastal plain, geophysical and geological studies (D. H. Eargle, Austin)
Tilden-Loma Alta area (K. A. Dickinson, D)
Uranium disequilibrium studies (F. E. Senftle, NC)
Texas-Wyoming, Roll-type deposits (E. N. Harshman, D)
Utah-Colorado (D):
Moab quadrangle (A. P. Butler, Jr.)
Uinta and Piceance Creek basin (L. C. Craig)
Washington, Midnite uranium mine (J. T. Nash, D)

Uranium—Continued
States—Continued
Wyoming (D):
Badwater Creek (R. E. Thaden)
Crooks Peak quadrangle (L. J. Schmitt, Jr.)
Granite as a source rock of uranium (J. S. Stuckless)
Northeastern Great Divide Basin (L. J. Schmitt, Jr.)
Powder River Basin (E. S. Santos)
Sagebrush Park quadrangle (L. J. Schmitt, Jr.)
Stratigraphic analysis of Tertiary uranium basins of Wyoming (D. A. Seeland)
Stratigraphic analysis of Western Interior Cretaceous uranium basins (H. W. Dodge, Jr.)

Urban geology:
States:
Alaska, Anchorage area (H. R. Schmoll, D)
Arizona, Phoenix-Tucson region resources (T. G. Theodore, M)
California (M, except as otherwise noted):
Coastal geologic processes (K. R. Lajoie)
Flatlands materials and their land use significance (E. J. Helley)
Geologic factors in open space (R. M Gulliver)
Hillside materials and their land use significance (C. M. Wentworth, Jr.)
Pacific Palisades landslide area, Los Angeles (J. T. McGill, D)
Palo Alto, San Mateo, and Montara Mountain quadrangles (E. H. Pampeyan)
Quaternary framework for earthquake studies, Los Angeles Basin (J. C. Tinsley III)
Regional slope stability (T. H. Nilsen)
San Francisco Bay region, environment and resources planning study:
Bedrock geology (M. C. Blake)
Marine geology (D. S. McCulloch)
Open space (C. S. Danielson)
Palo Alto, San Mateo, and Montara Mountain quadrangles (E. H. Pampeyan, M)
San Andreas fault:
Basement studies (D. C. Ross)
Basin studies (J. A. Bartow)
Regional framework (E. E. Brabb)
Tectonic framework (R. D. Brown)
San Mateo County cooperative (H. D. Gower)
Sargent-Berrocal fault zone (R. J. McLaughlin, D. H. Sorg)
Seismicity and ground motion (W. B. Joyner)
Southern:
Eastern part (D. M. Morton, Riverside)
Western part (R. F. Yerkes)
Colorado, Denver urban area, regional geochemistry (H. A. Tourtelot, D)
Georgia, Geochemical map of Savannah (H. A. Tourtelot, D)
Massachusetts, Boston and vicinity (C. A. Kaye, Boston)
Montana, geology for planning, Helena region (R. G. Schmidt, NC)
New York, Engineering geology of New York City (C. A. Baskerville, NC)
Pennsylvania (NC, except as otherwise noted):
Geochemistry of Pittsburgh urban area (H. A. Tourtelot, D)
Susceptibility to landsliding:
Allegheny County (J. S. Pomeroy)
Beaver, Butler, and Washington Counties (J. S. Pomeroy)

Urban geology—Continued
States—Continued
Utah:
Salt Lake City and vicinity (Richard VanHorn, D)
Wasatch Front surficial geology (R. D. Miller, D)
Virginia, Geohydrologic mapping of Fairfax County (A. J. Froelich, NC)
Washington:
Engineering properties of unconsolidated materials in Port Townsend quadrangle (R. D. Miller)
Map showing depth to bedrock in Port Townsend quadrangle (F. Pessl, Jr.; S. A. Safioles)
Slope stability in Port Townsend quadrangle (R. D. Miller)

Urban hydrology:
Analysis of urban flood data in United States (V. B. Sauer, w, Atlanta, Ga.)
Estuarine ecology (R. L. Cory, w, Edgewater, Md.)
Urban runoff networks (H. H. Barnes, Jr., w, NC)
States:
Alaska:
Anchorage geohydrology (Derrill Cowing, w, Anchorage)
Anchorage runoff study (R. S. George, w, Anchorage)
Colorado:
Denver-Boulder metro urban runoff (R. K. Livingston, w, D)
Front Range urban corridor (D. E. Hillier, w, D)
Storm runoff quality, Denver (S. R. Ellis, w, D)
Urban runoff (S. R. Blakely, w, D)
Connecticut:
Connecticut valley urban pilot study (R. L. Melvin, w, Hartford)
Urbanization effect, small streams (L. A. Weiss, w, Hartford)
Florida:
Bay Lake area (E. R. German, w, Orlando)
Detention pond (E. R. German, w, Orlando)
Evaluation of pollution control measures, Pinellas County (M. A. Lopez, w, Tampa)
Leon County (M. A. Franklin, w, Tallahasse)
Small streams flooding (R. D. Hayes, w, Tampa)
Stormwater quality, south Florida (H. C. Mattraw, w, Miami)
Tampa Bay region (M. A. Lopez, w, Tampa)
Hawaii, hydrology, sediment in Mauna Loa (C. J. Ewart, w, Honolulu)
Illinois, Effects of detention ponds on water quality (R. G. Striegl, w, DeKalb)
Kansas:
Urban runoff, Wichita (D. B. Richards, w, Lawrence)
Urban stormwater quality (L. M. Pope, w, Lawrence)
Maryland, Baltimore urban hydrology (B. G. Katz, w, Towson)
Minnesota:
Quality of runoff, Twin Cities area (M. A. Ayers, w, St. Paul)
Water quality assessment, Coon Creek watershed (A. D. Arntson, w, St. Paul)
Missouri:
Stream hydrology, St. Louis (T. W. Alexander, w, Rolla)
Urban runoff in Kansas City (J. H. Barks, w, Rolla)
New Mexico, urban flood hydrology, Albuquerque (J. P. Borland, w, Albuquerque)
New York:
Floods in urbanized basins (R. Lumia, w, Albany)
Irondequoit urban runoff study (W. M. Kappell, w, Ithaca)
Solid waste sites, Suffolk (G. E. Kimmel, w, Mineola)
Urban data transfer (W. M. Kappel, w, Ithaca)
Urban hydrology of Long Island (H. F. Ku, w, Syosset)

Urban hydrology—Continued
States—Continued
North Carolina, Urban hydrology, Coastal Plain (H. C. Gunter, w, Raleigh)
Ohio (R. P. Hawkinson, w, Columbus)
Oregon (W, Portland):
Salem storm-water quality (T. L. Miller)
Salem urban runoff (Antonius Laenen)
Pennsylvania (w, Malvern):
Philadelphia (T. G. Ross)
Storm-water measurements (T. G. Ross)
Urban hydrology, Warminster Township (R. A. Sloto)
South Dakota, Rapid City urban hydrology (K. E. Goddard, w, Rapid City)
Tennessee:
Effects of urbanization on floods and quality of water (F. N. Lee, w, Nashville)
Memphis urban flood frequency (B. L. Neely, w, Memphis)
Texas (w, Fort Worth, except as otherwise noted):
Austin (M. L. Maderak, w, Austin)
Dallas urban study (B. B. Hampton)
Fort Worth urban study (B. B. Hampton)
Houston urban study (Fred Liscum, w, Houston)
San Antonio urban study (Lynn Harmsen, w, San Antonio)
Utah, Salt Lake County urban runoff study (T. Arnow, w, Salt Lake City)
Washington:
Bellevue urban runoff study (W. L. Haushild, w, Tacoma)
Coastal erosion and sediment transport along shorelines in Port Townsend quadrangle (R. F. Kueler)

Vegetation:
Element availability:
Soils (R. C. Severson, D)
Vegetation (L. P. Gough, D)
Elements in organic-rich material (F. N. Ward, D)
Plant geochemistry, urban areas (H. A. Tourtelot, D)
Western coal regions, geochemical survey of vegetation (J. A. Erdman, D)
See also Plant ecology.

Volcanic-terrane hydrology. *See* Artificial recharge.

Volcanology:
Caldron and ash-flow studies (R. L. Smith, NC)
Cascade volcanoes, geodimeter studies (D. A. Swanson, M)
Columbia River basalt (D. A. Swanson, M)
Kimberlites (B. C. Hearn, Jr.)
Regional volcanology (R. L. Smith, NC)
Tephra hazards from Cascade Range volcanoes (D. R. Mullineaux, D)
Volcanic-ash chronology (R. E. Wilcox, D)
Volcanic hazards (D. R. Crandell, D)
States:
Arizona, San Francisco volcanic field (J. F. McCauley, M)
Hawaii:
Hawaiian Volcano Observatory (Hawaii National Park)
Seismic studies (P. L. Ward, M)
Submarine volcanic rocks (J. G. Moore, M)
Idaho (D):
Central Snake River Plain, volcanic petrology (H. E. Malde)
Eastern Snake River Plain region (M. A. Kuntz, H. R. Covington)
Montana, Wolf Creek area, petrology (R. G. Schmidt, NC)
New Mexico, Valles Mountains, petrology (R. L. Smith, NC)
Wyoming, deposition of volcanic ash in the Mowry Shale and Frontier Formation (G. P. Eaton, D)

Water budget:
Hydrologic reconnaissance, west-central Utah (J. S. Gates, w, Salt Lake City, Utah)

Water resources:
Central region field coordination (H. H. Hudson, w, D)
Clinker-water interaction (J. R. Herring, D)
Coal hydrology services (H. H. Hudson, w, D)
Columbia-North Pacific ground water (B. L. Foxworthy, w, Tacoma, Wash.)
Computational hydraulics (V. C. Lai, w, NC)
Data coordination, acquisition, and storage:
NAWDEX Project (M. D. Edwards, w, NC)
Water Data Coordination (P. E. Ward, w, NC)
Evaluation of land treatment (R. F. Hadley, w, D)
Foreign assistance, Section 607 (J. R. Jones, w, NC)
Foreign countries, Saudi Arabia, Saudi Arabian advisory services (G. C. Tibbits, Jr., w, NC)
Ground water, Missouri Basin (O. J. Taylor, w, D)
Hydrology of land use change (D. J. Lystrom, w, NC)
Infiltration and drainage (J. Rubin, w, M)
Information transfer (D. A. Rickert, w, NC)
International activities (J. R. Jones, w, NC)
Monitoring design, coal regions (H. H. Hudson, w, D)
Modeling principles (J. P. Bennett, w, NC)
National assessment (D. W. Moody, w, NC)
National quality of water networks design (R. A. Smith, w, NC)
Network design (M. E. Moss, w, NC)
Northeastern region field coordination (J. F. McCain, w, NC)
Off-road vehicle use (C. T. Snyder, w, M)
Polaris operations (T. T. Conomos, w, M)
Potomac estuary benthic ecology (R. L. Cory, w, Edgewater, Md.)
Potomac estuary dissolved oxygen (W. E. Webb, w, NC)
Potomac estuary submersed vegetation (V. P. Carter, w, NC)
Potomac phytoplankton (R. R. Cohen, w, NC)
Powell arid lands centennial (R. F. Hadley, w, D)
Quality of clinker aquifer (J. R. Herring, D)
Quality-of-water accounting network (R. J. Pickering, w, NC)
Rehabilitation potential, energy lands (L. M. Shown, w, D)
Snow chemistry reconnaisance (H. R. Feltz, w, NC)
Southeastern region field coordination (C. L. Holt, w, Atlanta, Ga.)
Southeast sand aquifer study (H. B. Counts, w, Atlanta, Ga.)
State aid, miscellaneous (J. R. Jones, w, NC)
2D finite element modeling (J. K. Lee, w, Bay St. Louis, Miss.)
Water for coal conversion, Upper Missouri River basin (O. O. Taylor, w, D)
Water-resource activities (J. P. Monis, w, D)
Waterway treaty engineering studies (J. A. Bettendorf, w, NC)
Western Region field coordination (L. E. Newcomb, w, M)
States and territories:
Alabama:
Drainage areas (J. C. Scott, w, Montgomery)
Plans, reports, and information (C. A. Pascole, w, Tuscaloosa)
Alaska (w, Anchorage, except as otherwise noted):
Arctic resources (J. M. Childers)
Coal resources study (D. R. Scully)
Collection of basic records analysis (D. R. Lamke)
Geohydrology, Delta-Clearwater area (D. E. Wilcox)
National Petroleum Reserve hydrology (C. E. Sloan)
North Star project (A. P. Krumbardt, w, Fairbanks)
Northwest Alaska gas pipeline (C. E. Sloan)
St. Paul Island (A. N. Feulner)

Water resources—Continued

States and territories—Continued

Arizona:
- Black Mesa hydrologic study (C. K. Bell, w. Tucson)
- Black Mesa monitoring program (J. H. Eychaner, w. Flagstaff)
- Verde Valley water resources (S. J. Owen, w, Tucson)
- Water resources of the Papago Reservation (L. J. Mann, w, Tucson)

Arkansas (w, Little Rock):
- Cache River aquifer-stream system (M. E. Broom)
- Investigations and hydrologic information (R. T. Sniegocki)
- Lignite hydrology (J. E. Terry, w, Little Rock)
- Lignite water resources (J. E. Terry)
- Time-of-travel study (T. E. Lamb)

California:
- Borrego Valley ground-water study (W. R. Moyle, w, Laguna Niguel)
- Ground water, Santa Cruz (K. S. Muir, w, M)
- Madera area, ground-water model (C. J. Landquist w, Sacramento)
- Monterey County network evaluation (M. J. Johnson, w, M)
- San Antonio Creek ground water appraisal (M. J. Mallory, w, Laguna Niguel)
- Santa Ynez ground-water quality (L. A. Eccles, w, Laguna Niguel)
- Surface water network study (J. R. Crippen, w, M)
- Water, Redwood National Park (S. H. Hofford, w, M)

Colorado (w, D, except as otherwise noted):
- Arkansas River basin (J. L. Hughes, w, Pueblo)
- Evaluation deep well sites (F. A. Welder, w, Meeker)
- Ground water:
  - Potentiometric surface mapping (F. A. Welder)
  - U.S. Bureau of Mines prototype mine (J. B. Weeks)
- Hydrology:
  - El Paso County (J. L. Hughes, w, Pueblo)
  - Naval Oil Shale Reserve No. 1 (D. L. Collins)
  - Parachute-Roan Creek Basin (O. B. Adams, w, Grand Junction)
  - South Platte Valley (D. C. Hall)
- Intensive monitoring, Raton, Colorado (D. P. Bauer)
- Larimer-Weld hydrology (D. C. Hall)
- Manual for hydrologic monitoring (R. Brennan, w, D)
- Popularized Piceance Basin report (O. O. Taylor, w, D)
- Regional monitoring (Gerhard Kuhn)
- Regional monitoring, Raton Mesa (A. P. Hall, w, Pueblo)
- Rio Grande Compact Commission (J. F. Blakey)
- San Luis Valley (J. L Hughes, w, Pueblo)
- Sediment yield, Piceance Basin (V. C. Norman)
- Southwest alluvial valleys—Upper Rio Grande (T. M. Crouch, w, Pueblo)
- Spring hydraulics (R. L. Tobin)
- Study plan for oil shale hydrology (O. O. Taylor, w, D)
- Upper Arkansas River basin (D. L. Cain, w, Pueblo)
- Warm-water sloughs (A. W. Burns)
- Water monitoring—coal mining, Colorado (T. R. Dosch, w, D)
- White River basin, Colorado and Utah (D. P. Bauer, w, D)
- Yampa River basin assessment (T. D. Steele)

Connecticut (w, Hartford):
- Ground water, Southbury-Woodbury (D. L. Mazzaferro)
- Hydrogeology, south-central Connecticut (F. P. Haeni)
- Integrated hydrologic network (R. L. Melvin)
- Part 7, Upper Connecticut River basin (R. B. Ryder)
- Part 9, Farmington River basin (E. H. Handman)
- Short-term studies (C. E. Thomas, Jr.)

Water resources—Continued

States and territories—Continued

Florida:
- Caloosahatchee River study (B. F. McPerson, w, Miami)
- City of Sarasota, monitoring (H. R. Sutcliffe, w, Sarasota)
- East Boundary area investigation (B. G. Waller, w, Miami)
- Ground water in Citrus, Hernando, and Levy Counties (J. D. Fretwell, w, Tampa)
- Hydrogeology, middle Peace Basin (W. E. Wilson III, w, Tampa)
- Hydrology of lakes in southwest Florida (S. E. Henderson, w, Tampa)
- Hydrology, Manatee County (D. P. Brown, w, Sarasota)
- Ochlockonee River basin investigation (C. A. Pascale, w, Tallahassee)
- Potentiometric surface, St. Petersburg-Tampa (R. M. Wolansky, w, Tampa)
- Sand-gravel aquifer, Pensacola (Henry Trapp, w, Tallahassee)
- Santa Fe River basin (J. D. Hunn, w, Tallahassee)
- Seismic surveys, west central Florida (R. M. Wolansky, w, Tampa)
- Sewage effluent disposal, irrigation (M. C. Yurewics, Tallahassee)
- Hydrogeologic maps, Seminole County (W. D. Wood, w, Winter Park)
- Landfill and sewage effluent (M. R. Fernandez, w, Tampa)
- Lee County (D. H. Boggess, w, Ft. Myers)
- Loxahatchee River assessment (G. W. Hill, w, Miami)
- Solid waste, Hillsborough County (Mario Fernandez, Jr., w, Tampa)
- Special studies, technical assistance (John Vecchioli, w, Tallahassee)
- Technical assistance, Suwanee River Water Management District (J. C. Rosenau, w, Tallahassee)
- Trend analysis, southeast Florida (W. J. Haire, w, Miami)
- Water Atlas (S. D. Leach, w, Tallahassee)
- Water resource assessment, statewide (J. D. Simmons, w, Tallahassee)
- Water resources, Duval and Nassau counties (E. C. Hayes, w, Jacksonville)
- Water resources, Hendry County (J. E. Fish, w, Miami)
- Water resources of Manasota Basin (D. P. Brown, w, Tampa)
- Withlacoochee River region (R. A. Miller, w, Orlando)

Georgia (w, Doraville):
- Water resources information system (R. F. Carter)

Hawaii (w, Honolulu):
- Biology-morphology, Wailuku River (J. J. S. Yee)
- Data management, Guam (C. J. Huxel, Jr.)
- Topical studies (B. L. Jones)

Idaho (w, Boise):
- Effects of ash (S. A. Frenzel, w, Boise)
- Kootenai Board—WWT (E. F. Hubbard)
- Special studies (C. A. Thomas)
- Streamflow evaluation, Upper Snake River (C. A. Thomas)

Indiana, Water resources, Kokomo area (J. C. Peters, w, Indianapolis)

Iowa (w, Iowa City), Low flow, Iowa streams (O. G. Lara)

Kansas (w, Lawrence, except as otherwise noted):
- Geohydrology Arkansas River valley southwest Kansas (L. E. Dunlap, w, Garden City)
- Glacial deposits (J. E. Denne)
- Special hydrologic investigations (H. G. O'Conner)

Water resources—Continued

States and territories—Continued

Kentucky (w, Louisville):
- Big Sandy River basin, Levisa Fork (R. W. Davis, w, Louisville)
- Ground water, Ohio River valley (J. M. Kernodle)
- Hydrology of oil shale areas (R. W. Davis, w, Louisville)
- Somerset hydrology (R. W. Davis)

Louisiana (w, Baton Rouge):
- Baton Rouge area (C. D. Whiteman, Jr.)
- Ground water, Kisatchie Forest area (J. E. Rogers, w, Alexandria)
- Lignite hydrology (J. L. Snider, w, Alexandria)
- New Orleans area (D. C. Dial)
- Reports on special topics (M. J. Forbes)
- Site studies (J. E. Rogers)
- Surface water:
  - Flood hydraulics and hydrology (F. N. Lee)
  - Velocity of Louisiana streams (G. J. Arcement)

Maine, Hydrology of peat bogs (W. J. Nichols, w, Augusta)

Massachusetts:
- French-Quinebaug study (B. J. Ryan, w, Boston)
- Ground-water quality network (B. J. Ryan, w, Boston)
- Water resources, Chicopee River basin (B. E. Krejmas, w, Boston)

Michigan (w, Lansing, except as otherwise noted):
- Construction of wells (F. R. Twenter)
- Geohydrology, environmental planning (F. R. Twenter)
- Ground water:
  - Models, Muskegon County (M. G. McDonald)
  - West Uppir Peninsula (C. J. Doonan)
- Water resources of Pictured Rocks (A. H. Handy)
- Water resources of Sleeping Bear Dunes (A. H. Handy)

Minnesota (w, St. Paul):
- Sherburne Wildlife Refuge (B. M. Wrege, w, St. Paul)
- Twin Cities ground-water study (J. H. Guswa)

Mississippi (w, Jackson):
- Flood studies, statewide (K. V. Wilson)
- Salt Dome hydrology in Mississippi (C. A. Spiers)
- Water assimilation (G. A. Bednar)

Missouri:
- Irrigation water, Audrian County (L. F. Emmett, w, Rolla)
- Water in northwestern Missouri (John Skelton, w, Rolla)

Montana (w, Helena, except as otherwise noted):
- Ground water, Fort Belknap (R. D. Feltis, w, Billings)
- Hydrology, lower Flathead (A. J. Boettche)
- Special investigations (J. A. Moreland)

Nebraska:
- Hydrogeology of south central Nebraska (J. M. Peckenpaugh, w, Lincoln)
- Time-of-travel data (L. R. Petri, w, Lincoln)

Nevada (w, Carson City):
- Aquifers in the Fallon area (P. A. Glancy)
- Surface water network evaluation (R. R. Squires)
- Topical studies (P. A. Glancy)
- Water supply:
  - Cold Spring Valley (A. S. Van Denburgh)
  - Mining districts (H. A. Shamberger)

New Jersey (w, Trenton):
- Cohansey Model (A. W. Harbaugh, w, Trenton)
- Problem river studies (J. C. Schornick, Jr.)
- Geophysical logging (R. L. Walker)
- Sole source aquifer system (E. F. Vowinkel, w, Trenton)
- Water resources, Wharton Tract (A. W. Harbaugh)

Water resources—Continued

States and territories—Continued

New Mexico (w, Albuquerque):
- Coal-lease areas, northwest New Mexico (J. R. Hejl)
- Ground water:
  - Harding County (F. D. Trauger)
  - Miscellaneous activities, State Engineering (W. A. Mourant)
  - White Sands Missile Range, water levels and pumpage (H. D. Hudson)
- Liaison—U.S. Geological Survey-Bureau of Land Management (Kim Ong)
- Pojoaque River analyses (G. A. Hearne)
- Southwest alluvial valleys (east) (D. W. Wilkins)

New York (w, Syosset, except as otherwise noted):
- Ground-water resources, Montauk area (K. R. Prince, w, Syosset)
- Ground-water yields (J. Soren, w, Syosset)
- Hydrogeology of Nassau County (Chabot Kilburn)
- Snow survey (R. V. Allen, w, Albany)
- Surface-water network evaluation (T. J. Zembrzuski, Jr., w, Albany)
- Water resources, South Fork, Long Island (Bronius Nemickas)

North Dakota (w, Bismarck, except as otherwise noted):
- Airborne snow surveys (D. G. Emerson, w, Bismarck)
- Ground water:
  - Dickey-Lamoure (C. A. Armstrong)
  - Hydrologic changes due to mining (W. F. Horak)
  - Ransom-Sargent (C. A. Armstrong)
  - Special investigations (K. F. Brinster)
- Rattlesnake Butte area hydrology (W. F. Horak, Jr.)
- Wibaux-Beach deposit hydrology (W. F. Horak, Jr.)

Northern Mariana Islands, Water resources information—Northern Marianas (D. A. Davis, w, Honolulu, Hawaii)

Ohio, Water for coal conversion (A. C. Razem, w, Columbus)

Oklahoma (w, Oklahoma City):
- Ground water, Antlers Sand (D. L. Hart, Jr.)
- Monitor Oklahoma coal field (R. K. Corley)
- Requests, special investigations (J. H. Irwin)

Oregon:
- Coal hydrology (G. G. Parker, w, Portland)
- Mount St. Helens (S. W. McKenzie, w, Portland)

Pennsylvania (w, Harrisburg, except as otherwise noted):
- Chemistry of precipitation (T. G. Ross, w, Malvern)
- Gaging network (H. N. Flippo, Jr.)
- Ground water:
  - Cumberland Valley (A. E. Beecher)
  - Ground-water resources of the Williamsport area (O. B. Lloyd)
- Highway construction effects on streams (J. F. Truhlar, Jr.)
- Western Pennsylvania (G. R. Schiner)

Puerto Rico (w, San Juan):
- Contingent requests (E. D. Cobb)
- Geohydrology of landfills, (Fernando Gomez-Gomez)
- St. Thomas water-resources appraisal (H. J. McCoy)

South Carolina (w, Columbia):
- Effectiveness of Cooper River rediversion (G. G. Patterson, w, Columbia)
- Reconnaissance of estuaries (F. A. Johnson)

South Dakota (w, Huron, except as otherwise noted):
- Cheyenne and Standing Rock Indian Reservations (L. W. Howells)

SUBJECT INDEX

A

B

C

D

E

F

G

H

I

J

K

L

M

N

O

P

Q

R

S

T

U

V

W

X

Y

INVESTIGATOR INDEX

D

E

F

G

H

N

O

P

R

S

T

U

V

W

Y

Z

☆ U.S. GOVERNMENT PRINTING OFFICE: 1982 — 361-614/10